

Office of Research and Development

Crosstalk in Stereoscopic Displays

Andrew J. Woods

**This thesis is presented for the Degree of
Doctor of Philosophy
of
Curtin University**

November 2013

“To the best of my knowledge and belief this exegesis contains no material previously published by any other person except where due acknowledgment has been made. This exegesis contains no material which has been accepted for the award of any other degree or diploma in any university.”



Andrew J. Woods

Abstract

The research presented in this thesis examines the image quality attribute of stereoscopic displays called crosstalk.

Stereoscopic 3D displays function by presenting a separate perspective view to each of an observer's two eyes, thereby allowing most observers to perceive an image containing realistic depth by way of binocular stereopsis. Ideally the left eye will only see the left perspective image, and the right eye only see the right perspective image. However, when crosstalk is present in a stereoscopic display, in addition to each eye seeing its intended view, it is also able to see some of the view(s) not intended for that eye. Crosstalk, sometimes known as ghosting, is usually perceived as a ghost-like doubling of features across the image. High levels of crosstalk degrade the perceived image quality of a stereoscopic image, and if crosstalk levels are particularly high, binocular fusion of the stereoscopic image can be adversely affected or even prevented.

Crosstalk occurs with most stereoscopic displays and the mechanisms that cause crosstalk can vary widely from one display technology to another, and from one 3D method to another. The thesis examines these mechanisms and also describes the development of models and simulations to predict the occurrence of crosstalk on a selection of stereoscopic displays. The development of a simulation to predict crosstalk performance is an important step in the analysis of crosstalk as it allows the relative contribution of the different crosstalk mechanisms to be determined – an aspect which cannot be determined by crosstalk measurement alone. A crosstalk simulation also allows "what-if" scenarios to be conducted virtually and quickly to determine the efficacy of different crosstalk reduction strategies.

Stereoscopic display technologies considered in this thesis include: time-sequential 3D and anaglyph 3D methods on liquid crystal displays (LCDs), plasma displays, digital light projection (DLP) displays, and cathode ray tube (CRT) displays; as well as anaglyph 3D in printed images.

The thesis includes a wide range of recommendations and guidance on techniques that will allow crosstalk levels to be reduced, including: increasing the addressing rate on time-sequential 3D LCDs, using printing inks with improved spectral characteristics for printed anaglyph 3D images, using anaglyph 3D glasses that have good spectral characteristics, disabling colour management on anaglyph 3D displays, and reducing phosphor persistence on time-sequential 3D plasma displays.

The ability to present stereoscopic images with low levels of crosstalk is an important goal in producing high-quality stereoscopic images, hence there is a motivation to develop stereoscopic

displays that exhibit low levels of crosstalk. This thesis provides a range of new insights which are critical to a detailed understanding of crosstalk and consequently to the development of effective crosstalk reduction techniques.

(439 words)

Acknowledgements

There are many, many people I wish to acknowledge and thank for their support, advice, guidance, direction and understanding whilst working towards the PhD holy grail.

Firstly, my gratitude to my supervisor and mentor, Dr Alec Duncan, and my co-supervisor, Dr Peter Fearn, for reading numerous drafts and providing expert guidance – your input has been invaluable.

I am grateful to the former and current Directors of the Centre for Marine Science and Technology (CMST) at Curtin University: John Penrose, Kim Klaka, and Christine Erbe – your support and encouragement have been very much appreciated. To my colleagues at CMST, you're a great team to work with – a wonderful family of marine researchers!

Over the years I have had the privilege of working with a number of people on projects that have contributed to this PhD. Thank you to the many collaborators and co-authors whom I have worked with directly on various aspects of this work: Stanley Tan, Tegan Rourke, Ka Lun Yuen, Kai Karvinen, Adin Sehic, Chris Harris, Dean Leggo, Jesse Helliwell, and Mike Weissman.

On the technical front, I am indebted to the many individuals who have assisted with test equipment, lab space, and software: Glen Lawson, Mal Perry, Frank Thomas, Ming Lim and Dan Marrable. Thanks also to those who helped with user testing: Bob Loss, Iain Parnum, Jesse Helliwell, Alec Duncan, Angela Recalde Salas, Michael Bittle, Matthew Koessler, and Ming Lim.

Various parts of the work conducted in this thesis was supported by iVEC, WA:ERA, and JumboVision – to these groups, a very big thank you. I would also like to acknowledge everyone who provided assistance with fine-tuning the published manuscripts: John Merritt, John Stern, plus the editors and anonymous reviewers of the journals in which the papers of this thesis were published.

To the Deans of Research at Curtin: Leonie Rennie, Graeme Wright and Kate Wright – I appreciate the important guidance you provided along the PhD pathway. To Andrew Hutchison, John Byron and Graeme Wright, your support in the latter stages of the PhD program was crucial for its completion.

My gratitude goes out to the friends I have made through the Stereoscopic Displays and Applications (SD&A) conference over the last 24 years, your friendship and enthusiasm for all things stereoscopic have been a big part of my academic career. And to those whom I may not have mentioned specifically but have shared ideas and suggestions along the way, thank you too!

Most importantly, the completion of this PhD would not have been possible without the support of my family. To my wife, Denise, for her incredible support and understanding through this very time-consuming process. To my kids, Jasmine and Jade, for allowing their dad to become absorbed in his work especially during the closing stages of the thesis submission process. Yes girls, Daddy has FINALLY finished the thesis and you can have him back now.

Table of Contents

Abstract.....	ii
Acknowledgements.....	iv
Table of Contents	vi
List of Publications	vii
List of Additional Publications by the Candidate Relevant to the Thesis.....	x
Refereed Status Statement	xiv
Copyright Permission Statement	xv
List of Stereoscopic Terminology	xvi
1. Introduction.....	1
1.1 Novelty.....	7
1.2 Exegesis/Publications Roadmap	8
1.3 Chronology.....	9
1.4 Impact.....	12
2. Literature Review	13
3. Research Design	16
4. Overview and Results	19
4.1 Crosstalk Mechanisms	19
4.2 Time-Sequential 3D using Active Shutter Glasses	20
4.2.1 Time-Sequential 3D on CRT Displays	22
4.2.2 Time-Sequential 3D on Plasma Displays.....	24
4.2.3 Time Sequential 3D on LCDs	26
4.2.4 Time-Sequential 3D on DLP Projectors.....	30
4.3 Anaglyph 3D.....	32
4.3.1 Anaglyph 3D on Emissive Displays.....	32
4.3.2 Anaglyph 3D in Printed Images.....	38
5. Review and Discussion	42
6. Conclusion	48
7. List of References (Exegesis only).....	49
8. Bibliography (from Exegesis and Included Publications).....	57
9. Published Papers	78
Appendix 1 – Additional Publications Relevant to the Thesis.....	A1-1
Appendix 2 – Statement of Contribution of Candidate to Submitted Publications	A2-1
Appendix 3 – Evidence of Peer-Review Status of Included Publications	A3-1
Appendix 4 – Copyright Permissions.....	A4-1
Appendix 5 – Full List of All Included Publications.....	A5-1

List of Publications

The full list of publications included in the body of the thesis is as follows.

The publications are grouped by type (refereed journal, refereed conference) and then in the order in which they will appear.

Refereed Journal Articles

Paper 1 A. J. Woods (2012) "Crosstalk in Stereoscopic Displays: a review" Journal of Electronic Imaging, IS&T/SPIE, 21(4), pp. 040902-1 to 040902-21, Oct-Dec 2012.

This paper serves as both a literature review for the field, and also presents new work on the mechanisms of crosstalk, and the measurement of crosstalk using test charts. A precursor of this paper was presented as a keynote presentation at the 3DSA conference in Japan in 2010.¹

Paper 2 A. J. Woods, K. L. Yuen, K. S. Karvinen (2007) "Characterizing crosstalk in anaglyphic stereoscopic images on LCD monitors and plasma displays" Journal of the Society for Information Display, 15(11), pp. 889-898, November 2007.

This paper presents early work on characterising anaglyph crosstalk on a selection of emissive displays, the development of an early simulation, and the results of the simulation. A simple validation was also performed.

Paper 3 A. J. Woods, C. R. Harris (2012) "Using cross-talk simulation to predict the performance of anaglyph 3-D glasses" in Journal of the Society for Information Display, 20(6), pp. 304-315.

This paper presents a mathematical model, and a revised and improved simulation for anaglyph crosstalk on emissive displays. The paper also presents a comprehensive validation of the crosstalk model which provides high confidence in the model, and subsequently the simulation is used to investigate a number of scenarios which can significantly reduce the presence of crosstalk in anaglyph 3D images on emissive displays.

Paper 4 A. J. Woods, C. R. Harris, D. B. Leggo, T. M. Rourke (2013) "Characterizing and Reducing Crosstalk in Printed Anaglyph Stereoscopic 3D Images" (Journal of Optical Engineering, SPIE, 52(4), pp. 043203-1 to 043203-19, April 2013.

Despite the printed anaglyph 3D technique having been invented in 1853, it appears this paper is the first to comprehensively analyse the mechanisms of crosstalk in printed anaglyph 3D images. The printed anaglyph has notable differences to crosstalk in anaglyph 3D on emissive displays, and ordinarily presents much more crosstalk than anaglyphs on emissive displays. The paper also describes a mathematical model to simulate printed anaglyph 3D crosstalk, a program which implements the model, and a comprehensive validation test which provides a high level of confidence in the accuracy of the model. Finally the simulation is used to consider a number of scenarios that can reduce the presence of crosstalk in printed anaglyph 3D images.

Refereed Conference Papers

Paper 5 A. J. Woods, K. L. Yuen (2006) "Compatibility of LCD Monitors with Frame-Sequential Stereoscopic 3D Visualisation" (Invited Paper), IMID/IDMC '06 Digest, (The 6th International Meeting on Information Display, and The 5th International Display Manufacturing Conference), pp. 98-102, Daegu, South Korea, 22-25 August 2006.

This paper appears to have been the first published manuscript to comprehensively analyse the time-domain performance of LCD monitors and describe why high levels of crosstalk occur with non-3D-ready LCD monitors. This work was the first published manuscript to disclose a way of reducing crosstalk when using the time-sequential 3D method on LCD monitors by increasing the image update addressing rate. My early papers used to term "compatibility" to refer to the display's capability to present 3D images with low levels of crosstalk.

Paper 6 A. J. Woods, K. S. Karvinen (2008) "The compatibility of consumer plasma displays with time-sequential stereoscopic 3D visualization" Stereoscopic Displays and Applications XIX, Proceedings of IS&T/SPIE Electronic Imaging, SPIE Vol. 6803, pp. 68030X-1 to 68030X-9, San Jose, California, January 2008.

This paper presents a comprehensive analysis of the ability for consumer plasma displays to display low crosstalk images when used with active shutter 3D glasses. Although a search of the literature found two papers which described an earlier effort to develop an experimental plasma display which exhibited low-crosstalk performance, the methods they used were not disclosed.

Paper 7 A. J. Woods, A. Sehic (2009) "The compatibility of LCD TVs with time-sequential stereoscopic 3D visualization" Stereoscopic Displays and Applications XX, Proceedings of IS&T/SPIE Electronic Imaging, SPIE Vol. 7237, pp. 72370N-1 to 72370N-9, San Jose, California, January 2009.

This paper described the analysis of several new backlight and LCD addressing technologies and their effect on the ability for low-crosstalk images to be achieved on these displays.

Paper 8 A. J. Woods, C. R. Harris (2010) "Comparing levels of crosstalk with red/cyan, blue/yellow, and green/magenta anaglyph 3D glasses" in Stereoscopic Displays and Applications XXI, Proceedings of IS&T/SPIE Electronic Imaging, SPIE Vol. 7253, pp. 75240Q-1 to 75240Q-12, San Jose, California, January 2010.

*This work was conducted as a continuation of the work conducted in (refereed journal paper) **Paper 2**. It extended the simulation to consider the performance of other colour-combination types of anaglyph glasses. A rudimentary validation was also performed.*

Referencing of Thesis Papers

Throughout this exegesis, references to each of the papers included in the thesis is done by way of bold italic text "**Paper #**" where "#" is the actual paper number. For ease of reference when reading this exegesis, a condensed list of all paper numbers, linking them to the paper titles is provided in Appendix 5.

List of Additional Publications by the Candidate Relevant to the Thesis

Several additional manuscripts by me (one refereed journal paper, one invited refereed article, one refereed conference paper, and six non-refereed conference papers) which are also relevant to this topic, but not part of the body of the thesis, are included as an appendix to the thesis – see Appendix 1 (as per section 4.7 of “Curtin University of Technology - Guidelines for Thesis by Publication”).

Paper 9 A. J. Woods, S. Tan (2002) “Characterising Sources of Ghosting in Time-Sequential Stereoscopic Video Displays” presented at Stereoscopic Displays and Applications XIII (SD&A), published in Stereoscopic Displays and Virtual Reality Systems IX, Proceedings of IS&T/SPIE Electronic Imaging, SPIE Vol. 4660, pp. 66-77, San Jose, California, January 2002. [Non-Refereed Conference Paper]

*This paper reported on an analysis of the mechanisms of crosstalk when using active shutter glasses with CRT displays to present stereoscopic 3D images. The results of this work are reported in refereed journal format in **Journal Paper 1**. **Paper 1** is the first appearance of the work of **Paper 9** in refereed journal format.*

Paper 10 A. J. Woods, T. Rourke (2004) “Ghosting in Anaglyphic Stereoscopic Images” presented at Stereoscopic Displays and Applications XV (SD&A), published in Stereoscopic Displays and Virtual Reality Systems XI, Proceedings of IS&T/SPIE Electronic Imaging, SPIE Vol. 5291, pp. 354-365, San Jose, California, January 2004. [Non-Refereed Conference Paper]

*This paper reported an early analysis of crosstalk in anaglyph 3D images on emissive displays. The results of this work are reported in refereed journal format in (refereed journal) **Paper 1**, and contributed valuable background research to (refereed journal) **Paper 2**.*

Paper 11 A. J. Woods (2005) "Compatibility of Display Products with Stereoscopic Display Methods" International Display Manufacturing Conference (IDMC), pp. 290-293, Taiwan, February 2005. [Non-Refereed Conference Paper]

This paper was an early attempt to classify the display performance characteristics of a wide range of emissive displays and their ability to present low-crosstalk stereoscopic images using a selection of stereoscopic display methods. In this context, "compatibility" refers to the display's ability to present low-crosstalk stereoscopic images.

Paper 12 A. J. Woods, T. Rourke, K. L. Yuen (2006) "The Compatibility of Consumer Displays with Time-Sequential Stereoscopic 3D Visualisation" (Invited Plenary Paper), Proceedings of the K-IDS Three-Dimensional Display Workshop 2006, pp. 7-10, Seoul National University, Seoul, South Korea, 21 August 2006. [Non-Refereed Conference Paper]

*This paper presented an analysis of the display performance characteristics of LCD monitors and DLP projectors and their ability to display low-crosstalk stereoscopic images. Again in this context, "compatibility" refers to the display's ability to present low-crosstalk stereoscopic images. This work was subsequently presented in more detail in (refereed conference paper) **Paper 5** and (non-refereed conference paper) **Paper 12**.*

Paper 13 A. J. Woods, T. Rourke (2007) "The compatibility of consumer DLP projectors with time-sequential stereoscopic 3D visualization" presented at Stereoscopic Displays and Applications XVIII, published in Stereoscopic Displays and Virtual Reality Systems XIV, Proceedings of IS&T/SPIE Electronic Imaging, SPIE Vol. 6490, pp. 64900V-1 to 64900V -7, San Jose, California, January 2007. [Non-Refereed Conference Paper]

*This paper presented a more detailed analysis of the display performance characteristics of DLP projectors and their ability to display low-crosstalk stereoscopic images. Again in this context, "compatibility" refers to the display's ability to present low-crosstalk stereoscopic images. Aspects of this work are subsequently reported in (refereed journal) **Paper 1**.*

Paper 14 A. J. Woods (2009) "3-D Displays in the Home" *Information Display*, 25(07), pp 8-12, July 2009. [Invited Refereed Article]

*This paper reviewed the five technologies that were being used for consumer released 3DTVs and 3D monitors at the time the article was written – DLP time-sequential, LCD micro-polarised, LCD time-sequential, PDP (plasma display panel) time-sequential, and LCD variable-polarisation-angle. The second half of the paper discussed the compatibility of conventional (non-3D-Ready) displays with stereoscopic display methods, drawing from **Paper 5**, **Paper 6**, **Paper 7**, and **Paper 11**.*

Paper 15 M. A. Weissman, A. J. Woods (2011) "A simple method for measuring crosstalk in stereoscopic displays" *Stereoscopic Displays and Applications XXII, Proceedings of IS&T/SPIE Electronic Imaging, SPIE Vol. 7863*, pp. 786310-1 to -11, Burlingame, California, January 2011. [Non-Refereed Conference Paper]

*This paper describes the development of a test chart method of measuring crosstalk in stereoscopic displays. The results of this work are reported in **Journal Paper 1**.*

Paper 16 A. J. Woods (2011) "How are crosstalk and ghosting defined in the stereoscopic literature?" *Stereoscopic Displays and Applications XXII, Proceedings of IS&T/SPIE Electronic Imaging, SPIE Vol. 7863*, pp. 78630Z-1 to 78630Z-12, Burlingame, California, January 2011. [Non-Refereed Conference Paper]

*This paper investigated the published literature on the terms crosstalk and ghosting and related terms to determine accepted meanings, as well as descriptive and mathematical definitions. This paper informs the literature review of the thesis and its results are also reported in (refereed journal) **Paper 1**.*

Paper 17 A. J. Woods, J. Helliwell (2012) "Investigating the cross-compatibility of IR-controlled active shutter glasses" Stereoscopic Displays and Applications XXIII, Proceedings of IS&T/SPIE Electronic Imaging, SPIE Vol. 8288, pp. 82881C-1 to 82881C-10, Burlingame, California, January 2012. [Refereed Conference Paper]

*This paper investigates the infra-red signalling which is used to control and synchronise the operation of liquid-crystal shutter glasses with the light output of time-sequential 3D displays. Aspects of this work, primarily the phase and duty cycle of the glasses, provide background knowledge for the analysis of crosstalk in shutter glasses 3D displays as reported in (refereed journal) **Paper 1** and (refereed conference) **Paper 5**, **Paper 6** and **Paper 7**.*

Paper 18 A. J. Woods (2013) "3D or 3-D: A study of terminology, usage and style" European Science Editing, 39(3), pp. 59-62, August 2013. [Refereed Journal Paper]

This paper investigates the terminology and usage of the two acronyms "3D" and "3-D" and in particular examines the publication styles which prescribe their usage in various technical publications. Both acronyms are accepted abbreviations for the term "three-dimensional" but when publishing the works of this thesis, several different publication styles were encountered with different publishers. I felt it was important to understand the background behind the various publication styles as they can have a significant effect on the ambiguity and preciseness of language related to stereoscopic displays.

Refereed Status Statement

This listing outlines the refereed status of all the publications included with this thesis.

[Core Publications]

Papers 1 to 4 are published in refereed journals:

- the IS&T/SPIE Journal of Electronic Imaging (JEI)
- the Journal of the Society for Information Display (JSID)
- the SPIE journal of Optical Engineering (OE)

Papers 5 to 8 are refereed papers published in conference proceedings:

- the IS&T/SPIE Stereoscopic Displays and Applications conference
- the International Meeting on Information Display (IMID)

[Additional Publications]

Paper 18 is published in a refereed journal – European Science Editing.

Paper 14 is published in a refereed society periodical – Information Display.

Paper 17 is a refereed paper published in a conference proceedings – IS&T/SPIE Stereoscopic Displays and Applications.

Paper 9, Paper 10, Paper 11, Paper 12, Paper 13, Paper 15 and **Paper 16** were published in conference proceedings and were not refereed.

Evidence of peer-review of the refereed papers is provided in Appendix 3.

Copyright Permission Statement

I warrant that I have obtained, where necessary, permission from the copyright owners to use any third-party copyright material reproduced in the thesis (e.g. questionnaires, artwork, unpublished letters), or to use any of my own published work (e.g. journal articles) in which the copyright is held by another party (e.g. publisher, co-author).

Copies of the copyright permission statements for each of the papers included in this thesis are included in Appendix 4.

List of Stereoscopic Terminology

3D	An acronym for 'three-dimensional'. Is often used to specifically refer to stereoscopic 3D technologies or methods (such as 3D Movies, 3D Displays, 3D cameras, 3D glasses, etc.) which invoke a person's binocular vision to experience depth perception, however it can also be used to refer to non-stereoscopic 3D technologies (such as 3D computer graphics, 3D animation, 3D modelling, 3D printing, DirectX 3D, etc.).
3DTV	A television display that is capable of displaying stereoscopic 3D images and video. Short for "Three-Dimensional Television".
3-D	see 3D
Anaglyph	A method of presenting stereoscopic 3D images where the left and right images are multiplexed using complementary colour channels of the display (usually red for the left eye and cyan for the right eye, although other colour combinations are possible) and the observer wears 3D glasses fitted with colour filters matched to the chosen colour channels. From Late Latin 'anaglyphus', carved in low relief.
Crosstalk	The incomplete isolation of the left and right image channels in a stereoscopic display so that the content from one channel is partly present in another channel. ² For multi-view displays this can be simplified to: The incomplete isolation of the image channels in a stereoscopic display so that the content from one channel is partly present in another channel.
CRT	Cathode ray tube – as in the original technology used for television displays
DLP	Digital light processing – as used in some projectors and rear-projection televisions. The core technology in a DLP based display is a digital micro-mirror device (DMD).
Ghosting	The perception of crosstalk – see crosstalk. ²
Leakage	The (amount of) light that leaks from one stereoscopic image channel to another – see crosstalk. ²
LCD	Liquid-crystal display
LCS	Liquid-crystal shutter - as used in LCS 3D glasses (or active shutter glasses) with time-sequential stereoscopic displays.
PDP	Plasma display panel
s3D	Stereoscopic 3D – see '3D' and 'Stereoscopic'
Stereoscopic	'Solid looking': having visible depth as well as height and width. May refer to any experience or device that is associated with binocular depth perception. ³

Time-sequential A method of presenting stereoscopic 3D images where the left and right images are displayed alternately as a sequence of left and right images (usually at 120 or 100fps) and some type of 3D glasses or autostereoscopic apparatus is used to gate left and right images to the left and right eyes. The most common implementation has the observer wearing a pair of active shutter glasses (usually fitted with liquid crystal (LC) shutters) which alternately block the left and right eyes in sequence with the presented left and right images. Also known as time-multiplexed, the term is a superset of: field-sequential, frame-sequential, alternate field, alternate frame, and active-stereo.

1. Introduction

The research presented in this thesis examines the image quality attribute of stereoscopic displays called crosstalk.

Stereoscopic displays are a special class of display which are capable of presenting stereoscopic 3D images to an observer. There is an incredibly wide variety of stereoscopic display technologies that have been conceived, demonstrated or are commercially available^{4,5} (**Paper 14** provides a description of 3D displays available to home consumers in 2009). Stereoscopic 3D displays function by presenting a separate perspective image to each of an observer's two eyes, thereby allowing most observers to perceive an image containing realistic depth, by way of binocular stereopsis. It is worth noting that an estimated 2% of the population do not have normal stereoscopic image perception and hence won't be able to experience the full benefit of a stereoscopic display.⁶ For those that do have good binocular vision, stereoscopic displays provide a heightened sense of realism and a visually attractive form of image reproduction.

The ways in which various stereoscopic displays relay different perspective images to the two eyes of an observer are amazingly wide and varied. Examples include:

- 'Time-Sequential 3D' where the observer(s) wear a pair of active shutter glasses (containing liquid crystal shutters (LCS)) which alternately block and pass a discrete sequence of left and right images from the display to the observers' left and right eyes;
- 'Polarised 3D' where the left and right images are presented with different light polarisation and the observer(s) wear a pair of polarised 3D glasses which direct the correct image to each eye;
- 'Anaglyph 3D' (also known as spectral-multiplexing) where the left and right images are encoded into different colour ranges of the visible spectrum (The Infitec,⁷ Dolby 3D,⁸ and Panavision 3D cinema techniques are a special cases of anaglyph); and
- 'Lenticular 3D' and 'Parallax Barrier 3D' where a special lens sheet or barrier sheet is placed over the face of a display which creates multiple viewing zones in different directions so that the observers' left and right eyes receive different perspective images.

Display technologies which can be used as the basis for stereoscopic display include liquid crystal displays (LCD), plasma display panels (PDP), cathode ray tubes (CRT), digital light projection (DLP), organic light emitting diode (OLED), light emitting diode (LED) arrays, film projection and also the printed page.

Stereoscopic displays are now deployed very widely in consumer, business, and industry environments. In 2012 there were an estimated 43 thousand 3D cinema screens worldwide,⁹ and an estimated cumulative 45 million 3DTVs (Three-Dimensional Televisions) sold worldwide.¹⁰

Additionally, there is a growing number of stereoscopic 3D display devices including 3D monitors, 3D projectors, 3D mobile phones, 3D cameras, 3D glasses, 3D tablets and other 3D devices.¹¹

The substantive topic of this thesis is crosstalk in stereoscopic displays. Crosstalk is a display performance characteristic of stereoscopic displays. In an ideal stereoscopic display, the left image is only sent to the left eye and the right image is only sent to the right eye. However, due to various imperfections with most stereoscopic display technologies, some of the left image can leak to the right eye, and some of the right image leaks to the left eye. This leakage of one image into the other eye will usually be seen as a slight doubling or ghosting of the image, and is generally known as ghosting or crosstalk. Different displays will exhibit different amounts of crosstalk, and depending on the amount of crosstalk, it can degrade the perceived image quality of stereoscopic 3D images. If crosstalk levels are sufficiently high, the fusion of stereoscopic image pairs by the human observer's visual system can fail, preventing the successful perception of a stereoscopic 3D image. Crosstalk is one of the primary determinants of image quality in stereoscopic displays. Ideally, crosstalk levels for any high-quality stereoscopic display will be low – preferably much less than 5%.²

The terms 'stereoscopic' and '3D' are often used interchangeably in the published literature, as they sometimes are in this exegesis and the included papers, however these two terms do have important differences. The term '3D' is short for 'three-dimensional' and technically can be used to refer to any device containing, or concept referring to, three dimensions. The term "three-dimensional" has been used in relation to stereoscopic photography at least since 1936.¹² The first use of the abbreviation "3-D" in the published literature appears to be Spottiswoode, et al. in 1952 in reference to 3D Movies.¹³ "3D" has been used in reference to all stereoscopic technologies ever since. In the 1970s and 1980s the terms 3D computer graphics and 3D animation started to be used to refer to the computer generation of images which contained monocular depth cues to enhance the realism of the images, but were not necessarily stereoscopic.¹⁴ Other uses of the 3D term include 3D printing (additive manufacturing), 3D laser scanning, 3D Computer Aided Design (CAD), 3D modelling (3D reconstruction), DirectX 3D, and others. In essence stereoscopic 3D is a subset of all possible uses of the term 3D. For clarity, some authors use the abbreviation s3D to explicitly describe the stereoscopic form of 3D, but in many instances the distinction will be obvious. In this thesis "3D" will always be used in reference to stereoscopic 3D, unless stated otherwise.

The term three-dimensional can be abbreviated as either "3-D" or "3D". Many journals and most newspapers apply a house style requiring the use of the hyphenated "3-D" form, whereas younger publications generally use the non-hyphenated "3D" form. This exegesis and most of the papers included with the thesis use the non-hyphenated "3D" form. Some of the papers in this thesis have been published in journals which prescribe the use of the hyphenated form, and hence these papers

use the “3-D” form. The usage of the two forms “3D” and “3-D” in the wider published literature is examined in more detail in *Paper 18*.¹⁵

In the published literature the term crosstalk can sometimes be written as ‘cross-talk’,¹⁶ ‘cross talk’¹⁷ or even ‘X-talk’.¹⁶ The term ‘crosstalk’ without any intermediate space or hyphen, is the more commonly used variant so that is what will be used in this exegesis (as described in *Paper 16*).¹⁸ One of the journals that published two of the papers contained in this thesis prescribed the use of the ‘cross-talk’ form, so those two papers (*Paper 2* and *Paper 3*) vary from the style of the other papers contained in this thesis.

There is also some ambiguity about the definition of the term “stereoscopic display” in the published literature. The three terms “stereoscopic display”, “autostereoscopic display”, and “three-dimensional display” are related but distinct.

In the first definition:

“stereoscopic display” refers to any display that is capable of displaying stereoscopic images to an observer (either a display requiring the observer to wear some type of 3D glasses or a display capable of presenting separate views to the left and right eyes without requiring the user to wear some form of 3D glasses).^{19,20}

In the second definition:

“stereoscopic display” refers to displays that are capable of presenting stereoscopic images to the observer that require the observer to wear some form of viewing apparatus, e.g. 3D glasses.²¹

In both definitions, “autostereoscopic displays” are displays capable of presenting stereoscopic images to an observer without the observer needing to wear any form of viewing apparatus – sometimes referred to as being “glasses-free”. In definition 1, “stereoscopic display” is a superset of “autostereoscopic display” whereas in definition 2, “stereoscopic display” and “autostereoscopic display” are mutually exclusive terms. The term “three-dimensional display” usually refers to a superset of “stereoscopic display” and “autostereoscopic display” to additionally include volumetric displays, and holographic displays.²⁰ Definition 1 is what will be used in this thesis.

The human visual system determines depth and dimensionality from images using a range of depth cues.²² These depth cues can be classified into ‘binocular depth cues’ – those requiring the image to be viewed stereoscopically using two eyes – and ‘monocular depth cues’ – those depth cues that can be perceived with only one eye. Monocular depth cues include interposition or occlusion, linear perspective, aerial perspective, familiar size, shadows and shading, motion parallax, texture gradient,

and accommodation (focus).²² Binocular depth cues comprise convergence (the inward and outward rotation of the eyes to align on particular objects in a scene) and binocular disparity (the difference in image location of an object seen by the left and right eyes, resulting from the horizontal separation of the two eyes).²² Convergence and binocular disparity are the two cues that are missing from regular 2D displays – but are specifically invoked in stereoscopic displays. Two eyes (and functioning binocular vision) are required to see and utilize binocular depth cues – they cannot be seen with only one eye. Binocular depth cues usually provide the strongest sense of depth amongst all depth cues.

One of the fascinating aspects about crosstalk is that the mechanisms by which it occurs vary considerably from one stereoscopic display technology to another. Even within one stereoscopic display: there will be multiple contributors to the overall crosstalk present in a display, the relative proportion of those contributors to the overall crosstalk can vary considerably, and the overall amount of crosstalk can also vary depending on screen position, viewing angle, viewing position, and other factors. Crosstalk is a complicated topic and the work described in this thesis has attempted to make sense and provide some order to the incredible variability of this topic.

In order to achieve the low crosstalk levels that characterise a high-quality stereoscopic display, it is important to understand the relative contributions of the various crosstalk mechanisms of a stereoscopic display, know the display properties (such as pixel response rate, or pixel spectra) that determine how crosstalk occurs, and finally identify the combination of display properties and technologies that will economically allow low-crosstalk levels. In order to understand the interplay of all these crosstalk-causing factors, it is highly advantageous to develop an algorithm and simulation which will allow the prediction of crosstalk based on the display specifications. For a display designer, the power of an accurate and functioning simulation is that it allows a range of what-if scenarios to be performed to research low-crosstalk combinations without needing to perform exhaustive physical testing.

The aims of the research described in this thesis are therefore to:

- (a) Characterise the mechanisms by which crosstalk occurs in a selection of stereoscopic display technologies,
- (b) Mathematically model and simulate the presence of crosstalk in a selection of stereoscopic display technologies, and validate those models,
- (c) Use crosstalk simulation to investigate how different display parameters affect the presence of crosstalk, and
- (d) Recommend ways in which crosstalk can be reduced in a selection of stereoscopic display technologies.

This thesis describes the investigation of crosstalk in the following stereoscopic display technologies:

1. time-sequential 3D on CRT displays,
2. time-sequential 3D on plasma TVs,
3. time-sequential 3D on LCD monitors and TVs,
4. time-sequential 3D on DLP projectors,
5. anaglyph 3D on emissive displays (CRT, plasma, LCD, DLP), and
6. anaglyph 3D in printed images.

The work of this thesis concentrates on two particular stereoscopic display methods, time-sequential 3D and anaglyph 3D, and the application of these methods to a selection of display technologies.

The time-sequential 3D technique relies on the alternating presentation of stereo-pair images on a single display surface – also sometimes described as time-multiplexing. The anaglyph 3D technique uses different parts of the visible spectrum to code two perspective images onto the same display surface – sometimes described as spectral-multiplexing. The mixing of the left and right perspective views in any step of the encoding, transmission, and/or decoding process is what leads to crosstalk in both of these systems.

In the list above, the analysis of the anaglyph 3D method on CRT, plasma, LCD, and DLP displays have been grouped into one topic because the same analysis technique can be applied across all four of these emissive display technologies. In contrast, the time-sequential 3D method has been considered as four separate topics when applied to these same four emissive display technologies because there are considerable differences between the analysis technique and results between these four cases.

The work reported in this thesis has consisted of identifying the physical properties of the displays (time domain response, spectral domain performance) and determining how these parameters affect crosstalk. With some of the technologies we have extended the analysis to develop a mathematical model of the presence of crosstalk. This in turn allows a simulation to be developed that can be used to conduct a range of what-if scenarios. With some of the stereoscopic displays modelled, visual comparison tests were also conducted to validate the accuracy of the simulation models.

This work has ridden an important wave in the development of high-quality stereoscopic displays. The work started at a time when CRTs were fast being replaced by LCDs, but at that stage there was no way of displaying time-sequential 3D images on LCDs. At this particular point in time there was considerable concern in the industry that the fast replacement of CRTs with LCDs would rob us of the ability to display high-quality stereoscopic images on consumer displays. Similarly, when this work started, plasma displays and DLP projectors were also mostly incompatible with time-sequential 3D.

Fortunately that situation has now completely changed, and high-quality time-sequential 3D presentation is possible with a wide range of display technologies. My hope is that this early work on the compatibility of new display technologies with stereoscopic display methods and the ability to display low-crosstalk images may have influenced the development efforts of new stereoscopic display technologies. At the very least we know that some of the work of this thesis was conducted at the very fast advancing edge of stereoscopic display developments.

In 2005 and 2006, *Paper 11* and *Paper 12* considered the compatibility of then current display technologies with the various stereoscopic display methods. These papers sought to establish a framework for understanding which displays would and would not support stereoscopic imaging, draw attention to the fact that there were gaps in compatibility that needed further research, and identify the aspects that limited 3D compatibility. Stereoscopic systems have long piggy-backed on existing technologies, hence considering compatibility of stereoscopic methods with existing technologies has been an important process.

Despite the high level of deployment of stereoscopic display technologies in consumer and industrial settings to date, there still remain many gaps of knowledge in this area and there are opportunities for research to address these gaps.

The organisation of this thesis is as follows. Following this introduction (Chapter 1), the literature in the field of crosstalk in stereoscopic displays is reviewed (Chapter 2). Next, the framework for the research into crosstalk is discussed (Chapter 3). The results of the research into crosstalk (Chapter 4) is then provided by way of a discussion of the published works – providing an overview of the findings and linking the published works into a coherent theme. The results and findings of the previous chapter are then reviewed and opportunities for future research discussed (Chapter 5). Finally the thesis draws conclusions from the published works (Chapter 6).

In preparing this exegesis my aim has been to provide a detailed explanatory framework which links the published papers without unnecessarily duplicating the content presented in the publications.

Copies of the publications which form the core of this thesis are included in Chapter 9. Additional publications by me that are relevant to the thesis, and in some cases have informed the refereed publications included in Chapter 9, are included in Appendix 1. A full listing of papers included in the thesis is provided in Appendix 5 in paper number, chronological and title alphabetical order.

Some comments regarding typographical aspects in this exegesis: em-dashes have been typeset with surrounding spaces to give the different statement sections better visual separation; citations to papers in the references list are shown in superscript form; if citations coincide with punctuation, the

citation will generally be placed after the punctuation; where quotations are used, the following punctuation will be placed outside the quotation marks unless the punctuation originally appeared in the quotation; and the exegesis is written in first person voice.

As the reader proceeds through this exegesis, “Chapter #” will refer to chapters in this exegesis, and “Section #” will refer to particular sections in the included publications.

This thesis submission consists of two parts – the ‘exegesis’ and the compendium of published works. The purpose of the ‘exegesis’ is to link the separate published works and to place them into a logical research framework in the context of an established body of knowledge. Hence ‘thesis’ refers to the full PhD submission, whereas ‘exegesis’ refers to the part excluding the published papers.

1.1 Novelty

There are several aspects of this work that are novel:

- (a) this work was the first to investigate and present the sources (mechanisms) of crosstalk for a wide selection of stereoscopic display technologies,
- (b) this work appears to be the first to illustrate the power of developing a simulation of crosstalk in that it allows the various components which contribute to the overall crosstalk to be considered and analysed independently, and allows methods of reducing crosstalk to be investigated quickly,
- (c) this work was the first to comprehensively examine crosstalk for the anaglyph 3D method on emissive displays (such as LCDs, CRTs) and printed images (a notably different problem) – by identifying the sources of crosstalk, describing it mathematically, developing a simulation of crosstalk, validating the simulation, using the simulation to explore a number of hypothetical scenarios, and suggest ways of reducing crosstalk,
- (d) this work was the first to present a spatio-temporal-domain graph of the time-sequential 3D method on LCDs that was a key to understanding the limitations of using the time-sequential 3D technique on LCDs, and
- (e) this work was the first to publish a technique for reducing crosstalk for the time-sequential 3D method on LCD monitors by increasing the image update addressing rate – NVIDIA privately lodged a patent²⁴ on this topic, separate to our efforts, just two weeks before our public disclosure.

In writing this exegesis, I have aimed to demonstrate that my research and published manuscripts have made a valuable contribution to the body of knowledge about crosstalk in stereoscopic displays.

Exegesis/Publications Roadmap

Brief Title	Year	Paper #	Exegesis Chapters																						
			1	2	3	4	4.1	4.2																	
			Introduction	Literature Review	Research Design	crosstalk measurement	CRT	LCDs	DLP	Plasma	LCD TVs	emissive anaglyph	printed anaglyph	Overview and Results	4	4.1	4.2	4.2.1	4.2.2	4.2.3	4.2.4	4.3.1	4.3.2	5	6
Crosstalk review	2012	1	all	5										4, 4.7	4	4.1	4.1	4.1	4.1	4.1	4.5		2, 4, 5		
Emissive Anaglyph Crosstalk 2	2007	2										2										3, 4		3, 4	
Emissive Anaglyph Crosstalk 3	2012	3										3										2-5		5	
Printed Anaglyph Crosstalk	2013	4	1										4									all		5, 6, 7	
Time-sequential on LCDs	2006	5				2																		3	
Time-sequential Plasma	2008	6					2											1, 3, 4						1, 3	
Time-sequential on LCD VTs red/cyan, green/magenta, blue/yellow	2009	7									4													5	
time-sequential on CRTs	2002	9				2									2, 1, 3	all								2	
Emissive Anaglyph Crosstalk 1	2004	10										2										2, 3, 4			
Compatibility of 3D emissive displays	2005	11	all																						
Time-sequential compatibility	2006	12	all																						
time-sequential on DLP	2007	13					2																3		
3D displays summary	2009	14	all																						
crosstalk chart	2011	15			all																			all	
crosstalk in the literature	2011	16	all																					2	
active shutter glasses	2012	17														all									
3D or 3-D	2013	18	all																						

key: 2,3 = relevant section numbers of respective papers

1.2 Chronology

The following listing provides a chronology of significant events in the stereoscopic (and broader) display industry and how the published works of this thesis fit into that chronology. The chronology starts in 1838 when Sir Charles Wheatstone²⁵ published his pivotal paper which described stereoscopic vision. Following this there was a gradual process of development of technologies which allowed stereoscopic display – particularly the invention and combination of CRT displays and LCS 3D glasses. The period from 2003 to 2010 was a particularly significant period of rapid change in the stereoscopic display industry. The CRT, which had been the mainstay of the display industry for almost 100 years, was rapidly being replaced by the LCD, which at that time was not stereoscopic 3D compatible. In 2003 there was considerable concern amongst the stereoscopic imaging community that if the CRT ceased to be produced, the display of stereoscopic imagery on commodity display hardware would become very difficult. Fortunately in quick succession (as can be seen in the chronology), 3D compatible single-chip DLP projectors (2005), 3D compatible DLP TVs (2007), 3D compatible plasma displays (2008), 3D compatible LCD monitors (2009) and 3D compatible LCD TVs (2010) were released into the market.

[YYYY-MM-DD]

- 1838 The theory of stereoscopic vision described (Sir Charles Wheatstone, UK)²⁵
- 1891 Anaglyph printing invented (Louis Ducos duHauron, France)^{26,27,28}
- 1897 The CRT invented (Ferdinand Braun, Germany)²⁹
- 1922 First theatre with time-sequential 3D projection (Teleview, USA)^{30,31}
- 1934 CRT TVs commercially released into homes (Telefunken, Germany)
- 1936 British Broadcasting Corporation (BBC) commences television broadcasting in UK to CRT televisions in homes³²
- 1975 PLZT (lead lanthanum zirconate titanate) shutters used for time-sequential 3D on CRTs (Roese, USA)³³
- 1983 First commercially released LCD TV (Casio, Japan)³⁴ (not 3D compatible)
- 1987 DLP invented (Larry Hornbeck, Texas Instruments, USA)³⁵
- 1989 First commercial wireless LCS 3D glasses for use with CRTs (StereoGraphics, USA)³⁶
- 1995 First commercial DLP projector ships (Texas Instruments, USA)³⁵ (not 3D compatible)
- 1998 First published example of time-sequential 3D on PDP³⁷
- 2001 Author's work investigating stereoscopic crosstalk commenced (published in **Paper 9**)
- 2001 First published example of time-sequential 3D DLP projection³⁸
- 2002-01 **Paper 9** – CRT Crosstalk
- 2003 LCD sales surpass CRT sales for first time³⁹
- 2004-01 **Paper 10** – Anaglyph crosstalk
- 2005 Matsushita/Panasonic announced they will cease CRT production in Europe
- 2005-02 **Paper 11** – Compatibility of display products with 3D methods

2005-03	First 3D compatible single-chip DLP projector commercially released (DepthQ, USA) ⁴⁰
2005-11	DLP 3D projection commences in commercial theatres (RealD, USA) ¹¹
2006-08-04	NVIDIA files time-sequential 3D LCD Patent (USA) ²⁴
2006-08-21	Paper 12 – Compatibility of display products with time-sequential 3D
2006-08-22	Paper 5 – Compatibility of LCDs with time-sequential 3D
2007-01	Paper 13 – Compatibility of DLP displays with time-sequential 3D
2007-04	3D-Ready DLP HDTVs commercially released (Samsung, USA) ⁴¹
2007-11	Paper 2 – Anaglyph crosstalk on LCD, plasma and CRT displays
2008	Sony announce they will cease CRT production ^{42,32}
2008-01	Paper 6 – Compatibility of plasma displays with time-sequential 3D
2008-03	3D-Ready plasma HDTVs commercially released (Samsung, USA) ⁴¹
2009-01	Paper 7 – Compatibility of LCD TVs with time-sequential 3D
2009-02	first consumer-grade 3D-Ready single-chip DLP projector released (Viewsonic) ^{43,44}
2009-02	first 3D-Ready LCD monitors commercially released (Samsung & Viewsonic, USA) ⁴⁵
2009-07	Paper 14 – “3-D Displays in the Home”
2010-01	Paper 8 – Anaglyph crosstalk with different colour primaries
2010-03	first 3D-Ready LCD HDTVs commercially released (Samsung, USA) ⁴¹
2011-01	Paper 15 – A simple method for measuring crosstalk
2011-01	Paper 16 – “How are crosstalk and ghosting defined in the stereoscopic literature?”
2012-01	Paper 17 – 3D shutter glasses IR protocols
2012-06	Paper 3 – Anaglyph crosstalk simulation on emissive displays
2012-12	Paper 1 – “Crosstalk in stereoscopic displays: a review”
2013-04	Paper 4 – Printed anaglyph crosstalk
2013-08	Paper 18 – “3D or 3-D: A study of terminology, usage and style”

As can be seen from the chronology, the published works of this thesis have followed closely (and sometimes foreshadowed) several notable events in the stereoscopic display industry:

- At a time when the market share of CRTs was in decline and being replaced by other display technologies, **Paper 11**, **Paper 12** and **Paper 5** considered the compatibility of the broader range of display technologies (CRT, and non-CRT) with various stereoscopic display methods.
- Following the release of DLP 3D projectors for business and theatre usage in 2005, **Paper 13** in 2007 considered the compatibility of consumer grade (commodity) DLP projectors with time-sequential 3D, just a few months before the release of consumer-grade rear-projection DLP 3D HDTVs into the market, and two years before the release of consumer grade DLP 3D projectors (Feb 2009).
- Two years prior to the commercial release of 3D compatible LCD monitors in 2009, but 18 days after NVIDIA privately lodged a patent on the topic, **Paper 5** proposed a method of achieving high-quality time-sequential 3D with LCDs.

- Two months prior to the commercial release of 3D compatible plasma HDTVs, **Paper 6** examined the compatibility of plasma displays with the time-sequential 3D method (reporting on work commenced some 12 months earlier).
- 14 months prior to the commercial release of 3D compatible LCD HDTVs, **Paper 7** considered the compatibility of LCD TVs (and advanced LCD display technologies) with the time-sequential stereoscopic display method.
- In 2011, when considerable research activity was being conducted into stereoscopic displays and crosstalk but there remained a notable 'disparity' in terminology definitions and usage, **Paper 16** investigated the historical usage of terms related to crosstalk and provided recommended definitions and usage for these terms. This work was later included in (Refereed Journal) **Paper 1**. Both of these papers, and an intermediate paper¹ (a precursor to **Paper 1**), have been well cited in the academic literature to date (109 citations to 20 October 2013).⁴⁶

1.3 Impact

One of the simplest ways of measuring the impact of academic research is to perform a citation analysis. The following table provides a listing of the citation count of the publications included in this thesis (plus one precursor paper) derived from Google Scholar.⁴⁶ The total citation count is 357 as of 20 October 2013.

Table 1 Citation count statistics for publications included in this thesis (plus one precursor paper) as derived from Google Scholar.⁴⁶ Data valid as of 20 October 2013. Latest data is available at: <http://scholar.google.com.au/citations?user=J-9YiCkAAAAJ>
NB: Google Scholar results include self-citations.

Paper #	Paper Title	Year	Cites
n/a	"Understanding Crosstalk in Stereoscopic Displays" ¹ precursor to Paper 1 "Crosstalk in Stereoscopic Displays: a review"	2010	69
Paper 9	"Characterising sources of ghosting in time-sequential stereoscopic video displays"	2002	52
Paper 16	"How are crosstalk and ghosting defined in the stereoscopic literature?"	2011	32
Paper 8	"Comparing levels of crosstalk with red/cyan, blue/yellow, and green/magenta anaglyph 3D glasses"	2010	31
Paper 10	"Ghosting in anaglyphic stereoscopic images"	2004	30
Paper 11	"Compatibility of display products with stereoscopic display methods"	2005	25
Paper 5	"Compatibility of LCD monitors with frame-sequential stereoscopic 3D visualisation"	2006	22
Paper 15	"A simple method for measuring crosstalk in stereoscopic displays"	2011	15
Paper 7	"The compatibility of LCD TVs with time-sequential stereoscopic 3D visualization"	2009	15
Paper 2	"Characterizing crosstalk in anaglyphic stereoscopic images on LCD monitors and plasma displays"	2007	15
Paper 14	"3-D Displays in the Home"	2009	14
Paper 1	"Crosstalk in stereoscopic displays: a review"	2012	8
Paper 6	"The compatibility of consumer plasma displays with time-sequential stereoscopic 3D visualization"	2008	8
Paper 13	"The compatibility of consumer DLP projectors with time-sequential stereoscopic 3D visualisation"	2007	7
Paper 12	"The compatibility of consumer displays with time-sequential stereoscopic 3D visualisation"	2006	7
Paper 17	"Investigating the cross-compatibility of IR-controlled active shutter glasses"	2012	3
Paper 3	"Using cross-talk simulation to predict the performance of anaglyph 3-D glasses"	2012	3
Paper 4	"Characterizing and reducing crosstalk in printed anaglyph stereoscopic 3D images"	2013	1
TOTAL			<u>357</u>

2. Literature Review

The topic of crosstalk has a long history. In electronics and telecommunications the term “crosstalk” has been used as far back as the 1880s⁴⁷ to describe the leakage of signals between parallel laid telephone cables. In the field of stereoscopic displays, “crosstalk” has been a recognised term at least since the 1930s⁴⁸ to describe the leakage of images between the image channels of a stereoscopic display.

An extensive review article, “Crosstalk in Stereoscopic Displays: A Review”² (**Paper 1**), written by me and forming part of this thesis submission, provides a detailed background and literature review of the field of crosstalk in stereoscopic displays up to 2012.

My research into stereoscopic crosstalk commenced in 2001 (for **Paper 9** published in 2002) and hence in preparing this literature review there is necessarily some overlap between the published literature as it stood in 2001, the published literature as it stands now, and my works which have been published over the period 2002 to 2013. Several of my papers are believed to have been the first to publish an investigation of crosstalk in a number of topic areas and hence now form an important part of the published literature. In preparing this literature review, I have been careful to identify and distinguish which works are by me and the papers that are by other authors.

The terminology, descriptive definitions, and mathematical definitions of “crosstalk” and related terms “ghosting”, “leakage”, “system crosstalk”, “viewer crosstalk”, “grey-to-grey crosstalk”, “autostereoscopic crosstalk”, “extinction ratio”, and “3D contrast” are set out in Section 2 of **Paper 1** and will not be repeated here. A brief summary of the particular terms relevant to the field of stereoscopic displays and crosstalk that are important for the understanding of this exegesis are presented in “List of Stereoscopic Terminology” on page xvi.

An investigation of how the related terms “crosstalk” and “ghosting” have been historically used in the published literature is presented in **Paper 16** and was used to inform the content of **Paper 1**. “Crosstalk” and “ghosting” are often used interchangeably in general discussion but do have separate and distinct definitions as laid out by Lipton in 1987⁴⁹ and summarised on page xvi. My own early papers tended to use the two terms interchangeably, however as my work has matured and understanding of the area has increased, the later papers mostly use the term crosstalk, except where it is appropriate to use the term ghosting.

It is broadly acknowledged that the presence of high levels of crosstalk is detrimental to the perception of stereoscopic images and a large number of papers have studied this

effect.^{50,51,52,53,54,55,56} A summary of the perceptual effects of crosstalk is provided in Section 3 of **Paper 1**.

Crosstalk occurs via a wide range of different mechanisms – Section 4 of **Paper 1** provides a detailed overview of the various methods by which crosstalk can occur in a wide selection of stereoscopic display technologies. Up to 2001, when my work on crosstalk began, most of the literature on the subject of crosstalk was based on the time-sequential 3D CRT displays available at the time.^{57,58,59,60,61,62} The literature cited three main contributors to crosstalk: phosphor afterglow, shutter leakage, and the effect of angle of view through the liquid-crystal shutter glasses. In 2002, CRTs were the only emissive desktop display capable of working with the time-sequential 3D technique – LCDs and plasma displays were gaining increased market penetration, but commercially released displays based on these technologies were not compatible with the time-sequential 3D display technique.⁶⁴ In quick succession, time-sequential 3D compatible displays based on DLP⁶⁵ (2005), PDP⁴¹ (2008) and LCD⁴⁵ (2009) technologies were released to market. The work of this thesis has therefore ridden a wave of new stereoscopic display technology development. Background literature on LCDs,^{66,67,68} PDPs^{37,69,70} and DLPs^{71,38,72} have played an important part in understanding these display technologies but generally did not directly address any crosstalk related aspects (Sections 4.1.2 to 4.1.4 of **Paper 1**).

Chapter 4 of this thesis provides detailed coverage of the new work conducted by me and collaborators on the mechanisms by which crosstalk occurs with the following types of stereoscopic displays: time-sequential 3D on CRT displays, time-sequential 3D on LCD monitors, time-sequential 3D on DLP projectors, time-sequential 3D on plasma TVs, time-sequential 3D on LCD TVs, anaglyph 3D on emissive displays, and anaglyph 3D in printed images. The crosstalk mechanisms for polarised 3D projection, micro-polarised LCDs, and autostereoscopic displays, constitute work by other authors and are described as part of the background literature in Sections 4.2 to 4.4 of **Paper 1**.

Other background topics relating to crosstalk available in the published literature include: methods of measuring crosstalk (Section 5 of **Paper 1**), ways in which crosstalk can be reduced (Section 6 of **Paper 1**), a summary of the technique of crosstalk cancellation (Section 7 of **Paper 1**), and coverage of the role of simulation in crosstalk analysis (Section 8 of **Paper 1**).

A full copy of **Paper 1** is included in Chapter 9 of this thesis.

Although **Paper 1** is ostensibly a review paper, the major content of the paper - Section 4 “Crosstalk Mechanisms” along with Section 5.2 “Visual Measurement Charts” - are based on original works by me, and represent the first refereed journal publication of a number of research topics investigated by me. Approximately 46% of **Paper 1** (mostly in the crosstalk mechanisms section) is based on

original work conducted by me in cooperation with collaborators. My work now forms a valuable contribution to the published literature on this topic. It is worth noting that much of my early works on crosstalk were published in non-refereed publications. The passage of time would now preclude the publication of those original works in refereed journals (e.g. CRTs are now an almost extinct technology). **Paper 1** therefore represents the first refereed journal publication of those topics. My unrefereed papers (**Paper 9, Paper 10, Paper 13, Paper 15, Paper 16, and Paper 17**)^{73,74,64,75,76,77,18,78} which contribute to and inform refereed journal **Paper 1** are included in Appendix 1 as “additional publications by the candidate relevant to the thesis” – the contribution of these works to the overall thesis will be discussed in further detail in Chapter 4 of this exegesis.

Full copies of **Paper 9, Paper 10, Paper 13, Paper 15, Paper 16, and Paper 17** are included in Appendix 1 of this thesis.

Lastly, background information on the topic of printed anaglyphs is provided in Section 1 of **Paper 4**. Despite the printed anaglyph 3D technique being one of the oldest 3D methods, invented by Louis Ducos duHauron in 1891,^{26,27,28} there has seemingly been relatively little technical analysis of this very widely used 3D technique. Manuscripts by Norling⁷⁹ in 1937, Harrington⁸⁰ et al in 2002, Tran⁸¹ in 2005, and Labbe⁸² in 2009 have examined various aspects of the traditional printed anaglyph, but there remained significant gaps in the understanding of this widespread 3D technique. One significant aspect that separates the printed anaglyph 3D technique from the other 3D techniques considered in this thesis is that the printed anaglyph uses the subtractive colour model whereas the other 3D techniques all follow the additive colour model – this single aspect requires a different analysis technique to the other 3D methods.

A full copy of **Paper 4** is included in Chapter 9 of this thesis.

3. Research Design

The genesis of this thesis was asking the seemingly simple question as to how crosstalk occurs in a stereoscopic display. This subsequently led onto the next question: What are the relative contributions of the different crosstalk mechanisms towards the total crosstalk present in a stereoscopic display.

In order to answer these questions, it was necessary to design an analysis technique which examined the fundamental light output operation of a display, and considered how this interacts with the selection device (e.g. 3D glasses) used to multiplex and de-multiplex the different views to the two human eyes. The analysis technique also needed to be designed within the technical limitations of the measurement equipment which was available at the time, and tailored to the particular requirements and characteristics of each display device and stereoscopic display technique.

The application of a particular stereoscopic display technique across different displays can produce very different crosstalk performance results so it is important for the chosen analysis technique to be able to capture the characteristics of each display that may affect crosstalk performance. Similarly, the application of different stereoscopic display techniques to the one display can produce very different crosstalk performance results, so ideally the display analysis technique will measure all necessary display characteristics for multiple stereoscopic display methods.

Once the fundamental display characteristics are known, the performance attributes (of the display and the glasses) can then be examined with a view to understanding how they interact, and how crosstalk occurs. A mathematical model then needs to be developed and implemented to simulate the presence of crosstalk in a particular stereoscopic display and start answering questions about the relative contribution of different crosstalk mechanisms to the overall crosstalk present in a particular stereoscopic display.

The basic design philosophy used for the project therefore led to the use of the following research steps:

- (a) Develop initial block diagram of crosstalk performance for a particular stereoscopic display,
- (b) **Measure** the temporal, spatial, angular, and spectral performance attributes of the display (as required),
- (c) Measure the temporal, spatial, angular, and spectral performance of the selection device (e.g. 3D glasses) (as required),
- (d) Develop a mathematical **Model** which characterises occurrence of crosstalk for a particular stereoscopic display,

- (e) Implement the mathematical model in a computer program and use the program to **Simulate** a selection of different scenarios,
- (f) **Validate** the mathematical model against measurements of total crosstalk and/or human perception testing of crosstalk performance, and finally
- (g) Use the developed mathematical model to **Extrapolate** how crosstalk occurs when different performance attributes are changed and therefore find cost-effective solutions for reducing crosstalk performance in a particular stereoscopic display.

I am calling this the measure/model/simulate/validate/extrapolate process.

Each of the steps above can be performed iteratively as needed to improve the accuracy of the model.

Three main classes of test equipment have been used in this work to characterise the optical performance characteristics of the displays and selection devices:

- (a) a photodiode and oscilloscope to measure time-domain performance,
- (b) a spectroradiometer to measure the spectrum of the emitted light from the display (in each of the three colour channels), and
- (c) a spectrophotometer to measure the spectral transmission of the anaglyph glasses or reflective spectrum of printed inks.

Spatial and angular performance is usually characterised by configuring the above equipment to collect measurements at different spatial locations and/or alignment angles. In the case of spatio-temporal performance, it is important to correctly measure the phase of the measured signal (in relation to the input video signal), because in some instances the shape of the waveform remains the same, but the phase changes with changes in spatial location – e.g. with CRTs and LCDs.^{83,85,73}

In order to characterise the time-domain performance of the LC cells in LCS glasses, LEDs of three different colours were usually used to provide a constant output light source and a photodiode was used to measure the light transmission through the LC shutter⁷³ (per Section 2.1.3 of **Paper 9**).

Specific examples of the equipment used during this study are as follows:

- (a) Photodiode: IPL10530DAL Integrated Photodiode Amplifier.^{86,73,76,83,87,85}
- (b) Spectroradiometers: Ocean Optics S1000,⁷³ Zeiss Monolithic Miniature-Spectrometer,⁷⁴ and Ocean Optics USB2000.^{88, 89, 90,91}
- (c) Spectrophotometers: Hitachi model 150-20 Spectrophotometer,⁷⁴ PG Instruments T90+ UV/VIS spectrophotometer,⁸⁹ and Perkin Elmer Lambda 35 spectrophotometer.^{88,90, 91}

In order to measure total crosstalk levels directly, it is necessary to use a photosensor that has a weighted spectral sensitivity that is equivalent to the sensitivity of the human eye – or in the case of a spectroradiometer, able to be calibrated to human eye sensitivity in post-processing. I did experiment with using a USB2000 spectroradiometer to measure total crosstalk, however that work has not been published at this stage.

Crosstalk measurement charts were also experimented with as a technique for end-users to easily determine crosstalk levels (as outlined in **Paper 15**),⁷⁷ however these results do not have high-levels of measurement accuracy (due to the difficulty of characterising and fixing display gamma, contrast, brightness, and black-level settings) and hence were not used directly in the crosstalk characterisation stages of this work.

Other authors have used a wide range of other equipment to measure crosstalk levels and display performance – as outlined in Section 5 of **Paper 1**.

This thesis examines the crosstalk performance and crosstalk mechanisms of seven specific categories of stereoscopic displays and the reader is referred to specific sections of the included papers for further specific information of the methodology used to study each of those displays:

- (a) time-sequential 3D on CRT displays – Section 2 of **Paper 9**
- (b) time-sequential 3D on LCD monitors – Section 2 of **Paper 5**
- (c) time-sequential 3D on DLP projectors – Section 2 of **Paper 13**
- (d) time-sequential 3D on plasma displays – Section 2 of **Paper 6**
- (e) time-sequential 3D on LCD TVs – Section 4 of **Paper 7**
- (f) anaglyph 3D on emissive displays (CRTs, LCDs, DLPs, PDPs) – Section 2 of **Paper 10**, Section 2 of **Paper 2**, Section 3 of **Paper 3**, and Section 2 of **Paper 8**
- (g) anaglyph 3D in printed images – Section 4 of **Paper 4**

4. Overview and Results

As stated in the introduction, this thesis describes the examination of the factors that contribute to and determine the amount of crosstalk that occurs in a broad selection of stereoscopic display technologies.

The particular types of stereoscopic display technologies about which the work of this thesis provides contributions to the body of knowledge are itemised below, along with a corresponding list of the papers and section numbers which contain the published record of the results of this work:

- (a) Time-sequential 3D using liquid-crystal shutter glasses – Section 4.1 of *Paper 1*; *Paper 9* and *Paper 17*
- (b) time-sequential 3D on CRT displays – Section 4.1.1 of *Paper 1*; and *Paper 9*
- (c) time-sequential 3D on plasma displays – Section 4.1.2 of *Paper 1*; and *Paper 6*
- (d) time-sequential 3D on LCDs – Section 4.1.3 of *Paper 1*; *Paper 5* and *Paper 7*
- (e) time-sequential 3D on DLP projectors – Section 4.1.4 of *Paper 1*; and *Paper 13*
- (f) anaglyph 3D on emissive displays (CRTs, LCDs, DLPs, PDPs) – Section 4.5 of *Paper 1*; *Paper 2*; *Paper 3*; *Paper 8* and *Paper 10*
- (g) anaglyph 3D in printed images – *Paper 4*

The following subsections of this chapter expand the discussion on crosstalk mechanisms generally, and then specifically for all of the stereoscopic display technologies investigated in this study. For each of the stereoscopic display technologies considered the results of the measure/model/simulate/validate/extrapolate process are explained and explored where applicable.

4.1 Crosstalk Mechanisms

Underpinning the analysis of crosstalk, it is an important step to determine the mechanisms that cause crosstalk in each stereoscopic display technology. Figure 1 below shows the flow of images in a stereoscopic system - from capture, through storage, editing, transmission and display, to perception by the observer. The figure is presented for a two-view system (a stereoscopic display system that presents two views – one for each eye), however the same theory could be applied to a multi-view system (a multi-view stereoscopic display system presents multiple-views and depending on where the observer is located, ideally only one of the views will be seen by the left eye and another of the views will be seen by the right eye. Multi-view systems are usually autostereoscopic). Although crosstalk can occur in all of the stages shown in Figure 1 (except perception), this thesis primarily investigates crosstalk in the display and image separation stages, due to the fact that crosstalk can generally be easily avoided in the capture, storage, editing and transmission stages (per

Section 4.7 of **Paper 1**). Stereoscopic displays that maintain complete separation between the image channels and therefore have zero crosstalk are discussed in Section 4.6 of **Paper 1**.

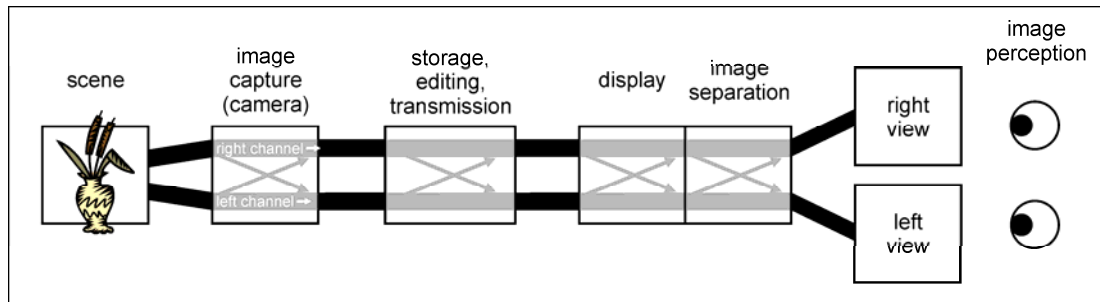


Figure 1 A flow diagram showing the transfer of stereoscopic images from image capture through to image viewing and perception by the observer (from Figure 3 of **Paper 1**). Firstly, a stereoscopic camera captures left and right images. Next, the left and right images are ideally kept separate during the storage, editing and transmission stage. With many stereoscopic displays, the left and right images are presented on the same display surface (so called 'plano-stereoscopic displays') and then a selection device is used to separate the left and right images to the left and right eyes. Crosstalk between the left and right image channels (indicated by the crossing arrows) can occur in the capture (camera) stage, storage/editing/transmission stage, image display (light generation), and image separation (3D glasses or autostereoscopic optical layer) stages. Most crosstalk usually occurs in the display and image separation stages.

The mechanisms which cause crosstalk (in the image display and separation stages) can vary considerably from one stereoscopic display technology to another. The following sub-chapters of this exegesis describe the examination of a selection of different stereoscopic display technologies to determine the crosstalk mechanisms for each of these displays, and present the results of the measure/model/simulate/validate/extrapolate process.

4.2 Time-Sequential 3D using Active Shutter Glasses

Active shutter glasses, also known as liquid-crystal shutter (LCS) glasses, are used in most time-sequential 3D displays to gate the left and right perspective images to the observer's left and right eyes. Most active shutter glasses are constructed using liquid-crystal (LC) cells in the left and right lenses of the glasses. As explained in Section 4.1 of **Paper 1**, LC cells have a number of non-ideal performance characteristics that can contribute to crosstalk in stereoscopic displays. Figure 2 below shows the time-domain performance of the LC cell in an example pair of active shutter glasses. It can be seen in this figure that the LC shutters have: a non-zero transmission in the opaque state, a non-instantaneous rise- and fall-time, and different optical performance at different optical wavelengths. Additionally, the optical performance of the LC cell varies with viewing angle, and the timing of the switching of the LC cells (phase and duty-cycle) also needs to be considered. The actual effect that these characteristics have on crosstalk will depend upon the performance characteristics (particularly the time domain response) of the emissive display with which the LCS glasses are used. Section 4.1.1 of **Paper 1** (informed by **Paper 9**) examined the interaction of LCS glasses with CRT

displays, and other papers in this thesis (and described in subsections of this exegesis below) report on the interaction of LCS glasses with other emissive displays.

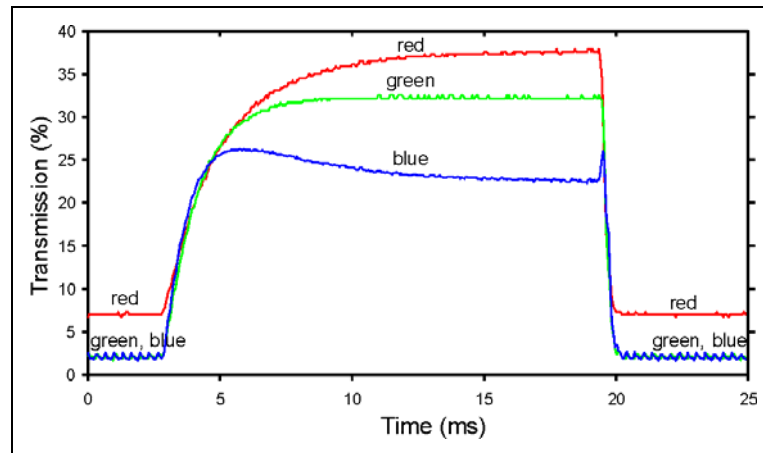


Figure 2 The optical transmission versus time response of an example pair of active shutter glasses at red, green and blue wavelengths. (from Figure 4 of **Paper 1** and explained further in Section 2.1.3 of **Paper 9**).

The phase and duty cycle of a pair of LCS glasses is determined by the driving circuitry of the glasses and system timing determined by the display system electronics. **Paper 17** examined the protocols which are used to control the timing of wireless active shutter glasses. Infra-red (IR), visible optical band, and radio-frequency (RF) are commonly used techniques to signal the correct timing to the active shutter glasses. Although it should be a fairly easy process to ensure that the active shutter glasses switch at the appropriate time, the results of **Paper 17** showed that there were a number of circumstances under which crosstalk could occur due to incorrect timing – specifically phase differences between different protocols (Section 4.3 of **Paper 17**) and inability of some protocols to operate with anything but a 50% duty cycle (Section 4.1 of **Paper 17**).

Paper 1 is included in Chapter 9 of this exegesis as a core manuscript of the thesis.

Paper 9 and **Paper 17** are included in Appendix 1 as additional publications relevant to the thesis.

The next four sub-chapters of this exegesis now examine the performance of active shutter glasses with four different emissive display technologies.

4.2.1 Time-Sequential 3D on CRT Displays

Section 4.1.1 of **Paper 1** provides a description of the sources of crosstalk in the time-sequential 3D method on CRT displays and lists them as:

- the performance of the liquid crystal shutters in the active shutter glasses (as discussed in detail in Chapter 4.2 of this exegesis),
- the amount of phosphor persistence,
- the timing of the shuttering of the glasses with respect to the displayed images, and
- the x-y coordinates on the screen.

Expanding on the information presented in Section 4.1.1 of **Paper 1**, **Paper 9** “Characterising Sources of Ghosting in Time-Sequential Stereoscopic Video Displays” went into further detail on this topic by:

- describing a model for crosstalk in time-sequential 3D CRT displays (Section 2.2 of **Paper 9**),
- implementing the model in a computer simulation (Section 3.1 of **Paper 9**),
- conducting measurements to populate the simulation (Section 2.1 of **Paper 9**), and
- performing a rudimentary validation of the simulation (Section 3.2 of **Paper 9**).

The process by which crosstalk occurs in time-sequential 3D on CRT displays is illustrated in Figure 3. The top part of this figure illustrates the light output when the phosphor is energised by the scanned electron beam and the time-domain transmission response of the LC shutter – the phosphor is energized during the first frame (L-eye) period, when the shutter is closed, and exponentially decays. The bottom part of the figure illustrates the multiplication of phosphor response by the shutter response to give the amount of leakage. The area under the solid orange curve from end of VBI1 (vertical blanking interval) to the start of VBI2 represents crosstalk due to the incomplete extinction of the shutter, and the area under the solid red curve from start of VBI2 onwards represents crosstalk due to long phosphor persistence.

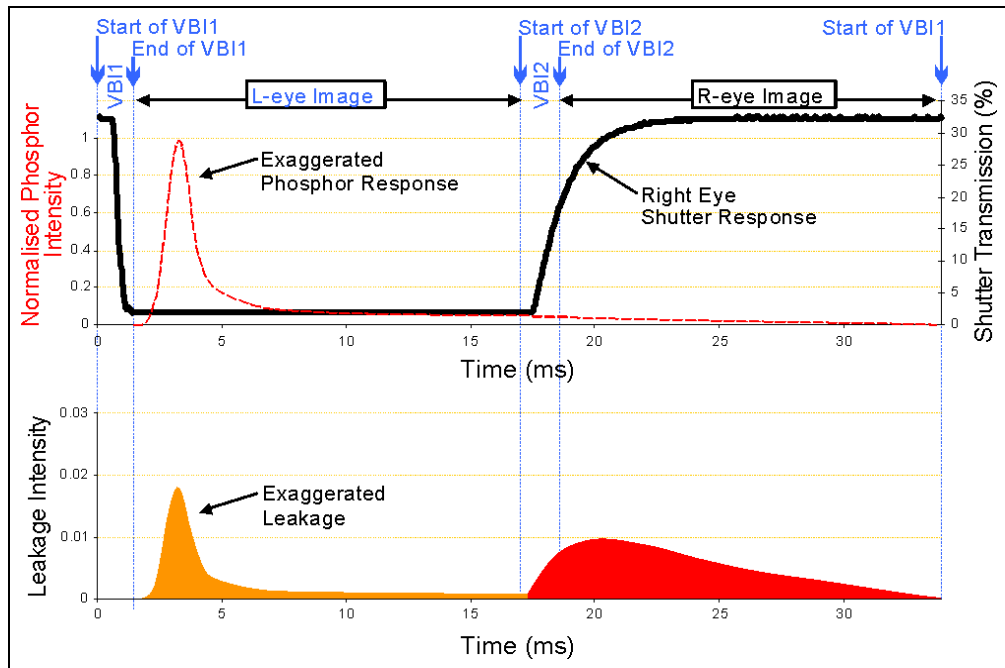


Figure 3 Illustration of crosstalk on a CRT (with exaggerated phosphor response for illustrative purposes). Top: phosphor response and shutter response. Bottom: multiplication of phosphor response by the shutter response to give the amount of leakage. (from Figure 8 of **Paper 1** and explained further in Section 2.2 of **Paper 9**).

There is considerable variability in the amount of crosstalk present in this category of stereoscopic displays due to different factors: optical quality of different shutter glasses, the spatial position on the display surface, and the timing of the shutter glasses. There is very little variation in phosphor persistence between CRT displays – as a result it is presumed that most commercially released CRT displays use the same display phosphor formulation. This work also found that crosstalk at different positions on the screen can be dominated by different crosstalk mechanisms – crosstalk at the top of the display is usually dominated by shutter leakage whereas crosstalk at the bottom of the display is usually dominated by phosphor decay – as illustrated in Figure 8 of **Paper 9** and explained in Section 3.1 of **Paper 9**.

Paper 9 appears to be the first publication to illustrate the power of developing a simulation of crosstalk in that it allows the various components which contribute to the overall crosstalk to be considered and analysed independently. This is an important step because the relative contributors to overall crosstalk cannot be determined individually by solely measuring the overall crosstalk.

Paper 1 is included in Chapter 9 of this exegesis as a core manuscript of the thesis.

Paper 9 is included in Appendix 1 of this thesis as an additional publication relevant to the thesis.

4.2.2 Time-Sequential 3D on Plasma Displays

This class of stereoscopic display presents stereoscopic images on a plasma display panel while the observer wears active shutter glasses.

As described in Section 4.1.2 of **Paper 1**, the sources of crosstalk when using the time-sequential 3D method on plasma displays are as follows:

- the performance of the liquid crystal shutters in the active shutter glasses (as discussed in detail in Section 4.2 of this exegesis),
- the amount of phosphor persistence,
- the timing of the shuttering of the glasses with respect to the displayed images, and
- the particular grey level value of a displayed pixel and therefore which sub-frames are fired.

Expanding on the information presented in **Paper 1, Paper 6** “The compatibility of consumer plasma displays with time-sequential stereoscopic 3D visualization”,⁸⁷ a refereed conference paper by me, goes into further detail on this topic by:

- examining the detailed operation of plasma displays to determine the factors which determine their compatibility (or incompatibility) with time-sequential 3D display (Section 1 of **Paper 6**),
- measuring the time-domain performance of 14 consumer released plasma displays to determine phosphor decay, sub-frame sequencing, time delay, and display synchronisation of plasma displays (Section 3 of **Paper 6**),
- describing a method for modelling crosstalk of time-sequential 3D on plasma displays and calculating crosstalk values for the tested displays (Section 3.4 of **Paper 6**), and
- recommending ways of reducing crosstalk and improving compatibility of plasma displays with the time-sequential 3D technique (Section 4 of **Paper 6**).

The research for **Paper 6** was conducted just before the release of 3D-Ready time-sequential 3D plasma displays into the consumer market. At this time the red and green phosphors of the tested displays typically had much longer time constants (longer phosphor decay) than the blue phosphor (as shown in Figure 4 of **Paper 6**). The presence of a long phosphor decay means that the image from one frame will still be present in the time period for the next frame which leads to leakage between stereoscopic image channels and therefore increased levels of crosstalk. Figure 4 below illustrates the occurrence of crosstalk with the time-sequential 3D method on plasma displays. In this particular example (for the red channel) the contribution to total crosstalk due to shutter leakage is roughly equivalent to the contribution due to the phosphor decay. Other plasma display and LCS glasses combinations will produce different crosstalk results.

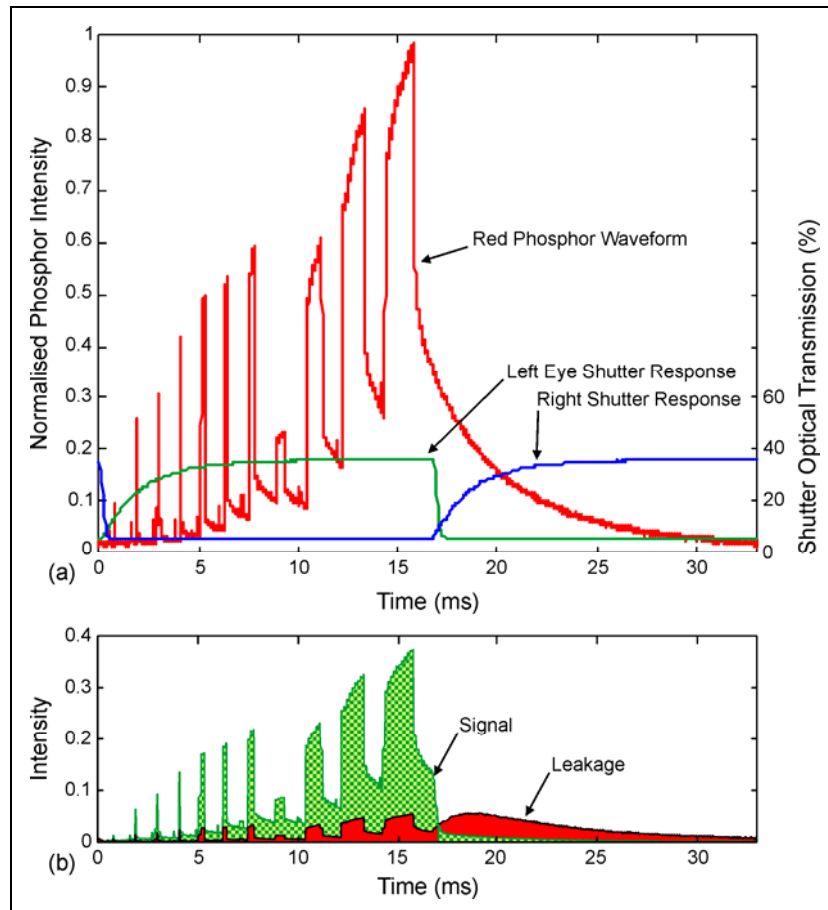


Figure 4 Timing diagram showing the relative timing of a pair of shutter glasses being used to view a time-sequential 3D image on an example conventional plasma display. Part (a) shows the time-domain transmission of the left and right shutters along with the time-domain light output of the display (showing alternating frames of 100% red and black). Part (b) shows the intensity of light through the shutters as will be viewed by the left and right eyes. The desired signal to the left eye through the shutter glasses is shown in hatched green, and the leakage to the right eye through the shutter glasses is shown in solid red. (from Figure 11 of **Paper 1** and explained further in Section 3.4 of **Paper 6**)

Although not directly reported in **Paper 6**, a crosstalk simulation program implementing the described crosstalk model was written in Matlab.⁹² One aspect of the operation of plasma displays which considerably complicates the implementation of an accurate crosstalk model is the way in which plasma displays reproduce different grey levels by firing different sub-frames in a binary sequence corresponding to the brightness of each individual sub-frame (per Section 1.1 of **Paper 6**). The bit order of the PDP pulse sequence of a particular display, and also the grey level of a particular pixel, will contribute to the amount of crosstalk present. This aspect was not implemented in the crosstalk simulation of this particular paper but was considered as an option for future work.

Paper 1 and **Paper 6** are included in Chapter 9 of this exegesis as core manuscripts of the thesis.

4.2.3 Time Sequential 3D on LCDs

This class of stereoscopic display present stereoscopic images on an LCD panel while the observer wears active shutter glasses.

As described in Section 4.1.3 of **Paper 1**, there are a number of unique performance characteristics of LCDs that determine compatibility and crosstalk levels when using the time-sequential 3D technique on LCDs. Of particular note is that LCDs use a scanned update method to update pixels from one frame to the next – new pixels are updated row by row from the top to the bottom of the display. Additionally, most LCDs are a hold-type display – the image is held and light is output continuously for the entire frame period. This is in contrast to CRT and plasma displays which emit pulses of light with an exponential decay of light between pulses. In CRT or plasma displays, the so-called ‘blanking interval’ between frames provides an interval of low-light output when the LC shutters can change from one state to another with minimised influence, however most conventional LCDs do not have a blanking period hence the switching time of the LC shutters is an important consideration in crosstalk performance.

At the time of embarking on this part of the research, commercial LCDs were incapable of being used for high-quality time-sequential stereoscopic display because considerable crosstalk was present. Due to the considerable difference between the operation of LCDs and CRTs, or even plasma displays, the conventional wisdom about the interaction of LC shutters with CRTs did not directly apply to LCDs. A re-examination of the operation of LCDs in relation to the time-sequential stereoscopic display method was therefore necessary.

*Slow pixel response (the time that it takes for a pixel to change from one grey level to another) had historically been considered to be the main reason that LCD monitors could not be used for time-sequential stereoscopic 3D viewing. Although pixel response rate is important, **Paper 5** revealed that the image update method of the panel is also an important consideration. Even if the pixel response rate is improved, the scan-like image update method of most conventional LCDs would still cause problems for the frame-sequential 3D method. This was an important realisation and informed the next step which was to devise a technique of presenting low crosstalk stereoscopic images on LCDs.*

Based upon the performance analysis of LCDs, Section 4.1.3 of **Paper 1** describes the sources of crosstalk in time-sequential 3D on LCDs as:

- the performance of the liquid crystal shutters in the active shutter glasses (as discussed in detail in Section 4.2 of this exegesis),
- the timing of the scanned image update method of the LCD (including the effects of Black Frame Insertion (BFI), increased frame rate, and backlight modulation discussed below),
- the pixel response rate of the LCD,
- the timing of the shuttering of the glasses with respect to the displayed images,
- the particular grey level value of a displayed pixel, and
- the x-y position on the screen.

Paper 5 and **Paper 7** provide further detail on the original research presented in **Journal Paper 1** (listed above).

Paper 5, “Compatibility of LCD Monitors with Frame-Sequential Stereoscopic 3D Visualisation”,⁸³ an invited refereed conference paper, was published in 2006 before the commercial release of time-sequential 3D compatible LCDs in 2009.⁴⁵ On the basis of this chronology, **Paper 5** provided the following insights:

- It examined and outlined the key performance attributes which determine the compatibility (or incompatibility) of LCDs with the time-sequential 3D method (Section 3 of **Paper 5**),
- It presented a spatio-temporal-domain graph of the time-sequential 3D method on LCDs that was a key to understanding the limitations of using the time-sequential 3D technique on LCDs (Section 3.4 of **Paper 5**),
- It identified the scanned image update method and the LCD pixel response rate (in combination with the hold-type display characteristic) as the primary factor causing high crosstalk levels with the time-sequential 3D display method on conventional LCDs (Sections 3.4 and 4 of **Paper 5**), and
- It presented two techniques to allow low-crosstalk stereoscopic images to be presented on LCDs using the time-sequential 3D display method (Section 4 of **Paper 5**).

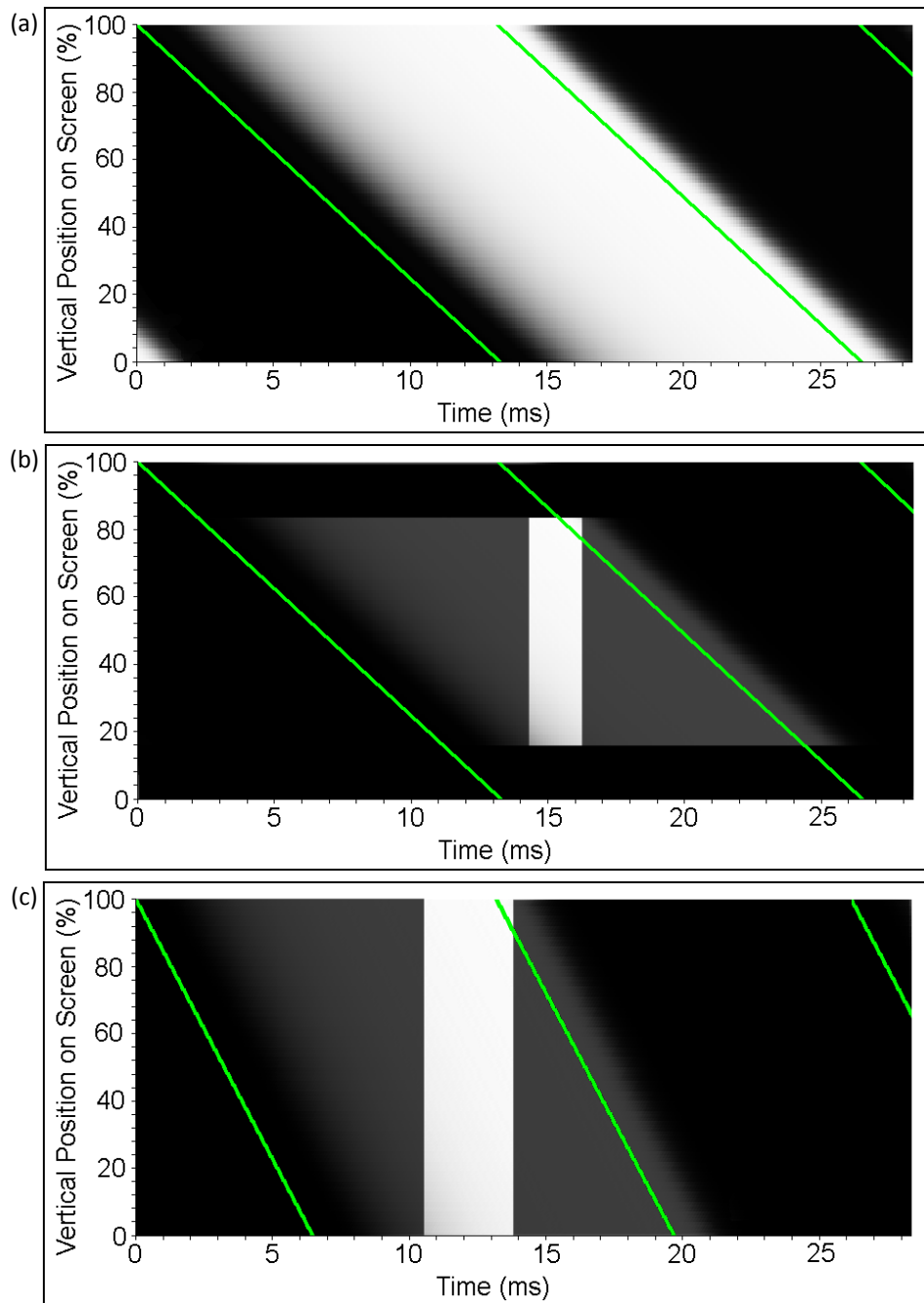


Figure 5 (a) Spatio-temporal-domain graph for an example LCD panel (with a pixel response rate of 5.7ms) being driven with a test time-sequential signal alternating between black and white frames at 75Hz. The diagonal green line illustrates the time at which each row of pixels on the display is addressed. (from Figure 2(b) of *Paper 5*).

(b) An illustration of the use of a reduced duty cycle LCS 3D glasses and letterboxing to achieve low-crosstalk with frame-sequential 3D on a commodity LCD monitor, albeit with low image brightness. Please note that the switching of the LCS also has a response rate⁷³ but this has not been fully illustrated in this figure (from Figure 3 of *Paper 5*).

(c) An illustration of the use of a fast addressing rate, fast pixel response rate LCD, and reduced duty cycle LCS 3D glasses to achieve a low crosstalk frame-sequential 3D image across the whole LCD surface (from Figure 4(b) of *Paper 5*).

The development of a spatio-temporal-domain graph of the performance of the time-sequential 3D technique on LCDs was a critical step to understanding the limitations and developing solutions for reducing crosstalk with this 3D display method. Figure 5 shows a series of spatio-temporal graphs for the time-sequential 3D technique on LCDs. Figure 5(a) illustrates the scan-like image update of a conventional LCD monitor. If standard 50% duty cycle LCS 3D glasses (opaque for 50% of the time, and transmissive for 50% of the time) are used with such a display, considerable crosstalk will be present across most of the display surface because there is no one time when one image is visible across the entire display surface. Figure 5(b) illustrates the first technique developed to reduce the amount of crosstalk on screen by (i) reducing the duty cycle of the open time of the LCS 3D glasses, (ii) letterboxing the displayed image, and (iii) using an LCD with a fast pixel response rate. Although crosstalk is reduced using this technique, the image brightness is considerably reduced and the requirement to blacken the top and bottom sections of the display is inconvenient. Figure 5(c) illustrates a more robust (second) technique to reduce crosstalk by (i) using a fast addressing rate, and two other techniques listed above (ii) using a reduced duty cycle of the LCS 3D glasses, and (iii) using a fast pixel response rate LCD. These techniques were presented in **Paper 5** published in 2006. Displays which used the second technique, but developed independently of me, were first released to market in 2009.⁴⁵

Paper 7, “The compatibility of LCD TVs with time-sequential stereoscopic 3D visualization”,⁸⁵ a refereed conference paper, was published in 2009, just as the first 3D-Ready time-sequential 3D compatible LCD monitors were being released.⁴⁵ By way of background, the first LCD TVs (as opposed to LCD monitors) to use the time-sequential 3D technique were released into the consumer market in 2010.⁴¹ On the basis of this chronology, **Paper 7** provided the following insights:

- It examined and identified the key performance attributes of three new LCD technologies: black frame insertion (BFI) (Sections 2.1 and 5.1 of **Paper 7**), 120Hz refresh (Sections 2.2 and 5.2 of **Paper 7**), and modulated backlight (Sections 2.3 and 5.3 of **Paper 7**) and outlined how these new LCD technologies affected compatibility with the time-sequential 3D display method and offered opportunities to reduce crosstalk (Section 6 of **Paper 7**),
- It reported that the new LCD technologies of BFI and 120Hz display (as implemented in the displays released at that time) when used in isolation were not of a sufficient technical change to allow high-quality (low crosstalk) stereoscopic display using the time-sequential 3D display method. For example, Figure 6 of **Paper 7** indicates that BFI reduces the crosstalk minimum and broadens the spatial range of the display which will have lower crosstalk, however the top and bottom of the display would still have excessive crosstalk.

Paper 1, **Paper 5** and **Paper 7** are included in Chapter 9 of this exegesis as core manuscripts of the thesis.

4.2.4 Time-Sequential 3D on DLP Projectors

DLP (Digital Light Processing) technology is based on the digital micro-mirror device (DMD) – a MEMS (micro-electrical mechanical system) developed by Texas Instruments (TI) in 1998.³⁵ The DMD is essentially a silicon chip onto which has been etched millions of tiny cantilevered mirrors – 17µm or smaller³⁸ – one for each pixel on the projected display. Each mirror can be electrically driven to swivel $\pm 10^\circ$ to either output light at that pixel location, or send the light to an absorber.

Displays based on DLP technology have an almost ideal temporal performance characteristic for time-sequential 3D because they do not exhibit any image persistence or image decay from one display frame period to the next. This is in contrast to CRTs, PDPs and LCDs which either exhibit afterglow or take a discrete period of time to change from one state to another. The mirrors which control the individual pixel brightness in a DMD can completely switch from the on state to the off state (and vice versa) in approximately $2\mu\text{s}$ ⁷¹ meaning that the display technology itself does not contribute to crosstalk between alternately presented frames.

The time domain performance of an example single-chip DLP projector is illustrated in Figure 6. Single-chip DLP projectors present full-colour images by using the colour-sequential technique, and this is evident in the top line of Figure 6 as the red, blue, green sequence. All of the mirrors are turned off at one point to create a blanking interval – as indicated. The time-domain performance of the active shutter glasses is shown on the bottom graph of Figure 6. As can be seen, the shutters are commanded to switch from one state to another during the blanking interval.

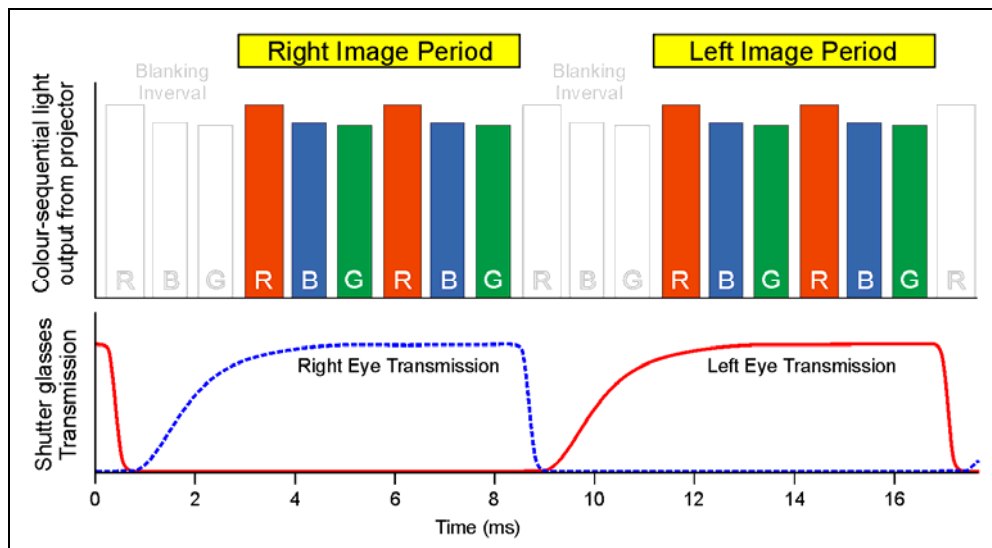


Figure 6 Illustration of the time-domain performance of an example 120 Hz 3D compatible single-chip DLP projector. (from Figure 14 in *Paper 1*)

Despite the ideal time-domain performance of the DMD chip itself, there are still some factors that can affect compatibility with the time-sequential 3D method and cause crosstalk.

Based upon the performance analysis of DLP displays, Section 4.1.4 of **Paper 1** describes the sources of crosstalk in time-sequential 3D on DLP displays as:

- the performance of the liquid crystal shutters in the active shutter glasses (as discussed in detail in Section 4.2 of this exegesis),
- the timing of the shuttering of the glasses with respect to the displayed images, and
- the duration of the blanking interval.

Paper 13 provides further detail on the findings presented in **Paper 1** (listed above). The research work for **Paper 13** was conducted in 2006, roughly one year after the first 3D compatible single-chip DLP projector was commercially released for the business market (by DepthQ),⁴⁰ but three years before the first consumer-grade 3D compatible single-chip DLP projector was released to market (by Viewsonic).^{43,44} Section 3 of **Paper 13** reported on the measurement of 45 commodity (non-3D-certified) single-chip DLP projectors for 3D compatibility. There are a range of additional factors which affect 3D compatibility and levels of crosstalk when the time-sequential 3D method is used with commodity (non-3D-certified) DLP projectors:

- Synchrony of the output display with the input video signal – some projectors do not synchronise the display output sequence with the video input sequence which can lead to an inability for LCS 3D glasses to correctly isolate left and right images and hence introduce severe crosstalk (see Table 2 in Section 3 of **Paper 13**),
- De-interlacing performance (particularly for field-sequential sources) – some projectors use a de-interlacing algorithm which mixes odd and even fields, which in turn causes severe crosstalk (see Table 2 in Section 3 of **Paper 13**),
- Time-offset (phase) between the input video signal and the displayed image sequence – invariably there is a one-frame delay between the input video sequence and the image display output however with some projectors there is a notable additional time offset of up to 1ms which can introduce crosstalk (see Table 3 in Section 3 of **Paper 13**), and
- colour-wheel speed and sequencing – some combinations of colour wheel speed (the number of colour sequence cycles per frame) and the sequence of filter segments on the colour wheel (such as Red/Green/Blue, Red/Green/Blue/White, or Red/Green/Blue/Yellow/Cyan) can cause problems such as colour bias or blanking interval duration when switching into a high-frequency 3D mode (see Figure 6 above).

3D-certified DLP projectors have largely solved these problems now, however there are still occasionally some irregularities with compatibility for some models. For example some projectors frame convert a 50Hz input signal to 60Hz for display which can cause cadence and motion reproduction issues (but generally does not affect crosstalk performance), and some projectors have a time offset between the infra-red token and the displayed image which can cause an incorrect

sequencing of aftermarket 3D glasses and therefore introduce crosstalk - “notably, the Sharp protocol has a 1ms offset” as reported in Section 3 of *Paper 17*.

Paper 1 is included in Chapter 9 of this exegesis as a core manuscript of the thesis.

Paper 13 and *Paper 17* are included in Appendix 1 as additional publications relevant to the thesis.

4.3 Anaglyph 3D

Anaglyph 3D displays work by multiplexing the left and right image views into complementary colour channels of the display and viewing the display through glasses that have colour filters designed to separate these colour channels (Section 4.5 of *Paper 1*). Traditional colour displays have three colour channels: red, green and blue. These colour channels very roughly correspond to the following spectral ranges: blue 400-500nm, green 500-600nm, and red 600-700nm. As described in Section 1 of *Paper 8*, the most commonly used colour combination for the anaglyph 3D technique is red for the left channel and cyan (blue + green) for the right channel, but other colour combinations are possible including blue/yellow and green/magenta.⁸⁸

The anaglyph 3D technique is substantially different from the time-sequential 3D method that has been described so far in this exegesis. Not only is the multiplexing technique different (based on different wavelengths of light as opposed to a left-right sequence of images alternating in time), the mechanisms which cause crosstalk are also completely different – these aspects dictate a full re-examination of crosstalk for the anaglyph 3D technique.

4.3.1 Anaglyph 3D on Emissive Displays

This chapter of the exegesis examines the application of the anaglyph 3D technique to emissive displays – specifically LCDs, CRTs, plasma displays (directly emissive) and DLPs (indirectly emissive). Emissive displays are a class of displays that emit light from their display surface and do not rely on the presence of ambient light (as opposed to reflective displays such as paper or some e-book readers which do rely on ambient light). The operation of the anaglyph technique, and the mechanisms which cause anaglyph crosstalk, are essentially the same across all four of the tested emissive displays (LCD, CRT, DLP, PDP) hence this section is written to encompass all four displays. The analysis method developed here is expected to be applicable to all full-colour emissive displays which use three colour channels. The anaglyph 3D technique when applied to printed images has significant differences to anaglyph 3D on emissive displays and hence it is discussed separately in the following exegesis chapter.

The analysis of anaglyph crosstalk is the most comprehensively investigated topic in this thesis – both for emissive displays in this section, and for printed images in the following section.

Based upon the performance analysis of the anaglyph 3D technique on emissive displays, Section 4.5 of **Paper 1** describes the sources of crosstalk as:

- The spectral quality of the display,
- The spectral quality of the anaglyph glasses and how well they match the spectral output of the display, and
- The properties of the anaglyph image generation algorithm.

These results are based upon a series of work presented in the following papers: **Paper 10** (2004), **Journal Paper 2** (2007), **Paper 8** (2010), and **Journal Paper 3** (2012). **Paper 10**, a non-refereed conference paper, reported on some early work which measured the spectra of a selection of displays (CRT, LCD, DLP), developed an initial crosstalk model and simulation, and conducted a brief validation experiment. This paper demonstrates an early attempt to implement the crosstalk measure/model/simulate/validate/extrapolate process as described in Section 3 of this exegesis. Most of **Paper 10** concentrated on the 'measure' phase of the five phase process, and described some initial work on modelling, validation and simulation of anaglyph crosstalk.

The process of anaglyph 3D crosstalk in emissive displays is illustrated in Figure 7 below - **Paper 10** was the first paper to set this out. Light from the three colour channels of the display have a certain spectral distribution (a) which passes through the colour filters of the anaglyph glasses which have a known spectral transmission (b). The spectral sensitivity of the human visual system affects how the different spectral frequencies are perceived (c). A simulation (d), based upon the anaglyph crosstalk model, can then be used to predict the amount of crosstalk as illustrated in (e) and (f).

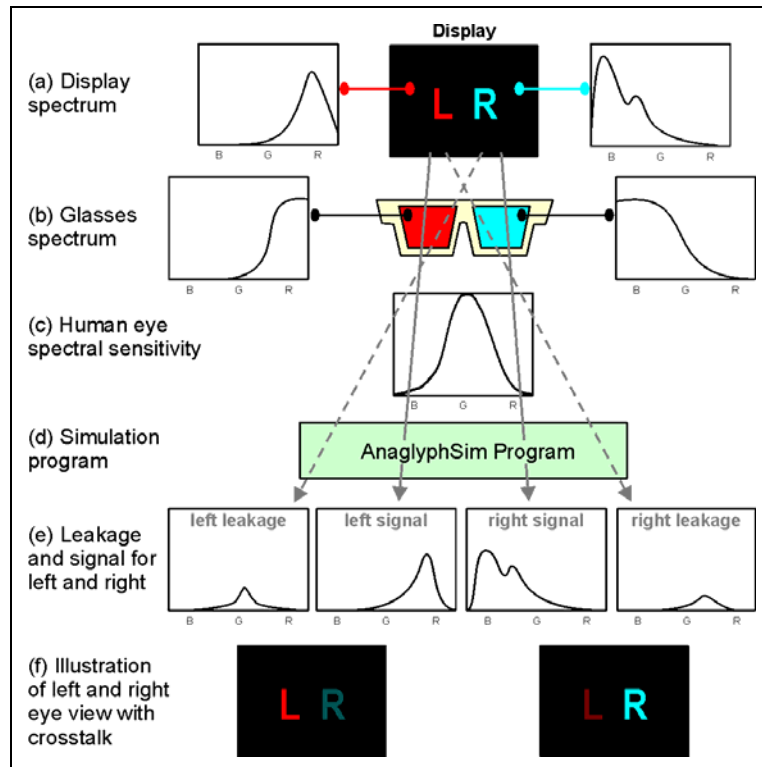


Figure 7 Illustration of the process and simulation of crosstalk of the anaglyph 3D method with emissive displays. From the top: (a) Spectral response of the display, (b) spectral response of the anaglyph 3D glasses, (c) human eye spectral sensitivity, (d) simulation of crosstalk using a computer program, (e) spectral output characteristic of the unintended (leakage) and intended (signal) image for both eyes, and (f) visual illustration of left eye and right eye view with crosstalk present. (from Section 4.5 of **Paper 1**)

Journal Paper 2 was the first publication of this anaglyph crosstalk research in a refereed journal. This paper expanded the work on anaglyph crosstalk by measuring a much wider selection of displays (13 LCDs and 14 PDPs) and glasses (now up to 32 pairs), it improved the crosstalk model and simulation program, conducted a more detailed validation (although still only in a single dimension), and predicted optimum combinations of glasses and displays for minimised crosstalk. This was the first of my publications in refereed journal format to outline the crosstalk measure/model/simulate/validate/extrapolate process.

The technique used to measure the spectral properties of the displays and glasses which form an input to the anaglyph crosstalk simulation model is outlined in Section 2 of **Paper 2** and the results of those measurements are illustrated in Figures 3-8 of **Paper 2** (in Sections 3.1 and 3.2). The anaglyph crosstalk model, which was developed in this body of work and illustrated in Figure 2 above, is described in Section 2 of **Paper 2**. The anaglyph crosstalk model was then used to predict low crosstalk combinations of displays and glasses as presented in Section 3.3 of **Paper 2**. A simple one-dimensional validation of the anaglyph crosstalk model using one subject was conducted and provided some confidence in the accuracy of the model, as explained in Section 3.4 of **Paper 2**. As described in Section 4 of **Paper 2**, the crosstalk simulation predicted that of the three display

technologies tested (LCDs, CRTs and PDPs), LCD monitors had the lowest average anaglyph crosstalk factor (18.6), and also the global minimum anaglyph crosstalk factor (7.0). The plasma displays were very similar with an average overall crosstalk factor of 18.6 but with a global minimum of only 8.1. The CRT had much worse anaglyph crosstalk with an average overall crosstalk factor of 27.0 and global minimum of 18.2. On average, the CRT had 45% more crosstalk than the LCD and plasma displays. The simulation revealed that there was a huge difference between the best and worst performing anaglyph glasses, but the best choice of anaglyph glasses depended upon which display was being considered. Overall the paper revealed that anaglyph crosstalk could be reduced by the selective choice of displays and glasses with optimum spectral characteristics, although crosstalk levels were still relatively high with an overall minimum crosstalk factor of 7.0. The further ability for crosstalk simulation to be able to predict (extrapolate) the performance of hypothetical configurations was not discussed in this paper and was left for following papers.

The previous papers (**Paper 10** and **Paper 2**) only considered red/cyan anaglyphs, whereas **Paper 8**, a refereed conference paper, extended the anaglyph crosstalk model and simulation to consider and compare other anaglyph colour combinations – specifically the blue/yellow and green/magenta anaglyph 3D methods. The generalisation of the model to predict other anaglyph colour primary combinations is described in Section 2 of **Paper 8**. The generalised model uses the same anaglyph simulation process illustrated in Figure 7 above for the red/cyan case, but now the left and right channels can be arbitrarily associated with different primary colour channels, to allow it to support the blue/yellow and green/magenta combinations. The spectral performance of a representative selection of glasses and displays is provided in Sections 3.1 and 3.2 of **Paper 8** - spectral data for more than 70 pairs of anaglyph glasses had now been sampled (including four green/magenta and six blue/yellow glasses). Section 3.4 of **Paper 8** described a slightly more detailed, but still rudimentary, validation process intended to compare the results of a human process of visually ranking the glasses to a simulated ranking performed using the generalised crosstalk simulation. The validation was conducted in one dimension (ranking a set of glasses when viewing a single display at a time) and with up to two observers. The validation results were noisy and only provided a moderate level of confidence in the ability of the model to accurately predict the comparison of crosstalk between different colour combination anaglyphs. Sections 3.4 and 4.2 of **Paper 8** went on to outline the limitations and complications of trying to compare different colour combination anaglyphs – particularly that the process of visually comparing anaglyph glasses of different colours was found to be a very difficult task and is also possibly highly subjective. Section 3.3 of **Paper 8** presented the results of the anaglyph crosstalk simulation across the three different anaglyph colour combinations (red/cyan, blue/yellow and green/magenta), 16 different pairs of glasses, and 30 different displays (14 LCDs, 1 CRT and 15 PDPs). Section 4 of **Paper 8** reported that the simulation predicted the red/cyan glasses to have the lowest average crosstalk factor but cautioned that the limitations of the study needed to be considered carefully when reviewing the simulation results.

This paper started to explore the real power of crosstalk simulation – using the crosstalk simulation to explore the crosstalk performance of hypothetical cases – by simulating the performance of an example set of dichroic filters for anaglyph purposes. The spectral performance of the dichroic filters was obtained from datasheets and the simulation was conducted without having physical samples of the dichroic filters in hand. The results of the simulation (presented in Sections 3.3 and 4.1 of **Paper 8**) predicted that the example red/cyan dichroic filter anaglyph glasses (with the spectral performance specified in Figures 3-8 of **Paper 8**) would offer a further two to four percentage point reduction in anaglyph crosstalk compared to the other tested anaglyph glasses. A good result in the simulation provides some motivation for the user to further investigate the option of using dichroic filters for anaglyph glasses filters. Whether the high cost of a pair of dichroic filter anaglyph glasses can be justified to achieve a two to four percentage point reduction in crosstalk is a separate decision.

In contrast, the simulation predicted that the example blue/yellow dichroic filter pair would produce considerably worse crosstalk than the existing blue/yellow anaglyph glasses and the difference was so large that there would be high confidence in deciding that in this case the extra cost of dichroic blue/yellow anaglyph glasses would not be justified. This example demonstrated that an accurate crosstalk simulation can be very useful in deciding the appropriate research direction to undertake when attempting to produce low crosstalk stereoscopic display solutions. The reason for the poor performance of the dichroic blue/yellow glasses was because of the particular cut-off wavelength of these filters. If the cut-off location occurred at a different wavelength, a much better result may have been possible, but this was not specifically investigated. Further analysis and discussion of the crosstalk results for different colour combination anaglyphs is provided in Section 4 of **Paper 8** and is not repeated here.

The most substantive work of all the four papers examining anaglyph crosstalk with emissive displays is **Journal Paper 3**. Although this paper draws from the work reported in the previous three papers, this paper extended the work to demonstrate the important role that crosstalk simulation can have in guiding research to reduce crosstalk in stereoscopic display systems. The algorithm for anaglyph crosstalk is expressed mathematically in Section 2 of **Paper 3**. The measurement of display and glasses spectrums (presented in Sections 3.1, 3.2, 4.1 and 4.2 of **Paper 3**) followed essentially the same process as reported in **Paper 2** however more effort was expended to calibrate the instruments and ensure the accuracy of the measurements. A new comprehensive validation experiment was devised and conducted across five observers (presented in Sections 3.4, 4.4 and 4.5 of **Paper 3**). Each of the five observers conducted 40 separate crosstalk ranking tasks across 12 pairs of glasses and four different displays, resulting in a total of 480 separate observations.⁹⁰ The results of the validation experiment (presented graphically in Figure 5 of **Paper 3**) revealed good agreement between the simulation and the visual ranking results. The validation experimental results were also

subjected to statistical analysis which calculated the Spearman rank correlation (r_s) values comparing the visual ranking results with the simulation results. These statistics (shown in Table 5 of *Paper 3*) provide a high level of confidence in the accuracy of the simulation model with 78% of the ranking tests having an r_s value of 0.9 or higher, and 18% having an r_s value of 0.99 or higher.⁹⁰

The availability of an accurate crosstalk model and simulation now allows the investigation of hypothetical options for reducing crosstalk in this stereoscopic display system. Section 5 of *Paper 3* provides two scenarios that were simulated using the anaglyph crosstalk model for emissive displays. The first simulation scenario compares the performance of the real-world anaglyph 3D glasses with idealised colour filters exhibiting a theoretical ‘brick-wall’ frequency response. ‘Brick-wall’ response colour filters are not achievable in reality, but using the model to simulate their theoretical effect on crosstalk allows an understanding of how close the real-world filters are to an ideal performance and therefore know how much scope there is for their improvement. As can be seen in Table 2 below, the use of ideal ‘brick-wall’ filters would make little difference to anaglyph crosstalk performance on LEDDLP1 – therefore it would be better to invest research into methods other than changes to the glasses performance to improve crosstalk performance. On the other hand, the simulation predicts that ‘brick-wall’ red filters could provide a 55% improvement for LCD15 (a Samsung 2233RZ LCD monitor) and a 65% improvement for CRT30 (a Mitsubishi Diamond View 1771ie CRT monitor) (per Table 2 below) indicating that there may be scope for improved crosstalk performance by investigating different real-world performance red filters. Further research would be needed to determine whether a cost-effective improvement could be achieved using available spectral filter technologies.

Table 2 Simulated improvement in anaglyph crosstalk performance by the use of theoretical “brick-wall” colour filters as compared to the best real-world filters tested in the study (from Table 6 of *Paper 3*).

(a) Red:				(b) Cyan:			
Display ID	simulated crosstalk (%)		improvement	Display ID	simulated crosstalk (%)		improvement
	Best Tested Red Filter	Best 'Brick-Wall' Red Filter			Best Tested Cyan Filter	Best 'Brick-Wall' Cyan Filter	
LCD15	8.7% (3DG74)	3.9% [620-700nm]	55%	LCD15	1.4% (3DG73)	0.3% [400-550nm]	31%
PDP15	16.6% (3DG88)	13.9% [610-700nm]	16%	PDP15	2.3% (3DG73)	1.4% [400-555nm]	39%
CRT30	16.6% (3DG74)	5.9% [625-700nm]	65%	CRT30	3.1% (3DG73)	2.4% [400-550nm]	20%
LEDDL1	19.7% (3DG88)	19.4% [615-700nm]	2%	LEDDL1	7.5% (3DG88)	7.2% [400-550nm]	4%

The second simulation scenario considered attempts to improve the crosstalk performance of display LEDDLP1 (a Samsung LED DLP rear-projection HDTV). “Most LEDs have fairly narrow spectral emission and very little out-of-band light output” but “in the case of LEDDLP1 ... there is a lot of out-of-band light output, particularly in the green channel”.⁹⁰ It is believed the out-of-band light output is due to the use of a colour management algorithm in the video-processing path of the display. The

colour management algorithm cannot be disabled via the user accessible controls of this display, so the anaglyph crosstalk simulation was used to predict the performance as if colour management could be disabled. The process used for this simulation is outlined in Section 5 of *Paper 3*. The results of the simulation (see Table 3 below) are remarkable – “a reduction of crosstalk by as much as 97%.”⁹⁰ The results indicate that if colour management “was able to be disabled on LEDDLP1, instead of exhibiting the most crosstalk, it could be exhibiting the least crosstalk”⁹⁰ of the four displays tested. This one simulation demonstrates the power of crosstalk simulation and its ability to provide direction for research effort. The detrimental effect that colour management can have on anaglyph crosstalk is explored further in the next sub-chapter of this exegesis.

Table 3 Comparison of simulated crosstalk performance of the LED DLP rear-projection HDTV with colour management (LEDDL1) and without colour management (LEDDL2). (from Table 7 of *Paper 3*)

Crosstalk(%)		Display ID		improvement
Glasses		LEDDL1	LEDDL2	
3DG88	red	19.7	0.6	97%
	cyan	7.5	0.6	92%
	overall	27.2	1.2	96%
3DG74	red	20.1	0.9	96%
	cyan	7.8	1.0	87%
	overall	27.9	1.9	93%
3DG73	red	20.3	1.1	95%
	cyan	7.6	0.8	90%
	overall	27.9	1.9	93%

A further sub-topic of *Paper 3* was an examination of the efficacy of using hand-made anaglyph 3D glasses. The experimental results shown in Table 3 of *Paper 3* (and validated in the visual ranking test presented in Section 4.4 of *Paper 3*) illustrate “that hand-made anaglyph glasses can exhibit significantly worse crosstalk performance than the better commercially available anaglyph 3-D glasses. Hence, good commercially available anaglyph 3D glasses [should be used] rather than hand-made glasses.”⁹⁰ This finding was not unexpected, but it was good to validate this hypothesis, especially because there are many examples of people/groups/sites (including NASA⁹³) recommending people make their own anaglyph glasses.

Paper 1, Paper 2, Paper 3 and *Paper 8* are included in Chapter 9 as core papers of the thesis. *Paper 10* is included in Appendix 1 as an additional publication relevant to the thesis.

4.3.2 Anaglyph 3D in Printed Images

The final stereoscopic display technique to be analysed as part of this thesis is the printing of anaglyph 3D images, as presented in *Journal Paper 4*. Printed anaglyph images often exhibit considerably higher levels of crosstalk than other stereoscopic display methods so there is some motivation to improve this very widely used stereoscopic display technique.

The way in which crosstalk occurs with printed anaglyph 3D images has similarities to the way in which crosstalk occurs with anaglyph 3D images on emissive displays, but there are a number of distinct differences which required a new crosstalk model to be developed and new equations for calculating crosstalk for printed anaglyphs to be devised. Figure 8 illustrates the model of printed anaglyph crosstalk developed for this thesis. With reference to Figure 8 (and explained in Section 3 of *Paper 4*) the model uses the spectrum of the light source (a), paper (b), ink(c), and colour filters in the anaglyph glasses (d). The simulation program (f) combines the above spectra with the spectral sensitivity of the human visual system (e) to generate curves for signal and leakage (g-h) and an illustration of crosstalk (i). The mathematical expression of the printed anaglyph crosstalk model is provided as Equations (1)-(13) in Section 3 of *Paper 4* and is not repeated here.

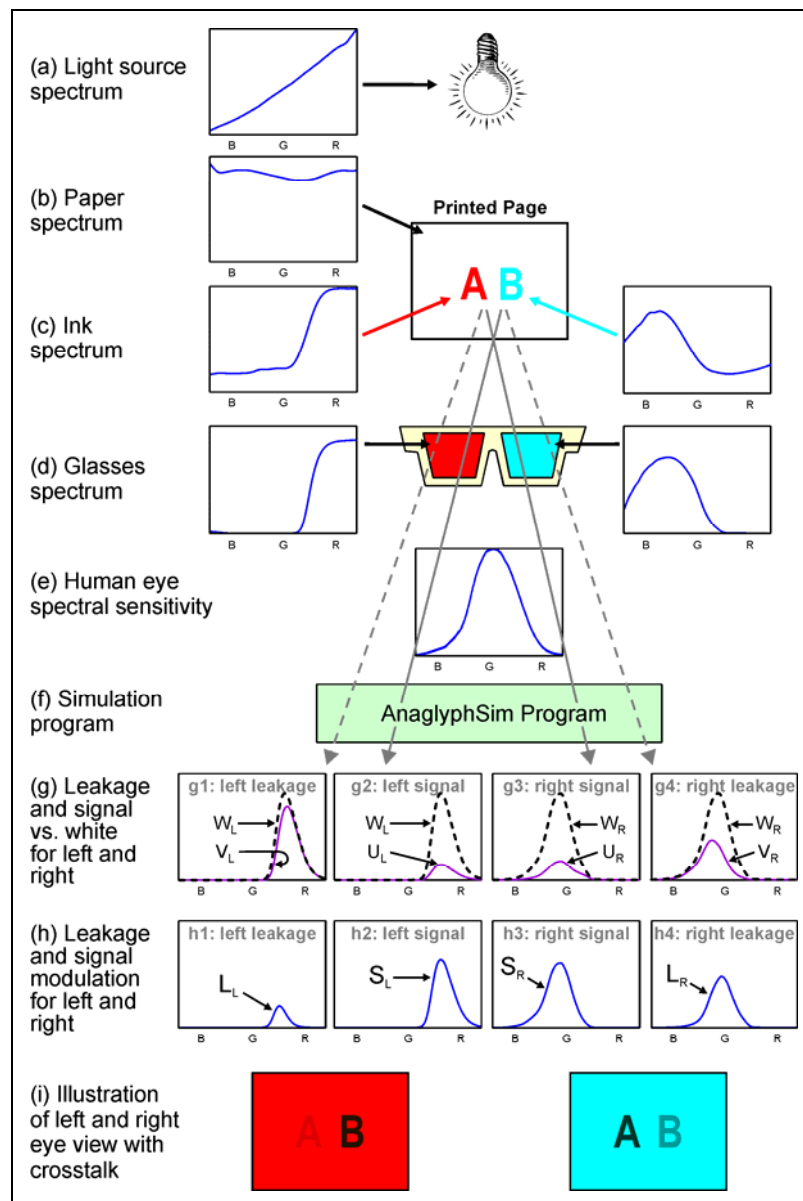


Figure 8 Illustration of the process of printed anaglyph crosstalk simulation. Each spectral graph shows wavelength on the horizontal axis (400 to 700nm, B=Blue, G=Green, R=Red) and intensity on the vertical axis. (from Figure 3 of *Paper 4*)

As can be seen from Figure 8, the crosstalk model has four input dimensions - light source, paper, ink type, and glasses – which means that the number of unique combinations of different inputs can escalate very rapidly. **Paper 4** considers three different light sources, one paper type, four different ink types, and 12 different anaglyph glasses resulting in 144 unique combinations. The crosstalk simulation provides a very quick way to compare all these different combinations and the results of these comparisons are illustrated in Figure 6 of **Paper 4**. The simulation predicted that the lowest crosstalk would be achieved using the combination of the RGB LED light source, the Epson printer ink set, and a commercial pair of red/blue anaglyph glasses identified as 3DG3 (as described in Section 5.5 of **Paper 4**). This particular input combination has an estimated 30% crosstalk, which is huge compared to other stereoscopic display methods, demonstrating a need to investigate options to lower printed anaglyph crosstalk, and prospectively a hint that there may exist a technique that could significantly reduce crosstalk in printed anaglyphs.

The printed anaglyph crosstalk model was validated by performing an extensive visual ranking validation experiment involving 780 separate crosstalk ranking observations across five observers in three domains (glasses, ink, lamp type) as outlined in Section 5.6 of **Paper 4**. The results of the validation experiment are illustrated in Figures 7-9 of **Paper 4**, and statistically analysed in Section 5.7 of **Paper 4**. The validation experiment results were analysed using both the Spearman rank correlation and the Pearson product-moment correlation techniques. The statistical analysis results provide a high level of confidence in the accuracy of the crosstalk simulation algorithm - in the glasses domain 96% of the ranking tests have an r_s value (Spearman's rank correlation) of 0.9 or better, 94% have an r^2 value (Coefficient of Determination using the Pearson product-moment correlation technique) of 0.9 or better, 60% have an r^2 value of 0.99 or better, and 20% have an r_s value of 0.99 or better. Statistical results in the ink and lamp domains also showed good correlation between the visual observations and the crosstalk simulation as described at the end of Section 5.7 of **Paper 4**.

With a high level of confidence in the developed printed anaglyph crosstalk model, Section 6 of **Paper 4** used the model to investigate options for reducing crosstalk. The simulation was used to investigate the effect of making changes in three different input dimensions – glasses, light source, and ink type. In a similar manner to **Paper 3**, the real-world glasses were compared to hypothetical 'brick-wall' filter anaglyph glasses (so called 'ideal' glasses). The use of a hypothetical RGB laser light source that provides very spectrally pure light was also examined, along with considering a new hypothetical ink type with an optimised spectral performance. Further detail of this analysis is provided in Section 6 of **Paper 4** and is not repeated here. The result of simulating these three scenarios is illustrated in Figure 9 below, which shows that although changes in the glasses and light source domain do make a difference, the biggest improvement in crosstalk was achieved by the changes made in the ink domain (down from 44% to 8.6%). Although there are no guarantees that it

will be possible to achieve a new ink set with the proposed spectrum, the simulation results certainly provide motivation to conduct further research in this direction.

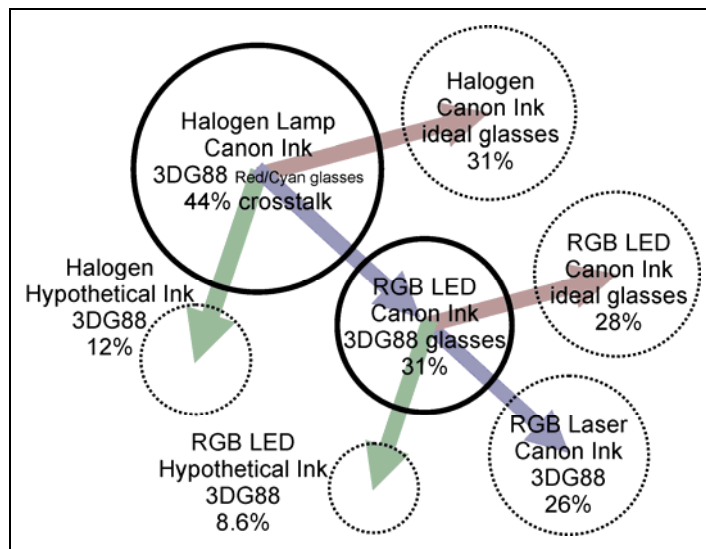


Figure 9 An illustration of the effect of making changes in the various input dimensions of printed anaglyph images (glasses dimension, ink set dimension, and light source dimension) has on the amount of crosstalk. The circle sizes (area) are proportional to the simulated amount of crosstalk for each condition. The simulation-only conditions are shown with dotted circles (from Figure 12 of *Paper 4*).

Another important finding of this research was the significant detrimental effect that colour management can have on printed anaglyph crosstalk levels. I believe that there needs to be provision to allow colour management to be disabled, or overridden by a different anaglyph-aware colour management algorithm, when printing anaglyph 3D images. Section 2.3 of *Paper 4* provides further discussion of this aspect.

Journal Paper 4 is included in Chapter 9 of this exegesis as a core manuscript of the thesis.

5. Review and Discussion

This thesis has identified the sources of crosstalk for six stereoscopic display technologies – time-sequential 3D on CRT displays, time-sequential 3D on plasma TVs, time-sequential 3D on LCD monitors and TVs, time-sequential 3D on DLP projectors, anaglyph 3D on emissive displays (CRT, plasma, LCD, DLP), and anaglyph 3D in printed images. In two cases (anaglyph 3D on emissive displays (*Paper 3*), and anaglyph 3D in printed images (*Paper 4*)) a full simulation of crosstalk was developed, validated, and extrapolated, and presented in refereed publications. In three cases (time-sequential 3D on CRTs (*Paper 9*), time-sequential 3D on LCDs (*Paper 5*), and time-sequential 3D on plasma displays (*Paper 6*)) a rudimentary crosstalk simulation was developed for the purposes of analysis and generating figures, but was not specifically presented in the publications.

The development of an accurate crosstalk simulation has allowed the relative contribution of different crosstalk mechanisms to the total crosstalk present in a display to be determined. In the case of time-sequential 3D on LCDs, this work identified that even if the pixel response time could be reduced, the scanned image update method would still be a significant contributor to crosstalk (particularly at the top and bottom of the screen) (Section 3.4 and 4 of *Paper 5*) unless work was performed to increase the speed of image update. In two cases (anaglyph 3D on emissive displays, and anaglyph 3D in printed images) crosstalk simulation has been used to identify conditions under which low levels of crosstalk would be observed (Sections 3.3 and 4 of *Paper 2*, and Section 5.5 of *Paper 4*) and additionally identify ways in which crosstalk could be reduced by making further changes to the display technologies used – e.g. by disabling colour management in an LED DLP HDTV (Section 5 of *Paper 3*) and by using improved spectral quality inks (Section 6 of *Paper 4*). This latter aspect of these two papers demonstrates the power of crosstalk simulation to quickly and cheaply identify ways in which crosstalk can be reduced and therefore improve the image quality of stereoscopic displays.

In terms of future work, a unified simulation for time-sequential 3D crosstalk across all of the emissive display technologies would be advantageous. I have already performed some development work towards this goal, however this work has not been finalised or published at this stage. In the prior chapters of this exegesis, the investigation of the time-sequential 3D method on the CRT, LCD, plasma and DLP display technologies have been considered and presented separately because the time-domain performance of each of these displays is notably different and produces sometimes radically different crosstalk mechanisms. However there is an opportunity to combine these separate analyses to develop a unified simulation across all time-sequential 3D displays. A unified simulation would include and combine all of the time-domain characteristics of the various emissive displays to estimate crosstalk performance of all of these displays. These characteristics include:

- image persistence (Section 2.1.2 of *Paper 9*)

- pixel response (Section 4.1.1 and 4.1.3 of **Paper 1**)
- image update method (Section 3.4 of **Paper 5**)
- impulse vs. hold-type display method (Section 3 of **Paper 5**)
- grey level generation technique (e.g. CRTs and LCDs produce different grey levels in an analog fashion (Sections 4.1.1 and 4.1.3 of **Paper 1**), DLP uses pulse width modulation (Section 4.1.4 of **Paper 1**), and plasma displays use a binary combination of different intensity pulses (Section 1.1 of **Paper 6**))
- blanking interval performance (Section 5 of **Paper 7**), and
- the time-domain properties of the LCS 3D glasses (Section 2.1.3 of **Paper 9**).

Such a simulation would be fairly complicated which is part of the reason that the work on the unified simulation has not yet been completed. The implementation of the plasma display grey level method would be the most challenging aspect of the unified crosstalk simulation because of the significant interplay between grey-level, time-domain pulse sequence (determined by the bit order of the PDP pulses, and the binary representation of each grey level), and phosphor persistence (Sections 1.1, 3.3 and 3.4 of **Paper 6**). A fully validated unified simulation of time-sequential 3D crosstalk would be beneficial because it would allow additional display technologies to be simulated (e.g. OLED, or other future display technologies) and the different time-sequential display technologies to be compared under the same model.

Section 5 of **Paper 3** explained that there was an opportunity to achieve an as yet unobtainably low level of anaglyph crosstalk (for emissive displays) by disabling the colour management in an LED DLP HDTV, however this prediction is yet to be validated using the actual display. The paper predicted that crosstalk levels as low as 0.6% in each eye are feasible even using current generation gel-filter anaglyph glasses. The override of colour management in this display will at the very least require access to the service menu and service controls of the display and may additionally require firmware changes to the display. The particular LED DLP HDTV in question is already time-sequential 3D compatible so it may seem pointless to enable the display of low-crosstalk anaglyph 3D images on this display, however it would be valuable to perform this investigation to validate the prediction of **Paper 3** and therefore confirm the academic validity of the crosstalk simulation process.

Section 7 of **Paper 4** proposed a range of techniques that could be used to improve the crosstalk performance of printed anaglyph 3D images. The best prospect for improving crosstalk performance is thought to be achieved by the use (or development) of inks which have better spectral purity – particularly the cyan ink. The first step would be to review current ink technologies available in the printing industry to determine whether printing inks with better spectral performance are already available – however, my initial investigations indicate that this is not the case. Measuring the spectra of a range of commercially obtainable inks and running these through the simulation would

be a worthwhile process to answer this question. In the event that better inks are not available, it may be necessary to develop new narrow spectral performance inks, perhaps by using quantum dot technology,⁸⁴ or modifying the chemical processes by which printing inks are produced.

Section 5 of **Paper 3** and Section 7 of **Paper 4** both identified that colour management can have a detrimental effect on crosstalk in printed anaglyph 3D images. The purpose of colour management is to achieve colour consistency between displays and it achieves this by mixing the colour channels to achieve the desired perceived output colour – much like a painter mixes paints on his or her palette. Unfortunately mixing colour channels causes crosstalk in anaglyph 3D images (for both emissive displays and printed images) therefore colour management directly leads to anaglyph crosstalk. Therefore there exists an opportunity to develop an anaglyph compatible colour management process which respects the need to keep colour channels separate after anaglyph multiplexing has occurred. In most current desktop printing systems, colour management is performed at the very last stage before ink is laid onto the paper and cannot be disabled. It would be desirable to implement anaglyph multiplexing after the colour management stage, however this would require significant changes to the colour management pipeline. The development of an anaglyph compatible colour management system would require low-level access to the desktop printing drivers and perhaps the programming of a new printer driver entirely. Section 2.2 of **Paper 4** also recommends the use of a new RGB to CMYK colour conversion algorithm, and the disabling (or optimisation) of “gray (grey) component replacement” (GCR) which will also likely need low-level access to the desktop printing drivers for implementation. One way to test these techniques is by using offset printing, however offset printing will ordinarily only be used for high printing volumes due to the high setup costs.

Section 6 of **Paper 4** proposed a new crosstalk calculation equation for printed anaglyph 3D images (Equations (14) and (15) of **Paper 4**). A new equation is necessary for printed anaglyph 3D images because of the different way in which anaglyph printing works compared to emissive displays. Future work could study the validation of these equations.

I would like to see the anaglyph crosstalk simulation software, titled “AnaglyphSim”, developed in these works (as explained in **Paper 3** and **Paper 4**) made available to other researchers in this field. The usual problem of research software is that it has been written for a very specific purpose, for use in a very specific way, and for use by a specific person. Such code will often not meet the immediate needs of other researchers – unless they are familiar with the software environment (in this case Matlab) and are happy to get their fingers deep in the code. A useful collection of input data (for use in the simulation software) has been collected as part of the works and has been invaluable in answering the questions posed. It would be desirable to make this available to other researchers

too. Future work could include the use of this software and data collection to answer a wide range of further questions about crosstalk in stereoscopic displays.

Paper 8 proposed the use of anaglyph glasses based on dichroic filters and used crosstalk simulation to predict that such glasses could provide a small but noticeable reduction of crosstalk (for the red/cyan and green/magenta cases) (Section 4.1 of **Paper 8**). It would be a valuable academic exercise to validate this prediction by purchasing a sample set of dichroic filters for constructing into a pair of anaglyph glasses to enable some human visual testing to be performed. The high cost of a set of anaglyph glasses based on dichroic filters would reduce the likelihood of commercial success, but there may be a selection of stereoscopic enthusiasts willing to pay a premium for increased viewing quality. As has been described in **Paper 2**, **Paper 3**, **Paper 4**, and **Paper 10** there are additional display specifications which can also be considered to reduce crosstalk and hence improve stereoscopic image quality in anaglyph 3D images.

Paper 1 and **Paper 16** identified several points of disagreement and inconsistency in the mathematical definition of crosstalk and grey-to-grey (gray-to-gray) crosstalk between various authors which I believe merits further investigation. Section 2.2.3 of **Paper 1** highlights that Huang et al.⁹⁴ provide a transfer function based approach to the mathematical definition of crosstalk, whereas several other authors^{88,18,50,20,95,96} provide observer-centric or output-luminance centric mathematical definitions of crosstalk. The difference between the transfer function based approach and the output-luminance approach is illustrated in Figure 10. The output-luminance centric definitions (shown in Figure 10 (a) and (b)) are based only on measurements of luminance at the viewer location – measurements which are easily obtained – whereas the transfer function based definition (Figure 8(c)) needs the source luminances ‘A’ and ‘B’ output by the display (before the effect of the multiplexing system, such as 3D glasses, lenticular sheet, or parallax barrier) as well as the luminance measurements at the viewer location. In cases where ‘A’ and ‘B’ cannot be measured directly, these must be calculated from the eight ‘L_{xxx}’ measurements (Figure 8(b)). The four transfer functions α_1 , α_2 , β_1 and β_2 are then calculated from ‘A’, ‘B’ and the eight ‘L_{xxx}’ measurements. Section 2.2.4 of **Paper 1** and Section 2.6 of **Paper 16** highlight similarities and differences between three different mathematical definitions of grey-to-grey crosstalk.^{97,98,99} The seemingly minor differences between the various grey-to-grey crosstalk definitions, mainly pertaining to the choice of variables on the denominator and the use of absolute values, still require some investigation to determine the pros and cons of each approach and hopefully propose a single equation which is most appropriate to use by all authors. More recently, a transfer function based mathematical definition of grey-to-grey crosstalk has also been proposed^{100,101} – in contrast to the output-luminance centric mathematical definitions discussed in the previous sentence. The cited advantage of the transfer function based approach is that it can be used to model intermediate values,¹⁰¹ however I remain concerned that such a model only simulates the effect of crosstalk in one display

and is not modelling the underlying causes of crosstalk, which is what the approach proposed in this thesis attempts to do. This area is still in a state of development and there remains an opportunity and a need to critically compare and unify the various mathematical definitions of crosstalk.

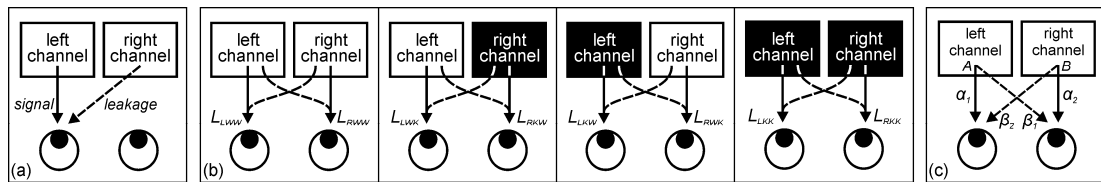


Figure 10 Illustration of the variables used in (a) crosstalk definition 1, (b) crosstalk definition 2, and (c) system crosstalk (from Figure 1 and Section 2.2 of **Paper 1**). The observer-centric or output-luminance centric mathematical definitions of crosstalk are shown in (a) and (b) whereas the transfer function based definition is used in (c). The subscripts of the eight luminance 'L' variables are defined as follows: The first subscript is the eye position (Left or Right) that the luminance is measured from, the second subscript is the value (black or White) of the desired image channel, and the third subscript is the value (black or White) of the undesired image channel. For example, L_{RWW} specifies the luminance measured at the right eye position when the right image (desired) channel is set to white and the left image (undesired) channel is also set to white, which corresponds to the summation of light from the right channel plus a (hopefully) small amount of light from the left channel.

The publicly released product specifications for 3D monitors and other 3D displays do not currently include a listing for the amount of crosstalk present for each display. It would be a useful specification to know when purchasing a new stereoscopic display since it has such a critical influence on image quality, but currently display manufacturers do not feel the need to reveal this particular specification to the public. It would be nice to be able to crowd-source this information from owners of these displays but unfortunately fairly specific optical measuring equipment is necessary to obtain accurate results (as described in Chapter 3). Although I have jointly proposed a simple method to measure crosstalk using display charts (**Paper 15**) the results are not sufficiently accurate to allow a reliable comparison of this crosstalk value between different displays due to potential gamma variation and black level variation between displays. The ability to accurately measure crosstalk values across displays is therefore limited to people (or laboratories or companies) with the right test equipment, and access to a range of 3D displays. Although the test equipment to measure crosstalk is not prohibitively expensive (as detailed in Section 5 of **Paper 1**) there is a limitation whereby the test results obtained using one set of test equipment cannot necessarily be directly compared with the test results obtained using a different set of test equipment – therefore there remains a need to ensure that test results obtained are consistent with human perception (i.e. perceptually relevant).¹⁰² Failing that, using the same test equipment to characterise a wide selection of displays would be a worthwhile effort to develop a better understanding of relative performance of different display systems.

The research design outlined in Chapter 3 proposed the use of the measure/model/simulate/validate/extrapolate process. The published works referenced in this

exegesis have shown this process to be an effective way of understanding and analysing crosstalk. **Paper 3** and **Paper 4** have tested this process right out to the extrapolate step for the anaglyph 3D technique. Other included papers have conducted work towards this step for the time-sequential 3D technique, however, as discussed above, further work is required to develop a unified model for all time-sequential 3D systems.

This thesis describes a wide range of knowledge about crosstalk in stereoscopic displays that has been investigated by me and collaborators, and summarises a wide range of information from other sources. Despite the breadth of work in this thesis, there remains considerable opportunity to conduct further research in this field, to allow us to understand the crosstalk performance of various displays, how crosstalk can be effectively reduced in different stereoscopic display technologies, and to allow us to fully understand the human perception of crosstalk.

6. Conclusion

This thesis has presented an examination of the definitions, presence, occurrence, measurement, mechanisms, simulation, reduction and perception of crosstalk in stereoscopic displays. The thesis has presented an investigation of crosstalk in the following stereoscopic display technologies: time-sequential 3D and anaglyph 3D methods on liquid crystal displays (LCDs), plasma displays, digital light projection (DLP) displays, and cathode ray tube (CRT) displays; as well as anaglyph 3D in printed images.

In addressing the aims of this thesis, a body of work has been presented which has:

- (a) Characterised the mechanisms by which crosstalk occurs in a wide range of stereoscopic display technologies,
- (b) Mathematically modelled and simulated the presence of crosstalk in a selection of stereoscopic display technologies,
- (c) Validated the models developed and used those models to investigate (extrapolate) how different display parameters affect the presence of crosstalk, and
- (d) Recommended ways in which crosstalk can be reduced in a range of stereoscopic display technologies.

This exegesis has drawn the collected publications into a structured framework and has included sufficient detail to explain the significance of the work without unnecessary duplication of the content presented in the included publications.

Stereoscopic displays are now an important segment of the display industry and crosstalk remains an important stereoscopic display performance attribute that needs to be minimised to allow the presentation of high-quality stereoscopic images. The work presented in this thesis has been conducted in a very active and dynamic period of the stereoscopic display industry, and I believe the works of this thesis have performed an important role in the maturation of the understanding of crosstalk in this developing field.

I originally commenced investigating crosstalk in stereoscopic displays because I felt that it was an important display attribute that I wanted to know more about and there was relatively little published literature which answered the questions that I wanted answered. Looking back at the published works now as I conclude this thesis, I recognise that it has been a truly fascinating journey and the questions that I originally asked have been answered, and so much more! As you, the reader, have worked through this exegesis and the included published works, I hope it has provided a useful and sound base on which to launch further research in this important field.

7. List of References (Exegesis only)

1. A. J. Woods (2010) "Understanding Crosstalk in Stereoscopic Displays" (Keynote Presentation) at 3DSA (Three-Dimensional Systems and Applications) conference, Tokyo, Japan, 19-21 May 2010.
2. A. J. Woods (2012) "Crosstalk in stereoscopic displays: a review" *Journal of Electronic Imaging* 21(4), 040902 (Oct-Dec 2012)
[included in Chapter 9 of this thesis as Paper 1]
3. International Stereoscopic Union (undated) "A Glossary of Stereoscopic Terms" [online] <http://www.stereoscopy.com/isu/glossary-index.html> Accessed: 20 October 2013.
4. A. J. Woods (2009) "3-D Displays in the Home" *Information Display*, 25(07), pp 8-12, July 2009. http://informationdisplay.org/Portals/InformationDisplay/IssuePDF/07_2009.pdf
[included in Appendix 1 of this thesis as Paper 14]
5. B. Lee (2013) "Three-dimensional displays, past and present" *Physics Today*, 44(6), pp. 36, April 2013. DOI: <http://dx.doi.org/10.1063/PT.3.1947>
6. B. Julesz (1983) "Texton Theory of Two-Dimensional and Three-Dimensional Vision" *Processing and Display of Three-Dimensional Data*, Proc. SPIE 367, pp. 2 (April 8, 1983); DOI: <http://dx.doi.org/10.1117/12.934294>
7. H. Jorke, M. Fritz (2006) "Stereo projection using interference filters" *Proc. SPIE 6055, Stereoscopic Displays and Virtual Reality Systems XIII*, 60550G (January 27, 2006); doi:10.1117/12.650348
8. M. J. Richards, and G. D. Gomes (2011) "Spectral Separation Filters for 3D Stereoscopic D-Cinema Presentation," United States Patent US 7,959,295 B2.
9. T. Gunnarsson (2012) "Global 3-D Market Flourishes Across Cinema, Home Video and TV VoD Platforms" Press Release, IHS/iSuppli, 20 December 2012.
URL: <http://www.isuppli.com/media-research/news/pages/global-3-d-market-flourishes-across-cinema-home-video-and-tv-vod-platforms.aspx> Accessed 18 May 2013.
10. M. Kozuka (2012) "Panasonic's Stereoscopic 3D Technologies, Standardization and Business Strategy" Keynote Presentation, *Stereoscopic Displays and Applications XXIII*, Burlingame, California, January 2012. (Presentation only) Video:
http://www.youtube.com/watch?v=7oy_lVTBLC4 Accessed 18 May 2013.
11. A. J. Woods (2013) "The Illustrated 3D Movie List" [online] May 2013. URL: <http://www.3dmovielist.com> Accessed 18 May 2013.
12. C. Kennedy (1936) "The Development and Use of Stereo Photography for Educational Purposes", Vol. 26, pp. 3-17, January 1936.
13. R. Spottiswoode, N. L. Spottiswoode and Charles Smith (1952) "Basic Principles of the Three Dimensional Film" *Journal of the SMPTE*, Vol. 59, pp. 249-286, October 1952.

14. B. Mendiburu (2010) "3D Movie Making: Stereoscopic Digital Cinema from Script to Screen" Focal Press.
15. A. J. Woods (2013) "3D or 3-D: A study of terminology, usage and style", *European Science Editing*, 39(3), pp. 59-62, August 2013.
[included in Appendix 1 of this thesis as **Paper 18**]
16. Y.-C. Chang, C.-Y. Chiang, K.-T. Chen, Y.-P. Huang (2009) "Investigation of Dynamic Crosstalk for 3D Display" in 2009 International Display Manufacturing Conference, 3D Systems and Applications, and Asia Display (IDMC/3DSA/Asia Display 2009), Taipei, Taiwan.
17. B. Lane (1982) "Stereoscopic displays" in *Proc. SPIE Processing and Display of Three-Dimensional Data*, ed. J.J. Pearson, 0367, 20-32.
18. A. J. Woods (2011) "How are crosstalk and ghosting defined in the stereoscopic literature?" in *Stereoscopic Displays and Applications XXII, Proceedings of IS&T/SPIE Electronic Imaging*, SPIE Vol. 7863, pp. 78630Z-1 to -12, Burlingame, California, January 2011.
[included in Appendix 1 of this thesis as **Paper 16**]
19. SMPTE (2009) "Report of SMPTE Taskforce on 3D to the Home" Society of Motion Picture and Television Engineers (SMPTE), New York.
20. International Committee for Display Metrology (2012) "Information display measurements standard (version 1.03)," Society for Information Display. [online] <http://icdm-sid.org/>
21. IEC (2009) "TC110/220/NP - New Work Proposal - 3D Displays - Terminology and letter symbols" International Electrotechnical Commission, dated: 2009-12-18.
22. L. Lipton (1978) "Foundations of the Stereoscopic Cinema – A Study in Depth" Van Nostrand Reinhold Company, New York.
23. L. Lipton (1989) "Compatibility of Stereoscopic Video Systems with Broadcast Television Standards" *Three-Dimensional Visualization and Display Technologies*, Proc. SPIE 1083, pp. 95.
24. G. A. Slavenburg, T. F. Fox, and David R. Cook (2007) "System, method, and computer program product for increasing an LCD display vertical blanking interval," United States Patent Application Publication 20070229487 A1, publication date 4 October, 2007.
25. C. Wheatstone (1838) "Contributions to the Physiology of Vision.—Part the First. On some remarkable, and hitherto unobserved, Phenomena of Binocular Vision" in *Philosophical Transactions of the Royal Society of London*, Vol. 128, pp. 371 – 394.
26. Encyclopædia Britannica (2012) "Louis Ducos du Hauron" in *Encyclopædia Britannica*, Encyclopædia Britannica Online, Encyclopædia Britannica Inc. Accessed: 22 Jul 2012 URL: <<http://www.britannica.com/EBchecked/topic/172961/Louis-Ducos-du-Hauron>>
27. L. D. duHauron (1891) "Estampes, photographies et tableaux stéréoscopiques, produisant l'air effect en plein jour, sans l'aide du stereoscope" French Patent No. 216465 (1891) in S. A. Benton (editor) "Selected Papers on Three-Dimensional Displays" SPIE Milestone Series, MS162 (2001)
28. L. D. duHauron (1895) "Stereoscopic print" U.S. Patent No. 544666.

29. M. Macedonia (2006) "It's the end of the tube as we know it" IEEE Computer, June 2006, Vol.39(6), pp.83-85.
30. D. L. Symmes (2006) "The Chopper" Online: [ARCHIVED]
<http://web.archive.org/web/20110707063258/http://www.3dmovingpictures.com/chopper.html> Dated: 14 November 2006, Accessed: 4 August 2013.
31. Laurence Hammond (1924) "Stereoscopic motion picture device," U.S. Patent No. 1506524.
32. T. Takahashi (2010) "A Review of Electronic Paper Display Technologies from the Standpoint of SID Symposium Digests" FDP 2010 Symposium Digest, (2010)
33. J. A. Roese (1975) "PLZT stereoscopic television system," U.S. Patent No. 3903358.
34. Casio (undated) "Casio Corporate History - Chronology of Products" Online: http://www.casio-europe.com/euro/corporate/chronologyofproducts/detail/1983_3/ Accessed: 11 August 2013.
35. L. J. Hornbeck (1995) "Digital Light Processing and MEMS: Timely Convergence for a Bright Future" (Invited Plenary Paper), Proceedings SPIE, Vol. 2639, Micromachining and Microfabrication Process Technology.
36. L. Lipton (2012) "Brief history of electronic stereoscopic displays" Optical Engineering 51(2), 021103, February 2012.
37. K. Hamada, T. Yamamoto, T. Kurita, Y. Takano, I. Yuyama (1998) "A field-sequential stereoscopic display system with 42-in. HDTV DC-PDP" Proc. Intl. Display Workshop IDW'98, pp. 555–558, IDW, Japan.
38. I. McDowall, M. Bolas, D. Corr, T. Schmidt (2001) "Single and Multiple Viewer Stereo with DLP Projectors" Stereoscopic Displays and Virtual Reality Systems VIII, Proc. SPIE Vol. 4297, pg 418-425, San Jose, California.
39. M. Hanlon (2003) "LCD sales surpass CRT sales for first time" GizMag, online:
<http://www.gizmag.com/go/2427/> dated: 15 December 2003, Accessed: 6 August 2013.
40. Projector Central (undated) "Lightspeed DepthQ Projector" Online:
<http://www.projectorcentral.com/Lightspeed-DepthQ.htm> Accessed: 11 August 2013.
41. A. J. Woods (2012) "The Illustrated 3D HDTV List", URL:
<http://www.3dmovielist.com/3dhdtvs.html> dated: 24 May 2012, accessed: 19 June 2013.
42. J. M. Lytle (2008) "Pioneer pulls plasma plug, Sony cans CRTs" TechRadar, online:
<http://www.techradar.com/au/news/television/pioneer-pulls-plasma-plug-sony-cans-crts-256211> dated: March 4th 2008, accessed: 12 August 2013.
43. A. J. Woods (2012) "The Illustrated 3D Compatible Projectors List",
URL: <http://www.3dmovielist.com/projectors.html> , dated: 6 Feb 2012, accessed: 19 June 2013.
44. Projector Central (undated) "Viewsonic PJD5111" Online:
<http://www.projectorcentral.com/ViewSonic-PJD5111.htm> Accessed: 11 August 2013.

45. A. J. Woods (2012) "The Illustrated 3D Monitor List",
URL: <http://www.3dmovielist.com/3dmonitors.html> , dated: 13 May 2012, accessed: 19 June 2013.
46. Google Inc. (2013) "Google Scholar (citations for: Andrew J. Woods)" [online] URL:
<http://scholar.google.com.au/citations?user=J-9YiCkAAAAJ> Dated: 13 October 2013,
Accessed: 13 October 2013.
47. W. W. Jacques (1885) "Underground wires," *Science* 6(126), pp. 6–7.
48. C. W. Earp (1941) "Carrier wave transmission system," U.S. Patent No. 2256317.
49. L. Lipton (1987) "Factors affecting 'ghosting' in time-multiplexed planostereoscopic CRT display systems," in *True 3D Imaging Techniques and Display Technologies*, Proc. SPIE 761, pp. 75–78.
50. S. Pala, R. Stevens, and P. Surman (2007) "Optical crosstalk and visual comfort of a stereoscopic display used in a real-time application," in *Stereoscopic Displays and Virtual Reality Systems XIV*, Proc. SPIE 6490, 649011.
51. K.-C. Huang, J.-C. Yuan, C.-H. Tsai, W.-J. Hsueh, N.-Y. Wang (2003) "A study of how crosstalk affects stereopsis in stereoscopic displays," in *Stereoscopic Displays and Virtual Reality Systems X*, Proc. SPIE 5006, 247–253.
52. S. Pastoor (1995) "Human factors of 3D images: Results of recent research at Heinrich-Hertz-Institut Berlin," in *Proc. IDW'95*, Vol. 3D-7, pp. 69–72, IDW, Japan.
53. Y. Nojiri et al. (2004) "Visual comfort/discomfort and visual fatigue caused by stereoscopic HDTV viewing," in *Stereoscopic Displays and Virtual Reality Systems XI*, Proc. SPIE 5291, 303–313.
54. F. L. Kooi and A. Toet (2004) "Visual comfort of binocular and 3D displays," *Displays* 25(2–3), 99–108.
55. P. J. H. Seuntiëns, L. M. J. Meesters, and W. A. Ijsselsteijn (2005) "Perceptual attributes of crosstalk in 3D images," *Displays* 26(4–5), 177–183.
56. K. Ukai and P. A. Howarth (2008) "Visual fatigue caused by viewing stereoscopic motion images: background, theories, and observations," *Displays* 29(2), 106–116.
57. T. J. Haven (1987) "A liquid-crystal video stereoscope with high extinction ratios, a 28% transmission state, and 100 μ s switching", in *True Three-Dimensional Imaging Techniques & Display Technologies*, D.F. McAllister, W.E. Robbins, Editors, Proceedings of SPIE vol. 761, pp. 23-26, Bellingham Washington USA, 1987.
58. L. Lipton, J. Halnon, J. Wuopio, B. Dorworth (2000) "Eliminating it-cell artefacts", in *Stereoscopic Displays & Virtual Reality Systems VII*, JO. Merritt, S.A. Benton. A.J. Woods, MT. Bolas, Editors, Proceedings of SPIE vol.3957, pp. 264-270, Bellingham Washington USA.
59. P.J. Bos, T. Haven (1989) "Field-Sequential Stereoscopic Viewing Systems using Passive Glasses", in *SID Vol. 30/1*, pp. 39-43.

60. J. S. Lipscomb, W. L. Wooten (1994) "Reducing Crosstalk between Stereoscopic Views", in Stereoscopic Displays & Virtual Reality System, S. S. Fisher, J. O. Merritt, M. T. Bolas, Editors, Proceedings of SPIE vol.2177, pp. 92-96, Bellingham Washington USA.
61. P. J. Bos (1991) "Time Sequential Stereoscopic Displays: The Contribution of Phosphor Persistence to the 'Ghost' Image Intensity", in Three-Dimensional Image Technologies, H. Kusaka, Editor, Proceedings of ITEC'91, ITE Annual Convention, pp. 603-606, Institute of Television Engineering of Japan, Tokyo, Japan, July 1991.
62. L. Lipton (2011) "The Stereoscopic Cinema: From Film to Digital Projection", in SMPTE Journal, pp. 586-593, Sept 2001.
63. L. Lipton (1992) "High Dynamic Range Electro-Optical Shutter for Stereoscopic and other Applications", United States Patent #5 1 17 302, May 1992.
64. A. J. Woods (2005) "Compatibility of Display Products with Stereoscopic Display Methods" International Display Manufacturing Conference (IDMC), pp. 290-293, Taiwan, February 2005. [included in Appendix 1 of this thesis as **Paper 11**]
65. Projector Central (2013) "InFocus DepthQ Projector" URL: <http://www.projectorcentral.com/InFocus-DepthQ.htm> , dated: 18 June 2013, accessed: 18 June 2013.
66. H. Pan, X.-F. Feng, S. Daly (2005) "LCD motion blur modeling and analysis" IEEE Int'l. Conf. Image Processing, Vol. 2, pp. 21-24.
67. A. A. S. Sluyterman, E. P. Boonekamp (2005) "Architectural Choices in a Scanning Backlight for Large LCD TVs" SID 05 Digest, pg 996-998.
68. H.-C. Hung, C.-W. Shih (2005) "Improvement in Moving Picture Quality Using Scanning Backlight System" Proceedings of the International Display Manufacturing Conference (IDMC'05), Taipei, Taiwan.
69. K. Hamada, T. Kurita, M. Kanazawa, K. Yamamoto (2001) "A 3D Hi-Vision Display with 50-in. AC PDP" Asia Display/Intl. Display Workshop IDW'01, pp. 785-788, IDW, Japan.
70. K.-D. Cho (2004) "New Address and Sustain Waveforms for AC Plasma Display Panel", PhD Thesis, Kyungpook National University.
71. L. J. Hornbeck (1998) "Current status and future applications for DMD based projection displays" Proc. Fifth Intl. Display Workshop IDW'98, Japan, pp. 1-4.
72. M. Husak, J. D. Lawrence, R. Mueller, C. Ward (2011) "System and method for synchronizing a 3D video projector" U.S. Patent No. 8066377.
73. A. J. Woods, S. Tan (2002) "Characterising Sources of Ghosting in Time-Sequential Stereoscopic Video Displays" presented at Stereoscopic Displays and Applications XIII (SD&A), published in Stereoscopic Displays and Virtual Reality Systems IX, Proceedings of IS&T/SPIE Electronic Imaging, SPIE Vol. 4660, pp. 66-77, San Jose, California, January 2002. [included in Chapter 9 of this thesis as **Paper 9**]

74. A. J. Woods, T. Rourke (2004) "Ghosting in Anaglyphic Stereoscopic Images" presented at Stereoscopic Displays and Applications XV (SD&A), published in Stereoscopic Displays and Virtual Reality Systems XI, Proceedings of IS&T/SPIE Electronic Imaging, SPIE Vol. 5291, pp. 354-365, San Jose, California, January 2004.
[included in Appendix 1 of this thesis as **Paper 10**]
75. A. J. Woods, T. Rourke, K.-L. Yuen (2006) "The Compatibility of Consumer Displays with Time-Sequential Stereoscopic 3D Visualisation" (Invited Plenary Paper), in Proceedings of the K-IDS Three-Dimensional Display Workshop 2006, pp. 7-10, Seoul National University, Seoul, South Korea, 21 August 2006.
[included in Appendix 1 of this thesis as **Paper 12**]
76. A. J. Woods, T. Rourke (2007) "The compatibility of consumer DLP projectors with time-sequential stereoscopic 3D visualization", presented at Stereoscopic Displays and Applications XVIII, published in Stereoscopic Displays and Virtual Reality Systems XIV, Proceedings of IS&T/SPIE Electronic Imaging, SPIE Vol. 6490, pp. 64900V-1 to -7, San Jose, California, January 2007.
[included in Appendix 1 of this thesis as **Paper 13**]
77. M. A. Weissman, Andrew J. Woods (2011) "A simple method for measuring crosstalk in stereoscopic displays" in Stereoscopic Displays and Applications XXII, Proceedings of IS&T/SPIE Electronic Imaging, SPIE Vol. 7863, pp. 786310-1 to -11, Burlingame, California, January 2011.
[included in Appendix 1 of this thesis as **Paper 15**]
78. A. J. Woods, Jesse Helliwell (2012) "Investigating the cross-compatibility of IR-controlled active shutter glasses" in Stereoscopic Displays and Applications XXIII, Proceedings of IS&T/SPIE Electronic Imaging, SPIE Vol. 8288, pp. 82881C-1 to -10, Burlingame, California, January 2012.
*[included in Appendix 1 of this thesis as **Paper 18**]*
79. J. A. Norling (1937) "Anaglyph Stereoscopy," U.S. Patent No. 2,135,197.
80. S. J. Harrington, R. P. Loce, and G. Sharma (2006) "Systems for spectral multiplexing of source images to provide a composite image, for rendering the composite image, and for spectral demultiplexing of the composite image to animate recovered source images," U.S. Patent No. 7,136,522 B2.
81. G. Sharma, R. P. Loce, S. J. Harrington, Y. Zhang (2003) "Illuminant multiplexed imaging: special effects using GCR," in Proc. 11th Color Imaging Conference: Color Science and Engineering Systems, Technologies, and Applications, pp. 266–271, IS&T (Society for Imaging Science & Technology), Springfield, Virginia.
82. R. Labbe, D. E. Klutho (2009) "Publishing stereoscopic images" Stereoscopic Displays and Applications XX, Proc. SPIE Vol. 7237, 72370J.

83. A. J. Woods, Ka Lun Yuen (2006) "Compatibility of LCD Monitors with Frame-Sequential Stereoscopic 3D Visualisation" (Invited Paper), in IMID/IDMC '06 Digest, (The 6th International Meeting on Information Display, and The 5th International Display Manufacturing Conference), pp. 98-102, Daegu, South Korea, 22-25 August 2006.
*[included in Chapter 9 of this thesis as **Paper 5**]*
84. L. Cui, Y. Li, J. Wang, E. Tian, X. Zhang, Y. Zhang, Y. Song, Lei Jianga (2009) "Fabrication of large-area patterned photonic crystals by ink-jet printing" Journal of Material Chemistry, Vol. 19, pp. 5499-5502.
85. A. J. Woods, A. Sehic (2009) "The compatibility of LCD TVs with time-sequential stereoscopic 3D visualization" in Stereoscopic Displays and Applications XX, Proceedings of IS&T/SPIE Electronic Imaging, SPIE Vol. 7237, pp. 72370N-1 to -9, San Jose, California, January 2009.
*[included in Chapter 9 of this thesis as **Paper 7**]*
86. IPL 10530 Integrated Photodiode Amplifiers, Product Data Sheet, Integrated Photomatrix Limited, Dorchester, United Kingdom.
87. A. J. Woods, K. S. Karvinen (2008) "The compatibility of consumer plasma displays with time-sequential stereoscopic 3D visualization" in Stereoscopic Displays and Applications XIX, Proceedings of IS&T/SPIE Electronic Imaging, SPIE Vol. 6803, pp. 68030X-1 to -9, San Jose, California, January 2008.
*[included in Chapter 9 of this thesis as **Paper 6**]*
88. A. J. Woods, C. R. Harris (2010) "Comparing levels of crosstalk with red/cyan, blue/yellow, and green/magenta anaglyph 3D glasses" in Stereoscopic Displays and Applications XXI, Proceedings of IS&T/SPIE Electronic Imaging, SPIE Vol. 7253, pp. 75240Q-1 to -12, San Jose, California, January 2010.
*[included in Chapter 9 of this thesis as **Paper 8**]*
89. A. J. Woods, K. L. Yuen, and K. S. Karvinen, (2007) "Characterizing crosstalk in anaglyphic stereoscopic images on LCD monitors and plasma displays" in Journal of the Society for Information Display, Volume 15, Issue 11, pp. 889-898, November 2007.
*[included in Chapter 9 of this thesis as **Paper 2**]*
90. A. J. Woods, C. R. Harris (2012) "Using cross-talk simulation to predict the performance of anaglyph 3-D glasses" in JSID (Journal of the Society for Information Display), Vol. 20, No. 6, pp. 304-315.
*[included in Chapter 9 of this thesis as **Paper 3**]*
91. A. J. Woods, C. R. Harris, Dean B. Leggo, Tegan M. Rourke (2013) "Characterizing and Reducing Crosstalk in Printed Anaglyph Stereoscopic 3D Images" in (Journal of) Optical Engineering, SPIE, Vol. 52, No. 4, pp. 043203-1 to 043203-19, April 2013.
*[included in Chapter 9 of this thesis as **Paper 4**]*
92. www.matlab.com

93. NASA (2012) "Build your own 3d glasses" National Aeronautics and Space Administration [online] <http://stereo.gsfc.nasa.gov/classroom/glasses.shtml> Dated: 5 December 2012. Accessed: 27 October 2013.
94. K.-C. Huang, C.-H. Tsai, K.-J. Lee, W.-J. Hsueh (2000) "Measurement of Contrast Ratios for 3D Display" in *Input/Output and Imaging Technologies II*, Proc. SPIE 4080, pp. 78–86.
95. P. Boher, T. Leroux, T. Bignon, V. Collomb-Patton (2010) "Multispectral polarization viewing angle analysis of circular polarized stereoscopic 3D displays" *Stereoscopic Displays and Applications XXI*, Proc. SPIE 7253, 72530R.
96. J.-C. Liou, K. Lee, F.-G. Tseng, J.-F. Huang, W.-T. Yen, W.-L. Hsu (2009) "Shutter glasses stereo LCD with a dynamic backlight" *Stereoscopic Displays and Applications XX*, Proc. SPIE 7237, 72370X.
97. S. Shestak, D.-S. Kim, S.-D. Hwang (2010) "Measuring of gray-to-gray crosstalk in a LCD based time-sequential stereoscopic displays," *Society for Information Display Symposium Digest Technical Papers* 41(1), 132–135.
98. S.-M. Jung, Y.-B. Lee, H.-J. Park, S.-C. Lee, W.-N. Jeong, J.-K. Shin, I.-J. Chung (2010) "Improvement of 3-D crosstalk with over-driving method for the active retarder 3-D displays" *Society for Information Display Symposium Digest Technical Papers*, 41(1), pp. 1264–1267.
99. C.-C. Pan, Y.-R. Lee, K.-F. Huang, T.-C. Huang (2010) "Cross-talk evaluation of shutter-type stereoscopic 3D display" *Society for Information Display Symposium Digest Technical Papers*, 41(1), pp. 128–131.
100. F.-H. Chen, J.-C. Yang, Y.-H. Chou, K.-C. Huang, K. Lee (2012) "Gray-to-gray crosstalk model" *3DSA (Three Dimensional Systems and Applications) Confence*, pp. 213–216.
101. K.-C. Huang, F.-H. Chen, L.-C. Lin, H.-Y. Lin, Y.-H. Chou, C.-C. Liao, Y.-H. Chen, K. Lee (2013) "A crosstalk model and its application to stereoscopic and autostereoscopic displays" *Journal of the Society for Information Display*, 21(6), pp. 249-262.
102. K. Teunissen, A. Sevo, A. van Daltsen, and H. van Parys (2011) "Perceptually Relevant Characterization of Stereoscopic Displays" *Society for Information Display Symposium Digest Technical Papers*, 42(1), pp. 994-997.

Every reasonable effort has been made to acknowledge the owners of copyright material. I would be pleased to hear from any copyright owner who has been omitted or incorrectly acknowledged.

8. Bibliography (from Exegesis and Included Publications)

As a courtesy to the reader, this list includes, in one place, all of the references cited in the published papers plus any additional references cited in the exegesis.

The circled number refers to the paper number(s) which cite this particular reference. e.g. ① = this reference was cited in **Paper 1**. ⑤ = this reference was cited in the Exegesis.

1. ⑬ A. Abileah (2011) "3D Displays – Technologies & Testing Methods" at 3D Imaging Workshop, Stanford University.
2. ③ Agarwal (2010) "Make your own 3D glasses in 10 seconds," Digital Inspiration [online]. URL: <http://www.labnol.org/home/make-3dglasses/13776/> Dated: 2 June 2010. Accessed: 6 July 2011.
3. ⑭ W. Allen, R. Ulichney (2005) "Wobulation: Doubling the Addressed Resolution of Projection Displays," SID Symposium Digest 36, 1514-1517.
http://www.hpl.hp.com/personal/Robert_Ulichney/papers/2005-wobulation-SID.pdf
4. ① American Polarizers Inc (undated) "Circular Polarizers - APNCP37" American Polarizers, Inc. [online] accessed 28 March 2010.
<http://www.apioptics.com/pdf/APNCP37-010-STD.pdf>
5. ⑱ Associated Press (2013) "The Associated Press Stylebook and Briefing on Media Law" New York: Associated Press. ISBN 978-0-917360-57-2.
6. ③④ V. C. Barber, D. A. Brett (1982) "'Colour bombardment" - a human visual problem that interferes with the viewing of anaglyph stereo material" in Scanning electron microscopy, 2, pp.495-498.
7. ① M. Barkowsky, S. Tourancheau, K. Brunnström, K. Wang, and B. Andrén (2011) "Crosstalk Measurements of Shutter Glasses 3D Displays" SID 11 Digest, 812-815.
8. ⑰ G. R. Basile, F. J. Poradish (2006) "System and Method for Synchronizing a Viewing Device" US Patent Application 2008/0151112 A1, dated 22 Dec 2006.
9. ③④ R. Blake R. Sekuler (2006) "Perception (5th edn.);" McGraw Hill, Boston, pp. 92.
10. ① L. Blondé, J.-J. Sacré, D. Doyen, Q. Huynh-Thu, and C. Thébault (2011) "Diversity and Coherence of 3D Crosstalk Measurements," SID 11 DIGEST, 804-807.
11. ①⑮ W. Bloos (2008) "Ghosting test - standard method for determining ghost image," Stereo Forum, online, dated 5 June 2008, accessed 25 March 2010.
<http://www.stereoforum.org/viewtopic.php?f=16&t=53>
12. ①⑬ A. Boev, A. Gotchev, and K. Egiazarian (2007) "Crosstalk measurement methodology for autostereoscopic screens" 3DTV Conference, 1-4.

13. ③ K. R. Boff, J. E. Lincoln (1988) Engineering data compendium: Human perception and performance, AAMRL, Wright-Patterson AFB, OH, pp. 370.
14. ①⑤⑥ P. Boher, T. Leroux, T. Bignon, V. Collomb-Patton (2010) "Multispectral polarization viewing angle analysis of circular polarized stereoscopic 3D displays" in Proc. SPIE Stereoscopic Displays and Applications XXI, 7253, 0R1-0R12.
15. ⑥ P. Boher (2010) ELDIM, personal communication, 13 April 2010.
16. ⑤ P.J. Bos, T. Haven (1989) "Field-Sequential Stereoscopic Viewing Systems using Passive Glasses", in SID Vol. 30/1, pp. 39-43.
17. ⑤⑥ P. J. Bos (1991) "Time Sequential Stereoscopic Displays: The Contribution of Phosphor Persistence to the 'Ghost' Image Intensity", in Three-Dimensional Image Technologies, H. Kusaka, Editor, Proceedings of ITEC'91, ITE Annual Convention, pp. 603-606, Institute of Television Engineering of Japan, Tokyo, Japan, July 1991.
18. ① P. J. Bos (1991) "Performance limits of stereoscopic viewing systems using active and passive glasses," IEEE Virtual Reality Annual International Symposium, 371-376 (1993). (NB: same as P. J. Bos, "Time sequential stereoscopic displays: The contribution of phosphor persistence to the "ghost" image intensity," Proc. ITEC'91 Annual Conf., Three-Dimensional Image Tech., (H. Kusaka, ed.), 603-606.
19. ⑦ C. Bungert (2005) "Shutterglasses Comparison Chart" Online: <http://stereo3d.com/shutter.htm> Dated: 1 April 2005. Accessed: 29 March 2011.
20. ⑤ Casio (undated) "Casio Corporate History - Chronology of Products" Online: http://www.casio-europe.com/euro/corporate/chronologyofproducts/detail/1983_3/ Accessed: 11 August 2013.
21. ⑦ Consumer Electronics Association (CEA) (2011) "R4WG16: Active Eyewear Standards IR Sync Request for Proposal (RFP)"
22. ⑧ Consumer Electronics Association (CEA) (2013) It Is Innovation (i3), 1(3), May 2013. Arlington, Virginia. Available at <http://www.ce.org/i3>
23. ① J. Chang, H. J. Kim, J. W. Choi, and K. Y. Yu (2008) "Ghosting reduction method for color anaglyphs," in Stereoscopic Displays and Applications XIX, Proceedings of SPIE-IS&T Electronic Imaging, 6803, 68031G.1-68031G.10.
24. ⑤①⑥ Y.-C. Chang, C.-Y. Chiang, K.-T. Chen, Y.-P. Huang (2009) "Investigation of Dynamic Crosstalk for 3D Display" in 2009 International Display Manufacturing Conference, 3D Systems and Applications, and Asia Display (IDMC/3DSA/Asia Display 2009), Taipei, Taiwan.
25. ① L. Chen, Y. Tu, W. Liu, Q. F. Li, K. Teunissen, and I. Heynderickx (2008) "Investigation of Crosstalk in a 2-View 3D Display," SID 08 Digest, 1138-1141.

26. ⑤ F.-H. Chen, J.-C. Yang, Y.-H. Chou, K.-C. Huang, K. Lee (2012) "Gray-to-gray crosstalk model" 3DSA (Three Dimensional Systems and Applications) Conference, pp. 213–216.
27. ① F.-H. Chen, J.-C. Yang, Y.-H. Chou, K.-C. Huang, and K. Lee (2012) "Gray-to-Gray Crosstalk Model," 3DSA (Three-Dimensional Systems and Applications) conference, 213-216.
28. ⑬ Chien, K.-W. and Shieh, H.-P. D., "3D Mobile Display Based on Sequentially Switching Backlight with Focusing Foil" in SID 2004 Digest, 1434-1437 (2004).
29. ⑭ C. Chinnock (2009) "Philips Decides to Shut Down 3D Operation," Display Daily [online] at <http://displaydaily.com/2009/03/27/>
30. ⑤⑥ K.-D. Cho (2004) "New Address and Sustain Waveforms for AC Plasma Display Panel", PhD Thesis, Kyungpook National University.
31. ⑮⑯ Y.-M. Chu, K.-W. Chien, H.-P. D. Shieh, J.-M. Chang, A. Hu, V. Yang (2005) "3D Mobile Display Based on Dual Directional Lightguides" in 4th International Display Manufacturing Conference, Taipei, Taiwan, 799-801.
32. ①②⑧ CIE (1932) "Commission Internationale de l'Eclairage Proceedings" Cambridge University Press.
33. ⑩ C. Connolly (2003) "Colorimetry: Anatomical Studies Advance", Photonics Spectra, Issue Aug 2003, pp 56-66.
34. ⑬ D. Cook (2004) "Stereoscopic Gaming: Technology and Applications", Keynote Presentation at Stereoscopic Displays and Applications XV conference, 19-21 January 2004, San Jose, California. (Presentation only).
35. ① M. Cowan, J. Greer, and L. Lipton (2011) "Ghost-compensation for improved stereoscopic projection," US Patent Application Publication 2011/0025832 A1.
36. ⑤ L. Cui, Y. Li, J. Wang, E. Tian, X. Zhang, Y. Zhang, Y. Song, Lei Jianga (2009) "Fabrication of large-area patterned photonic crystals by ink-jet printing" Journal of Material Chemistry, Vol. 19, pp. 5499-5502.
37. ③ Daleh (undated) "Build your own 3D glasses" [online]. URL: http://www.daleh.id.au/3d_glasses.html Accessed: 26 August 2011.
38. ⑮ DataColor AG, <http://spyder.datacolor.com/product-mc-s3elite.php>
39. ⑱ J. Dennis (2011) National Stereoscopic Association, personal communication, 1 September 2011.
40. ①③④ E. Dubois (2001) "A projection method to generate anaglyph stereo images," IEEE Intl. Conf. Acoustics, Speech, and Signal Processing, Proc. (ICASSP '01), 3, 1661–1664.

41. ④ L. D. duHauron (1891) "Estampes, photographies et tableaux stéréoscopiques, produisant l'air effect en plein jour, sans l'aide du stereoscope" French Patent No. 216465 (1891) in S. A. Benton (editor) "Selected Papers on Three-Dimensional Displays" SPIE Milestone Series, MS162 (2001)
42. ④ L. D. duHauron (1895) "Stereoscopic print" U.S. Patent No. 544666.
43. ④ K. Ealasubramonian, R. P. Rajappan (1983) "Compatible 3-D television: the state of the art" in Proc. SPIE Three-Dimensional Imaging, ed. J.P. Ebbeni, A. Monfils, 0402, 100-106.
44. ④ C. W. Earp (1941) "Carrier wave transmission system," U.S. Patent No. 2256317.
45. ① J. B. Eichenlaub (1990) "An autostereoscopic display for use with a personal computer," in Stereoscopic Displays and Applications, Proceedings of SPIE-IS&T Electronic Imaging, 1256, 156-163.
46. ④ Encyclopædia Britannica (2012) "Louis Ducos du Hauron" Encyclopædia Britannica, Encyclopædia Britannica Online, Encyclopædia Britannica Inc. Accessed: 22 Jul 2012 URL: <<http://www.britannica.com/EBchecked/topic/172961/Louis-Ducos-du-Hauron>>
47. ① S. M. Faris (1991) "Micro-Polarizer Arrays Applied to a New Class of Stereoscopic Imaging," SID 91 Digest, 840-843.
48. ①①④ S. M. Faris (1994) "Novel 3-D stereoscopic imaging technology" in Stereoscopic Displays and Virtual Reality Systems, Proceedings of SPIE vol. 2177, San Jose, California, February 1994.
49. ⑧ M. Fihn (2013) Veritas et Visus, personal communication, 28 May 2013.
50. ① S. S. Fisher, M. McGreevy, J. Humphries, and W. Robinett (1986) "Virtual Environment Display System," Proceedings of the Workshop on Interactive 3D Graphics, 1-11.
51. ④ B. Fraser, C. Murphy, and F. Bunting, "Real world color management," Peachpit press (2004).
52. ④ J. E. Gaudreau, "Stereoscopic displaying method and device" US Patent 5629798 (1997).
53. ④ J. E. Gaudreau, et al., "Innovative stereoscopic display using variable polarized angle" Stereoscopic Displays and Virtual Reality Systems XIII, Proc. SPIE 6055, 605518 (2006).
54. ① J. Goodman (2003) "Development of the 960p stereoscopic video format" in Stereoscopic Displays and Virtual Reality Systems X, Proceedings of SPIE-IS&T Electronic Imaging, 5006, 187-194.
55. ④ Google Inc. (2013) "Google Scholar (citations for: Andrew J. Woods)" [online] URL: <http://scholar.google.com.au/citations?user=J-9YiCkAAAAJ> Dated: 13 October 2013, Accessed: 13 October 2013.

56. ⑱ Google Inc. (2013) "Google Trends" [online] URL: www.google.com/trends Dated: 30 May 2013, Accessed: 30 May 2013
57. ⑲ A. M. Gorski (1992) "User evaluation of a stereoscopic display for space training applications" Proc. SPIE Stereoscopic Displays and Applications III, 1669, 236-243.
58. ⑳ T. Gunnarsson (2012) "Global 3-D Market Flourishes Across Cinema, Home Video and TV VoD Platforms" Press Release, IHS/iSuppli, 20 December 2012. URL: <http://www.isuppli.com/media-research/news/pages/global-3-d-market-flourishes-across-cinema-home-video-and-tv-vod-platforms.aspx> Accessed 18 May 2013.
59. ㉑ K. Hamada, T. Yamamoto, T. Kurita, Y. Takano, I. Yuyama (1998) "A field-sequential stereoscopic display system with 42-in. HDTV DC-PDP" Proc. Intl. Display Workshop IDW'98, pp. 555–558, IDW, Japan.
60. ㉒ K. Hamada, T. Kurita, M. Kanazawa, K. Yamamoto (2001) "A 3D Hi-Vision Display with 50-in. AC PDP" Asia Display/Intl. Display Workshop IDW'01, pp. 785–788, IDW, Japan.
61. ㉓ L. Hammond (1924) "Stereoscopic Motion Picture Device" U.S. Patent No. 1,506,524, 26 August 1924.
62. ㉔ M. Hanlon (2003) "LCD sales surpass CRT sales for first time" GizMag, online: <http://www.gizmag.com/go/2427/> dated: 15 December 2003, Accessed: 6 August 2013.
63. ④ S. J. Harrington, R. P. Loce, G. Sharma "Systems for spectral multiplexing of source images to provide a composite image, for rendering the composite image, and for spectral demultiplexing of the composite image to animate recovered source images" U.S. Patent US 7,136,522 B2 (Filed 2002, Issued 2006)
64. ㉕ S. J. Harrington, R. P. Loce, and G. Sharma (2006) "Systems for spectral multiplexing of source images to provide a composite image, for rendering the composite image, and for spectral demultiplexing of the composite image to animate recovered source images" U.S. Patent No. 7,136,522 B2.
65. ㉖㉗㉘㉙ T. J. Haven (1987) "A liquid-crystal video stereoscope with high extinction ratios, a 28% transmission state, and 100 μs switching" True Three-Dimensional Imaging Techniques & Display Technologies, D.F. McAllister, WE. Robbins, Editors, Proceedings of SPIE vol. 761, pp. 23-26, Bellingham Washington USA, 1987.
66. ㉚ HCinema (undated) "HCinema (projector database)" [online] Available: <http://www.projektoren-datenbank.de/pro> [accessed 21st Dec 2003]
67. ⑲ S. P. Hines (1984) "Three-Dimensional Cinematography" Proc. SPIE Optics in Entertainment II, ed. C.S. Outwater, 0462, 41-47 (1984).
68. ⑲ L. F. Hodges (1991) "Basic principles of stereographic software development" in Proc. SPIE Stereoscopic Displays and Applications II, 1457, 9-17 (1991).

69. ⑩ M. Hollins (1990) "Medical Physics" Thomas Nelson & Sons, London, pp26-27.
70. ①⑮⑯ H.-K. Hong, J.-W. Jang, D.-G. Lee, M.-J. Lim, and H.-H. Shin (2010) "Analysis of angular dependence of 3-D technology using polarized eyeglasses" *Journal of the SID*, 18(1), 8-12.
71. ⑤ L. J. Hornbeck (1995) "Digital Light Processing and MEMS: Timely Convergence for a Bright Future" (Invited Plenary Paper), *Proceedings SPIE*, Vol. 2639, Micromachining and Microfabrication Process Technology.
72. ⑤①⑫⑬ L. J. Hornbeck (1998) "Current Status and Future Applications for DMD-Based Projection Displays" *Proceedings of the Fifth International Display Workshop IDW '98*, Kobe, Japan.
73. ⑤①⑮⑯ K.-C. Huang, C.-H. Tsai, K.-J. Lee, W.-J. Hsueh (2000) "Measurement of Contrast Ratios for 3D Display" in *Input/Output and Imaging Technologies II*, *Proc. SPIE* 4080, pp. 78–86.
74. ⑤①⑯ K.-C. Huang et al. (2003) "A study of how crosstalk affects stereopsis in stereoscopic displays" *Stereoscopic Displays and Virtual Reality Systems X*, *Proc. SPIE* 5006, 247–253.
75. ⑮⑯ K.-C. Huang, K. Lee, H.-Y. Lin (2009) "Crosstalk issue in stereo/autostereoscopic display" in *Proc. Int. Display Manufacturing Conference*, 2–18.
76. ⑤ K.-C. Huang, F.-H. Chen, L.-C. Lin, H.-Y. Lin, Y.-H. Chou, C.-C. Liao, Y.-H. Chen, K. Lee (2013) "A crosstalk model and its application to stereoscopic and autostereoscopic displays" *Journal of the Society for Information Display*, 21(6), pp. 249-262.
77. ⑤⑥⑦ H.-C. Hung, C.-W. Shih (2005) "Improvement in Moving Picture Quality Using Scanning Backlight System" *Proceedings of the International Display Manufacturing Conference (IDMC'05)*, Taipei, Taiwan.
78. ⑤① M. Husak, J. D. Lawrence, R. Mueller, C. Ward (2011) "System and method for synchronizing a 3D video projector" U.S. Patent No. 8066377.
79. ⑤ D. C. Hutchison (2007) "Introducing DLP 3-D TV" Texas Instruments white paper. [http://dlp.com/downloads/Introducing DLP 3-D HDTV Whitepaper.pdf](http://dlp.com/downloads/Introducing_DLP_3-D_HDTV_Whitepaper.pdf)
80. ⑤ International Committee for Display Metrology (2012) "Information display measurements standard (version 1.03)" Society for Information Display. [online] <http://icdm-sid.org/>
81. ③④ I. Ideses, L. Yaroslavsky (2005) "Three methods that improve the visual quality of colour anaglyphs" *Journal of Optics A: Pure and Applied Optics*, 7(12), p.755-762.
82. ⑤ IEC (2009) "TC110/220/NP - New Work Proposal - 3D Displays - Terminology and letter symbols" International Electrotechnical Commission, dated: 2009-12-18.
83. ⑱ Institute of Electrical and Electronics Engineers (IEEE) (2013) "IEEE Spectrum" 50(5) (INT), May 2013, New York. Available at <http://spectrum.ieee.org/>

84. ©⁹ Integrated Photomatrix Limited (undated) "IPL 10530 Integrated Photodiode Amplifiers, Product Data Sheet" Integrated Photomatrix Limited, Dorchester, United Kingdom.
85. ① ISO (2012) "Ergonomics of human-system interaction – Part 331: Optical characteristics of autostereoscopic displays" Technical Report ISO/TR 9241-331.
86. © International Stereoscopic Union (undated) "A Glossary of Stereoscopic Terms" [online] <http://www.stereoscopy.com/isu/glossary-index.html> Accessed: 20 October 2013.
87. ©¹ W. W. Jacques (1885) "Underground wires" *Science* 6(126), pp. 6–7.
88. ①¹⁶ A. Jain, and J. Konrad (2007) "Crosstalk in automultiscopic 3-D displays: Blessing in disguise?" in *Stereoscopic Displays and Virtual Reality Systems XIV, Proceedings of SPIE-IS&T Electronic Imaging*, 6490, 649012.1-649012.12.
89. ① T. Järvenpää, M. Salmimaa (2007) "Optical Characterization Methods for Autostereoscopic 3D Displays" *Proc. of EuroDisplay*, 132-135.
90. ① T. Järvenpää, M. Salmimaa, T. Levola (2010) "Qualified Viewing Spaces for Near-to-Eye and Autostereoscopic Displays" *SID 10 Digest*, 335-338.
91. ©¹ ¹⁴ H. Jorke, M. Fritz (2006) "Stereo projection using interference filters" *Proc. SPIE 6055, Stereoscopic Displays and Virtual Reality Systems XIII*, 60550G (January 27, 2006); doi:10.1117/12.650348
92. © B. Julesz (1983) "Texton Theory of Two-Dimensional and Three-Dimensional Vision" *Processing and Display of Three-Dimensional Data, Proc. SPIE 367*, pp. 2 (April 8, 1983); DOI: <http://dx.doi.org/10.1117/12.934294>
93. ©¹ ¹⁵ ¹⁶ S.-M. Jung, Y.-B. Lee, H.-J. Park, S.-C. Lee, W.-N. Jeong, J.-K. Shin, I.-J. Chung (2010) "Improvement of 3-D crosstalk with over-driving method for the active retarder 3-D displays" *Society for Information Display Symposium Digest Technical Papers*, 41(1), pp. 1264–1267.
94. © Kaptein, R. and Heynderickx, I., "Effect of Crosstalk in Multi-View Autostereoscopic 3D Displays on Perceived Image Quality" in *SID '07 Digest*, 1220-1223 (2007).
95. ©² K. S. Karvinen, A. J. Woods (2007) "The Compatibility of Plasma Displays with Stereoscopic Visualisation" *CMST Technical Report CMST2007-04*, Curtin University of Technology, Perth Australia, February 2007.
96. ©⁸ C. Kennedy (1936) "The Development and Use of Stereo Photography for Educational Purposes" Vol. 26, pp. 3-17, January 1936.
97. ① T. Kim, J. M. Ra, J. H. Lee, S. H. Moon, and K.-Y. Choi (2011) "3D Crosstalk Compensation to Enhance 3D Image Quality of Plasma Display Panel" *IEEE Transactions on Consumer Electronics*, 57(4), 1471-1477.
98. ① S. Klimenko, P. Frolov, L. Nikitina, and I. Nikitin (2003) "Crosstalk reduction in passive stereo-projection systems" *Proc. of Eurographics'03*, 235–240.

99. ①⑩ J. Konrad, B. Lacotte, and E. Dubois (2000) "Cancellation of image crosstalk in time-sequential displays of stereoscopic video" *IEEE Transactions on Image Processing*, 9(5), 897-908.
100. ① J. Konrad, and M. Halle (2007) "3-D Displays and Signal Processing: An Answer to 3-D Ills?" *IEEE Signal Processing Magazine*, 24, 97-111.
101. ⑤①③④ F. L. Kooi, A. Toet (2004) "Visual comfort of binocular and 3D displays" *Displays* 25(2-3), 99-108.
102. ⑮ N. Koren (undated) "Making Fine Prints" [online]
<http://www.normankoren.com/makingfineprints1A.html>
103. ⑤ M. Kozuka (2012) "Panasonic's Stereoscopic 3D Technologies, Standardization and Business Strategy" Keynote Presentation, Stereoscopic Displays and Applications XXIII, Burlingame, California, January 2012. (Presentation only) Video:
http://www.youtube.com/watch?v=7oy_IvTBLC4 Accessed 18 May 2013.
104. ⑱ E. Kurland (2013) 3-DIY, personal communication, 28 May 2013.
105. ⑤④ R. Labbe, D. E. Klutho (2009) "Publishing Stereoscopic Images" in *Stereoscopic Displays and Applications XX*, Proc. SPIE 7237, pp. 72370J-1 to 72370J-5
106. ⑤⑱ B. Lane (1982) "Stereoscopic displays" in *Proc. SPIE Processing and Display of Three-Dimensional Data*, ed. J.J. Pearson, 0367, 20-32.
107. ① S. J. Lee, M. J. Kim, K. H. Lee, and K. H. Park (2009) "Review of Wire Grid Polarizer and Retarder for Stereoscopic Display," in *Stereoscopic Displays and Applications XX*, Proceedings of SPIE-IS&T Electronic Imaging, 7237, 72370P.1-72370P.10.
108. ① Y. H. Lee, and Y. B. Jung, (2010) "Stereoscopic image projecting system using circularly polarized filter module," US Patent Application Publication No. US 2010/0079728 A1.
109. ① J. Lee, J. Lee, S. Kim, J. Han, T. Jun, and S. Shin (2010) "Optical Performance Analysis Method of Auto-stereoscopic 3D Displays," *SID 10 Digest*, 327-330.
110. ⑤ B. Lee (2013) "Three-dimensional displays, past and present" *Physics Today*, 44(6), pp. 36, April 2013. DOI: <http://dx.doi.org/10.1063/PT.3.1947>
111. ⑱ J. Levine, IEEE, personal communication, 23 September 2011.
112. ① B. Li, and J. Caviedes (2012) "Evaluating the Impact of Crosstalk on Shutter-type Stereoscopic 3D Displays," *Sixth International Workshop on Video Processing and Quality Metrics*, 1-6.
113. ⑤①⑦⑮⑱ J.-C. Liou, K. Lee, F.-G. Tseng, J.-F. Huang, W.-T. Yen, W.-L. Hsu (2009) "Shutter glasses stereo LCD with a dynamic backlight" *Stereoscopic Displays and Applications XX*, Proc. SPIE 7237, 72370X.

114. [Ⓔ][Ⓘ][Ⓙ] J. S. Lipscomb, W. L. Wooten (1994) "Reducing Crosstalk between Stereoscopic Views", in *Stereoscopic Displays & Virtual Reality System*, S. S. Fisher, J. O. Merritt, M. T. Bolas, Editors, Proceedings of SPIE vol.2177, pp. 92-96, Bellingham Washington USA.
115. [Ⓔ][Ⓘ] L. Lipton (1978) "Foundations of the Stereoscopic Cinema – A Study in Depth" Van Nostrand Reinhold Company, New York.
116. [Ⓔ][Ⓘ][Ⓚ] L. Lipton (1987) "Factors affecting 'ghosting' in time-multiplexed planostereoscopic CRT display systems," in *True 3D Imaging Techniques and Display Technologies*, Proc. SPIE 761, pp. 75–78.
117. [Ⓘ] L. Lipton, A. Berman, L. D. Meyer, and J. L. Fergason (1988) "Method and system employing a push-pull liquid crystal modulator," U.S. Pat. No. 4,792,850.
118. [Ⓔ] L. Lipton (1989) "Compatibility of Stereoscopic Video Systems with Broadcast Television Standards" *Three-Dimensional Visualization and Display Technologies*, Proc. SPIE 1083, pp. 95.
119. [Ⓚ] L. Lipton (1991) "Selection devices for field-sequential stereoscopic displays: a brief history" Proc. SPIE *Stereoscopic Displays and Applications II*, 1457, 274-282 (1991).
120. [Ⓔ][Ⓙ] L. Lipton (1992) "High Dynamic Range Electro-Optical Shutter for Stereoscopic and other Applications", United States Patent #5 1 17 302, May 1992.
121. [Ⓘ] L. Lipton (1992) "The Future of autostereoscopic electronic displays," in *Stereoscopic Displays and Applications III*, Proceedings of SPIE-IS&T Electronic Imaging, 1669, 156-162.
122. [Ⓔ][Ⓙ] L. Lipton, J. Halnon, J. Wuopio, B. Dorworth (2000) "Eliminating it-cell artefacts", in *Stereoscopic Displays & Virtual Reality Systems VII*, JO. Merritt, S.A. Benton. A.J. Woods, MT. Bolas, Editors, Proceedings of SPIE vol.3957, pp. 264-270, Bellingham Washington USA.
123. [Ⓙ] L. Lipton, "The Stereoscopic Cinema: From Film to Digital Projection", in *SMPTE Journal*, pp. 586-593, Sept 2001.
124. [Ⓘ][Ⓚ][Ⓛ][Ⓜ][Ⓝ][Ⓘ] L. Lipton (2009) "Glossary," Lenny Lipton's Blog, online, dated 16 March 2009, accessed 19 March 2010. <http://lennylipton.wordpress.com/2009/03/16/glossary/>
125. [Ⓔ] L. Lipton (2011) "The Stereoscopic Cinema: From Film to Digital Projection", in *SMPTE Journal*, pp. 586-593, Sept 2001.
126. [Ⓘ] L. Lipton (2011) Leonardo IP, personal communication, 8 Nov 2011.
127. [Ⓔ][Ⓘ] L. Lipton (2012) "Brief history of electronic stereoscopic displays" *Optical Engineering* 51(2), 021103, February 2012.
128. [Ⓚ] D. Lovy (1996) "WINDIG 2.5" [software], Dept of Physical Chemistry, University of Geneva, Switzerland.

129. ⑤ J. M. Lytle (2008) "Pioneer pulls plasma plug, Sony cans CRTs" TechRadar, online: <http://www.techradar.com/au/news/television/pioneer-pulls-plasma-plug-sony-cans-crts-256211> dated: March 4th 2008, accessed: 12 August 2013.
130. ① C.-Y. Ma, Y.-C. Chang, Y.-P. Huang, and C.-H. Tsao (2011) "A Simulation Platform and Crosstalk Analysis for Patterned Retarder 3D Display," *SID 11 Digest*, 808-811.
131. ⑩ S. G. G. MacDonald, D. M. Burns (1975) "Physics for the Life and Health Sciences" Addison Wesley, USA.
132. ⑤ M. Macedonia (2006) "It's the end of the tube as we know it" *IEEE Computer*, June 2006, Vol.39(6), pp.83-85.
133. ① A. Marraud, and M. Bonne (1983) "Restitution of a Stereoscopic Picture by Means of a Lenticular Sheet," in *Three-Dimensional Imaging, Proceedings of SPIE-IS&T Electronic Imaging*, 402, 129-132.
134. ①③④ D. F. McAllister, Y. Zhou, and S. Sullivan (2010) "Methods for computing color anaglyphs," in *Stereoscopic Displays and Applications XXI, Proceedings of SPIE-IS&T Electronic Imaging*, 7524, 75240S.1–75240S.12.
135. ③④ J. H. McDonald (2009) "Handbook of biological statistics (2nd ed.)" Sparky House Publishing, Baltimore, Maryland, pp. 221-223 (2009).
<http://udel.edu/~mcdonald/statspearman.html>
136. ⑤⑫⑬ I. McDowall, M. Bolas, D. Corr, T. Schmidt (2001) "Single and Multiple Viewer Stereo with DLP Projectors" *Stereoscopic Displays and Virtual Reality Systems VIII, Proc. SPIE Vol. 4297*, pg 418-425, San Jose, California.
137. ① D. J. McKnight (2010) "Enhanced ghost compensation for stereoscopic imagery," US Patent Application Publication US 2010/0040280 A1.
138. ⑤ B. Mendiburu (2010) "3D Movie Making: Stereoscopic Digital Cinema from Script to Screen" Focal Press.
139. ⑤ L. Meyer (1992) "Monitor selection criteria for stereoscopic displays" *Proc. SPIE Stereoscopic Displays and Applications III*, 1669, 211-214.
140. ③ S. Miles (2009) "How to make your own 3D glasses" Pocket-lint [online] URL: <http://www.pocket-lint.com/news/27268/how-to-make-3d-glasses> Dated: 22 September 2009. Accessed: 6 July 2011.
141. ① A. Millin, P. Harman (2001) "Three-dimensions via the Internet," in *Stereoscopic Displays and Virtual Reality Systems VIII, Proceedings of SPIE-IS&T Electronic Imaging*, 4297, 328-333.
142. ⑬ D. J. Montgomery, G. J. Woodgate, A. Jacobs, J. Harrold, D. Ezra (2001) "Analysis of the performance of a flat panel display system convertible between 2D and autostereoscopic 3D modes" in *Proc. SPIE Stereoscopic Displays and Virtual Reality Systems VIII*, 4297, 148-159.

143. ⑩ H. Morishama, H. Nose, N. Taniguchi, K. Inoguchi, S. Matsumura, (1998) "An Eyeglass-Free Rear-Cross-Lenticular 3-D Display" in SID Digest 1998, 923-926.
144. ⑩ J. Morreale (2011) SID, personal communication, 1 September 2011.
145. ⑤ National Aeronautics and Space Administration (NASA) (2012) "Build your own 3d glasses" [online] <http://stereo.gsfc.nasa.gov/classroom/glasses.shtml> Dated: 5 December 2012. Accessed: 27 October 2013.
146. ⑩ National Stereoscopic Association (NSA) (2013) "Stereo World" 38(6), May/June 2013, Portland, Oregon. Available at <http://www.stereoworld.org/>
147. ⑤① Y. Nojiri, H. Yamanoue, A. Kanazato, M. Emoto, and F. Okano (2004) "Visual comfort / discomfort and visual fatigue caused by stereoscopic HDTV viewing," in Stereoscopic Displays and Virtual Reality Systems XI, Proceedings of SPIE-IS&T Electronic Imaging, 5291, 303-313.
148. ⑤④ J. A. Norling (1937) "Anaglyph Stereoscropy," U.S. Patent No. 2,135,197.
149. ⑩ Y. Ohno (1999) "OSA Handbook of Optics, Volume III: Visual Optics and Vision" National Institute of Standards and Technology, Maryland USA.
150. ① Optical Filters (undated) "XP42 Linear Polarizer Filters datasheet" Optical Filters UK. <http://www.opticalfilters.co.uk>
151. ① J. Osterman, T. Scheffer (2011) "Contrast-Enhanced High-Speed Polarization Modulator for Active-Retarder 3D Displays," SID 11 DIGEST, 93-96.
152. ⑤①⑩⑫ S. Pala, R. Stevens, and P. Surman (2007) "Optical crosstalk and visual comfort of a stereoscopic display used in a real-time application," in Stereoscopic Displays and Virtual Reality Systems XIV, Proc. SPIE 6490, 649011.
⑤①⑤⑦ H. Pan, X.-F. Feng, S. Daly (2005) "LCD motion blur modeling and analysis" IEEE Int'l. Conf. Image Processing, Vol. 2, pp. 21-24.
153. ⑤①⑩⑫ C.-C. Pan, Y.-R. Lee, K.-F. Huang, T.-C. Huang (2010) "Cross-talk evaluation of shutter-type stereoscopic 3D display" Society for Information Display Symposium Digest Technical Papers, 41(1), pp. 128-131.
154. ① S.-M. Park, H.-S. Lee, J.-H. Jeong, S. Shestak, and D.-S. Kim (2010) "Method and Apparatus for Displaying Stereoscopic Image," United States Patent Application Publication 2010/0066820 A1, publication date 18 March 2010.
155. ⑤① S. Pastoor (1995) "Human factors of 3D images: Results of recent research at Heinrich-Hertz-Institut Berlin," in Proc. IDW'95, Vol. 3D-7, pp. 69-72, IDW, Japan.
156. ① R. Patterson (2007) "Human factors of 3-D displays," Journal of the SID, 15(11), 861-871.
157. ③ R. Patterson, et al (2007) "Binocular rivalry and head-worn displays," Human Factors 49(6), 1083-1096.
158. ③ R. Patterson (2009) "Review Paper: Human factors of stereo displays: An update," J. Soc. Info. Display, 17(12), 987-996.

159. ⑰ Petrus (2011) "Universal sutterglasses controller" (sic) in MTBS3D Forums. Online: <http://www.mtbs3d.com/phpBB/viewtopic.php?p=55149#p55149> Dated: 10 Jan 2011. Accessed: 29 March 2011.
160. ⑤ Projector Central (undated) "Viewsonic PJD5111" Online: <http://www.projectorcentral.com/ViewSonic-PJD5111.htm> Accessed: 11 August 2013.
161. ⑤ Projector Central (2013) "InFocus DepthQ Projector" URL: <http://www.projectorcentral.com/InFocus-DepthQ.htm> , dated: 18 June 2013, accessed: 18 June 2013.
162. ⑤ Projector Central (undated) "Lightspeed DepthQ Projector" Online: <http://www.projectorcentral.com/Lightspeed-DepthQ.htm> Accessed: 11 August 2013.
163. ② C. Pulfrich (1922) "Die Stereoskopie im Dienste der isochromem und herterochromen Photometrie," *Naturwissenschaft* 10, 553–564.
164. ③④ M. A. Purnell (2003) "Casting, replication, and anaglyph stereo imaging of microscopic detail in fossils, with examples from conodonts and other jawless vertebrates," *Palaeontologia Electron.* 6(2), 1–11, (see Appendix 1).
165. ④ M. Ramstad (2009) "High-Fidelity Printed Anaglyphs and Viewing Filters," United States Patent Application Publication, No.: US 2009/0278919 A1, Pub. Date: 12 Nov 2009.
166. ⑤① M. J. Richards, G. D. Gomes (2011) "Spectral Separation Filters for 3D Stereoscopic D-Cinema Presentation," United States Patent US 7,959,295 B2.
167. ⑤① J. A. Roese (1975) "PLZT Stereoscopic Television System," US Patent No. 3903358, Filing date: 22 May 1974, Issue date: 2 September 1975
168. ① J. A. Roese, A. S. Khalafalla (1976) "Stereoscopic viewing with PLZT ceramics," *Ferroelectrics*, 10(1), 47-51.
169. ⑫⑬ T. Rourke, A. J. Woods (2006) "Compatibility of Consumer DLP Projectors with Time-Sequential Stereoscopic Visualisation", Technical Report CMST 2006-17, Curtin University of Technology.
170. ④ J. R. Rupkalvis (2012) personal communication, July 2012.
171. ⑨ A. Ryer (1997) "International Light Handbook" pp. 11, International Light Corporation, Newburyport, Massachusetts, USA. [online]: <http://www.intl-light.com/lhandbook>
172. ⑥ Samsung (2008) "SAMSUNG Debuts The First 3D Ready Flat-Panel HDTV With Its 2008 Entry-Level Plasma HDTV Line-Up" Press Release 7 January 2008, Retrieved on 9 January 2008 from http://www.samsung.com/us/news/newsRead.do?news_seq=6449&page=1

173. ①③④⑩ W. R. Sanders, D. F. McAllister (2003) "Producing anaglyphs from synthetic images" in *Stereoscopic Displays and Virtual Reality Systems X, Proceedings of SPIE-IS&T Electronic Imaging*, 5006, 348–358.
174. ①③④ H. Sanftmann, D. Weiskopf (2011) "Anaglyph stereo without ghosting" *Computer Graphics Forum*, 30(4), 1251–1259.
175. ④ J. Scarpetti, "Stereoscopic Photographic Print, Method of Making, and Apparatus for Viewing" United States Patent, Filed: 11 Sept 1972, Issued: 28 June 1974.
176. ⑤① P. J. H. Seuntiëns, L. M. J. Meesters, and W. A. Ijsselsteijn (2005) "Perceptual attributes of crosstalk in 3D images," *Displays* 26(4–5), 177–183.
177. ⑤④ G. Sharma, R. P. Loce, S. J. Harrington, Y. Zhang (2003) "Illuminant multiplexed imaging: special effects using GCR," in *Proc. 11th Color Imaging Conference: Color Science and Engineering Systems, Technologies, and Applications*, pp. 266–271, IS&T (Society for Imaging Science & Technology), Springfield, Virginia.
178. ⑩ K. Sheehan (2013) SPIE, personal communication, 29 May 2013.
179. ① S. Shestak, D.-S. Kim (2007) "Application of Pi-cells in Time-Multiplexed Stereoscopic and Autostereoscopic Displays, Based on LCD Panels," in *Stereoscopic Displays and Virtual Reality Systems XIV, Proceedings of SPIE-IS&T Electronic Imaging*, 6490, 64900Q.1-64900Q.9.
180. ⑤①⑩⑬⑯ S. Shestak, D.-S. Kim, S.-D. Hwang (2010) "Measuring of gray-to-gray crosstalk in a LCD based time-sequential stereoscopic displays," *Society for Information Display Symposium Digest Technical Papers* 41(1), 132–135.
181. ① S. Shestak, D. Kim, and Y. Kim (2012) "How much crosstalk can be allowed in a stereoscopic system at various grey levels?" in *Stereoscopic Displays and Applications XXIII, Proceedings of SPIE-IS&T Electronic Imaging*, 8288, 828810.1-828810.10.
182. ①④ International Committee for Display Metrology (ICDM) (2012) "Information Display Measurements Standard (version 1.03)" Society for Information Display (SID). URL: <http://icdm-sid.org/>
183. ⑩ Society for Information Display (SID) (2013) "Information Display" 9(3), May/June 2013. Campbell, California. Available at <http://informationdisplay.org/>
184. ⑤① G. A. Slavenburg, T. F. Fox, and D. R. Cook (2007) "System, method, and computer program product for increasing an LCD display vertical blanking interval," United States Patent Application Publication 20070229487 A1, publication date 4 October 2007.
185. ① G. A. Slavenburg, T. F. Fox, and D. R. Cook (2011) "System, Method, and Computer Program Product for Compensating for Crosstalk During the Display of Stereo Content," US Patent 8085217 B2.

186. ⑤⑦⑫ A. A. S. Sluyterman, E. P. Boonekamp (2005) "Architectural Choices in a Scanning Backlight for Large LCD TVs" SID 05 Digest, pg 996-998.
187. ⑤ SMPTE (2009) "Report of SMPTE Taskforce on 3D to the Home" Society of Motion Picture and Television Engineers (SMPTE), New York.
188. ⑫ SPIE (2013) "SPIE Professional" 8(2), April 2013, Bellingham, Washington.
189. ⑤⑫ R. Spottiswoode, N. L. Spottiswoode, C. Smith (1952) "Basic Principles of the Three Dimensional Film" Journal of the SMPTE, Vol. 59, pp. 249-286, October 1952.
190. ③④ S. S. Stevens (1957) "On the psychophysical law" Psychological Review, 64(3), pp. 153-181.
191. ①⑫ R. F. Stevens (2004) "Cross-talk in 3D displays" Report CETM 56, National Physical Laboratory, UK.
192. ①⑫ H. Stevenson, M. Khazova (2004) "Patterned Grating Alignment of Reactive Mesogens for Phase Retarders," Proceedings of the 24th International Display Research Conference (IDRC) with the 4th International Meeting on Information Display (IMID), 1-4.
193. ①③④ A. Stockman, L. T. Sharpe (2007) "Luminous energy function (2 degree, linear energy)" [online]. URL: <http://www.cvrl.org/cvrlfunctions.htm> and <http://www.cvrl.org/database/text/lum/CIE2008v2.htm> Accessed: 29 July 2011.
194. ①③④ A. Stockman, H. Jägle, M. Pirzer, L. T. Sharpe (2008) "The dependence of luminous efficiency on chromatic adaptation," J. Vision, 8(16):1, 1–26. <http://journalofvision.org/8/16/1/>
195. ⑫ W. Strunk, E. B. White, The Elements of Style. 4th ed. Boston, Massachusetts: Allyn & Bacon; 2000. ISBN: 0-205-30902-X
196. ⑤⑫ D. L. Symmes (2006) "The Chopper" {Online} [ARCHIVED] <http://web.archive.org/web/20110707063258/http://www.3dmovingpictures.com/chopper.html> Dated: 14 November 2006, Accessed: 4 August 2013.
197. ⑤ T. Takahashi (2010) "A Review of Electronic Paper Display Technologies from the Standpoint of SID Symposium Digests" FDP 2010 Symposium Digest, (2010)
198. ⑨⑩ S. S. L. Tan (2001) "Sources of Crosstalk in Stereoscopic 3D Displays" Centre for Marine Science & Technology, Curtin University of Technology, Perth, Australia, 2001.
199. ① W. Tan, S. Z. Zhou, S. C. Read (2011) "Methods and Systems for Reducing or Eliminating Perceived Ghosting in Displayed Stereoscopic Images" US Patent Application Publication 2001/0080401 A1.
200. ④ L. A. Taplin (2001) "Spectral Modeling of a Six-Color Inkjet Printer" Master of Science Thesis, Rochester Institute of Technology.

201. ⑤① K. Teunissen, A. Sevo, A. van Dalen, H. van Parys (2011) "Perceptually Relevant Characterization of Stereoscopic Displays" Society for Information Display Symposium Digest Technical Papers, 42(1), pp. 994-997.
202. ① G. Themelis (2003) "Comparison of Stereo Projection Screens," online, dated April 2003, accessed 28 March 2010. <http://www.drt3d.com/info/ScreenTesting.htm>
203. ① S. Tourancheau, K. Wang, L. Janowski, J. Bułat, K. Brunnström, and M. Barkowsky (2012) "Reproducibility of crosstalk measurements on active glasses 3D LCD displays based on temporal characterization," in Stereoscopic Displays and Applications XXIII, Proceedings of SPIE-IS&T Electronic Imaging, 8288, 82880Y.1-82880Y.17.
204. ④ V. M. Tran, "New methods of rendering anaglyph stereoscopic images on CRT displays and photo-quality ink-jet printers" M.A.Sc. Thesis, University of Ottawa, December 2005.
205. ①③④ I. Tsirlin, L. M. Wilcox, R. S. Allison (2011) "The Effect of Crosstalk on the Perceived Depth from Disparity and Monocular Occlusions," IEEE Transactions on Broadcasting, 57(2), 445-453.
206. ① I. Tsirlin, L. M. Wilcox, R. S. Allison (2012) "Effect of crosstalk on depth magnitude in thin structures," J. Electron. Imaging, 21(1), 011003-1-011003-7.
207. ① I. Tsirlin, R. S. Allison, L. M. Wilcox (2012) "Crosstalk reduces the amount of depth seen in 3D images of natural scenes," in Stereoscopic Displays and Applications XXIII, Proceedings of SPIE-IS&T Electronic Imaging, 8288, 82880W.1-82880W.9.
208. ② H. Uchiike, T. Hirakawa, "Color plasma displays" Proc IEEE 90, Issue 4, 533-539 (2002).
209. ⑬ Uehara, S., Hiroya, T., Kusanagi, H., Shigemura, K. and Asada, H., "High-visibility 2D/3D LCD with HDDP Arrangement and its Optical Characterization Methods" IMID/IDMC/ASIA DISPLAY '08 Digest, 147-150 (2008).
210. ⑬ Uehara, S., Ujike, H., Hamagishi, G., Taira, K., Koike, T., Kato, C., Nomura, T., Horikoshi, T., Mashitani, K., Yuuki, A., Izumi, K., Hisatake, Y., Watanabe, N., Umezu, N., Nakano, Y., "Standardization based on human factors for 3D display: performance characteristics and measurement methods" Proc. SPIE Stereoscopic Displays and Applications XXI, 7524 , 7524071-12 (2010).
211. ⑬ Uehara, S., Koike, T., Kato, C., Uchidoi, M., Horikoshi, T., Hamagishi, G., Hisatake, Y., Ujike, H., "Development of Performance Characteristics for 3D Displays" IMID/IDMC/ASIA DISPLAY 2010 DIGEST, 245-246 (2010).
212. ⑤① K. Ukai and P. A. Howarth (2008) "Visual fatigue caused by viewing stereoscopic motion images: background, theories, and observations," Displays 29(2), 106-116.
213. ⑱ Veritas et Visus (2013) "3rd Dimension" 8(2), May 2013, Temple, Texas. Available at http://www.veritasetvisus.com/3rd_dimension.htm

214. ⑩ H. Veron, D. A. Southard, J. R. Leger, J. L. Conway (1990) "Stereoscopic Displays for Terrain Database Visualization" in Proc. SPIE Stereoscopic Displays and Applications, 1256, 124-135.
215. ③④ R. E. Walpole, R. H. Myers (1985) "Probability and Statistics for Engineers and Scientists" Collier Macmillan, pp. 347.
216. ①⑩ V. Walworth, S. Bennett, and G. Trapani (1984), "Three-dimensional projection with circular polarizers" in Optics in Entertainment II, Proceedings of SPIE, 0462, 64-68.
217. ④ V. K. Walworth "Light polarization in support of stereoscopic display" Optical Engineering 51(2), 021104 (February 2012)
218. ② B. A. Wandell, L. D. Silverstein (2003) "Digital color reproduction" in The Science of Color, Elsevier, pp. 296.
219. ① L. Wang, Y. Tu, L. Chen, P. Zhang, T. Zhang, K. Teunissen, and I. Heynderickx (2012) "Effect of Display Technology on the Crosstalk Perception in Stereoscopic Video Content," IEEE Transactions on Circuits and Systems for Video Technology, 22(9), 1257-1265.
220. ④ A. F. Watch (1895) "The Anaglyph: A New Method Of Producing The Stereoscopic Effect," Journal of the Franklin Institute, CXL(6), pp. 401-405, December.
221. ⑮ M. A. Weissman (2007) "A simple measurement of extinction ratio" presented at Stereoscopic Displays and Applications XVIII, San Jose.
222. ⑤①⑩ M. A. Weissman, A. J. Woods (2011) "A simple method for measuring crosstalk in stereoscopic displays" in Stereoscopic Displays and Applications XXII, Proceedings of IS&T/SPIE Electronic Imaging, SPIE Vol. 7863, pp. 786310-1 to -11, Burlingame, California, January 2011.
223. ⑤① C. Wheatstone (1838) "Contributions to the Physiology of Vision.—Part the First. On some remarkable, and hitherto unobserved, Phenomena of Binocular Vision" in Philosophical Transactions of the Royal Society of London, Vol. 128, pp. 371 – 394.
224. ① D. Wickens, A. Kramer, J. Andersen, A. Glasser, K. Sarno (1990) "Focused and divided attention in stereoscopic depth" in Stereoscopic Displays and Applications, Proceedings of SPIE-IS&T Electronic Imaging, 1256, 28-34.
225. ① L. M. Wilcox, J. A. D. Stewart (2003) "Determinants of perceived image quality: Ghosting vs. brightness" in Stereoscopic Displays and Virtual Reality Systems X, Proc. of SPIE-IS&T Electronic Imaging, 5006, 263-268.
226. ④ P. Wimmer (undated) "Anaglyph Methods Comparison" [online] URL: http://www.3dtv.at/knowhow/anaglyphcomparison_en.aspx Accessed: 6 Mar 2013.

227. ① A. J. Woods, K.-L. Yuen, K.S. Karvinen (2007) "Characterizing crosstalk in anaglyphic stereoscopic images on LCD monitors and plasma displays," *Journal of the SID*, 15(11), 889-898.
228. ① W. Woo, N. Kim, Y. Iwadata (2000) "Stereo imaging using a camera with stereoscopic adapter," *Proc. IEEE - Systems, Man, and Cybernetics (SMC) 2000*, 1512-1517.
229. ① G. J. Woodgate, J. Harrold, A. M. S. Jacobs, R. R. Moseley, and D. Ezra (2000) "Flat panel autostereoscopic displays – characterisation and enhancement" in *Stereoscopic Displays and Virtual Reality Systems VII, Proceedings of SPIE-IS&T Electronic Imaging*, 3957, 153-164.
230. ⑪ A. J. Woods, T. Docherty, and R. Koch (1991) "The Use of Flicker-Free Television Products for Stereoscopic Display Applications" *Stereoscopic Displays and Applications II, Proceedings of SPIE Vol. 1457*, San Jose, California, February 1991. www.curtin.edu.au/cmst/publicat/1991-18.pdf
231. ⑤①②⑤⑥⑧⑩⑪⑫⑬⑯ A. J. Woods, S. Tan (2002) "Characterising Sources of Ghosting in Time-Sequential Stereoscopic Video Displays" presented at *Stereoscopic Displays and Applications XIII (SD&A)*, published in *Stereoscopic Displays and Virtual Reality Systems IX, Proceedings of IS&T/SPIE Electronic Imaging*, SPIE Vol. 4660, pp. 66-77, San Jose, California, January 2002.
232. ⑤①②③④⑧⑪ A. J. Woods, T. Rourke (2004) "Ghosting in Anaglyphic Stereoscopic Images" presented at *Stereoscopic Displays and Applications XV (SD&A)*, published in *Stereoscopic Displays and Virtual Reality Systems XI, Proceedings of IS&T/SPIE Electronic Imaging*, SPIE Vol. 5291, pp. 354-365, San Jose, California, January 2004.
233. ⑤⑤⑥⑫ A. J. Woods (2005) "Compatibility of Display Products with Stereoscopic Display Methods" *International Display Manufacturing Conference (IDMC)*, pp. 290-293, Taiwan, February 2005. [included in Appendix 1 of this thesis as Paper 11]
234. ⑤①⑥⑦⑧⑫⑭⑰ A. J. Woods, K. L. Yuen (2006) "Compatibility of LCD Monitors with Frame-Sequential Stereoscopic 3D Visualisation" (Invited Paper), in *IMID/IDMC '06 Digest*, (The 6th International Meeting on Information Display, and The 5th International Display Manufacturing Conference), pp. 98-102, Daegu, South Korea, 22-25 August 2006.
235. ⑤ A. J. Woods, T. Rourke, K.-L. Yuen (2006) "The Compatibility of Consumer Displays with Time-Sequential Stereoscopic 3D Visualisation" (Invited Plenary Paper), in *Proceedings of the K-IDS Three-Dimensional Display Workshop 2006*, pp. 7-10, Seoul National University, Seoul, South Korea, 21 August 2006.

236. ⑤⑧ A. J. Woods, K. L. Yuen, K. S. Karvinen, (2007) "Characterizing crosstalk in anaglyphic stereoscopic images on LCD monitors and plasma displays" in *Journal of the Society for Information Display*, Volume 15, Issue 11, pp. 889-898, November 2007.
237. ⑤①⑥⑧⑫ A. J. Woods, T. Rourke (2007) "The compatibility of consumer DLP projectors with time-sequential stereoscopic 3D visualization", presented at *Stereoscopic Displays and Applications XVIII*, published in *Stereoscopic Displays and Virtual Reality Systems XIV*, Proceedings of IS&T/SPIE Electronic Imaging, SPIE Vol. 6490, pp. 64900V-1 to -7, San Jose, California, January 2007.
238. ③④⑭ A. J. Woods, K. L. Yuen, K. S. Karvinen (2007) "Characterizing crosstalk in anaglyphic stereoscopic images on LCD monitors and plasma displays" in *JSID*, 15(11), pp. 889-898.
239. ⑤①⑦⑧⑭⑰ A. J. Woods, K. S. Karvinen (2008) "The compatibility of consumer plasma displays with time-sequential stereoscopic 3D visualization" *Stereoscopic Displays and Applications XIX*, Proceedings of IS&T/SPIE Electronic Imaging, SPIE Vol. 6803, pp. 68030X-1 to -9, San Jose, California, January 2008.
240. ⑤① A. J. Woods (2009) "3-D Displays in the Home," *Information Display*, 25(07), 8-12.
241. ⑤①⑧⑭ A. J. Woods, A. Sehic (2009) "The compatibility of LCD TVs with time-sequential stereoscopic 3D visualization" in *Stereoscopic Displays and Applications XX*, Proceedings of IS&T/SPIE Electronic Imaging, SPIE Vol. 7237, pp. 72370N-1 to -9, San Jose, California, January 2009.
242. ⑤①③④⑮⑯ A. J. Woods, C. R. Harris (2010) "Comparing levels of crosstalk with red/cyan, blue/yellow, and green/magenta anaglyph 3D glasses" in *Stereoscopic Displays and Applications XXI*, Proceedings of IS&T/SPIE Electronic Imaging, SPIE Vol. 7253, pp. 75240Q-1 to -12, San Jose, California, January 2010.
243. ⑤①③⑬ A. J. Woods (2010) "Understanding Crosstalk in Stereoscopic Displays" (Keynote Presentation) at 3DSA (Three-Dimensional Systems and Applications) conference, Tokyo, Japan, 19-21 May 2010.
244. ①⑯⑱ A. J. Woods, J. O. Merritt, S. S. Fisher, M. T. Bolas, S. A. Benton, N. S. Holliman, N. A. Dodgson, I. E. McDowall, M. Dolinsky, eds. (2010) "Stereoscopic Displays and Applications 1990-2009: A Complete 20-Year Retrospective and The Engineering Reality of Virtual Reality 1994-2009 (Special Collection)" (DVD-ROM), SPIE, 51. ISBN 987-0-8194-7659-3.
245. ⑤①③④⑮ A. J. Woods (2011) "How are crosstalk and ghosting defined in the stereoscopic literature?" in *Stereoscopic Displays and Applications XXII*, Proceedings of IS&T/SPIE Electronic Imaging, SPIE Vol. 7863, pp. 78630Z-1 to -12, Burlingame, California, January 2011.

246. ⑰ A. J. Woods, J. Helliwell (2011) "White Paper: A Survey of 3D Sync IR Protocols", Curtin University, March 2011.
<http://www.cmst.curtin.edu.au/local/docs/pubs/2011-17-woods-helliwell-3D-Sync-IR.pdf>
247. ④ A. J. Woods (2012) "Crosstalk in stereoscopic displays: a review" *Journal of Electronic Imaging* 21(4), 040902 (Oct–Dec 2012)
248. ⑤ A. J. Woods, J. Helliwell (2012) "Investigating the cross-compatibility of IR-controlled active shutter glasses" in *Stereoscopic Displays and Applications XXIII, Proceedings of IS&T/SPIE Electronic Imaging, SPIE Vol. 8288*, pp. 82881C-1 to -10, Burlingame, California, January 2012.
249. ⑤ A. J. Woods (2012) "The Illustrated 3D Compatible Projectors List", URL:
<http://www.3dmovielist.com/projectors.html> , dated: 6 Feb 2012, accessed: 19 June 2013.
250. ⑤①⑰ A. J. Woods (2012) "The Illustrated 3D HDTV List", URL:
<http://www.3dmovielist.com/3dhdtvs.html> dated: 24 May 2012, accessed: 19 June 2013.
251. ⑤① A. J. Woods (2012) "The Illustrated 3D Monitor List", URL:
<http://www.3dmovielist.com/3dmonitors.html> , dated: 13 May 2012, accessed: 19 June 2013.
252. ⑤ A. J. Woods (2013) "The Illustrated 3D Movie List" [online] May 2013. URL:
<http://www.3dmovielist.com> Accessed 18 May 2013.
253. ⑤①④ A. J. Woods, C. R. Harris (2012) "Using cross - talk simulation to predict the performance of anaglyph 3 - D glasses" in *JSID (Journal of the Society for Information Display)*, Vol. 20, No. 6, pp. 304 - 315.
254. ⑤ A. J. Woods (2013) "3D or 3-D: A study of terminology, usage and style", *European Science Editing*, 39(3), pp. 59-62, August 2013.
255. ⑤ A. J. Woods, C. R. Harris, Dean B. Leggo, Tegan M. Rourke (2013) "Characterizing and Reducing Crosstalk in Printed Anaglyph Stereoscopic 3D Images" in *(Journal of) Optical Engineering, SPIE, Vol. 52, No. 4*, pp. 043203-1 to 043203-19, April 2013.
256. ⑪ A. J. Woods (undated) "Proposed Standard for Field-Sequential 3D Television" [online] www.stereoscopic.org/standards
257. ③④ Z. Xie, T. G. Stockham Jr. (1989) "Toward the unification of three visual laws and two visual models in brightness perception" *IEEE Transactions on Systems, Man and Cybernetics*, 19(2), pp. 379 - 387.
258. ⑱ Yahoo (2010) "The Yahoo! Style Guide" New York, Yahoo! Inc, pp. 483. ISBN 978-0312569846.

259. ⑩ Y.-Y. Yeh, L. D. Silverstein (1989) "Using electronic stereoscopic color displays: Limits of fusion and depth discrimination" in Proc. SPIE Three-Dimensional Visualization and Display Technologies, ed. S S Fisher, W E Robbins, 1083, 196-204.
260. ①③④ Y.-Y. Yeh, L. D. Silverstein (1990) "Limits of fusion and depth judgment in stereoscopic color displays" Human Factors, 32, 45-60.
261. ① Y. Yoshihara (2003) "3D-LCD用マイクロポールについて" ("About Micro-Pol for 3D LCD"), 3D Consortium, June 2003. (presentation only)
262. ②⑫ K. L. Yuen (2006) "Compatibility of LCD Monitors with Stereoscopic Display Methods", Technical Report CMST 2006-34, Curtin University of Technology.
263. ④ R. Z. Zeng, H. Z. Zeng (2011) "Printing Anaglyph Maps Optimized for Display" in Color Imaging XVI: Displaying, Processing, Hardcopy, and Applications, Proc. of Electronic Imaging, SPIE Vol. 7866, pp. 78661S-1-5.
264. ②③④⑧ R. Zone (2002) "Good old fashion anaglyph: High tech tools revive a classic format in spy kids 3-D," Stereo World 29, No. 5, 11–13 and 46 (2002–2003).
265. ④ R. Zone (2012) personal communication, July 2012.
266. ⑩ The Macquarie Encyclopedic Dictionary, Macquarie University, Australia (1990).
267. ⑰ The Full HD 3D Glasses Initiative. Online: <http://www.fullhd3dglASSES.com/> Accessed: 16 December 2011.
268. ④ "Louis Ducos du Hauron" Encyclopædia Britannica, Encyclopædia Britannica Online, Encyclopædia Britannica Inc. (2012). Accessed: 22 Jul 2012 URL: <<http://www.britannica.com/EBchecked/topic/172961/Louis-Ducos-du-Hauron>>
269. ⑥⑦⑬ NVIDIA 3D Stereo Driver http://www.nvidia.com/object/3d_stereo.html
270. ⑥⑦⑬ Powerstrip software <http://entechtaiwan.net/util/ps.shtm>
271. ⑮ Wikipedia, http://en.wikipedia.org/wiki/SRGB_color_space
272. ⑬ Stereoscopic Player software http://www.3dtv.at/Products/Player/Index_en.aspx
273. ⑤⑧ www.matlab.com
274. ⑦ unknown author (2007) "Philips ditches Aptura backlight tech for LED" PC PRO, 13 March 2007, <http://www.pcpro.co.uk/news/107108/philips-ditches-aptura-backlight-tech-for-led.html>
275. ⑦ unknown author (2009) "NVIDIA Geforce 3D Vision Review" OverClockersClub, 7 January 2009, http://www.overclockersclub.com/reviews/nvidia_3d_vision/
276. ③ unknown author (undated) "How to make 3D glasses" [online] URL: http://www.ehow.com/how_4455680_make-3d-glasses.html Accessed: 26 August 2011.
277. ③ unknown author (undated) "How to make a pair of 3D glasses for 3D Anaglyphs" [online] URL: <http://www.haworth-village.org.uk/3d/3d-glasses.asp> Accessed: 26 August 2011.

278. ③ unknown author (undated) "Make your own 3-D glasses" [online]. URL: <http://paperproject.org/3dglASSES.html> Accessed: 26 August 2011.
279. ③ unknown author (undated) "How to make your own 3D glasses" Wikihow [online] URL: <http://www.wikihow.com/Make-Your-Own-3D-Glasses> Accessed: 6 July 2011.
280. ③ unknown author (undated) "Make 3-D glasses" Wired How-to Wiki [online] URL: http://howto.wired.com/wiki/Make_3-D_Glasses Accessed: 6 July 2011.
281. ⑥ unknown author (undated) "The plasma behind the plasma TV screen" [online] <http://www.plasmatvscience.org/theinnerworkings.html> Accessed: 28 November 2006

9. Published Papers

“An original reprint of each paper must be bound directly into the thesis, or photocopied on A4 size paper. Papers should be separated by a sheet of coloured paper on which is stated the full bibliographic citation of the publication.”

Refereed Journal Articles

- Paper 1** A. J. Woods (2012) “Crosstalk in Stereoscopic Displays: a review” in Journal of Electronic Imaging, IS&T/SPIE, Vol. 21, No. 4, pp. 040902-1 to 040902-21 (December 2012).
- Paper 2** A. J. Woods, K. L. Yuen, and K. S. Karvinen (2007) “Characterizing crosstalk in anaglyphic stereoscopic images on LCD monitors and plasma displays” in Journal of the Society for Information Display, Volume 15, Issue 11, pp. 889-898, November 2007.
- Paper 3** A. J. Woods, C. R. Harris (2012) “Using cross-talk simulation to predict the performance of anaglyph 3-D glasses” in Journal of the Society for Information Display, Vol. 20, No. 6, pp. 304-315.
- Paper 4** A. J. Woods, C. R. Harris, D. B. Leggo, T. M. Rourke (2013) “Characterizing and Reducing Crosstalk in Printed Anaglyph Stereoscopic 3D Images” in (Journal of) Optical Engineering, SPIE, Vol. 52, No. 4, pp. 043203-1 to 043203-19, April 2013.

Refereed Conference Papers

- Paper 5** A. J. Woods, K. L. Yuen (2006) "Compatibility of LCD Monitors with Frame-Sequential Stereoscopic 3D Visualisation" (Invited Paper), in IMID/IDMC '06 Digest, (The 6th International Meeting on Information Display, and The 5th International Display Manufacturing Conference), pp. 98-102, Daegu, South Korea, 22-25 August 2006.
- Paper 6** A. J. Woods, K. S. Karvinen (2008) "The compatibility of consumer plasma displays with time-sequential stereoscopic 3D visualization" in Stereoscopic Displays and Applications XIX, Proceedings of IS&T/SPIE Electronic Imaging, SPIE Vol. 6803, pp. 68030X-1 to -9, San Jose, California, January 2008.
- Paper 7** A. J. Woods, A. Sehic (2009) “The compatibility of LCD TVs with time-sequential stereoscopic 3D visualization” in Stereoscopic Displays and Applications XX, Proceedings of IS&T/SPIE Electronic Imaging, SPIE Vol. 7237, pp. 72370N-1 to -9, San Jose, California, January 2009.
- Paper 8** A. J. Woods, C. R. Harris (2010) “Comparing levels of crosstalk with red/cyan, blue/yellow, and green/magenta anaglyph 3D glasses” in Stereoscopic Displays and Applications XXI, Proceedings of IS&T/SPIE Electronic Imaging, SPIE Vol. 7253, pp. 75240Q-1 to -12, San Jose, California, January 2010.

Paper 1 [Refereed Journal Article]

A. J. Woods (2012) "Crosstalk in Stereoscopic Displays: a review" in Journal of Electronic Imaging, IS&T/SPIE, Vol. 21, No. 4, pp. 040902-1 to 040902-21 (December 2012).

Crosstalk in stereoscopic displays: a review

Andrew J. Woods

Curtin University

Centre for Marine Science & Technology

GPO Box U1987, Perth 6845 Australia

Abstract. Crosstalk, also known as ghosting or leakage, is a primary factor in determining the image quality of stereoscopic three dimensional (3D) displays. In a stereoscopic display, a separate perspective view is presented to each of the observer's two eyes in order to experience a 3D image with depth sensation. When crosstalk is present in a stereoscopic display, each eye will see a combination of the image intended for that eye, and some of the image intended for the other eye—making the image look doubled or ghosted. High levels of crosstalk can make stereoscopic images hard to fuse and lack fidelity, so it is important to achieve low levels of crosstalk in the development of high-quality stereoscopic displays. Descriptive and mathematical definitions of these terms are formalized and summarized. The mechanisms by which crosstalk occurs in different stereoscopic display technologies are also reviewed, including micro-polar 3D liquid crystal displays (LCDs), autostereoscopic (lenticular and parallax barrier), polarized projection, anaglyph, and time-sequential 3D on LCDs, plasma display panels and cathode ray tubes. Crosstalk reduction and crosstalk cancellation are also discussed along with methods of measuring and simulating crosstalk. © 2012 SPIE and IS&T. [DOI: [10.1117/1.JEI.21.4.040902](https://doi.org/10.1117/1.JEI.21.4.040902)]

1 Introduction

Stereoscopic three dimensional (3D) displays present a 3D image to an observer by sending a slightly different perspective view to each of an observer's two eyes. The visual system of most observers is able to process the two perspective images so as to interpret an image containing a perception of depth by invoking binocular stereopsis so they can see it in 3D.

There are a wide range of technologies available to present stereoscopic 3D images to an audience, and the discussion in this paper will be limited to so-called "planostereoscopic" displays¹—i.e., displays that present both left and right perspective images on the same planar surface and then use a coding/decoding scheme (e.g., glasses) to present the correct image to each eye. Examples of such planostereoscopic displays include liquid crystal display (LCD) or plasma display panel (PDP) 3D TVs viewed using active shutter 3D glasses, 3D LCD monitors or 3D cinema systems viewed using passive polarized 3D glasses, or autostereoscopic displays utilizing either a parallax barrier or lenticular lens sheet to allow the 3D image to be viewed without 3D glasses. The aim of all of these displays is to send separate left- and right-eye views to each eye, but due to various inaccuracies, which will be described in detail later in the

paper, the image intended only for one eye may be leaked to the other eye. This leakage of one image channel to the other in a stereoscopic display system is known as crosstalk or sometimes ghosting or leakage. Crosstalk is a primary factor affecting the image quality of stereoscopic 3D displays and is the focus of this review paper.

This paper starts by providing a summary of descriptive and mathematical definitions of crosstalk and related terms as they are now in common usage, along with a short summary of the perceptual effects of crosstalk. The bulk of the paper describes the various methods by which crosstalk can occur in various stereoscopic display technologies. This is followed by a description of the methods of measuring crosstalk, a discussion of ways in which crosstalk can be reduced, and last, some coverage of the role of simulation of crosstalk analysis.

2 Terminology and Definitions

In electronic engineering, the term "crosstalk" has been used as far back as the 1880s² to describe the leakage of signals between parallel laid telephone cables. Crosstalk in stereoscopic displays has been a recognized term at least since the 1930s,³ if not earlier.

The use of the term "crosstalk" in the stereoscopic literature is very common—present in over 15% of all documents in a major stereoscopic literature collection.^{4,5} The term is also often written as "cross talk,"⁶ "cross-talk,"⁷ or "X-talk,"⁶ but "crosstalk" (without an intermediate space or hyphen) is the most commonly used variant, so that is the form that will be used in this paper.⁴ Other variants with the same meaning include "interocular crosstalk,"^{8,9} "crosstalk ratio,"¹⁰ and "3D crosstalk."¹¹

Despite the term's long history of usage in the stereoscopic technical literature, many papers in the past have simply used the term without providing a descriptive or mathematical definition, nor citing a reference to such. The terms crosstalk and ghosting have been used interchangeably in some of the published literature, whereas modern usage provides separate definitions for these terms—this will be explained in the following sections. Unfortunately there are also some contradictory uses of the terminology in the literature.

The technical field of stereoscopic displays has grown considerably even in just the past five years and in order to foster the continued development of the field, it is important to have a common knowledge of the terminology and definitions of crosstalk and related terms. The following subsections provide a summary of definitions of the important terms in this field and identify ambiguities that still remain

Paper 12214V received Jun. 4, 2012; revised manuscript received Oct. 12, 2012; accepted for publication Oct. 16, 2012; published online Dec. 5, 2012.

0091-3286/2012/\$25.00 © 2012 SPIE and IS&T

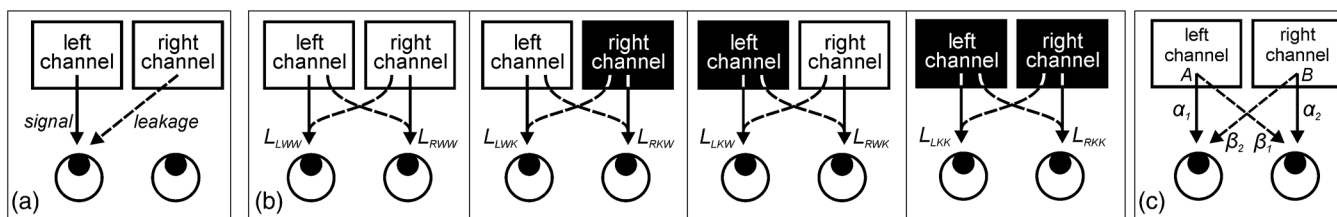


Fig. 1 An illustration of the terms and luminance measurement variables used in this paper with respect to the left and right image channels and left and right eyes. The left and right image channels are shown separated here for illustrative purposes but would be visually overlaid on a stereoscopic display. (a) Illustration of the terms signal and leakage. (b) Illustration of the eight luminance variable L variants. The first subscript is the eye position (Left or Right) that the luminance is measured from. The second subscript is the value (black or White) of the desired image channel, and the third subscript is the value (black or White) of the undesired image channel. For example, LRWW specifies the luminance measured at the right eye position when the right image (desired) channel is set to white and the left image (undesired) channel is also set to white, which corresponds to the summation of light from the right channel plus a (hopefully) small amount of light from the left channel. (c) Illustration of the transfer function variables used in Huang’s definition of “system crosstalk” (see Sec. 2.2.3).¹⁶

and could otherwise cause confusion for those reading the published literature.

Stereoscopic terminology can be used to describe a principle in general terms and can also be used to quantify a physical property—this paper will review both the descriptive and mathematical definitions where applicable.

2.1 Descriptive Definitions

A selection of descriptive definitions of crosstalk from the literature (1987 to 2009) were previously examined.⁴ It was found that despite some variations in wording, there was a common theme—i.e., light from one image channel leaking into another. The following descriptive definition will be used in this paper (based on Lipton¹²):

Crosstalk: the incomplete isolation of the left and right image channels so that the content from one channel is partly present in another channel.

There is also a mathematical definition of crosstalk, which will be provided in the following section. In the general stereoscopic literature and the lay media, the terms “crosstalk” and “ghosting” have often been used interchangeably,⁴ but in scientific discussion it is worthwhile to differentiate these terms. Crosstalk and ghosting appear to have been first documented as separate terms in 1987 by Lipton,¹³ which leads us to the following definition:

Ghosting: the perception of crosstalk.

The term “leakage” is also commonly used in discussions about crosstalk, however, a formal definition was not found in the stereoscopic literature.⁴ The following definition was developed based on dictionary definitions and current usage in the field:⁴

Leakage: the (amount of) light that leaks from one stereoscopic image channel to another.

Leakage is also known as “crosstalk luminance” and “unintended luminance.”¹⁴

2.2 Mathematical Definitions

Crosstalk can be used as a metric to express how much crosstalk occurs in a particular stereoscopic display system. There are several mathematical definitions of crosstalk in common usage as explained below.

2.2.1 Crosstalk definition 1

In its simplest form crosstalk can be mathematically defined¹⁵ as:

$$\text{Crosstalk}(\%) = \frac{\text{leakage}}{\text{signal}} \times 100, \quad (1)$$

where “leakage” is the luminance of light that leaks from the unintended channel to the intended channel, and “signal” is the luminance of the intended channel, as illustrated in Fig. 1(a).

In common practice, two luminance measurements are usually taken (from the intended eye position) with: (a) full-black in the intended channel and full-white in the unintended channel (this corresponds with “leakage” above) and (b) full-white in the intended channel and full-black in the unintended channel (this corresponds with “signal” above).

This can also be expressed as:

$$C_L = \frac{L_{LKW}}{L_{LWK}} \quad (2)$$

and

$$C_R = \frac{L_{RKW}}{L_{RWK}}, \quad (3)$$

where C_L and C_R are crosstalk for the left and right eyes (which can be presented as a number or a percentage), and L_{LKW} , L_{LWK} , L_{RWK} , L_{RKW} are the luminance measured from the Left or Right eye position (first subscript) with White or black in the desired image channel (second subscript) and White or black in the undesired image channel (third subscript) as illustrated in Fig. 1(b).^{*†‡} The shortcoming of this definition is that it does not consider the effect of a non-zero

^{*}It is worth noting that some publications use variable C to denote crosstalk, whereas other publications use variable C for contrast¹⁷ and variable X or χ for crosstalk.^{14,18}

[†]Some papers define the subscripts for the luminance measurement variables differently than we have used in this paper. Specifically, sometimes the second luminance (L) subscript is the setting (White or black) of the “left channel” (as opposed to the “desired channel”), and the third subscript is the setting (White or black) of the “right channel” (as opposed to the “undesired channel”). This makes no difference for the left-eye luminance variables, but results in a transposition of the second and third subscript meanings for the right-eye luminance variables. The “desired, undesired” definition is the more common, and is more extensible for crosstalk in multi-view displays, so this is what has been used in this paper.

[‡]When testing PDPs, test images should only fill a small portion of the screen in order to avoid triggering the automatic brightness limiter (ABL) (which reduces the intensity of high-brightness scenes to reduce peak power consumption) which would otherwise bias measurement results.¹⁹

black level of the display. Some displays are incapable of outputting zero luminance for full-black (e.g., LCDs)—this non-zero black level does not contribute to visible crosstalk (ghosting) and hence would bias the crosstalk calculation using this first definition. If the display black level is set at zero luminance, definition 1 is entirely valid, but definition 1 should only be used with displays which can have zero black level, and are set up that way.

2.2.2 Crosstalk definition 2

The second mathematical definition removes the effect of non-zero black level by subtracting the black level luminance:

$$\text{Crosstalk}(\%) = \frac{\text{leakage} - \text{black level}}{\text{signal} - \text{black level}} \times 100. \quad (4)$$

Several papers support this second formulation (but with different variable names).^{4,10,14,17,20}

This equation can also be expressed as:

$$C_L = \frac{L_{LKW} - L_{LKK}}{L_{LWK} - L_{LKK}} \quad (5)$$

and

$$C_R = \frac{L_{RKW} - L_{RKK}}{L_{RWK} - L_{RKK}}, \quad (6)$$

where the variables are as defined in Sec. 2.2.1 and L_{LKK} and L_{RKK} are the black level of the display.^{†‡}

Both of these definitions use what is commonly referred to as a black-white crosstalk test because full-black and full-white test signals are used.^{21‡} Full-white and full-black signals are used because maximum ghosting usually occurs when the pixels in the desired-eye channel are full-black and the same pixels in the opposite eye-channel are full-white.

The differences between these two mathematical definitions of crosstalk (definitions 1 and 2) create an ambiguity—therefore when quoting crosstalk values it is important to specify which definition is being used, and similarly if reading a report or technical paper, it is important to determine which definition has been used to calculate the results quoted.

2.2.3 System crosstalk and viewer crosstalk

In 2000, Huang et al.,¹⁶ defined two new terms in an attempt to disambiguate the terminology relating to crosstalk:

System crosstalk: the degree of the unexpected leaking image from the other eye.

Viewer crosstalk: the crosstalk perceived by the viewer.²²

As defined, system crosstalk is independent of the image content (determined only by the display), whereas viewer crosstalk varies depending upon the content. These definitions are similar to the definitions of crosstalk and ghosting provided in Sec. 2.1 (based on Lipton¹²)—but are not exactly the same. The definition of viewer crosstalk includes the effect of image contrast (and indirectly the effect of parallax) but Lipton’s definition of ghosting includes any perception effect.

These are defined mathematically as:¹⁶

$$\text{System crosstalk (left eye)} = \beta_2/\alpha_1, \quad (7)$$

$$\text{Viewer crosstalk (left eye)} = B\beta_2/A\alpha_1, \quad (8)$$

where “ α_1 describes the percentage part of the left-eye image observed at the left eye position,” and “ β_2 describes the percentage part of the right-eye image leaked to the left-eye position”¹⁶ and vice versa for the other eye. A is the luminance of a particular point in the left-eye image, and B is the luminance of the same corresponding point (same x, y location on the screen) in the right-eye image, as illustrated in Fig. 1(c). It is worth noting that Eq. (7) does not include the effect of black level—as is also the case with crosstalk definition 1 in Sec. 2.2.1.

The philosophy upon which system crosstalk is defined is quite different to crosstalk definitions 1 and 2 provided earlier. Variables α_1 and β_2 are essentially transfer functions which characterize the optical performance of the entire system (from image display, through the glasses or image separation stage, to viewed luminance) and hence is probably the reason that the authors called it system crosstalk. In comparison, definitions 1 and 2 are observer-centric or output-luminance centric—based only on measurements of luminance at the viewer location. In order to calculate the system performance variables α_1 and β_2 , both the source and output luminance need to be measured, but with some displays the source luminance cannot be directly measured (e.g., lenticular or parallax barrier displays). Fortunately, if some assumptions are made, the equation can be converted to an equation based on properties that can be easily measured, and hence can be expressed similarly to Eq. (1).

In 2009, Huang et al.²² provided a revised definition of system crosstalk that includes the effect of black level.[§]

$$\text{SCT}_L = \frac{L_{LKW} - L_{LKK}}{L_{LWK} - L_{LKK}} \quad (9)$$

and

$$\text{SCT}_R = \frac{L_{RKW} - L_{RKK}}{L_{RWK} - L_{RKK}}, \quad (10)$$

where SCT_L and SCT_R are the system crosstalk for the left and right eyes, and L_{LKW} , etc. are defined per Sec. 2.2.1.[†]

As a result of this change of definition, it is important to establish which definition of system crosstalk (2000¹⁶ or 2009²²) is being used when it appears in a publication. Equations (9) and (10) are equivalent to crosstalk definition 2 provided above [Eqs. (5) and (6)].

2.2.4 Gray-to-gray crosstalk

In most stereoscopic displays crosstalk is an additive process and roughly linear, so using the black-white test to measure crosstalk and expressing the result as a simple percentage is representative of the display’s overall crosstalk, but this is not true for all stereoscopic displays, particularly 3D LCDs or 3D PDPs using shutter glasses, and hence a more detailed definition is needed. For displays in which the crosstalk process is highly nonlinear, the gray-to-gray crosstalk measurement should be used.

In 2010, three papers^{21,23,24} all separately defined a new term: “gray-to-gray crosstalk.”

[§]These equations have been reworked (from that published by the original authors) to a scheme which matches the notation used throughout in this paper.

Shestak et al.,²¹ provided the following definition.[§]

$$C_{Lij} = \frac{L_{Lij} - L_{Lii}}{L_{Ljj} - L_{Lii}} \quad (11)$$

and

$$C_{Rij} = \frac{L_{Rij} - L_{Rii}}{L_{Rjj} - L_{Rii}}, \quad (12)$$

where C_{Lij} is crosstalk for the **L**eft eye (first subscript) calculated for the matrix of the desired image channel (second subscript) and the undesired image channel (third subscript) gray level combinations i and j ,[†] L_{Lij} is the luminance measured from the **L**eft eye position (first subscript) with i gray level in the desired image channel (second subscript) and i gray level in the undesired image channel (third subscript), and so on.

Jung,²³ Pan,²⁴ ICDM,¹⁴ and Chen²⁵ have also provided definitions for gray-to-gray crosstalk which vary from that of Shestak,²¹ so again, it is important to know which definition is used when gray-to-gray crosstalk values are published. Apart from variable notation differences, the main difference between definitions of gray-to-gray crosstalk is the choice of variables on the denominator and the use of absolute values. It would be useful to see a comparison between these definitions to know the pros and cons of each and help decide on the most useful definition—like Järvenpää et al., have done for autostereoscopic crosstalk definitions.²⁶

There are some difficulties of these gray-to-gray crosstalk definitions—first, a singularity is present when $i = j$ with some definitions, and secondly, the crosstalk values are not perceptually relevant. Teunissen et al.,²⁷ and Shestak et al.,²⁸ have described an extension of this work to provide a perceptually relevant measure of the visibility of crosstalk (ghosting) in relation to the gray-to-gray crosstalk measurement.

2.2.5 Multi-view autostereoscopic (inter-view) crosstalk

The crosstalk definitions described so far only apply to two-view stereoscopic displays, but the definition can be extended to apply to multiview autostereoscopic displays, where it can also be called inter-view, adjacent-view or inter-zone crosstalk.

Järvenpää et al.^{18,29} have provided the following definition of crosstalk for multi-view autostereoscopic displays.[§]

$$C_i(\theta) = \frac{\sum_{j=1}^{\text{\# of views}} [L_j(\theta) - L_K(\theta)] - [L_i(\theta) - L_K(\theta)]}{L_i(\theta) - L_K(\theta)}, \quad (13)$$

where $C_i(\theta)$ is the calculated crosstalk curve for each view i as a function of the horizontal viewing angle θ , $L_j(\theta)$ is the measured luminance curve for view j when that view is white and the other views are black, $L_i(\theta)$ is the measured luminance curve for view i (the view for which the crosstalk is being determined) when that view is white and the other views are black, and $L_K(\theta)$ is the measured luminance curve when all display pixels (all views) are black.

Crosstalk can also vary with pixel position on the screen and vertical viewing angle of the observer, and the crosstalk

equation can be extended to include these variables if needed.¹⁸

The above definition applies only to autostereoscopic displays with discrete views—a different formula would be needed for autostereoscopic displays with continuous views.¹⁸

2.2.6 Extinction and 3D contrast

Two other related terms are:

Extinction and extinction ratio: “The ratio of the luminance of the correct eye [view] to the luminance of the unwanted ‘ghost’ from the image intended for the opposite eye”⁹—usually expressed as a ratio, for example ‘50:1.’

3D contrast: Unfortunately multiple definitions exist. Boher¹⁷ and ISO¹⁸ define 3D contrast as the inverse of (black-white) 3D crosstalk (definition 2 above). ISO¹⁸ also defines 3D contrast for multi-view autostereoscopic displays as the inverse of multi-view autostereoscopic crosstalk [Eq. (13) above]. However, ICDM¹⁴ defines 3D contrast as the arithmetic mean of the two (left and right) monocular contrasts, where monocular contrast is defined as the luminance ratio of both channels’ white level to both channels’ black level. ICDM¹⁴ defines system contrast as L_{LWK}/L_{LKW} (the inverse of crosstalk definition 1 above).

3 Perception of Crosstalk

The perception of crosstalk in stereoscopic displays has been studied widely.^{10,22,30-34} It is broadly acknowledged that the presence of high levels of crosstalk in a stereoscopic display is detrimental. Wilcox and Stewart³⁵ reported that crosstalk was the most important attribute in determining image quality for 75% of their observers. The effects of crosstalk in a stereoscopic image include ghosting and loss of contrast, loss of 3D effect and depth resolution, viewer discomfort,³⁶ reduced limits of fusion, reduced image quality and reduced visual comfort,⁹ and reduced perceived magnitude of depth.³⁷

The perception of crosstalk (ghosting) increases with increasing image contrast and increasing binocular parallax of the image.^{21,30,33} This principle is illustrated in Fig. 2 which summarizes an experiment performed by Pastoor.³⁰ One example of this principle is that a stereoscopic image with high contrast (lots of bright whites against a deep black background—e.g., a star field image) will exhibit more ghosting on a particular stereoscopic display than will an image with low contrast. Other image content aspects that can also affect perception of crosstalk include focus and motion blur (blur can disguise crosstalk)³⁸ and the extent of objects (crosstalk is more visible on thin objects).³⁹

The stereoscopic literature provides various advice on the amounts of crosstalk that are acceptable and unacceptable. Some examples include:

- “Difference [change] in crosstalk between [from] 2% and [to] 6% significantly affected image quality and visual comfort” (Ref. 40 paraphrasing Ref. 9)
- “In order to reproduce a reasonable depth range (up to 40 minarc) on a high-contrast display (100:1), crosstalk should be as low as 0.3%”³⁰

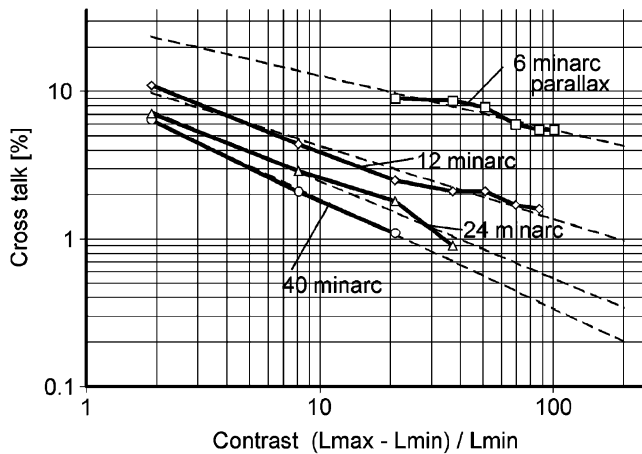


Fig. 2 Visibility thresholds for crosstalk as a function of local image contrast and binocular parallax as conducted by Pastoor.³⁰ The graph shows that “visibility of crosstalk increases (i.e., the threshold value is lowered) with increasing contrast and increasing binocular parallax (depth) of the stereoscopic image.”³⁰ The four line segments on the graph show the threshold of visibility of crosstalk for four different values of stereoscopic image parallax (6, 12, 24, and 40 min of arc) and a selection of different image contrast levels (ranging from 2:1 to 100:1). With the same image contrast (e.g., 20:1), it can be seen that the threshold of visibility of crosstalk decreases for increasing levels of parallax, meaning that ghosting is more visible with higher levels of stereoscopic image parallax. Keeping parallax constant (e.g., following the 12 minarc line), it can be seen that the threshold of visibility of crosstalk decreases with increasing image contrast, meaning that crosstalk is more visible with higher levels of image contrast. Image: © ITE and SID.³⁰

- “Crosstalk . . . visibility threshold of about 1% to 2%” (Ref. 40 paraphrasing Ref. 31)
- “Crosstalk level of about 5% is sufficient to induce visual discomfort in half of the population”³²
- “Results show that a 1% increment in crosstalk is visible, while 5.8% crosstalk is perceptible, but not annoying”⁴⁰
- “For optimal image quality, crosstalk levels should be held below 1%. However, most of the depth percept is maintained at crosstalk levels of up to 4%”³⁷
- “A significant decrease in perceived depth was observed with as little as 2–4% crosstalk”⁴¹

As can be seen above, unfortunately there is considerable variability between the results and guidelines of different papers. This might just be a reflection of the nature of perception-based studies, but results can also be influenced by differences between stereoscopic display technologies, measurement methods, experimental conditions, and display content. There may also be different acceptability thresholds for different usage types—entertainment viewing may be more tolerant of crosstalk than an industrial fine tele-operation task. It is also important to understand that most of the current measures of crosstalk are not perceptually relevant—hence more research is needed in this area.^{27,28}

The reason for determining the threshold of visibility of crosstalk is that it can be very difficult to totally eliminate crosstalk in a particular stereoscopic display technology, whereas if the level of crosstalk can be reduced to a point at which it is not noticeable to the observer, this may allow a more technically and economically viable solution. There is still a great

deal to be learnt about the perception of crosstalk and there is considerable scope for more research in this area.^{27,28}

4 Crosstalk Mechanisms

Figure 3 shows the flow of images from the capture of the perspective images with a camera, through to the display of the images on a stereoscopic display, and subsequently viewing and perception by an observer. Crosstalk can occur in the capture, storage/transmission, display and separation stages—this paper focuses most of its attention on how crosstalk occurs in the display and separation stages.

One of the fascinating things about crosstalk is that the mechanisms by which it occurs can vary considerably from one stereoscopic display technology to another.

The sections below summarize the important performance attributes for various stereoscopic display technologies and the mechanisms by which crosstalk occurs in each. This list of 3D displays is not intended to be exhaustive—people are incredibly inventive and there are literally hundreds of different stereoscopic display technologies, so it is not possible to discuss all possible stereoscopic display technologies in one short paper. This paper provides the reader with information about the factors which cause crosstalk in a selection of the most common stereoscopic displays and hopefully provide clues as to the crosstalk mechanisms in other displays not specifically discussed.

4.1 Time-Sequential 3D Using Active Shutter Glasses

The time-sequential 3D display method is a widely used technique to display stereoscopic images to an observer.¹¹ It relies on the alternate presentation of left and right images on the display surface combined with a pair of active shutter 3D glasses to gate the appropriate image to each eye.¹ In the past, mechanical shutters⁴² and lead-lanthanum-zirconate-titanate (PLZT) shutters^{43,44} have been used in the glasses, but current shutter glasses almost exclusively use a liquid crystal (LC) cell in front of each eye to sequentially occlude the images.⁴⁵ The optical transmission properties of the liquid crystal shutter are a key determinant in the amount of crosstalk present with the time-sequential 3D displays which use shutter glasses.

The optical transmission performance of an example pair of shutter glasses is shown in Fig. 4. In this figure it can be seen that:

- the LC shutters have non-zero transmission in the opaque state, which means that some light still leaks through when the shutter is nominally in the blocking condition,
- the rise-time and fall-time are not instantaneous—sometimes taking several milliseconds to change from one state to another, and
- the performance at different optical wavelengths is not all the same.

¹¹The time-sequential stereoscopic 3D method is also known as time-multiplexed, field-sequential, frame-sequential, alternate frame, or active-stereo.

¹3D shutter glasses are also known as active shutter glasses, liquid crystal shutter (LCS) glasses, and sometimes incorrectly as LCD shutter glasses. The LC cells in 3D shutter glasses are not displays (just shutters), so the term “LCD shutter glasses” is incorrect.

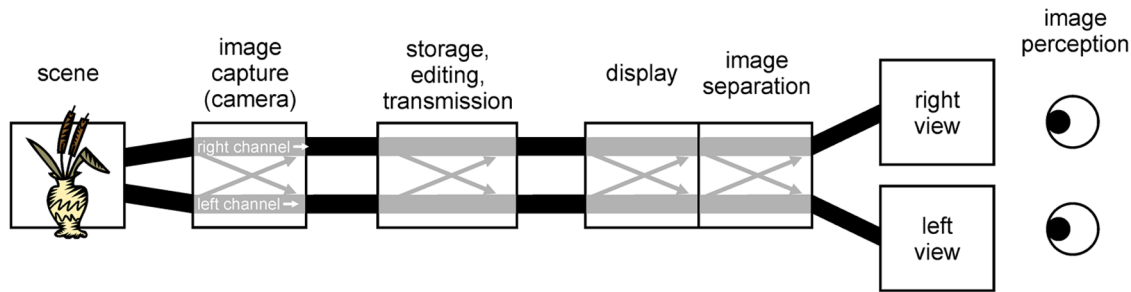


Fig. 3 A flow diagram showing the transfer of stereoscopic images from image capture through to image viewing and perception by the observer. Crosstalk between the left and right image channels can occur in the capture (camera) stage, storage/editing/transmission stage, image display (light generation), and image separation (3D glasses or autostereoscopic optical layer) stages. Most crosstalk usually occurs in the display and image separation stages.

In addition to the attributes listed above, the optical performance of the LC cell also varies with viewing angle through the cell. The best performance is usually achieved when the visual angle is perpendicular to the cell and drops off as the viewing angle varies from perpendicular.

There can also be considerable variability in the optical performance of the LC shutter between various makes of shutter glasses. Figure 5 provides an example of the performance of eight different pairs of shutter glasses and highlights the large differences possible. These optical differences can also affect crosstalk performance.

Next it is necessary to consider how the shutters operate in coordination with the sequence of the displayed left and right images. Figure 6 provides an illustration of how a pair of shutter glasses interacts with the image output sequence of a theoretical time-sequential stereoscopic display. Figure 6(a) provides an illustration of the light output of the left-right image sequence, with around 1 millisecond of blanking time between images. Figure 6(b) shows the transmission response of the left-hand LC shutter (the green response from Fig. 4). Figure 6(c) is an illustration of the image intensity that the left-eye will see when viewing the display through the shutter glasses. The intensity of the desired image (signal) is indicated in green and it can be seen that the intensity of the beginning of the left image is reduced because of the long rise-time of the shutter. The intensity of the undesired image (leakage) is indicated in red—in this

case this represents the intensity of the right image as seen by the left eye caused by the shutter not fully switching to 0% transmission in the opaque state. The amount of crosstalk illustrated in Fig. 6(c) is approximately 7% (calculated by dividing the red area by the green area—assuming a zero black level display).

Another aspect to consider in reference to Fig. 6 is that if the shutters switch too early or too late relative to the sequence of displayed images, the incorrect image will be gated to each eye, hence causing crosstalk.

Another item to note in the example of Fig. 6 is that the transition of the left LC shutter from open to closed occurs within the blanking interval between the display of the left and right images. The presence of a blanking interval is useful in helping to hide the transition of the LC shutters. Some displays don't have a blanking interval, which can compromise crosstalk performance.

Very few stereoscopic displays are able to achieve the theoretical time-sequential display output illustrated in Fig. 6(a)—Digital light projection (DLP) or organic light emitting diode (OLED) displays come close to this performance, but there will typically be three deviations from this ideal performance:

- **Image persistence.** In cathode ray tube (CRT) and PDP displays, the phosphors which emit light have an exponential decay in light output from when they are first energized, meaning that the image on the

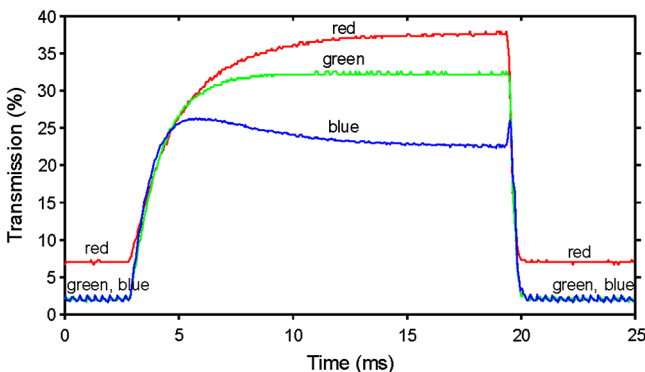


Fig. 4 The transmission versus time response of an example pair of active shutter glasses at red, green and blue wavelengths (measured using red, green and blue light emitting diode (LED) continuous light sources).⁴⁶

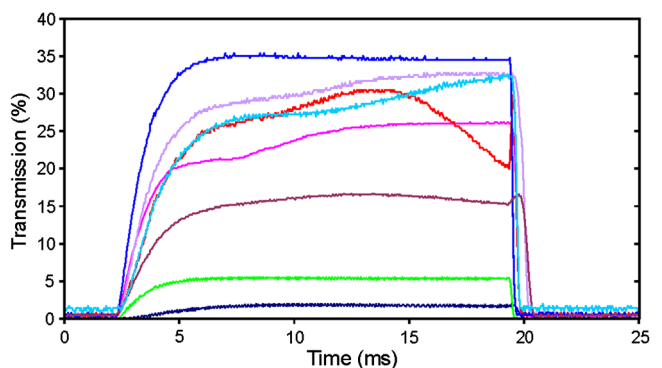


Fig. 5 The transmission versus time response of a selection of different LCS glasses at green wavelengths (measured using a green LED continuous light source). There can be a wide variability of performance between different shutter glasses.⁴⁶

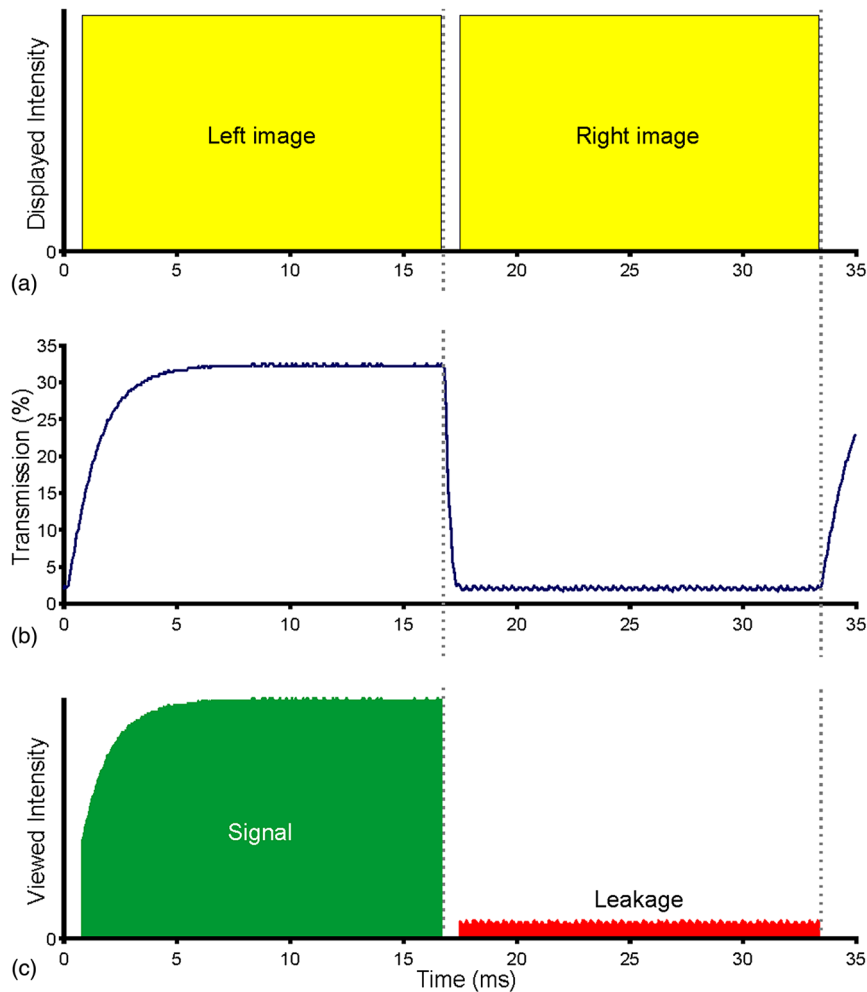


Fig. 6 An illustration of how a pair of shutter glasses interacts with the left/right image sequence of a theoretical time-sequential stereoscopic display. (a) The sequence of left and right images output by a theoretical display with instantaneous pixel response. (b) The transmission versus time of the left-eye LC shutter. (c) The image intensity as viewed through the left-eye of the LC glasses.

display persists for a nominal period of time.^{46,47} Displays which exhibit long image persistence will typically exhibit more crosstalk because light from one frame is still being output during the period of the following frame.

- **Pixel response rate.** In LCDs it takes a measurable period of time for a pixel to change from one gray level to another and this is referred to as the pixel response rate.⁴⁸ A display with a slow pixel response rate will typically exhibit more crosstalk than a display with a fast pixel response rate.
- **Image update method.** This term describes the way in which the screen is updated from one image to another. In some displays, new images are scanned or addressed from the top to bottom (e.g., CRTs⁴⁶ and LCDs⁴⁸), whereas some displays update all pixels on the screen at the same time (e.g., DLPs⁴⁹ and PDPs⁴⁷). In simple terms, it will be easier to synchronize a shutter to a display whose pixels all update at the same moment. When shutter glasses are used with a scanned display, the amount of crosstalk present will usually vary with screen position due to the different phase of the

switching of the shutter relative to the time the pixels change at different screen coordinates.

These display performance attributes will affect crosstalk performance by varying amounts as will be discussed in more detail in Secs. 4.1.1 through 4.1.4 in relation to specific display technologies.

In summary, the methods by which crosstalk can occur in systems using shutter glasses are:

- The optical performance of the liquid crystal cells—the amount of transmission in the opaque state, the rise-time, the fall-time, and the amount of transmission in the clear state.
- The relative timing (synchronization) of the glasses with respect to the displayed images.
- The angle of view through the liquid crystal cells—the optical performance of the cells usually falls off with viewing angles which are off perpendicular.
- The temporal performance of the particular display being used and how this interacts with the temporal performance of the shutters.

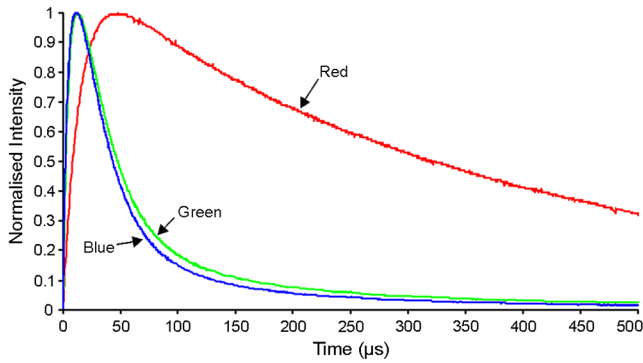


Fig. 7 Phosphor intensity versus time response for the three phosphors of a typical cathode ray tube (CRT) display.⁴⁶

The display-particular aspects will now be discussed in Secs. 4.1.1 through 4.1.4.

4.1.1 Time-sequential 3D on CRTs

CRT displays were the first display technology to be used with liquid crystal shutter glasses when they were introduced in the 1980s so that is where we will start our discussion. CRTs generate an image by scanning an electron beam over a phosphor-coated surface on the inside the screen. As the electron beam is scanned across the display surface from top to bottom, the phosphors emit light as they are hit by the electron beam and exponentially decay over time, as illustrated in Fig. 7. In this figure it can be seen that the red phosphor has a longer decay (persistence) than the green and blue phosphors. CRT displays are considered to be an impulse-type display because the displayed image is generated by a series of pulses of light.⁵⁰

The interaction of shutter glasses with the light output of a CRT is illustrated in Fig. 8. As the electron beam energizes the phosphor it outputs a peak of light which then decays exponentially (exaggerated here for illustrative purposes). This figure considers the leakage from the left-image channel into the right-eye view, so the phosphor is shown energized during the left-eye period when the right-eye shutter is closed. When the right-eye shutter opens during the second vertical blanking interval (VBI2), the phosphor is still outputting some light from the previous image period—particularly for pixel positions at the bottom of the screen, which are energized shortly before VBI2. The bottom of Fig. 8 illustrates the amount of light leakage from the left image channel into the right-eye view—the area under the solid red curve from end of the first vertical blanking interval (VBI1) to the start of VBI2 represents leakage due to the incomplete extinction of the shutter, and the area under the solid red curve from start of VBI2 onwards represents leakage due to long phosphor persistence.

Figure 9 illustrates the spatial variation of crosstalk on a time-sequential CRT display. CRTs will exhibit more crosstalk at the bottom of the screen because phosphors at the bottom of the screen will be energized soon before the shutter is opened for the other eye and therefore more of that phosphor’s decay tail will be visible to the other eye.

With time-sequential 3D on a CRT, the important factors which cause crosstalk^{13,46,51} are therefore:

- the performance of the liquid crystal cells in the shutter glasses (see Sec. 4.1),
- the amount of phosphor persistence—the time that it takes for the phosphors to stop glowing after they have been energized (see Fig. 7) (Long phosphor persistence will cause more crosstalk because the light

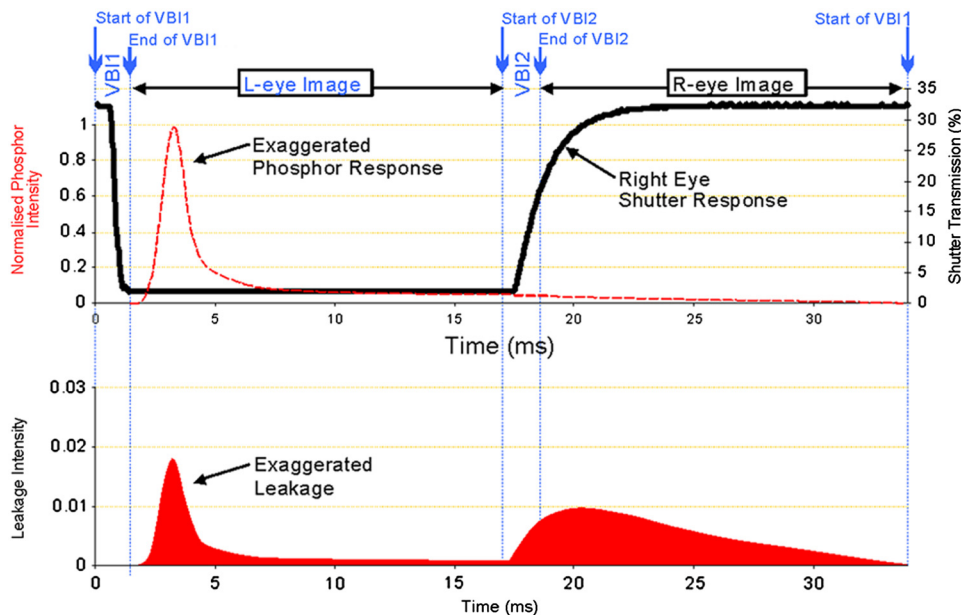


Fig. 8 Illustration of crosstalk on a cathode ray tube (CRT) (with exaggerated phosphor response for illustrative purposes).⁴⁶ Top: phosphor response and shutter response. The phosphor is energized during the first frame (L-eye) period, when the shutter is closed, and exponentially decays. Bottom: multiplication of phosphor response by the shutter response to give the amount of leakage. The area under the solid red curve from end of VBI1 (vertical blanking interval) to the start of VBI2 represents crosstalk due to the incomplete extinction of the shutter, and the area under the solid red curve from start of VBI2 onwards represents crosstalk due to long phosphor persistence.

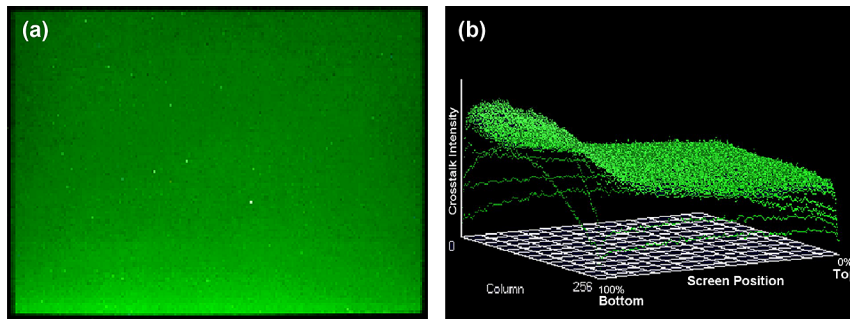


Fig. 9 Illustration of spatial variation of crosstalk on a cathode ray tube (CRT), with increased crosstalk at the bottom of the screen: (a) actual screen photograph of CRT crosstalk through a pair of active shutter glasses, and (b) histogram of measured CRT crosstalk.⁴⁶

from the first frame is still being output during the period of the following frame),

- the timing of the shuttering of the glasses with respect to the display of images on the screen—it is important that the switching of the shutters occurs during the vertical blanking interval (VBI) to minimize crosstalk (see Fig. 8), and
- the x - y coordinates on the screen—the bottom of the screen will exhibit more crosstalk than the top of the screen due to the way that the electron beam scans the display from top to bottom (see Fig. 9).

4.1.2 Time-sequential 3D on PDPs

PDPs with time-sequential 3D display capability were first experimentally demonstrated in 1998^{52,53} and first commercially released in 2008 by Samsung.⁵⁴ PDPs generate light using phosphors which are energized up to 10 times per frame (see Fig. 10). These 10 pulses (subframes) per frame have different durations (sustain time) and hence luminance, in a binary sequence from longest duration to shortest duration. Different gray levels are achieved for each pixel by firing or not firing the phosphors for each pixel in none, some, or all of the 10 subframes per frame. This is quite different from the way that gray-levels are produced on a CRT which has analog control over the intensity of the pulse of light from the phosphors, whereas with a PDP each individual pulse of light per pixel per subframe can only be on or off—there is no in-between. Therefore, ten individual pulses of pre-determined intensity are fired selectively to collectively produce different gray levels.⁴⁷

With further reference to Fig. 10, it can be seen that the phosphors in PDPs also (like CRTs) exhibit an exponential decay in light output after they have been energized—this is particularly visible in the period between 16 ms and 33 ms with the red and green color channels. Figure 11 illustrates the interaction of shutter glasses with the light output of another conventional PDP display (different than Fig. 10). In Fig. 11(a) it can be seen that the long phosphor persistence from 17 ms onwards causes there to be light output from the previous frame when the right shutter opens which will in turn cause crosstalk. Figure 11(b) illustrates the relative intensity of the signal (left image channel into the left-eye view) and leakage (left image channel into the right-eye view) components. Additionally, the area under the red leakage curve from 0 to 17 ms represents leakage due to the incomplete extinction of the shutter, and the area under

the red leakage curve from 17 ms onwards represents leakage due to long phosphor persistence.

With time-sequential 3D on a PDP, the important contributors to crosstalk⁴⁷ are therefore:

- the performance of the liquid crystal cells in the shutter glasses (see Sec. 4.1),
- the amount of phosphor persistence—the time that it takes for the phosphors to stop glowing after they have been energized (see Fig. 10),
- the timing of the shuttering of the glasses relative to the display of images on the screen (see Fig. 11), and
- the particular gray level value of a displayed pixel and therefore which subframes are fired—a subframe fired immediately before the transition point will dump more light into the following frame due to phosphor persistence than for a subframe which is fired earlier whose phosphor persistence will have had more time to decay before the next frame (see Fig. 11).

Crosstalk does not vary with screen position on PDPs except where the visual angle through the shutter glasses might be non-perpendicular for viewing the corners of the screen.

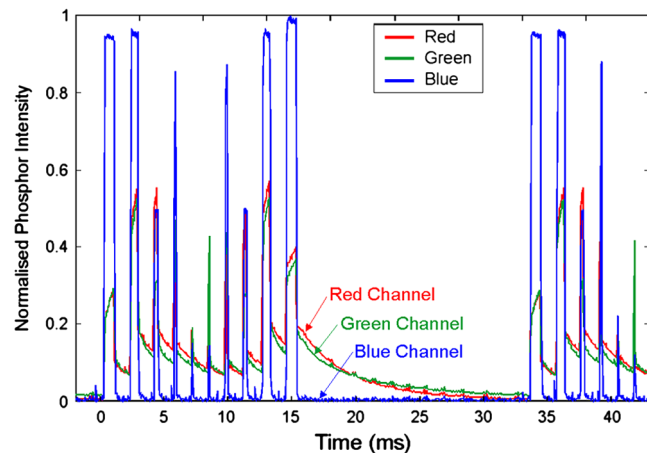


Fig. 10 The time-domain light output of an example plasma display (showing alternating frames of 100% white and black). The vertical axis is the normalized phosphor intensity.⁴⁷ This graph illustrates the 10 pulses per frame used to construct images with various gray levels and the long phosphor persistence of the red and green channels (of this particular display).

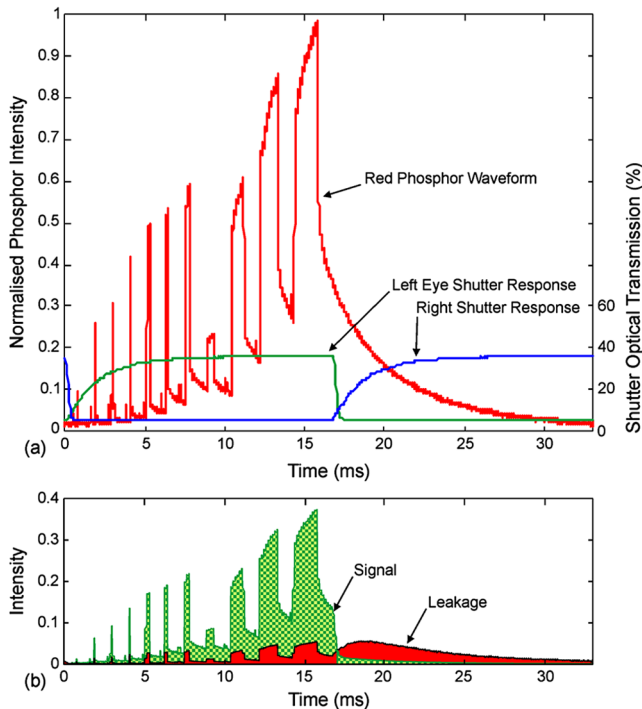


Fig. 11 Timing diagram showing the relative timing of a pair of shutter glasses being used to view a time-sequential 3D image on an example conventional PDP display (a different display than Fig. 10). Part (a) shows the time-domain transmission of the left and right shutters along with the time-domain light output of the display (showing alternating frames of 100% red and black). Part (b) shows the intensity of light through the shutters as will be viewed by the left and right eyes. The desired signal to the left eye through the shutter glasses is shown in hatched green, and the leakage to the right eye through the shutter glasses is shown in solid red.⁴⁷ This figure shows severe crosstalk for illustrative purposes and is not intended to be representative of all 3D PDPs.

It should be noted that the examples of Figs. 10 and 11 are derived from older conventional non-3D-Ready PDPs—newer 3D-Ready PDPs will typically exhibit less phosphor persistence and use better shutter glasses than shown in these figures, and also operate at 120 fps with a resultant fewer subframes per frame.

4.1.3 Time-sequential 3D on LCDs

Liquid-crystal displays (LCDs) generate an image by back-lighting an LCD panel containing an array of individually addressable cells (usually three cells for each pixel—one for each of red, green and blue color primaries). Each LC cell gates the light from the backlight, either passing light, blocking light or somewhere in between for different gray levels. Traditionally, the backlight in LCDs has been based on a cold-cathode fluorescent lamp (CCFL) but light emitting diode (LED) backlights are now increasingly being used. The light source for an LCD projector may be a metal-halide arc lamp, LED, or laser. Conventional LCDs are known as a hold-type display because they output light for the entire frame period.⁵⁰

Figure 12 illustrates the light output of a conventional (non-3D-Ready) LCD monitor driven with a video signal alternating between white and black frames—a common time-sequential 3D test signal. The green line indicates the

row of pixels of the display that is being addressed (updated) as time progresses—starting at the top of the screen and scanning down to the bottom in the period of one frame. Looking horizontally from a point on the green line, it can be seen that as each pixel is addressed to change (either from black-to-white, or white-to-black) the pixels at that row take a finite period of time to change from one state to another—this is known as the pixel response time, as discussed in Sec. 4.1 in relation to LC shutters. The scanned image update method of a conventional LCD presents some problems for the use of the time-sequential stereoscopic display method, namely there is no time period available when one frame is visible exclusively across the entire display—this can be seen by referring to Fig. 12 and considering a vertical sector of the graph at a particular time. For example, it can be seen that at 8 ms, the top of the screen will be one frame (white), the bottom of the screen will be the previous frame (black) and a horizontal band in the middle of the screen will be a mix of both frames—this is obviously an unsuitable time to open the shutter. The closest moment to having a single frame visible across the entire screen is at 15 ms, however, there is still some darkening of the display at the very top and bottom (indicating some crosstalk), and additionally this is only for a very short instant (a much longer time period is necessary).⁴⁸

Starting in 2009, a new class of 3D LCD monitors was commercially released which successfully supported the time-sequential 3D method.⁵⁵ This was achieved primarily by modifying (increasing the speed of) the image update method—either by increasing the frame rate, or increasing the vertical blanking interval, or both.^{48,56-59}

Figure 13(a) illustrates the light output of an example time-sequential 3D LCD monitor or TV using a modified image update method—driven with a video signal alternating between white and black frames. In this figure, the green line (indicating the row of pixels on the display which is being addressed at one point in time) can be seen to complete the full screen update in a much shorter time period, leaving part of the frame-period for the image to stabilize and show a full image across the entire display. For example, in Fig. 13(b), the highlighted period indicates the period when the shutters of a pair of active shutter glasses could be timed to open to

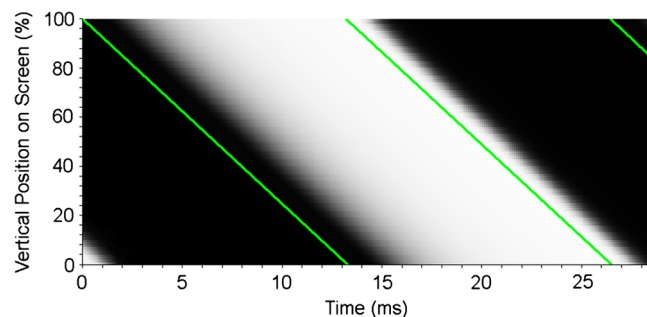


Fig. 12 Time domain response of a conventional LCD monitor with a 4% vertical blanking interval between alternating black and white frames at 85 fps. The vertical axis represents the vertical position on the screen with 100% being the top of the screen and 0% being the bottom of the screen. The green line represents the time at which a particular row of pixels is addressed (updated). It can be seen that there is no time period when a white frame is visible across the entire display (by considering a vertical sector of the graph at a particular time).⁴⁸

present a stereoscopic image, however the gray tinting at the bottom of this area indicates that some crosstalk will still be present. Technologies such as black frame insertion (BFI) and modulated (or scanned) backlight can also be used with LCDs to improve 3D performance.⁵⁶

With time-sequential 3D on an LCD, the important contributors to crosstalk are therefore:

- the performance of the liquid crystal cells in the shutter glasses (see Sec. 4.1);
- the specific timing of the image update method on the screen (see Figs. 12 and 13) including the effects of BFI, increased frame rate, and/or modulated backlight;
- the pixel response rate of the LCD (black-to-white, white-to-black, and gray-to-gray);
- the timing of the shuttering of the glasses with respect to the display of images on the screen (see Fig. 13) including the duty cycle of the shutters;
- the particular gray level value of a displayed pixel (pixel response rate varies with the input and output pixel gray level—small changes in gray level often take the longest to complete);²⁸ and
- the x - y position on the screen—depending upon shutter timing, the top and bottom of the screen may exhibit more crosstalk than the middle of the screen (see Fig. 13).⁴⁸

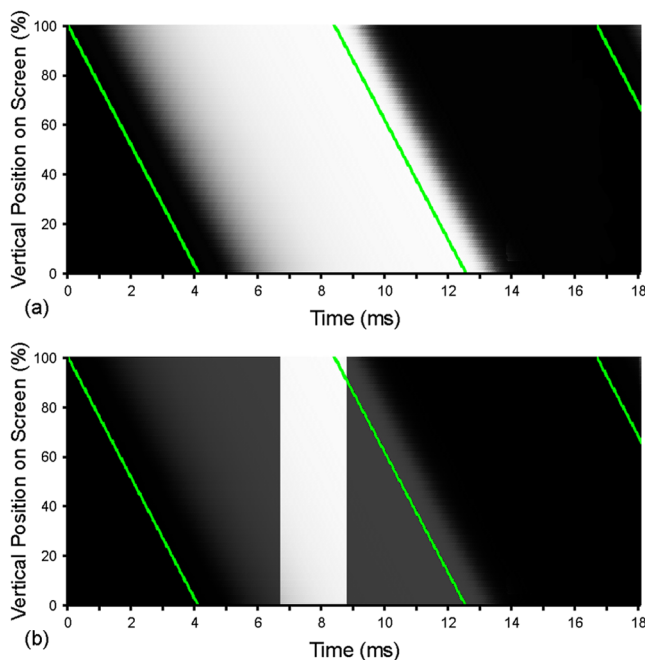


Fig. 13 (a) Time domain response of a simulated time-sequential 3D LCD monitor with a fast addressing rate and fast pixel response rate. Note that the entire screen is updated in only 4.2 ms (the time period of the green line) versus 13 ms with a conventional LCD (Fig. 12). (b) The same monitor as (a) being viewed through shutter glasses with reduced duty cycle switching (the response rate of shutters are not shown).⁴⁸ The highlighted period between 6.7 ms and 8.8 ms is almost exclusively white, which means one of the views will dominate, but there is a bit of gray tinting at the bottom of this area, which suggests some crosstalk will be evident at the bottom of the screen.

4.1.4 Time-sequential 3D on DLPs

DLP projectors and DLP rear-projection TVs work by shining a light source (e.g., a metal halide arc lamp or LEDs) onto a DMD (digital micro-mirror device—an array of tiny mirrors that can each be individually commanded to tilt $\pm 12^\circ$ at very fast speeds). The reflection off the DMD is sent through a lens and focused on a screen and each mirror on the DMD corresponds to one pixel on the screen. In single-chip DLP projectors, a color-sequential technique is used to achieve a full-color image⁴⁹ as illustrated in Fig. 14. DLPs operate most like a hold-type display—except that gray levels are achieved by a duty cycle modulation process and it is also possible to introduce a blanking interval between frames.⁶⁰

With reference to Fig. 14 it can be seen that the right perspective image is displayed over the period 3 to 8.5 ms with an approximately 3 ms blanking interval before and after the image display period. The blanking interval provides a period during which the left and right shutters in the active shutter glasses can stabilize after state change before light is displayed on the screen for the left and right eyes.

DLPs have very good performance characteristics for time-sequential 3D display—in essence there is no crosstalk introduced by the actual DLP display itself.⁴⁹ This is due to two key points: there is no phosphor decay (the DMD mirrors can switch completely from one state to another in $\sim 2 \mu\text{s}$),⁶¹ and the entire image changes from one frame to the next at effectively the same time. Crosstalk does not vary with screen position with DLP displays—except where the viewing angle through the shutter glasses might be different for viewing different parts of the screen. Ordinarily the only crosstalk present with time-sequential 3D on DLP is due to the performance of the shutter glasses. It is also important that the video electronics path in the DLP display does not mix the left and right images and presents the images in a correct left/right image sequence,⁴⁹ but this is now fairly standard with a wide range of 3D DLP projectors and TVs available commercially.

The important factors that cause crosstalk with time-sequential 3D on DLP displays are therefore:

- the performance of the liquid crystal cells in the shutter glasses (see Sec. 4.1),
- the timing (and phase) of the shuttering of the glasses with respect to the image display sequence on the screen (if the LC shutters switch at the wrong time, the glasses can direct images to the wrong eye and hence cause crosstalk), and
- the duration of the blanking interval (the blanking interval should ideally be long enough to hide the transition time of the LC shutters).

4.2 Polarized 3D Projection

Polarization is an optical property of light that can be used to encode separate left and right images for presentation to the two eyes of an observer for stereoscopic display purposes.⁶² Conceptually, the simplest method of achieving polarized 3D projection involves the use of two projectors, a polarizer fitted to the front lens of each projector, a silvered screen, and matching polarized 3D glasses for the audience. The polarizers can either be linear polarizers or circular polarizers.⁶²

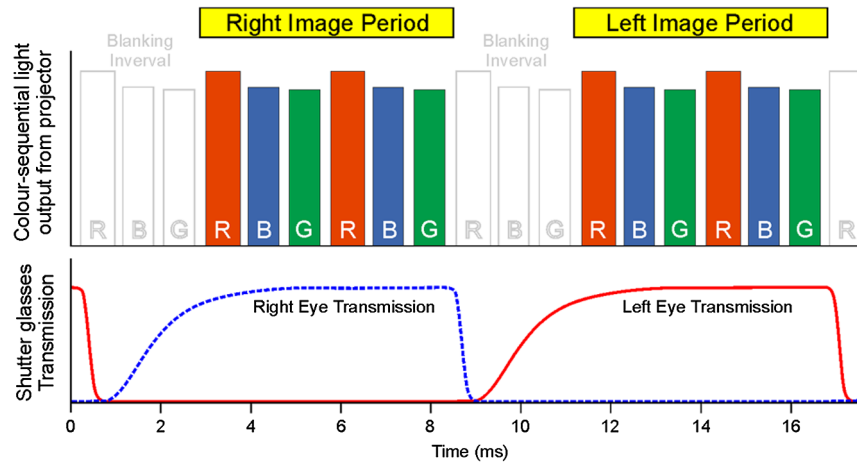


Fig. 14 Illustration of the time-domain performance of an example 120 Hz 3D single-chip digital light projection (DLP) projector. In this figure, a stereoscopic image pair is being presented at 120 frames per second (60 frames for the left and 60 for the right in alternating sequence) and viewed using a pair of shutter glasses. The top of the figure shows the sequence of left and right images built up by a red, blue, green color sequence to construct a full-color image. The bottom half of the figure shows the optical transmission of the shuttering eyewear which must synchronize correctly with the sequence of left and right images. This particular projector is operating with a 6x color cycle speed [6 RGB color cycles per 60 fps frame period (16.7 ms)] and in this case one color cycle per left/right frame period is extinguished to create a blanking interval.

For stereoscopic display purposes the left image channel is encoded with one polarization state, and the right image channel will be encoded with an orthogonal polarization state (for example +45 deg and -45 deg, or 0 deg and 90 deg for linear polarizers; or left-handed and right-handed for circular polarizers). Ideally the left and right image channels will be maintained separately, but due to various limitations of the filters, some leakage will occur between the channels and cause crosstalk.

Polarizing filters are not perfect devices and unfortunately do not perfectly polarize the light that passes through them, which is an avenue for the presence of crosstalk. Figure 15 illustrates the optical performance of an example linear polarizer filter. The key factor to consider for establishing the amount of crosstalk that will be present due to imperfect polarizers is the amount of light that passes through a pair of crossed polarizers [indicated by the transmission crossed (T_c) curve in the figure] compared to the amount of light that passes through a pair of parallel polarizers (T_p in the figure). In this example, the amount of light passed in the crossed polarizer state is very low, which would indicate the potential for very low crosstalk. Figure 16 illustrates the optical performance of an example circular polarizer. In this case, the “double pass reflected” curve provides an indication of the amount of crosstalk to be expected, which is higher than the linear polarizer example of Fig. 15.

These examples are indicated for perfectly orthogonal projection polarizers and perfectly oriented decoding polarizers, however, in a real-life situation the orientation of the decoder polarizers in the glasses may not perfectly match the orientation of the projector polarizers (e.g., due to head tilt or improperly worn glasses) which will adversely affect crosstalk performance.⁶⁵ Circular polarizers are less sensitive to rotational misalignment between encoder and decoder polarizers than linear polarizers, but are still adversely affected—the orientation of the rear linear layers must match for optimal performance.

Projection screen properties can also affect crosstalk performance. Different screen materials have different polarized light preservation properties⁶⁶ and front projection screens

have different polarization performance characteristics compared to rear-projection screens. The quality of the preservation of polarization of light of the screen will affect crosstalk performance.

In summary, the factors which affect crosstalk in dual-projector polarized 3D projection systems are:

- the optical polarization quality of the polarizers,
- the polarization preservation properties of the projection screen, and
- incorrect orientation of the coding or decoding polarizers (perhaps due to head tilt).

Polarized 3D projection can also be achieved time-sequentially with the use of a polarization modulator (as used by StereoGraphics/RealD,⁶⁷ NuVision,⁶⁸ and DepthQ⁶⁹), or a circular polarization filter wheel (as used by MasterImage⁷⁰). In these systems, the polarization modulator (or filter wheel) is configured to switch between two

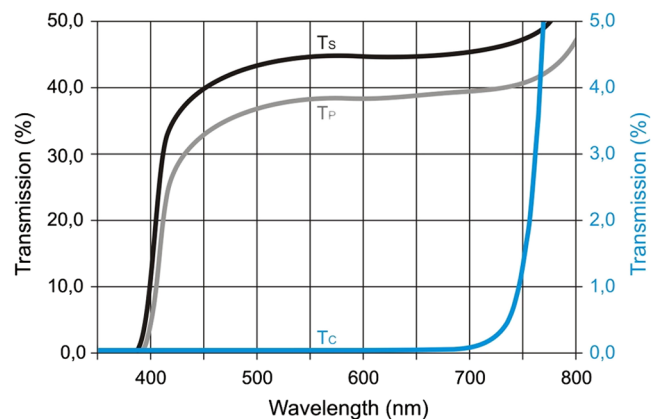


Fig. 15 Spectral response of an example linear polarizer in single T_s , parallel T_p and crossed T_c configurations.⁶³ The blue “crossed” curve is a close approximation of the amount of leakage that will occur between two linear polarized channels of a polarized stereoscopic display (excluding the effect of head tilt and screen depolarization).

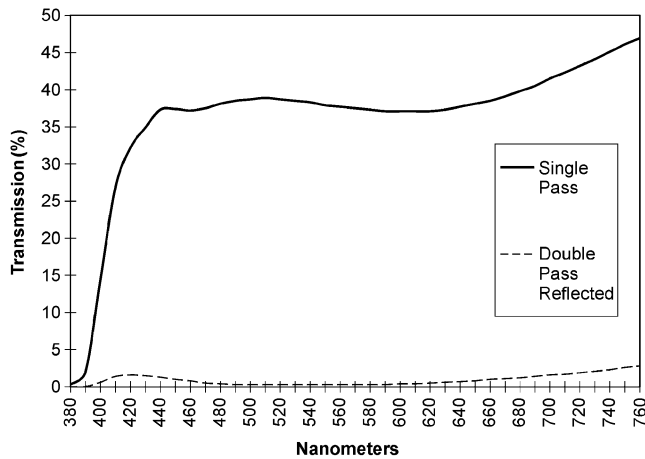


Fig. 16 Spectral response of single and “crossed” circular polarizers.⁶⁴ The dashed curve is a representation of the amount of leakage that will occur between two circular polarized channels of a polarized stereoscopic display due exclusively to the polarization quality of the polarizers.

orthogonal polarization states in synchronization with the sequence of left and right images output by the display. There are two additional factors which can affect crosstalk performance^{57,71} in these systems, namely:

- the phase and temporal performance of the polarization modulator with respect to the image sequence of the display, and
- the optical polarization quality of the polarization modulator.

4.3 Micro-Polarized 3D LCDs

Micro-polarized 3D LCD monitors (also known as micro-pol, μ Pol, Xpol, film patterned retarder, or FPR) work by the application of a special optical filter to the front of a conventional LCD panel in order to polarize odd-numbered rows of pixels with one polarization state, and even-numbered rows with the opposite polarization state (see Fig. 17).⁷² The two polarization states may either be two orthogonal linear polarization directions, or circular polarization (left-handed circular for one eye and right-handed circular for the other eye)—circular is the most commonly used in commercially available products currently. When the observer wears the appropriate 3D glasses, one eye will see the odd-numbered rows and the other eye will see the even-numbered rows.

Micro-polarized 3D LCD monitors have the advantage that they are viewed using lightweight passive polarized 3D glasses, but have the disadvantage that the vertical spatial resolution per eye is half that of the full display resolution. The construction of a micro-polarized 3D display is illustrated in Fig. 18, where it can be seen that micro-polarizer film is usually applied to the face of the LCD monitor at the viewer side of the LCD optical stack. There is sensitivity of the viewing position of the observer caused by the micro-polarizer film and the LCD cells being separated by a glass layer that is usually approximately 0.5 mm thick. As shown in Fig. 18, if the observer is positioned correctly, the micro-polarizer rows line up correctly with the rows of LCD pixels, however, if the observer were to view the

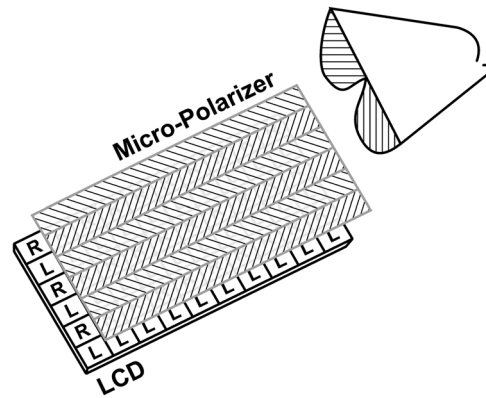


Fig. 17 The optical layout of a micro-polarized 3D LCD. A micropolarizer layer over the front of the LCD polarizes alternate rows of pixels into two different polarization states.^{73,74} In this example an observer wearing a pair of polarized 3D glasses will see the odd-numbered rows of pixels through the right eye, and the even-numbered rows of pixels through the left eye.

display from a different vertical viewing position, a parallax error would be introduced since the micro-polarizer rows would not correspond correctly with the underlying LCD pixels rows, and hence crosstalk would be introduced. A parallax error also exists if the observer views the display from a different viewing distance. Several methods have been developed to reduce or eliminate the viewing position sensitivity, including the use of a black mask between micro-polarizer strips (this method is usually called X-Pol) and in-cell micro-polarization.⁷⁵

With a micro-polarized 3D LCD, the factors that contribute to crosstalk are therefore:

- the optical polarization quality of the micro-polarizer film and hence the polarization quality of the two polarization states;
- the orientation,⁶⁵ optical polarization quality, and optical match of the polarized 3D glasses to the output polarization of the display;
- the accuracy of the alignment of the micro-polarizer strips to the rows of pixels on the display;
- the pitch of the micro-polarizer strips relative to the pitch of rows of pixels on the display and the distance between the LCD cells and the micro-polarizer film (usually determined by the thickness of the front glass layer)—which will determine the optimum viewing distance;
- the presence (or absence) of a black mask between micro-polarizer strips—the presence of black mask improves the size of the viewing zones but at the sacrifice of screen luminance;
- the x - y pixel position on the screen—different areas of the screen may exhibit more crosstalk than others;
- the viewing position of the observer—most current micro-pol monitors are highly sensitive to vertical viewing position, and also sensitive to the viewing distance from the monitor;¹⁷ and
- the horizontal viewing angle of the observer—viewing angles off perpendicular can affect the polarization performance.⁷⁷

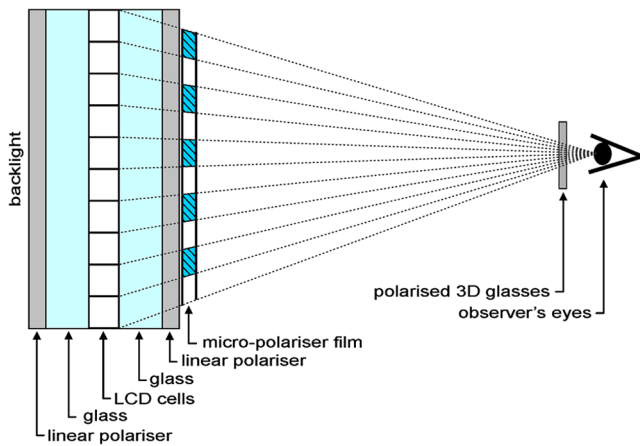


Fig. 18 The side view of a micro-polarized 3D LCD monitor showing the arrangement of the optical layers.⁷⁶ It can be seen that the display is sensitive to vertical viewing position since in the indicated viewing position, the micro-polarizer strips line up precisely with the LCD pixels behind them (indicated by the dotted lines), but from a different viewing height the micro-polarizer strips will not optically overlap with the same rows of LCD pixels as the viewing position shown in the diagram, which will lead to crosstalk between the two stereoscopic image channels.

4.4 Autostereoscopic Displays

A wide range of technologies are used to achieve autostereoscopic displays (3D without special eyewear). The most common autostereoscopic technologies in current use are based on lenticular⁷⁸ and parallax barrier⁷ technologies, which both make use of an optical element to direct multiple perspective views in different angular directions out of the display. With reference to Fig. 19, a lenticular autostereoscopic display uses a special lenticular lens sheet containing an array of (usually) vertical column convex lenses placed over the face of the monitor, whereas a parallax barrier autostereoscopic display has a vertical barrier grid (consisting of an alternating series of opaque black vertical strips and clear gaps) placed over the face of the monitor (or in some cases behind the display LCD⁷⁹). If the observer's eyes are located in the correct sweet spots of the display (indicated by the gray diamond shaped polygons in Fig. 19), the observer should be able to see an optimal stereoscopic image across the entire display with minimal crosstalk. If the observer's eyes move away from the sweet spots, a measurable amount of view mixing will occur and this will be visible as crosstalk. Head or eye tracking can be used to steer the views such that the observer's eyes are always in the correct sweet spot, but this is not available with all autostereoscopic displays. In addition to two-view autostereoscopic displays (as illustrated in Fig. 19), multiview autostereoscopic displays are also possible which send out a multitude of views out of the display.⁸⁰

The geometry of the optical element in relation to the display panel will determine the geometry of the view output of the autostereoscopic display, and hence the location of the sweet spots. The properties which determine the view geometry of the autostereoscopic display are the pitch, thickness, curvature and refractive index of the lenticular lens array;⁷⁸ the pitch, mounting distance, aperture width, and aperture design of the parallax barrier;⁷ all in relation to the display properties of pixel pitch, fill factor, and sub-pixel

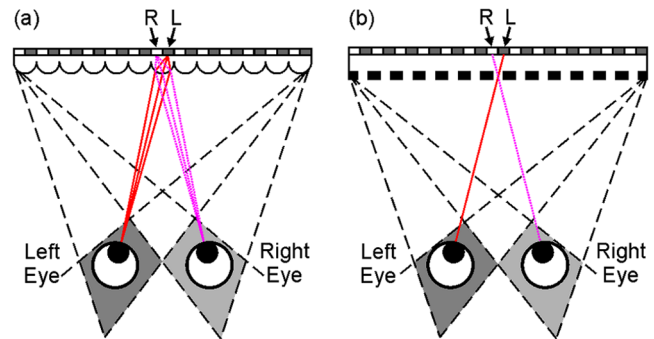


Fig. 19 Example configuration of (a) two-view lenticular autostereoscopic display and (b) two-view parallax barrier autostereoscopic display (top view). The optical elements ideally act to allow the left eye to see only the left image pixels, and the right eye to only see the right image pixels. The 'sweet spots' where this optical isolation works best are shown in gray.

arrangement. These properties not only determine the location and geometry of the sweet spots but also the amount of crosstalk present in the optimal viewing position(s). Additional factors that can affect crosstalk performance are the general optical quality of the lenticular lens or parallax barrier as well as diffraction⁷ and possibly chromatic aberration effects.⁸¹

An illustration of the optical output of a lenticular multi-view autostereoscopic display is provided in Fig. 20 for an example slanted lenticular multi-view autostereoscopic display.⁸⁰ The relative luminance of each view is plotted for a selection of observation positions across the display from a range of viewing positions (simulating a person moving from side to side), at a pre-determined viewing distance. It can be seen in this particular example display the mixing of views is considerable, even at the sweet spot locations, which will be visible as crosstalk.

In summary the important causes of crosstalk in lenticular and parallax barrier autostereoscopic displays are:

- the geometry and optical quality of the optical element (lenticular lens or parallax barrier) including:
- the accuracy of alignment of the optical element to the layout of pixels on the display including the alignment angle of the lens/barrier;
- (for lenticular autostereoscopic displays) the pitch, thickness, curvature and refractive index of the lenticular lens sheet;
- (for parallax barrier autostereoscopic displays) the pitch, mounting distance, aperture width and aperture design of the parallax barrier;
- the pitch, fill factor, and RGB sub-pixel layout of the display;
- the viewing position (in x , y , and z directions) of the observer(s); and
- the x - y pixel position on the screen—different areas of the screen may exhibit different levels of crosstalk.

Other types of autostereoscopic displays will have additional and different mechanisms of crosstalk generation than those listed above.

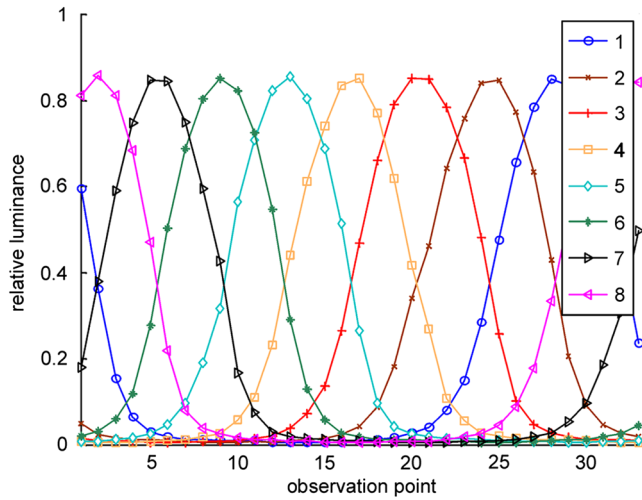


Fig. 20 The visibility of different perspective views as output by an example lenticular multi-view autostereoscopic display when viewed from different horizontally spaced observation points.⁸⁰ For example, from viewing position (observation point) 20, view 3 is dominant, but some of views 2 and 4 are also visible which causes crosstalk. This figure shows severe crosstalk for illustrative purposes and is not intended to be representative of all modern autostereoscopic displays.

It has been proposed that some crosstalk is advantageous to the operation of multi-view autostereoscopic displays in order to hide abrupt switches between views when the observer moves from one sweet spot to another.⁸² In this case, some crosstalk at view boundaries would be considered desirable, but crosstalk between views at sweet spot locations would be undesirable. This is different to the way crosstalk is considered with other stereoscopic displays, where all crosstalk is usually considered undesirable.

4.5 Anaglyph 3D

Anaglyph 3D displays work by coding the left and right image channels into complementary color channels of the display and viewing the display through glasses that have color filters matched to these colors (e.g., red for the left eye and cyan (blue + green) for the right eye).

The process of crosstalk in anaglyph 3D displays is illustrated in Fig. 21.¹⁵ If the spectrum of the display or glasses do not match well, crosstalk will occur. Ideally the spectral output of the display will have a narrow range of light output in the desired spectral range and very little light output out of this region. However, in reality, many displays have spectral output across a broad range of wavelengths—particular in the spectral range dedicated to the other eye. Similarly, in the ideal case, the spectrum transmission of the glasses will pass light in the desired spectral range (which corresponds with the peak output spectral range of the display) and zero transmission immediately out of this range. However, in reality, anaglyph glasses will usually have peak transmission in the desired spectral range with a gradual (slowly changing) reduction in transmission through to a low transmission spectral range which may not totally extinguish light in the undesired spectral range—see Fig. 21(b). These two non-ideal spectral performance aspects will mean that some light from one channel of the display will leak through the filter of the glasses for the other channel and

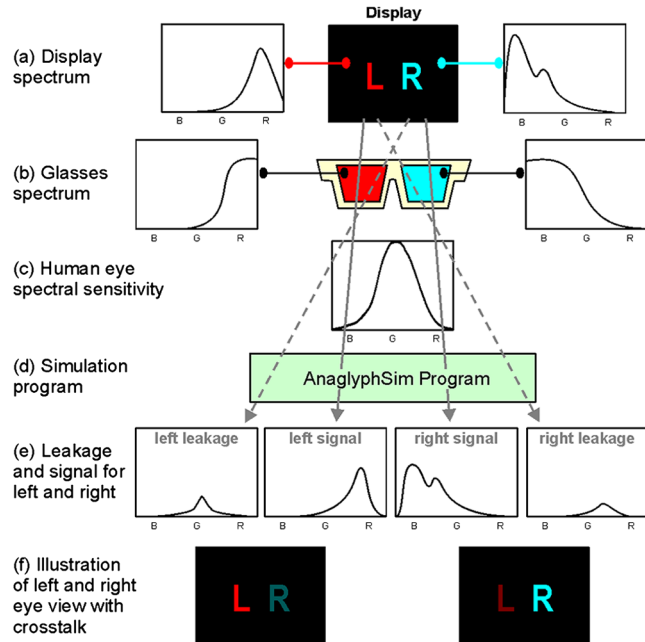


Fig. 21 Illustration of the process (and simulation) of crosstalk in anaglyph 3D displays. From the top: (a) Spectral response of display, (b) spectral response of anaglyph glasses, (c) human eye spectral sensitivity, (d) simulation of crosstalk using a computer program, (e) spectral output characteristic of crosstalk and intended image, and (f) visual illustration of left eye and right eye view with crosstalk.¹⁵

hence lead to crosstalk. There are a range of algorithms that can be used to generate the anaglyph image from a stereoscopic image pair,⁸³⁻⁸⁵ and in some circumstances some image mixing can occur during this stage, which can be interpreted as crosstalk.

With anaglyph 3D displays, the important factors that contribute to crosstalk are therefore:

- the spectral quality of the display,
- the spectral quality of the anaglyph glasses and how well it matches the spectral output of the display, and
- the properties of the anaglyph image generation algorithm.

Crosstalk in anaglyph 3D images generally does not vary with screen position or viewing angle, except where the spectral characteristics of the display or glasses change with viewing angle or screen position. Several papers have analyzed crosstalk in anaglyph 3D images.^{15,19,86,87}

The Infitec,⁸⁸ Dolby 3D,⁸⁹ and Panavision 3D cinema techniques are a special case of anaglyph and can be analyzed in a similar manner.

4.6 Zero Crosstalk 3D Displays

Some 3D displays are inherently free of crosstalk. There is no opportunity for image mixing to occur in 3D displays that have completely separate display channels for the left and right eyes. Examples of zero crosstalk 3D displays include the mirror stereoscope (originally developed by Sir Charles Wheatstone in 1838⁹⁰) and some HMDs (head mounted displays).⁹¹ Zero crosstalk 3D displays have been used to study the perception of crosstalk because they allow the amount of crosstalk to be simulated electronically from 0% to 100%.³³

4.7 Non-Display Related Sources of Crosstalk

It is important to note that crosstalk can also occur in the capture, storage, manipulation and transmission of stereoscopic images prior to arrival at the stereoscopic display. In this case the crosstalk can be caused by the mixing of the left and right images instead of keeping them separate and distinct.

For example, some image crosstalk is possible during stereoscopic image capture using the NuView 3D camera attachment⁹² or the prototype 3D lens adapter for the Canon XL-1 video camera.⁹³ In these examples the crosstalk occurs because the two imaging capture paths share a common optical path before they reach the single imaging sensor and the optical isolation of the two views in this common optical path is not perfect.

Another example is during stereoscopic image manipulation or storage. If a row-interleaved or anaglyph 3D image is stored in JPEG format, the left and right images can become mixed (because JPEG is a lossy compression method), resulting in image crosstalk. This type of crosstalk can be reduced or eliminated by avoiding the use of lossy compression of row-interleaved images, or in the case of anaglyph JPEGs, using the RGB color-space rather than the YUV color-space.⁹⁴

Steps should be taken to avoid crosstalk or image mixing in the stereoscopic source images before they are presented on the stereoscopic display.

5 Measurement of Crosstalk

Two methods exist for the measurement of crosstalk: optical sensors and visual measurement charts.

5.1 Optical Sensors

An optical measurement device, such as a photometer or a radiometer, can be used to measure crosstalk. The spectral sensitivity of the sensor(s) used should match the spectral sensitivity of the human visual system (photopic vision) so that the measurements are representative of what a human observer would see.⁹⁵⁻⁹⁷ Examples of sensors that have been used to measure crosstalk include: Integrated Photomatrix Inc. IPL10530 DAL photo-diode,⁴⁶ Ocean Optics USB2000 spectroradiometer,⁸⁷ Konica Minolta CS1000 spectroradiometer,⁶⁵ Konica Minolta CS-100 spot chroma meter,^{20,22} Eldim EZContrastMS,¹⁷ and Photo Research PR-705.⁹⁸ Many other devices can also be used for this purpose.

In the first instance, the optical sensor will be placed at the left eye position (either behind the left eye of the 3D glasses, or in the left eye viewing zone for an autostereoscopic display) and a series of measurements taken with a cross-combination of the image channels set at various specified levels. This is then repeated for the other eye position(s). In the case of black-white crosstalk, the two gray-levels will be black and white (see Sec. 2.2.2) and for gray-to-gray crosstalk a much greater number of measurements will be taken for a selection of gray-level combinations (Sec. 2.2.4). Crosstalk may also be characterized spatially across the display,^{99,100} or for different horizontal and vertical viewing angles,¹⁴ in which case the number of measurements can increase significantly, resulting in a much more complex crosstalk dataset—in which case the automation of the taking of the measurements can be advantageous.

Efforts to standardize crosstalk measurement methods are currently under way and being published by ICDM,¹⁴ IEC, ISO, and others.^{4,27} Ensuring the accuracy and reproducibility of crosstalk measurements between different measurement sensors, measurement methods and laboratories is an important problem and work is continuing in this area.^{99,101,102}

5.2 Visual Measurement Charts

Visual measurement charts provide a very quick and effective way of evaluating crosstalk in a stereoscopic display without the need for expensive optical test equipment. Two examples of such charts are shown in Figs. 22 and 23. The method of using the charts is to display the left and right panels of the chart in the left and right channels of the stereoscopic display. The user then visually compares the amount of crosstalk visible on screen for each eye separately in nominated areas of the chart against a scaled gray level ramp.

Unfortunately, there are some limitations with this method: (a) the gamma curve of the monitor should be calibrated using an appropriate sensor (such as the Spyder 3 from Datacolor), (b) the chart does not account for the non-zero black level of some monitors (e.g., LCDs), (c) the chart only measures white-to-black crosstalk, and (d) crosstalk can be different in different parts of the screen. These charts only measure crosstalk in relatively small portions of the screen, although this can be easily addressed with changes or multiple versions of the charts.

Due to the limitations of the visual measurement charts, appropriate electro-optic tools should be used to quantify crosstalk when accurate crosstalk data are needed that are not subject to the possible inaccuracies described above.

6 Crosstalk Reduction

In order to reduce the amount of crosstalk present on a particular stereoscopic display, it is necessary to reduce the effect of one or more of the crosstalk mechanisms of that particular display (as described in Sec. 4). First, develop a detailed listing of the crosstalk mechanisms of that display, their relative contribution to overall crosstalk, and an assessment of cost/benefit tradeoffs of any changes. In order to determine the relative contribution of the crosstalk mechanisms to overall crosstalk, it is necessary to perform a detailed analysis and optical measurement of the display and glasses in the temporal, spatial, and spectral domains. It is also beneficial to develop a simulation of crosstalk on a particular display in order to better understand the interrelationship of the individual display properties and how they affect the crosstalk mechanisms, and ultimately their relative contribution to overall crosstalk (see Sec. 8).

Once the relative contributions of each crosstalk mechanism are known, the main causes of crosstalk should be assessed first to see whether there are any changes that could be made to reduce the effect of these particular crosstalk mechanisms. There will also likely be cost/benefit tradeoffs with any changes made to reduce crosstalk. In some cases the trade-off might be increased cost of manufacture of the display or glasses, or a reduction in some other display performance characteristic. There will probably be an optimum balance between crosstalk and other display performance characteristics (including cost of manufacture,

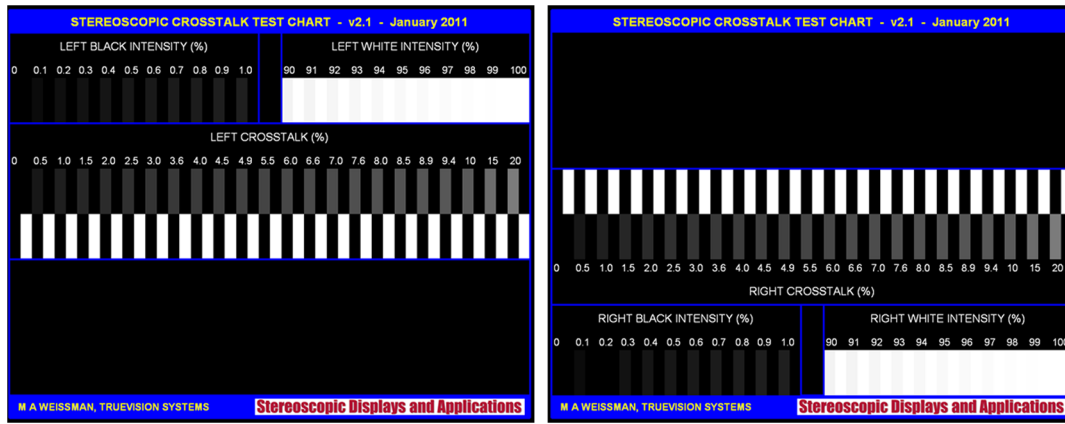


Fig. 22 Crosstalk measurement test chart designed by Weissman.¹⁰³

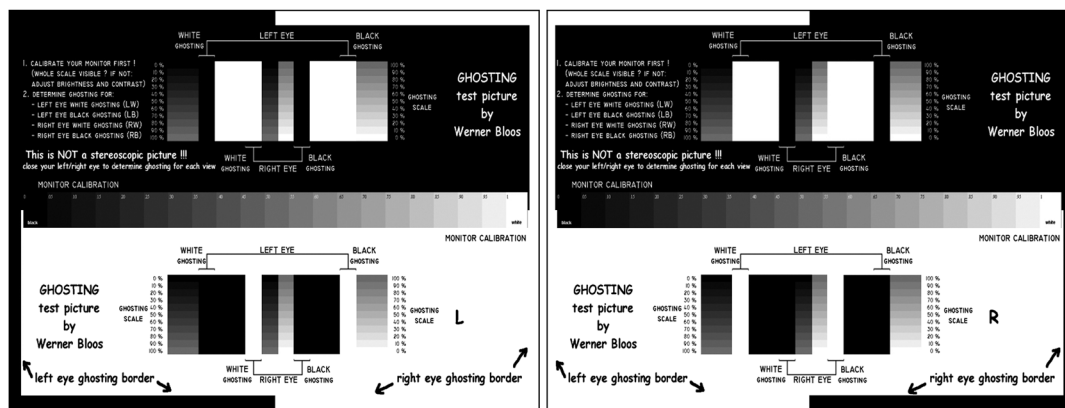


Fig. 23 Crosstalk measurement test chart designed by Bloos.¹⁰⁴

flicker, luminance, contrast, black level, etc.). For example, with the conventional plasma displays tested in Ref. 47, the study suggested using shorter persistence phosphors in plasma displays—but this might result in the increased cost or reduced luminance of the display. With time-sequential 3D on LCDs, a reduction in the duty cycle of the shutter glasses could reduce crosstalk, but this might be at the cost of reducing the image luminance.⁴⁸ With micro-polarized 3D LCDs, the addition of a black mask will increase the size of the viewing zones (i.e., increasing the size of the zones where low crosstalk is evident), but this might reduce the luminance of the display and possibly increase the cost of manufacture.

Some crosstalk reduction methods may only be possible to be performed by the display manufacturer (requiring a fundamental change to the display hardware), whereas other techniques might be able to be performed by the user (for example fine-tuning the timing of the glasses).

Another way to reduce the visibility of crosstalk (ghosting) is to reduce the contrast ratio of the image or display and/or reduce the luminance of the display (see Sec. 3)—but both of these actions would also reduce the overall quality of the displayed image and fundamentally this does not actually reduce the crosstalk, just the visibility of the crosstalk. Crosstalk cancellation is another way of reducing the visibility of crosstalk and is discussed in the next section.

7 Crosstalk Cancellation

Crosstalk cancellation (also known as anti-crosstalk, cross-talk compensation or ghost-busting) can be used to reduce the visibility of crosstalk.^{105–107} When crosstalk cancellation is used, the crosstalk is still present but it is concealed by the cancellation process.

Crosstalk cancellation involves the pre-distortion of the stereoscopic image in a specially controlled manner before display. A simple example of the process of crosstalk cancellation is illustrated in Fig. 24. Part (a) shows the leakage of the right image (unintended) channel into the left-eye view in a system without crosstalk cancellation. Part (b) shows the crosstalk cancellation process—the amount of leakage that is expected to occur from the right channel to the left channel is evaluated and this amount is subtracted from the left image creating a modified left image (shown as anti-crosstalk in the figure). When the modified left image is displayed on screen and viewed, the addition of the modified left image plus the leakage from the right image results in the equivalent of the original left image (since the anti-crosstalk and the leakage cancel each other out).

A simple illustration of the process of crosstalk cancellation on a stereoscopic display. (a) An example of a stereoscopic display with crosstalk visible to the left eye from the leakage of light from the right image channel. (b) An example of anti-crosstalk being applied to the left image so that

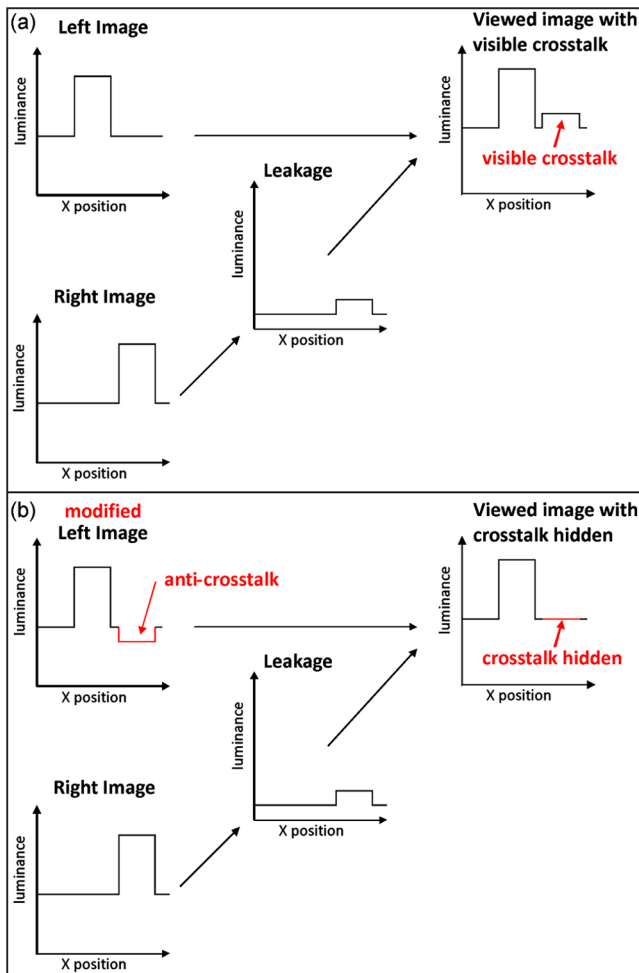


Fig. 24 A simple illustration of the process of crosstalk cancellation on a stereoscopic display. (a) An example of a stereoscopic image with crosstalk visible to the left eye from the leakage of light from the right image channel. (b) An example of anti-crosstalk being applied to the left image so that when leakage occurs from the right image channel, it cancels with the anti-crosstalk to hide the crosstalk.

when leakage occurs from the right image channel, it cancels with the anti-crosstalk to hide the crosstalk.

In practice, the full crosstalk cancellation process is more complicated than this simple explanation—a more detailed algorithm will normally be used which includes an inverse-transformation of crosstalk¹⁰⁶ and consideration of psychovisual effects,¹⁰⁶ pixel position,¹⁰⁵ display gamma,¹⁰⁸ previous-frame content,¹⁰⁹ and black-level adjustment.^{110,111}

Crosstalk cancellation has been evaluated for a wide range of stereoscopic display technologies, including anaglyph,^{107,112} polarized projection,^{108,113} and time-sequential 3D on CRTs,^{105,106} PDPs,^{52,114} and LCDs.^{57,115}

In most stereoscopic displays, crosstalk is primarily an additive process (the leakage adds to the intended signal), however, as mentioned in Sec. 5.1, the crosstalk process in time-sequential 3D LCDs is quite different—it is highly nonlinear and is a mix of additive and subtractive (in some instances the leakage subtracts from the intended signal).²¹ In this instance the crosstalk cancellation algorithm will need to be much more complicated and multi-dimensional and may be more easily implemented using a look-up table.^{21,99,106}

Crosstalk cancellation has limitations—one particular challenge is with high contrast images containing bright details against a black or dark background. If anti-crosstalk is applied to a black or dark background, it may require the modified image to go darker than black (i.e., negative), which is not possible with current displays. In this situation, one solution is to raise the black level of the image to accommodate the level of anti-crosstalk that is needed, but this will reduce image contrast and may give the image an undesirable washed-out look.^{105,106,110,111}

Crosstalk cancellation works best when the amount of crosstalk that needs to be cancelled is already relatively small. Large amounts of crosstalk may not be able to be fully hidden by crosstalk cancellation. It is also important to note that crosstalk cancellation may not work effectively when the amount of crosstalk in a particular 3D display can change significantly due to a change in viewing position²² or head tilt, or when the crosstalk is not pixel-aligned in both views—as occurs with micro-polarized 3D LCDs.

8 Simulation of Crosstalk

The development of an algorithm to predict crosstalk in a particular stereoscopic display allows a range of what-if scenarios to be explored without going to the expense of performing physical tests or building physical models. For example, how much crosstalk will occur if a particular pixel update method is used, if a particular shutter timing is used, or if a new design of 3D glasses is used. Hundreds or thousands of what-if scenarios can be simulated at minimal expense allowing new crosstalk reduction scenarios to be easily explored.

In order to develop a crosstalk simulation algorithm it is necessary to perform an optical measurement of the display and glasses in the temporal, spatial, and spectral domains. The accuracy of the crosstalk model will also need to be validated. Crosstalk simulations for parallax barrier 3D,⁷ anaglyph 3D,^{15,19,87} and time-sequential 3D on CRT,⁴⁶ PDP,⁴⁷ and LCD⁵⁶ have been developed.

9 Conclusion

This paper has provided a review of knowledge about stereoscopic display crosstalk with regard to terminology, definitions, mechanisms, measurement, and minimization. Crosstalk is a very important attribute in determining image quality in stereoscopic displays. In order for the stereoscopic display field to grow it is important that there be a common understanding of crosstalk. This field is still evolving and several efforts are currently under way to provide standardized methods of defining and measuring crosstalk^{4,27}—one of which has recently been released.¹⁴ Ultimately we want stereoscopic displays with low levels of crosstalk and in order to meet this goal, display designers will need to minimize the various crosstalk mechanisms described in this paper. Currently, crosstalk is not a specification that is regularly released by display manufacturers, but it is hoped that in the near future this important determinant of stereoscopic display quality will be readily available (along with which definition has been used to calculate it)—this will empower consumers to be able to intelligently choose 3D displays with lower crosstalk and hence better 3D image quality.

Acknowledgments

The author would like to thank WA:ERA, iVEC, and Jumbo Vision International as well as Stanley Tan, Tegan Rourke, Ka Lun Yuen, Kai Karvinen, Adin Sehic, Chris Harris and Jesse Helliwell for their support of and contributions to some of the projects described in this paper. This paper is a significantly expanded version of an earlier published manuscript.¹¹⁶

References

- L. Lipton, "The future of autostereoscopic electronic displays," in *Stereoscopic Displays and Applications III*, *Proc. SPIE* **1669**, 156–162 (1992).
- W. W. Jacques, "Underground wires," *Science* **6**(126), 6–7 (1885).
- C. W. Earp, "Carrier wave transmission system," U.S. Patent No. 2256317 (1941).
- A. J. Woods, "How are crosstalk and ghosting defined in the stereoscopic literature?" in *Stereoscopic Displays and Applications XXII*, *Proc. SPIE* **7863**, 78630Z (2011).
- A. J. Woods et al., Eds., "Stereoscopic displays and applications 1990–2009: a complete 20-year retrospective and the engineering reality of virtual reality 1994–2009 (Special Collection)," *Selected SPIE/IS&T Papers on DVD-ROM*, Vol. 51 (2010).
- Y.-C. Chang et al., "Investigation of dynamic crosstalk for 3D display," presented at 2009 Int'l. Display Manufacturing Conf., 3D Systems and Applications, and Asia Display (IDMC/3DSA/Asia Display 2009), Taipei, Taiwan, SID, California (2009).
- G. J. Woodgate et al., "Flat panel autostereoscopic displays—characterisation and enhancement," in *Stereoscopic Displays and Virtual Reality Systems VII*, *Proc. SPIE* **3957**, 153–164 (2000).
- C. D. Wickens et al., "Focused and divided attention in stereoscopic depth," in *Stereoscopic Displays and Applications*, *Proc. SPIE* **1256**, 28–34 (1990).
- Y.-Y. Yeh and L. D. Silverstein, "Limits of fusion and depth judgment in stereoscopic color displays," *Hum. Factors* **32**(1), 45–60 (1990).
- S. Pala, R. Stevens, and P. Surman, "Optical crosstalk and visual comfort of a stereoscopic display used in a real-time application," in *Stereoscopic Displays and Virtual Reality Systems XIV*, *Proc. SPIE* **6490**, 649011 (2007).
- H. Stevenson and M. Khazova, "Patterned grating alignment of reactive mesogens for phase retarders," in *Proc. 24th Int'l. Display Research Conf. with the 4th Int'l. Meeting on Information Display*, Daegu, South Korea, pp. 1–4 (2004).
- L. Lipton, "Glossary," *Lenny Lipton's Blog*, 16 March 2009, <http://lennylipton.wordpress.com/2009/03/16/glossary/> (19 March 2010).
- L. Lipton, "Factors affecting 'ghosting' time-multiplexed planostereoscopic CRT display systems," in *True 3D Imaging Techniques and Display Technologies*, *Proc. SPIE* **761**, 75–78 (1987).
- International Committee for Display Metrology, "Information display measurements standard (version 1.03)," Society for Information Display, <http://icdm-sid.org/> (2012).
- A. J. Woods and C. R. Harris, "Comparing levels of crosstalk with red/cyan, blue/yellow, and green/magenta anaglyph 3D glasses," in *Stereoscopic Displays and Applications XXI*, *Proc. SPIE* **7253**, 72530Q (2010).
- K.-C. Huang et al., "Measurement of Contrast Ratios for 3D Display," in *Input/Output and Imaging Technologies II*, *Proc. SPIE* **4080**, 78–86 (2000).
- P. Boher et al., "Multispectral polarization viewing angle analysis of circular polarized stereoscopic 3D displays," in *Stereoscopic Displays and Applications XXI*, *Proc. SPIE* **7253**, 72530R (2010).
- ISO, "Ergonomics of human-system interaction—Part 331: Optical characteristics of autostereoscopic displays," Technical Report ISO/TR 9241-331 (2012).
- A. J. Woods and C. R. Harris, "Using cross-talk simulation to predict the performance of anaglyph 3-D glasses," *J. Soc. Inform. Display* **20**(6), 304–315 (2012).
- J.-C. Liou et al., "Shutter glasses stereo LCD with a dynamic backlight," in *Stereoscopic Displays and Applications XX*, *Proc. SPIE* **7237**, 72370X (2009).
- S. Shestak, D.-S. Kim, and S.-D. Hwang, "Measuring of gray-to-gray crosstalk in a LCD based time-sequential stereoscopic displays," *Soc. Inform. Display Symp. Digest Tech. Papers* **41**(1), 132–135 (2010).
- K.-C. Huang et al., "A study of how crosstalk affects stereopsis in stereoscopic displays," in *Stereoscopic Displays and Virtual Reality Systems X*, *Proc. SPIE* **5006**, 247–253 (2003).
- S.-M. Jung et al., "Improvement of 3-D crosstalk with over-driving method for the active retarder 3-D displays," *Soc. Inform. Display Symp. Digest Tech. Papers* **41**(1) 1264–1267 (2010).
- C.-C. Pan et al., "Cross-talk evaluation of shutter-type stereoscopic 3D display," *Soc. Inform. Display Symp. Digest Tech. Papers* **41**(1), 128–131 (2010).
- F.-H. Chen et al., "Gray-to-gray crosstalk model," in *3DSA (Three Dimensional Systems and Applications) Conf.*, pp. 213–216 (2012).
- T. Järvenpää, M. Salmimaa, and T. Levola, "Qualified viewing spaces for near-to-eye and autostereoscopic displays," *Soc. Inform. Display Symp. Digest Tech. Papers* **41**(1), 335–338 (2010).
- K. Teunissen et al., "Perceptually relevant characterization of stereoscopic displays," *Soc. Inform. Display Symp. Digest Tech. Papers* **42**(1), 994–997 (2011).
- S. Shestak, D. Kim, and Y. Kim, "How much crosstalk can be allowed in a stereoscopic system at various grey levels?" in *Stereoscopic Displays and Applications XXIII*, *Proc. SPIE* **8288**, 828810 (2012).
- T. Järvenpää and M. Salmimaa, "Optical characterization methods for autostereoscopic 3D displays," in *Proc. EuroDisplay*, pp. 132–135, SID, California (2007).
- S. Pastoor, "Human factors of 3D images: Results of recent research at Heinrich-Hertz-Institut Berlin," in *Proc. IDW'95*, Vol. 3D-7, pp. 69–72, IDW, Japan (1995).
- Y. Nojiri et al., "Visual comfort/discomfort and visual fatigue caused by stereoscopic HDTV viewing," in *Stereoscopic Displays and Virtual Reality Systems XI*, *Proc. SPIE* **5291**, 303–313 (2004).
- F. L. Kooi and A. Toet, "Visual comfort of binocular and 3D displays," *Displays* **25**(2–3), 99–108 (2004).
- P. J. H. Seuntjens, L. M. J. Meesters, and W. A. Ijsselstein, "Perceptual attributes of crosstalk in 3D images," *Displays* **26**(4–5), 177–183 (2005).
- K. Ukai and P. A. Howarth, "Visual fatigue caused by viewing stereoscopic motion images: background, theories, and observations," *Displays* **29**(2), 106–116 (2008).
- L. M. Wilcox and J. A. D. Stewart, "Determinants of perceived image quality: Ghosting versus brightness," in *Stereoscopic Displays and Virtual Reality Systems X*, *Proc. SPIE* **5006**, 263–268 (2003).
- R. F. Stevens, "Cross-talk in 3D displays," Report CETM 56, National Physical Laboratory, United Kingdom (2004).
- I. Tsirlin, L. M. Wilcox, and R. S. Allison, "The effect of crosstalk on the perceived depth from disparity and monocular occlusions," *IEEE Trans. Broadcast.* **57**(2), 445–453 (2011).
- L. Wang et al., "Effect of display technology on the crosstalk perception in stereoscopic video content," *IEEE Trans. Circuits Syst. Video Technol.* **22**(9), 1257–1265 (2012).
- I. Tsirlin, L. M. Wilcox, and R. S. Allison, "Effect of crosstalk on depth magnitude in thin structures," *J. Electron. Imaging* **21**(1), 011003 (2012).
- L. Chen et al., "Investigation of crosstalk in a 2-view 3D display," *Soc. Inform. Display Symp. Digest Tech. Papers* **39**(1), 1138–1141 (2008).
- I. Tsirlin, R. S. Allison, and L. M. Wilcox, "Crosstalk reduces the amount of depth seen in 3D images of natural scenes," in *Stereoscopic Displays and Applications XXIII*, *Proc. SPIE* **8288**, 82880W (2012).
- L. Hammond, "Stereoscopic motion picture device," U.S. Patent No. 1506524 (1924).
- J. A. Roese, "PLZT stereoscopic television system," U.S. Patent No. 3903358 (1975).
- J. A. Roese and A. S. Khalafalla, "Stereoscopic viewing with PLZT ceramics," *Ferroelectrics* **10**(1), 47–51 (1976).
- L. Lipton, "Brief history of electronic stereoscopic displays," *Opt. Eng.* **51**(2), 021103 (2012).
- A. J. Woods and S. S. L. Tan, "Characterising sources of ghosting in time-sequential stereoscopic video displays," in *Stereoscopic Displays and Virtual Reality Systems IX*, *Proc. SPIE* **4660**, 66–77 (2002).
- A. J. Woods and K. S. Karvinen, "The compatibility of consumer plasma displays with time-sequential stereoscopic 3D visualization," in *Stereoscopic Displays and Applications XIX*, *Proc. SPIE* **6803**, 68030X (2008).
- A. J. Woods and K.-L. Yuen, "Compatibility of LCD monitors with frame-sequential stereoscopic 3D visualisation," *IMID/IDMC'06 Digest 6th Int'l. Meeting on Information Display and 5th Int'l. Display Manufacturing Conf.*, pp. 98–102, SID, California (2006).
- A. J. Woods and T. Rourke, "The compatibility of consumer DLP projectors with time-sequential stereoscopic 3D visualization," *Stereoscopic Displays and Virtual Reality Systems XIV*, *Proc. SPIE* **6490**, 64900V (2007).
- H. Pan, X.-F. Feng, and S. Daly, "LCD motion blur modeling and analysis," *IEEE Int'l. Conf. Image Processing*, Vol. 2, pp. 21–24 (2005).
- P. J. Bos, "Performance limits of stereoscopic viewing systems using active and passive glasses," *IEEE Virtual Reality Annual Intl. Symp.*, pp. 371–376, IEEE, Washington (1993); H. Kusaka, "Time sequential stereoscopic displays: the contribution of phosphor persistence to the 'ghost' image intensity," in *Proc. ITEC'91 Annual Conf. Three-Dimensional Image Tech.*, pp. 603–606 (1991).
- K. Hamada et al., "A field-sequential stereoscopic display system with 42-in. HDTV DC-PDP," in *Proc. Intl. Display Workshop IDW'98*, pp. 555–558, IDW, Japan (1998).

53. K. Hamada et al., "A 3D Hi-Vision Display with 50-in. AC PDP," in *Asia Display/Intl. Display Workshop IDW'01*, pp. 785–788, IDW, Japan (2001).
54. A. J. Woods, "The illustrated 3D HDTV list," (28 March 2012), www.3dmovielist.com/3dhdtvs.html (15 May 2012).
55. A. J. Woods, "The Illustrated 3D monitor list," (2012), <http://www.3dmovielist.com/3dmonitors.html> (13 May 2012).
56. A. J. Woods and A. Sehic, "The compatibility of LCD TVs with time-sequential stereoscopic 3D visualization," in *Stereoscopic Displays and Applications XX*, *Proc. SPIE* **7237**, 72370N (2009).
57. S. Shestak and D.-S. Kim, "Application of pi-cells in time-multiplexed stereoscopic and autostereoscopic displays, based on LCD panels," in *Stereoscopic Displays and Virtual Reality Systems XIV*, *Proc. SPIE* **6490**, 64900Q (2007).
58. G. A. Slavenburg, T. F. Fox, and D. R. Cook, "System, method, and computer program product for increasing an LCD display vertical blanking interval," U.S. Patent Application Publication 20070229487 A1 (2007).
59. S.-M. Park et al., "Method and apparatus for displaying stereoscopic image," U.S. Patent Application Publication 2010/0066820 A1 (2010).
60. M. Husak et al., "System and method for synchronizing a 3D video projector," U.S. Patent No. 8066377 (2011).
61. L. J. Hornbeck, "Current status and future applications for DMD-based projection displays," in *Proc. Fifth Intl. Display Workshop IDW'98*, Japan, pp. 1–4 (1998).
62. V. Walworth, S. Bennett, and G. Trapani, "Three-dimensional projection with circular polarizers," in *Optics in Entertainment II*, *Proc. SPIE* **0462**, 64–68 (1984).
63. "XP42 linear polarizer filters datasheet," Optical Filters United Kingdom, <http://www.opticalfilters.co.uk>.
64. "Circular Polarizers—APNCP37," American Polarizers, Inc., <http://www.apoptics.com/pdf/APNCP37-010-STD.pdf> (28 March 2010).
65. H.-K. Hong et al., "Analysis of angular dependence of 3-D technology using polarized eyeglasses," *J. Soc. Inform. Display* **18**(1), 8–12 (2010).
66. G. Themelis, "Comparison of stereo projection screens," (April 2003), <http://www.drt3d.com/info/ScreenTesting.htm> (28 March 2010).
67. L. Lipton et al., "Method and system employing a push-pull liquid crystal modulator," U.S. Patent No. 4792850 (1988).
68. T. Haven, "A liquid crystal stereoscope with high extinction ratios, a 28% transmission state, and one hundred microsecond switching," in *True Three-Dimensional Imaging Techniques and Display Technologies*, *Proc. SPIE* **761**, 23–26 (1987).
69. J. Osterman and T. Scheffer, "Contrast-enhanced high-speed polarization modulator for active-retarder 3D displays," *Soc. Inform. Display Symp. Digest Tech. Papers* **42**(1), 93–96 (2011).
70. Y. H. Lee and Y. B. Jung, "Stereoscopic image projecting system using circularly polarized filter module," U.S. Patent Application Publication 2010/0079728 A1 (2010).
71. J. Konrad and M. Halle, "3-D displays and signal processing: an answer to 3-D Ills?" *IEEE Signal Process. Mag.* **24**(6), 97–111 (2007).
72. S. M. Faris, "Micro-polarizer arrays applied to a new class of stereoscopic imaging," in *SID 91 Digest*, pp. 840–843 (1991).
73. A. J. Woods, "3-D displays in the home," *Inform. Display* **25**(7), 8–12 (2009).
74. S. M. Faris, "Novel 3D stereoscopic imaging technology," in *Stereoscopic Displays and Virtual Reality Systems XI*, *Proc. SPIE* **5291**, 180–195 (2004).
75. S. J. Lee et al., "Review of wire grid polarizer and retarder for stereoscopic display," in *Stereoscopic Displays and Applications XX*, *Proc. SPIE* **7237**, 72370P (2009).
76. Y. Yoshihara, "About Micro-Pol for 3D LCD" (English translation of Japanese title), *3D Consortium* (June 2003) (presentation only).
77. C.-Y. Ma et al., "A simulation platform and crosstalk analysis for patterned retarder 3D display," *Soc. Inform. Display Symp. Digest. Tech. Papers* **42**(1), 808–811 (2011).
78. A. Marraud and M. Bonne, "Restitution of a stereoscopic picture by means of a lenticular sheet," in *Three-Dimensional Imaging*, *Proc. SPIE* **402**, 129–132 (1983).
79. J. B. Eichenlaub, "An autostereoscopic display for use with a personal computer," in *Stereoscopic Displays and Applications*, *Proc. SPIE* **1256**, 156–163 (1990).
80. A. Boev, A. Gotchev, and K. Egiazarian, "Crosstalk measurement methodology for autostereoscopic screens," in *3DTV Conference*, pp. 1–4, IEEE, Kos Island (2007).
81. R. Patterson, "Human factors of 3-D displays," *J. Soc. Inform. Display* **15**(11), 861–871 (2007).
82. A. Jain and J. Konrad, "Crosstalk in automultiscopic 3-D displays: blessing in disguise?" in *Stereoscopic Displays and Virtual Reality Systems XIV*, *Proc. SPIE* **6490**, 649012 (2007).
83. E. Dubois, "A projection method to generate anaglyph stereo images," in *IEEE Intl. Conf. Acoustics, Speech, and Signal Processing Proc. ICASSP'01*, Vol. 3, pp. 1661–1664, IEEE, Salt Lake City, Utah (2001).
84. W. R. Sanders and D. F. McAllister, "Producing anaglyphs from synthetic images," *Stereoscopic Displays and Virtual Reality Systems X*, *Proc. SPIE* **5006**, 348–358 (2003).
85. D. F. McAllister, Y. Zhou, and S. Sullivan, "Methods for computing color anaglyphs," in *Stereoscopic Displays and Applications XXI*, *Proc. SPIE* **7524**, 75240S (2010).
86. A. J. Woods and T. Rourke, "Ghosting in anaglyphic stereoscopic images," in *Stereoscopic Displays and Virtual Reality Systems XI*, *Proc. SPIE* **5291**, 354–365 (2004).
87. A. J. Woods, K.-L. Yuen, and K. S. Karvinen, "Characterizing crosstalk in anaglyphic stereoscopic images on LCD monitors and plasma displays," *J. Soc. Inform. Display* **15**(11), 889–898 (2007).
88. H. Jorke and M. Fritz, "Stereo projection using interference filters," in *Stereoscopic Displays and Virtual Reality Systems XIII*, *Proc. SPIE* **6055**, 60550G (2006).
89. M. J. Richards and G. D. Gomes, "Spectral separation filters for 3D stereoscopic D-cinema presentation," U.S. Patent No. 7,959,295 B2 (2011).
90. C. Wheatstone, "Contributions to the physiology of vision—Part the first on some remarkable, and hitherto unobserved, phenomena of binocular vision," *Philos. Trans. Roy. Soc. Lond.* **128**, 371–394 (1838).
91. S. S. Fisher et al., "Virtual Environment Display System," *Proc. Workshop Interactive 3D Graphics*, pp. 1–11, ACM, New York (1986).
92. W. Woo, N. Kim, and Y. Iwadata, "Stereo imaging using a camera with stereoscopic adapter," *Proc. IEEE Syst., Man Cybern.*, pp. 1512–1517, IEEE, Nashville, Tennessee (2000).
93. J. Goodman, "Development of the 960p stereoscopic video format," in *Stereoscopic Displays and Virtual Reality Systems X*, *Proc. SPIE* **5006**, 187–194 (2003).
94. A. Millin and P. Harman, "Three-dimensions via the Internet," in *Stereoscopic Displays and Virtual Reality Systems VIII*, *Proc. SPIE* **4297**, 328–333 (2001).
95. CIE, Commission Internationale de l'Eclairage Proceedings, Cambridge University Press, Cambridge, England (1932).
96. A. Stockman and L. T. Sharpe, "Luminous energy function (2 degree, linear energy)," (2007), <http://www.cvrl.org/cvrlfunctions.htm> and <http://www.cvrl.org/database/text/lum/CIE2008v2.htm> (29 July 2011).
97. A. Stockman et al., "The dependence of luminous efficiency on chromatic adaptation," *J. Vision* **8**(16), 1–26 (2008).
98. M. Barkowsky et al., "Crosstalk measurements of shutter glasses 3D displays," *Soc. Inform. Display Digest Tech. Papers* **42**(1), 812–815 (2011).
99. S. Tourancheau et al., "Reproducibility of crosstalk measurements on active glasses 3D LCD displays based on temporal characterization," in *Stereoscopic Displays and Applications XXIII*, *Proc. SPIE* **8288**, 82880Y (2012).
100. J. Lee et al., "Optical performance analysis method of auto-stereoscopic 3D displays," *Soc. Inform. Display Digest Tech. Papers* **41**(1), 327–330 (2010).
101. L. Blondé et al., "Diversity and coherence of 3D crosstalk measurements," *Soc. Inform. Display Digest Tech. Papers* **42**(1), 804–807 (2011).
102. M. Barkowsky et al., "Crosstalk measurements of shutter glasses 3D displays," *Soc. Inform. Display Digest Tech. Papers* **42**(1), 812–815 (2011).
103. M. A. Weissman and A. J. Woods, "A simple method for measuring crosstalk in stereoscopic displays," in *Stereoscopic Displays and Applications XXII*, *Proc. SPIE* **7863**, 786310 (2011).
104. W. Bloos, "Ghosting test—standard method for determining ghost image," Stereo Forum, 5 June 2008, <http://www.stereoforum.org/viewtopic.php?f=16&t=53> (25 March 2010).
105. J. S. Lipscomb and W. L. Wooten, "Reducing crosstalk between stereoscopic views," in *Stereoscopic Displays and Virtual Reality Systems*, *Proc. SPIE* **2177**, 92–96 (1994).
106. J. Konrad, B. Lacotte, and E. Dubois, "Cancellation of image crosstalk in time-sequential displays of stereoscopic video," *IEEE Trans. Image Process.* **9**(5), 897–908 (2000).
107. A. J. Chang et al., "Ghosting reduction method for color anaglyphs," in *Stereoscopic Displays and Applications XIX*, *Proc. SPIE* **6803**, 68031G (2008).
108. M. Cowan, J. Greer, and L. Lipton, "Ghost-compensation for improved stereoscopic projection," U.S. Patent Application Publication 2011/0025832 A1 (2011).
109. G. A. Slavenburg, T. F. Fox, and D. R. Cook, "System, method, and computer program product for compensating for crosstalk during the display of stereo content," U.S. Patent No. 8085217 B2 (2011).
110. W. Tan, S. Z. Zhou, and S. C. Read, "Methods and systems for reducing or eliminating perceived ghosting in displayed stereoscopic images," U.S. Patent Application Publication 2001/0080401 A1 (2011).

111. D. J. McKnight, "Enhanced ghost compensation for stereoscopic imagery," U.S. Patent Application Publication 2010/0040280 A1 (2010).
112. H. Sanftmann and D. Weiskopf, "Anaglyph stereo without ghosting," *Comput. Graphics Forum* **30**(4), 1251–1259 (2011).
113. S. Klimenko et al., "Crosstalk reduction in passive stereo-projection systems," in *Proc. Eurographics'03*, pp. 235–240 (2003).
114. T. Kim et al., "3D crosstalk compensation to enhance 3D image quality of plasma display panel," *IEEE Trans. Consum. Electron.* **57**(4), 1471–1477 (2011).
115. B. Li and J. Caviedes, "Evaluating the impact of crosstalk on shutter-type stereoscopic 3D displays," in *Sixth Int'l. Workshop on Video Processing and Quality Metrics*, pp. 1–6 (2012).
116. A. J. Woods, "Understanding crosstalk in stereoscopic displays," in *3DSA (Three-Dimensional Systems and Applications) Conf.*, pp. 34–44 (2010).



Andrew J. Woods is a consultant and research engineer at Curtin University's Centre for Marine Science and Technology in Perth, Australia. He has more than 20 years of experience in the design, application, and evaluation of stereoscopic video equipment for industrial and entertainment applications. He has bachelor's and master's degrees in electronic engineering, specializing in stereoscopic imaging. He is also co-chair of the annual Stereoscopic Displays and Applications Conference—the largest and longest running technical stereoscopic 3D imaging conference.

Paper 2 [Refereed Journal Article]

A. J. Woods, K. L. Yuen, and K. S. Karvinen (2007) "Characterizing crosstalk in anaglyphic stereoscopic images on LCD monitors and plasma displays" in Journal of the Society for Information Display, Volume 15, Issue 11, pp. 889-898, November 2007.

Characterizing crosstalk in anaglyphic stereoscopic images on LCD monitors and plasma displays

Andrew J. Woods
Ka Lun Yuen
Kai S. Karvinen

Abstract — In 1853, William Rollman¹ developed the inexpensive and easy to use anaglyph method for displaying stereoscopic images. Although it can be used with nearly any type of full-color display, the anaglyph method compromises the accuracy of color reproduction, and it often suffers from crosstalk (or ghosting) between the left- and right-eye image channels. Crosstalk degrades the ability of the observer to fuse the stereoscopic image, and hence reduces the quality of the 3-D image. Crosstalk is present in various levels with most stereoscopic displays; however, it is often particularly evident with anaglyphic 3-D images. This paper summarizes the results of two projects that characterized the presence of anaglyphic crosstalk due to spectral issues on 13 LCD monitors, 14 plasma displays, and a CRT monitor when used with 25 different pairs of anaglyph 3-D glasses. A mathematical model was used to predict the amount of crosstalk in anaglyphic 3-D images when different combinations of displays and glasses are used, and therefore highlight displays, glasses, and combinations thereof which exhibit lower levels of crosstalk when displaying anaglyphic 3-D images.

Keywords — Anaglyph, 3-D, stereoscopic, crosstalk, ghosting, LCD monitors, plasma displays, CRT displays.

1 Introduction

The anaglyph method of displaying stereoscopic images uses a complementary color-coding technique to send separate left and right views to an observer's two eyes. The two perspective images of a stereo-pair are stored in complementary color channels of the display, and the observer wears a pair of glasses containing color filters which act to pass the correct image but block the incorrect image to each eye.

For example, if a red/cyan anaglyph is used, the left perspective image is stored in the red color channel and the right perspective image is stored in the blue and green color channels (blue + green = cyan), and the observer wears a pair of anaglyph 3-D glasses with the left-eye filter red and the right-eye filter cyan.

The main advantages of the anaglyph 3-D method are its simplicity, low cost, and compatibility with any full-color display. The main disadvantages are its inability to accurately depict full-color images, and commonly the presence of crosstalk. Crosstalk (or ghosting) is the leaking of an image to one eye when it is intended exclusively for the other eye. For example, the left eye should only be able to see the left perspective image, but due to crosstalk, the left eye may see a small proportion of the right perspective image. Crosstalk occurs with most stereoscopic displays and results in reduced image quality and difficulty of fusion if the amount of crosstalk is large.

This paper considers the two spectral contributors to anaglyphic crosstalk: display spectral response and anaglyph glasses spectral response. Two other possible contributors to

anaglyph ghosting, image compression and image encoding/transmission,² are not explored in this paper.

Figure 1 provides an illustration of the process of crosstalk in anaglyph stereoscopic images due to spectral leakage (as illustrated for the red/cyan method). Firstly, the display has a specific spectral output for the red, green, and blue color channels. Usually the left perspective image is stored in the red color channel and the right perspective image is stored in the green and blue color channels (cyan). Second, the red/cyan anaglyph 3-D glasses used to view the anaglyph display also have a certain spectral transmission response for the left and right eye filters. Here the left filter predominantly transmits red light but with a little bit of transmission in the green band, and the right filter predominantly transmits blue and green light but with a little bit of transmission in the red band. Due to the non-ideal nature of the display and the glasses, some light from the right (cyan) color channel leaks through the left (red) eye filter. Similarly, some light from the left (red) color channel leaks. This is in addition to the transmission of the intended image through the left- and right-eye filters. Therefore, the left eye predominantly sees the left perspective image but with a small amount of the right perspective image visible, and the right eye predominantly sees the right perspective image but with a small amount of the left perspective image visible.

This paper carries on from the work of Woods and Rourke² which considered anaglyph ghosting with cathode-ray tube (CRT) monitors, one liquid-crystal display (LCD) monitor, and a mixture of LCD and digital light processing (DLP) projectors. This paper focuses on anaglyph ghosting on LCD monitors and plasma displays with 13 LCD moni-

The authors are with the Centre for Marine Science & Technology, Curtin University of Technology, GPO Box U1987, Perth, WA 6845 Australia; telephone +61-8-9266-7920, fax -4799, e-mail: A.Woods@cmst.curtin.edu.au.

© Copyright 2007 Society for Information Display 1071-0922/07/1511-0889\$1.00

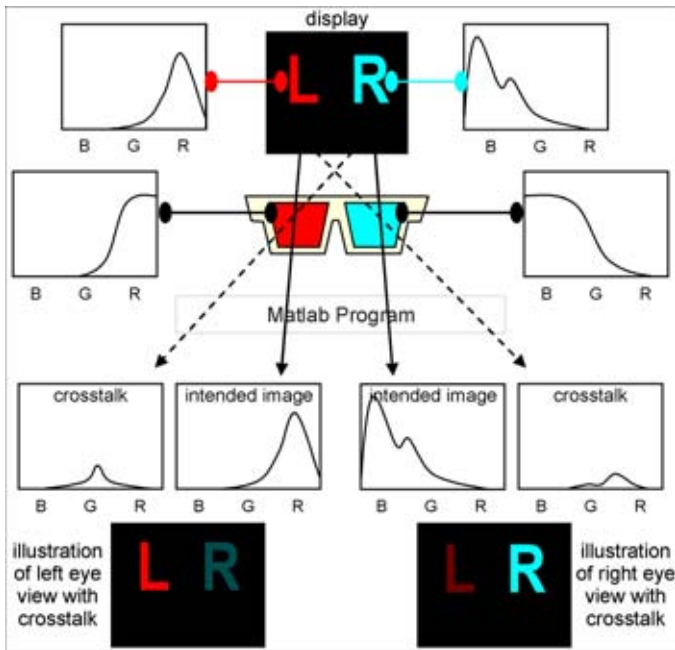


FIGURE 1 — Illustration of the process of anaglyph spectral ghosting and its simulation in this project. From the top: (1) Spectral response of display, (2) spectral response of anaglyph glasses, (3) simulation of ghosting using a computer program, (4) spectral output characteristic of crosstalk and intended image, and (5) visual illustration of left- and right-eye view with crosstalk.

tors and 14 plasma-displays panels (PDPs) tested. A CRT monitor was also tested for comparison purposes. All data for this project was measured using more accurate equipment than was available in the previous study.²

This paper only examines crosstalk in red/cyan anaglyph stereoscopic images, although the simulation methods discussed could also be applied to blue/yellow or green/magenta anaglyphs.

2 Experimental method

The first step was to measure the spectral output of the displays using a manually calibrated Ocean Optics USB2000 spectroradiometer. Table 1 itemizes the displays tested – consisting of 13 LCD computer monitors, 14 PDPs, and one CRT monitor.

Each display was connected to a PC which displayed a slide show consisting of a plain white slide ($R = G = B = 255$), a plain red slide ($R = 255, G = B = 0$), a plain green slide ($R = B = 0, G = 255$), a plain blue slide ($R = G = 0, B = 255$), and a plain black slide ($R = G = B = 0$). The spectroradiometer was used to measure the spectrum of each of these slides (as displayed on each display) and the data collected on a PC.

The second step was to measure the transmission spectrum of a large selection of anaglyph 3-D glasses using a PG Instruments T90+ UV/Vis spectrophotometer. A total of 50 pairs of anaglyph glasses were tested³; however, only 25 pairs are reported here for the sake of brevity.

TABLE 1 — Listing of the tested displays.

Tag	Display Make and Model
LCD01	Samsung SyncMaster 171s
LCD02	Benq FP731
LCD03	NEC MultiSync LCD 1760V
LCD04	Acer AL1712
LCD05	Acer FP563
LCD06	Benq FP71G
LCD07	Benq FP71G+S
LCD08	Philips 150S3
LCD09	Hewlett Packard HPL1706
LCD11	Samsung SyncMaster 740N
LCD12	Philips 190s
LCD13	Samsung SyncMaster 913B
LCD14	ViewSonic VX922
PDP01	LG DT-42PY10X
PDP02	Fujitsu P50XHA51AS
PDP03	NEC PX-50XR5W
PDP04	Panasonic TH-42PV60A
PDP05	Samsung PS-42C7S
PDP06	LG RT-42PX11
PDP07	NEC PX-42XM1G
PDP08	Sony PFM-42V1
PDP09	Sony FWD-50PX2
PDP10	Hitachi 55PD8800TA
PDP11	Hitachi 42PD960BTA
PDP12	Pioneer PDP-507XDA
PDP13	Pioneer PDP-50HXE10
PDP14	Fujitsu PDS4221W-H
CRT	Mitsubishi Diamond View VS10162

Note: Due to manufacturing variation or experimental error, the results provided in this paper should not be considered to be representative of all displays of that particular brand or model.

The third step was to use a specially developed Matlab computer program to calculate the presence of crosstalk in the anaglyph images for different display and glasses combinations. With reference to Fig. 1, the program first loads and resamples the display and filter spectral data so that all data is on a common x -axis coordinate system. Next, the program determines the display's cyan spectral output by adding the green and blue color channel data of the display. The program then multiplies the red display spectrum with the red filter's spectral response to obtain the intended image curve for the red eye, multiplies the cyan display spectrum with the cyan filter's spectrum to obtain the intended image curve for the cyan eye, multiplies the red display spectrum with the cyan filter's spectral response to obtain the crosstalk curve for the cyan eye, and multiplies the cyan display spectrum with the red filter's spectrum to obtain the crosstalk curve for the red eye.

The program also scales these result curves to include the human-eye response to light by multiplying by the curve shown in Fig. 2, which shows the CIE (International Commission on Illumination) model for simulating photopic (bright light) human-eye sensitivity to light.⁴

The crosstalk percentage for each eye is then calculated by dividing the area under the crosstalk curve by the area under the intended signal curve for each eye and multiplying by 100. The overall crosstalk factor for a particular

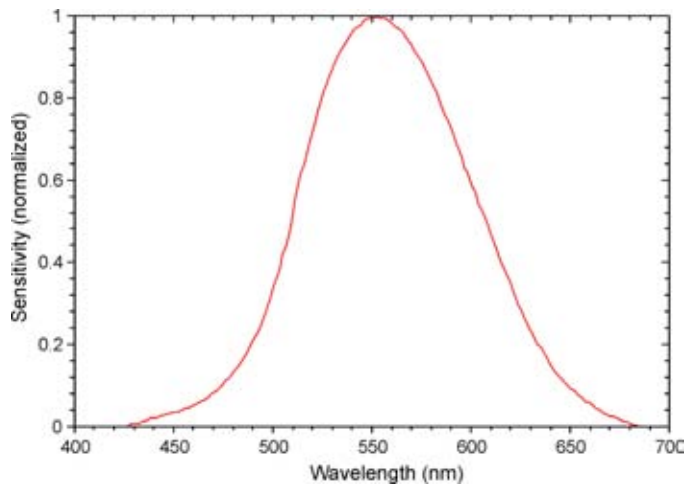


FIGURE 2 — CIE 1931 standard normalized photopic human-eye response.

pair of glasses in combination with a particular display is the sum of the left- and right-eye percentage crosstalk values. It should be noted that the overall crosstalk factor is not a percentage, but rather a number that allows the comparison of different glasses/display combinations. The program also automates the process of performing a cross comparison of all the displays against all of the glasses.

3 Results

3.1 Display device results

The spectral output measurement of 13 different LCD monitors, 14 different PDP monitors, and one CRT monitor are reported in this study.

Figure 3 shows the spectral output of an example LCD monitor (LCD04). All of the LCD monitors tested used cold cathode fluorescent lamp (CCFL) backlights. CCFLs are a form of mercury-vapor fluorescent lamp that generate visible light by energizing the gas in the fluorescent tube so that it emits ultraviolet rays which in turn causes the phosphor material that coats the inside surface of the tube to emit visible light. The spectrum of a CCFL is fairly broad but with many notable narrow peaks. Although the spectral output of the raw CCFL was not measured in any of the LCDs tested, its general form can be approximated from the summation of the three traces shown in Fig. 3. The three individual color primaries (red, green, and blue) are created by placing color filters over the individual subpixel groups in the LCD pixel grid.⁵ The light spectrum output by each color channel is primarily a multiplication of the backlight spectrum by the spectrum of the color filters used in each subpixel. In the example LCD monitor shown in Fig. 3, there is a considerable amount of overlap between each of the three color channels. The amount of overlap varied from monitor to monitor.

The combined spectral results for the 13 LCD monitors tested are shown in Appendix B (Figs. B1, B2, and B3).

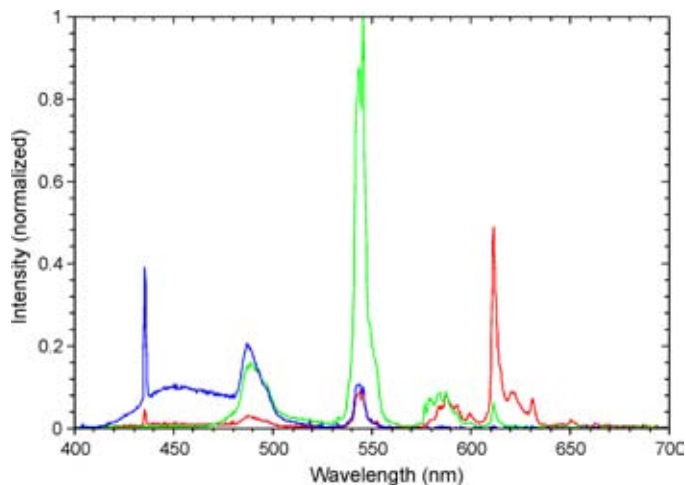


FIGURE 3 — Color spectrum of an example LCD monitor (LCD04).

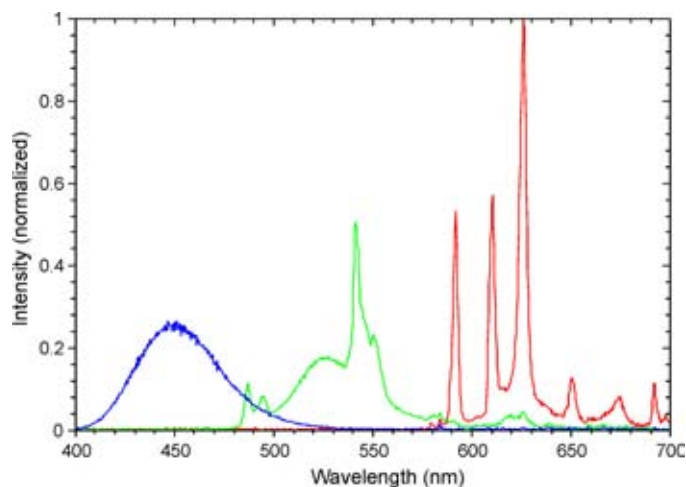


FIGURE 4 — Color spectrum of an example plasma display (PDP08).

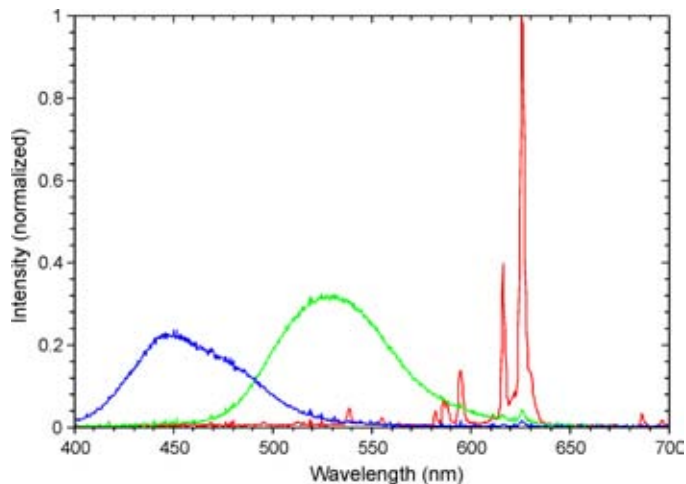


FIGURE 5 — Color spectrum of the example CRT monitor.

A separate graph is provided for each of the three color primaries. There is a lot of similarity between the spectral characteristics of all the LCD monitors; however, some dif-

ferences occur in the out-of-band rejection (*e.g.*, the amount of green light present in the red color primary) which will probably be related to the quality of color filters used for each of the color primaries.

Figure 4 shows the spectral output of an example plasma display (PDP08). Color plasma displays generate visible light by energizing a gas mixture in each cell so that it emits ultraviolet light rays which in turn causes the phosphor material that coats the inside of each cell to emit visible light. The spectral output of each of the color channels is determined by the phosphor formulation used for each group of subpixels.⁶ The blue output has a classic bell-shaped curve centered around 450 nm. The red output is a mixture of several narrow peaks and the green output is a mixture of a bell curve and another major narrow peak.

The combined spectral results for all of the 14 plasma displays tested are shown in Appendix B (Figs. B4, B5, and B6). A separate graph is provided for each of the three color primaries. The color spectrum of the red and blue color primaries are very similar across all the tested plasma displays; however, there is a lot of variation of the spectral response of the green color primary which will probably relate to the formulation of the phosphors used.

Figure 5 shows the spectral output of an example CRT monitor. A previous paper by Woods and Tan⁷ reported that 11 tested CRT monitors had almost exactly the same spectral response which suggests that most CRTs use the same phosphor formulation for each of the color primary channels. The blue and green output have a bell-shaped curve whereas the red output is made up of several narrow peaks.

3.2 Anaglyph 3-D glasses results

Figure 4 shows the spectral transmission of an example pair of red-cyan anaglyph glasses. In this example the red filter has a pass band of wavelengths roughly 600–700 nm. The cyan filter has a pass band of wavelengths roughly 550–400 nm. As can be seen in Fig. 4, a little bit of light at the wavelength of around 590 nm will be transmitted through both the red and cyan filters, therefore arriving at both eyes. When this overlap occurs it is another possible source of crosstalk.

All of the anaglyph glasses reported in this paper are listed in Table 2. This list is substantially similar to that reported in Woods and Rourke² except that all pairs of glasses have been retested using a more accurate instrument.

The spectral transmission of all the glasses from Table 2 are shown overlaid in Fig. 7 (red filters) and Fig. 8 (cyan filters). It can be seen that there is considerable variation between the spectral response of the various glasses tested. There is some clustering of some of the data, however, this is probably due to some glasses being from the same manufacturer or manufacturing process.

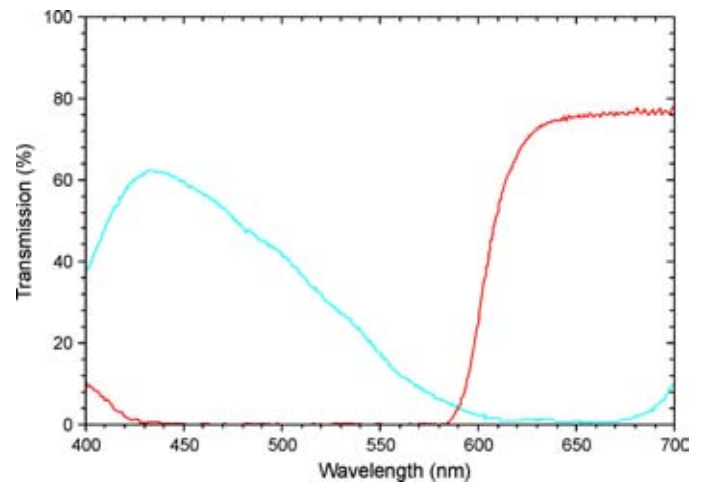


FIGURE 6 — Spectral transmission of an example pair of anaglyph 3-D glasses (3DG16).

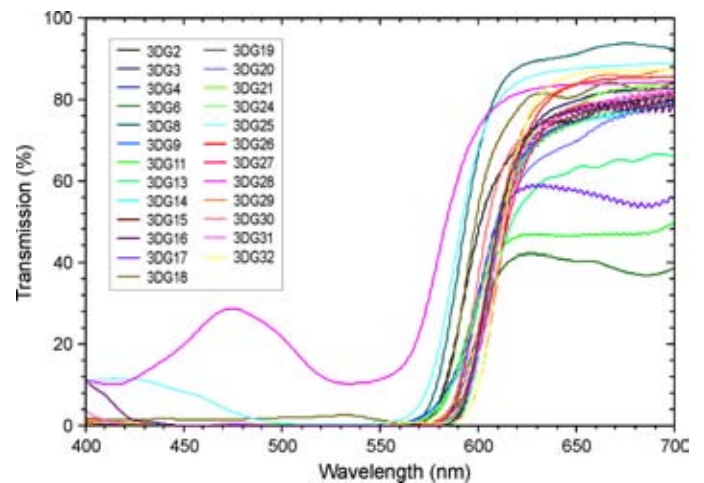


FIGURE 7 — Spectral transmission for all the red filters.

3.3 Crosstalk calculation results

The crosstalk and uncertainty results calculated by the Matlab program for the combination of all displays against all anaglyph glasses are shown in Tables C1 and C2 in Appendix C. For each display/glasses combination, the table lists the percentage crosstalk for the red eye (top left), the percentage crosstalk for the cyan eye (top right), and the overall crosstalk factor for both eyes combined (bottom). The overall crosstalk factor is the sum of the left- and right-eye percentages, and as such is not a percentage. The uncertainty figures are only shown for the overall crosstalk factor. The uncertainty figures were calculated for the individual red and cyan crosstalk but are omitted here due to space limitations.

3.4 Validation test

A first-order validation test was performed to confirm that the results from the crosstalk model were sensible. A set of

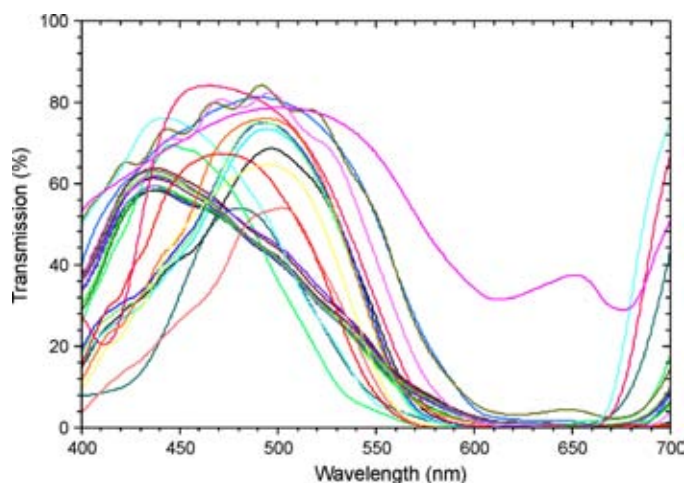


FIGURE 8 — Spectral transmission for all the cyan filters.

test images were viewed on a CRT monitor and subjectively ranked in order of increasing crosstalk. The results of the subjective ranking were then compared with the crosstalk ranking generated by the MATLAB program and this is shown in Table 2.

As can be seen from the table, the subjective ranking agrees extremely well with the calculated results, which provides some confidence in the validity of the crosstalk calculation results. Two of the differences occurred where the crosstalk percentage difference was just 0.1, and two differences occurred where the crosstalk percentage difference was 0.4. Crosstalk differences of 0.1 and 0.4 are very small and are hard to discern by the naked eye.

4 Discussion

Crosstalk in anaglyph images acts to degrade the 3-D image quality by making them hard to fuse. One important way to optimize the quality of anaglyph 3-D images is therefore to minimize the presence of crosstalk. In most circumstances, the easiest way to minimize crosstalk would be with the choice of anaglyph 3-D glasses, but in some circumstances it may also be possible to choose different display monitors. This project aims to highlight possible low-crosstalk combinations so crosstalk can be reduced.

Across all of the displays, the LCD monitors had the lowest overall crosstalk, both from an average (18.6) and also a global minimum (7.0) perspective. The plasma displays were very close behind with an average overall crosstalk of 18.6 and global minimum of 8.1. The CRT had much worse anaglyph crosstalk with an average overall crosstalk of 27.0 and global minimum of 18.2. On average, the CRT had 45% more crosstalk than the LCD and plasma displays.

As cited earlier, there is a reasonable amount of variation of the color spectrum across all LCD monitors and across all plasma displays. Similarly, there is a fairly large variation in overall crosstalk factor across all of the LCD monitors and all of the plasma displays. For example, the

TABLE 2 — Subjective testing of anaglyph glasses and comparison with calculated results. Lines join matching entries.

Red filter			Cyan		
Subjective	Calculated		Subjective	Calculated	
Glasses	Glasses	Cross-talk	Glasses	Glasses	Cross-talk
3DG32	3DG32	14.4	3DG26	3DG26	3.6
3DG26	3DG26	14.8	3DG30	3DG32	3.8
3DG3	3DG3	14.8	3DG32	3DG30	3.8
3DG31	3DG31	15.4	3DG24	3DG24	4.0
3DG19	3DG16	15.6	3DG14	3DG14	4.0
3DG16	3DG19	16.0	3DG4	3DG4	4.0
3DG21	3DG21	16.2	3DG2	3DG2	4.1
3DG15	3DG15	16.2	3DG27	3DG27	4.1
3DG27	3DG27	16.4	3DG8	3DG8	4.3
3DG20	3DG20	16.9	3DG25	3DG25	4.3
3DG29	3DG29	17.3	3DG29	3DG29	4.4
3DG30	3DG30	19.7	3DG31	3DG31	4.7
3DG17	3DG17	20.0	3DG11	3DG11	4.9
3DG6	3DG6	20.6	3DG6	3DG6	4.9
3DG14	3DG24	22.4	3DG20	3DG17	5.3
3DG24	3DG14	22.8	3DG17	3DG20	5.4
3DG9	3DG9	22.8	3DG3	3DG3	5.5
3DG4	3DG4	23.4	3DG19	3DG9	5.7
3DG2	3DG2	25.6	3DG21	3DG19	5.7
3DG11	3DG11	27.0	3DG16	3DG21	5.8
3DG8	3DG8	28.9	3DG15	3DG16	5.8
3DG18	3DG18	35.1	3DG9	3DG15	5.8
3DG25	3DG25	37.8	3DG18	3DG18	6.1
3DG28	3DG28	112.8	3DG28	3DG28	15.1

LCD monitor with the highest crosstalk factors (LCD04) only performs marginally better than a CRT, and the plasma display with the highest crosstalk factors (PDP02) had slightly worse performance than a CRT.

The best performing LCD monitor was LCD14 which provided an average crosstalk factor of only 13.8 and achieved the lowest crosstalk factor across all displays of 7.0 (when combined with glasses 3DG32). The best performing plasma display was the PDP12 with an average crosstalk factor of 11.9 which achieved the third lowest crosstalk factor across all plasma displays of 8.1 (when used with glasses 3DG13).

The worst pair of anaglyph glasses across all displays by far was 3DG28 – the ink-jet-printed transparency filters. This is not an unexpected result since these filters have such poor performance in the out-of-band wavelengths and very poor contrast.

The choice of best glasses depends upon which display is being considered. For the LCD monitors, 3DG32, 3DG26, and 3DG13 usually had the lowest overall crosstalk (all were within the uncertainty limits of each other). For the plasma displays, 3DG30, 3DG13, and 3DG32 usually

had the lowest overall crosstalk (within the uncertainty limits). For the CRT case, the best glasses were 3DG32, 3DG26, and 3DG13. It is interesting to note that the “cyan” filters of 3DG13 and 3DG26 have a more blue appearance than those of 3DG30 and 3DG32 that have a more cyan appearance. These differences may have some effect on color perception which is discussed below.

As can be seen in Tables C1 and C2, red crosstalk is usually significantly greater than cyan crosstalk – on average almost four times greater. Red crosstalk usually therefore dominates the overall crosstalk value. This can be attributed to the shape of the spectral curves for the display and glasses, but will also be due to the fact that the green channel is usually much brighter than the red channel.

It is usually possible to obtain a slightly lower overall crosstalk figure for a particular display by mixing and matching filters from different glasses; however, the improvement achieved is usually less than the calculated overall uncertainty value.

It is worth mentioning that even a perfect filter (one that transmits 100% of light in the desired wavelength domain and 0% outside it) would still have crosstalk if the display’s color channels overlap in the spectral domain (as most displays do).

Three further items are worth considering. First, intensity. If the filter cuts out most of the light, the image will be very dim and hard to see. Lower light levels also make the effect of even small ghosting levels proportionally greater than they might otherwise be. A brightness imbalance between left and right eye can also result in the Pulfrich effect⁸ whereby horizontal motion can be interpreted as binocular depth, which is generally undesirable. Brightness levels and imbalance have not been considered in this paper.

Second, color perception. Truly full-color stereoscopic images are not possible with anaglyphs, but a properly constructed anaglyph using complimentary colors can approximate a full-color image. This distorted color image is usually referred to as a “pseudo-color anaglyph” or a “polychromatic anaglyph” as opposed to a “full-color anaglyph” (which is not possible). If a non-complimentary combination is used (*e.g.*, red/blue or red/green), pseudo-color anaglyphs are impossible because a large portion of the visible spectrum is missing. The overall image may also be darker. This paper has only considered red/cyan anaglyphs, although it is sometimes hard to draw a line between what is classified as a cyan filter and what is classified as a blue filter.

Third, color balance and color temperature. Most monitors allow the color balance or color temperature of the display to be adjusted. This allows the user to change the relative intensities of the three color channels (but not the spectral output of each color channel). We have found that such adjustments do affect the results of the crosstalk calculations; however, as yet we have not used this knowledge to choose an optimum color balance, or performed any validation experiments to confirm whether the simulation of color

balance changes matches human perception. For the purposes of this study, the default color profiles were used for each monitor.

5 Conclusion

Although there are a range of stereoscopic display technologies available that produce much better 3-D image quality than the anaglyph 3-D method, the anaglyph remains widely used because of its simplicity, low cost, and compatibility with all full-color displays. This paper highlights one particular way of improving the image quality of anaglyph 3-D images specifically relating to spectral crosstalk.

This study has revealed that crosstalk in anaglyphic 3-D images can be minimized by the appropriate choice of anaglyphic 3-D glasses. The study has revealed that there can be considerable variation in the amount of crosstalk present when an anaglyphic 3-D display is viewed with different anaglyphic 3-D glasses.

The study has also revealed that there is considerable variation in the amount of anaglyphic crosstalk exhibited by different displays. For example, on average CRT monitors exhibit approximately 45% more crosstalk than LCD monitors and plasma displays.

An anaglyphic crosstalk calculation algorithm has been developed that appears to work well and generates outputs that agree well with subjective assessments of anaglyphic 3-D crosstalk.

It should be noted that the results of this paper are not intended to be a leader board of one glasses manufacturer versus another – we have not tested all glasses from all manufacturers, nor have we tested a large sample of each manufacturers glasses. This paper does, however, highlight that there is significant variation between different anaglyph 3-D glasses and displays. Further crosstalk optimization may be possible by using the anaglyphic crosstalk calculation algorithm and working with 3-D glasses manufacturers.

Acknowledgments

We would like to thank the multitude of companies and individuals who lent LCD monitors and plasma displays for testing.^{3,9} We also wish to thank iVEC (the hub of advanced computing in Western Australia) and Jumbo Vision International for their support of the plasma displays phase of this project.

References

- 1 R Zone, “Good old fashion anaglyph: High tech tools revive a classic format in spy kids 3-D,” *Stereo World* **29**, No. 5, 11–13 and 46 (2002–2003).
- 2 A J Woods and T Rourke, “Ghosting in anaglyphic stereoscopic images,” *Stereoscopic Displays and Virtual Reality Systems XI, Proc SPIE* **5291**, 354–365 (2004).
- 3 K S Karvinen and A J Woods, “The compatibility of plasma displays with stereoscopic visualization,” *Technical Report CMST2007-04* (Curtin University of Technology, Australia, 2007).

- 4 CIE, *Commission Internationale de l'Eclairage Proceedings* (Cambridge University Press, 1932).
- 5 B A Wandell and L D Silverstein, "Digital color reproduction," *The Science of Color* (Elsevier, 2003), pp. 296.
- 6 H Uchiike and T Hirakawa, "Color plasma displays," *Proc IEEE* **90**, Issue 4, 533–539 (2002).
- 7 A J Woods and S S L Tan, "Characterizing sources of ghosting in time-sequential stereoscopic video displays," *Stereoscopic Displays and Virtual Reality Systems IX, Proc SPIE* **4660**, 66–77 (2002).
- 8 C Pulfrich, "Die Stereoskopie im Dienste der isochromem und herterochromen Photometrie," *Naturwissenschaft* **10**, 553–564 (1922).
- 9 K L Yuen, "Compatibility of LCD monitors with stereoscopic display methods," *Undergraduate Student Project Report* (Curtin University of Technology, 2006).

Appendix A: Red/cyan anaglyph glasses

Appendix B: Spectral results for all tested LCD monitors and plasma displays

The figures below show the spectral results for each color channel of all tested LCD monitors and plasma displays. Figure B1 is normalized on the average value between 450 and 455 nm. Figures B2 and B3 are normalized on the peak value. Figures B4–B6 are normalized on the area under the

TABLE A1 — Red/cyan anaglyphic 3-D glasses measured.

Glasses Number	Name	Other information on glasses
3DG 2	IMAX/OMNIMAX	"Fujitsu presentation of "We are born of stars"; © IMAX Systems Corp., 1986; Made in USA by Theatric Support, Studio City, California."
3DG 3	National Geographic	Distributed with August 1998 edition of National Geographic Magazine
3DG 4	Sports Illustrated	Distributed with Winter 2000 edition of Sports Illustrated magazine (US edition). "MFGD by Theatric Support."
3DG 6	3D Greetings	Attached to a pseudo-color anaglyph postcard of a Tiger.
3DG 8	Spectacles	"Theatric Support, Studio City CA" Plastic hard-framed spectacles purchased from Reel-3D.
3DG 9	Bugs!	From <i>Bugs!</i> magazine series
3DG 11	[no name]	[no identification or writing on glasses – white cardboard]
3DG 13	Toyota	"Seeing is believing – The New Toyota Camry" advertising flyer.
3DG 14	Reel 3D	#1 Purchased from Reel-3D – apparently made by Theatric Support.
3DG 15	Reel 3D	#2 Purchased from Reel-3D.
3DG 16	Freddy's Dead	" <i>The Final Nightmare</i> ; New Line Cinema 1991" Distributed at showings of the movie "Freddy's Dead: The Final Nightmare"
3DG 17	3D Video Glasses	"© 1982 3D Video Corp., N. Hollywood, California; for use with 3D Video electronically processed TV programs"
3DG 18	Rhino Home Video	" <i>Cat Women of the Moon</i> ", " <i>Robot Monster</i> " & " <i>The Mask</i> "
3DG 19	DDD	"www.ddd3d.com Dynamic Digital Depth". Supplied by American Paper Optics.
3DG 20	ABC	"96/97 new season premiere; http://abc.com "
3DG 21	Optic Boom	"A DDD Product; ddd.com "
3DG 24	Studio 3D	"Stereoscopic imaging; www.studio3d.com "
3DG 25	Sports Illustrated Australian Edition	Distributed with March 2000 edition of Sports Illustrated magazine (Australian edition).
3DG 26	Substance Comic	Distributed with "3-D Substance #2" Comic, by Jack C. Harris and Steve Ditko and The 3-D Zone. ©1991.
3DG 27	Deep Vision 3D of Hollywood	"For Deep Vision 3-D TV"
3DG 28	Canon ink	Canon Ink (BCI-3e C/M/Y) printed on inkjet transparency sheet
3DG 29	Spy Kids 3D	"© 2003 Miramax Film Corp.; www.spykids.com ; Troublemaker Studios; Dimension Films; Manufactured by Playwerks Inc., USA" As supplied at movie theatres.
3DG 30	The Adventures of Shark Boy and Lava Girl	"© 2004 Miramax Film Corp.; Troublemaker Studios; Dimension Films; Columbia Pictures; Playwerks Premium Solutions" As supplied at movie theatres.
3DG 31	Shrek 3-D	Glasses blank white. As supplied with the Shrek 3-D DVD Region 4
3DG 32	World 3-D Film Expo	"WORLD 3-D FILM EXPO is a SubuCat Productions presentation www.sabucat.com " "REAL 3D is a trademark of and glasses made in U.S.A. by Dimension 3" As supplied with the World 3-D Film Expo Souvenir Book.

Note: Although a wide selection of glasses was tested, generally only a single pair of glasses of each particular style/brand was sampled. As such, due to manufacturing variations or experimental error, the results provided in this paper should not be considered to be representative of all glasses of that particular style/brand.

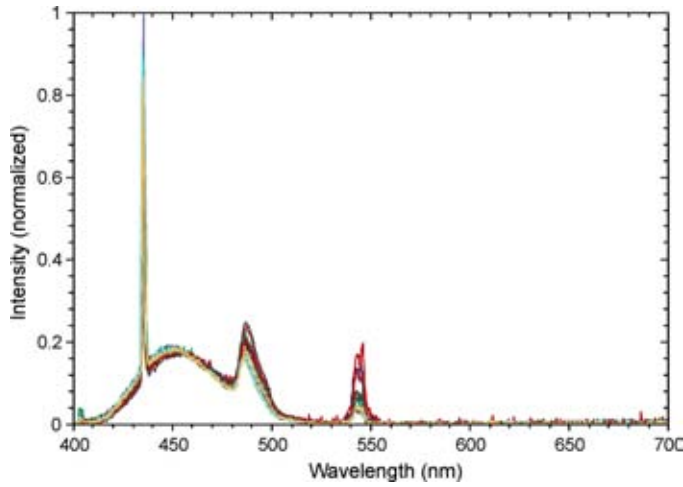


FIGURE B1 — Blue-color-primary spectral output for 13 LCD monitors.

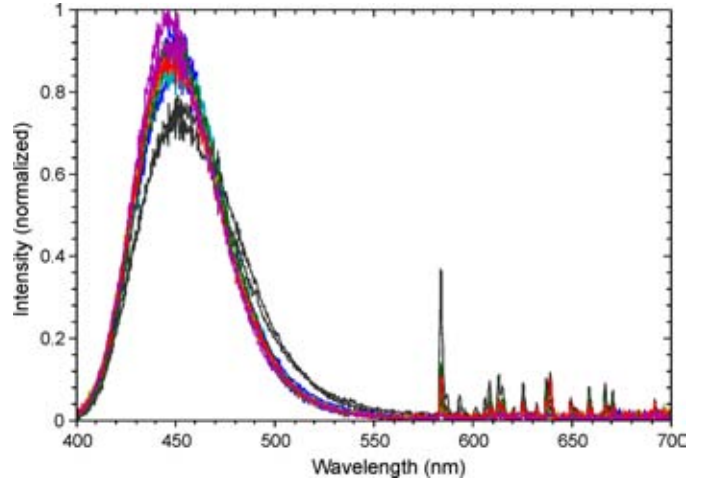


FIGURE B4 — Blue-color-primary spectral output for 14 plasma displays.

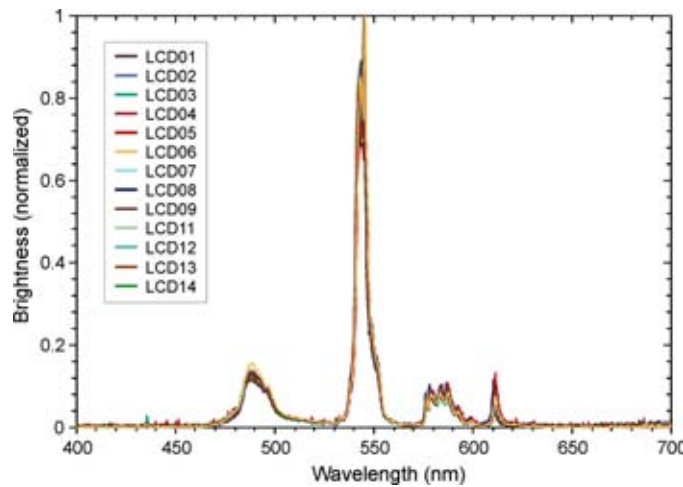


FIGURE B2 — Green-color-primary spectral output for 13 LCD monitors.

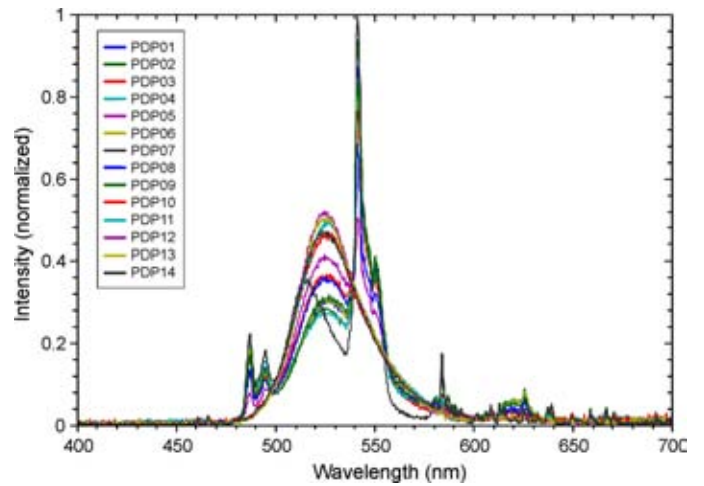


FIGURE B5 — Green-color-primary spectral output for 14 plasma displays.

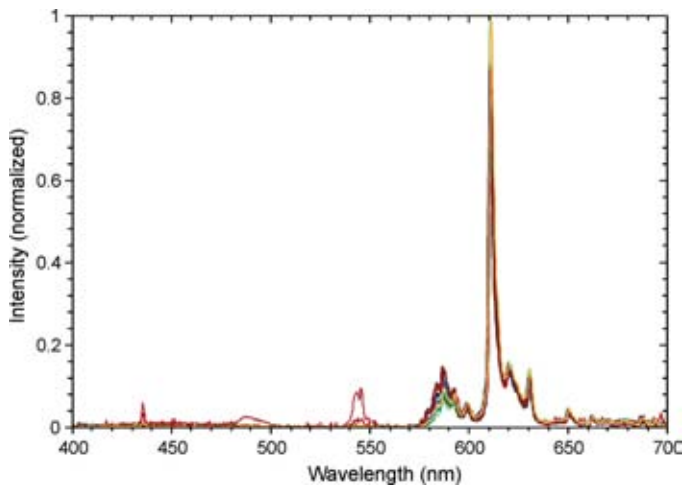


FIGURE B3 — Red-color-primary spectral output for 13 LCD monitors.

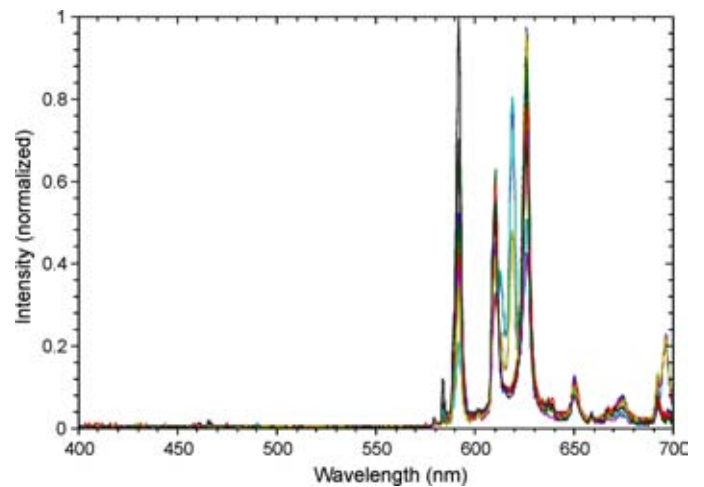


FIGURE B6 — Red-color-primary spectral output for 14 plasma displays.

curve. These normalizations were chosen so as to more easily reveal the similarities and differences between the various traces.

Appendix C: Crosstalk calculation results for LCD monitors and plasma displays

The following tables contain the results from the crosstalk calculation program. Every combination of anaglyph glasses and display has been calculated. The lowest overall crosstalk combinations are highlighted in bright green and the worst overall crosstalk results are highlighted in orange. Overall

crosstalk results of less than 15 have been highlighted in light green. Red crosstalk percentages less than nine have been highlighted in pink, and cyan crosstalk percentages less than 1.5 have been highlighted in cyan. These threshold figures do not have any significance apart from allowing us to highlight the lower crosstalk results.

TABLE C1 — Crosstalk calculation results for the LCD and CRT monitors. The top left cell of each combination is red crosstalk %, the top right cell of each combination is cyan crosstalk %, and the bottom cell of each combination is the overall crosstalk factor and uncertainty.

	LCD01	LCD02	LCD03	LCD04	LCD05	LCD06	LCD07	LCD08	LCD09	LCD11	LCD12	LCD13	LCD14	CRT
3DG02	17.7 0.9 18.6 ± 1.6	15.9 0.9 16.8 ± 1.5	17.1 0.8 17.7 ± 1.6	20.1 7.8 27.9 ± 2.4	23.8 2.6 26.5 ± 2.4	14.2 0.8 15.0 ± 1.3	17.8 1.0 18.8 ± 1.7	24.0 1.5 25.6 ± 2.3	18.1 1.7 17.8 ± 1.6	13.8 1.4 15.2 ± 1.3	16.5 1.2 17.8 ± 1.6	15.3 0.4 15.7 ± 1.4	14.1 0.6 14.8 ± 1.3	25.6 4.1 29.7 ± 1.4
3DG03	8.3 3.5 11.7 ± 1.0	7.6 3.3 10.9 ± 1.0	10.7 3.0 13.6 ± 1.2	9.6 9.7 20.8 ± 1.9	15.4 5.4 20.8 ± 1.9	7.8 3.4 11.3 ± 1.0	9.6 3.5 13.1 ± 1.2	16.3 4.3 20.6 ± 1.8	10.1 5.0 15.0 ± 1.4	7.6 3.8 11.4 ± 1.0	9.4 4.2 13.6 ± 1.2	7.0 2.4 9.4 ± 0.8	6.6 2.8 9.5 ± 0.8	14.8 5.5 20.3 ± 0.9
3DG04	16.0 0.7 16.7 ± 1.5	14.4 0.7 15.1 ± 1.3	15.9 0.5 16.4 ± 1.5	18.0 7.6 25.7 ± 2.2	22.2 2.4 24.7 ± 2.2	13.0 0.7 13.7 ± 1.2	16.5 0.9 17.4 ± 1.6	22.8 1.4 24.1 ± 2.1	15.3 1.4 16.8 ± 1.5	12.8 1.3 14.1 ± 1.2	15.4 1.1 16.5 ± 1.5	13.9 0.3 14.2 ± 1.3	12.9 0.5 13.4 ± 1.2	23.4 4.0 27.5 ± 1.3
3DG06	12.0 2.6 14.6 ± 1.3	10.8 2.4 13.2 ± 1.2	13.1 2.1 15.2 ± 1.4	13.8 9.0 22.8 ± 2.0	18.8 4.4 23.2 ± 2.1	10.2 2.5 12.7 ± 1.1	12.5 2.7 15.2 ± 1.4	19.2 3.3 22.5 ± 2.0	11.9 3.8 15.8 ± 1.4	9.7 2.9 12.7 ± 1.1	11.9 3.2 15.0 ± 1.3	9.9 1.7 11.6 ± 1.0	9.3 2.0 11.4 ± 1.0	20.6 4.9 25.5 ± 1.2
3DG08	20.4 1.6 22.1 ± 1.9	18.3 1.7 20.1 ± 1.8	19.1 1.5 20.5 ± 1.8	23.2 8.2 31.4 ± 2.7	26.2 3.3 29.5 ± 2.6	16.2 1.8 17.9 ± 1.6	20.3 1.9 22.2 ± 2.0	26.3 2.4 28.7 ± 2.5	17.9 2.6 20.5 ± 1.8	15.8 2.5 18.3 ± 1.6	18.7 2.3 21.0 ± 1.9	17.9 1.1 19.0 ± 1.7	16.5 1.5 18.0 ± 1.6	28.9 4.3 33.1 ± 1.5
3DG09	15.2 3.5 18.7 ± 1.6	13.6 3.2 16.8 ± 1.5	15.3 2.8 18.1 ± 1.6	17.1 9.7 26.8 ± 2.3	21.5 5.4 26.9 ± 2.4	12.4 3.2 15.7 ± 1.4	15.8 3.5 19.2 ± 1.7	22.1 4.3 26.4 ± 2.3	14.9 5.0 19.9 ± 1.8	12.2 3.5 15.7 ± 1.4	14.8 4.1 18.9 ± 1.7	13.2 2.3 15.5 ± 1.4	12.2 2.7 14.9 ± 1.3	22.8 5.7 28.5 ± 1.3
3DG10	24.8 0.7 25.5 ± 2.2	22.2 0.8 23.0 ± 2.0	22.4 0.5 22.9 ± 2.0	27.7 7.3 35.0 ± 3.1	29.8 2.3 32.1 ± 2.9	23.8 1.3 20.1 ± 1.8	24.0 1.0 25.1 ± 2.2	29.7 1.4 31.2 ± 2.7	21.1 1.4 22.5 ± 2.0	18.8 1.7 20.5 ± 1.8	22.0 1.3 23.2 ± 2.1	21.9 0.3 22.2 ± 2.0	20.1 0.6 20.8 ± 1.8	32.2 3.4 35.6 ± 1.6
3DG11	18.4 2.5 20.9 ± 1.8	16.4 2.3 18.7 ± 1.6	17.6 2.0 19.6 ± 1.7	20.7 8.9 29.6 ± 2.6	24.3 4.3 28.6 ± 2.5	14.6 2.4 17.0 ± 1.5	18.2 2.6 20.8 ± 1.9	24.5 3.2 26.3 ± 1.8	16.6 3.7 17.0 ± 1.5	14.1 2.8 20.3 ± 1.8	16.9 3.1 19.9 ± 1.8	15.8 1.6 17.4 ± 1.5	14.6 2.0 16.6 ± 1.5	27.0 4.9 31.8 ± 1.5
3DG13	8.1 0.9 9.0 ± 0.8	7.5 1.0 8.5 ± 0.8	10.5 0.7 11.3 ± 1.0	9.4 7.5 16.9 ± 1.5	15.3 2.5 17.8 ± 1.6	7.7 1.0 8.7 ± 0.8	9.4 1.2 10.6 ± 1.0	16.1 1.6 17.8 ± 1.6	9.8 1.6 11.5 ± 1.0	7.5 1.9 9.3 ± 0.8	9.2 1.5 10.7 ± 1.0	6.8 0.5 7.3 ± 0.7	6.4 0.8 7.4 ± 0.7	15.5 3.5 19.1 ± 0.9
3DG14	15.5 0.7 16.2 ± 1.4	13.9 0.7 14.7 ± 1.3	15.5 0.5 16.0 ± 1.4	17.5 7.6 25.1 ± 2.2	21.8 2.4 24.2 ± 2.2	12.7 0.7 13.3 ± 1.2	16.0 0.9 16.9 ± 1.5	22.3 1.4 23.7 ± 2.1	15.0 1.4 16.4 ± 1.5	12.4 1.3 13.7 ± 1.2	15.0 1.1 16.1 ± 1.4	13.4 0.3 13.7 ± 1.2	12.4 0.5 13.0 ± 1.2	22.8 4.0 26.8 ± 1.2
3DG15	9.4 3.9 13.3 ± 1.2	8.6 3.7 12.3 ± 1.1	11.4 3.4 14.8 ± 1.3	10.8 10.1 20.9 ± 1.8	16.4 5.9 22.3 ± 2.0	8.5 3.9 12.4 ± 1.1	10.5 4.0 14.5 ± 1.3	17.2 4.8 22.0 ± 1.9	10.7 5.5 16.3 ± 1.5	8.3 4.2 12.5 ± 1.1	10.1 4.7 14.8 ± 1.3	7.9 2.8 10.7 ± 0.9	7.4 3.3 10.7 ± 1.0	16.2 5.8 22.1 ± 1.0
3DG16	8.4 3.9 12.4 ± 1.1	7.8 3.7 11.5 ± 1.0	10.8 3.4 14.2 ± 1.3	9.8 10.1 19.9 ± 1.7	15.6 5.9 21.5 ± 1.9	7.9 3.9 11.9 ± 1.0	9.6 4.0 13.7 ± 1.2	16.4 4.8 21.2 ± 1.9	10.0 5.5 15.6 ± 1.4	7.7 4.3 11.9 ± 1.1	9.4 4.7 14.2 ± 1.3	7.1 2.8 9.9 ± 0.9	6.7 3.3 10.0 ± 0.9	15.6 5.8 21.4 ± 1.0
3DG17	11.5 3.2 14.7 ± 1.3	10.4 3.0 13.4 ± 1.2	12.8 2.7 15.5 ± 1.4	13.3 9.4 22.7 ± 2.0	18.4 5.0 23.5 ± 2.1	9.9 3.1 13.0 ± 1.1	12.1 3.2 15.4 ± 1.4	18.8 4.0 22.8 ± 2.0	11.7 4.6 16.3 ± 1.5	9.5 3.5 13.0 ± 1.2	11.6 3.8 15.4 ± 1.4	9.6 2.1 11.7 ± 1.0	9.0 2.6 11.5 ± 1.0	20.0 5.3 25.3 ± 1.2
3DG18	27.6 3.9 31.5 ± 2.7	24.3 3.6 27.9 ± 2.4	24.4 3.4 27.8 ± 2.4	29.7 10.1 39.8 ± 3.5	31.9 5.9 37.3 ± 3.3	21.0 3.8 28.0 ± 2.2	26.3 3.9 30.2 ± 2.7	32.1 4.8 36.9 ± 3.2	24.3 5.5 29.8 ± 2.6	20.5 4.1 24.6 ± 2.2	23.9 4.6 28.5 ± 2.5	24.3 2.7 27.0 ± 2.4	22.3 3.2 25.4 ± 2.2	35.1 6.1 41.2 ± 1.9
3DG19	9.0 3.8 12.8 ± 1.1	8.3 3.6 11.9 ± 1.1	11.1 3.3 14.4 ± 1.3	10.4 10.0 20.4 ± 1.8	16.1 5.7 21.8 ± 2.0	8.3 3.8 12.1 ± 1.1	10.2 3.8 14.1 ± 1.3	16.9 4.6 21.6 ± 1.9	10.5 5.4 15.9 ± 1.4	8.1 4.1 12.2 ± 1.1	10.0 4.5 14.5 ± 1.3	7.6 2.6 10.3 ± 0.9	7.2 3.1 10.3 ± 0.9	16.0 5.7 21.7 ± 1.0
3DG20	9.6 3.4 13.0 ± 1.1	8.8 3.2 12.0 ± 1.1	11.5 2.8 14.4 ± 1.3	11.1 9.6 20.7 ± 1.8	16.7 5.2 21.9 ± 2.0	8.7 3.3 12.0 ± 1.1	10.7 3.4 14.1 ± 1.3	17.4 4.2 21.6 ± 1.9	10.8 4.8 15.6 ± 1.4	8.4 3.7 12.1 ± 1.1	10.3 4.0 14.4 ± 1.3	8.1 2.3 10.4 ± 0.9	7.6 2.7 10.4 ± 0.9	16.9 5.4 22.3 ± 1.0
3DG21	9.4 3.8 13.2 ± 1.2	8.6 3.6 12.2 ± 1.1	11.4 3.3 14.7 ± 1.3	10.8 10.0 20.8 ± 1.8	16.4 5.7 22.2 ± 2.0	8.5 3.8 12.4 ± 1.1	10.5 3.9 14.4 ± 1.3	17.2 4.7 21.9 ± 1.9	10.8 5.4 16.2 ± 1.4	8.3 4.2 12.5 ± 1.1	10.2 4.6 14.8 ± 1.3	7.9 2.7 10.6 ± 0.9	7.5 3.2 10.6 ± 0.9	16.2 5.8 21.9 ± 1.0
3DG24	15.2 0.7 15.8 ± 1.4	13.6 0.7 14.3 ± 1.3	15.3 0.5 15.8 ± 1.4	17.1 7.6 24.7 ± 2.2	21.5 2.4 23.9 ± 2.1	12.4 0.6 13.1 ± 1.1	15.7 0.8 16.5 ± 1.5	22.1 1.3 23.4 ± 2.1	14.8 1.3 16.1 ± 1.4	12.2 1.3 13.4 ± 1.2	14.8 1.0 15.8 ± 1.4	13.1 0.2 13.4 ± 1.2	12.2 0.5 12.6 ± 1.1	22.4 4.0 26.3 ± 1.2
3DG25	27.8 1.6 29.4 ± 2.6	25.2 1.7 26.9 ± 2.3	24.9 1.5 26.3 ± 2.3	31.2 8.1 39.3 ± 3.4	32.6 3.3 35.9 ± 3.2	21.5 1.8 23.3 ± 2.0	27.2 1.9 29.1 ± 2.6	32.8 2.4 35.1 ± 3.1	23.6 2.6 26.2 ± 2.3	21.4 2.6 24.0 ± 2.1	24.6 2.3 26.9 ± 2.4	25.4 1.1 26.5 ± 2.3	23.1 1.5 24.6 ± 2.2	37.8 4.3 42.1 ± 1.9
3DG26	8.4 0.5 8.9 ± 0.8	7.8 0.7 8.4 ± 0.8	10.7 0.4 11.2 ± 1.0	9.5 7.3 16.8 ± 1.5	15.3 2.2 17.5 ± 1.6	7.9 0.6 8.5 ± 0.8	9.8 0.8 10.6 ± 1.0	16.4 1.3 17.7 ± 1.6	10.6 1.2 11.8 ± 1.1	7.8 1.4 9.2 ± 0.8	9.7 1.0 10.7 ± 1.0	7.2 0.2 7.4 ± 0.7	6.8 0.5 7.2 ± 0.7	14.8 3.6 18.4 ± 0.8
3DG27	10.3 1.0 11.3 ± 1.0	9.5 0.9 10.4 ± 0.9	12.0 0.7 12.7 ± 1.1	11.8 7.8 19.6 ± 1.7	17.2 2.7 19.9 ± 1.8	9.2 0.9 10.1 ± 0.9	11.5 1.1 12.6 ± 1.1	18.1 1.6 19.8 ± 1.8	11.8 1.8 13.5 ± 1.2	9.1 1.5 10.5 ± 0.9	11.1 1.3 12.5 ± 1.1	8.9 0.4 9.3 ± 0.8	8.3 0.7 9.0 ± 0.8	16.4 4.1 20.5 ± 0.9
3DG28	92.7 14.5 107.2 ± 9.2	84.5 15.0 99.5 ± 8.6	78.7 15.7 94.4 ± 8.2	97.0 19.5 116.5 ± 10.0	87.5 18.1 105.5 ± 9.2	70.9 17.2 88.1 ± 7.6	85.7 15.4 101.1 ± 8.8	87.9 17.1 105.1 ± 9.1	74.2 18.9 93.1 ± 8.1	71.1 17.4 88.5 ± 7.6	75.5 17.8 93.3 ± 8.1	90.8 13.0 103.8 ± 9.0	81.8 14.6 96.5 ± 8.3	112.8 15.1 127.9 ± 5.7
3DG29	10.9 1.6 12.5 ± 1.1	9.9 1.5 11.5 ± 1.0	12.4 1.3 13.7 ± 1.2	12.5 8.2 20.7 ± 1.8	17.8 3.3 21.1 ± 1.9	9.6 1.5 11.1 ± 1.0	11.9 1.7 13.6 ± 1.2	18.5 2.3 20.8 ± 1.8	11.9 2.5 14.4 ± 1.3	9.3 2.1 11.4 ± 1.0	11.4 2.0 13.5 ± 1.2	9.3 0.9 10.2 ± 0.9	8.7 1.2 9.9 ± 0.9	17.3 4.4 21.6 ± 1.0
3DG30	11.3 0.5 11.8 ± 1.0	10.3 0.6 10.9 ± 1.0	12.7 0.4 13.1 ± 1.2	13.1 7.4 20.5 ± 1.8	18.3 2.2 20.5 ± 1.8	9.8 0.5 10.4 ± 0.9	12.0 0.7 12.8 ± 1.2	18.7 1.2 19.9 ± 1.8	11.7 1.2 12.9 ± 1.2	9.4 1.3 10.7 ± 1.0	11.5 0.9 12.4 ± 1.1	9.4 0.2 9.6 ± 0.9	8.9 0.4 9.3 ± 0.8	19.7 3.8 23.4 ± 1.1
3DG31	8.7 1.9 10.7 ± 0.9	8.0 1.7 9.8 ± 0.9	11.0 1.4 12.4 ± 1.1	10.1 8.5 18.6 ± 1.6	15.8 3.7 19.5 ± 1.8	8.1 1.7 9.8 ± 0.9	9.9 1.9 11.9 ± 1.1	16.7 2.6 19.3 ± 1.7	10.4 3.0 13.4 ± 1.2	7.9 2.1 10.0 ± 0.9	9.7 2.3 12.0 ± 1.1	7.4 1.1 8.5 ± 0.8	7.0 1.4 8.4 ± 0.7	15.4 4.7 20.1 ± 0.9
3DG32	8.1 0.6 8.7 ± 0.8	7.5 0.7 8.2 ± 0.7	10.6 0.4 11.0 ± 1.0	9.2 7.5 16.7 ± 1.5	15.1 2.3 17.4 ± 1.6	7.7 0.6 8.3 ± 0.7	9.6 0.8 10.4 ± 0.9	16.2 1.3 17.4 ± 1.6	10.4 1.2 11.6 ± 1.1	7.7 1.3 9.0 ± 0.8	9.5 1.0 10.4 ± 0.9	7.0 0.2 7.2 ± 0.6	6.6 0.5 7.0 ± 0.6	14.4 3.8 18.2 ± 0.8

Paper 3 [Refereed Journal Article]

A. J. Woods, C. R. Harris (2012) "Using cross-talk simulation to predict the performance of anaglyph 3-D glasses" in Journal of the Society for Information Display, Vol. 20, No. 6, pp. 304-315.

Using cross-talk simulation to predict the performance of anaglyph 3-D glasses

Andrew J. Woods (SID Member)
Chris R. Harris

Abstract — The anaglyph 3-D method is a widely used technique for presenting stereoscopic 3-D images. Its primary advantage is that it will work on any full-color display (LCDs, plasmas, and even prints) and only requires that the user view the anaglyph image using a pair of anaglyph 3-D glasses with usually one lens tinted red and the other lens tinted cyan (blue plus green). A common image-quality problem of anaglyph 3-D images is high levels of cross-talk – the incomplete isolation of the left and right image channels such that each eye sees a “ghost” of the opposite perspective view. An anaglyph cross-talk simulation model has been developed which allows the amount of anaglyph cross-talk to be estimated based on the spectral characteristics of the anaglyph glasses and the display. The model is validated using a visual cross-talk ranking test which indicates good agreement. The model is then used to consider two scenarios for the reduction of cross-talk in anaglyph systems and finds that a considerable reduction is likely to be achieved by using spectrally pure displays. The study also finds that the 3-D performance of commercial anaglyph glasses can be significantly better than hand-made anaglyph glasses.

Keywords — *Stereoscopic, 3-D, cross-talk, ghosting, leakage, anaglyph.*

DOI # 10.1889/JSID20.6.304

1 Introduction

The anaglyph 3-D display technique dates back to 1853 when it was developed by William Rollman.¹ The technique involves the presentation of the left and right perspective images in complementary color channels of the display – usually with the left perspective image stored in the red color channel and the right perspective image in the blue and green color channels. To see the anaglyph 3-D image, the observer wears a pair of glasses fitted with color filters in front of each eye – usually red for the left eye and cyan (blue plus green) for the right eye. The color filters act to separate the components of the presented anaglyph 3-D image so that the left perspective image is only seen by the left eye, and the right perspective image is only seen by the right eye, and hence the observer can see a stereoscopic 3-D image.

Anaglyph 3-D has several limitations in terms of the quality of the presented 3-D images – particularly the inability to produce accurate full-color 3-D images (since color is used as the separation or multiplexing technique), binocular rivalry^{2,3} (sometimes known as retinal rivalry) (because each eye sees a different color), and often the presence of high levels of cross-talk (also known as crosstalk or cross talk).⁴ Despite the availability of stereoscopic 3-D display technologies which offer much higher-quality 3-D presentation (*e.g.*, polarized and active shutter glasses), anaglyph continues to be used today in a wide range of applications because it will work with any full-color display and the glasses are very cheap and commonly available, whereas polarized and active shutter 3-D methods require specialized equipment which may not be available to the user. The anaglyph 3-D technique is also seeing high levels of usage because of the current high level of interest in 3-D technologies generally.

Given the continued widespread use of the anaglyph 3-D technique, there is value in efforts to improve the image-quality of this technique. This paper concentrates on the 3-D image quality metric of cross-talk which can be defined as the “incomplete isolation of the left and right image channels”^{5,6} such that one eye can see a ghost image from the other channel. Cross-talk is one of the main determinants of 3-D image quality⁷ and stereoscopic viewing comfort.^{8,9}

Although there is very little literature on the perceptual effects of cross-talk in anaglyph 3-D images, there is a good body of work on the perceptual effects of cross-talk in other stereoscopic 3-D display technologies. Cross-talk has been found to “strongly affect subjective ratings of display image quality and visual comfort” in an active-shutter stereoscopic display.¹⁰ Cross-talk was found to “significantly degrade viewing comfort” in a polarized projected 3-D display.⁸ Cross-talk has also been found to have “a detrimental effect on the perceived magnitude of depth from disparity and monocular occlusions” using a mirror-stereoscope display.¹¹ Studies have found cross-talk levels of 5–9% can significantly affect visual comfort and image quality.^{8,10} Our own anecdotal evidence indicates that anaglyph 3-D images are similarly adversely affected by cross-talk.

Several methods have been proposed for improving the perceived quality of anaglyph 3-D images: applying cross-talk cancellation to reduce the perception of ghosting due to cross-talk,¹² registering the parallax of foreground objects,¹³ using different primary color combinations,¹⁴ and using different algorithms to calculate the RGB values of the anaglyph image.^{15–18} This paper uses the technique of optimizing the spectral curves of the display and/or glasses

Received 10-18-11; accepted 04-12-12.

The author is with Curtin University, GPO Box U1987, Perth, WA 6845, Australia; telephone +61-8-9266-7920, e-mail: A.Woods@curtin.edu.au.

© Copyright 2012 Society for Information Display 1071-0922/12/2006-0304\$1.00.

as a way of reducing anaglyph cross-talk,^{4,19} which is different but complementary to the improvement techniques listed above.

In particular, this paper describes the validation of a cross-talk simulation model which can be used to predict the cross-talk performance of anaglyph 3-D glasses when used with various full-color displays. The availability of an accurate cross-talk simulation model allows a better understanding of anaglyph cross-talk to be gained and also allows the investigation of new techniques which might offer lower cross-talk without needing to perform physical testing.

The test set of anaglyph glasses used in this study provides a good range of cross-talk values over which to validate the cross-talk simulation model (as will be seen in Sec. 4.3). The glasses test set is rather unique in that it can also be used to test another hypothesis. The test set consists of a selection of commercially sourced anaglyph 3-D glasses and also a number of “hand-made” glasses. The hypothesis is that “hand-made” glasses will have inferior 3-D performance compared to that of commercial anaglyph glasses.

Despite the widespread availability of anaglyph 3-D glasses, there will still be circumstances when a user may not have a pair readily available, and to solve this situation there are several sources which recommend constructing a pair of anaglyph 3-D glasses using some simple parts that may be available around the home – notably using colored “cellophane”^a plastic wrap^{20–23} for the red and cyan filters, or using marker pens^{24–27} and clear plastic sheet to construct the color filters. Anecdotal evidence indicated that hand-made anaglyph 3-D glasses would suffer from poor 3-D performance by exhibiting high levels of stereoscopic cross-talk. Visual testing and simulation have been used to verify this hypothesis and validate the cross-talk simulation model.

The analysis is conducted across a broad selection of display devices in order to generalize the results.

2 Cross-talk simulation

The cross-talk simulation used in this study builds on past work conducted by the authors and earlier collaborators.^{4,14,19} The program uses spectral data from the displays and glasses in combination with a cross-talk simulation model to estimate the presence of 3-D cross-talk when anaglyph 3-D images presented on emissive full-color displays are viewed using anaglyph 3-D glasses.

The program uses the following cross-talk simulation algorithm:

$$S_L = \int_{\lambda_{\min}}^{\lambda_{\max}} e(\lambda)g_L(\lambda)(m_L(\lambda)-b(\lambda))d\lambda \quad (1)$$

^aAlthough the term “cellophane” is commonly used to refer to any colored plastic wrap, in many countries it is a registered trademark of Innovia Films, Ltd., UK.

$$S_R = \int_{\lambda_{\min}}^{\lambda_{\max}} e(\lambda)g_R(\lambda)(m_R(\lambda)-b(\lambda))d\lambda \quad (2)$$

$$L_L = \int_{\lambda_{\min}}^{\lambda_{\max}} e(\lambda)g_L(\lambda)(m_R(\lambda)-b(\lambda))d\lambda \quad (3)$$

$$L_R = \int_{\lambda_{\min}}^{\lambda_{\max}} e(\lambda)g_R(\lambda)(m_L(\lambda)-b(\lambda))d\lambda \quad (4)$$

$$C_L = L_L/S_L \quad (5)$$

$$C_R = L_R/S_R \quad (6)$$

$$C = C_L + C_R \quad (7)$$

where S is the signal intensity (*e.g.*, intensity of the image intended for the left eye as seen at the left eye position, and similar for the right eye); e is the normalized photopic spectral sensitivity of the human eye²⁸ as illustrated in Fig. 3(a); g is the spectral transmission of the left or right eye filters of the glasses; m is the emission spectrum of the appropriate color channel(s) of the display monitor; b is the emission spectrum of the black level of the display; L is the leakage intensity (intensity of the image intended for the left eye as seen at the right eye position, or vice versa); C is the cross-talk at each eye (or combined) and usually expressed as a percentage; λ_{\min} and λ_{\max} describe the wavelength range – for the human eye the range of visible light sensitivity is approximately 400–700 nm; and subscripts L and R refer to the left-eye channel and right-eye channel, respectively. In a conventional red/cyan anaglyph, L will refer to the red channel and R will refer to the cyan (blue plus green) chan-

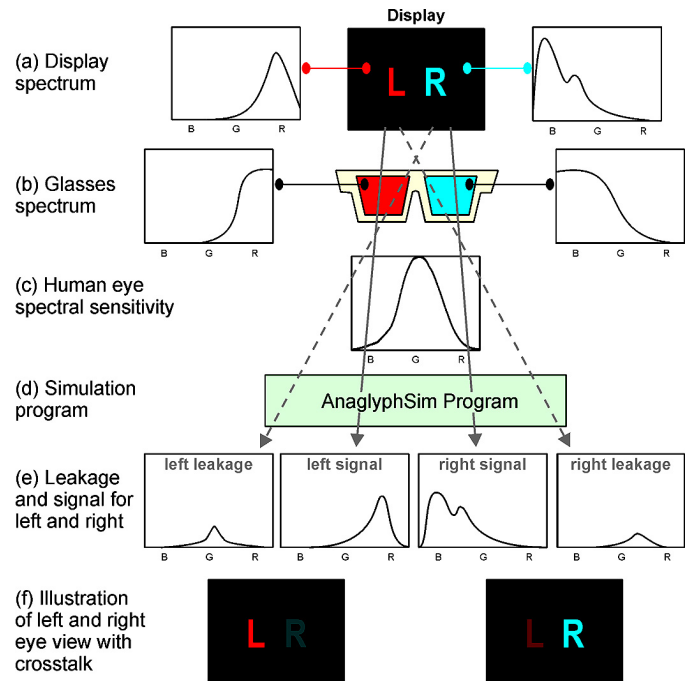


FIGURE 1 — Illustration of the process of anaglyph cross-talk simulation used in this project.

nel, but other color variations are possible (*e.g.*, blue/yellow or green/magenta¹⁴).

There is no requirement to use a calibrated device to measure m and b – the only requirement is that the same device and scaling is used between measurements. Additionally, S and L can be in arbitrary units because they are only used as a ratio in Eqs. (5) and (6).

This anaglyph cross-talk simulation algorithm is illustrated in Fig. 1 for the example case of a red/cyan anaglyph. Firstly, (a) the emission spectrum of red channel of the display, (b) the spectrum of the red filter of the glasses, and (c) the human-eye spectral sensitivity are multiplied to obtain (e) the spectrum of the intended signal seen by the left eye, and similar for the right eye. The spectrum of the leakage seen by the left eye is obtained by multiplying the spectrum of the blue plus green channels of the display, the spectrum of the red filter of the glasses, and the human eye spectral sensitivity. A similar process is used to determine the right-eye leakage. The luminance of each of these signals is obtained by integrating the resulting curves, which is illustrated by the bottom row (f) of this figure. The cross-talk percentage is obtained by dividing the leakage luminance by the signal luminance for each eye as set out in Eqs. (5) and (6). A very similar process would be used if different anaglyph color primaries were used.

The cross-talk performance of anaglyph glasses can vary quite widely from one pair of glasses to another and between different displays. The cross-talk simulation program can very quickly provide an estimate of cross-talk performance across a very large number of combinations of glasses and displays – a process that would be extremely time-consuming and logistically difficult if performed with physical displays and glasses. Another advantage of using a cross-talk simulation program is that it can be used to estimate the cross-talk performance of new or theoretical filters or displays without needing to perform physical testing.

Since the last paper on this topic,¹⁴ the simulation program, has been updated to use a more recent model of the human-eye spectral sensitivity^{28,29} and optimized to significantly increase the speed of operation.

3 Experimental method

The cross-talk simulation model was validated using a four-step process.

3.1 Spectral emission of displays

The spectral-emission properties of a selection of displays (LCD, PDP, CRT, and LED DLP)^b were measured using an Ocean Optics USB2000 spectroradiometer and also obtained

^bLCD = liquid-crystal display; PDP = plasma-display panel; CRT = cathode-ray tube; LED = light-emitting diode; DLP = digital light processing, which uses a digital micro-mirror device (DMD); CCFL = cold-cathode fluorescent lamp.

TABLE 1 — Register of tested displays.

Display ID	Display Make and Model (type of display)
LCD15	Samsung 2233RZ (LCD with CCFL ^b backlight)
PDP15	Samsung PS50A450 (Plasma Display Panel)
CRT20	Mitsubishi Diamond View 1771ie (Cathode Ray Tube)
LEDDL1	Samsung HLT5689 (rear projection DLP using an LED light engine)

from previous studies.^{4,14} Table 1 lists the displays used in this study.

The “Glasses IDs” and “Display IDs” used here correspond to the identification series first started in Ref. 19 and continued in Refs. 14 and 4 and are consistent among these studies.

It should be noted that particular care must be exercised when measuring the spectrum of the displays in order to minimize measurement error due to the measurement technique. In the case of the PDP and CRT monitors, their impulse-type operation can create synchronization issues with the sampling period of the sensor. Although all of the tested displays have some time-varying light output, PDP and CRT have the most variation. Long integration times should be used to minimize the effect of the time-varying light output. In the case of PDPs, another factor to consider is the presence of an automatic brightness limiter (ABL) which reduces the intensity of high-brightness scenes (to reduce power consumption). Full-screen test charts should not be used in order to avoid triggering the ABL, which would otherwise affect the measurement of the relative balance of the red, green, and blue color channels. The test charts should therefore be limited to a small portion of the screen, against a black background. The sensing head of the spectroradiometer should also not be placed too close to the surface of the screen such that the spatial separation of the color subpixels would be detected by the sensor.

3.2 Spectral transmission of glasses

The 12 pairs of anaglyph glasses tested in this study are listed in Table 2. The selection of glasses consists of three commercial pairs, three pairs constructed using marker pens, and six pairs constructed using colored plastic wrap (“cellophane”). This selection of glasses provided a wide range of cross-talk values which was useful for validating the cross-talk simulation model.

The three pairs of marker pen anaglyph glasses were constructed by using red/blue pairs of marker pens purchased from retail outlets. The marker pens were used to draw red and blue filter samples on a fresh sheet of overhead transparency film. The overhead transparency film used had good clarity and optical performance, in keeping with its manufacture for use in an optical projection application.

TABLE 2 — Register of anaglyph glasses tested in this study.

Glasses ID	Description
Commercial anaglyph glasses	
3DG73	NVIDIA 3D Vision Discover
3DG74	Stereoscopic Displays and Applications 2006 – manufactured by American Paper Optics
3DG88	Top Gear – manufactured by OZ3D Optics
Hand-made marker-pen anaglyph glasses	
3DG77	"hand-drawn" using Sharpie Fine Point Permanent Marker- red and blue (on clear overhead transparency film)
3DG78	"hand-drawn" using Artline 70 - red and blue (on clear overhead transparency film)
3DG79	"hand-drawn" using Artline 854 OHP Permanent Marker - red and blue (on clear overhead transparency film)
Hand-made 'Cellophane' anaglyph glasses	
3DG80	John Sands "Plain Cello" - red and blue
3DG81	John Sands "Plain Cello" (two layers) - red and blue
3DG82	Henderson Greetings "cello" - red and blue
3DG83	Henderson Greetings "cello" (two layers) - red and blue
3DG84	Unbranded "clear wrap" - red and blue
3DG85	Unbranded "clear wrap" (two layers) - red and blue

The “cellophane” glasses were constructed from three different brands of red and blue sets of colored plastic wrap purchased at retail outlets. Each brand of wrap was used to construct two pairs of anaglyph glasses; firstly, with a single layer of plastic film in each eye (red in one eye and blue/cyan in the other eye), and, secondly, with two layers of the plastic wrap.

The optical spectral transmission of the anaglyph filters were measured with a Perkin Elmer Lambda 35 spectrophotometer.

It should be noted that some of the hand-made glasses have some non-ideal optical properties other than their spectral transmission performance – specifically, the clarity of the lens [which degrades the modulation transfer function (MTF)], dispersion, and variability of the ink density. The marker-pens tend to have a considerable amount of variability of ink density (across the filter and from filter to filter) due to the manual way in which the ink is applied. Glasses 3DG81, 3DG84, and 3DG85 have the worst clarity of all the glasses making the image soft focused.

3.3 Cross-talk simulation

The spectral data from the displays and glasses was processed using the anaglyph cross-talk simulation program described in Sec. 2. This provides a cross-talk percentage estimate for both filters of every pair of glasses when used with each display – in this particular project a total of 96 values.

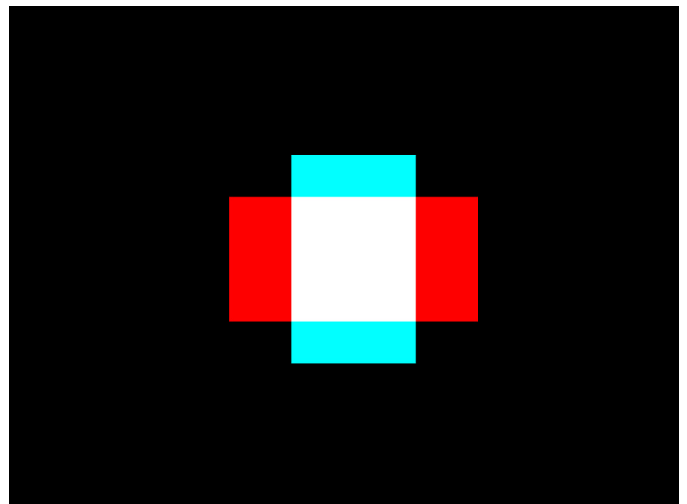


FIGURE 2 — The visual test target used during the anaglyph cross-talk visual ranking tests.

3.4 Visual ranking

The cross-talk performance of the various anaglyph filters were visually ranked to allow a comparison with the cross-talk simulation results. The glasses listed in Table 2 were mounted in similar white frames, ordered randomly, and each observer was asked to rank the glasses from lowest cross-talk to highest cross-talk whilst looking at the test graphic (see Fig. 2) presented on each target display (from Table 1). Five observers (labeled Ob1 to Ob5) took part in the visual ranking tests. Each observer was provided with a randomly ordered stack of glasses. The observers were asked to compare two glasses at a time using the test graphic and to place the glasses on the table in front of them with the lowest cross-talk glasses on the left to the highest cross-talk on the right. Each observer made multiple passes through the set of glasses in front of them, comparing two glasses at a time using the test graphic, to sort the glasses into the correct order, and finally confirm that the glasses were in the correct order. Each observer performed separate sorting tasks for the red and cyan filters across each of the four displays, so that each observer performed eight sorting tasks. The room was dimly lit to reduce the likelihood of ambient light or frame luminance affecting the results.³⁰

The visual validation test was conducted on the basis of the relative ranking of the cross-talk performance of the glasses because the human-visual system is not accurate at determining absolute measurement of brightness (known as “lightness constancy”),³¹ whereas the human-visual system is usually very good at performing relative brightness comparisons.

The test target used in this study (Fig. 2) allows two types of cross-talk comparison to be performed. In the case of a validation test with the red filters: Firstly, the relative brightness of the leaked cyan rectangle relative to the brightness of the passed red rectangle will give one indication of the cross-talk level, and, secondly, the relative brightness of the center white square relative to the brightness of the passed red rectangle will also give an indication of cross-

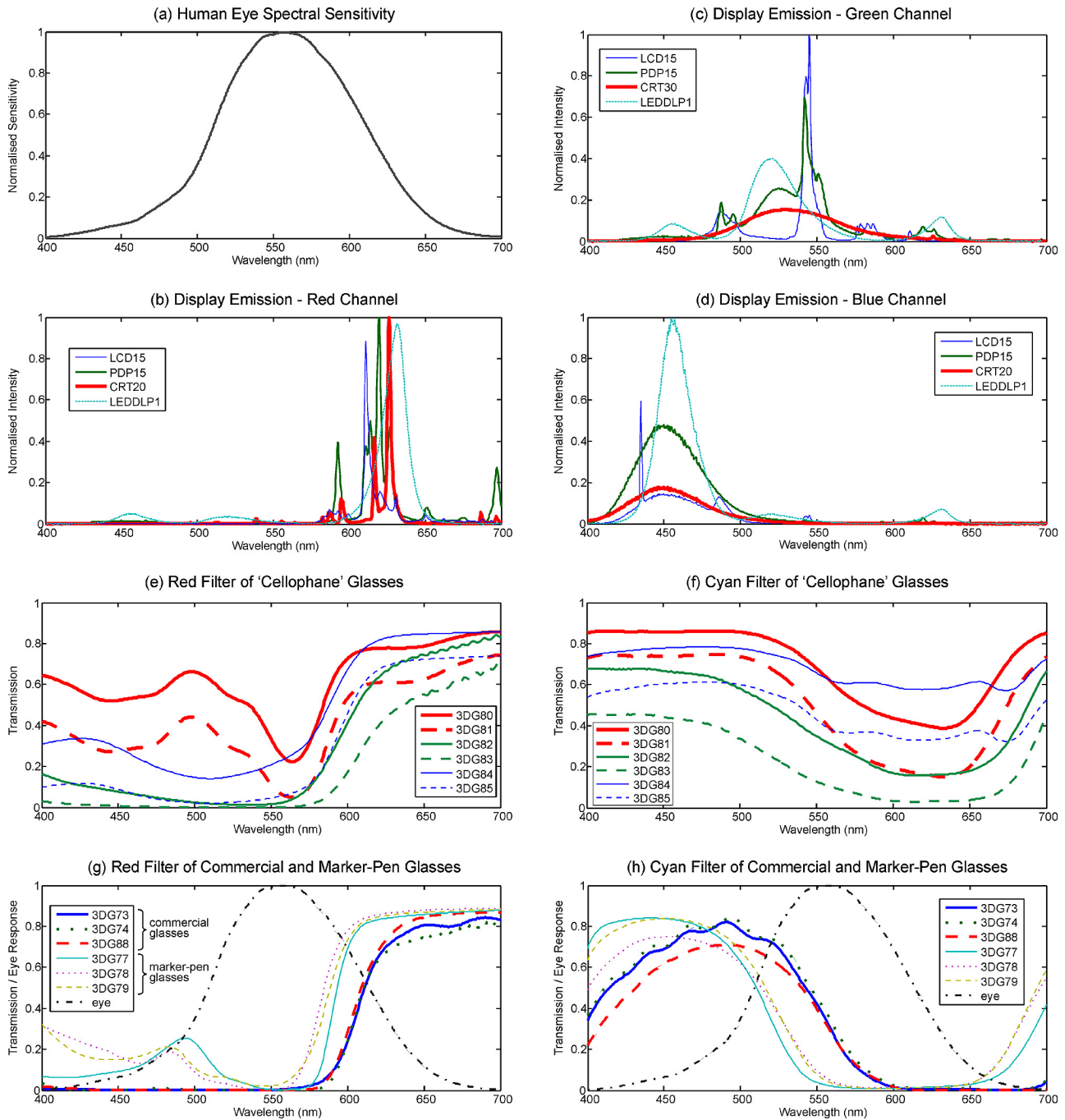


FIGURE 3 — Spectral plots of (a) human-eye spectral sensitivity, (b) the emission spectrum of the red channel of the tested displays, (c) the emission spectrum of the green channel of the tested displays, (d) the emission spectrum of the blue channel of the tested displays, (e) red filter of the tested “cellophane” glasses, (f) cyan filter of the tested “cellophane” glasses, (g) red filter of the commercial and marker-pen glasses with the human-eye response also indicated, and (h) cyan filter of the commercial and marker-pen glasses with human-eye response also indicated. The plots are shown vertically stacked with the same horizontal axis to allow easy comparison between different plots of the same color range.

talk level. It is usually easier to use the first method to compare glasses with low cross-talk levels and the second method for mid-to-high levels of cross-talk. The observers were briefed accordingly, but were free to use whichever method they found easiest.

The observers were asked to try to only consider cross-talk differences between the glasses and ignore other optical differences such as relative brightness, relative clarity, and

variability of the filter pigments. The marker pen filters usually had a high level of pigment variability. Some of the “cellophane” filters had very poor clarity and softened the image considerably. Several of the observers commented that it was difficult to compare cross-talk levels between two filters which had vastly different clarity, particularly when the cross-talk levels were seemingly close, which may lead to ranking error.

4 Results

4.1 Display spectra

The spectra of the four sampled emissive displays are shown in Figs. 3(b)–3(d) for each of the three color channels. The three curves for each display have been scaled such that the maximum of the three curves for each display is normalized to one. It can be seen that there is a considerable variation between the spectral curves of different displays for each color primary. This is due to each of the displays using very different light-generation and modulation techniques.

When considering the anaglyph performance of various emissive displays, of key importance is the amount of light emitted in the “out of band” areas for each color channel. For example, a green color primary would ideally only emit light in the approximate range 500–570 nm, but as can be seen in Fig. 3(c), most of the displays output a significant amount of light outside this range. More light output in the out-of-band areas for each color channel will contribute to higher levels of anaglyph cross-talk – this is considered further in Sec. 4.3.

4.2 Glasses spectral transmission

The spectral transmission of the glasses tested in this study are shown in Figs. 3(e)–3(h). The spectral transmission of the hand-made “cellophane” glasses are shown in Figs. 3(e) and 3(f). The spectral transmission of the commercial anaglyph glasses and the hand-made marker-pen glasses are shown in Figs. 3(g) and 3(h).

The spectral performance limitations of the “cellophane” glasses are clearly evident in Figs. 3(e) and 3(f). In an ideal pair of anaglyph glasses, the filters should pass the intended color band and block the unwanted color bands, with the blocking of the unwanted channels being the most important. For example, with a red filter, it should pass the red part of the spectrum (roughly 590–700 nm) and block the blue and green parts of the spectrum (roughly 400–570 nm). With most of the “cellophane” glasses, it can be seen that the unwanted color ranges are not well attenuated. Referring to the plots of the red filter of 3DG80, 3DG81, and 3DG84 in Fig. 3(e), it can be seen that these filters do not provide very much attenuation of wavelengths from 400 to 570 nm (the blue and green areas of the visible spectrum) which will result in significant leakage and therefore high cross-talk. This can be compared with the spectral performance of the red commercial filter 3DG88 in Fig. 3(g), which has very low transmission in the blue-green wavelength range. The marker-pen filters shown in Figs. 3(e) and 3(f) also show a similar insufficient attenuation in the 400–570-nm range which will also point to poor cross-talk performance. The cross-talk performance of the glasses will be discussed further from a simulation standpoint below.

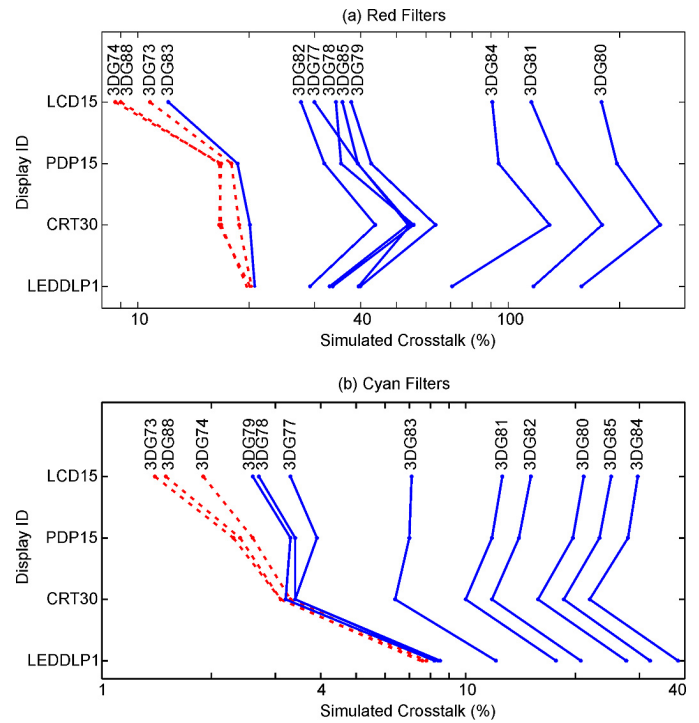


FIGURE 4 — Illustration of the results of the cross-talk simulation of the 12 sets of glasses across the four tested displays for (a) red filters and (b) cyan filters. The commercial anaglyph glasses are plotted in dashed red.

4.3 Cross-talk simulation

The cross-talk simulation program results for the 12 sets of anaglyph glasses (three commercial pairs and nine hand-made pairs) are shown in Table 3 for each of the four displays. The simulation program calculates the cross-talk for the left and right eyes separately, as shown in the table, and in addition provides an estimate of overall cross-talk (the sum of the cross-talk value from the left and right eyes). Table 3 has been sorted from lowest mean overall cross-talk to highest mean overall cross-talk.

The cross-talk simulation program results for the separate red and cyan filters for each display are also illustrated in Fig. 4. This figure allows an inter-display comparison of the relative performance of the different filters across different displays to be easily seen. The horizontal axis of both of these plots is shown on a logarithmic scale because it reduces the bunching of the results on the left-hand side of the plots, and the human-visual response has been described as having a logarithmic-like response to light over a limited range.^{32,33}

With reference to Fig. 4, it can be seen that the rank order of the simulated cross-talk of the tested filters is mostly the same from one display to another as illustrated by the mostly non-intersecting line segments. A few cross-overs do occur, and these will be caused by the differences between the shapes of the spectral curves of the different displays and the way these interact with the different shaped spectral curves of the filters.

With only a few exceptions, the simulation predicts that the commercial anaglyph filters will offer substantially

TABLE 3 — Cross-talk calculation results of the four displays. The lowest “overall cross-talk” for each display has been highlighted in rich green. “Overall cross-talk” of less than 15 has been highlighted in light green. The highest “overall cross-talk” for each display has been highlighted in orange.

Crosstalk (%)		Displays				mean
		LCD15	PDP15	CRT30	LED DLP1	
3DG88 commercial	Red	9.0	16.6	16.8	19.7	19.1
	Cyan	1.5	2.4	3.1	7.5	
	Overall	10.5	19.0	19.9	27.2	
3DG74 commercial	Red	8.7	16.8	16.6	20.1	19.5
	Cyan	1.9	2.6	3.3	7.8	
	Overall	10.6	19.5	19.9	27.9	
3DG73 commercial	Red	10.8	17.9	18.8	20.3	20.5
	Cyan	1.4	2.3	3.1	7.6	
	Overall	12.2	20.2	21.9	27.9	
3DG83 'cellophane'	Red	12.1	18.6	20.1	20.7	26.0
	Cyan	7.1	7.0	6.4	12.1	
	Overall	19.2	25.6	26.5	32.8	
3DG78 marker-pen	Red	34.3	35.4	55.6	33.6	44.2
	Cyan	2.7	3.4	3.4	8.4	
	Overall	37.0	38.8	58.9	42.0	
3DG77 marker-pen	Red	30.0	39.2	54.5	39.5	45.6
	Cyan	3.3	3.9	3.4	8.5	
	Overall	33.3	43.1	57.9	48.0	
3DG82 'cellophane'	Red	27.6	31.9	43.8	29.2	48.5
	Cyan	15.1	14.0	11.8	20.7	
	Overall	42.7	45.9	55.6	49.9	
3DG79 marker-pen	Red	37.7	42.7	63.7	39.9	50.3
	Cyan	2.6	3.3	3.2	8.2	
	Overall	40.3	46.0	66.9	48.1	
3DG85 'cellophane'	Red	35.7	39.3	53.7	33.0	65.2
	Cyan	25.1	23.3	18.6	32.1	
	Overall	60.8	62.6	72.4	65.0	
3DG84 'cellophane'	Red	90.6	94.3	129.4	70.6	125.7
	Cyan	29.7	27.9	21.9	38.3	
	Overall	120.3	122.2	151.3	108.9	
3DG81 'cellophane'	Red	115.5	135.8	179.4	117.1	149.9
	Cyan	12.6	11.8	10.0	17.7	
	Overall	128.1	147.6	189.3	134.8	
3DG80 'cellophane'	Red	178.7	196.7	257.3	157.8	218.7
	Cyan	21.1	19.7	15.8	27.6	
	Overall	199.8	216.4	273.1	185.4	

lower cross-talk than the other filters. With the better performing glasses (the commercial glasses), the simulation also points to some big differences in cross-talk performance from one display to another – for example, the simulation predicts that the commercial glasses will provide much lower cross-talk when used with LCD15 than the other displays, for both filter colors.

The simulation also predicts a good spread in the cross-talk performance of the selection of test filters used in this study – which in turn will aid in the validation of the simulation algorithm.

Some of the cross-talk simulation values presented in Table 3 are greater than 100% (*i.e.*, the worst performing filters) – the reader might at first think this is impossible, but this can occur with anaglyph cross-talk because the blue and green channels combined (one eye) have a much higher luminance than the red channel (the other eye).

It can be seen from Fig. 4(a) that the red filter of 3DG83 has a predicted cross-talk performance very close to that of the commercial filters; however, the cyan filter of 3DG83 has quite poor predicted cross-talk performance. Additionally, both of these marker-pen ink filters have high ink-density variability which degrade the visual quality of the glasses as a whole.

4.4 Visual ranking and validation

The visual ranking experiment involved 40 separate cross-talk ranking tasks across five observers, 12 pairs of glasses (two filters in each pair of glasses), and four different displays, resulting in 480 separate observations. The results of the visual ranking experiment are illustrated in Fig. 5. The glasses ranking results for each display, observer, and filter color combination are plotted against the corresponding simulated cross-talk ranking for that display and filter color. A line segment joins the visual ranking with the simulated ranking for each pair of glasses.

When plotting the ranking results, we had the option of showing the ranking observations with an equal spacing between observations; however, this would give an unrealistic equal visual emphasis on ranking observations regardless of how close or disparate the cross-talk is between those particular filters. We therefore decided to plot the results on horizontal axis values which correspond to the simulated

TABLE 4 — Example of the ranking representation technique used in Fig. 5 for Observer 2 ranking the cyan filters on LEDDLP1.

simulated rank order	visual rank order	simulated rank order on simulated crosstalk scale (%)	visual rank order on simulated crosstalk scale (%)
1	1	7.5	7.5
2	6	7.6	8.5
3	5	7.8	8.4
4	4	8.2	8.2
5	3	8.4	7.8
6	2	8.5	7.6
7	7	12.1	12.1
8	8	17.7	17.7
9	9	20.7	20.7
10	11	27.6	32.1
11	10	32.1	27.6
12	12	38.3	38.3

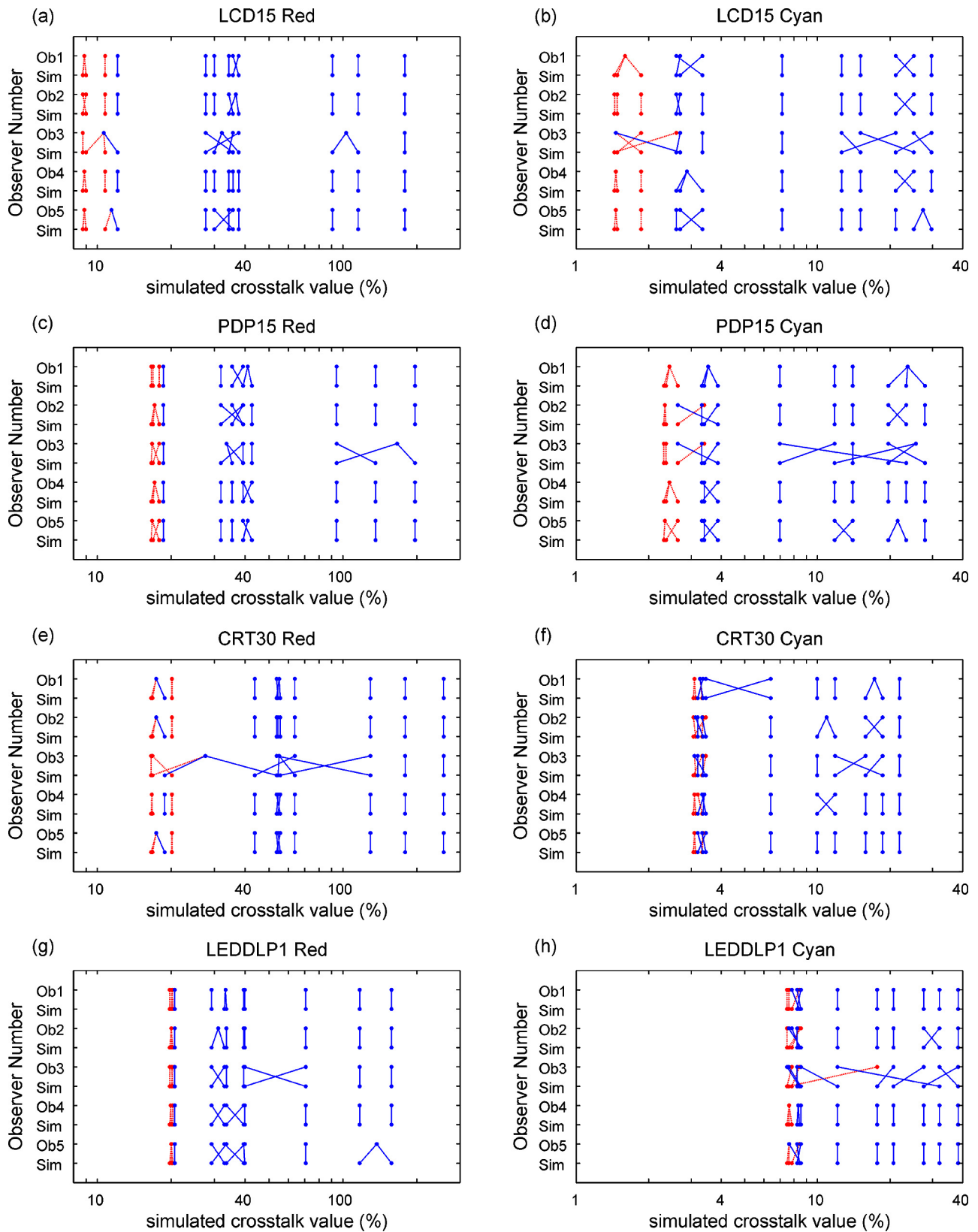


FIGURE 5 — The results of the cross-talk visual validation experiment compared to the simulated rankings. The red filter results are shown on the left column, and the cyan filter results on the right. The results for each display are plotted per row. The ranking results for each of the five observers are each plotted against the corresponding simulated ranking. The ranking of the commercial glasses are indicated in dashed red.

TABLE 5 — Results of the statistical analysis of the visual ranking results. The table shows the correlation data for each of the display, observer, and filter-color combinations, and also the average correlation for each observer using the Spearman’s rank correlation (r_s) technique as described in Sec. 4.5. (1 indicates good agreement, 0 indicates poor agreement).

Display ID	Observer	r_s of ranking results		
		red filters	cyan filters	average r_s for each observer
LCD15	Ob1	0.991	0.965	0.977
	Ob2	0.981	0.986	0.941
	Ob3	0.876	0.862	0.849
	Ob4	0.998	0.984	0.978
	Ob5	0.968	0.989	0.947
PDP15	Ob1	0.991	0.979	
	Ob2	0.930	0.942	
	Ob3	0.921	0.827	
	Ob4	0.972	0.965	
	Ob5	0.965	0.951	
CRT30	Ob1	0.981	0.967	
	Ob2	0.993	0.851	
	Ob3	0.818	0.862	
	Ob4	0.977	0.951	
	Ob5	0.972	0.935	
LEDDL1	Ob1	0.996	0.944	
	Ob2	0.991	0.853	
	Ob3	0.979	0.650	
	Ob4	0.984	0.991	
	Ob5	0.887	0.908	

cross-talk values for each pair of glasses. This plotting technique provides more visual emphasis on ranking errors which have greater simulated cross-talk differences than ranking errors between filters which have small simulated cross-talk differences. We believe this plotting technique allows a more useful analysis of the data.

This process is further illustrated in Table 4 for one observer, display, and filter-color-combination ranking test. The first two columns show rank order as calculated by the simulation program *vs.* the rank order as seen by the observer. Line segments have been shown between columns 1 and 2 to illustrate the quality of the comparison. Unity separation between ranking observations has been used in these first two columns. Columns 3 and 4 change the unity spacing of the observations to a spacing corresponding to the calculated cross-talk values. The values illustrated in columns 3 and 4 are then used to generate Fig. 5 – in this specific example observer Ob2 of Fig. 5(h).

The horizontal axis of Fig. 5 is shown on a logarithmic scale because the eye has a logarithmic-like response to light. The use of a logarithmic scale also reduces the bunching of the results on the left-hand side of the plots.

In cases where the observer was unable to distinguish any difference between different filters (*i.e.*, they looked to have the same amount of cross-talk), observers were allowed to group those glasses together. Glasses that have been grouped together by an observer are plotted with the same horizontal axis value (using the mean of the corresponding simulated cross-talk values).

The commercial glasses results are plotted in dashed red, whereas the hand-made glasses are plotted in solid blue – thus allowing the commercial glasses to be easily identified. This also highlights the better performance (lower cross-talk) of the commercial glasses.

Referring to Fig. 5, in cases where the visual ranking agrees with the simulated ranking, the line segments are vertical and do not intersect. In cases where the visual and simulated rankings disagree, there will be a cross-over of the line segments.

In general terms, the validation results, as depicted in Fig. 5, agree very well with the cross-talk simulation ranking results. Across all of the tests, a high proportion (66%) of the observations were ranked perfectly. It can be seen from the figure that ranking errors (indicated by crossing line-segments) rarely occurred across large simulated cross-talk value differences. The vast number of ranking errors occurred between filters with very similar values of simulated cross-talk. These results are statistically analyzed in the next section.

We should note that the visual ranking tests were only conducted within each display and not between displays. The cross-talk simulation results of Table 3 and Fig. 4 do indicate that LCD15 is expected to provide noticeably lower cross-talk than the other displays when using the commercial glasses. This scenario was tested visually using red filter 3DG88 and LCD15 could be seen to have significantly lower cross-talk than PDP15, CRT30, and LEDDL1 as predicted by the cross-talk simulation model; however, this test was only conducted informally and hence this aspect has not been validated in this particular study.

4.5 Statistical analysis

The quality of agreement between the visual ranking and the simulated ranking was assessed using the Spearman’s rank correlation³⁵ technique. The Spearman’s rank correlation is often used in biological statistics when one or more of the variables in a dataset consist of only ranks, as is the case with the human-visual ranking of cross-talk of anaglyph glasses as described in Sec. 4.4. The Spearman rank correlation (r_s) values were calculated for all of the visual validation observations across each display, observer, and filter color combination, and these are presented in Table 5 along with the average correlation for each observer.

The average r_s value for each observer was calculated as the mean of the eight correlation results for each observer (across four displays and two filter colors). The results of

TABLE 6 — Simulated improvement in anaglyph cross-talk performance by the use of theoretical “brick-wall” color filters as compared to the best real-world filters tested in this study.

(a) Red:

Display ID	simulated crosstalk (%)		improvement
	Best Tested Red Filter	Best 'Brick-Wall' Red Filter	
LCD15	8.7% (3DG74)	3.9% [620-700nm]	55%
PDP15	16.6% (3DG88)	13.9% [610-700nm]	16%
CRT30	16.6% (3DG74)	5.9% [625-700nm]	65%
LEDDL1P1	19.7% (3DG88)	19.4% [615-700nm]	2%

(b) Cyan:

Display ID	simulated crosstalk (%)		improvement
	Best Tested Cyan Filter	Best 'Brick-Wall' Cyan Filter	
LCD15	1.4% (3DG73)	0.3% [400-550nm]	31%
PDP15	2.3% (3DG73)	1.4% [400-555nm]	39%
CRT30	3.1% (3DG73)	2.4% [400-550nm]	20%
LEDDL1P1	7.5% (3DG88)	7.2% [400-550nm]	4%

observer three differed the most from the other four observers and also differed the most from the simulated rankings.

Despite the authors’ initial concern about the difficulties of validating the cross-talk simulation results using the visual validation experiment, the plots of the results (Fig. 5) and the statistical analysis (Table 5) provide a high level of confidence in the accuracy of the cross-talk simulation algorithm. It can be seen in Table 5 that 78% of the ranking tests have an r_s value of 0.9 or better, and 18% have an r_s value of 0.99 or better.

The plotting technique used in Fig. 5 provides good insight into the visual validation results. The technique works very well with this relatively small number of observers but would not work well with a larger number of observers. For a larger number of observers, it would be better to focus solely on the statistical analysis.

5 Discussion

Given that we have established a high level of confidence in the accuracy of the anaglyph cross-talk simulation model, we can now use the model to predict the performance of a number of anaglyph cross-talk scenarios we would not otherwise be able to physically replicate. Let us consider two such scenarios.

The first scenario is to consider the performance of a pair of anaglyph glasses which have a theoretical “brick-wall” filter performance (*i.e.*, 100% transmission in the pass region and 0% transmission in the blocking region). It will not be possible to physically test “brick-wall” filters in reality because they only exist in theory, but we believe that these simulation results will provide an indication of the absolute limit of lowest cross-talk performance achievable by optimization of the glasses alone. Table 6 lists the simulated anaglyph cross-talk performance of the four tested displays with simulated theoretical “brick-wall” anaglyph filters shown in comparison to the best tested filters for each display. The cut-off wavelength of the “brick-wall” filters were optimized for the least cross-talk for each display at 5 nm intervals and are indicated within square brackets on Table 6.

The simulation results indicate that even with a perfect pair of anaglyph glasses, none of the displays were able to exhibit zero cross-talk – this is because most displays output light in out-of-band wavelengths for each of the three color channels. The average anaglyph cross-talk improvement with perfect glasses across all of the displays was only 29% – the best improvement being 65% and the least improvement was 2%. The lowest cross-talk achievable with a perfect filter set was with LCD15 (3.9% for the red channel, and 0.3% for the cyan channel) – but these results are only achievable in theory. With LEDDL1P1, the lowest cross-talk achieved even with theoretically perfect glasses was particularly poor at 19.4% red and 7.2% cyan. The red channel of PDP15 also had a poor minimum cross-talk of 13.9% with perfect glasses. The simulation indicates that on CRT30 a fairly large reduction of cross-talk is achievable in the red channel using perfect glasses (65% reduction), but the actual cross-talk amount would still be fairly high at 5.9% for that eye.

The second scenario considers the cross-talk performance of LEDDL1P1. Most LEDs have fairly narrow spectral emission and very little out-of-band light output. In the case of LEDDL1P1, the half-intensity-width of the red, green, and blue LEDs are 17, 35, and 24 nm, respectively (which is good), but there is a lot of out-of-band light output, particularly in the green channel as can be seen in Fig. 3(c). The authors speculate that this out-of-band light output is due to the presence of a color-accuracy algorithm within the video-processing path of the display which drives the display color channels based on a mix of the color-channel inputs. Since LEDs have a very narrow spectrum, they are capable of generating very richly saturated colors, so in order for the image shown on an LED TV not to be shown with overtly rich colors it will be necessary to desaturate the image by mixing the color channels. Unfortunately, this process will be detrimental for anaglyph images because it will lead to cross-talk. The authors were unable to disable this color-mixing algorithm on LEDDL1P1 using the accessible menu options, but it was possible to calculate an estimation of the three-channel color spectrum of the display as if the color-mixing process was disabled (this has been given the designation

TABLE 7 — Comparison of the simulated cross-talk performance of LEDDLP1 with the theoretical LEDDLP2 for the three commercial anaglyph glasses.

Glasses		Display ID		improvement
		LEDDL1	LEDDL2	
3DG88	red	19.7	0.6	97%
	cyan	7.5	0.6	92%
	overall	27.2	1.2	96%
3DG74	red	20.1	0.9	96%
	cyan	7.8	1.0	87%
	overall	27.9	1.9	93%
3DG73	red	20.3	1.1	95%
	cyan	7.6	0.8	90%
	overall	27.9	1.9	93%

LEDDL2) and this can be fed into the cross-talk simulation model.

The cross-talk simulation results for LEDDL2, as shown in Table 7, are remarkable – a reduction of cross-talk by as much as 97%. These simulation results indicate that if the color mixing was able to be disabled on LEDDL1, instead of exhibiting the most cross-talk, it could be exhibiting the least cross-talk. The simulated overall cross-talk of 1.2% for LEDDL2 using the best tested glasses (3-DG88) is 71% less than even the lowest cross-talk achievable using the theoretical “brick-wall” filters on LCD15. If this is true, it will be a notable achievement. Work will continue to physically demonstrate this result.

The results of these two simulation scenarios illustrate the advantages that cross-talk simulation can provide – not only in anaglyph 3-D displays but also other stereoscopic displays. In this case, the simulations indicate that there is significantly more scope for reduction in anaglyph cross-talk by the use of more spectrally pure displays than might be gained from further improvements to the spectral performance of anaglyph glasses.

6 Conclusion

This paper has presented the validation of an anaglyph cross-talk simulation model which can be used to assess the improvement of 3-D image quality of anaglyph 3-D images viewed on emissive displays.

The paper has found that hand-made anaglyph glasses can exhibit significantly worse cross-talk performance than the better commercially available anaglyph 3-D glasses. Hence, the authors recommend using good commercially available anaglyph 3-D glasses rather than hand-made glasses.

The anaglyph cross-talk simulation program has also allowed us to explore the possibilities for reducing cross-talk in anaglyph systems and has found that (a) there is significant scope for reducing cross-talk by using spectrally pure emissive displays, (b) the choice of anaglyph glasses can have a significant effect on anaglyph cross-talk levels, and (c) there is only limited scope for reducing cross-talk levels

by further improvements to the anaglyph glasses (compared to existing good quality commercial anaglyph glasses).

With further refinement the anaglyph cross-talk simulation program discussed in this paper could also be used to simulate and investigate the cross-talk performance of other wavelength multiplexed 3-D techniques such as Infitec, Dolby 3D, and Panavision 3D.

Acknowledgments

The authors wish to acknowledge the support of the visualization facilities from iVEC; the collaboration of Stanley Tan, Tegan Rourke, Ka Lun Yuen, Kai Karvinen, Dean Leggo, and Jesse Helliwell on various aspects of this topic; Robert Loss, Alec Duncan, Iain Parnum, and Jesse Helliwell for their assistance with the visual validation tests; and Alec Duncan and John Merritt for their assistance with the manuscript.

References

- 1 R. Zone, “Good old fashion anaglyph: High tech tools revive a classic format in Spy Kids 3-D,” *Stereo World* **29**(5), 11–13, 46 (2002–2003).
- 2 V. C. Barber and D. A. Brett, “‘Colour bombardment’ – A human visual problem that interferes with the viewing of anaglyph stereo material,” *Scanning Electron Microscopy* **2**, 495–498 (1982).
- 3 R. Patterson *et al.*, “Binocular rivalry and head-worn displays,” *Human Factors* **49**(6), 1083–1096 (2007).
- 4 A. J. Woods *et al.*, “Characterizing crosstalk in anaglyphic stereoscopic images on LCD monitors and plasma displays,” *J. Soc. Info. Display* **15**(11), 889–898 (2007).
- 5 L. Lipton, “Glossary,” Lenny Lipton’s Blog, [online] (2009). URL: <http://lennylipton.wordpress.com/2009/03/16/glossary/> Dated 16 March 2009. Accessed 19 March 2010.
- 6 A. J. Woods, “How are crosstalk and ghosting defined in the stereoscopic literature?” *Proc. SPIE Stereoscopic Displays and Applications XXII* **7863**, 78630Z (2011).
- 7 A. J. Woods, “Understanding crosstalk in stereoscopic displays (Key-note Presentation),” *Proc. Intl. Conf. on 3D Systems and Applications (3DSA)*, 34–44 (2010).
- 8 F. L. Kooi and A. Toet, “Visual comfort of binocular and 3D displays,” *Displays* **25**, 99–108 (2004).
- 9 R. Patterson, “Review Paper: Human factors of stereo displays: An update,” *J. Soc. Info. Display* **17**(12), 987–996 (2009).
- 10 Y.-Y. Yeh and L. D. Silverstein, “Limits of fusion and depth judgment in stereoscopic color displays,” *Human Factors* **32**(1), 45–60 (1990).
- 11 I. Tsirlin *et al.*, “The effect of crosstalk on the perceived depth from disparity and monocular occlusions,” *IEEE Trans. Broadcasting* **57**(2), 445–453 (2011).
- 12 H. Sanftmann and D. Weiskopf, “Anaglyph stereo without ghosting,” *Computer Graphics Forum* **30**(4), 1251–1259 (2011).
- 13 I. Ideses and L. Yaroslavsky, “Three methods that improve the visual quality of colour anaglyphs,” *J. Opt. A: Pure Appl. Opt.* **7**(12), 755–762 (2005).
- 14 A. J. Woods and C. R. Harris, “Comparing levels of crosstalk with red/cyan, blue/yellow, and green/magenta anaglyph 3D glasses,” *Proc. SPIE Stereoscopic Displays and Applications XXI* **7253**, 0Q1–0Q12 (2010).
- 15 M. A. Purnell, “Casting, replication, and anaglyph stereo imaging of microscopic detail in fossils, with examples from conodonts and other jawless vertebrates,” *Palaeontologia Electron.* **6**(2), 1–11 (2003) (see Appendix 1).
- 16 E. Dubois, “A projection method to generate anaglyph stereo images,” *IEEE Intl. Conf. Acoustics, Speech, and Signal Processing, Proc. (ICASSP ’01)* **3**, 1661–1664 (2001).
- 17 W. R. Sanders and D. F. McAllister, “Producing anaglyphs from synthetic images,” *Proc. SPIE Stereoscopic Displays and Virtual Reality Systems X* **5006**, 348–358 (2003).

- 18 D. F. McAllister *et al.*, "Methods for computing color anaglyphs," *Proc. SPIE Stereoscopic Displays and Applications XXI* **7524**, 75240S-1-75240S-12 (2010).
- 19 A. J. Woods and T. Rourke, "Ghosting in anaglyphic stereoscopic images," *Proc. SPIE Stereoscopic Displays and Virtual Reality Systems XI* **5291**, 354-365 (2004).
- 20 Daleh, "Build your own 3D glasses" [online]. URL: http://www.daleh.id.au/3d_glasses.html Accessed: 26 August 2011.
- 21 Various authors, "How to make 3D glasses" [online]. URL: http://www.ehow.com/how_4455680_make-3d-glasses.html Accessed: 26 August 2011.
- 22 Author unknown, "How to make a pair of 3D glasses for 3D Anaglyphs" [online]. URL: <http://www.haworth-village.org.uk/3d/3d-glasses.asp> Accessed: 26 August 2011.
- 23 Author unknown, "Make your own 3-D glasses" [online]. URL: <http://paperproject.org/3dglases.html> Accessed: 26 August 2011.
- 24 A. Agarwal, "Make your own 3D glasses in 10 seconds," *Digital Inspiration* [online] (2010). URL: <http://www.labnol.org/home/make-3d-glasses/13776/> Dated: 2 June 2010. Accessed: 6 July 2011.
- 25 Various authors, "How to make your own 3D glasses," *Wikihow* [online]. URL: <http://www.wikihow.com/Make-Your-Own-3D-Glasses> Accessed: 6 July 2011.
- 26 Various authors, "Make 3-D glasses," *Wired How-to Wiki* [online]. URL: http://howto.wired.com/wiki/Make_3-D_Glasses Accessed: 6 July 2011.
- 27 S. Miles, "How to make your own 3D glasses," *Pocket-lint* [online] (2009). URL: <http://www.pocket-lint.com/news/27268/how-to-make-3d-glasses> Dated: 22 September 2009. Accessed: 6 July 2011.
- 28 A. Stockman and L. T. Sharpe, "Luminous energy function (2 degree, linear energy)" [online] (2007). URL: <http://www.cvrl.org/cvrlfunctions.htm> and <http://www.cvrl.org/database/text/lum/CIE2008v2.htm> Accessed: 29 July 2011.
- 29 A. Stockman *et al.*, "The dependence of luminous efficiency on chromatic adaptation," *J. Vision* **8**(16):1, 1-26 (2008). <http://journalofvision.org/8/16/1/>
- 30 K. R. Boff and J. E. Lincoln, *Engineering data compendium: Human perception and performance*, AAMRL, Wright-Patterson AFB, OH, pp. 370 (1988).
- 31 R. Blake and R. Sekuler, *Perception* (5th edn.) (McGraw Hill, Boston, 2006), pp. 92.
- 32 S. S. Stevens, "On the psychophysical law," *Psychological Rev.* **64**(3), 153-181 (1957).
- 33 Z. Xie and T. G. Stockham Jr., "Toward the unification of three visual laws and two visual models in brightness perception," *IEEE Trans. Systems, Man and Cybernetics* **19**(2), 379-387 (1989).
- 34 R. E. Walpole and R. H. Myers, *Probability and Statistics for Engineers and Scientists* (Collier Macmillan, 1985), pp. 347.
- 35 J. H. McDonald, *Handbook of Biological Statistics* (2nd edn.) (Sparky House Publishing, Baltimore, Maryland, 2009), pp. 221-223. <http://udel.edu/~mcdonald/statspearman.html>



Andrew J. Woods is a research engineer at Curtin University's Centre for Marine Science & Technology in Perth, Australia. He has MEng and BEng (Hons1) degrees in electronic engineering. He has expertise in the design, application, and evaluation of stereoscopic imaging systems for industrial and entertainment applications. He has served as co-chair of the Stereoscopic Displays and Applications conference since 2000.



Chris R. Harris is a graduate of Curtin University with a B.S. degree in applied physics and has interests in electronics and information technology. He is currently employed by Murdoch University.

Paper 4 [Refereed Journal Article]

A. J. Woods, C. R. Harris, D. B. Leggo, T. M. Rourke (2013) "Characterizing and Reducing Crosstalk in Printed Anaglyph Stereoscopic 3D Images" in (Journal of) Optical Engineering, SPIE, Vol. 52, No. 4, pp. 043203-1 to 043203-19, April 2013.

Characterizing and reducing crosstalk in printed anaglyph stereoscopic 3D images

Andrew J. Woods

Curtin University
Centre for Marine Science and Technology
GPO Box U1987
Perth, Western Australia 6845, Australia

Chris R. Harris

Murdoch University
90 South Street
Murdoch, Western Australia 6150, Australia

Dean B. Leggo

LabTech Training
25 Colray Avenue
Osborne Park, Western Australia 6017, Australia

Tegan M. Rourke

Sir Charles Gairdner Hospital
Hospital Avenue
Nedlands, Western Australia 6009, Australia

Abstract. The anaglyph three-dimensional (3D) method is a widely used technique for presenting stereoscopic 3D images. Its primary advantages are that it will work on any full-color display and only requires that the user view the anaglyph image using a pair of anaglyph 3D glasses with usually one lens tinted red and the other lens tinted cyan. A common image quality problem of anaglyph 3D images is high levels of crosstalk—the incomplete isolation of the left and right image channels such that each eye sees a “ghost” of the opposite perspective view. In printed anaglyph images, the crosstalk levels are often very high—much higher than when anaglyph images are presented on emissive displays. The sources of crosstalk in printed anaglyph images are described and a simulation model is developed that allows the amount of printed anaglyph crosstalk to be estimated based on the spectral characteristics of the light source, paper, ink set, and anaglyph glasses. The model is validated using a visual crosstalk ranking test, which indicates good agreement. The model is then used to consider scenarios for the reduction of crosstalk in printed anaglyph systems and finds a number of options that are likely to reduce crosstalk considerably. © The Authors. Published by SPIE under a Creative Commons Attribution 3.0 Unported License. Distribution or reproduction of this work in whole or in part requires full attribution of the original publication, including its DOI. [DOI: [10.1117/1.OE.52.4.043203](https://doi.org/10.1117/1.OE.52.4.043203)]

Subject terms: stereoscopic; three-dimensional; crosstalk; ghosting; leakage; anaglyph.

Paper 121666 received Nov. 15, 2012; revised manuscript received Mar. 6, 2013; accepted for publication Mar. 7, 2013; published online Apr. 5, 2013.

1 Introduction

The anaglyph three-dimensional (3D) method is the most commonly used technique for printing stereoscopic 3D images, with it being used in a wide range of technical and entertainment publications. The anaglyph technique uses spectral multiplexing to encode left and right views within a single printed image. The left and right perspective images are encoded in complementary color channels of the image—usually the left image in the red channel and the right image in the blue and green color channels. To see the anaglyph 3D image, the observer wears a pair of glasses fitted with color filters in front of each eye—usually red for the left eye and cyan (blue plus green) for the right eye. The color filters act to separate the components of the presented anaglyph 3D image with the aim that the left-perspective image is only seen by the left eye, and the right-perspective image is only seen by the right eye, and allow the observer to see a compelling stereoscopic 3D image.

There are many techniques which can be used to print 3D images¹ (e.g., lenticular, free-view stereo-pairs, stereo-pairs viewed with mirror or lensed viewers, parallax barrier, polarized vectographs,² and polarized StereoJet prints²), however anaglyph printing is the most commonly used 3D printing technique, primarily because of its economy and ease of use. Despite its popularity, anaglyph 3D printing suffers from probably the lowest 3D quality of all the 3D printing methods. Given the continued widespread use of the anaglyph 3D technique, there is value in efforts to improve the image quality of this technique.

Anaglyph 3D has several limitations in terms of the quality of the presented 3D images—particularly the inability to

produce accurate full-color 3D images (since color is used as the separation or multiplexing technique), binocular rivalry³ (sometimes known as retinal rivalry) (because each eye sees a different color), and often the presence of high levels of crosstalk.⁴ This paper concentrates on the 3D image quality metric of crosstalk, which can be defined as the “incomplete isolation of the left and right image channels”^{5,6} such that one eye can see a ghost image from the other channel. Crosstalk is one of the main determinants of 3D image quality⁷ and stereoscopic viewing comfort.⁸

Although there is very little literature on the perceptual effects of crosstalk in anaglyph 3D images, there is a good body of work on the perceptual effects of crosstalk in other stereoscopic 3D display technologies. Crosstalk has been found to “strongly affect subjective ratings of display image quality and visual comfort” in an active shutter stereoscopic display,⁹ “significantly degrade viewing comfort” in a polarized projected 3D display,⁸ and have “a detrimental effect on the perceived magnitude of depth from disparity and monocular occlusions” using a mirror-stereoscope display.¹⁰ Studies have found crosstalk levels of 5% to 9% can significantly affect visual comfort and image quality.^{8,9} Our own anecdotal evidence indicates that anaglyph 3D images are similarly adversely affected by crosstalk.

Several methods have been proposed for improving the perceived quality of anaglyph 3D images: applying crosstalk cancellation to reduce the perception of ghosting due to crosstalk,¹¹ registering the parallax of foreground objects,¹² using different primary color combinations,¹³ and using different anaglyph multiplexing algorithms to calculate the RGB values of the anaglyph image.^{14–20} The choice of

anaglyph multiplexing algorithm will determine the amount and quality of color reproduction in the anaglyph image and inversely, the amount of binocular rivalry. For example, a highly saturated scene can cause high levels of binocular rivalry if a high color reproduction anaglyph algorithm is used. However, binocular rivalry can be reduced by using an anaglyph algorithm which desaturates the input images, but this reduces the quality of color reproduction.²⁰

This paper uses the technique of optimizing the spectral curves of the “display” and glasses, and maintaining purity of the color channels, as a way of reducing anaglyph crosstalk,^{4,21} which is different but complementary to the improvement techniques listed above. In the context of printed anaglyphs discussed in this paper, the term “display” will be used to refer to the printed image which is displayed to the observer—and indirectly the specific ink set and paper used to generate the print, and the light source used to illuminate it.

The anaglyph 3D technique dates back to 1853 when it was developed by William Rollman²²—although it is believed he only used solid blocks of color in his work and not continuous tone images. Louis Ducos Duhauron is credited as inventing the continuous tone printed anaglyph in 1891.^{23–25} In 1895, Alfred Watch²⁶ presented a descriptive article introducing the printed anaglyph process.

Despite anaglyph 3D prints having been with us for over a hundred years, it is surprising that there have been relatively few technical publications to have described the science and technique of the printed anaglyph 3D image over this period, and several fundamental problems remain unsolved.

In 1937, John Norling²⁷ identified that “inks, pigments and dyes commonly used in printing the red and blue pictures are not pure colors” and hence “a residual image or ghost image” will be present, and patented a technique of overprinting with yellow ink to improve the printed spectra.

In 2002, Steven Harrington et al.^{28,29} disclosed a series of work on Illuminant Multiplexed Images, encoding separate images in the separate ink colors, and decoding the images using narrow-band light sources. This topic has some relevance to anaglyph imaging however their work did not specifically address printed anaglyphs viewed through anaglyph glasses.

In 2005, Vu Tran¹⁸ described the development of an anaglyph multiplexing algorithm for printed anaglyphs which aimed to improve the color rendition of printed anaglyphs (using dichopic color mixture theory)¹⁸ and reduce crosstalk. In this dissertation, he identified that in-built color management can disrupt the quality of printed anaglyphs (which agrees with our findings) and developed a detailed algorithm to cope with this effect. He also wrote “the illuminant light does not have a strong effect on overall 3D perception” which disagrees with our findings. In 2011, Ru Zhu Zeng¹⁹ described another algorithm to color correct anaglyph 3D images for printing, but the paper did not disclose the details.

In 2009, Ron Labbe¹ provided a summary of 3D printing techniques and a timeline of the use of the printed anaglyph in publicly released publications. He also correctly identified that “the inks in the CMYK process do not lend themselves to a perfectly ghost-free image, especially the cyan”¹—this is discussed in further detail later in Sec. 5.3.

Moving on from the traditional printed anaglyph, in 1974 Jay Scarpetti³⁰ proposed a printed anaglyph technique based

on a front and back lit printed transparency, and in 2009, Monte Ramstad³¹ disclosed an extension of the conventional anaglyph printing process using fluorescent inks, but these techniques do not offer any direct benefit to the conventional printed anaglyph.

Attempts to optimize the performance of printed anaglyph images by the appropriate choice of printing inks and filters in the anaglyph glasses has also been performed for some time but mainly in an empirical manner.^{32,33} This paper proposes a similar optimization, but using a technical analysis and simulation to guide the choice of glasses and inks, with an additional variable which is the choice of light source.

The work on printed anaglyphs described in this paper builds upon previous work that some of the authors of this paper published on crosstalk with anaglyph images on emissive displays such as liquid crystal displays (LCDs), plasma display panels (PDPs), digital light projection televisions (DLP TVs) and cathode ray tubes (CRTs).^{4,13,21,34} Emissive displays and printed images differ in the way that the image and color is generated. Emissive displays use the additive color model (by additive mixing of red, green and blue color primaries) whereas printing uses the subtractive color model (by subtractive mixing of cyan, magenta and yellow inks).³⁵ Figure 1 provides an illustration of the difference between the additive color and subtractive color models. With an emissive display, the screen starts from a black base and then red, green or blue light is added in various combinations to produce a wide range of colors. For example, when red and blue light are added together [Fig. 1(a)] the result is a magenta color, and when red, green, and blue light are used together (in an appropriate balance), the additive result is white. In contrast to emissive displays, the starting point with color printing is a blank white page. The most commonly used primary color inks are cyan, magenta and yellow—commonly called “process inks.”³⁵ With reference to Fig. 2, it can be seen that the yellow ink mostly attenuates (subtracts) light in the blue spectral region (~400 to 500 nm) whilst not substantially attenuating light in the green (~500 to ~600 nm) and red (~600 to ~700 nm) regions. Ideally the magenta ink attenuates (subtracts) light in the green spectral region, and cyan ink attenuates (subtracts) light in the red spectral region, while not attenuating light outside these regions. In printing, the application of cyan ink attenuates the red spectral band so it can be

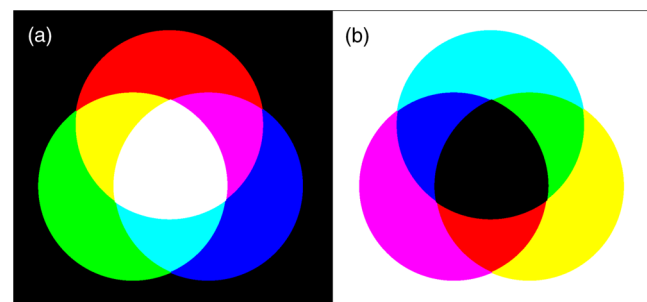


Fig. 1 An illustration of (a) the additive color model as used in emissive displays with red, green and blue color primaries, and (b) the subtractive color model as used in printing with cyan, magenta, and yellow color primaries. The combination of the different color primaries in varying amounts in the two models results in a wide range of possible colors.

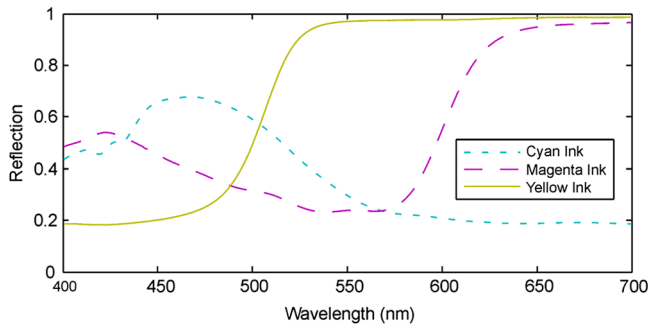


Fig. 2 The reflectance spectra of an example set of cyan, magenta, and yellow printing inks.

thought of as “minus-red,” and similarly magenta ink can be thought of as “minus-green,” and yellow ink as “minus-blue.” The combined printing of the three printing inks (cyan, magenta and yellow) in varying density allows a wide range (gamut) of colors to be presented. For example, when cyan and magenta inks are printed together [Fig. 1(b)], a blue color is generated. When ideal cyan, magenta and yellow inks are printed together, all light reflected off the white page is absorbed and a black area is created. This description serves to illustrate that the process of generating printed anaglyph 3D images is similar but has notable differences to anaglyph images on emissive displays, and these differences mean that the analysis and optimization of printed anaglyphs need to be different.

The body of this paper starts by providing a summary of the mechanisms by which crosstalk occurs in printed anaglyph 3D images. This is followed by the introduction of a mathematical model that describes and predicts the occurrence of printed anaglyph 3D crosstalk due to spectral characteristics. Next, the paper describes a visual validation experiment that was conducted to determine the accuracy of the developed model. In the discussion, the paper describes the advantages that the availability of an accurate crosstalk simulation model affords, and uses the model to investigate three methods of reducing crosstalk in anaglyph 3D prints, one of which on its own could significantly reduce anaglyph crosstalk.

2 Sources of Crosstalk in Printed Anaglyphs

This work has identified four main contributors to crosstalk in printed anaglyph images:

2.1 Spectral Characteristics

Since the anaglyph 3D process uses spectral multiplexing to separate the left and right image channels, the spectral characteristics of the lighting, paper, printing inks and 3D glasses and how they interact will determine how light from the left and right image channels will reach the left and right eyes. The specific spectral width and cut-off wavelength of each of the printing inks in relation to the cut-off wavelength of the color filters in the anaglyph glasses will affect how well the color channels are isolated, and therefore the amount of crosstalk present.

Ideally each of the cyan, magenta, and yellow inks will strongly attenuate light in the red, green, and blue color bands, respectively, while leaving the other color bands unattenuated, but in reality, the printing inks deviate from this

ideal response considerably and, for example, cyan ink commonly attenuates a considerable amount of the green and blue light bands. This nonideal spectral response of the printing inks, as illustrated in Fig. 2, limits the ability to maintain isolation between the color channels and hence is another source of crosstalk.

The spectral characteristics of the specific blank “white” paper used to print anaglyph 3D images can also affect anaglyph crosstalk, but in normal circumstances we expect this to be a small effect. We have also found that the spectral characteristics of the lighting used to illuminate the printed anaglyph can affect the amount of crosstalk present.

The smart choice of lighting, printing inks and 3D glasses can reduce the presence of anaglyph crosstalk and this will be explored further in Sec. 3 by the use of the simulation model.

2.2 Color Space Conversion

Most image editing is conducted in the RGB (red-green-blue) color space, because this is the color space needed for most emissive displays, however for printing, images must be converted to the CMYK (cyan-magenta-yellow-black) color space. When working with anaglyph images, ideally the color channels of the image will be maintained separate through the entire imaging chain, but the default RGB to CMYK color space conversion process used by most software will often mix the color channels in order to maintain color accuracy (see also Sec. 2.3.). Optimally the *R* (red) channel (of the RGB color space) will be mapped to the *C* (cyan) channel (of the CMYK color space), *G* (green) to *M* (magenta), and *B* (blue) to *Y* (yellow), however this is often not the way the conversion is performed. If some mixing of the color channels occurs during the color space conversion, this will contribute to crosstalk.

2.3 Color Management

Color management is a mathematical process that attempts to ensure that when an image is printed or displayed on different devices that the colors of the image appear the same between all of those devices.³⁵ Many readers will be familiar with the situation where an image displayed on the screen of their computer can look substantially different from the same image printed using their desktop printer. Color management attempts to solve these color consistency problems by a process of characterizing and calibrating the color characteristics of the devices used to capture, present and print color images.³⁵ In summary, each device used to capture, display or print color images needs to be characterized and a profile [often known as an International Color Consortium (ICC) profile] will be defined for each device. When a color image is transferred from one device to another, the ICC profile is used by the color management module (CMM) to “convert” the color values of the image so that the colors will look the same on the target device as they do on the source device.

The process of color management usually achieves its task by mixing the color channels of the color image to achieve the desired colors—much like a painter mixes inks to achieve a desired color. This process can produce very pleasing color accurate images when used for regular two-dimensional color images; however, it is our proposition

that this mixing is detrimental when applied to anaglyph 3D images and will lead to the presence of crosstalk.

Although color management still has some importance with anaglyph images, the color spectrum received by each eye is distorted by the anaglyph glasses worn by the observer (which are designed to de-multiplex the different color bands to each eye) and hence the perception of color is substantially biased. The color channel mixing process used by color management also conflicts with the need to maintain isolation between the color channels in anaglyph images. We therefore suggest that there needs to be a different color management process for anaglyph images, one that maintains isolation between the color channels, perhaps by integrating the color management and color multiplexing steps into a single process.^{15,18}

For the purposes of this project it would have been helpful if color management could be totally disabled, but we were unable to find a reliable way of achieving this with common desktop printers. Even programs which purported to offer an option to disable color management, did not actually disable color management fully. We only found one reference to a printer driver which allowed direct control of the individual inks,³⁶ however we did not have access to this driver during the work of this paper. Interestingly, anaglyph images presented on emissive displays connected to a computer ordinarily do not suffer from any anaglyph image degradation due to color management, because many image editing applications simply directly map the RGB values of each pixel in the image to the pixels on the display without any color management. On the other hand, more advanced image editing programs may include color management and hence may introduce problems for anaglyph images. In offset printing it is possible to bypass color management because the individual separations (individual color plates for each ink color) can be controlled separately and hence avoid crosstalk caused by color management—unfortunately desktop printers do not operate using separations.

2.4 Gray Component Replacement

Although we referred earlier to printing commonly using only three primary inks to produce a full-color image, a fourth printing ink, black, is usually used to improve the contrast range of printed images. The problem is that the combination of real cyan, magenta and yellow inks usually produces a dark muddy brown rather than a deep black, so it is beneficial to use black ink in dark areas to improve the image quality in dark regions of the image.^{29,35} Black ink also has the advantage that it is cheaper than color inks so there is a financial incentive to use black ink in preference to heavy concentrations of cyan, magenta and yellow inks. Black ink can also be used in mid-gray areas of the image instead of using a combination of cyan, magenta and yellow inks. “The two basic black generation strategies are Under Color Removal (UCR), and Gray Component Replacement (GCR). UCR separations use black only in the neutral and near-neutral areas, while GCR is a more aggressive strategy that replaces the amount of CMY that would produce a neutral with K , even in colors that are quite a long way from neutral.”³⁵

If an aggressive amount of GCR is used, it can compromise the separation between the left and right image channels in near-neutral gray areas of the image and hence cause

crosstalk. It is also our experience that even small amounts of black ink replacement can compromise anaglyph images, even if the black ink is only used in very dark parts of the image, for two reasons. First, the black ink is often used to expand the dark range of the image into areas of darkness that the individual color inks are not able to achieve on their own, and when viewed through anaglyph glasses this transition from a color ink area to a black ink replacement area may be noticeable, and because the introduction of black replacement can be triggered by the image content in the other perspective image channel, it can lead to crosstalk (in dark areas of the image). Second, the black ink can look quite different to equivalent density of the color primary inks when viewed through the anaglyph glasses due to subtle differences in the spectral curves of the black and color inks, which in turn can also lead to crosstalk.

Our experience to date suggests that less crosstalk will be observed in printed anaglyph images if GCR and UCR can be switched off. Unfortunately we were unable to find a reliable way of disabling GCR and UCR on the color inkjet and color laser printers that we tested.

3 Simulation of Spectral Crosstalk

We have developed a crosstalk simulation model to predict the occurrence of crosstalk in printed anaglyph images due to the spectral properties of the light source, paper, inks and anaglyph glasses. The simulation used in this study builds on the crosstalk model for anaglyph images on emissive displays developed by the authors and earlier collaborators.^{4,13,21,34}

The analysis in this paper is performed for the red/cyan color combination, but it could equally be applied to other color combinations.¹³

The printed anaglyph crosstalk simulation algorithm is illustrated in Fig. 3 for the example case of a red-left/cyan-right anaglyph. With reference to Fig. 3, the model uses (a) the emission spectrum of the light source (in this example an incandescent lamp), (b) the spectrum of the blank paper, (c) the spectrum of the “red” and cyan inks, (d) the spectrum of the red and cyan filters of the glasses, and (e) the human eye spectral sensitivity.

In this particular study we chose to simplify the analysis by considering the use of red ink (which is the combination of yellow and magenta inks) for the right eye channel rather than presenting the performance of yellow and magenta inks separately. It should be noted that an actual red ink is not usually available in many printers and instead it is produced by combining yellow and magenta inks. The simulation can calculate the performance of yellow and magenta inks separately but we are only reporting the results of “red” ink performance here.

The anaglyph crosstalk simulation program [see Fig. 3(f)] multiplies the spectra [(a) through (e)] together to obtain the spectral plots shown in Fig. 3(g). In the four plots [Fig. 3(g1) through 3(g4)], the dashed black line represents the luminance spectrum that is visible when the blank white page is viewed through the left or right colored lens, and the solid line represents the spectrum visible when the “red” or cyan inks are printed on the page and viewed through the left or right lenses of the glasses. Specifically, the black dashed lines shown in Fig. 3(g1) and 3(g2) are identical and show the luminance spectrum when the white page is viewed

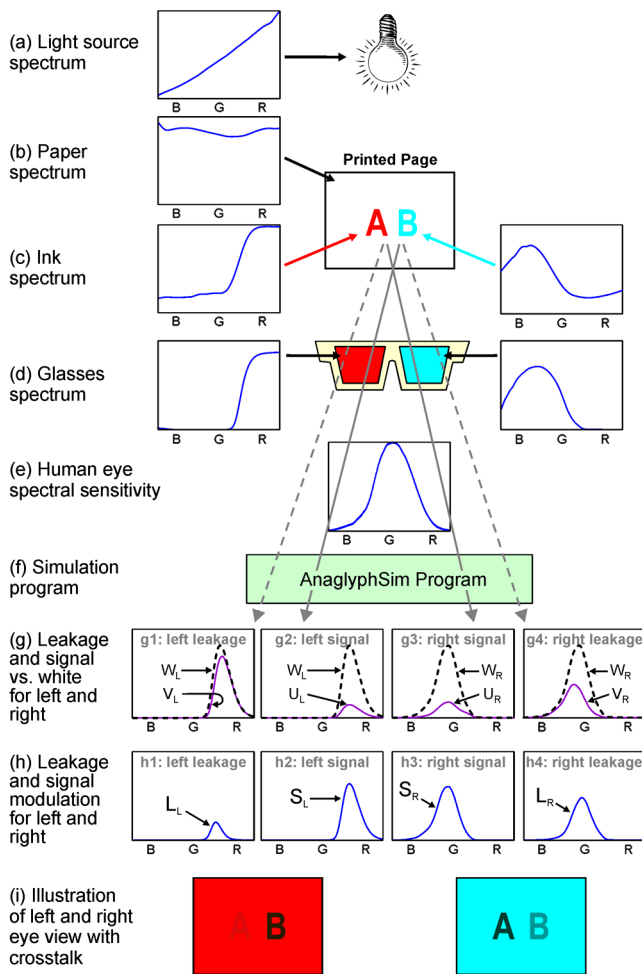


Fig. 3 Illustration of the process of printed anaglyph crosstalk simulation described in this paper. Each spectral graph shows wavelength on the horizontal axis (400 to 700 nm, *B* = blue, *G* = green, *R* = red) and intensity on the vertical axis.

through the red lens of the glasses, and the black dashed line shown in Fig. 3(g3) and 3(g4) are identical and show the luminance spectrum when the white page is viewed through the cyan lens. The solid curves of Fig. 3(g) represent the luminance spectrum of: (g1) the “red” ink viewed through the red lens, (g2) the cyan ink viewed through the red lens, (g3) the “red” ink viewed through the cyan lens, and (g4) the cyan ink viewed through the cyan lens. The difference between the dashed and solid curves in each of these plots (g1) through (g4) represent how well each ink modulates that particular eye color channel. For example, in Fig 3(g2) there is a big gap between the dashed and solid curves which means that when cyan ink is printed on a white page it will be highly visible against the blank white page when viewed through the red lens, and in Fig. 3(g1) the small difference between the dashed and solid curves means that when this particular “red” ink is printed on a white page it will be nearly invisible against the blank white page when viewed through the red lens.

The spectral plots shown in Fig. 3(h) represent the difference between the dashed and solid curves shown in the spectral plots of Fig. 3(g) immediately above. These plots represent the ability of each ink to modulate the light in each eye channel—specifically, (h1) the ability of the “red”

ink to modulate the red eye channel, (h2) the ability of the cyan ink to modulate the red eye channel, (h3) the ability of the “red” ink to modulate the cyan (right-eye) channel, and (h4) the ability of the cyan ink to modulate the cyan (right-eye) channel. The areas under each of these curves represent the luminance difference that each ink is able to provide for each eye channel compared to a blank white page. For example, graphs (h2) and (h3) have the largest area under the curve which further demonstrates that “red” ink should be used to modulate the cyan-eye (right-eye) channel, and cyan ink should be used to modulate the red-eye (left-eye) channel. This is equivalent to the signal component in the analysis of an emissive display.³⁴ The areas under the curves in graphs (h1) and (h4) are equivalent to the leakage component and should ideally be small. Graph (h1) has the smallest area under the curve representing that this particular “red” ink only slightly modulates the red (left-eye) channel, which will mean that it does not produce much leakage, which is preferred. In contrast, the area under the curve in graph (h4) is relatively large [compared to the area under (h3)], representing that the cyan ink modulates the cyan (right-eye) channel by a fairly large amount, so there will be a fair amount of leakage of the left-image channel into the right-eye.

The two diagrams in Fig. 3(i) provide a diagrammatic representation of how much crosstalk will be visible for the left and right eyes in this particular example. The left-eye view appears dominated by red because the white page is being viewed through the red filter, and the right-eye view has a dominant cyan color because the white page is being viewed through the cyan filter. For the left eye, the letter “B” will be highly visible (dark) against the red background because the cyan ink does a good job of extinguishing the red part of the spectrum, and the letter “A” is only faintly visible as a light red-grey because the “red” ink only lightly attenuates the red (left-eye) channel. For the right eye, the letter “A” is highly visible because the “red” ink does a good job of extinguishing the cyan part of the spectrum, and the letter “B” will appear partly visible as a medium cyan-gray because the cyan ink moderately attenuates the cyan (right-eye) channel.

In the special case of printed anaglyphs it is proposed that the crosstalk percentage is calculated by dividing the leakage luminance difference [e.g., $W_L - V_L$ in Fig. 3(g)] by the signal luminance difference [e.g., $W_L - U_L$ in Fig. 3(g)] for each eye as will be set out mathematically below.

The printed anaglyph crosstalk simulation algorithm can be expressed as follows in equation form. In the first instance the amount and spectrum of light which reaches the left and right eyes, through the anaglyph glasses, off the blank (white) page is calculated:

$$W_L(\lambda) = I(\lambda)p(\lambda)e(\lambda)g_L(\lambda) \tag{1}$$

$$W_R(\lambda) = I(\lambda)p(\lambda)e(\lambda)g_R(\lambda) \tag{2}$$

Second, the amount and spectrum of light that reaches the left and right eyes through the anaglyph glasses off the red and cyan printed areas are calculated:

$$U_L(\lambda) = I(\lambda)p(\lambda)i_L(\lambda)e(\lambda)g_L(\lambda) \tag{3}$$

$$U_R(\lambda) = I(\lambda)p(\lambda)i_R(\lambda)e(\lambda)g_R(\lambda) \tag{4}$$

$$V_L(\lambda) = I(\lambda)p(\lambda)i_R(\lambda)e(\lambda)g_L(\lambda) \quad (5)$$

$$V_R(\lambda) = I(\lambda)p(\lambda)i_L(\lambda)e(\lambda)g_R(\lambda) \quad (6)$$

Thirdly, the signal and leakage components are calculated:

$$S_L = \int_{\lambda_{\min}}^{\lambda_{\max}} (W_L(\lambda) - U_L(\lambda))d\lambda \quad (7)$$

$$S_R = \int_{\lambda_{\min}}^{\lambda_{\max}} (W_R(\lambda) - U_R(\lambda))d\lambda \quad (8)$$

$$L_L = \int_{\lambda_{\min}}^{\lambda_{\max}} (W_L(\lambda) - V_L(\lambda))d\lambda \quad (9)$$

$$L_R = \int_{\lambda_{\min}}^{\lambda_{\max}} (W_R(\lambda) - V_R(\lambda))d\lambda \quad (10)$$

And last the crosstalk is calculated:

$$C_L = \text{leakage/signal} = L_L/S_L \quad (11)$$

$$C_R = \text{leakage/signal} = L_R/S_R \quad (12)$$

$$C = (C_L + C_R)/2, \quad (13)$$

where W_L and W_R are the luminance spectrum of light which reaches the left and right eyes off an unprinted blank (white) page when it is illuminated using a specified light source, and viewed through a specified pair of anaglyph glasses. I is the normalized spectral emission of the light source; p is the spectral reflectance of the paper; e is the normalized photopic spectral sensitivity of the human visual system^{37,38} as illustrated in Fig. 4(g); g_L and g_R are the spectral transmission of the left and right eye filters of the glasses; λ is the light wavelength (usually expressed in nm); λ_{\min} and λ_{\max} describe the wavelength range—for the human eye the range of visible light sensitivity is approximately 400 to 700 nm; i_L and i_R are the spectral reflectance of the inks which modulate the left and right eye channels, respectively (for red-left/cyan-right anaglyphs, i_L will be the spectrum of the cyan ink, and i_R will be the spectrum of the “red” ink). U_L and U_R are the luminance spectrum of light which reaches the left and right eyes from areas that have had the *desired* channel ink applied to the paper when viewed through the nominated anaglyph filter for that eye; V_L and V_R are the luminance spectrum of light which reaches the left and right eyes from areas that have had the *undesired* channel ink applied to the paper when viewed through the nominated anaglyph filter for that eye; S_L and S_R are effectively the signal intensity for the left and right eyes, respectively (or the ability of the appropriate ink to modulate its corresponding left or right eye channel); L_L and L_R are effectively the leakage intensity for the left and right eyes, respectively (or the ability of the left-channel ink to modulate light in the right eye channel, and vice versa—ideally this would

be low); C is the crosstalk at each eye (or combined left and right eyes)—often expressed as a percentage; and Subscripts L and R refer to the left-eye channel and right-eye channel, respectively. In a traditional red/cyan anaglyph, L will refer to the red channel and R will refer to the cyan (blue + green) channel, but other color variations are possible (e.g., blue/yellow or green/magenta¹³).

Equations (1) through (6) correspond with steps (a) through (g) in Fig. 3. Equations (7) to (10) correspond with step (h) in Fig. 3 and represent an extra step that is needed for printed anaglyphs which is not needed with anaglyphs on emissive displays. Finally Eqs. (11) through (13) calculate the amount of crosstalk present in the anaglyph printing process (for a particular light, paper, ink, glasses combination).

In addition to the need for the crosstalk simulation algorithm to be an accurate portrayal of the optical processes involved, it is also important that accurate spectral data is obtained for use in the simulation—which is detailed in the next section.

The anaglyph crosstalk simulation algorithm is implemented in a program we have called “AnaglyphSim” which is written in MATLAB. The program imports the spectral data for the various lights, papers, inks and glasses and implements the algorithm for the various combinations. The program calculates the percentage crosstalk and a range of other statistics for each of the combinations.

It should be noted that the current simulation excludes the direct effect of GCR, color management and color space conversion, although the use of spectral data from the impure ink swatches (due to color management) in the model indirectly includes some effect of color management. Ideally, the undesirable effects of GCR, color management and color space conversion will be disabled separately and hence not need to be part of the simulation.

4 Validation of the Printed Anaglyph Crosstalk Simulation Model

The crosstalk simulation model was validated using a four step process.

4.1 Spectral Emission of Light Sources

The spectral emission properties of a selection of light sources were measured using an Ocean Optics USB2000 spectroradiometer. Table 1 lists the light sources used in this study.

4.2 Spectral Reflectance of Papers and Inks

The spectral reflectance of the papers and printing inks used in this study were measured using a PerkinElmer Lambda 35 spectrophotometer in combination with Labsphere RSA-PE-20 integrating sphere. In order to limit the number of variables in this study, a single paper type from a single batch was used throughout all the testing—a ream of “Fuji Xerox Performer+ 80 gsm A4” paper.

Table 2 lists the four printers whose inks were tested in this study. The spectral reflectances of the inks of the various printers were obtained by printing the inks on a blank sheet of the nominated paper stock and loading them into the spectrophotometer. Each of the ink spectra was then calculated by expressing each measured ink swatch spectrum as a

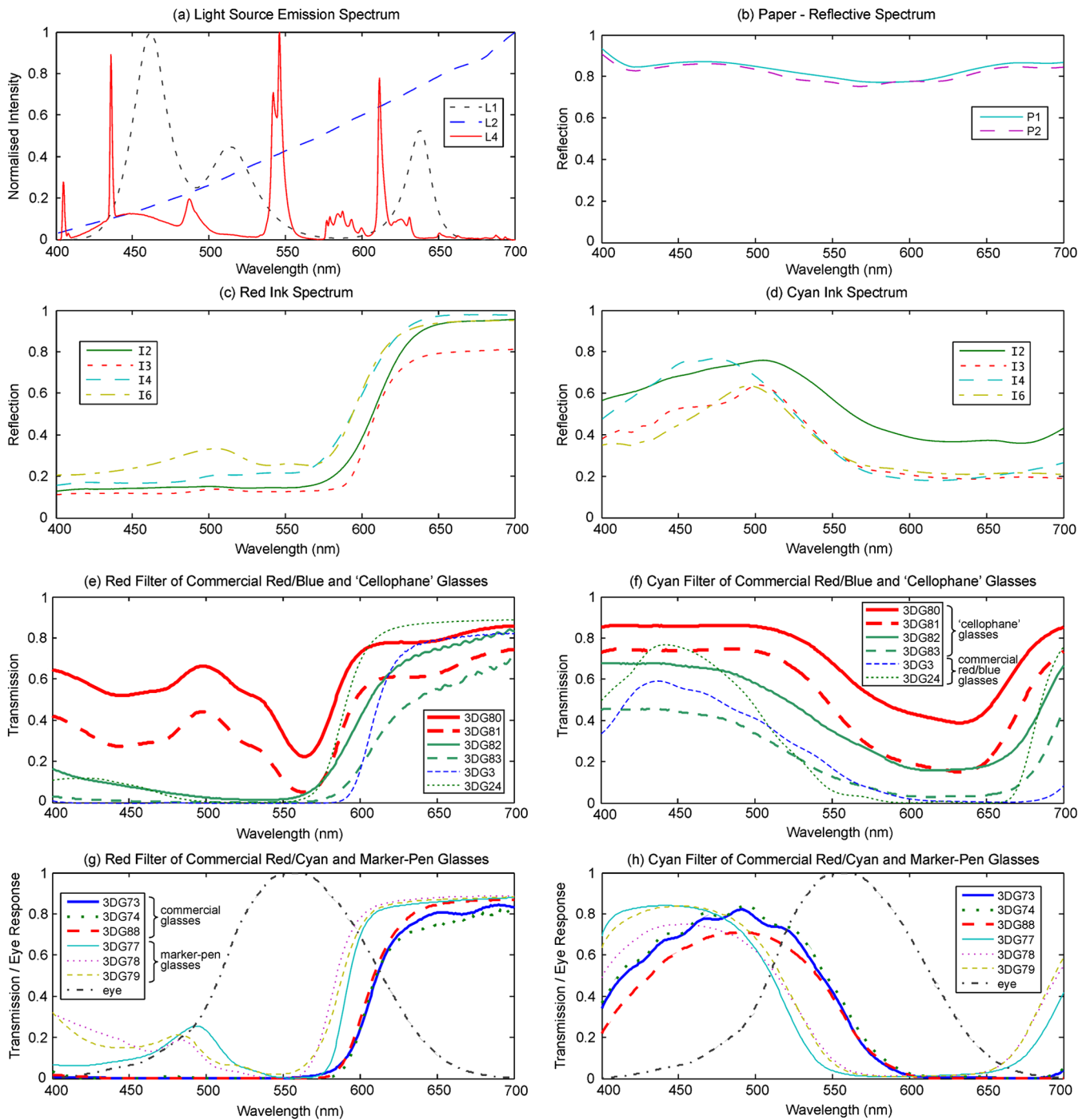


Fig. 4 Spectral plots of (a) the three light sources, (b) two paper stocks, (c) the “red” ink from the four tested printers, (d) the cyan ink from the four tested printers, (e) the red filter of commercial red/blue and “cellophane” glasses (six pairs), (f) the cyan or blue filter of the commercial red/blue and “cellophane” glasses (six pairs), (g) the red filter of the commercial red/cyan and “marker-pen” glasses (six pairs) with the human visual system response also indicated, and (h) the cyan filter of the commercial red/cyan and “marker-pen” glasses (six pairs) with the human visual system response also indicated.

percentage of the spectrum of the unprinted “white” paper. Obtaining pure printed swatches of the individual inks was sometimes a difficult task. Only one of the printers that we tested (I6) was able to print a test page containing pure swatches of each ink. With the other printers it was necessary to use experimentation with various color management settings and different imaging applications to try to obtain pure test swatches, however it was not possible to obtain pure swatches using this technique and there was always some

level of contamination from other inks. This contamination may not be visible to the naked eye, but can be seen with a microscope as “scum dots”³⁵ of undesired color ink in the swatch of the desired ink color.

4.3 Spectral Transmission of Glasses

Twelve pairs of anaglyph glasses were used in this study—listed in Table 3. This is the same list of glasses used in the

Table 1 Register of light sources.

Lamp ID	Description
L1	RGB LED spotlight
L2	Halogen lamp (Philips Eco Classic 70 W)
L4	Fluorescent lamp (Crompton 6 W T4 tube)

Table 2 Listing of the printers and ink sets tested.

Ink ID	Description
I2	Canon S820 inkjet printer (original inks)
I3	Fuji Xerox DocuCentre-IV C3375 color laser printer/multifunction device (original toners)
I4	Epson Artisan 835 inkjet printer (original inks)
I6	Kodak ESP 5250 inkjet printer (original inks)

study reported in Ref. 34 except with the inclusion of two commercially manufactured red/blue anaglyph glasses (3DG3 and 3DG24) and the removal of two of the worst performing “cellophane” filter glasses (3DG84 and 3DG85). The selection of glasses consists of three red/cyan commercial pairs, two red/blue commercial pairs, three pairs constructed using marker pens, and four pairs constructed using colored “cellophane” plastic wrap. Please note that the term “cellophane” is commonly used to refer to any colored plastic wrap, however, in many countries it is a registered trademark of Innovia Films Ltd., United Kingdom. This selection of glasses provided a wide range of color filter performance which was useful for validating the crosstalk simulation model. Two pairs of red/blue anaglyph glasses were included in the set to test whether they might provide better crosstalk performance, albeit at the sacrifice of perceived color fidelity.

The seven pairs of hand-made glasses were constructed as previously described.³⁴ The optical spectral transmission of the anaglyph filters were measured with a Perkin Elmer Lambda 35 spectrophotometer.

It should be noted that some of the hand-made glasses have some nonideal optical properties other than their spectral transmission performance—specifically the clarity of the lens [which degrades the modulation transfer function (MTF)], dispersion, and variability of the ink density. The marker-pens tend to have a considerable amount of variability of ink density (across the filter and from filter-to-filter) due to the manual way in which the ink is applied. Glasses 3DG81 had the worst clarity of all the glasses making the image soft focused.

The “Glasses IDs” used here correspond to the identification series used in previous studies.^{4,13,21,34}

4.4 Crosstalk Simulation

The spectral data from the lights, paper, inks and glasses was processed using the anaglyph crosstalk simulation program described in Sec. 3. The simulation provides a crosstalk

Table 3 Register of anaglyph glasses used in this study.

Glasses ID	Description
Commercial red/cyan anaglyph glasses	
3DG73	NVIDIA 3D Vision Discover
3DG74	Stereoscopic Displays and Applications 2006—manufactured by American Paper Optics
3DG88	Top Gear—manufactured by OZ3D Optics
Commercial red/blue anaglyph glasses	
3DG3	National Geographic—Distributed with August 1998 edition of National Geographic Magazine
3DG24	Sports Illustrated Australian Edition—Distributed with March 2000 edition of Sports Illustrated magazine (Australian edition)
Hand-made marker-pen anaglyph glasses	
3DG77	“hand-drawn” using Sharpie Fine Point Permanent Marker—red and blue (on clear overhead transparency)
3DG78	“hand-drawn” using Artline 70—red and blue (on clear overhead transparency)
3DG79	“hand drawn” using Artline 854 OHP Permanent Marker—red and blue (on clear overhead transparency film)
Hand-made “cellophane” anaglyph glasses	
3DG80	John Sands “Plain Cello”—red and blue
3DG81	John Sands “Plain Cello” (two layers)—red and blue
3DG82	Henderson Greetings “cello”—red and blue
3DG83	Henderson Greetings “cello” (two layers)—red and blue

percentage estimate for both filters of every pair of glasses when used with every combination of light, paper and ink set. Additionally the program provides intermediate results in the calculation—namely percentage visibility of “red” ink through the red lens, percentage visibility of the cyan ink through the red lens, percentage visibility of the “red” ink through the cyan lens, and percentage visibility of the cyan ink through the cyan lens—these conditions correspond to signal and leakage (L_L , S_L , S_R , and L_R), respectively in Fig. 3 and Eqs. (7) to (10).

These four intermediate values can also be thought as the ability for each of the inks to “modulate” each of the color channels. Somewhat counter-intuitively, the “red” ink ideally only modulates the cyan color channel (while not modulating the red color channel) and cyan ink ideally only modulates the red color channel (while not modulating the cyan color channel).

With the particular dataset used in this study the program calculates a total of 576 simulation result combinations (12 pairs of anaglyph glasses \times 2 lenses per pair of glasses \times 4

printer ink sets $\times 2$ inks per printer (“red” and cyan) $\times 1$ paper type $\times 3$ light sources = 576 values).

4.5 Visual Ranking

The crosstalk performance of the various anaglyph filters were visually ranked to allow a comparison with the crosstalk simulation model results. In a previous study,³⁴ the visual ranking was performed on the basis of the amount of crosstalk of each combination, but, it can be difficult for an observer to judge crosstalk visually because it is a derived value—that is, the luminance of the leakage component divided by the luminance of the signal component, whilst also ignoring the effect of overall luminance and any other lens effects such as defocus or filter pigment variability. For this particular project, it was decided to perform the visual ranking on the basis of a simpler intermediate value—i.e., the percentage visibility of a particular ink through a particular colored lens (i.e., modulation). This simplifies the comparison for the user, but still provides a useful ranking comparison in order to test the validity of the simulation.

Figure 5 shows the four different printed test targets used to perform the visual ranking. Each of the four test targets was printed separately on each of the four printers listed in Table 2 (resulting in 16 test sheets). Figure 5(a) is used to compare the percentage visibility of the “red” ink through the cyan lens—ideally “red” ink should appear dark or black when viewed through the cyan lens. The black surround in Fig. 5(a) and 5(b) was included because it was found to make it easier to judge the darkness of the colored ink area. Figure 5(b) is used to compare the percentage visibility of the cyan ink through the red lens—ideally cyan ink should appear dark or black when viewed through the red lens. Figure 5(c) is used to compare the percentage visibility of the “red” ink through the red lens, and Fig. 5(d) is used to compare the percentage visibility of the cyan ink through the cyan lens.

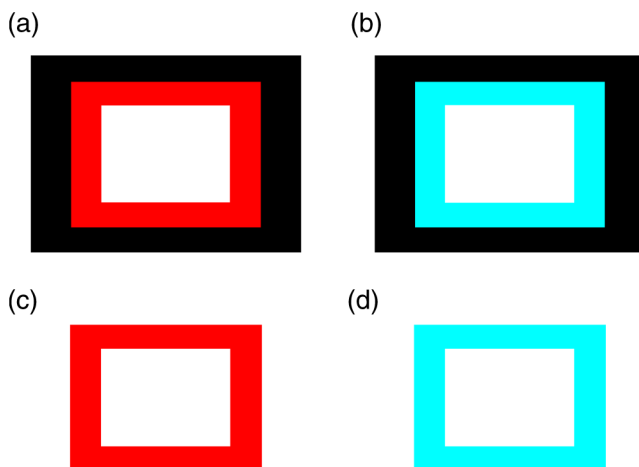


Fig. 5 The four printed visual test targets used during the anaglyph crosstalk visual ranking tests. Target (a) was used to measure the ability of “red” ink to modulate cyan light (as viewed through the cyan lens), (b) was used to measure the ability of cyan ink to modulate red light (as viewed through the red lens), (c) was used to measure the invisibility of the “red” ink when viewed through the red lens, and (d) was used to measure the invisibility of the cyan ink when viewed through the cyan lens. The test targets are printed one per page for each printer ink set.

In the authors’ previous study³⁴ of anaglyph crosstalk on emissive displays the visual ranking was performed across only a single dimension (i.e., across the 12 sets of anaglyph glasses for a particular display condition). This provided a good validation of the simulation’s ability to correctly estimate the relative performance of different sets of anaglyph glasses, however it did not specifically validate the model’s ability to correctly estimate the relative performance of different displays. In this study, the visual ranking process was expanded to include two additional conditions which ranked anaglyph performance between (a) the four different ink sets, and (b) the three different light sources—therefore the model is now being validated in three dimensions (glasses, ink set, and light source).

Five observers (labeled Ob1 to Ob5) took part in the visual ranking tests. Due to the large number of individual test combinations (576 as stated in the previous section) it was necessary to limit the number of test rank combinations performed by the observers. We feel that the range of rank tests performed (detailed below) allowed a reasonable assessment, whilst also limiting the time to undertake the experiment to avoid observer overload. The visual ranking process took approximately two hours for each observer.

The first test condition performed was a ranking in the glasses dimension. The 12 pairs of glasses listed in Table 3 were mounted in similar white frames, ordered randomly, and each observer was asked to rank the glasses whilst looking at a particular test target [Fig. 5(a)–5(d)] printed by a particular printer, illuminated by a nominated light source. The observers were asked to compare two glasses at a time using the printed test target and to place the glasses on the table in front of them with the lowest modulation (least visibility) on the left to the highest modulation (highest visibility) on the right. Each observer made multiple passes through the set of glasses in front of them to confirm that the glasses were in the correct order. Each observer performed a separate sorting task for each condition, so that each observer performed 10 glasses sorting tasks (labeled “A1” through “A10” in Table 4). The visual ranking test was conducted in a photographic dark room with the only source of lighting being the specified light source (from Table 1) so as to prevent ambient lighting affecting the results. The observers were briefed at the beginning of the visual trials as to the background of the project and the process they were to use in each visual rank test.

The second test condition performed was a ranking in the ink set dimension. A single pair of glasses (3DG74) was used to view and rank a set of four test prints (one from each of the four printers), whilst illuminated by a specified lamp. The six test conditions for this test are itemized in Table 5. Each observer was asked to rank the four test prints in terms of the amount of leakage each condition exhibited.

The third test condition performed was a ranking in the lamp illuminant dimension. A single pair of glasses (3DG74), was used to view a specified test print (printed by a nominated printer), and the observer was asked to rank the amount of leakage present whilst successively illuminated by the three lamp types (from Table 1). The four test conditions performed are itemized in Table 6.

The visual validation test was conducted on the basis of the relative ranking of visual performance because the human visual system is not accurate at determining absolute

Table 4 Listing of the 10 glasses ranking experimental conditions conducted. For example, condition “A1” is conducted with the “red” ink test target Fig. 5(c) in the L1P1I4 display condition viewed through the red lens of the 12 pairs of glasses, which equates to a comparison of the “Left Leakage” value. (L1P1I4 = Light 1 (RGB LED Lamp), Paper 1 (Fuji Xerox Performer+), Ink set 4 (Epson 835 printer)—per Tables 1 and 2).

Lens:	red lens		cyan lens	
	cyan ink	red ink	cyan ink	red ink
Test target:	Fig. 5(b)	Fig. 5(c)	Fig. 5(d)	Fig. 5(a)
Lamp/ ink				
L1P1I4	-	A1	A2	-
L2P1I4	A3	A4	A5	A6
L4P1I3	A7	A8	A9	A10
Value:	Signal _L	Leakage _L	Leakage _R	Signal _R

measurement of brightness (known as “lightness constancy”),³⁹ whereas the human visual system is usually very good at performing relative brightness comparisons.

While ranking the glasses, the observers were asked to try to only consider luminance modulation differences between each of the glasses and ignore other optical differences such as overall luminance, relative clarity, and variability of the filter pigments. The marker pen filters usually had a high level of pigment variability. Some of the “cellophane” filters had very poor clarity and softened the image considerably.

Table 5 Listing of the six printer ink set ranking experimental conditions. For example, condition “B1” is conducted with four printed test targets version Fig. 5(c) printed on each of the four printers with the “red” ink, illuminated by the RGB LED lamp (lamp 1) and viewed through the red lens of glasses 3DG74, which equates to a comparison of the “Left Leakage” value. (The meanings of L#, I# and 3DG# are itemized in Tables 1–3, respectively).

Ranking of Inks:	I2, I3, I4, I6	
Lens:	red lens	cyan lens
Ink:	red ink	cyan ink
Test targets:	Fig. 5(c) via I2, I3, I4, & I6	Fig. 5(d) via I2, I3, I4, & I6
Lamp/glasses		
L1, 3DG74	B1	B2
L2, 3DG74	B3	B4
L4, 3DG74	B5	B6
Value:	Leakage _L	Leakage _R

Table 6 Listing of the four light source ranking experimental conditions. For example, condition “C1” is conducted with test target version Fig. 5(c) printed with the “red” ink of the Canon Printer (ink set 2), viewed through the red lens of glasses 3DG74, and successively illuminated by each of the three lamp types, which equates to a comparison of the “Left Leakage” value. (The meanings of L#, I# and 3DG# are determined from Tables 1–3, respectively).

Ranking of Lamps:	L1, L2, L4	
Lens:	red lens	cyan lens
Ink:	red ink	cyan ink
Test target:	Fig. 5(c)	Fig. 5(d)
Ink/Glasses		
I2, 3DG74	C1	C2
I4, 3DG74	C3	C4
Value:	Leakage _L	Leakage _R

Luminance modulation of a particular ink swatch is visible as the darkness of the ink swatch relative to the luminance of the unprinted page.

5 Results and Discussion

5.1 Light Source Emission Spectra

The spectra of the three sampled light sources are shown in Fig. 4(a). The curves for each display have been scaled such that the maximum of the curve for each lamp is normalized to one. It can be seen that there is a considerable variation between the spectral curves of the different light sources, which is due to each of the lamps having a very different light generation technique.

One important aspect to notice in Fig. 4(a) is that the spectrum of the RGB LED lamp (L1) has a low point around 580 nm. This is a good characteristic because the crossover point between the red and the cyan parts of the visual spectrum occurs at around 580 nm. The significance of the correspondence will become more evident later.

5.2 Paper Reflective Spectra

The reflective spectra (independent of source illumination) for two paper stocks are shown in Fig. 4(b). All of the visual testing in this study was performed using a single paper stock (P1: “Fuji Xerox Performer+”). However, a second paper stock (P2: “Double A” 80 gsm A4) was measured and shown here to allow a brief comparison of how the spectra of a different paper stock might vary, but obviously this particular comparison is not exhaustive.

One aspect this data does not capture is the presence of fluorescent whitening agents which are sometimes used to “brighten” the look of the paper. These agents work by absorbing UV light and re-emitting blue light to make the paper look less yellow. The current measurement procedure does not capture the presence of fluorescent agents, although the measurement procedure could be modified to allow this effect to be included in the model.

5.3 Ink Set Reflective Spectra

The reflective spectrum (independent of the source illumination and the paper stock) of the “red” and cyan inks for the four printers tested are shown in Fig. 4(c) and 4(d), respectively.

One aspect that these graphs reveal is that the spectral performance of the cyan ink of all four printers is particularly poor. Ideally, the cyan ink would attenuate light in the red part of the spectrum (~600 to 700 nm) and not attenuate light in the blue and green parts of the spectrum (~400 to 600 nm). It can be seen that although the maximum attenuation (lowest amount of reflection) of the cyan ink is in the red region, the cyan ink also attenuates a substantial amount of light in the blue and green regions. This means that when cyan ink is applied, it not only modulates the red part of the spectrum, but also partly modulates the blue and green parts of the spectrum. The “red” ink has much better spectral shape than the cyan ink, in that it heavily attenuates the blue and green parts of the spectrum, but only lightly attenuates the red part of the spectrum (except for I3, which attenuates about 20% of the red region).

The poor spectral quality of the current printing inks is expected to have a large effect on the crosstalk performance of printed anaglyphs and this will be explored further later in the paper using the crosstalk simulation algorithm.

5.4 Glasses Spectral Transmission

The transmission spectra of the glasses tested in this study are shown in Fig. 4(e) through 4(h). The transmission spectra of the commercial red/blue glasses and hand-made “cellophane” glasses are shown in Fig. 4(e) and 4(f). The transmission spectra of the commercial red/cyan anaglyph glasses and the hand-made “marker-pen” glasses are shown in Fig. 4(g) and 4(h).

The poor spectral performance of the “cellophane” glasses are clearly evident in Fig. 4(e) and 4(f). In an ideal pair of anaglyph glasses, the filters would pass the intended color band and block the unwanted color bands, with the blocking of the unwanted channels being the most important. For example, with a red filter, it should pass the red part of the spectrum (~600 to 700 nm) and block the blue and green parts of the spectrum (~400 to 570 nm). With most of the “cellophane” glasses, it can be seen that the unwanted color ranges are not well attenuated. Referring to the plots of the red filter of 3DG80 and 3DG81 in Fig. 4(e), it can be seen that these filters do not provide very much attenuation of wavelengths from 400 to 570 nm (the blue and green regions) which will result in significant leakage and therefore high crosstalk. This can be compared with the spectral performance of the red commercial filter 3DG88 in Fig. 4(g), which has very low transmission in the blue-green wavelength range. The marker-pen filters shown in Fig. 4(g) also show a similar insufficient attenuation in the 400 to 570 nm range for the “marker-pen” red filter which will also point to poor crosstalk performance. The crosstalk performance of the glasses will be discussed further from a simulation standpoint below.

5.5 Crosstalk Simulation

The crosstalk simulation program allows a wide range of conditions to be simulated. The results of the crosstalk

simulation are illustrated in Fig. 6 across the 288 “display” conditions considered in this project. The simulation program calculates the crosstalk for the left and right eyes separately, and an estimate of the overall crosstalk (calculated as the arithmetic mean of the left and right crosstalk),⁴⁰ as shown in the figure. The figure allows an inter-condition comparison of the relative performance of the different filters to be easily seen. For example, it can be seen that for the red lens, the simulation predicts that the combination of the RGB LED lamp (L1), the Epson printer (I4) and red lens of glasses 3DG3 provides the lowest crosstalk condition at 11.7% crosstalk. For the cyan lens, the simulation predicts that the combination of the RGB LED lamp (L1), the Canon printer (I2) and the cyan lens of 3DG77 provide the lowest crosstalk condition at 33% crosstalk—which admittedly is a massive amount of crosstalk. More broadly, the simulation also predicts that: the crosstalk in the red lens is generally much lower than crosstalk in the cyan lens; and the RGB LED lamp (L1) generally provides lower crosstalk for both the red and cyan lenses than the other two lamp types (which is probably due to the dark area in the spectral emission of the RGB LED lamp at 580 nm as discussed in Sec. 5.1).

The horizontal axis of both of these plots is shown on a logarithmic scale because it reduces the bunching of the results on the left hand side of the plots, and the human visual response has been described as having a logarithmic-like response to light over a limited range.^{41,42}

With reference to Fig. 6, it can be seen that the rank order of the simulated crosstalk of the tested filters is generally the same from one “display” condition to another. Some crossovers do occur, and these will be caused by the differences between the shapes of the spectral curves of the different inks and lights and the way these interact with the different shaped spectral curves of the filters.

With only a few exceptions, the simulation predicts that the red lens of the commercial anaglyph glasses will offer substantially lower crosstalk than the “hand-made” anaglyph glasses. With the cyan lens, the predicted differences are less clear-cut as they are more closely bunched together, but it can be seen from Fig. 6(b) that the “cellophane” glasses are predicted to mostly have the worst performance.

The simulation predicts a good spread in the crosstalk performance of the selection of test filters used in this study—which in turn will aid in the validation of the simulation algorithm.

Some of the crosstalk simulation values presented in Fig. 6 are greater than 100% (i.e., the worst performing filters)—this might seem impossible, but this can occur with anaglyph crosstalk with poorly performing filters because the blue and green channels combined (one eye) have a significantly higher luminance than the red channel (the other eye).

The simulation also predicts that blue lenses (3DG77, 24, 79, 78, 3) will generally exhibit lower crosstalk than the lenses that have more of a cyan performance (3DG73, 88, 74, 83, 81, 82, 80). This is to be expected because a blue filter blocks more of the green part of the spectrum than a cyan filter does, and hence creates more of a blanking spectral range between the left and right spectral channels. The loss of light from the green part of the spectrum will result in a dimmer image and a loss of color fidelity. It is likely that designers will generally prefer to use cyan lenses due to the

brightness and color fidelity problems of blue filters, hence more work is needed to reduce the crosstalk of cyan filters.

Figure 6 reveals a further aspect that can affect crosstalk performance: the balancing of the density of the inks. The density of an ink determines how dark the ink appears when it is printed on the page. The density can be controlled either by the concentration of the ink formulation, or the

amount of ink which is deposited on the page during the printing process. By way of example, low crosstalk could be achieved in the cyan channel by printing the “red” ink with high density, and using only light density with the cyan ink. However, this will result in high levels of crosstalk in the other eye (in addition to a faint signal image) (due to a relatively darker leakage and a relatively faint signal). This is

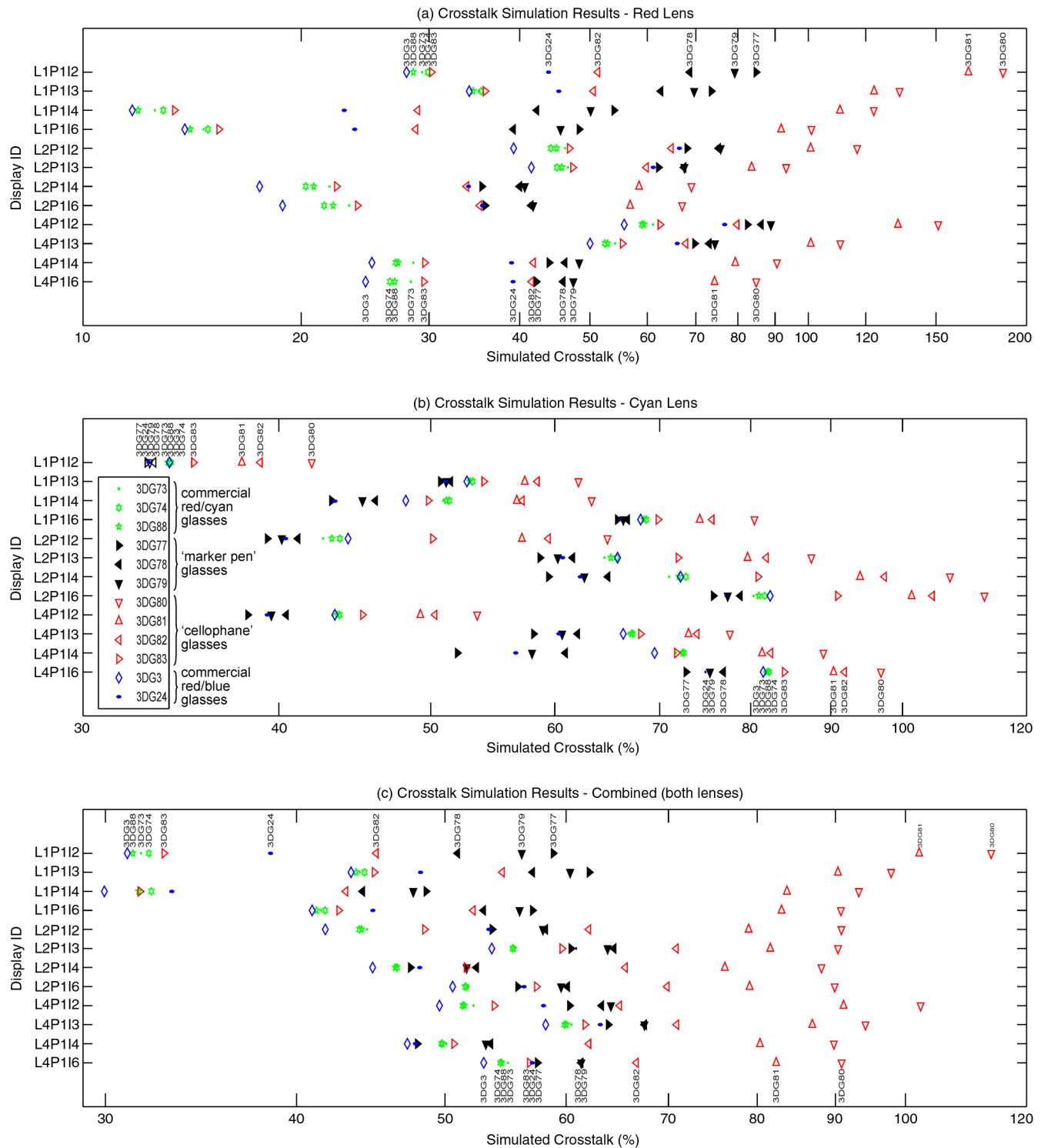


Fig. 6 Illustration of the results of the printed anaglyph crosstalk simulation for the 12 sets of anaglyph glasses, four printer ink sets and three light sources for (a) red lens, (b) cyan lens, and (c) combined. The symbol key shown in part (b) also applies to parts (a) and (c).

what could be occurring in the L1P1I2 “display condition” of Fig. 6. The cyan channel exhibits low relative crosstalk compared to the other crosstalk results, however in the red channel it exhibits the opposite with high relative crosstalk compared to the other crosstalk results of the red filters. This leads us to suggest that there may be some benefit in careful balancing of the relative density of the two inks so as to balance the amount of crosstalk in both eyes (while at the same time trying to match the darkness of both channels). We have conducted some work to predict the best density balance to minimize crosstalk, but this work is not ready for publication at this stage.

5.6 Visual Validation Results

The visual ranking experiment involved 100 separate crosstalk ranking tasks across five observers, 12 pairs of glasses (two filters in each pair of glasses), four different ink sets, and three different lamp types resulting in 780 separate observations (600 glasses rank observations, 120 ink set rank observations, and 60 lamp rank observations). The results of the visual glasses ranking experiment are illustrated in Fig. 7. The glasses ranking results for each “display” condition (lamp, paper, ink set), observer, and filter color combination are plotted against the corresponding simulated crosstalk ranking for that “display” condition and filter color. A line segment joins the visual ranking with the simulated ranking for each observation.

When plotting the ranking results, we had the option of showing the ranking observations with an equal spacing between observations; however, this would give an unrealistic

equal visual emphasis on ranking observations regardless of how close or disparate the value is between those particular filters. We therefore decided to plot the results with horizontal axis values which correspond to the simulated percentage modulation values for each pair of glasses. This plotting technique allows us to easily see which conditions the simulation expects to have similar values, and provides more visual emphasis on ranking errors which have greater simulated differences than ranking errors between filters which have small simulated differences. We believe this plotting technique allows a more useful analysis of the data. This same plotting technique was used in one of our previous papers.³⁴

In cases where the observer was unable to distinguish any difference between different filters (i.e., they looked to have the same amount of modulation), observers were allowed to group those glasses together. Glasses that have been grouped together by an observer are plotted with the same horizontal axis value (using the mean of the corresponding simulated crosstalk values).

The different groups of anaglyph glasses (commercial red/cyan, commercial red/blue, “marker-pen” and “cellophane”) have been plotted with different colors and line styles, thus allowing the different groups to be easily identified and reveal any trends.

Referring to Fig. 7, in cases where the visual ranking agrees with the simulated ranking, the line segments are vertical and do not intersect. In cases where the visual and simulated rankings disagree, there will be a cross-over of the line segments.

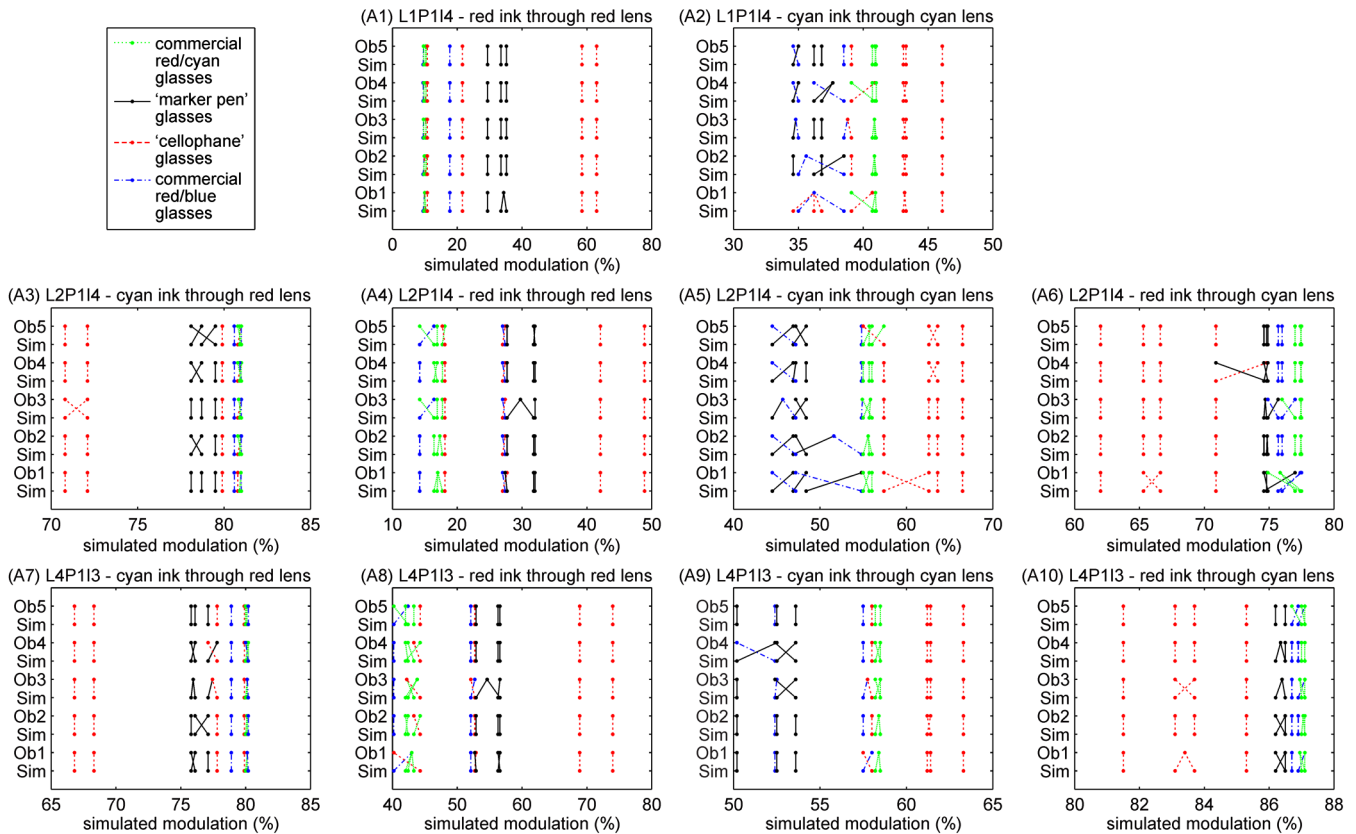


Fig. 7 The visual validation test results for the 12 sets of glasses showing observed rank order compared to simulated rank order on the scale of the simulated percentage modulation—per the experimental plan set out in Table 4. Ob1–Ob5 represents the five observers.

In general terms the validation results of the glasses ranking experiment, as depicted in Fig. 7, agree very well with the crosstalk simulation ranking results. Across all of the observations, a high proportion (70%) of the observations were ranked in direct agreement with the simulation. It can be seen from the figure that ranking errors (indicated by crossing line-segments) rarely occurred across large simulated modulation value differences. Ranking errors usually only occurred between filters with very similar simulated modulation values. These results are statistically analyzed in the next section.

As outlined in Sec. 4.5, two further ranking experiments were conducted—firstly comparing (ranking) the relative performance of the three different lamp types as illustrated in Fig. 8, and secondly comparing (ranking) the relative performance of the four different ink sets as illustrated in Fig. 9. Again it can be seen from these two figures that the validation results of the ink set and lamp ranking experiment agree very well with the crosstalk simulation ranking results. Again a high proportion of the observations were ranked in agreement with the simulation—75% for the ink set ranking

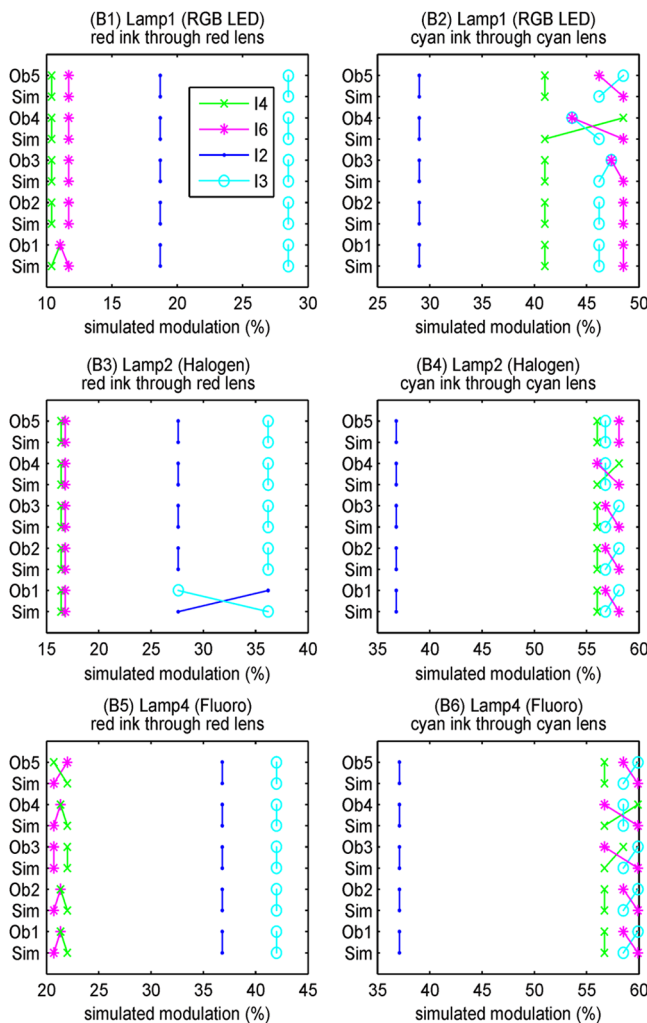


Fig. 8 The printer ink set ranking results showing observed rank order compared to simulated rank order on the scale of the percentage modulation—per the experimental plan set out in Table 5. These observations were performed using glasses 3DG74. Please note that cyan through red and red through cyan were not tested in this domain in order to reduce the experiment duration per Sec. 4.5.

and 87% for the lamp ranking. Ranking errors (indicated by crossing line-segments) again only usually occurred between observations with small differences between the simulated modulation values. These results are also statistically analyzed in the next section.

Looking at the plotted results (Figs. 7 to 9), there do not appear to be any consistent ranking reversals in the data across all observers, which would point to an error in the model. There is a consistent number of random rank reversals between observations which have close simulated modulation values, but this would be consistent with an increased difficulty for the observers to do this visual comparison, and not an error with the simulation.

5.7 Statistical Analysis

The quality of agreement between the visual ranking and the simulated ranking was assessed using two correlation techniques. The first technique, Spearman’s rank correlation,⁴³ is used in biological statistics when one or more of the variables in a dataset consist of only ranks, as is the case with the visual ranking data. The Spearman rank correlation (r_s) values were calculated for all of the visual validation observations across the various tested ink, lamp, observer, and filter color combinations and these are presented in Table 7.

The second analysis technique is based on the Pearson product-moment correlation coefficient⁴⁴ (also known as the sample correlation coefficient), and its square, the coefficient of determination (r^2). Normally the Pearson technique cannot be applied to ordinal rank order data, however for the purposes of this analysis, the ordinal visual ranks for each condition were transformed into an interval variable by assigning the ranks the values of the percentage modulation from the crosstalk simulation. One advantage of this analysis method is that all ranking errors are considered, but more

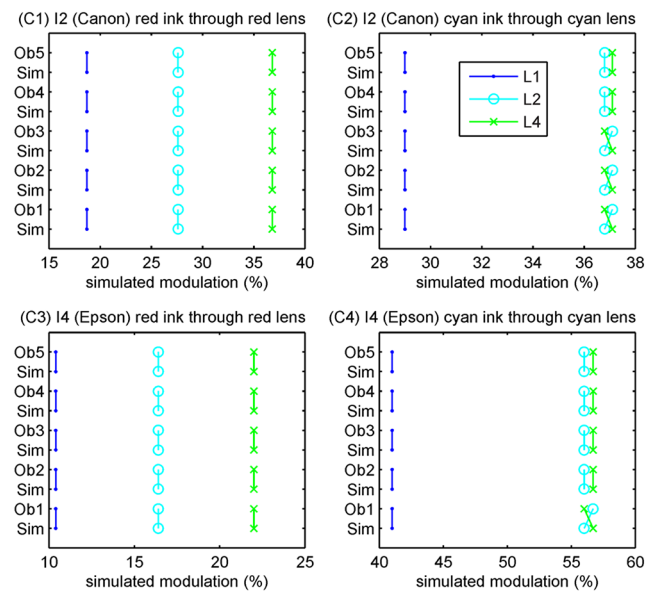


Fig. 9 The lamp light source ranking results showing observed rank order compared to simulated rank order on the scale of the percentage modulation—per the experimental plan set out in Table 6. These observations were performed using glasses 3DG74. Please note that cyan through red and red through cyan were not tested in this domain in order to reduce the experiment duration per Sec. 4.5.

emphasis is placed on ranking errors between observations with larger simulated crosstalk differences. This second technique is unconventional, however it corresponds well with the plotting technique used in Fig. 7. The Coefficient of Determination (r^2) values are presented in columns 8 through 11 of Table 7. The average r_s and r^2 value for each of the five observers are shown in columns 7 and 12, respectively of Table 7. The average r_s and r^2 values for each observer were calculated as the mean of the 10 correlation results for each observer for each correlation technique.

The statistical analysis (Table 7) of the visual ranking results (as plotted in Fig. 7) provides a high level of confidence in the accuracy of the crosstalk simulation algorithm in the glasses domain. It can be seen in Table 7 that 96% of the ranking tests have an r_s value of 0.9 or better, 94% have an r^2 value of 0.9 or better, 60% have an r^2 value of 0.99 or better, and 20% have an r_s value of 0.99 or better.

Another way of analyzing the data is to consider the correlation with the ranking results of each observer to each other in comparison to the correlation of the ranking results of each observer with the simulation. It can be seen in Table 8 that in all but one case, the best correlation for each observer

was with the simulation (and not the other observers). This provides further confidence in the glasses dimension of the simulation.

The visual ranking results across the ink set and lamp domains were also statistically analyzed and provide further confidence in the model in these domains. For the ink set domain results (shown in Fig. 8), the mean r_s was 0.805 and mean r^2 was 0.963. For the lamp domain results (illustrated in Fig. 9), the mean r_s was 0.900 and the mean r^2 was 0.999. It should be noted that there are less observations per domain for the ink (4) and lamp (3) domains compared to the glasses domain, which has 12 options—a factor that may limit the accuracy of the analysis.

The statistical analysis of the visual validation experiment has provided a high level of confidence in the accuracy of the printed anaglyph crosstalk simulation model.

6 Simulation of Alternative Scenarios

Now that we have established that the printed anaglyph crosstalk simulation model is operating with a high level of accuracy, we can use the model to predict the performance of a number of printed anaglyph crosstalk scenarios we

Table 7 Results of the statistical analysis of the glasses visual ranking results. The table shows the correlation data for each “display,” observer and filter color combination, and also the average correlation for each observer using the two correlation techniques. Columns 3-6 show the Spearman’s rank correlation (r_s). Columns 8-11 show the Coefficient of Determination (r^2) values calculated using the Pearson product-moment correlation technique as described in the text. Columns 7 and 12 show the average value for each of the observers across all ‘displays’ and filter types using the two techniques. (1 indicates good agreement, 0 indicates poor agreement).

Display ID	Observer	r_s of ranking results (Spearman)					r^2 of log of ranking results (Pearson)				
		cyan ink through red lens	red ink through red lens	cyan ink through cyan lens	red ink through red lens	average r_s for each observer	cyan ink through red lens	red ink through red lens	cyan ink through cyan lens	red ink through red lens	average r^2 for each observer
L1P114	Ob1	—	0.981	0.935	—	0.934	—	0.999	0.890	—	0.949
	Ob2	—	0.993	0.949	—	0.972	—	1.000	0.901	—	0.979
	Ob3	—	0.996	0.982	—	0.960	—	1.000	0.997	—	0.988
	Ob4	—	0.998	0.935	—	0.957	—	1.000	0.895	—	0.968
	Ob5	—	0.998	0.986	—	0.970	—	1.000	0.998	—	0.991
L2P114	Ob1	0.989	0.972	0.937	0.715		1.000	0.999	0.717	0.921	
	Ob2	0.908	0.991	0.949	0.996		0.994	1.000	0.915	1.000	
	Ob3	0.902	0.984	0.942	0.977		0.975	0.986	0.983	0.989	
	Ob4	0.901	0.986	0.972	0.937		0.994	0.999	0.973	0.902	
	Ob5	0.915	0.972	0.909	0.993		0.978	0.992	0.951	1.000	
L2P113	Ob1	0.977	0.897	0.988	0.945		0.999	0.979	0.997	0.989	
	Ob2	0.981	0.986	0.988	0.979		0.991	0.998	0.999	0.995	
	Ob3	0.981	0.921	0.961	0.950		0.999	0.986	0.984	0.978	
	Ob4	0.942	0.958	0.949	0.995		0.995	0.994	0.930	0.999	
	Ob5	1.000	0.972	1.000	0.952		1.000	0.992	1.000	0.995	

Table 8 Results of a Pearson cross-correlation between the ranking results of one observer against the other observers and the simulation results for the glasses ranking data illustrated in Fig. 7.

	Ob1	Ob2	Ob3	Ob4	Ob5
Sim	0.973	0.989	0.994	0.984	0.995
Ob1	1	0.975	0.969	0.968	0.967
Ob2	0.975	1	0.986	0.983	0.988
Ob3	0.969	0.986	1	0.981	0.992
Ob4	0.968	0.983	0.981	1	0.982
Ob5	0.967	0.988	0.992	0.982	1

would not otherwise be able to physically replicate easily. Let us consider several such scenarios to further reduce the crosstalk—using the best of the (red/cyan) glasses/ink/lamp combinations revealed in Fig. 6 (i.e., L1P1I2 3DG88) as a starting point.

The first scenario is to consider changing the light source used to illuminate the printed anaglyph image. We have already considered the effect of a small selection of light sources on the amount of crosstalk and found that changing from a halogen light source (L2) to an RGB LED light source (L1) resulted in a 13 percentage point drop in crosstalk (from 44% to 31% crosstalk, using ink set I2 and glasses 3DG88). We can also now use the simulation to consider the effect of using a light source which consists of red, green and blue lasers which will have very narrow spectral peaks in the red, green and blue sections of the visual spectrum (we will designate this light source “L5”). The spectrum of such a

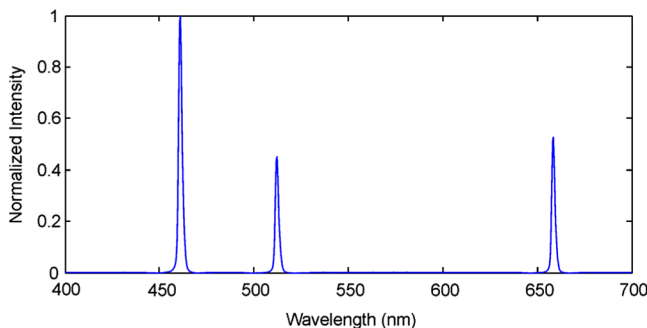


Fig. 10 The spectrum of a simulated RGB laser light source.

theoretical light is shown in Fig. 10. It is hoped that the wide spectral bands of no light output would afford a further reduction in crosstalk. Table 9 lists the simulated printed anaglyph crosstalk performance using such a RGB laser light source in comparison to the aforementioned configurations. The simulation predicts that using an RGB laser light source will result in a further drop of crosstalk (now down to 26%) but this is still an unacceptable level of crosstalk—other work suggests that crosstalk levels need to be at least less than 5% for comfortable 3D viewing.⁷ Further optimization of the actual frequency of the laser spectral peaks may result in a further small improvement, but it is unlikely we will be able to reach an acceptable level of crosstalk by any further changes to the light source alone.

The second scenario considers changing the anaglyph glasses to improve crosstalk. Here we simulate the performance of a pair of anaglyph glasses which have a theoretical “brick-wall” filter performance (i.e., 100% transmission in the pass region and 0% transmission in the blocking region). It would not be possible to physically test “brick-wall” filters in reality because they do not exist, but these simulation results will provide an indication of the absolute limit of lowest crosstalk performance achievable by optimization of the glasses alone. The pass-bands of the “brick-wall” filters were 620 to 700 nm for the red filter and 400 to 560 nm for the cyan filter with other wavelengths blocked. Table 10 lists the simulated anaglyph crosstalk performance of the four test conditions—two with glasses 3DG88 and two with the glasses changed to the “brick-wall” filters. The simulation results indicate that even with a perfect pair of anaglyph glasses, none of the anaglyph prints were able to exhibit zero crosstalk; this is because the inks we tested have significant attenuation in out-of-band wavelengths. For the better of the two conditions (L1P1I2), the use of “brick-wall” glasses only resulted in a 10% improvement of combined crosstalk (both eyes) but this improvement is only achievable in theory, which indicates that there is limited scope for the further reduction in crosstalk by any further changes to the anaglyph glasses alone.

The third scenario considers the effect of changing the spectral response of the printer inks. As can be seen in Fig. 2, the spectral response of a typical yellow ink has a good spectral characteristic for anaglyph purposes—it has low attenuation in the out-of-band range (~520 to 700 nm), it has high attenuation in the in-band range (~400 to 480 nm), and a reasonably fast change from high attenuation to low attenuation (in the region 480 to 520 nm). Unfortunately the cyan and magenta inks typically do not show such a good spectral performance, particularly the cyan. For the purposes of this scenario, hypothetical red and

Table 9 Simulated effect on printed anaglyph crosstalk of changing light sources.

	Simulated crosstalk			Improvement (from L2P1I2)	
	Red channel (%)	Cyan channel (%)	Combined (%)	Percent (%)	Percentage points
L2P1I2 3DG88	45.0	43.2	44.1	—	—
L1P1I2 3DG88	28.5	34.0	31.3	29%	12.8
L5P1I2 3DG88	20.6	31.9	26.2	41%	17.9

Table 10 Simulated effect on printed anaglyph crosstalk of using theoretical “brick-wall” filter anaglyph glasses.

		Simulated crosstalk		Improvement	
		3DG88 (%)	“Brick-wall” filters (%)	Percent (%)	Percentage points
L1P1I2	red	28.5	21.9	23	6.6
	cyan	34.0	34.5	-1	-0.5
	both	31.3	28.2	10	3.1
L2P1I2	red	45.0	21.1	53	23.9
	cyan	43.2	41.1	5	2.1
	both	44.1	31.1	29	13

cyan ink spectra were constructed based on the spectrum of an example yellow ink, such that the new hypothetical red and cyan inks have low attenuation in the out-of-band regions, high attenuation in the in-band regions, and a fast change from high-attenuation to low-attenuation, like that of the example yellow ink. The spectra of the proposed hypothetical red/cyan inks are shown in Fig. 11.

The simulation results of using the hypothetical inks are shown in Table 11. It can be seen that the hypothetical inks provide a substantial improvement in crosstalk performance—as much as an 84% reduction. The predicted overall crosstalk of the L2P1 3DG88 condition of only 8.6% is very encouraging and is approaching an acceptable level of crosstalk which other work suggests needs to be much less than 5%.⁷ It is probable that further optimization of the spectra of the red/cyan ink set can lead to further reductions in printed anaglyph crosstalk.

An illustration of how changes to the three domains of printed anaglyph 3D images have on the amount of crosstalk is provided in Fig. 12. It can be seen that the domain which has the biggest effect on reducing the amount of crosstalk is the ink set domain. It can also be seen that the RGB LED lighting and 3DG88 anaglyph glasses (middle circle of Fig. 12) seems to achieve near the maximum gain achievable by changes in the lighting and glasses domains, whereas we

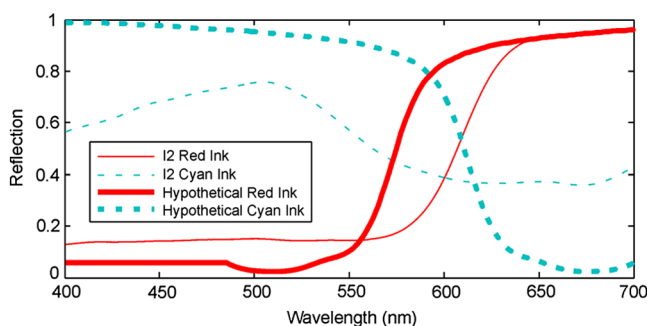


Fig. 11 The reflectance spectra of the hypothetical red/cyan ink set compared to the “red” and cyan inks of I2.

Table 11 Simulated effect on printed anaglyph crosstalk of using improved red/cyan inks.

		Simulated crosstalk		Improvement	
		I2 (Canon) (%)	Hypothetical inks (%)	Percentage (%)	Percentage points
L1P1 3DG88	Red	28.5	11.6	59	16.9
	Cyan	34.0	5.6	84	28.4
	Both	31.3	8.6	73	22.7
L2P1 3DG88	Red	45.0	16.0	64	29
	Cyan	43.2	9.0	79	34.2
	Both	44.1	12.5	72	31.6

believe there remains considerable scope for improvement in the ink set domain.

The results of these three simulation scenarios illustrate the advantages that crosstalk simulation can provide in predicting the crosstalk performance of printed anaglyph images. In this case, the simulations indicate that there is significantly more scope for reduction in anaglyph crosstalk by the use of more spectrally pure inks than might be gained from further improvements to the spectral performance of anaglyph glasses. The simulation and the visual validation experiment have also confirmed that there is some scope for improving crosstalk performance by using different light sources, however the simulation indicates that we are probably close to the maximum advantage obtainable with the tested RGB LED light source (in the case of red/cyan anaglyphs).

As mentioned in Sec. 3, the equations developed for calculating crosstalk in printed anaglyphs Eqs. (1) through (13)

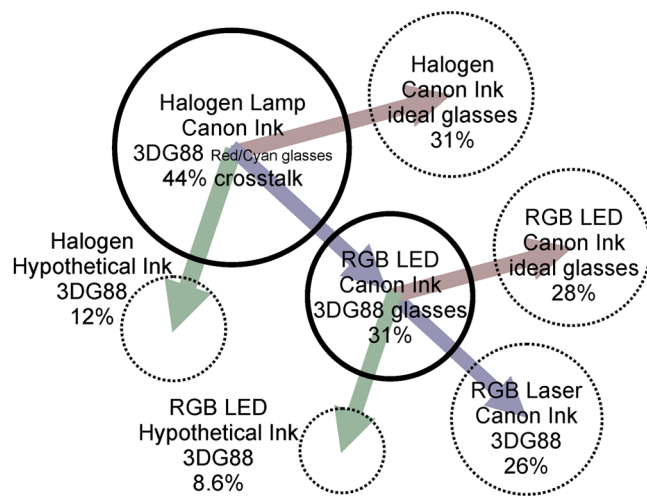


Fig. 12 An illustration of the effect of making changes in the various domains of printed anaglyph images (glasses domain, ink set domain, and illumination domain) has on the amount of crosstalk. The circle sizes (area) are proportional to the simulated amount of crosstalk for each condition. The simulation only conditions are shown as dotted circles.

are similar but notably different to the crosstalk equations for emissive displays.⁷ This difference also extends to the equations used to calculate crosstalk from light measurement device readings off an anaglyph print. Crosstalk Eqs. (11) and (12) can therefore be expressed as

$$C_L = (L_{LWW} - L_{LWK}) / (L_{LWW} - L_{LKW}), \quad (14)$$

$$C_R = (L_{RWW} - L_{RWK}) / (L_{RWW} - L_{RKW}), \quad (15)$$

where C_L and C_R are the crosstalk at each eye—often expressed as a percentage; and L_{LWW} , L_{LWK} , L_{LKW} , L_{RWW} , L_{RWK} , and L_{RKW} are the luminance as measured behind the glasses at the left or right eye position (first subscript), with the desired eye channel ink applied (K —black) or the desired eye channel ink not applied (W —white) (second subscript), and with the undesired eye channel ink applied (K —black) or the undesired eye channel ink not applied (W —white) (third subscript). For example, in the case of a red-left/cyan-right anaglyph print, L_{LWW} is the luminance measured from the left eye position behind the red lens when there is no ink applied to the white page, L_{LKW} is the luminance measured from the left eye position behind the red lens when only cyan ink (the desired ink for this eye channel) is applied to the page, and L_{RWK} is the luminance measured from the right eye position behind the cyan lens when only cyan ink (the undesired ink for this eye channel) is applied to the page. This particular luminance variable expression can appear confusing; however it is expressed this way in order to correspond with the variable definitions used to express the measurement of crosstalk in emissive displays.⁷

7 Conclusion

This paper has presented the development and validation of a crosstalk simulation model for printed anaglyph images. The model is significant in that it allows for the first time a detailed analysis of the process of crosstalk in printed anaglyph 3D images. Printed anaglyph 3D images can often exhibit a lot of crosstalk so it is very useful to have a tool that allows the exploration of techniques to reduce crosstalk in such images. The model has already allowed us to propose a solution that may reduce crosstalk to as low as 8.6%. The model can very quickly simulate the crosstalk performance of a huge number of input combinations (glasses, inks, papers, and lights) to determine optimum combinations—a process that would be impossible to conduct physically. The model can be used to intelligently guide research effort before time and money is expended on physical testing.

In summary, this paper has identified seven ways of reducing crosstalk with printed anaglyph 3D images:

1. use (or perhaps develop) inks which have better spectral purity;
2. use an optimized light source (such as the RGB LED lamp described in Sec. 4.1);
3. use anaglyph 3D glasses which exhibit good spectral performance (such as the commercial anaglyph 3D red/cyan glasses described in Sec. 4.3);
4. use an RGB to CMYK color conversion algorithm which does not mix color channels;
5. avoid the use of gray component replacement (GCR);

6. use (or perhaps develop) a color management process which respects the need to keep color channels separate after anaglyph multiplexing (perhaps by performing color management before anaglyph multiplexing);
7. use an anaglyph multiplexing algorithm that does not introduce crosstalk by mixing the left and right color channels.

Many of these items cannot be achieved with current ink-jet and color laser printers, but can with offset printing.

The information presented in this paper should facilitate a significant improvement in the 3D image quality of this very widely used 3D presentation technique.

Acknowledgments

The authors wish to acknowledge the support of Alec Duncan for his assistance with the manuscript; Dan Marrable, Ming Lim, and Glen Lawson for their assistance with the optical test equipment; and Angela Recalde, Matthew Koessler, Michael Biddle, and Ming Lim for their assistance with the visual validation tests.

References

1. R. Labbe and D. E. Klutho, "Publishing stereoscopic images," *Proc. SPIE*, **7237**, 72370J (2009).
2. V. K. Walworth, "Light polarization in support of stereoscopic display," *Opt. Eng.* **51**(2), 021104 (2012).
3. V. C. Barber and D. A. Brett, "Colour bombardment—a human visual problem that interferes with the viewing of anaglyph stereo material," *Scan. Electron Microsc.* **2**(Pt. 2), 495–498 (1982).
4. A. J. Woods, K. L. Yuen, and K. S. Karvinen, "Characterizing crosstalk in anaglyphic stereoscopic images on LCD monitors and plasma displays," *J. Soc. Inform. Disp.* **15**(11), 889–898 (2007).
5. L. Lipton, "Glossary" in Lenny Lipton's Blog, dated 16 March 2009, <http://lennylipton.wordpress.com/2009/03/16/glossary/> (19 March 2010).
6. A. J. Woods, "How are crosstalk and ghosting defined in the stereoscopic literature?," *Proc. SPIE* **7863**, 78630Z (2011).
7. A. J. Woods, "Crosstalk in stereoscopic displays: a review," *J. Electron. Imag.* **21**(4), 040902 (2012).
8. F. L. Kooi and A. Toet, "Visual comfort of binocular and 3D displays," *Displays* **25**(2–3), 99–108 (2004).
9. Y.-Y. Yeh and L. D. Silverstein, "Limits of fusion and depth judgement in stereoscopic color displays," *Hum. Factors* **32**(1), 45–60 (1990).
10. I. Tsirlin, L. M. Wilcox, and R. S. Allison, "The effect of crosstalk on the perceived depth from disparity and monocular occlusions," *IEEE Trans. Broadcast.* **57**(2), 445–453 (2011).
11. H. Sanftmann and D. Weiskopf, "Anaglyph stereo without ghosting," *Comput. Graph. Forum* **30**(4), 1251–1259 (2011).
12. I. Ideses and L. Yaroslavsky, "Three methods that improve the visual quality of colour anaglyphs," *J. Opt. A Pure Appl. Opt.* **7**(12), 755–762 (2005).
13. A. J. Woods and C. R. Harris, "Comparing levels of crosstalk with red/cyan, blue/yellow, and green/magenta anaglyph 3D glasses," *Proc. SPIE* **7524**, 75240Q (2010).
14. M. A. Purnell, "Casting, replication, and anaglyph stereo imaging of microscopic detail in fossils, with examples from conodonts and other jawless vertebrates," *Palaeont. Electron.* **6**(2), 1–11 (2003).
15. E. Dubois, "A projection method to generate anaglyph stereo images," in *Proc. IEEE Int. Conf. on Acoustics, Speech, and Signal Process.*, Vol. 3, pp. 1661–1664, IEEE, Piscataway, New Jersey (2001).
16. W. R. Sanders and D. F. McAllister, "Producing anaglyphs from synthetic images," *Proc. SPIE* **5006**, 348–358 (2003).
17. D. F. McAllister, Y. Zhou, and S. Sullivan, "Methods for computing color anaglyphs," *Proc. SPIE* **7524**, 75240S (2010).
18. V. M. Tran, "New methods of rendering anaglyph stereoscopic images on CRT displays and photo-quality ink-jet printers," MSc Thesis, University of Ottawa (2005).
19. R. Z. Zeng and H. Z. Zeng, "Printing anaglyph maps optimized for display," *Proc. SPIE* **7866**, 78661S (2011).
20. P. Wimmer, "Anaglyph methods comparison," http://www.3dvtv.at/knowhow/anaglyphcomparison_en.aspx (6 March 2013).
21. A. J. Woods and T. Rourke, "Ghosting in anaglyphic stereoscopic images," *Proc. SPIE* **5291**, 354–365 (2004).
22. R. Zone, "Good old fashion anaglyph: high tech tools revive a classic format in Spy Kids 3-D," *Stereo World* **29**(5), 11–13 and 46 (2002).

23. "Louis Ducos du Hauron," in *Encyclopædia Britannica*, Encyclopædia Britannica Online, Encyclopædia Britannica Inc., (2012), <http://www.britannica.com/EBchecked/topic/172961/Louis-Ducos-du-Hauron> (22 July 2012).
24. L. D. Duhauron, "Estampes, photographies et tableaux stéréoscopiques, produisant l'air effect en plein jour, sans l'aide du steroscope," French Patent No. 216465 (1891) in S. A. Benton, Ed., *Selected Papers on Three-Dimensional Displays*, SPIE Milestone Series, MS162, pp. 138–145 (2001).
25. L. D. Duhauron, "Stereoscopic print," U.S. Patent No. 544666 (1895).
26. A. F. Watch, "The anaglyph: a new method of producing the stereoscopic effect," *J. Franklin Inst.* **140**(6) 401–405 (1895).
27. J. A. Norling, "Anaglyph Stereoscropy," U.S. Patent No. 2,135,197 (1937).
28. S. J. Harrington, R. P. Loce, and G. Sharma, "Systems for spectral multiplexing of source images to provide a composite image, for rendering the composite image, and for spectral demultiplexing of the composite image to animate recovered source images," U.S. Patent No. 7,136,522 B2 (2006).
29. G. Sharma et al., "Illuminant multiplexed imaging: special effects using GCR," in *Proc. 11th Color Imaging Conference: Color Science and Engineering Systems, Technologies, and Applications*, pp. 266–271, IS&T (Society for Imaging Science & Technology), Springfield, Virginia (2003).
30. J. Scarpetti, "Stereoscopic photographic print, method of making, and apparatus for viewing," U.S. Patent 3820874 (1974).
31. M. Ramstad, "High-fidelity printed anaglyphs and viewing filters," U.S. Patent Application Publication No. US 2009/0278919 A1 (2009).
32. J. R. Rupkalvis, StereoScope International, Personal Communication (2012).
33. R. Zone, The 3D Zone, Personal Communication (2012).
34. A. J. Woods and C. R. Harris, "Using cross-talk simulation to predict the performance of anaglyph 3-D glasses," *J. Soc. Inform. Disp.* **20**(6), 304–315 (2012).
35. B. Fraser, C. Murphy, and F. Bunting, *Real World Color Management*, Peachpit Press, San Francisco, California (2004).
36. L. A. Taplin, "Spectral modeling of a six-color inkjet printer," MS Thesis, Rochester Institute of Technology (2001).
37. A. Stockman and L. T. Sharpe, "Luminous energy function (2 degree, linear energy)," (2007), <http://www.cvrl.org/cvrlfunctions.htm> and <http://www.cvrl.org/database/text/lum/CIE2008v2.htm> (29 July 2011).
38. A. Stockman et al., "The dependence of luminous efficiency on chromatic adaptation," *J. Vision* **8**(16), 1–26 (2008).
39. R. Blake and R. Sekuler, *Perception*, 5th ed., McGraw Hill, Boston, Massachusetts (2006).
40. International Committee for Display Metrology (ICDM), "Information display measurements standard (version 1.03)," SID, <http://icdm-sid.org/> (2012).
41. S. S. Stevens, "On the psychophysical law," *Psychol. Rev.* **64**(3), 153–181 (1957).
42. Z. Xie and T. G. Stockham Jr., "Toward the unification of three visual laws and two visual models in brightness perception," *IEEE Trans. Syst. Man Cybern.* **19**(2), 379–387 (1989).
43. J. H. McDonald, *Handbook of Biological Statistics*, 2nd ed., pp. 221–223, Sparky House Publishing, Baltimore, Maryland, <http://udel.edu/~mcdonald/statspearman.html> (2009).
44. R. E. Walpole and R. H. Myers, *Probability and Statistics for Engineers and Scientists*, p. 347, Collier Macmillan, New York (1985).



Andrew J. Woods is a research engineer at Curtin University's Centre for Marine Science & Technology in Perth, Australia. He has MEng and BEng (Hons1) degrees in electronic engineering. He has expertise in the design, application, and evaluation of stereoscopic imaging systems for industrial and entertainment applications. He has served as co-chair of the Stereoscopic Displays and Applications conference since 2000.



Chris R. Harris is a graduate of Curtin University with a bachelor's degree in applied physics and has interests in electronics and information technology. He is currently employed by Murdoch University.



Dean B. Leggo is a graduate of Curtin University with a Bachelor of Science in physics. He is currently employed as a trainer and assessor by LabTech Training. His interests are in frontier science, film production and volunteering.



Tegan M. Rourke is currently employed as a radiation physicist at Sir Charles Gairdner Hospital in Perth, Western Australia. She has a bachelor's degree in physics from Curtin University and is currently completing a PhD with the University of Western Australia.

Paper 5 [Refereed Conference Paper]
A. J. Woods, K. L. Yuen (2006) "Compatibility of LCD Monitors with Frame-Sequential Stereoscopic 3D Visualisation" (Invited Paper), in IMID/IDMC '06 Digest, (The 6th International Meeting on Information Display, and The 5th International Display Manufacturing Conference), pp. 98-102, Daegu, South Korea, 22-25 August 2006.

Compatibility of LCD Monitors with Frame-Sequential Stereoscopic 3D Visualisation

Andrew J. WOODS, Ka Lun YUEN

**Centre for Marine Science & Technology, Curtin University of Technology,
GPO Box U1987, Perth WA 6845, Australia**

Phone: +61 8 9266 7920, Fax: +61 8 9266 4799, E-mail: A.Woods@cmst.curtin.edu.au

Abstract

Historically, LCD monitors have not been able to be used for frame-sequential stereoscopic 3D visualisation due to their slow pixel response rate. With LCD pixel response rates now in the single-digit millisecond range it is natural to ask whether it is now possible to achieve frame-sequential stereoscopic 3D viewing on LCDs.

1. Introduction

Historically, LCD monitors have not been able to be used for frame-sequential stereoscopic 3D visualisation primarily due to their slow pixel response rate.

The frame-sequential stereoscopic display method (also known as field-sequential, time-sequential, or alternate field) works by displaying an alternating sequence of left and right perspective images on a display screen. The observer wears a pair of Liquid Crystal Shutter (LCS) 3D glasses which alternately occlude the left and right eyes, such that the left eye sees only the left perspective images as they are displayed on the screen, and the right eye sees only the right perspective images as they are displayed on the screen. In order for the frame-sequential stereoscopic viewing method to work on a particular display device, the display must be capable of displaying separate and discrete alternate images without noticeable crosstalk between images (and at a sufficiently high image update frequency to avoid visible flicker). If the display is not able to completely extinguish the previous image before displaying the next image, ghosting (aka: crosstalk) [1] will be visible in the stereoscopic image and this can significantly degrade stereoscopic image quality. A slow pixel response rate will have this effect.

With some currently available LCDs having pixel response rates in the single-digit millisecond range it

is natural to ask whether it is now possible to achieve frame-sequential stereoscopic viewing on LCDs.

We conducted a study to establish the important factors determining whether LCD monitors can or cannot be used for frame-sequential stereoscopic 3D visualisation.

These questions are particularly pertinent now because the production of CRTs is declining and the production of LCDs is increasing. CRTs have been the display of choice for use with the frame-sequential 3D method for many years, but there is a risk that at some point the production of CRTs could cease completely. The use of stereoscopic viewing is also increasing rapidly in a wide range of application areas – more people now want stereoscopic capability on their desktop or laptop PC.

2. Experimental Method

In this study we tested fifteen different LCD monitors from various manufacturers ranging from units that are several years old to units that have been just released in the last six months.

Equipment used for testing included: two custom built photodiode sensor pens (based on an Integrated Photomatrix Inc. IPL10530 DAL), an oscilloscope (Goldstar OS-3000), a PC equipped with an NVIDIA 6600GT (stereoscopic capable) graphics card for test image generation, and a custom built LCS 3D glasses driver box capable of adjustable phase and duty cycle.

The measurement method consisted of driving the LCD monitors with a range of video test signals via the VGA or DVI port, and monitoring the light output of the monitor with the photodiode sensor pens.

Data analysis was performed using a range of custom-written Maple programs and Excel spreadsheets.

3. Important LCD and LCS Properties

The frame-sequential stereoscopic display method has traditionally been used with CRT monitors, however LCD monitors have a very different mode of operation than CRTs. The main significant difference is that LCDs are a hold-type display whereas CRTs are an impulse-type display [2].

In this study five main properties of LCDs and/or LCS 3D glasses were identified which affect the stereoscopic image quality of frame-sequential stereoscopic 3D viewing on LCD monitors.

3.1 LCD and LCS Native Polarisation

The native polarisation of the display and the native polarisation of the LCS 3D glasses can affect whether both eyes can see a bright image. If the polarisation axis of either of the LCS glasses lenses is perpendicular to the polarisation axis of the display, that particular eye will appear dark at all times. Most of the LCD monitors that we tested had a native polarisation axis at -45° (from vertical). Some LCS glasses that we tested had the polarisation axes of the two eyes -45° and $+45^\circ$, therefore one eye would see an image and the other eye would not - but there are many other orientations in common circulation.

This problem is easy to overcome by the addition of a quarter wave or half wave retarder in front of the LCS glasses lenses. A half wave polariser can be used to rotate the native polarisation of each LCS to match the polarisation axis of a chosen LCD, or a quarter wave polariser can be used to effectively jumble the polarisation by converting linear polarisation to circular or elliptical polarisation. The half wave polariser method offers a brighter image but is tuned to a particular polarisation angle and hence won't work with all LCDs.

3.2 Refresh Rate

The maximum vertical refresh rate of a monitor determines the maximum speed at which it can display a sequence of images. When used for frame-sequential stereoscopic display, the frame rate per eye is half that of the overall monitor refresh rate. If the refresh rate is too slow, flicker will be visible in the stereoscopic image. An overall refresh rate of 100-120 Hz is usually considered necessary to obtain a fully flicker-free stereoscopic image, however this also depends upon image brightness.

Most of the LCD monitors that we tested were able to accept and display video signals with refresh rates between 60Hz and 75Hz. Two would work at 60Hz only, and four would work at up to 85Hz. At 60Hz significant flicker would usually be evident. At 85Hz a small amount of flicker would be evident.

3.3 LCD Pixel Response Rate

In LCDs the pixel response rate is a measure of how fast an individual pixel can switch from one state to another.

As can be seen in Figure 1, it takes a finite time for a pixel to switch from black-to-white (BTW) and from white-to-black (WTB) (in the example of Figure 1, BTW = 4.4ms (10% to 90%) and WTB = 1.3ms (90% to 10%)). In this study, BTW was always found to be longer than WTB. The transition time from one grey level to another (grey-to-grey (GTG)) can also be measured, however areas of high contrast between the two perspective views are usually the location of most stereoscopic ghosting [1]. Hence, the value for BTW response time seems to be more important than WTB or GTG for stereoscopic image quality.

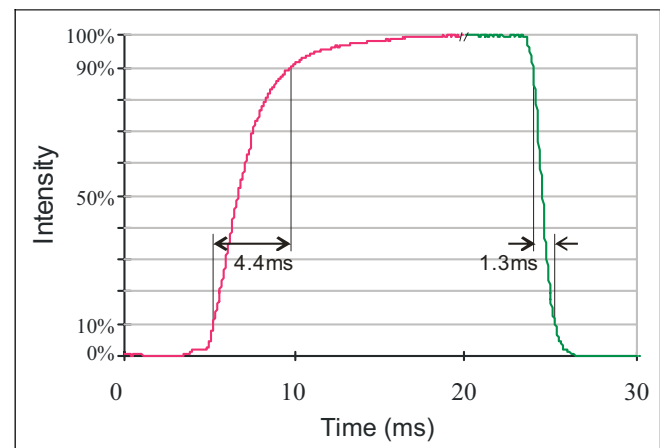


Figure 1: Example LCD pixel response (BTW and WTB)

For frame-sequential 3D viewing, the LCS shutter should not be opened until the switching of the pixel (from one state to another) has stabilised sufficiently. If the BTW pixel response time is too slow (i.e. greater than the period of one field or frame. e.g. $>17\text{ms}$ for 60Hz field rate) the image would never stabilise before the next image was displayed and hence it could not be used for frame-sequential 3D because too much ghosting would be present.

3.4 Image Update Method

The method by which the display updates from one image to the next also needs to be considered.

In all of the LCDs that we tested, a new image is written to the LCD one line at a time from the top of the screen to the bottom [3]. The time duration to update the whole screen was close to the time period of one frame ($1 / \text{frame rate}$) (e.g. the time period for 1 frame at 75Hz is 13.3ms).

This transition from one image to the next is similar in some respects to the way that an image is scanned on a CRT (except that an LCD is a hold-type display and not an impulse-type display like a CRT). This transition from one image to the next is also similar to the vertical wipe transition effect in video editing. Convolved on this scan-like image update is also the LCD pixel response.

The scan-like image update method is illustrated in Figure 2. The vertical axis shows the vertical position on the LCD panel. The horizontal axis shows time. The thin diagonal line represents the addressing of each row of the LCD. The top plot (a) shows the result for a LCD monitor with a slow pixel response

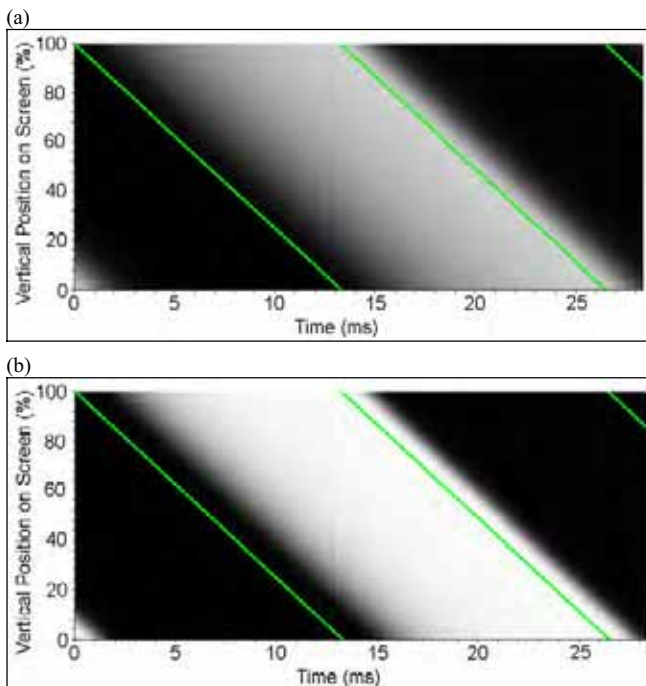


Figure 2: Time domain response of two LCD panels alternating between black and white at 75Hz for (a) a slow pixel response rate panel (21.7ms) and (b) a fast pixel response rate panel (5.7ms).

rate ($\text{BTW} + \text{WTB} = 21.7\text{ms}$) and the lower plot (b) shows the result for a LCD monitor with a fast pixel response rate ($\text{BTW} + \text{WTB} = 5.6\text{ms}$). It can be seen in the figure that the BTW transition is slower than the WTB transition.

It is evident from Figure 2 that there is no one time when a single image is shown exclusively on the whole LCD panel – this is particularly so for LCD monitors with a long pixel response rate but is also true for LCD monitors with a short pixel response rate. This means that there is not a time when the shutters in LCS glasses could open and see only a single perspective image (exclusively).

3.5 LCS Duty Cycle

Most driving electronics for LCS 3D glasses drive the glasses with a 50% duty cycle. The left shutter is open 50% of the time (when left perspective images are displayed on the screen) and opaque the other 50% of the time. The right shutter is driven in a similar fashion but out of phase with the left shutter. This scheme works fine with CRT monitors (impulse-type display) but not with conventional LCD monitors (hold-type display) because of the finite LCD pixel response time and image update method discussed above.

The option of using a reduced LCS duty cycle is discussed below.

4. Discussion

Slow pixel response rate has historically been considered to be the main reason that LCD monitors cannot be used for frame-sequential stereoscopic 3D viewing. Although pixel response rate is important, the section above has revealed that the image update method of the panel is also an important consideration. Even if the pixel response rate is improved, the scan-like image update method of most conventional LCDs will still cause problems for the frame-sequential 3D method.

Two methods are proposed to allow stereoscopic images to be displayed on LCD monitors using the frame-sequential method.

Firstly, we have been able to achieve a reasonable quality stereoscopic image on a fast pixel response rate LCD monitor by switching the LCS glasses with a very short duty cycle and by adding black bands to the top and bottom of the screen image (i.e. letter-boxing the screen image). This is illustrated in

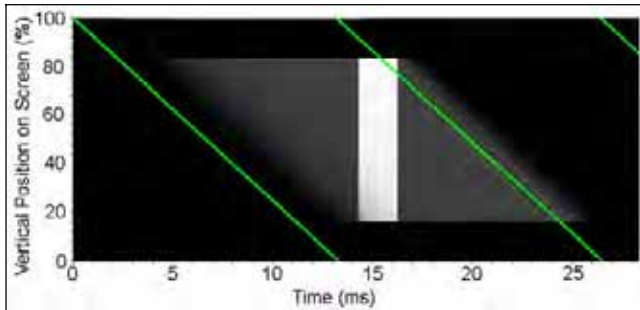


Figure 3: The use of a reduced duty cycle LCS 3D glasses[†] and letterboxing to achieve frame-sequential stereo on a fast pixel response rate LCD.

Figure 3. It should however be noted that the image will be fairly dim due to the reduced duty cycle and the letterboxing of the image may be problematic in some instances. There can also still be a slight amount of ghosting at the bottom of the stereoscopic image.

Secondly, if the addressing of the LCD panel could be sped up, perhaps completing a full panel update in 50% of the time period of one frame (rather than the full period of one frame), there would exist a period in time when a single image could be seen exclusively on the screen. This is illustrated in Figure 4. One way to achieve this might be to allow the LCD monitor to accept higher frequency video signals (e.g. twice the desired stereo frequency) and change only the image in the video signal once every second frame. Unfortunately this is not a solution for existing LCD monitors and will be limited by the maximum addressing speed of the LCD panel.

Fifteen different LCD monitors were tested during this study and although all of the monitors tested had very similar display properties, it is not suggested that all LCD monitors are the same. There are already some new LCD TVs which operate differently than the LCD monitors described above, namely LCD TVs which use a blinking backlight [3] or a scanning backlight [4]. These technologies which have been developed to improve motion image reproduction in normal television viewing.

[†] Please note that the switching of the LCS also has a response rate [1] but this has not been illustrated correctly in this figure.

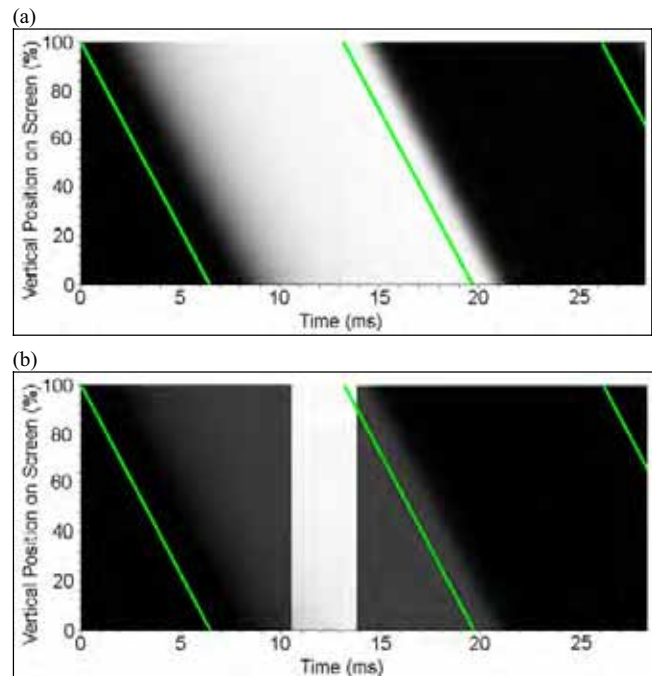


Figure 4: (a) Time domain response of a fictitious LCD monitor with a fast addressing rate and fast pixel response rate and (b) the same being used with reduced duty cycle LCS 3D glasses[†].

5. Conclusion

This study has identified five main properties of LCDs and LCS 3D glasses which affect the quality of stereoscopic images displayed using the frame-sequential stereoscopic display method on LCD monitors.

Despite the fact that the pixel response rate of new LCD monitors is falling, the scan-like image update method used by many/most conventional LCD monitors still prevents them being used with conventional LCS 3D glasses to achieve a full-screen stereoscopic image using the frame-sequential stereoscopic display method.

This paper has suggested two possible methods of achieving frame-sequential stereo on fast response LCD monitors. However both methods are not ideal.

LCD technology is developing fast and new drive methods may mean that new generation LCDs could be compatible with the frame-sequential stereoscopic display method by using a modified LCS drive technique.

LCD panels can be used for other stereoscopic viewing methods and these are summarised in reference [5].

6. Acknowledgements

We wish to thank the companies and individuals who lent LCD monitors for testing.

7. References

- [1] A. J. Woods, and S. S. L. Tan, "Characterising Sources of Ghosting in Time-Sequential Stereoscopic Video Displays", in *Stereoscopic Displays and Virtual Reality Systems IX*, Proc. SPIE Vol. 4660, San Jose, California (2002).
- [2] H. Pan, X.-F. Feng, and S. Daly, "LCD motion blur modelling and analysis", in *IEEE International Conference on Image Processing (ICIP 2005)*, Vol. 2, pp 21-24, (2005).
- [3] A. A. S. Sluyterman, and E. P. Boonekamp, "Architectural Choices in a Scanning Backlight for Large LCD TVs", in *SID 05 Digest*, pg 996- (2005)
- [4] H.-C. Hung, and C.-W. Shih, "Improvement in Moving Picture Quality Using Scanning Backlight System", in *Proceedings of the International Display Manufacturing Conference (IDMC'05)*, Taipei, Taiwan (2005).
- [5] A. J. Woods, "Compatibility of Display Products with Stereoscopic Display Methods", in *Proceedings of the International Display Manufacturing Conference (IDMC'05)*, ISBN 957-28522-2-1, Taipei, Taiwan (2005).

Paper 6 [Refereed Conference Paper]
A. J. Woods, K. S. Karvinen (2008) "The compatibility of consumer plasma displays with time-sequential stereoscopic 3D visualization" in Stereoscopic Displays and Applications XIX, Proceedings of IS&T/SPIE Electronic Imaging, SPIE Vol. 6803, pp. 68030X-1 to -9, San Jose, California, January 2008.

The compatibility of consumer plasma displays with time-sequential stereoscopic 3D visualization

Andrew J. Woods*, Kai S. Karvinen
Centre for Marine Science and Technology, Curtin University of Technology,
GPO Box U1987, Perth WA 6845, Australia.

ABSTRACT

Plasma display panels (PDP) are now a commonly used display technology for both commercial information display purposes and consumer television applications. Despite the widespread deployment of these displays, it was not commonly known whether these displays could be used successfully for time-sequential stereoscopic 3D visualization (i.e. using LCS 3D glasses). We therefore conducted a study to test a wide range of PDPs for stereoscopic compatibility. This paper reports on the testing of 14 consumer plasma displays. Each display was tested to establish whether the display synchronized with the incoming video signal, whether there was electronic crosstalk between alternate fields or frames, the maximum frequency at which the display would work, the time delay between the incoming video signal and the displayed images, whether the display de-interlaced interlaced video sources in a 3D compatible way, and the amount of phosphor decay exhibited by the display. The overall results show that plasma displays are not ideal for use with time-sequential stereo. While roughly half of the plasma displays tested do support the time-sequential 3D technique, all of the tested displays had a maximum display frequency of 60Hz and most had long phosphor persistence which produces a lot of stereoscopic crosstalk.

Keywords: stereoscopic, 3D, plasma displays, PDP, time-sequential.

1. INTRODUCTION

Plasma display panels (PDP) are now a commonly used display technology for both commercial information display purposes and consumer television applications. Despite the widespread deployment of these displays, prior to this study it was not commonly known whether plasma displays could be used successfully for time-sequential stereoscopic 3D visualization (i.e. using LCS (Liquid Crystal Shutter) 3D glasses).

There is an increasing awareness and demand for large stereoscopic displays, and it would be ideal if existing plasma displays could be used for this purpose.

We therefore undertook a research project to sample a wide range of consumer-grade plasma displays to determine their level of time-sequential 3D compatibility. The results of the project would provide an improved understanding of the level of 3D compatibility of consumer-grade plasma displays for those wishing to employ large direct-view stereoscopic displays, and also hopefully raise awareness of the potential stereoscopic capability of these displays in the hope that manufacturers would implement time-sequential stereoscopic display compatibility in future models as a standard feature (and list it in their specifications).

Previous work conducted at Curtin has included studies of the 3D compatibility¹ of CRT monitors², LCD monitors³, and DLP projectors⁴. This study is a natural progression of those previous studies.

1.1 Operation of a Plasma Display Panel

A plasma display consists of a two-dimensional array of millions of tiny cells, called sub-pixels. Each sub-pixel contains a mixture of noble gases and is lined with a phosphorescent material. Three sub-pixels driven together (a red sub-pixel, a green sub-pixel, and a blue sub-pixel) form a full color pixel. Figure 1a shows the structure of a typical AC plasma display sub-pixel. When a voltage is applied across a particular sub-pixel, plasma is created which emits ultraviolet light. The ultraviolet light is absorbed by the phosphor within the cell, which in turn emits light of a particular color.

* A.Woods@cmst.curtin.edu.au; phone +61 8 9266 7920; fax +61 8 9266 4799; www.cmst.curtin.edu.au

Unlike CRTs or LCDs, all the sub-pixels in a plasma display can be driven to output light at the same time. Figure 1b and 1c show the time-domain drive scheme of a plasma display panel. In these graphs, the horizontal axis is time and the vertical axis is the vertical position on screen (the pixel row number counting from the top down). In this example, during each field-period the plasma display can be energized up to 8 times – each of these 8 periods is called a sub-field. Figure 1c shows the structure of one sub-field (SF), comprising a reset period, the addressing period (each sub-pixel in the entire display is individually addressed for triggering or not-triggering), and the sustain period (the entire panel is energized, and those sub-pixels that have been triggered, will output light). It can be seen from Figure 1b that the sustain period is different for each of the sub-fields, in a binary pattern – i.e. SF1 has a sustain period of 1 ‘unit’ (0.01ms), SF2 has a sustain period of 2 ‘units’, SF3=4, SF4=8, ... , SF8=128 ‘units’ (1.28ms). In general terms, a sub-pixel triggered during sub-field 8 (SF8) will have double the brightness of a sub-pixel triggered during sub-field 7 (SF7). For each sub-pixel, different grey-levels are achieved by triggering the sub-pixel only in selected sub-fields. For example, in general terms, a black sub-pixel would be achieved by not triggering the sub-pixel during any of the sub-fields, a full-bright sub-pixel would be achieved by triggering the sub-pixel during all of the sub-fields, and a half-brightness sub-pixel would be achieved by only triggering the sub-pixel during sub-field 8 (SF8).

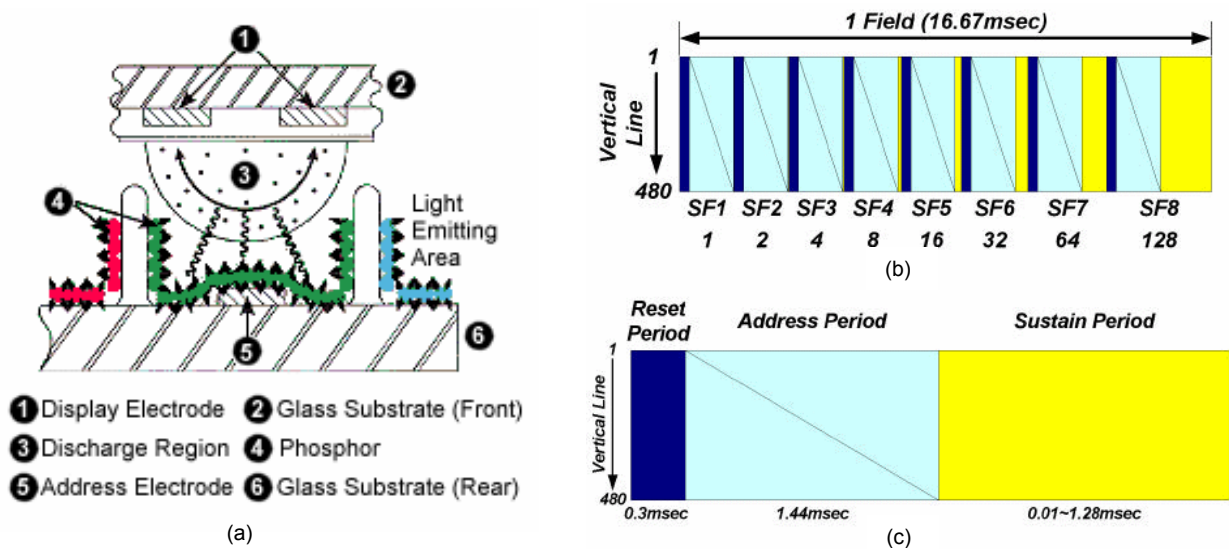


Figure 1: (a) The layout of a typical AC plasma display sub-pixel⁵, (b) an illustration of the time-domain drive scheme of an example plasma display panel using 8 sub-fields during one TV-field⁶, and (c) the time-domain structure of a single sub-field⁶.

As was mentioned above, all sub-pixels of a plasma display can be driven simultaneously, however unlike a CRT which only drives each pixel to emit light once per field, a plasma display can be driven to output light multiple times per field (8 times per field in the example above, although different plasma displays use a different number of sub-fields per TV-field, and different sub-field timing). This means that plasma displays act somewhat like a cross between a hold-type display and an impulse-type display. CRTs are an impulse-type display and LCDs are a hold-type display.

2. EXPERIMENTAL METHOD

In this study we tested 14 different consumer-grade plasma displays from nine different manufacturers. The age of the displays ranged from units that were several years old to units that had only been recently released at the time of the tests.

Equipment used for testing included: two custom-built photodiode sensor pens (based on an Integrated Photomatrix Inc. IPL10530 DAL), two oscilloscopes (a Goldstar OS-3000, and a TiePie Engineering Handyscope HS3 digital USB oscilloscope), and a custom-built LCS 3D glasses driver box capable of adjustable phase and duty cycle. Equipment used to generate the time-sequential 3D video signals consisted of a small form factor PC fitted with a stereoscopic capable graphics card (NVIDIA 6600GT) and a Panasonic 'DMR-E65' DVD recorder/player. The Panasonic DMR-E65 was chosen because it is known to convert interlaced video signals to progressive in a 3D compatible way when the component progressive output is selected via the internal menu. Software on the PC consisted of Windows XP, the NVIDIA 3D Stereo Driver⁷, the NVIDIA JPS Viewer⁷, and Powerstrip⁸. The test equipment layout is shown in Figure 2.

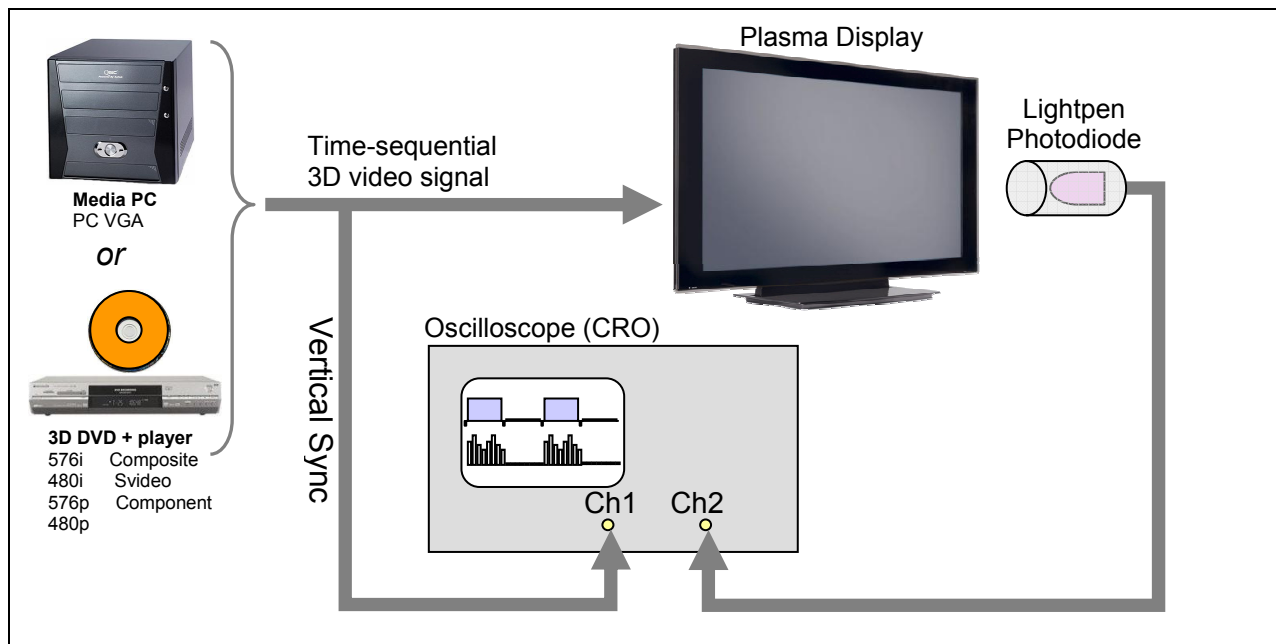


Figure 2: Schematic diagram of the experimental setup.

Test signals consisted of alternating sequences (at field or frame rate) of red and black, blue and black, green and black, white and black, or RGB color bars and black (i.e., in the case of "red and black", one field of red, one field of black, and repeat). In the case of the DVD player, custom written NTSC and PAL 3D DVDs were used. In the case of the PC, custom created JPS (Stereoscopic JPEG) files were used.

Each plasma display was tested to establish: (a) whether the output frame rate of the display synchronized with the incoming video signal, (b) whether there was electronic crosstalk between alternate fields or frames, (c) the maximum frequency at which the display would work in stereo (VGA only), (d) the time delay between the incoming video signal and the displayed images, (e) whether the display de-interlaced interlaced video sources in a 3D compatible way, and (f) the amount of phosphor decay exhibited by the display. These properties were tested for various video input connections (composite, SVideo, component, and VGA), various video formats (NTSC (480i), PAL (576i), 480P, 576P), and various VGA resolutions/frequencies.

Standard Definition (SD) video formats were tested because there is a reasonable range of commercially available field-sequential 3D DVDs and it is important to know which displays can be used with these 3D DVDs. VGA modes were tested because the projector can be driven at its native resolution and frame rate with this interface. DVI-D and HDMI input connections were not tested because a method of extracting the vertical sync signal from these interface cables was not available.

3. RESULTS AND DISCUSSION

The 14 plasma displays tested in this study are listed in Table 1 along with some basic specifications.

Table 1: The Plasma displays tested in this study, their basic specifications, and an arbitrary identification tag.

Tag	Manufacturer	Model	Screen Diagonal (inches)	Native Display Resolution	VGA Input Resolution
D01	LG	DT-42PY10X	42	1024 x 768	1024 x 768
D02	Fujitsu	P50XHA51AS	50	1366 x 768	1360 x 768
D03	NEC	PX-50XR5W	50	1366 x 768	1360 x 768
D04	Panasonic	TH-42PV60A	42	1024 x 768	1024 x 768
D05	Samsung	PS-42C7S	42	852 x 480	800 x 600
D06	LG	RT-42PX11	42	852 x 480	800 x 600
D07	NEC	PX-42XM1G	42	1024 x 768	1024 x 768
D08	Sony	PFM-42V1	42	852 x 480	800 x 600
D09	Sony	FWD-50PX2	50	1366 x 768	1360 x 768
D10	Hitachi	55PD8800TA	55	1366 x 768	1024 x 768
D11	Hitachi	42PD960BTA	42	1024 x 1080	1024 x 768
D12	Pioneer	PDP-507XDA	50	1366 x 768	1360 x 768
D13	Pioneer	PDP-50HXE10	50	1366 x 768	1360 x 768
D14	Fujitsu	PDS4221W-H	42	1024 x 1024	1024 x 768

3.1 Synchronization

In order for time-sequential 3D video to work correctly on a particular display, it is necessary for the display's update of video frames to synchronize with the input video signal. It has been found that in some cases the display has its own native frequency of display (usually ~60Hz) and all other input frequencies are resampled to this native frequency – this resampling process usually destroys the 3D video signal.

Table 2 lists the synchronization test results. The 'Component 50Hz Progressive' column indicates whether the display would correctly synchronize to 576P 50Hz frame-sequential 3D video (derived from a PAL 3D DVD) entered via the component connector. The 'Component 60Hz Progressive' column indicates whether the display would correctly synchronize to 480P 60Hz frame-sequential 3D video (derived from an NTSC 3D DVD) entered via the component connector. The VGA 60Hz column indicate whether the display would correctly synchronize to frame-sequential 3D video entered via the VGA connector (in almost all cases the video resolution was set to the native resolution of the display). The bottom row of the table indicates the percentage of all tested projectors that would synchronize in that video mode.

It is worth noting that none of the tested plasma displays were 3D compatible with interlaced video sources (576i or 480i field-sequential). This is undoubtedly due to the display using a 3D incompatible 'interlaced to progressive scan' converter. Fortunately the 3D incompatible 'interlaced to progressive scan converter' can be bypassed by inputting a progressive video signal into the display.

Regarding Table 2, it can be seen that some of the tested displays (D01, D04 and D06) would not synchronize to the incoming video signal in any video mode or video connection, and hence would not be time-sequential 3D compatible. It is surprising to see this result because non-synchronization would also cause problems for regular 2D content – in scenes of continuous smooth motion, a regular stutter or glitch in the motion would be visible.

Table 2: Display synchronization test results for the 14 plasma displays. (A green 'YES' indicates that the display did synchronize with the incoming video signal, a red 'NO' indicates that the display did not synchronize in those modes, and a dash indicates that mode was not tested (either because that mode was not available on that display, or a necessary cable or connector was not available).

Display	Component 50Hz progressive	Component 60Hz progressive	VGA	VGA input resolution
D01	No	No	No	1024 x 768
D02	Yes	Yes	Yes	1360 x 768
D03	No	Yes	No	1360 x 768
D04	No	No	No	1024 x 768
D05	Yes	Yes	No	800 x 600
D06	No	No	No	800 x 600
D07	Yes	Yes	Yes	1024 x 768
D08	-	-	Yes	800 x 600
D09	-	-	Yes	1360 x 768
D10	-	No	No	1024 x 768
D11	Yes	-	No	1024 x 768
D12	Yes	Yes	No	1360 x 768
D13	-	-	No	1360 x 768
D14	No	Yes	Yes	1024 x 768
% of displays that synchronize the display output to the input video signal	50%	60%	38%	

3.2 Time Delay

With some displays there is often a time delay between the video information being received at the display via one of the video input connectors, and light being output on the display for that particular frame. This effect is shown for an example plasma display in Figure 3. Table 3 lists the time delay measurement for the tested plasma displays with different input video sources.

Most drivers for LCS 3D glasses assume that there is no such delay (which is correct for CRTs). If LCS 3D glasses with no delay are used to view time-sequential 3D images on a display with a significant amount of time delay, a great deal of ghosting can be present. As mentioned earlier, we developed a smart dongle which allows the time delay of the LCS 3D glasses to be adjusted.

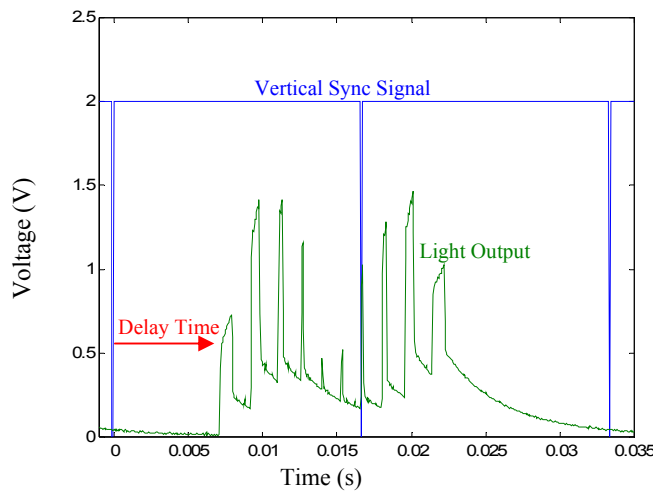


Figure 3: This graph illustrates the delay time between the vertical sync from the VGA video signal (blue trace) and light output on the display (green trace) was measured as 23.7ms for monitor D14. The vertical axis of the graph is brightness for the Light Output trace, and Voltage for the Vertical Sync trace. In this instance one frame period = 16.7ms (60Hz) and the delay time is approximately 7ms.

Table 3: This table shows the measured time delay between the trailing edge of the vertical sync and the start of light output on the screen, measured in milliseconds. ('N.S.' means the display would Not Synchronize with the video signal, and '-' means this video mode could not to be tested)

Display ID	Component (50Hz)	Component (60Hz)	VGA (60Hz)	Maximum Resolution
D01	N.S.	N.S.	N.S.	1024 x 768
D02	30.0	26.7	26.7	1360 x 768
D03	N.S.	26.0	N.S.	1360 x 768
D04	N.S.	N.S.	N.S.	1024 x 768
D05	22.0	19.0	N.S.	800 x 600
D06	N.S.	N.S.	N.S.	800 x 600
D07	39.2	32.4	33.9	1024 x 768
D08	-	-	30.0	800 x 600
D09	-	-	25.2	1360 x 768
D10	-	N.S.	N.S.	1024 x 768
D11	21.6	-	N.S.	1024 x 768
D12	40.2	45.6	N.S.	1360 x 768
D14	N.S.	23.4	23.7	1024 x 768

3.3 Phosphor Decay

Like CRTs, plasma displays also use phosphors to generate visible light. And as with CRTs, phosphor decay (aka: phosphor persistence, phosphor afterglow) can also be a problem with plasma displays. Figure 4 shows the time-domain response of an example plasma display (D14). It can be seen from the graph that this particular display has 10 sub-fields per TV-field (count the peaks), but more importantly for this section, after each peak the red and the green color primaries exhibit a significant amount of phosphor decay. In this example, the blue color primary doesn't have any noticeable phosphor decay. This type of graph was very common among the displays that were tested. The red and green phosphors typically had phosphor decays with long time constants, whereas blue usually exhibited almost no phosphor afterglow.

Long phosphor decay when combined with time-sequential 3D viewing produces ghosting since the light from one eye view leaks into the time period of the other eye view.

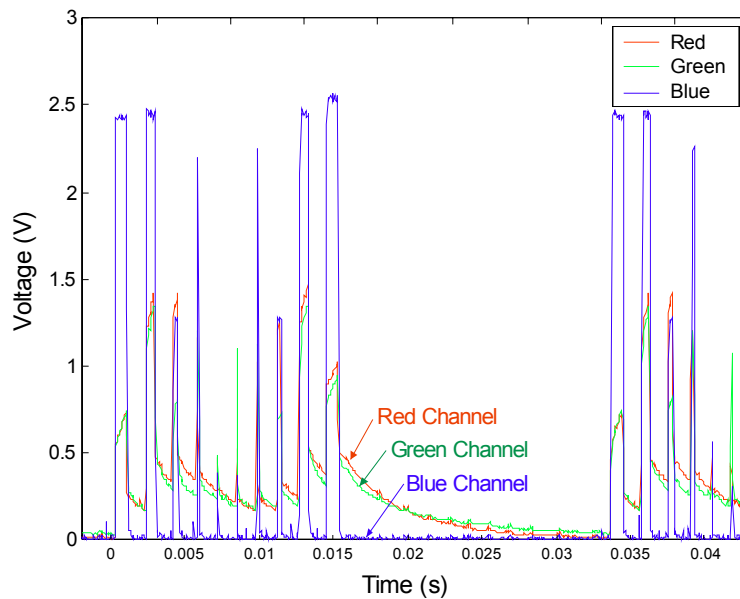


Figure 4: The time-domain light output of an example plasma display (D14) (for alternate frames of 100% red, green and blue with black). The vertical axis is brightness of the each of the color channels as measured in volts by the photo sensor, and the horizontal axis is time (seconds).

3.4 Crosstalk

Most of the plasma displays tested exhibited significant amounts of crosstalk when viewing time-sequential 3D images using LCS 3D glasses. The main reason for the excessive crosstalk is the significant amount of phosphor afterglow. Figure 5 below shows the time-domain light output for a red frame (followed by a black frame) for display D02, along with the transmission response of an example pair of LCS 3D glasses for both eyes (in this case a pair of NuVision 3Dspex glasses driven by the Curtin smart dongle). In Figure 5, it can be seen that from 0 to 17ms the left eye of the LCS glasses is transmissive and the right eye of the LCS glasses is opaque. At about 17ms, the LCS glasses switch from one state to the other, and in the example of Figure 5 the afterglow of the phosphors is still decaying from the first field, hence light from the left eye image will leak into the right eye producing crosstalk.

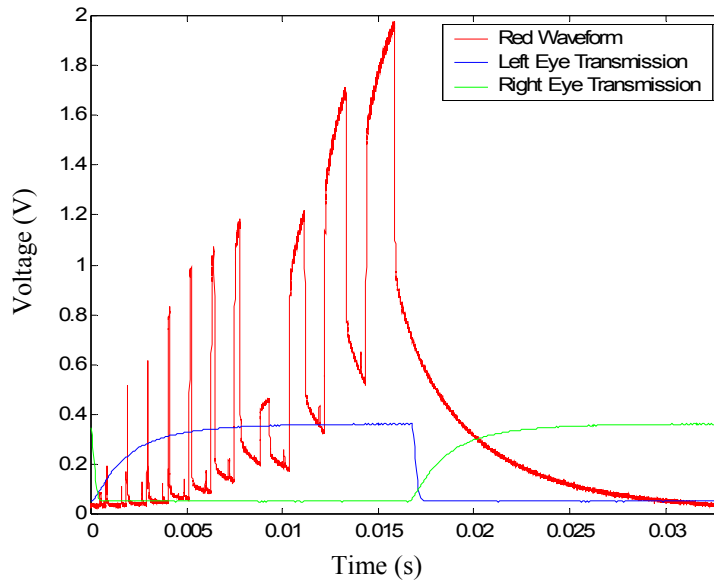


Figure 5: Diagram showing the LCS 3D glasses transmission states for both eyes and the time-domain light output for a red frame (followed by a black frame) for display D02. The vertical axis is brightness of the each of the color channels as measured in volts by the photo sensor, and the horizontal axis is time (seconds). In this instance one frame period = 16.7ms (60Hz).

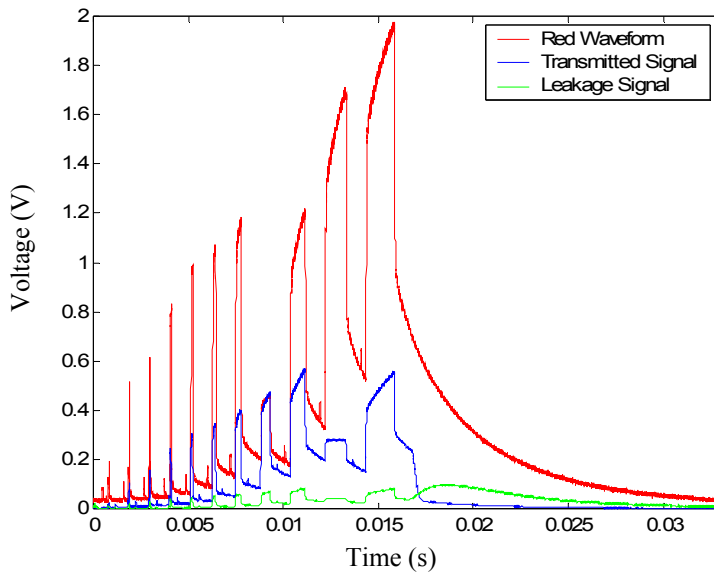


Figure 6: Diagram showing the original red waveform of monitor D02 (red), the transmitted signal to the left eye (blue), and the crosstalk signal to the right eye (green)

Figure 6 shows the result of multiplying the red waveform amplitude with the transmission response of the LCS glasses (left eye, and right eye) – firstly the transmitted (desired) signal in blue, along with the leakage (undesired) signal in green. Division of the area under the leakage curve by the area under the transmitted curve will give the crosstalk measure.

The calculated time-sequential 3D crosstalk factors for each of the plasma displays tested is listed in Table 4. As can be seen in the table, monitor D08 exhibits the least crosstalk, and monitor D10 exhibits the most crosstalk. The crosstalk performance for an example DLP projector is also provided for comparison purposes. The switching of DLP projectors is almost perfect with negligible leakage between frames due to the DLP engine, which means that essentially all of the crosstalk for DLP projectors is due to the glasses. The crosstalk factor for D08 is only a few points higher than DLP which is a reasonable result. On the other hand, results such as the 38.3 crosstalk factor figure for D10, will mean that a time-sequential 3D image would be severely affected by crosstalk.

Table 4: Calculated time-sequential crosstalk factors with 50% duty cycles (green, yellow and orange cells indicate overall crosstalks of <10%, 10-20% and >20% respectively)

<i>Display</i>	<i>Duty Cycle</i>	<i>Total Crosstalk</i>	<i>Red Crosstalk</i>	<i>Green Crosstalk</i>	<i>Blue Crosstalk</i>
D01	50	22.6 ± 2.1	11.7 ± 0.8	10.5 ± 1.2	0.4 ± 0.1
D02	50	27.9 ± 3.0	12.2 ± 1.3	15.1 ± 1.6	0.6 ± 0.1
D03	50	21.8 ± 2.3	8.6 ± 0.9	12.7 ± 1.4	0.5 ± 0.1
D04	50	26.9 ± 2.7	8.1 ± 0.8	18.3 ± 1.8	0.5 ± 0.1
D05	50	14.3 ± 1.5	7.2 ± 0.8	6.6 ± 0.6	0.6 ± 0.1
D06	50	21.6 ± 2.1	9.2 ± 1.0	12.0 ± 1.0	0.4 ± 0.2
D07	50	22.5 ± 2.4	9.6 ± 1.0	12.2 ± 1.3	0.7 ± 0.1
D08	50	9.9 ± 1.0	5.6 ± 0.6	3.3 ± 0.4	1.0 ± 0.1
D09	50	14.8 ± 1.5	6.5 ± 0.7	7.9 ± 0.8	0.5 ± 0.1
D10	50	38.3 ± 4.0	13.9 ± 1.5	23.8 ± 2.5	0.6 ± 0.1
D11	50	14.8 ± 1.5	6.0 ± 0.6	8.4 ± 0.9	0.4 ± 0.1
D45	50	23.2 ± 2.5	10.0 ± 1.1	12.5 ± 1.4	0.8 ± 0.1
DLP	50	5.5 ± 0.7	3.7 ± 0.4	1.3 ± 0.1	0.5 ± 0.1

In all of these examples, the glasses have been switched with a 50% duty cycle. Some simulations were also performed by reducing the duty cycle of the LCS glasses but these results are reported separately⁹.

4. CONCLUSION

The purpose of this study was to determine the compatibility of plasma displays with stereoscopic visualization. Results show that approximately half of all displays tested are partially compatible with progressive time-sequential stereoscopic viewing. Approximately half of the plasma displays tested were 3D incompatible because the display output did not synchronize to the input video signal. Of the displays that did synchronize with a time-sequential 3D video signal, most produced large amounts of crosstalk – only two displays exhibited acceptably low levels of crosstalk. None of the displays were able to refresh at frequencies above 60Hz, which would generally result in noticeable flicker. None of the plasma displays tested were compatible with interlaced time-sequential 3D video signals (as provided by field-sequential 3D DVDs). For the reasons mentioned above, it is unlikely that any of the tested plasma displays will be useful for commercial time-sequential stereoscopic applications.

Some plasma displays can be used for stereoscopic applications, however, the level of 3D compatibility is incredibly variable from one display to another. Flicker-free time-sequential 3D is not possible in the displays that we tested, as the maximum frame rate is limited to 60Hz. For this reason, the tested plasma displays would not be considered ideal for use with time-sequential 3D viewing.

It was ironic to find that the plasma display which offered the best performance of all the displays was a Sony (D08), but Sony decided to stop making plasma displays in 2006.

The research reported in this technical paper was completed in February 2007, and although we did not find any plasma displays that could be directly used for flicker-free time-sequential 3D display, the results did indicate that it was

technically feasible. It was therefore heartening to hear in early January 2008, when this technical paper was being completed, that Samsung will be releasing several consumer “3D Ready” plasma displays in March 2008¹⁰. The displays use LCS 3D glasses to view the time-sequential 3D image which updates at 120Hz. As yet we have not been able to test one of these new Samsung “3D Ready” plasma displays, but obviously Samsung have been able to successfully implement 120Hz synchronous operation in a plasma display, and presumably they have also been able to minimize phosphor afterglow which was identified as a problem with most of the commercial plasma displays that we tested.

ACKNOWLEDGEMENTS

This work was supported by iVEC (the hub of advanced computing in Western Australia), Jumbo Vision International, and Curtin University of Technology.

We wish to thank the companies and individuals who provided access to plasma displays for testing: Kim Kimenkowski, Jumbo Vision International (Kewdale, Western Australia); Peter Henley; Natalie Fenner; Con Parente, West Coast Hi-Fi (O'Connor, Western Australia); Alan Blackmore, CDM Optel Australia (Osborne Park, Western Australia); and Michael, and Matt Southgate from West Coast Hi-Fi (Cannington, Western Australia).

REFERENCES

1. Woods, A.J. (2005), “Compatibility of Display Products with Stereoscopic Display Methods”, International Display Manufacturing Conference, Taiwan, February 2005.
2. Woods, A., Tan, S.S.L. (2002) “Characterising Sources of Ghosting in Time-Sequential Stereoscopic Video Displays”, presented at Stereoscopic Displays and Applications XIII, published in Stereoscopic Displays and Virtual Reality Systems IX, Proceedings of SPIE Vol. 4660, San Jose, California, 21-23 January 2003.
3. Woods, A.J., Yuen, K.-L. (2006) "Compatibility of LCD Monitors with Frame-Sequential Stereoscopic 3D Visualisation" (Invited Paper), in IMID/IDMC '06 Digest, (The 6th International Meeting on Information Display, and The 5th International Display Manufacturing Conference), pg 98-102, Daegu, South Korea, 22-25 August 2006.
4. Woods, A.J., Rourke, T., (2007) "The compatibility of consumer DLP projectors with time-sequential stereoscopic 3D visualisation", presented at Stereoscopic Displays and Applications XVIII, published in Stereoscopic Displays and Virtual Reality Systems XIV, Proceedings of SPIE Vol. 6490, San Jose, California, 29-31 January 2007.
5. “The plasma behind the plasma TV screen” (n.d.). Retrieved on 28 November 2006 from <http://www.plasmatvscience.org/theinnerworkings.html>
6. Cho, K.-D., (2004) “New Address and Sustain Waveforms for AC Plasma Display Panel”, PhD Thesis, Kyungpook National University. Retrieved 7 February 2007, from http://palgong.knu.ac.kr/~plasma/Paperdata/thesis/Ph_Dr_Cho_2004.pdf
7. NVIDIA 3D Stereo Driver http://www.nvidia.com/object/3d_stereo.html
8. Powerstrip software <http://entechtaiwan.net/util/ps.shtm>
9. Karvinen, K.S., Woods, A.J. (2007) “The Compatibility of Plasma Displays with Stereoscopic Visualisation” CMST Technical Report CMST2007-04, Curtin University of Technology, Perth Australia, February 2007.
10. Samsung (2008) “SAMSUNG Debuts The First 3D Ready Flat-Panel HDTV With Its 2008 Entry-Level Plasma HDTV Line-Up”, Press Release 7 January 2008, Retrieved on 9 January 2008 from http://www.samsung.com/us/news/newsRead.do?news_seq=6449&page=1

Paper 7 [Refereed Conference Paper]
A. J. Woods, A. Sehic (2009) "The compatibility of LCD TVs with time-sequential stereoscopic 3D visualization" in Stereoscopic Displays and Applications XX, Proceedings of IS&T/SPIE Electronic Imaging, SPIE Vol. 7237, pp. 72370N-1 to -9, San Jose, California, January 2009.

The compatibility of LCD TVs with time-sequential stereoscopic 3D visualization

Andrew J. Woods*, Adin Sehic

Centre for Marine Science and Technology, Curtin University of Technology,
GPO Box U1987, Perth WA 6845, Australia.

ABSTRACT

Liquid Crystal Displays (LCD) are now a popular display technology for consumer television applications. Our previous research has shown that conventional LCD computer monitors are not well suited to time-sequential stereoscopic visualization due to the scanning image update method, the hold-type operation of LCDs, and in some cases slow pixel response rate. Recently some new technologies are being used in LCD TVs to improve 2D motion reproduction - such as black frame insertion and 100/120Hz capability. This paper reports on the testing of a selection of recent LCD TVs to investigate their compatibility with the time-sequential stereoscopic display method - particularly investigating new display technologies. Aspects considered in this investigation include image update method, pixel response rate, maximum input frame rate, backlight operation, frame rate up-conversion technique, synchronization, etc. A more advanced Matlab program was also developed as part of this study to simulate and characterize 3D compatibility and calculate the crosstalk present on each display. The results of the project show that black frame insertion does improve 3D compatibility of LCDs but not to a sufficient level to produce good 3D results. Unfortunately 100/120Hz operation of the tested LCD did not improve 3D compatibility compared to the LCD monitors tested previously.

Keywords: Stereoscopic, time-sequential 3D, LCD, compatibility, 100Hz, 120Hz, black frame insertion.

1. INTRODUCTION

The time-sequential (also known as: field-sequential, frame-sequential, time-multiplexed, alternate field) stereoscopic display technique has a long and successful history of use with CRT (Cathode Ray Tube) displays. High-quality full-color flicker-free stereoscopic images can be seen with the aid of Liquid Crystal Shutter (LCS) 3D glasses when operating at a display frequency of 120Hz. CRTs have now almost completely been replaced by LCDs (and Plasma) displays in the home television market, so naturally people are interested to know whether LCD TVs can be used with LCS 3D glasses to view stereoscopic 3D content. Our previous work has shown that conventional consumer LCD computer monitors [1] and Plasma displays [2] are not well suited to time-sequential stereoscopic 3D visualization. Some of the incompatibility reasons cited were fundamental to the way that the displays output light and generated images, but other factors were more specific to way that the specific display was implemented (usually related to video processing).

For the purposes of this discussion, we divide LCD TVs into three categories: (1) Commercially released displays in which the 3D compatibility of the display is unstated, (2) commercially released displays which are stated as being 3D Ready or Stereoscopic 3D capable, and (3) customized displays which are being developed in R&D labs but are not commercially released. This paper aims to establish whether any LCDs in Category 1 can be used for time-sequential 3D visualization. Obviously the 3D status of displays in Category 2 is already known. It is hoped that the analyses and results of this paper will be helpful for the innovations taking place in Category 3, but since such displays are not currently commercially available, it is outside the scope of this paper.

2. NEW LCD TECHNOLOGIES

Since the publication of our LCD compatibility paper [1] in 2006, a number of new technologies have been introduced into some commercially released LCD TVs. These new technologies are: Black Frame Insertion (BFI), 120Hz refresh,

* A.Woods@curtin.edu.au; phone +61 8 9266 7920; fax +61 8 9266 4799; www.3d.curtin.edu.au

and modulated backlight. These technologies have been introduced to improve the reproduction of moving images in 2D viewing (nothing to do with 3D viewing). Conventional LCDs suffer from a problem called image smear (often known as motion blur) which is caused by LCDs being a hold-type display [3]. These new technologies reduce the presence of image smear, but this paper considers how these technologies affect time-sequential 3D compatibility.

2.1 Black Frame Insertion (BFI)

Black Frame Insertion can be considered two ways, either (a) the display time of each individual frame is reduced and replaced with black, in effect reducing the duty cycle of each frame, or (b) the display adds a black frame between each original video input frame. Image smear will be reduced because the hold-time is reduced, however one problem with this technique is that if the backlight brightness isn't increased, the brightness of the display will be reduced in proportion to the amount of BFI introduced. It could be argued that the insertion of the intermediate black frames increases the display frequency up to 120Hz, but these extra frames are just black, not new image frames, so it is still 60 frames per second, but with a reduced on time per frame. BFI is sometimes compared to the modulated backlight technology, and although the effect on image smear is similar, BFI is different because it is implemented at the LCD panel, not the backlight.

2.2 120Hz Refresh

This technology works by interpolating extra frames between the original 60Hz frames provided at the video signal input. The 60 original frames per second plus the new interpolated frames interspersed between the original frames results in 120 frames per second (120Hz). At the new 120Hz image rate, the time on screen per frame is halved, and hence the integration time is halved which in turn reduces image smear for moving objects. With 60Hz input sources the display rate is doubled to 120Hz, and for 50Hz input sources the display rate is doubled to 100Hz.

2.3 Modulated Backlight

Also known as strobing backlight or scanning backlight, in this case image smear is reduced because the on-time of each frame is reduced by switching the backlight on and off (reducing the duty cycle). With a strobing backlight the entire backlight is turned on and off all at once. With a scanning backlight the on and off cycle is scanned down the display in segments, usually following the scan-like image update of the LCD.

3. IMPORTANT LCD AND LCS PROPERTIES

Our work in 2006 [1] identified several important properties of LCD monitors and LCS 3D glasses which determine the compatibility of a particular display with the time-sequential stereoscopic 3D display method.

3.1 LCD and LCS Native Polarization

The LCD and the LCS both have a native (linear) polarization angle – if these are orthogonal, the display will appear black when viewed through the LCS glasses. This is easily overcome by the use of a quarter or half-wave retarder, or designing the LCS with a different polarization orientation.

3.2 Refresh Rate

The maximum refresh rate of a monitor determines the maximum speed at which it can display a sequence of images. A refresh rate of 100-120Hz is usually considered necessary for flicker-free viewing with the time-sequential 3D method. The maximum refresh rate which can be used successfully for time-sequential 3D is determined by two factors: (a) the maximum rate at which the input electronic will accept a video signal, and (b) the maximum rate at which the internal display electronics will drive the LCD panel. Generally, the lower of these two maximums will be the important number for 3D purposes.

3.3 LCD Pixel Response Time

It takes a finite period of time for an individual pixel to be switched from one state to another. For time-sequential 3D viewing, the LCS should not be opened until the switching of the pixel (from one state to another) has stabilized sufficiently. If the pixel response time is too slow, the image would never stabilize before the next image was displayed, and hence could not be used for time-sequential 3D viewing.

3.4 Image Update Method

A new image is written to an LCD one line at a time from the top of the screen to the bottom. This transition from one image to the next is similar to the way that an image is scanned on a CRT, except that an LCD is a hold-type display whereas a CRT is an impulse-type display [3]. The scan-line image update method of a conventional LCD is illustrated in Figure 1. It is evident from this figure that there is no one time when a single image is shown exclusively on the whole LCD panel – this is particularly so for LCD monitors with a long pixel response rate, but is also true for LCDs with a short pixel response rate. In this example there is no single time when the shutters in the LCS glasses could open and see exclusively a single perspective image.

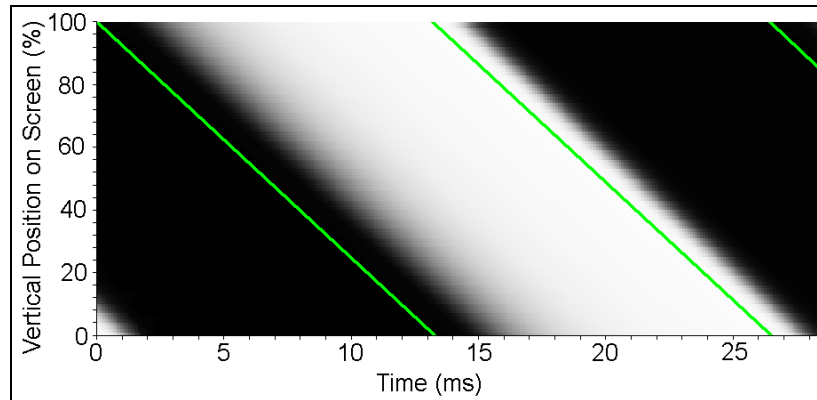


Figure 1: The time-domain response of an example conventional LCD panel alternating between black and white at 75Hz. The vertical axis shows the vertical position on the LCD panel. The horizontal axis shows time. The thin diagonal line represents the addressing of each row of the LCD.

3.5 LCS Duty Cycle

Most driving electronics for LCS 3D glasses drive the shutters with a 50% duty cycle which is problematic for time-sequential 3D on LCDs. In our previous work [1] we showed that reducing the LCS duty cycle can improve compatibility with the time-sequential 3D method.

3.6 Synchronization

In order for time-sequential 3D video to work correctly on a particular display, it is necessary for the display's update of video frames to synchronize with the input video signal. Somewhat surprisingly some commercial displays do not synchronize to the incoming video signal and instead resample the signal to the display's own native frequency (usually ~60Hz) – this resampling process usually destroys the time-sequential 3D video signal.

4. EXPERIMENTAL METHOD

In this study we attempted to test a display representing each of the three technologies described earlier. For the 100/120Hz LCD technology we tested a Sony “KDL46XBR” (46” LCD). For the BFI technology we tested a BenQ “FP241WZ” LCD. Unfortunately we were unable to obtain access to an LCD which used backlight modulation for our tests. Philips did commercially release a range of LCD HDTVs which incorporated a modulated backlight (under the trade name Aptura), however these had been discontinued when we began our testing [7] and we were unable to locate any second-hand displays for testing purposes.

Equipment used for testing included: two custom-built photodiode sensor pens (based on an Integrated Photomatrix Inc. IPL10530 DAL), an oscilloscope (a TiePie Engineering Handyscope HS3 digital USB oscilloscope), and a custom-built LCS 3D glasses driver box capable of adjustable phase and duty cycle. Equipment used to generate the time-sequential 3D video signals consisted of a small form factor PC fitted with a stereoscopic capable graphics card (NVIDIA 6600GT). Software on the PC consisted of Windows XP, Microsoft Powerpoint, the NVIDIA 3D Stereo Driver and JPS Viewer [8], and Powerstrip [9]. The test equipment layout is shown in Figure 2.

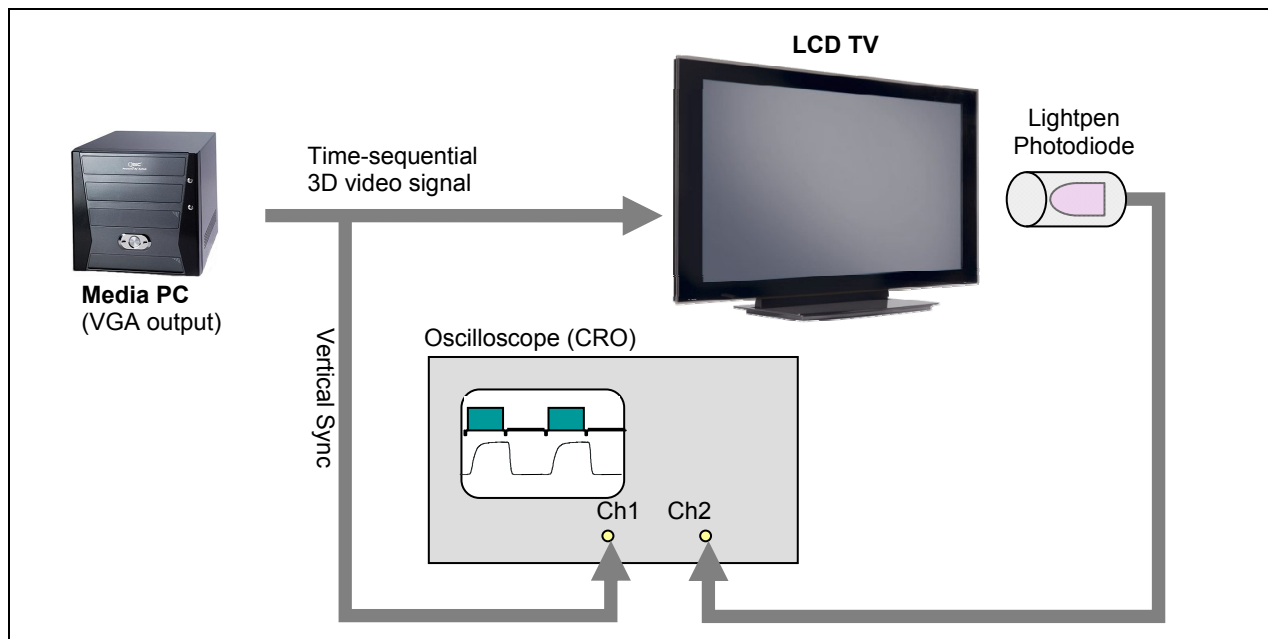


Figure 2: Schematic diagram of the experimental setup.

Test signals consisted of alternating sequences (at frame rate) of ‘red and black’, ‘blue and black’, ‘green and black’, or ‘white and black’ (i.e., in the case of ‘red and black’, one frame of red, followed by one frame of black, and repeat). Each display was tested to establish: (a) whether the output frame rate of the display synchronized with the incoming video signal, (b) whether there was electronic crosstalk between alternate frames, (c) the maximum frequency at which the display would work in stereo, and (d) the time-domain response of the display (to establish pixel response rate, etc). Only the VGA input of the displays was used - the DVI-D and HDMI input connections were not tested because a method of extracting the vertical sync signal from these interface cables was not available.

A custom written Matlab program was used to simulate and characterize 3D compatibility and calculate the crosstalk present on each display. This program was an improved version of the program previously used to simulate the operation and crosstalk performance of Plasma displays [2].

5. RESULTS

The test and simulation results for the tested LCD technologies (BFI and 120Hz refresh) are detailed below.

5.1 Black Frame Insertion

The first thing that should be noted about the particular BFI LCD display that we tested is that it did not synchronize to the incoming video signal. This is a requirement for correct time-sequential 3D operation so this particular display would not be able to be used for time-sequential 3D regardless of its other properties. In order to establish whether BFI had any advantages or disadvantages for time-sequential 3D, the monitor was simulated as if it did synchronize. The time-domain response of the BFI LCD is shown in Figure 3. The (BFI) black frames inserted by the display are indicated by the text labels. With this particular monitor the amount of BFI (or more correctly the duty cycle of the black frames) could be adjusted, from its maximum shown in Figure 3 to a minimum of zero (off). The more BFI that was selected, the dimmer the display became.

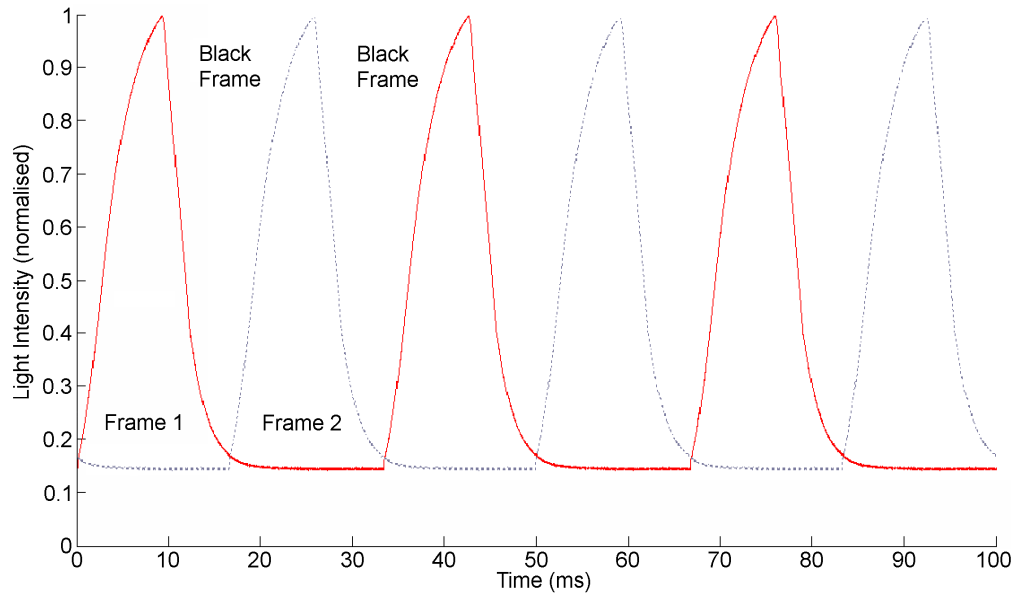


Figure 3: The time-domain response of the example BFI LCD operating at 60Hz. The vertical axis shows normalized light intensity. The solid red trace shows the display being driven with an alternating sequence of black and white input frames. The second dotted trace is the first trace delayed by one frame to show the existence of the (BFI) black frames inserted by the display.

Due to the scan-like image update method of LCDs a more useful way of representing the spatio-temporal output of the LCD is shown in Figure 4. With this particular figure it is easy to see the combination of the sequence of left and right perspective images, the introduction of the inserted black frames (BFI), and the scan-like image update method. It should be noted at this point that due to a technical oversight, the exact image update method of this BFI display was not measured; however we believe this figure to be a reasonable estimate of its operation with this display. It can be seen that the black “BFI” bands do a good job of separating sequential frames, however the presence of the scan-like image update method complicates matters for time-sequential 3D.

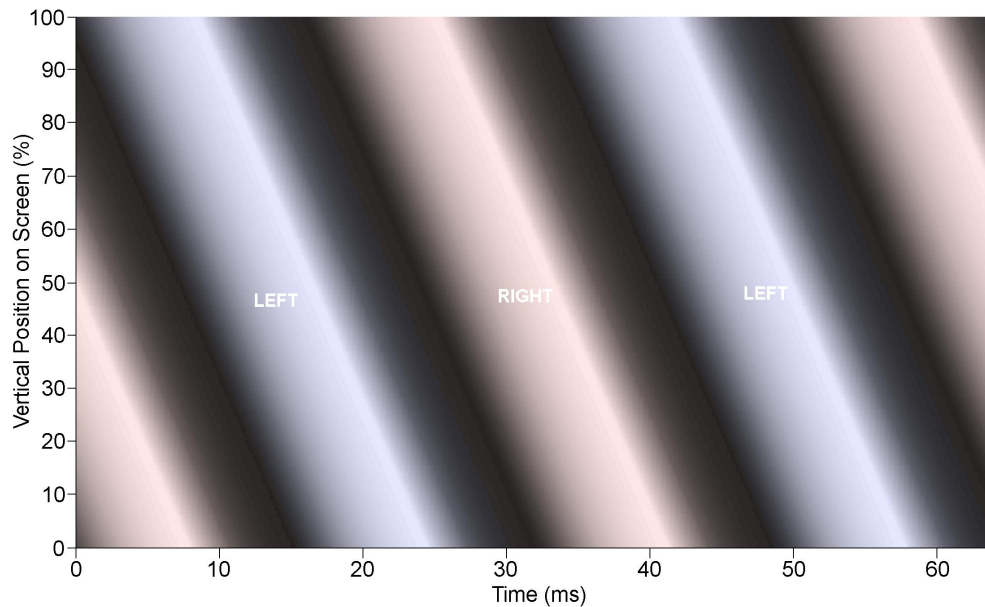


Figure 4: The spatial- and time-domain response of the example BFI LCD operating at 60Hz. The vertical axis shows the vertical position on the screen and the horizontal axis time. The LEFT and RIGHT labels and tinting represent a sequence of left and right perspective images shown sequentially.

Figure 5 illustrates this complication by showing the spatio-temporal output of the display when viewed through LCS 3D glasses. It can be seen that at the beginning of the shutter open period (for viewing the left perspective image) the right perspective image is still visible at the bottom of the screen, and at the end of the shutter open period the right perspective image is starting to be visible at the top of the screen. This will cause ghosting to be visible at the top and bottom of the screen.

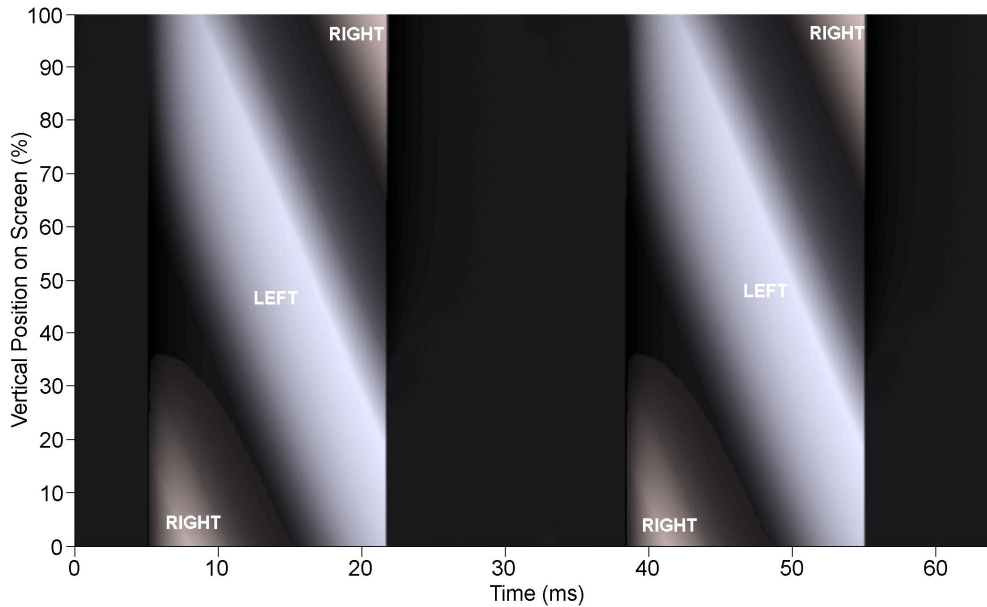


Figure 5: The spatial- and time-domain response of the example BFI LCD operating at 60Hz being viewed through LCS 3D glasses operating at 50% duty cycle. The LEFT and RIGHT labels represent the visibility of left and right perspective images.

Figure 6 shows a calculation of the amount of ghosting that would be visible on the screen when a time-sequential 3D image was viewed through LCS 3D glasses. The two traces on the graph show the amount of ghosting visible on the screen for the two different conditions of BFI on (at maximum) and BFI off – the same display was used for both conditions. With the ‘BFI off’ case, it can be seen that there is a ghosting minimum at the middle of the screen and

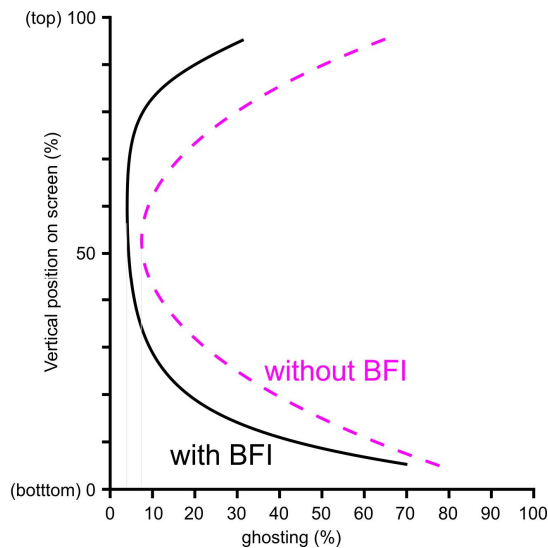


Figure 6: Ghosting simulation results for the BFI LCD monitor with BFI turned on and off. The vertical axis is the vertical position on the screen and the horizontal axis is the calculated amount of ghosting.

ghosting gets worse at the top and bottom of the screen. This is consistent with our previous work [1]. With the ‘BFI on’ case it can be seen that the ghosting minimum is lower than the previous case and also wider meaning that there would be less ghosting visible across more of the display. However, ghosting does still increase at the top and bottom of the display. Unfortunately it was not possible to visually validate these simulation results due to the fact that the tested monitor did not synchronize to the incoming video signal.

One other thing worth commenting on with this particular display is that the maximum frame rate video signal it was able to accept is 60Hz - it is not capable of accepting a 120 or 100Hz signal. A frame rate of 100 or 120Hz is usually considered necessary for flicker-free time-sequential viewing.

5.2 120Hz Refresh

The first thing that should be noted about the tested 120Hz LCD is that it is not possible to input a raw 100Hz or 120Hz video signal – it is only capable of receiving a signal up to 60Hz vertical frequency. For the display’s 120Hz modes, internal electronics in the display interpolate extra intermediate frames between the original 60Hz frames. As discussed earlier, this is designed to reduce the presence of image smear (also known as motion blur). Unfortunately this interpolation (or frequency doubling) process is not compatible with a time-sequential 3D video signal. Additionally with this display the 120Hz mode did not activate when using the VGA input.

The time domain response of the tested 120Hz LCD is shown in Figure 7. The drive signal in this case is a 60Hz video signal alternating between white and black frames. The solid blue trace shows the actual light output of the display. It can be seen that the dotted red trace (which represents the upper envelope of the first trace) alternates between two states (black and white) at 60Hz as expected. The additional regular dips (approximately every 6.3ms) in the blue solid trace are unsynchronized with the input video signal. The dips might be an attempt to improve motion reproduction, but since they are unsynchronized with the video rate they would not have a repeatable effect on time-sequential 3D display. The ghosting results of this monitor (operating at 60Hz) would therefore be very similar to the “without BFI” curve of Figure 6.

The spatio-temporal graphs have not been produced for this display since it could not be driven directly in 120Hz, and the 60Hz results would have been very similar to the results previously published [1].

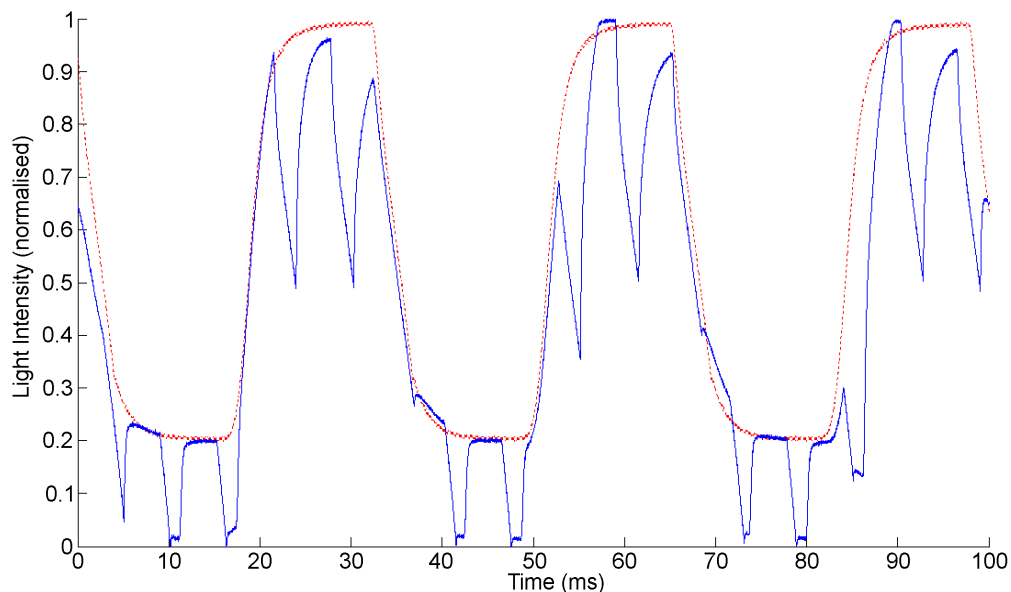


Figure 7: The time-domain response of the example 120Hz LCD operating at 60Hz. The display was being driven with an alternating sequence of black and white input frames. The blue solid trace shows the actual light output of the display. The red dotted trace indicates the upper envelope of the first trace.

5.3 Modulated Backlight

As indicated earlier, we were unable to obtain a modulated backlight LCD for testing during this project. Readers who are interested in considering this topic further are referred to Liou, et al [6].

6. DISCUSSION

Table 1 provides a tabular summary of the three technologies discussed in this paper and the compatibility or incompatibility of the various display properties as embodied in commercially released displays. The main problem of all of these displays is their inability to accept a true 120Hz video input signal. This is determined by the video input electronics and the bandwidth of the input video interface. Even if the ‘maximum input video rate’ problem was overcome, the scan-like image update method of most displays would still likely cause some problems for time-sequential 3D compatibility, although this seems to be less of an issue for BFI and modulated backlight displays. The details for the modulated backlight column in the table are extrapolated from product specifications and technical papers [3][4][5][6].

Table 1: A summary of the important LCD and LCS properties and compatibility or incompatibility for each of the three display technologies discussed in this paper.

	Black Frame Insertion	120Hz Refresh	Modulated Backlight
Native Polarization	○ easily overcome	○ easily overcome	○ easily overcome
Maximum Input Video Rate	× 60Hz only	× 60Hz only	× 60Hz only
Maximum Display Refresh Rate	× 60Hz only	✓ 120Hz	× 60Hz only
Pixel Response Time	✓ short	✓ short	✓ short
Synchronization	○ the particular display we tested didn't synchronize but this could be overcome with other displays	✓	✓ probably OK
Image Update Method	× the ‘scan-like’ image update method causes time-sequential 3D compatibility problems	× the ‘scan-like’ image update method causes time-sequential 3D compatibility problems	× the ‘scan-like’ image update method will probably cause some problems with time-sequential 3D compatibility
LCS Duty Cycle	○ reducing the duty cycle would be beneficial	○ reducing the duty cycle would probably be beneficial	○ reducing the duty cycle would probably be beneficial

Key: ✓ = this particular property does not cause any problems with time-sequential 3D compatibility for this display type.
 × = this particular property is a problem for time-sequential 3D for this display.
 ○ = this particular property may cause a slight problem with time-sequential 3D compatibility but it is easily overcome.

7. CONCLUSION

Unfortunately our investigations indicate that unless a commercially released LCD TV specifically designates 3D compatibility, it is highly unlikely to be capable of producing flicker-free low-ghost stereoscopic images using the time-sequential 3D method. Furthermore regular 120Hz LCD TVs (without a ‘Stereoscopic 3D Compatible’ designation) are unlikely to provide improved time-sequential 3D compatibility compared to regular LCD monitors - despite the enticing similarity to the “120Hz 3D” title. The results of the project show that black frame insertion does provide some improvement of 3D compatibility of LCDs but not to a sufficient level to produce flicker-free ghost-free 3D results.

It should be noted that while this manuscript was being finalized, but after the research work was completed, Viewsonic and Samsung each released 22” LCD monitors which are capable of being used for time-sequential 3D viewing in concert with the NVIDIA GeForce 3D Vision LCS glasses [10]. At this point it is not clear what technologies they have

implemented to achieve 120Hz time-sequential 3D, however they have certainly increased the maximum input video rate to 120Hz and implemented some other modifications from conventional LCD technology.

It is hoped that more LCDs will be released with stereoscopic 3D compatibility – which will be achieved by addressing the limitations discussed in this paper.

8. ACKNOWLEDGEMENTS

We wish to thank Stuart Parker at BenQ Australia and Con Parente at West Coast HiFi (O'Connor, Western Australia) who provided access to LCDs for testing during this project. We also wish to thank iVEC (the hub of advanced computing in Western Australia) and Jumbo Vision International for their financial and in-kind support of the project.

REFERENCES

- [1] Woods, A.J. and Yuen, K.-L., "Compatibility of LCD Monitors with Frame-Sequential Stereoscopic 3D Visualisation" (Invited Paper), in IMID/IDMC '06 Digest, (The 6th International Meeting on Information Display, and The 5th International Display Manufacturing Conference), pg 98-102, Daegu, South Korea (2006).
<http://www.cmst.curtin.edu.au/publicat/2006-30.pdf>
- [2] Woods, A. J. and Karvinen, K. S., "The compatibility of consumer plasma displays with time-sequential stereoscopic 3D visualization" in Stereoscopic Displays and Applications XIX, Proceedings of SPIE Vol. 6803, SPIE, Bellingham, WA, USA (2008).
http://www.cmst.curtin.edu.au/publicat/2008-01_3d-plasma_woods_karvinen.pdf
- [3] Pan, H., Feng, X.-F. and Daly, S., "LCD motion blur modelling and analysis", in IEEE International Conference on Image Processing (ICIP 2005), Vol. 2, pp 21-24, (2005).
- [4] Sluyterman, A. A. S. and Boonekamp, E. P., "Architectural Choices in a Scanning Backlight for Large LCD TVs", in SID 05 Digest, pg 996- (2005)
- [5] Hung, H.-C. , and Shih, C.-W., "Improvement in Moving Picture Quality Using Scanning Backlight System", in Proceedings of the International Display Manufacturing Conference (IDMC'05), Taipei, Taiwan (2005).
- [6] Liou, J.-C., Lee, K., Tseng, F.-G., Huang, J.-F., Yen, W.-T. and Hsu, W.-L., "Shutter Glasses Stereo LCD with a Dynamic Backlight", in Stereoscopic Displays and Applications XX, Proceedings of Electronic Imaging Vol. 7237, SPIE, Bellingham, WA, USA (2009) (in press).
- [7] "Philips ditches Aptura backlight tech for LED", PC PRO, 13 March 2007,
<http://www.pcpro.co.uk/news/107108/philips-ditches-aptura-backlight-tech-for-led.html>
- [8] NVIDIA 3D Stereo Driver http://www.nvidia.com/object/3d_stereo.html (accessed 22 December 2008)
- [9] Powerstrip software <http://entechtaiwan.net/util/ps.shtm> (accessed 22 December 2008)
- [10] "Nvidia Geforce 3D Vision Review", OverClockersClub, 7 January 2009,
http://www.overclockersclub.com/reviews/nvidia_3d_vision/

Paper 8 [Refereed Conference Paper]
A. J. Woods, C. R. Harris (2010) "Comparing levels of crosstalk with red/cyan, blue/yellow, and green/magenta anaglyph 3D glasses" in Stereoscopic Displays and Applications XXI, Proceedings of IS&T/SPIE Electronic Imaging, SPIE Vol. 7253, pp. 75240Q-1 to -12, San Jose, California, January 2010.

Comparing levels of crosstalk with red/cyan, blue/yellow, and green/magenta anaglyph 3D glasses

Andrew J. Woods, Chris R. Harris
Centre for Marine Science and Technology, Curtin University of Technology,
GPO Box U1987, Perth WA 6845, Australia

ABSTRACT

The Anaglyph 3D method of stereoscopic visualization is both cost effective and compatible with all full-color displays, however this method often suffers from poor 3D image quality due to poor color quality and ghosting (whereby each eye sees a small portion of the perspective image intended for the other eye). Ghosting, also known as crosstalk, limits the ability of the brain to successfully fuse the images perceived by each eye and thus reduces the perceived quality of the 3D image. This paper describes a research project which has simulated the spectral performance of a wide selection of anaglyph 3D glasses on CRT, LCD and plasma displays in order to predict ghosting levels. This analysis has included for the first time a comparison of crosstalk between different color-primary types of anaglyph glasses - green/magenta and blue/yellow as well as the more traditional red/cyan. Sixteen pairs of anaglyph 3D glasses were simulated (6 pairs of red/cyan glasses, 6 pairs of blue/yellow glasses and 4 pairs of green/magenta glasses). The spectral emission results for 13 LCDs, 15 plasma displays and one CRT Monitor were used for the analysis. A custom written Matlab program was developed to calculate the amount of crosstalk for all the combinations of different displays with different anaglyph glasses.

Keywords: stereoscopic, 3D, anaglyph, crosstalk, ghosting

1. INTRODUCTION

The anaglyph method of displaying stereoscopic 3D images relies on the multiplexing of left and right perspective views into complementary color channels of the display - the viewer then wears a pair of glasses containing color filters which intend to only pass the appropriate color channels for each eye (e.g. the red channel to the left eye and the blue and green channels to the right eye for the most common red/cyan anaglyph process), and therefore the correct perspective images for each eye. The anaglyph method has existed since 1853¹ and remains a common 3D display technique today because it works with any full-color display, is easy to encode images into anaglyph format, and the glasses are relatively cheap to produce. Unfortunately the anaglyph 3D method often suffers from relatively poor 3D image quality due to its inability to accurately display full-color 3D images, and commonly the presence of relatively high levels of 3D crosstalk.

The terms ghosting and crosstalk with respect to stereoscopic displays are often used interchangeably however we will use the definition by Lipton² in this discussion: Crosstalk is the "incomplete isolation of the left and right image channels so that one leaks or bleeds into the other - like a double exposure. Crosstalk is a physical entity and can be objectively measured, whereas ghosting is a subjective term" and refers to the "perception of crosstalk". We have used the following mathematical definition of crosstalk: $\text{crosstalk (\%)} = \text{leakage} / \text{signal} \times 100$ (where leakage is used here to mean the raw leakage of light from the unintended channel to the intended channel).

Anaglyph 3D encoding can be performed using any pair of complementary color channels to store the left and right perspective images. Red/cyan has traditionally been the most common choice of colors for anaglyph glasses, however recently blue/yellow and green/magenta color combinations have also been used widely.

Figure 1 graphically illustrates the principle behind the image separation used in anaglyphic image viewing, as well as the concept of crosstalk (ghosting or leakage) and signal (intended image). The display has a specific spectral output for each of the red, green and blue sub-pixels (color channels). With red/cyan glasses, the left image is stored in the red color channel, while the right image is stored in the cyan (green + blue) color channel. The red/cyan lenses in the glasses have

a specific spectral transmission response such that red filter predominantly transmits light from the red color channel while blocking light from the blue and green color channels (and vice versa for the other eye). Due to the imperfect nature of the spectral performance of the filters and the spectral emission of the color channels of the display, some of the right image will be visible to the left eye (and vice versa for the other eye) and this is referred to as leakage or crosstalk.

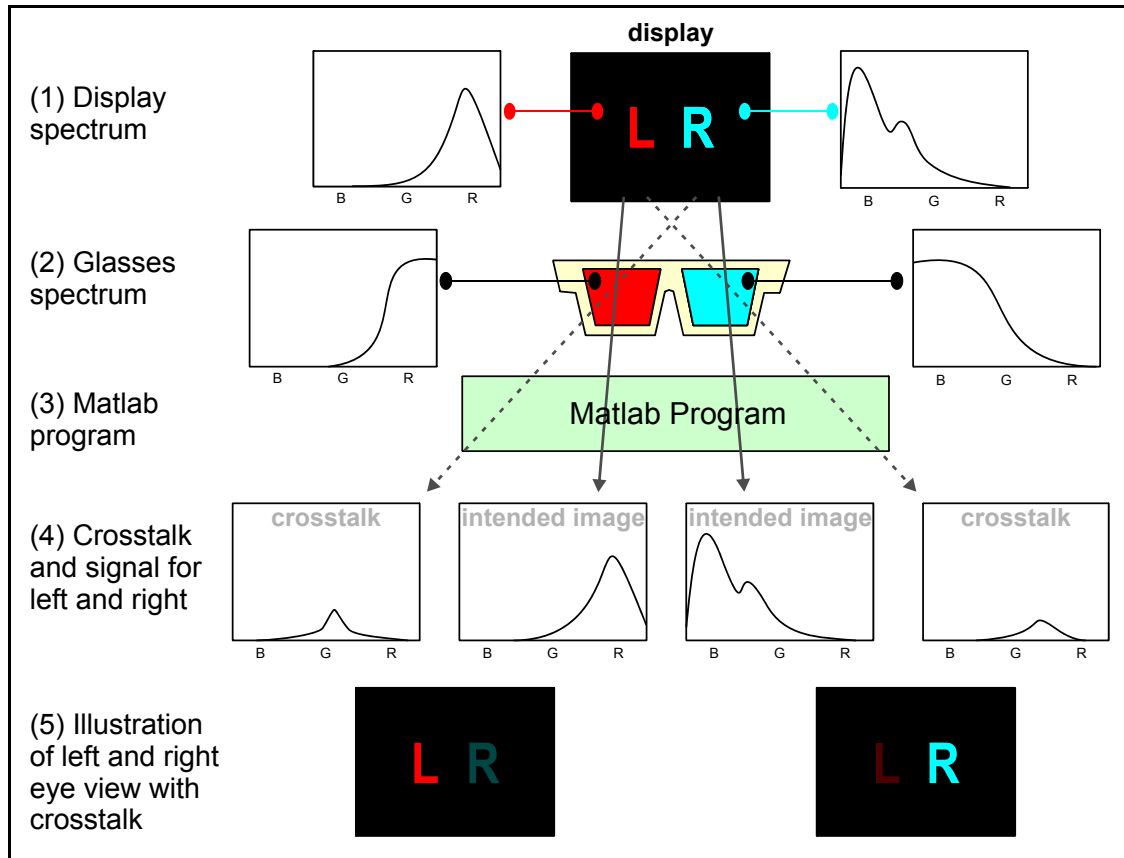


Figure 1: Illustration of the process of anaglyph spectral ghosting and its simulation in this project. From the top: (1) Spectral response of display, (2) spectral response of anaglyph glasses, (3) simulation of crosstalk using a computer program, (4) spectral output characteristic of crosstalk and intended image, and (5) visual illustration of left eye and right eye view with crosstalk.

This paper carries on from the work of Woods and Rourke³, and Woods, Yuen and Karvinen⁴ which considered red/cyan anaglyph crosstalk of various displays and developed an algorithm to estimate the amount of 3D crosstalk that will be present when a particular pair of anaglyph glasses is used to view an anaglyph 3D image on a particular full-color display. Past studies by the authors have also examined the sources of crosstalk in time-sequential 3D displays^{5,6,7,8,9}. This paper extends the developed algorithms and examines and compares the levels of crosstalk present between different color-primary types of anaglyph glasses (i.e. red/cyan, blue/yellow and green/magenta) with different displays.

It should be noted that this paper only examines and compares crosstalk in anaglyph images and does not examine other aspects of 3D image quality (including psychological effects). This aspect should be considered closely when reviewing the results of this paper, and is discussed in more detail in Section 4.2.

2. EXPERIMENTAL METHOD

Firstly, the spectral output of a large selection of displays has been measured using a manually calibrated Ocean Optics USB2000 spectroradiometer as part of this and previous studies^{3,4}. Table 1 lists the displays sampled - comprising 13 LCD monitors, 15 plasma-display panels (PDPs), and one CRT (Cathode Ray Tube) monitor.

Table 1: Listing of all the displays simulated in this particular study.

Display ID	Display Make and Model
LCD01	Samsung SynchronMaster 171s
LCD02	Benq FP731
LCD03	NEC MultiSync LCD 1760V
LCD04	Acer AL1712
LCD05	Acer FP563
LCD06	Benq FP71G
LCD07	Benq FP71G+S
LCD08	Philips 150S3
LCD09	Hewlett Packard HPL1706
LCD11	Samsung SynchronMaster 740N
LCD12	Philips 190s
LCD13	Samsung SynchronMaster 913B
LCD14	ViewSonic VX922
PDP01	LG DT-42PY10X
PDP02	Fujitsu P50XHA51AS
PDP03	NEC PX-50-XR5W
PDP04	Panasonic TH-42PV60A
PDP05	Samsung PS-42C7S
PDP06	LG RT-42PX11
PDP07	NEC PX-42XM1G
PDP08	Sony PFM-42V1
PDP09	Sony FWD-P50X2
PDP10	Hitachi 55PD8800TA
PDP11	Hitachi 42PD960BTA
PDP12	Pioneer PDP-507XDA
PDP13	Pioneer PDP-50HXE10
PDP14	Fujitsu PDS4221W-H
PDP15	Samsung PS50A450P1DXXY
CRT	Mitsubishi Diamond View VS10162

NB: Due to manufacturing variation or experimental error, the results in this paper should not be considered representative of all displays of that particular brand or model.

Secondly, the spectral transmission of a large selection of anaglyph glasses were collated - using a Perkin Elmer Lambda 35 spectrophotometer to measure newly acquired anaglyph 3D glasses and re-measure some older glasses, as well as using spectral data for anaglyph glasses from a previous study⁴. Spectral data for more than 70 pairs of anaglyph glasses have now been sampled, however, only 16 pairs are reported here for the sake of brevity (6 red/cyan, 6 blue/yellow, and 4 green/magenta). Table 2 lists the anaglyph glasses described in this study. Most of the glasses reported here consist of gel-type filters in a cardboard frame - the exceptions are 3DG70, 71 and 72 which are glass dichroic filters. Although at the time of this study we did not possess a physical sample of the dichroic filters, the spectral transmission curves of the filters were available and have been included in the simulations for comparison purposes. Another exception is 3DG28 which is a set red and cyan filters printed using a Canon inkjet printer onto transparency film – again, included for comparison purposes. The red/cyan glasses 3DG4, 32, 73 and 74 were chosen because of their good performance. The blue/yellow glasses 3DG22, 23, 51, 67, 69 and green/magenta glasses 3DG68, 75, 76 were chosen because they were the only samples of those color-type of anaglyph glasses that were able to be obtained by the authors for testing.

Table 2: Listing of all the anaglyph glasses simulated in this particular study.

Glasses ID	Color of Single Primary Filter	Color of Double Primary Filter	Description
3DG4	Red	Cyan	Sports Illustrated - MFGD By Theatric Support
3DG22	Blue	Yellow	Stereospace - SpaceSpex™ - 3DTV Corp
3DG23	Blue	Yellow	ColorCode 3.D. (Black/Grey cardboard Frame - no arms)
3DG28	Red	Cyan	Red/Cyan Canon Inkjet Printer Transparency
3DG32	Red	Cyan	World 3-D Film Expo (3D DVD) - "Real 3D" - SabuCat Productions
3DG51	Blue	Yellow	Ghosts of the Abyss (3D DVD) - Geneon Entertainment
3DG67	Blue	Yellow	ColorCode 3.D. (Blue Frame)
3DG68	Green	Magenta	Journey to the Centre of the Earth (3D DVD) - TrioScopics, LP
3DG69	Blue	Yellow	Monsters vs. Aliens - NBC - Intel - ColorCode 3D (Superbowl 2009)
3DG70	Red	Cyan	Edmund Optics Dichroic Filters - red U52-528, cyan U52-537
3DG71	Blue	Yellow	Edmund Optics Dichroic Filters - blue U52-531, yellow U52-543
3DG72	Green	Magenta	Edmund Optics Dichroic Filters - green U52-534, magenta U52-540
3DG73	Red	Cyan	3D Vision Discover - NVIDIA
3DG74	Red	Cyan	Stereoscopic Displays and Applications - American Paper Optics
3DG75	Green	Magenta	My Bloody Valentine (3D DVD) - LionsGate - Trioscopics LP
3DG76	Green	Magenta	Coraline (3D DVD) - LAIKA - Trioscopics LP

PLEASE NOTE: Generally only a single pair of glasses of each particular style/brand was sampled. As such, due to manufacturing variations or experimental error, the results provided in this paper should not be considered to be representative of all glasses of that particular style/brand.

The third step was to use a custom written Matlab¹⁰ program to calculate the amount of crosstalk in anaglyph images for different display, glasses, and color-primary combinations. With reference to Figure 1, the program first loads and resamples the display and glasses spectral data so that all data is on a common x-axis coordinate system. For each lens of the glasses, the program multiplies the spectrum of the display color channel(s) which match the lens with the spectrum of that lens to obtain the intended image curve for each eye. To obtain the crosstalk curve for each eye, the spectrum of the lens is multiplied by the spectrum of the color channel(s) which should not pass through that lens. Where the spectrum of two display color channels need to be combined for the calculation (e.g. cyan = blue + green) the two color spectrums are added before multiplying with the lens spectrum. For example: red signal curve = red lens spectrum multiplied by red display spectrum, and red crosstalk curve = red lens spectrum multiplied by the addition of the green display spectrum and the blue display spectrum. The program also scales these results curves to include the human-eye sensitivity to different wavelengths of light¹¹ (see Figure 2). The crosstalk percentage for each eye is then calculated by dividing the area under the crosstalk curve by the area under the intended signal curve for each eye and multiplying by 100. The overall crosstalk factor for a particular pair of glasses when used in combination with a particular display is the sum of the left- and right-eye percentage crosstalk values. It should be noted that the overall crosstalk factor is not a percentage, but rather a number that allows the comparison of different glasses/display combinations. The program automates the process of performing a cross comparison of all the displays against all of the glasses.

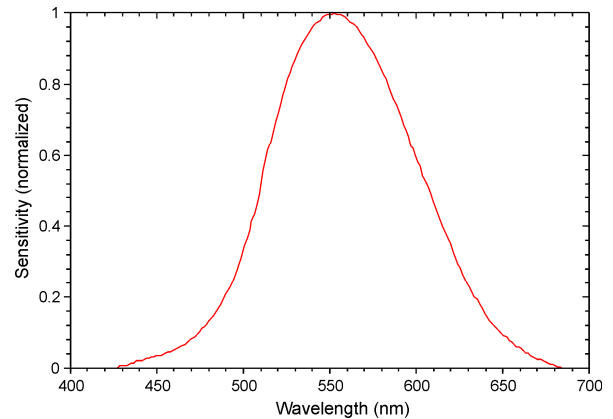


Figure 2: CIE 1931 photopic human eye response.

3. RESULTS

3.1 Anaglyph 3D Glasses Spectral Transmission

The spectral results for the anaglyph glasses analyzed in this paper are shown in Figures 3 through 8. It can be seen in all cases that the dichroic filters have a high-transmittance pass-band, a very low-transmittance stop-band, and generally

a very sharp transition. It can be seen that the inkjet filters in Figures 3 and 4 have very poor performance in the stop band which will negatively affect their use as anaglyph filters considerably. The remaining curves in Figures 3 through 8 are gel-filters and although there is some clustering, it can be seen that can be a lot of variation between individual filters.

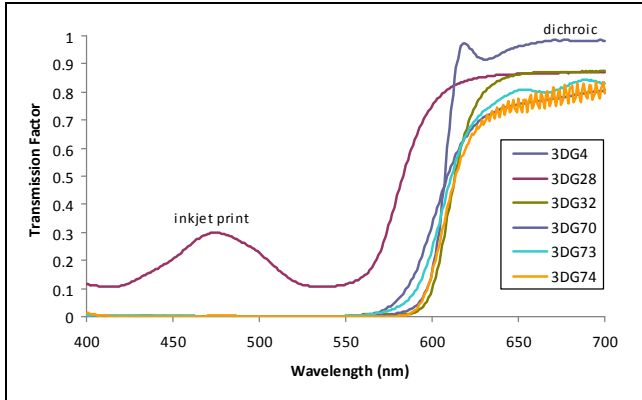


Figure 3 - Spectral transmission of the red filters.^α

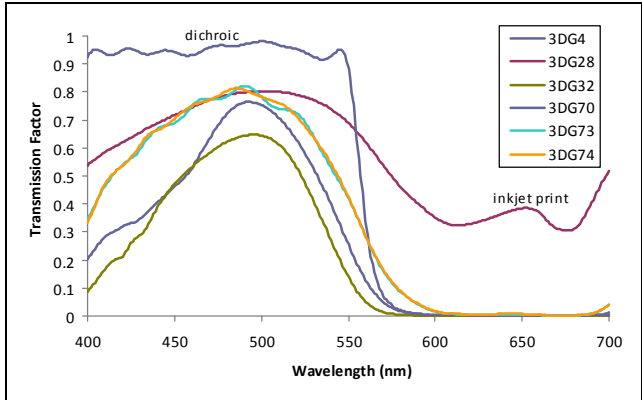


Figure 4 - Spectral transmission of the cyan filters.

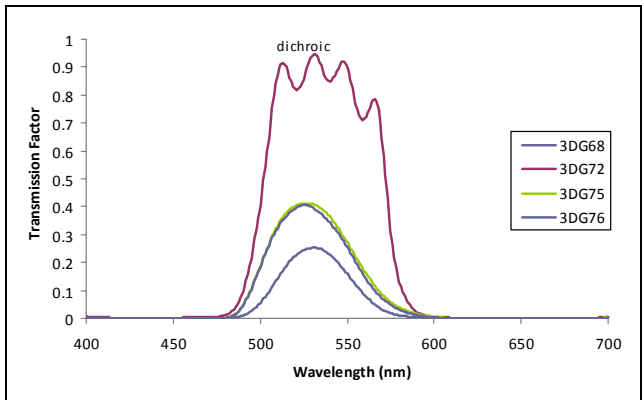


Figure 5 - Spectral transmission of the green filters.

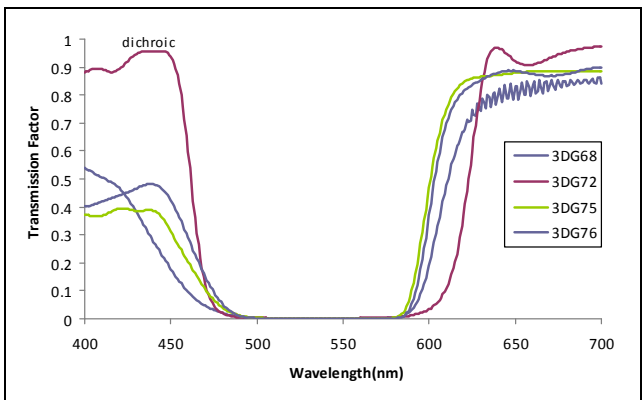


Figure 6 - Spectral transmission of the magenta filters.

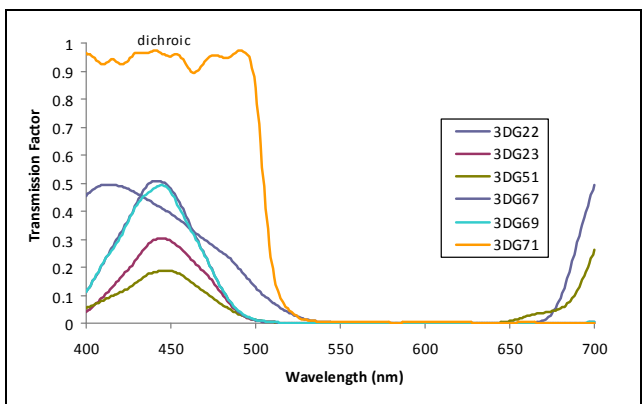


Figure 7 - Spectral transmission of the blue filters.

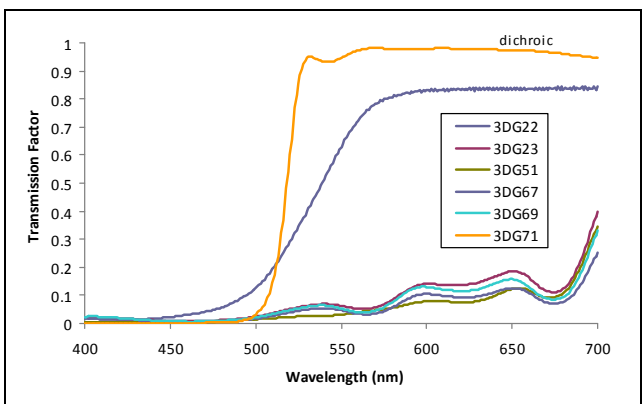


Figure 8 - Spectral transmission of the yellow filters.

^α The legends and colors of some of the figures and tables in this paper won't be distinguishable when printed in black and white. A color version of the figures and tables is available from the primary author's website.

3.2 Display Device Spectral Emission

The spectral emission measurements of the 29 different displays reported in this study (13 LCD monitors, 15 plasma displays, and one CRT monitor) are shown in Figures 9 through 11.

Figure 9 shows the spectral output of all the tested LCD monitors. All of the LCD monitors tested used CCFL (Cold Cathode Fluorescent Lamp) backlights and the spectral peaks of the light output by the backlight are clearly visible. There is a lot of similarity between the spectral characteristics of all the LCD monitors, however, some differences are evident in the out-of-band rejection (e.g. the amount of green light present in the red color primary) which will be related to the quality of color filters used for each of the color primaries.

Figure 10 shows the spectral output of all the tested plasma displays. The color spectrum of the red and blue color primaries are very similar across all the tested plasma displays, however, there is a lot of variation of the spectral response of the green color primary which will probably relate to the formulation of the phosphors used.

Figure 11 shows the spectral output of an example CRT monitor. A previous paper by Woods and Tan⁵ reported that 11 tested CRT monitors had almost exactly the same spectral response which suggests that most CRTs use the same phosphor formulation for each of the color primary channels. It is believed that this graph can therefore be considered representative of most CRTs.

3.3 Crosstalk Calculation Results

The crosstalk results as calculated by the Matlab crosstalk calculation program for the combination of all displays against all anaglyph glasses are shown in Table 3 and 4. For each display/glasses combination the table lists the percentage crosstalk for the single-color-primary eye (top cell), the percentage crosstalk for the double-color-primary eye (middle cell), and the overall crosstalk factor for both eyes combined (bottom cell). The overall crosstalk factor is the sum of the

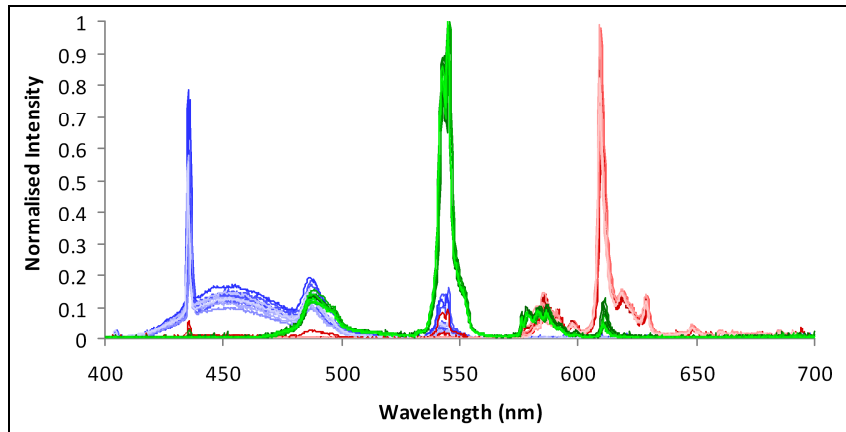


Figure 9: Color spectrum of the tested LCD monitors

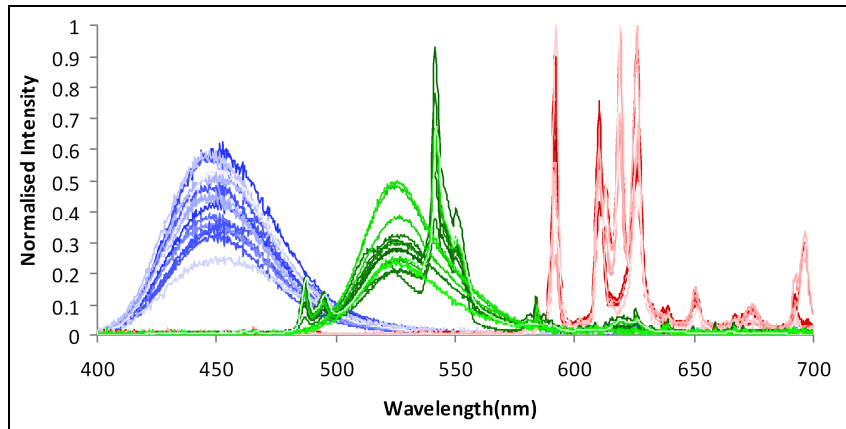


Figure 10: Color spectrum of the tested plasma displays

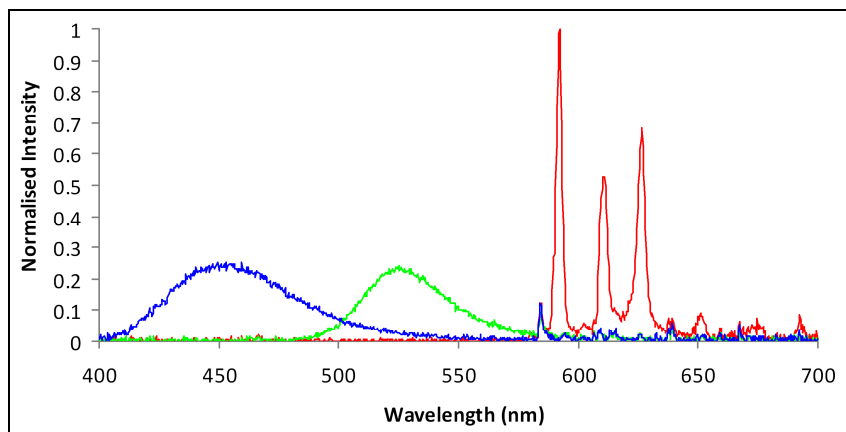


Figure 11: Color spectrum of an example CRT monitor

left and right eye percentages, and as such is not a percentage. To aid in the analysis of the tables, some of the overall crosstalk factors have been tagged/highlighted.

Table 3: Crosstalk calculation results for the LCD and CRT monitors. (The lowest overall crosstalk factors for each display have been highlighted in bright green and tagged with a '#' character, and the highest overall crosstalk factors are highlighted in orange and tagged with a '+' character. Overall crosstalk factors of less than 15 have been highlighted in light green - this threshold figure does not have any significance apart from allowing us to highlight the lower overall crosstalk factor results.)

Glasses		Displays													
		LCD1	LCD2	LCD3	LCD4	LCD5	LCD6	LCD7	LCD8	LCD9	LCD11	LCD12	LCD13	LCD14	CRT
3DG4	Red	16.1	14.5	16.0	18.1	22.3	13.1	16.6	22.9	15.4	12.8	15.5	14.0	12.9	26.8
	Cyan	0.8	0.8	0.5	7.7	2.5	0.7	0.9	1.4	1.5	1.3	1.1	0.3	0.6	4.9
	Overall	16.9	15.2	16.5	25.8	24.8	13.8	17.5	24.3	16.9	14.2	16.6	14.3	13.5	31.7
3DG22	Blue	65.5	68.7	72.0	70.9	59.0	110.2	78.6	55.8	67.9	90.6	89.1	68.4	65.9	129.5
	Yellow	3.9	3.1	3.0	6.1	10.0	1.9	3.0	8.7	4.8	2.9	2.3	2.3	4.2	4.5
	Overall	69.4	71.9	75.0	77.0	69.1	112.1	81.6	64.5	72.7	93.5	91.4	70.6	70.1	134.0 ⁺
3DG23	Blue	26.0	23.3	28.7	32.5	27.0	40.8	28.2	24.6	25.8	34.5	32.1	24.8	26.3	30.3
	Yellow	4.2	3.4	3.2	6.3	9.8	2.1	3.2	8.6	5.0	3.1	2.4	2.6	4.5	5.1
	Overall	30.2	26.7	31.9	38.7	36.8	42.9	31.4	33.2	30.8	37.6	34.5	27.4	30.8	35.4
3DG28 (inkjet)	Red	92.2	84.0	78.3	96.5	87.1	70.4	85.2	87.6	73.9	70.7	75.1	90.2	81.4	108.5
	Cyan	14.6	15.0	15.7	19.6	18.1	17.2	15.5	17.2	18.9	17.4	17.8	13.1	14.6	16.9
	Overall	106.8 ⁺	99.0 ⁺	94.0 ⁺	116.1 ⁺	105.2 ⁺	87.7	100.7 ⁺	104.7 ⁺	92.8 ⁺	88.1	92.9	103.3 ⁺	96.0 ⁺	125.4
3DG32	Red	8.8	8.1	11.0	9.9	15.6	8.2	10.1	16.7	10.9	8.1	9.9	7.6	7.1	18.1
	Cyan	0.6	0.7	0.5	7.5	2.3	0.6	0.8	1.3	1.3	1.3	1.0	0.2	0.5	4.7
	Overall	9.4	8.8	11.5	17.4 ⁺	18.0	8.8	10.9	18.0	12.2	9.4	10.9	7.8	7.6	22.8
3DG51	Blue	33.6	31.4	37.3	39.5	33.7	54.1	37.1	31.3	34.2	44.9	42.9	32.3	34.1	40.2
	Yellow	4.0	3.4	3.1	5.7	8.8	2.0	3.2	7.8	4.9	3.1	2.5	2.5	4.2	5.2
	Overall	37.6	34.8	40.4	45.3	42.5	56.1	40.3	39.1	39.1	48.0	45.4	34.9	38.3	45.4
3DG67	Blue	22.8	19.8	25.0	28.9	24.2	34.6	24.2	22.0	22.8	29.4	28.0	21.3	22.8	27.1
	Yellow	4.3	3.4	3.3	6.4	10.1	2.1	3.2	8.9	5.0	3.1	2.4	2.6	4.5	5.1
	Overall	27.07	23.2	28.2	35.3	34.2	36.7	27.4	30.9	27.9	32.5	30.4	23.9	27.4	32.2
3DG68	Green	7.7	5.5	5.9	20.6	23.3	4.0	5.2	19.0	9.1	5.0	4.2	4.0	7.8	10.9
	Magenta	8.9	7.5	11.0	10.4	14.4	8.2	9.0	15.5	8.2	6.8	9.2	7.7	6.7	14.1
	Overall	16.6	12.9	16.9	31.0	37.7	12.2	14.2	34.5	17.3	11.7	13.4	11.7	14.4	24.9
3DG69	Blue	24.3	21.3	26.5	30.3	25.4	37.0	25.7	23.1	24.2	31.2	29.7	22.7	24.2	28.7
	Yellow	4.2	3.4	3.2	6.2	9.8	2.1	3.2	8.7	5.0	3.1	2.4	2.6	4.4	5.1
	Overall	28.5	24.7	29.8	36.6	35.2	39.1	28.9	31.7	29.2	34.2	32.1	25.2	28.7	33.8
3DG70 (dichroic)	Red	8.6	7.7	10.9	9.9	15.4	8.0	9.5	16.0	9.7	7.6	9.3	7.1	6.7	18.3
	Cyan	0.6	0.6	0.4	7.7	2.3	0.6	0.7	1.1	1.2	1.1	0.9	0.2	0.4	5.0
	Overall	9.2 ⁺	8.3 ⁺	11.3 ⁺	17.7	17.7 ⁺	8.6 ⁺	10.2 ⁺	17.1 ⁺	10.8 ⁺	8.6 ⁺	10.2 ⁺	7.3 ⁺	7.1 ⁺	23.4
3DG71 (dichroic)	Blue	71.1	80.2	81.1	77.8	65.7	128.2	90.5	61.4	75.5	105.9	101.3	76.7	72.7	122.4
	Yellow	3.6	2.8	2.7	6.2	10.8	1.7	2.7	9.3	4.6	2.6	2.0	1.9	4.1	4.0
	Overall	74.7	83.0	83.8	84.0	76.4	129.9 ⁺	93.3	70.7	80.1	108.5 ⁺	103.3 ⁺	78.6	76.8	126.4
3DG72 (dichroic)	Green	8.5	6.1	6.4	20.8	23.7	4.4	6.0	19.8	10.3	5.6	5.1	4.5	8.2	11.6
	Magenta	6.0	5.3	8.8	6.4	10.5	6.5	7.5	13.0	8.2	6.1	8.5	6.4	5.1	10.0
	Overall	14.5	11.4	15.2	27.2	34.2	11.0	13.4	32.9	18.5	11.8	13.7	10.9	13.4	21.6 ⁺
3DG73	Red	14.1	12.7	14.7	15.8	20.5	11.7	14.7	21.2	14.3	11.5	13.9	12.2	11.3	24.0
	Cyan	1.9	1.7	1.4	8.5	3.7	1.7	1.9	2.6	2.9	2.1	2.3	1.1	1.4	5.7
	Overall	16.0	14.4	16.0	24.2	24.1	13.4	16.6	23.7	17.3	13.6	16.2	13.3	12.6	29.7
3DG74	Red	8.6	7.9	10.9	9.9	15.7	8.0	9.8	16.6	10.4	7.8	9.6	7.3	6.9	18.5
	Cyan	1.9	1.8	1.4	8.5	3.7	1.7	2.0	2.6	3.0	2.2	2.3	1.1	1.4	5.7
	Overall	10.5	9.7	12.3	18.4	19.4	9.7	11.8	19.2	13.4	10.0	12.0	8.4	8.3	24.2
3DG75	Green	9.4	6.7	7.2	21.9	25.0	5.0	6.4	20.8	10.8	6.0	5.4	5.0	9.0	11.9
	Magenta	10.4	8.7	12.0	12.2	16.0	9.2	10.2	16.7	8.9	7.6	10.2	8.8	7.8	17.1
	Overall	19.8	15.4	19.2	34.1	41.0	14.2	16.6	37.5	19.6	13.6	15.6	13.8	16.7	29.0
3DG76	Green	9.2	6.6	7.1	21.9	25.0	4.9	6.2	20.7	10.6	5.9	5.3	4.9	8.9	11.8
	Magenta	9.0	7.5	11.1	10.6	14.6	8.3	9.0	15.5	8.0	6.8	9.2	7.7	6.8	15.5
	Overall	18.3	14.1	18.2	32.5	39.6	13.2	15.3	36.2	18.6	12.7	14.4	12.6	15.7	27.3

Key: Overall Crosstalk Factor: 00.0⁺ = Highest, 00.0[#] = Lowest, 00.0 = Less than 15.

Table 4: Crosstalk calculation results for the PDP monitors.

Glasses		Displays														
		PDP1	PDP2	PDP3	PDP4	PDP5	PDP6	PDP7	PDP8	PDP9	PDP10	PDP11	PDP12	PDP13	PDP14	PDP15
3DG4	Red	14.9	24.8	9.8	15.6	10.9	17.9	13.6	16.9	16.7	12.8	11.1	8.4	10.2	16.5	13.5
	Cyan	1.1	1.0	2.1	2.4	2.1	1.5	1.3	2.2	1.2	2.8	1.6	1.4	1.9	1.5	0.7
	Overall	16.0	25.8	11.9	17.9	13.0	19.4	14.9	19.1	17.9	15.7	12.7	9.8	12.1	18.0	14.2
3DG22	Blue	72.3	49.4	78.2	73.8	54.7	72.2	68.5	60.1	59.1	59.9	57.7	88.9	70.7	61.9	54.6
	Yellow	2.9	5.9	3.8	3.5	4.7	3.5	7.3	6.4	4.1	6.2	6.6	3.6	4.8	10.8	3.5
	Overall	75.3	55.2	82.0*	77.3	59.5	75.7	75.8	66.6	63.2	66.1	64.3	92.5*	75.5	72.8	58.1
3DG23	Blue	11.2	8.0	12.3	15.3	7.4	11.9	12.8	10.4	9.1	8.1	6.8	8.9	8.0	8.5	9.4
	Yellow	3.4	6.8	4.2	4.0	5.2	4.0	7.7	7.0	4.7	6.8	7.1	4.0	5.3	10.9	4.2
	Overall	14.6	14.8	16.5	19.3	12.6	15.9	20.5	17.4	13.8	14.9	13.9	12.9	13.3	19.4	13.6
3DG28 (inkjet)	Red	66.8	92.0	59.5	67.4	59.5	77.8	61.7	72.7	74.7	62.5	69.5	67.7	72.4	58.0	74.2
	Cyan	17.7	14.5	20.0	19.2	20.7	15.9	20.5	18.1	16.4	21.1	16.3	15.7	15.7	24.7	14.8
	Overall	84.6*	106.5*	79.5	86.6*	80.2*	93.6*	82.2*	90.7*	91.1*	83.6*	85.8*	83.3	88.1*	82.7*	89.0*
3DG32	Red	14.1	23.7	9.0	14.7	9.3	17.0	13.1	15.8	15.5	11.7	9.6	7.1	8.7	15.4	12.2
	Cyan	1.0	0.9	1.9	2.2	2.0	1.4	1.2	2.1	1.1	2.6	1.5	1.2	1.8	1.3	0.7
	Overall	15.1	24.6	10.9	17.0	11.3	18.4	14.3	17.9	16.6	14.3	11.1	8.4	10.5	16.7	12.8
3DG51	Blue	18.9	13.0	19.7	23.1	12.1	19.2	20.2	16.5	15.1	13.8	11.7	16.2	13.9	14.8	14.3
	Yellow	3.5	7.1	4.3	4.0	5.2	4.1	8.0	7.2	4.8	6.9	7.3	4.1	5.4	11.1	4.2
	Overall	22.4	20.1	24.0	27.1	17.3	23.3	28.2	23.7	19.9	20.8	18.9	20.3	19.3	25.9	18.5
3DG67	Blue	9.9	7.1	11.2	13.8	6.8	10.5	11.4	9.6	8.1	7.6	6.3	8.2	7.4	8.6	8.2
	Yellow	3.3	6.7	4.1	3.9	5.2	4.0	7.7	6.9	4.6	6.7	7.1	4.0	5.2	10.8	4.1
	Overall	13.2*	13.7*	15.4	17.7	12.0	14.4*	19.1	16.5*	12.7*	14.3	13.3	12.1	12.7	19.4	12.4
3DG68	Green	5.1	7.7	7.3	7.9	9.3	6.2	12.6	10.6	6.6	10.4	9.8	6.0	8.1	15.6	6.2
	Magenta	11.4	15.3	6.3	12.1	6.5	13.4	8.0	10.1	11.6	6.4	5.5	5.1	5.9	6.6	10.1
	Overall	16.4	23.0	13.6	20.1	15.8	19.6	20.6	20.7	18.2	16.8	15.2	11.2	14.0	22.2	16.3
3DG69	Blue	10.8	7.7	12.1	14.7	7.4	11.3	12.3	10.3	8.8	8.2	6.8	9.0	8.1	9.2	8.9
	Yellow	3.4	6.8	4.2	4.0	5.2	4.0	7.7	7.0	4.7	6.7	7.1	4.0	5.3	10.8	4.2
	Overall	14.2	14.5	16.3	18.7	12.5	15.3	20.0	17.2	13.5	14.9	14.0	13.0	13.4	20.0	13.1
3DG70 (dichroic)	Red	13.4	22.6	8.2	13.9	8.3	16.1	12.3	15.0	14.7	10.9	8.5	6.4	7.9	14.7	10.9
	Cyan	1.0	0.9	2.0	2.2	2.2	1.4	1.3	2.2	1.1	2.9	1.7	1.4	1.9	1.5	0.7
	Overall	14.4	23.5	10.2*	16.1*	10.5*	17.5	13.6*	17.1	15.8	13.8*	10.2*	7.8*	9.8*	16.2*	11.6*
3DG71 (dichroic)	Blue	63.9	43.0	64.8	67.6	44.4	63.2	60.7	49.0	50.8	46.0	42.5	64.7	51.5	45.3	49.4
	Yellow	2.4	4.9	3.3	3.0	4.1	3.0	6.8	5.7	3.4	5.2	5.7	3.0	4.1	10.1	2.9
	Overall	66.3	47.8	68.1	70.7	48.5	66.2	67.5	54.7	54.3	51.2	48.2	67.7	55.6	55.4	52.2
3DG72 (dichroic)	Green	5.8	8.8	8.5	9.0	10.5	7.0	14.1	12.0	7.5	12.2	11.2	7.0	9.4	17.6	6.9
	Magenta	9.7	12.1	5.4	10.9	5.6	11.4	7.3	8.5	9.5	5.4	4.9	4.2	4.8	5.7	9.1
	Overall	15.5	20.8	13.9	19.9	16.1	18.4	21.4	20.5	17.0	17.6	16.0	11.2	14.1	23.4	16.0
3DG73	Red	15.2	25.1	10.1	15.8	10.8	18.2	13.9	17.1	16.9	12.9	11.0	8.5	10.3	16.6	13.6
	Cyan	2.0	1.8	3.2	3.3	3.2	2.3	2.6	3.1	2.0	4.0	2.3	2.1	2.6	3.2	1.4
	Overall	17.2	27.0	13.4	19.1	14.0	20.5	16.5	20.3	18.9	16.9	13.3	10.6	12.9	19.8	14.9
3DG74	Red	13.5	22.8	8.4	14.1	8.9	16.2	12.6	15.2	14.8	11.3	9.2	6.7	8.4	14.8	11.6
	Cyan	2.1	1.9	3.3	3.4	3.3	2.3	2.6	3.2	2.1	4.0	2.3	2.1	2.7	3.3	1.4
	Overall	15.5	24.7	11.8	17.5	12.2	18.5	15.2	18.4	16.9	15.3	11.5	8.8	11.0	18.2	13.1
3DG75	Green	6.3	9.6	8.8	9.5	10.9	7.4	14.9	12.4	8.1	12.2	11.3	7.1	9.4	18.3	7.6
	Magenta	11.1	14.7	6.2	11.8	6.6	13.1	7.6	10.0	11.4	6.4	5.5	5.3	6.0	6.6	10.0
	Overall	17.4	24.3	15.0	21.3	17.5	20.5	22.5	22.4	19.5	18.6	16.8	12.4	15.4	24.8	17.6
3DG76	Green	6.2	9.5	8.6	9.4	10.8	7.4	14.8	12.3	8.0	12.0	11.2	7.0	9.3	17.9	7.6
	Magenta	10.8	14.2	5.9	11.5	6.2	12.7	7.4	9.6	11.0	6.2	5.2	4.9	5.7	6.4	9.5
	Overall	17.0	23.7	14.6	20.9	17.0	20.0	22.2	22.0	19.0	18.2	16.5	12.0	15.0	24.3	17.1

Key: Overall Crosstalk Factor: 00.0* = Highest, 00.0* = Lowest, 00.0 = Less than 15.

3.4 Validation

A series of first-order validation tests were performed to check the accuracy of the crosstalk model. A set of test images were viewed on CRT and PDP monitors and subjectively ranked in order of increasing crosstalk by human observers. The results of the subjective ranking were then compared with the crosstalk ranking generated by the Matlab program and this is shown in Tables 5(a-f). The first group of validations (Tables 5 a-d) only compare a single filter color at a time. The second group of validations (Tables 5 e and f) compare the overall crosstalk ranking of the glasses (both left and right eye filters) as a whole.

It can be seen that the single lens subjective rankings agree extremely well with the calculated results (Tables 5 a-d). Most of the differences occur where the crosstalk percentage difference was 0.6 or less, which is a very small difference and would be hard to discern by the naked eye.

The validation of the overall crosstalk factor ranking for each overall pair of anaglyph glasses (combining left and right lenses) (Tables 5 e and f) indicates that we are on the right track but there is room for improvement (of either the algorithm or the validation procedure). The overall crosstalk validation experiment on a CRT monitor (Table 5e) was reasonably successful with only two glasses having large ranking differences (3DG4 and 3DG73). The other ranking differences generally had crosstalk factor ranking differences[†] less than 5 points. The ranking of the color groups of glasses also agrees fairly well except for the placement of 3DG4 and 3DG73. The overall crosstalk validation experiment on PDP15 (Table 5f) was seemingly more jumbled than the CRT ranking, but it is also important to note that most of the calculated crosstalk factors fall within a smaller range for PDP15 (12.4 to 18.5 → 6.1 range) than for the CRT case (where the equivalent range is 22.8 to 45.4 → 22.6 range). Our previous studies have found that when the crosstalk numbers are closer together it will be harder to visually distinguish the differences. The largest disagreement of ranking for PDP15 are with 3DG69, 3DG51, and 3DG67 – which are all blue/yellow glasses (this is based on the rank position difference, and also the crosstalk factor ranking difference). All of the other ranking differences for PDP15 have a crosstalk factor ranking difference of less than 2 (e.g. for 3DG73 is 14.9-13.1=1.8).

Tables 5(a-f): Anaglyph crosstalk validation tables. Validation of individual filters on a CRT monitor for (a) red filter, (b) cyan filter, (c) blue filter, and (d) yellow filter. Validation of overall ranking of anaglyph glasses on (e) a CRT monitor, and (f) a plasma display. Lines join matching entries. Key: R/C = Red/Cyan, G/M = Green/Magenta, B/Y = Blue/Yellow.

(a) Red Lens Validation (CRT)			(b) Cyan Lens Validation (CRT)		
Visual Rank	Computed Rank	Calculated Crosstalk	Visual Rank	Computed Rank	Calculated Crosstalk
3DG32	3DG32	18.1	3DG10	3DG26	4.6
3DG26	3DG26	18.5	3DG26	3DG32	4.7
3DG13	3DG13	19.2	3DG32	3DG10	4.84
3DG04	3DG04	26.8	3DG04	3DG13	4.88
3DG10	3DG10	35.1	3DG13	3DG04	4.91
3DG28	3DG28	108.5	3DG28	3DG28	16.9

(c) Blue Lens Validation (CRT)			(d) Yellow Lens Validation (CRT)		
Visual Rank	Computed Rank	Calculated Crosstalk	Visual Rank	Computed Rank	Calculated Crosstalk
3DG67	3DG67	27.1	3DG23	3DG22	4.5
3DG23	3DG69	28.7	3DG51	3DG67	5.09
3DG69	3DG23	30.3	3DG69	3DG23	5.10
3DG51	3DG51	40.2	3DG67	3DG69	5.12
3DG22	3DG22	129.5	3DG22	3DG51	5.2

(e) Anaglyph Glasses Validation (CRT)			(f) Anaglyph Glasses Validation (PDP15)		
Visual Rank	Computed Rank	Calculated Crosstalk	Visual Rank	Computed Rank	Calculated Crosstalk
3DG32	3DG32	22.8	3DG32	3DG67	12.4
3DG4	3DG74	24.2	3DG74	3DG32	12.8
3DG73	3DG68	24.9	3DG73	3DG74	13.1
3DG74	3DG76	27.3	3DG4	3DG69	13.1
3DG68	3DG75	29.0	3DG23	3DG23	13.6
3DG76	3DG73	29.7	3DG67	3DG4	14.2
3DG75	3DG4	31.7	3DG51	3DG73	14.9
3DG23	3DG67	32.2	3DG68	3DG68	16.3
3DG67	3DG69	33.8	3DG76	3DG76	17.1
3DG69	3DG23	35.4	3DG75	3DG75	17.6
3DG51	3DG51	45.4	3DG69	3DG51	18.5
3DG22	3DG28	125.4	3DG22	3DG22	58.1
3DG28	3DG22	134.0	3DG28	3DG28	89.0

It should be noted that the accuracy of these validation experiments are limited due to the limited number of conditions tested (CRT and PDP15) and the limited number of observers (1 or 2). The authors would like to expand the validation experiments (primarily by increasing the number of observers) in order to improve the accuracy of the crosstalk calculation model – particularly the calculation of the overall crosstalk factor. It is important to point out that visually comparing anaglyph glasses of different colors was found to be a very difficult task and is also possibly highly subjective. Some aspects discussed in Section 4.2 may also contribute to the accuracy of the validation.

[†] For the purposes of this discussion the crosstalk factor ranking difference is defined by example as follows: On a CRT the calculated crosstalk factor for 3DG4 is 31.7. When visually ranked on a CRT, 3DG4 has rank position 2, which is the same ranking position as 3DG74 in the computed rank column. The calculated crosstalk factor for 3DG74 is 24.2. Therefore the crosstalk factor ranking difference for 3DG4 on a CRT is 31.7-24.2=7.5.

4. DISCUSSION

4.1 General Observations

Crosstalk in anaglyph images acts to degrade the 3D image quality by making them hard to fuse – the corollary of this is that the image quality of anaglyph 3D images can be maximized by minimizing the amount of crosstalk. The simulations of this study predict that the choice of anaglyph glasses can have a major impact on the amount of crosstalk present, therefore a simple change of anaglyph glasses could significantly reduce the amount of crosstalk present. The simulations also predict that the spectral characteristics of a particular display can also have a significant effect on the amount of crosstalk present – one display can exhibit significantly less ghosting than the same image and glasses on another display. Understandably it will usually be harder for a user to swap to a different display to attempt to reduce crosstalk, than it will be to change glasses.

A number of interesting trends can be seen in the crosstalk simulation results of Tables 3 and 4. The crosstalk algorithm predicts that in most cases the pair of anaglyph glasses with the highest level of crosstalk (from the set of glasses considered in this paper across all of the displays considered in this paper) was the inkjet printed pair of glasses 3DG28 (average crosstalk 93.8, global maximum 125.4) – this was not totally unexpected given their very poor stop-band performance. In other words – don't use inkjet printed anaglyph filters. The algorithm predicts that the pair of anaglyph glasses with the lowest level of crosstalk (from the set of glasses considered in this paper across all of the displays considered in this paper) was the red/cyan dichroic-filter glasses 3DG70 (average crosstalk 13.6, global minimum 7.1). This result is probably attributable to the very low stop-band transmission, very high pass-band transmission, sharpness of the transition between stop-band and pass-band, and also the actual wavelength of the transition point for both eyes. Unfortunately a physical sample of these glasses was not available to conduct visual testing so these results should be considered with some skepticism.

The crosstalk algorithm predicts that the cyan and the yellow filters mostly have very low crosstalk figures (an average of 2.2% for the better four cyan gel-filters across all displays and 5.1% for the better four yellow gel-filters). Unfortunately the predicted crosstalk performance of the red and blue filters does not match the low crosstalk performance of the cyan and yellow filters they are usually matched with (red average 13.5% and blue average 20.1%).

Some further summarized data is available in Table 6 which shows that the algorithm predicts that the four better red/cyan gel-glasses will perform similarly on LCD and plasma displays but better than on CRT, that the four better blue/yellow gel-glasses will perform better on plasma displays than on LCD and CRT, and that the green/magenta gel-glasses will perform better on plasma and LCD than with CRT. The algorithm also predicts that CRT will generally exhibit about double the amount of anaglyph crosstalk compared to LCD or plasma. Across all of the better gel-glasses, plasma had the lowest average crosstalk (average of 17.0, global minimum of 8.4), followed by LCD (average of 22.9, global minimum of 7.6) and then CRT (average of 30.3, global minimum of 22.8).

Table 6: Summarized crosstalk simulation results showing average overall crosstalk factor for various anaglyph glasses across various displays.

Average overall crosstalk factor for:	Displays		
	LCD	PDP	CRT
Better four red/cyan gel-filter glasses	14.7	15.7	27.1
Better four blue/yellow gel-filter glasses	33.9	16.9	36.7
All three green/magenta gel-filter glasses	20.1	18.4	27.1
Dichroic red/cyan filter glasses (simulated only)	11.1	13.9	23.4
Dichroic blue/yellow filter glasses (simulated only)	87.9	58.3	126.4
Dichroic green/magenta filter glasses (simulated only)	17.5	17.4	21.6

Please note the limitations of this study as described in Section 4.2.

Comparing the levels of crosstalk between the various color-primary types of anaglyph glasses (choosing the best four gel-glasses of each type, or best three in the case of green/magenta), the algorithm predicts that for LCDs, red/cyan glasses will have the lowest average overall crosstalk (average 14.7, global minimum 7.6), followed by green/magenta (average 20.1, global minimum 11.7), then by blue/yellow (average 33.9, global minimum 24.7). For plasma displays the difference is less marked, with the algorithm predicting that on average the red/cyan glasses will have the lowest crosstalk (average 15.7, global minimum 8.4), closely followed by blue/yellow (average 16.9, global minimum 12.5),

and closely followed by green/magenta (average 18.4, global minimum 11.2). For CRT, the algorithm predicts that on average red/cyan and green/magenta have the same average lowest crosstalk (red/cyan average 27.1, global minimum 22.8) (green/magenta average 27.1, global minimum 24.9), followed by blue/yellow (average 36.7, global minimum 32.2). Across all of the tested displays, the algorithm predicts that red/cyan has the lowest average crosstalk (average 15.7), followed closely by green/magenta (average 19.5), and then blue/yellow (average 25.2).

It was mentioned above that the red/cyan dichroic filter glasses were predicted to have the lowest average crosstalk across all of the tested displays. Let's look more closely at the performance of the other dichroic filters. According to the simulation, the green/magenta dichroic filter glasses have slightly lower crosstalk levels (average 17.6) than the green/magenta gel-filter glasses (average 19.5). This would be for the same reasons cited for the good performance of the red/cyan dichroic filter glasses. On the other hand, the blue/yellow dichroic filter glasses are predicted to have grossly higher average crosstalk levels (average 73.9) than the better blue-yellow gel-filter glasses (average 25.2). Looking more closely at this result, the yellow dichroic filter is predicted to have slightly lower crosstalk than the better yellow gel-filters, but the algorithm predicts the blue dichroic filter to have almost three times the crosstalk as the better blue gel-filters. This will be the source of the high result overall dichroic crosstalk result. Looking at the spectrum of the blue dichroic filter shows that the transition wavelength is around 505nm which is probably too high. If the transition wavelength was closer to 480 or 490nm, the result would probably be very different. The simulation results indicate that dichroic filters have potential to offer lower crosstalk than equivalent gel-filters, providing the transition wavelengths are positioned optimally. It would be interesting to validate these predictions with visual tests on physical pairs of these glasses.

4.2 Limitations of this Study

The techniques used in this study have several limitations which should be considered when the results of this study are reviewed. The study only considers a limited number of displays – it is unclear whether these displays are a valid representation of all displays in common circulation. Furthermore recent model displays may have a different spectral emission performance – for example, LED backlit LCD TVs are likely to have different spectral characteristics and therefore very different crosstalk results.

The crosstalk calculation algorithm only considers crosstalk as an indicator for 3D image quality – there are a number of other factors which also contribute towards the perception of 3D image quality but are not included in the algorithm. For example: clarity or sharpness of the lenses (filters with a low MTF would reduce 3D image quality); brightness balance of the left and right lenses (high brightness imbalance can lead to the perception of the Pulfrich effect – our calculations indicate that the green/magenta glasses generally have better brightness balance and blue/yellow glasses have the greatest brightness imbalance although that work isn't reported here due to space limitations); color balance of the monitor (our tests have revealed that color balance does have an effect on crosstalk calculations but we have not been able to design this out of the algorithm at the present time); experimental variation and product manufacturing variation; the inherent difficulty of accurately visually comparing relative brightness of different colors; and other psychological effects (which can lead to subjective variation).

The current crosstalk simulation algorithm uses a simple addition of left eye crosstalk and right eye crosstalk to obtain the overall crosstalk factor for a pair of glasses. This may not be a good representation of how we perceive overall levels of crosstalk – particularly when there are large brightness differences and large crosstalk differences between the eyes. One example of this is glasses 3DG51 on a CRT – the crosstalk of the blue filter has almost eight times the amount of crosstalk of the yellow lens (which has quite low crosstalk). The yellow lens is also substantially brighter than the blue lens. When glasses 3DG51 are worn, the perception of the brighter yellow lens seems to dominate the perception of the 3D image and less crosstalk is perceived than a simple addition of yellow and blue individual crosstalk would suggest. Further work is required in this area and would be aided by an expanded validation experiment as mentioned in Section 3.4.

This study also ignores the introduction of anaglyph crosstalk by the use of lossy compression techniques on anaglyph images (e.g. JPEG compression), and the use of incorrect anaglyph generation algorithms (which may unwittingly mix left and right images). These effects are quite separate from the spectral techniques described in this paper and should be considered separately. Anaglyph content producers should work to ensure that their anaglyph 3D content is not adversely affected by these last two factors.

5. CONCLUSION

Although there are a range of other stereoscopic display technologies available that produce much better 3D image quality than the anaglyph 3D method (e.g. polarized, shutter glasses, and Infitec), the anaglyph 3D method remains widely used because of its simplicity, low cost, and compatibility with all full-color displays and prints. If anaglyph 3D is to be used, it would be best if it were used optimally which is one of the purposes of this paper.

This paper has revealed that crosstalk in anaglyphic 3-D images can be minimized by the appropriate choice of anaglyphic 3-D glasses. The study has also revealed that there is considerable variation in the amount of anaglyphic crosstalk exhibited by different displays. Compared to previous work that has only considered red/cyan anaglyph glasses, this paper has extended the work to include blue/yellow and green/magenta anaglyph glasses which are now also in common usage. The paper has also considered the effect of using dichroic filters and inkjet printed filters for anaglyph 3D viewing. The techniques used in the paper to simulate anaglyph crosstalk are by no means perfect at this stage, but they do confirm that there is considerable opportunity for the optimization of anaglyph viewing by the appropriate choice of anaglyph glasses and displays.

6. ACKNOWLEDGMENTS

The authors would like to thank WA:ERA, iVEC and Jumbo Vision International for their support of various aspects of this project.

REFERENCES

1. R Zone, "Good old fashion anaglyph: High tech tools revive a classic format in spy kids 3-D," *Stereo World* **29**, No. 5, 11–13 and 46 (2002–2003).
2. L Lipton "Glossary" in Lenny Lipton's Blog, dated: 16 March 2009, accessed: 16 December 2009. Online: <http://lennylipton.wordpress.com/2009/03/16/glossary/>
3. Woods, A.J., and Rourke T. (2004) "Ghosting in Anaglyphic Stereoscopic Images", presented at Stereoscopic Displays and Applications XV, published in Stereoscopic Displays and Virtual Reality Systems XI, Proceedings of SPIE-IS&T Electronic Imaging, SPIE Vol. 5291, San Jose, California.
4. Woods, A.J., Yuen, K.-L., and Karvinen, K.S. (2007) "Characterizing crosstalk in anaglyphic stereoscopic images on LCD monitors and plasma displays" in Journal of the Society for Information Display, Volume 15, Issue 11, pp. 889-898, November 2007.
5. Woods, A.J., and Tan, S.S.L. (2002) "Characterising Sources of Ghosting in Time-Sequential Stereoscopic Video Displays", presented at Stereoscopic Displays and Applications XIII, published in Stereoscopic Displays and Virtual Reality Systems IX, Proceedings of SPIE Vol. 4660, San Jose, California, 21-23 January 2003.
6. Woods, A.J., Yuen, K.-L. (2006) "Compatibility of LCD Monitors with Frame-Sequential Stereoscopic 3D Visualisation" (Invited Paper), in IMID/IDMC '06 Digest, (The 6th International Meeting on Information Display, and The 5th International Display Manufacturing Conference), pg 98-102, Daegu, South Korea, 22-25 August 2006.
7. Woods, A.J., and Rourke, T., (2007) "The compatibility of consumer DLP projectors with time-sequential stereoscopic 3D visualization", presented at Stereoscopic Displays and Applications XVIII, published in Stereoscopic Displays and Virtual Reality Systems XIV, Proceedings of IS&T/SPIE Electronic Imaging Vol. 6490, San Jose, California, 29-31 January 2007.
8. Woods, A.J., Karvinen, K. S. (2008) "The compatibility of consumer plasma displays with time-sequential stereoscopic 3D visualization" in Stereoscopic Displays and Applications XIX, Proceedings of SPIE Vol. 6803, San Jose, California.
9. Woods, A.J, and Sehic, A. (2009) "The compatibility of LCD TVs with time-sequential stereoscopic 3D visualization" in Stereoscopic Displays and Applications XX, Proceedings of Electronic Imaging, Proc SPIE Vol. 7237, San Jose, California, 19-21 January 2009.
10. www.matlab.com
11. CIE, Commission Internationale de l'Eclairage Proceedings (Cambridge University Press, 1932).

This is a separator page and is intentionally blank.

Appendix 1 – Additional Publications Relevant to the Thesis

- Paper 9** A. J. Woods, S. Tan (2002) "Characterising Sources of Ghosting in Time-Sequential Stereoscopic Video Displays" presented at Stereoscopic Displays and Applications XIII (SD&A), published in Stereoscopic Displays and Virtual Reality Systems IX, Proceedings of IS&T/SPIE Electronic Imaging, SPIE Vol. 4660, pp. 66-77, San Jose, California, January 2002.
- Paper 10** A. J. Woods, T. Rourke (2004) "Ghosting in Anaglyphic Stereoscopic Images" presented at Stereoscopic Displays and Applications XV (SD&A), published in Stereoscopic Displays and Virtual Reality Systems XI, Proceedings of IS&T/SPIE Electronic Imaging, SPIE Vol. 5291, pp. 354-365, San Jose, California, January 2004.
- Paper 11** A. J. Woods (2005) "Compatibility of Display Products with Stereoscopic Display Methods" International Display Manufacturing Conference (IDMC), pp. 290-293, Taiwan, February 2005.
- Paper 12** A. J. Woods, T. Rourke, K. L. Yuen (2006) "The Compatibility of Consumer Displays with Time-Sequential Stereoscopic 3D Visualisation" (Invited Plenary Paper), in Proceedings of the K-IDS Three-Dimensional Display Workshop 2006, pp. 7-10, Seoul National University, Seoul, South Korea, 21 August 2006.
- Paper 13** A. J. Woods, T. Rourke (2007) "The compatibility of consumer DLP projectors with time-sequential stereoscopic 3D visualization", presented at Stereoscopic Displays and Applications XVIII, published in Stereoscopic Displays and Virtual Reality Systems XIV, Proceedings of IS&T/SPIE Electronic Imaging, SPIE Vol. 6490, pp. 64900V-1 to -7, San Jose, California, January 2007.
- Paper 14** [Invited Reviewed Article]
A. J. Woods (2009) "3-D Displays in the Home" Information Display, 7(09), pp. 8-12.
- Paper 15** M. A. Weissman, A. J. Woods (2011) "A simple method for measuring crosstalk in stereoscopic displays" in Stereoscopic Displays and Applications XXII, Proceedings of IS&T/SPIE Electronic Imaging, SPIE Vol. 7863, pp. 786310-1 to -11, Burlingame, California, January 2011.
- Paper 16** A. J. Woods (2011) "How are crosstalk and ghosting defined in the stereoscopic literature?" in Stereoscopic Displays and Applications XXII, Proceedings of IS&T/SPIE Electronic Imaging, SPIE Vol. 7863, pp. 78630Z-1 to -12, Burlingame, California, January 2011.
- Paper 17** [Refereed Conference Paper]
A. J. Woods, J. Helliwell (2012) "Investigating the cross-compatibility of IR-controlled active shutter glasses" in Stereoscopic Displays and Applications XXIII, Proceedings of IS&T/SPIE Electronic Imaging, SPIE Vol. 8288, pp. 82881C-1 to -10, Burlingame, California, January 2012.
- Paper 18** [Refereed Journal Paper]
A. J. Woods (2013) "3D or 3-D: a study of terminology, usage and style" European Science Editing, 39(3), pp. 59-62, August 2013.

Paper 9 A. J. Woods, S. Tan (2002) "Characterising Sources of Ghosting in Time-Sequential Stereoscopic Video Displays" presented at Stereoscopic Displays and Applications XIII (SD&A), published in Stereoscopic Displays and Virtual Reality Systems IX, Proceedings of IS&T/SPIE Electronic Imaging, SPIE Vol. 4660, pp. 66-77, San Jose, California, January 2002.

Characterising Sources of Ghosting in Time-Sequential Stereoscopic Video Displays

Andrew J. Woods*, Stanley S. L. Tan
Centre for Marine Science and Technology (CMST), Curtin University of Technology

ABSTRACT

A common artefact of time-sequential stereoscopic video displays is the presence of some image ghosting or crosstalk between the two eye views. In general this happens because of imperfect shuttering of the Liquid Crystal Shutter (LCS) glasses used, and the afterglow of one image into another due to phosphor persistence. This paper describes a project that has measured and quantified these sources of image ghosting and developed a mathematical model of stereoscopic image ghosting. The primary parameters which have been measured for use in the model are: the spectral response of the red, green and blue phosphors for a wide range of monitors, the phosphor decay rate of same, and the transmission response of a wide range of LCS glasses. The model compares reasonably well with perceived image ghosting. This paper aims to provide the reader with an improved understanding of the mechanisms of stereoscopic image ghosting and to provide guidance in reducing image ghosting in time-sequential stereoscopic displays.

Keywords: Stereoscopic, Liquid Crystal Shutter glasses, Ghosting, Crosstalk, Phosphor Afterglow, Shutter Leakage.

1. INTRODUCTION

One of the most common stereoscopic display techniques is the use of liquid crystal shutter (LCS) glasses in combination with the sequential display of left and right perspective images on a common Cathode Ray Tube (CRT) display (e.g. most TVs and computer monitors). When the left perspective image is displayed on the screen, the right eye cell of the LCS glasses goes opaque and the left eye cell goes clear, and vice versa for when the right perspective image is displayed. Therefore the left eye sees only left perspective images and vice versa for the right eye. If the speed of repetition is sufficiently high, the eye will not notice the alternate presentation of the images nor any flicker.

This technique is often called field-sequential or frame-sequential 3D since sequential or alternate images contain the left and right image. The term field-sequential applies to interlaced video systems and frame-sequential applies to progressive mode video displays. An overall term that can be used to describe both field- and frame-sequential systems is "time-sequential".

An unfortunate property of these types of stereoscopic displays is the presence of a low level amount of image ghosting or crosstalk. Image ghosting or crosstalk is the leakage of one eye view into the other eye. For example, the left eye should only be able to see the left perspective image, but due to crosstalk, the left eye sees a small proportion of the right perspective image.

The amount of crosstalk is typically quite low and hence is usually mostly noticed on images that exhibit high contrast. For example, where a bright object appears against a dark background.

Most of the literature on the subject of crosstalk^{1,2,3,4,5,6} cites two main contributors to crosstalk:

- **Phosphor Afterglow**

Images are formed on a CRT display when the phosphor coating on the inside of the tube fluoresces upon excitation by an electron beam. The light output of these phosphors 'decay' after the initial excitation instead of extinguishing immediately. This phosphor persistence (or afterglow) enables one image to persist in time so that a faint 'afterglow image' may still be seen when the subsequent image is being displayed on the CRT. In this way, the left perspective

* A.Woods@cmst.curtin.edu.au; phone: +61 8 9266 7920; fax: +61 8 9266 4799; <http://www.cmst.curtin.edu.au> ; Centre for Marine Science & Technology, Curtin University of Technology, GPO Box U1987, Perth 6845, AUSTRALIA.

image is displayed simultaneously with an ‘afterglow image’ of the right perspective image, enabling the left eye to see both, and similarly for the right eye.

- **Shutter leakage**

Due to the physical limitations of LC (liquid crystal) technology, when an LC shutter occludes an eye, it does not become totally 100% opaque. Thus if the displayed image is bright, the occluded eye may still be able to see a small percentage of the image not intended for it.

Our questions were:

- How much do phosphor afterglow and shutter leakage actually contribute to crosstalk?
- Are there any other contributors to crosstalk? Some factors that we considered were: timing of the LCS drive signal (when in the Vertical Blanking Interval the switch occurs), the nature of the signal used to drive the LCS (voltage, modulation, etc), and the field/frame rate of the CRT display. Lipton⁷ also discusses angle of view through the LCS.

These questions weren’t entirely addressed in the literature so we set about performing some measurements to characterise the crosstalk.

2. CROSSTALK MEASUREMENT AND MODELING

2.1 CROSSTALK MEASUREMENT

Unfortunately, it wasn’t possible for us to separately measure the contribution of phosphor afterglow and incomplete extinction to ghosting directly in one measurement. Therefore we had to devise a method by which we could model the crosstalk process mathematically using the measured individual properties of the CRT phosphors and LCS glasses.

The three items that we measured to develop our model were:

- Phosphor spectral response,
- Phosphor time response, and
- LC shutter time/spectral response.

2.1.1 PHOSPHOR SPECTRAL RESPONSE

The colour image on a CRT display is constructed using three different colour phosphors: RED, GREEN, and BLUE. We used an Ocean Optics S1000 Spectoradiometer to measure the spectral output of the three colour phosphors. The results of this measurement (carried out on a selection of 11 different CRT computer monitors and TVs) are shown in Figure 1.

It can be seen that the blue and green phosphors exhibit a classic bell shape curve centred at around 450nm for blue and 520nm for green. In contrast the red phosphor has many peaks with the main peak at around 630nm. One further aspect of this result to note is the partial spectral overlap of the three phosphors.

We carried out this same measurement on 11 different CRT computer monitors and TVs in order to establish how much variation there was between different monitors. The overlaid results of all 11 CRT monitors are shown in Figure 2. We were surprised by the uniformity of the result, which obviously indicates that a standard set of phosphors is used in most CRT displays.

Note, however, that the one CRT projector that we measured had a very different spectrum than the CRT monitors that we measured. LCD displays also have a considerably different spectrum for each of the red, green and blue primaries, which is due to the entirely different display method used. However, it should be noted that LCS glasses would not normally be used with current LCD monitors.

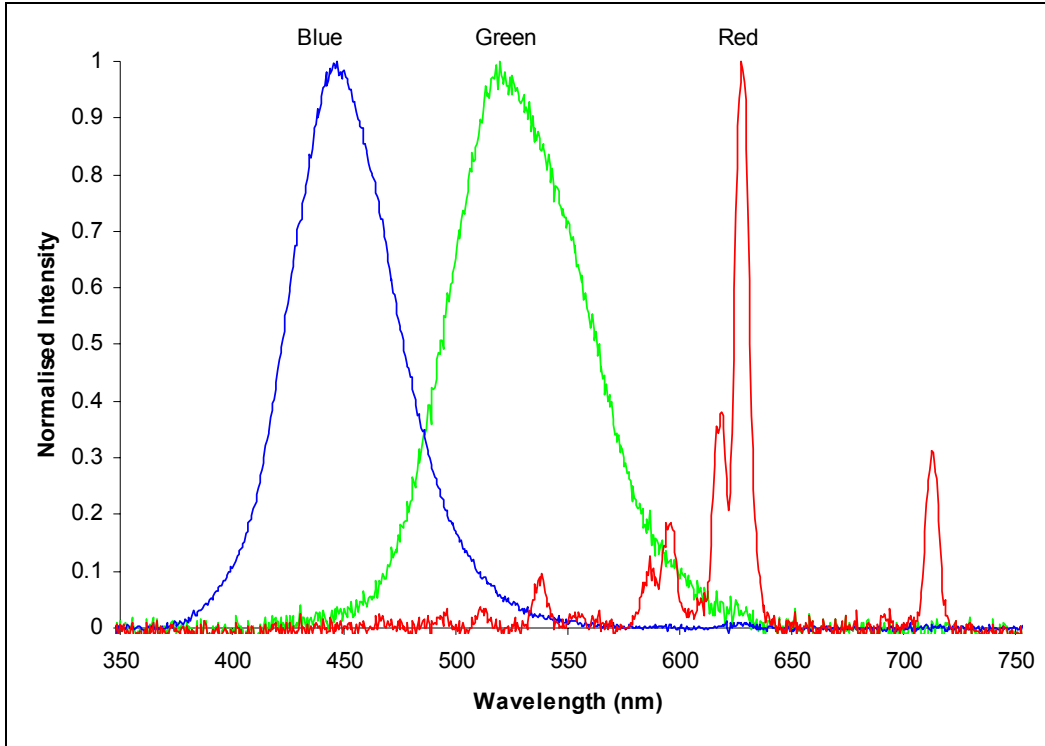


Figure 1: Spectral output of the phosphors of a typical CRT display.

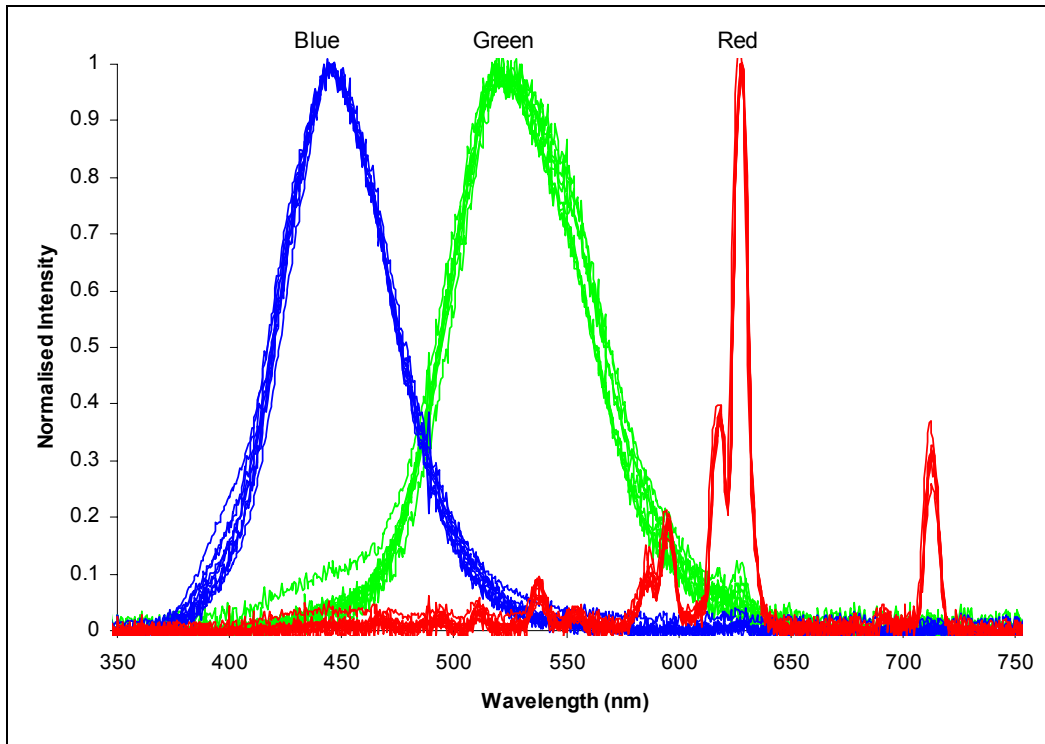


Figure 2: Overlaid spectral output of 11 different CRT monitors.

2.1.2 PHOSPHOR TIME RESPONSE

The phosphor intensity vs. time response of each of the three CRT phosphors was measured using an IPL10503DAL photodiode from Integrated Photomatrix Limited (Dorchester, UK)⁸. The results of this measurement for each of the three colour phosphors are shown in Figure 3. Again, blue and green have a very similar result. In contrast, the red phosphor has a much longer decay. The linearity of the IPL10503DAL was confirmed by a separate experiment⁹.

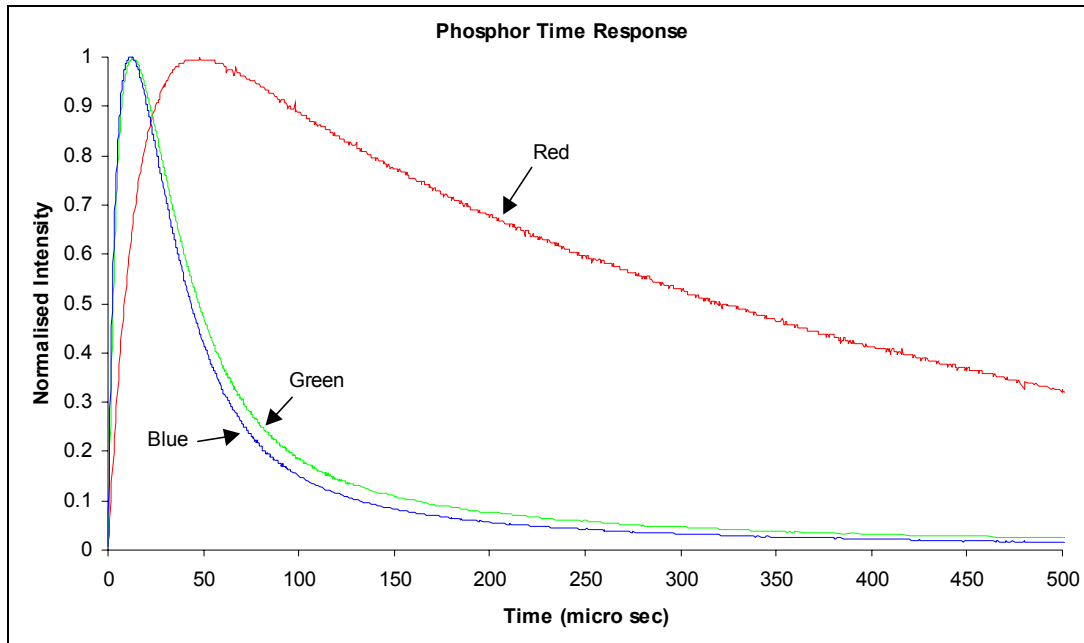


Figure 3: Phosphor intensity vs. time response for the three phosphors of a typical CRT display.

2.1.3 LC SHUTTER TIME/SPECTRAL RESPONSE.

Measuring the transmission vs. time response of the LCS glasses presented a slightly more difficult problem. The optical transmission of a filter (in our case an LC shutter) is normally measured by placing a source on one side of the filter and a detector on the opposite side. The percentage transmission of the filter is given by the percentage reduction in the reading of the detector when the filter is inserted into the optical path. It is possible to determine the optical transmission of the filter at particular spectral frequencies by using an optical source with a particular spectral output.

In our case we were primarily interested in the transmission vs. time response of the LCS glasses at the spectral frequencies output by the individual CRT phosphors. It would have made sense to use the CRT phosphors as the optical source for the transmission measurement, however we were also interested in isolating the time varying transmission response of the LCS shutters and therefore needed an optical source which had a constant optical output versus time. Unfortunately the optical output of the phosphors in a CRT monitor are not constant – the phosphors are modulated by the scanning electron beam – and therefore we could not directly use them as source.

Instead we decided to use LEDs (Light Emitting Diodes) as the optical source. LEDs have a constant optical output, have a fairly narrow spectral output, bright models are available, and they are easy to work with. However, our challenge was to select LEDs whose output was fairly well matched to the spectral output of the CRT phosphors. Figure 4 shows the spectral output of the LEDs that we chose to imitate the CRT phosphors plotted against the CRT phosphor spectral responses. It can be seen in Figure 4 that the blue and green LEDs are a fairly close match to the output of the blue and green phosphors – at least considered close enough for the purposes of this experiment. Unfortunately no single LED is ever going to match the multi-peaked spectral output of the red CRT phosphor so we chose a red LED whose centre frequency was fairly close to the red phosphor's main peak.

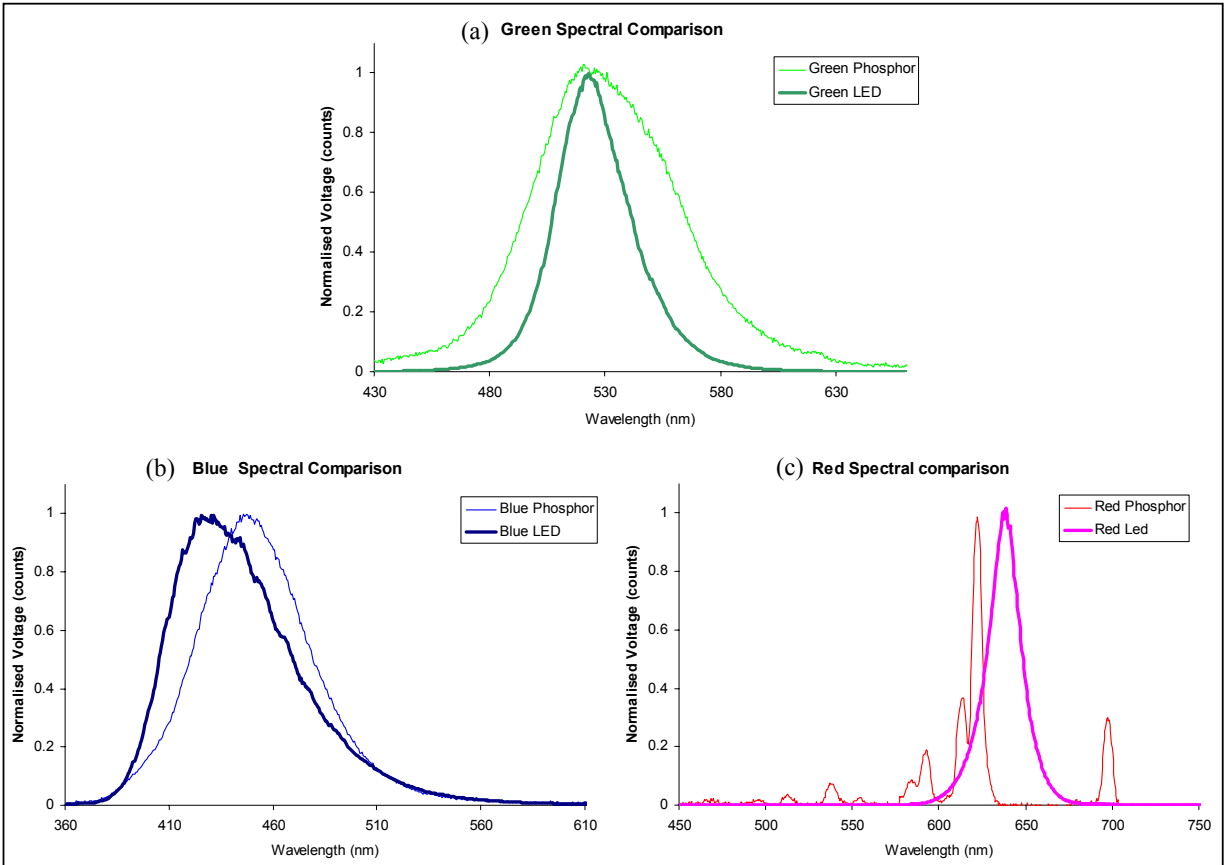


Figure 4: The spectral output of the chosen LEDs versus the spectral output of the CRT phosphors for (a) Green, (b) Blue and (c) Red.

The transmission vs. time response of a range of different LCS glasses was then measured using the LEDs chosen above as light sources (individually for red, green and blue) and the photodiode mentioned previously as the detector. A sample result of this measurement on a selected pair of LCS glasses is shown in Figure 5.

The results of Figure 5 show the opaque→transmissive→opaque cycle of a pair of LCS glasses for the selected red, green and blue wavelengths. At 0ms the glasses are in the opaque (extinction) state. At 2.5ms the drive signal of the glasses changes state triggering the glasses to change into the transmissive state. At 22.5ms the drive signal changes again and drives the LCS glasses into the opaque state. This is repeated at the cycle frequency of the drive signal – in this case 60Hz.

A number of things should be observed from Figure 5:

- The results for each of the three colours are not the same – although there are similarities.
- In the opaque state, there is still a measurable amount of transmission – it is not 0% transmission. (This is what we refer to as shutter leakage.)
- In the opaque state, the red transmission is considerably higher than the transmission of the other two colours.
- At the opaque to transmissive transition it can be seen that the glasses switch gradually to the transmissive state – the state change is not immediate.
- The percentage transmission during the transmissive state is not constant. In one case (blue) the transmission increases to a maximum and then decreases. For the other two colours (red and green) the transmissions monotonically increase to different equilibrium points.
- The transmissive to opaque state change is fairly sharp compared to the opaque to transmissive state change.

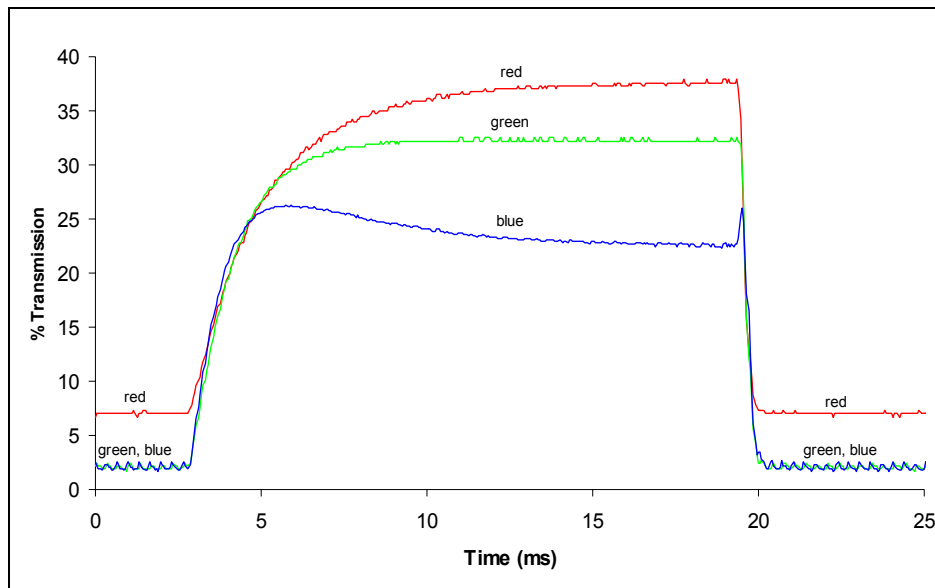


Figure 5: The transmission vs. time response of a selected pair of LCS glasses for the selected red, green and blue wavelengths.

This measurement process was repeated for a range of different pairs of LCS glasses. These results, shown in Figure 6, show a considerable amount of variation. This variation is probably due to differing types of materials used in the manufacture of the various LC shutters sampled. In this test the cycle frequency was 50Hz (except for one set of glasses which had to be cycled at 100Hz). Again the red spectral range exhibits the most leakage during the opaque shutter state.

2.2 THE CROSSTALK MODEL

The three properties described above (phosphor spectral response, phosphor time response, and LC shutter time/spectral response) were combined together in a mathematical model in order to simulate the function of the stereoscopic image crosstalk. The crosstalk model is illustrated in Figure 7.

The top half of Figure 7 shows the shutter response and the phosphor response overlaid on the same time scale. In this case the phosphor response has been exaggerated for illustrative purposes. In real life the phosphor response is considerably narrower. The horizontal axis shows the time for one complete shutter cycle – one image for the left eye and then one image for the right eye – with the shutters switching appropriately. This graph actually indicates the time cycle for the right eye – it can be seen that the shutter goes opaque during the display of the left image and is transmissive during the display of the right eye image. In this case the phosphor response curve is positioned to coincide with a pixel close to the top of the screen and for the left eye image.

The vertical dashed lines on the graph indicate the start and finish of the vertical blanking interval. This is the time in which no picture information is being drawn on the screen. For example, "End of VBI1"[†] coincides with the start (top) of the left image and "Start of VBI2" coincides with the end (bottom) of the left image.

From 18000 μ sec on the bottom half of Figure 7 shows the amount of light from a pixel on the left eye image that has leaked through the LC shutter and can be seen by the right eye. This has been calculated by multiplying the shutter response and phosphor response together. Ideally this curve would be zero, however its presence indicates the presence of crosstalk.

[†] VBI = Vertical Blanking Interval

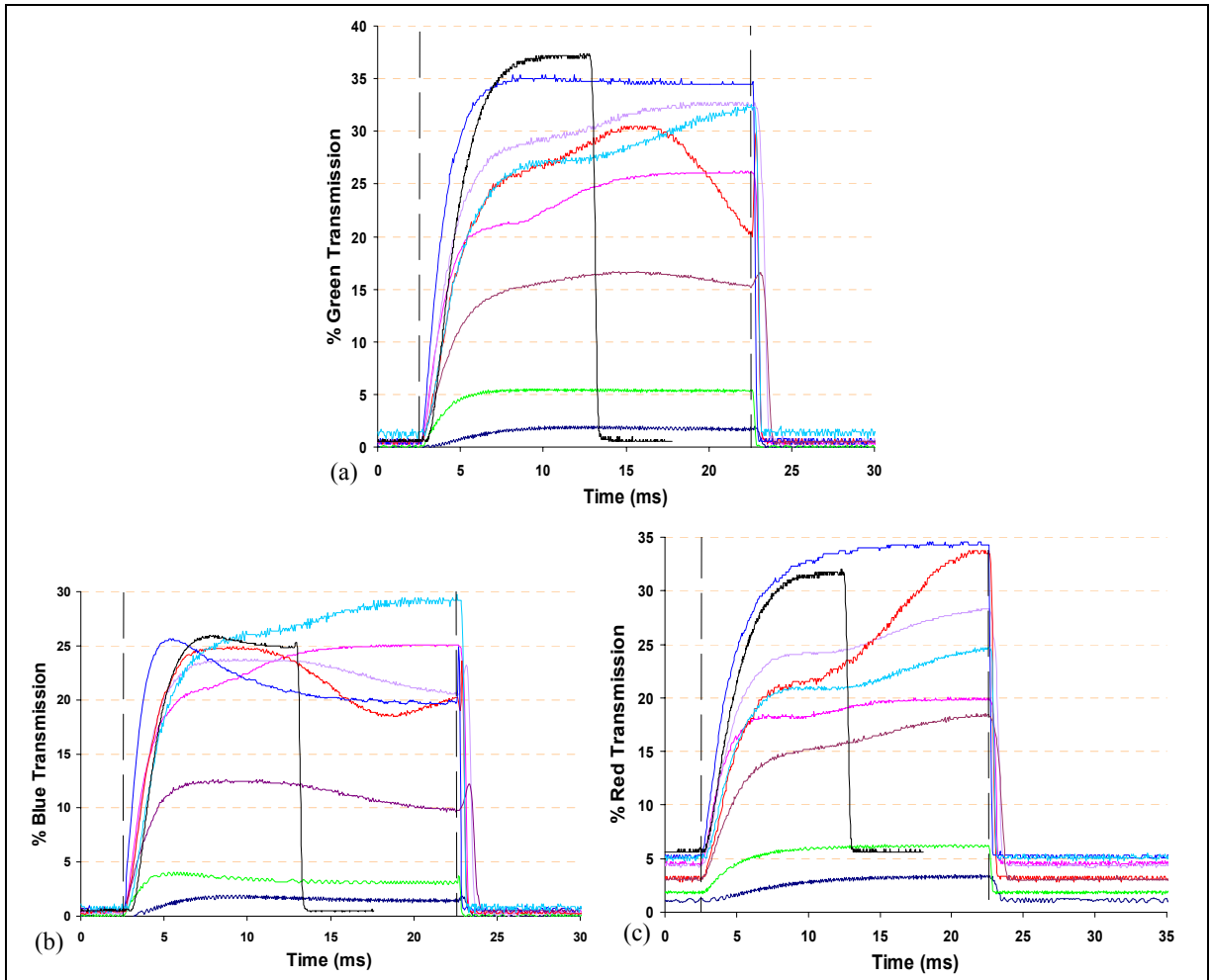


Figure 6: The transmission vs. time response of a selection of different LCS glasses[‡] in the (a) green, (b) blue, and (c) red spectral ranges.

The total amount of crosstalk (for this specific pixel position) is then calculated by integrating the area under the bottom curve.

To determine the contribution of each crosstalk source to total crosstalk, the time integration is divided into two regions, one encompassing the duration of the shutter's transmissive state, and the other encompassing the shutter's occlusion state. The time integration taken while the shutter is in its occlusion state represents the average crosstalk light energy 'leaking' through the 'imperfectly' occluded shutter and is due to shutter leakage. Similarly, the integration taken while the shutter is in its transmissive state, while none of the left image should have been visible, will represent the average crosstalk light energy received due to phosphor afterglow.

[‡] Please note that we have intentionally not listed the manufacturer and model of the various LCS glasses measured. In most cases we have measured only one pair of glasses and hence this may not be representative of all LCS glasses of this model. The basis of this graph is that there can be considerable variation between different LCS glasses.

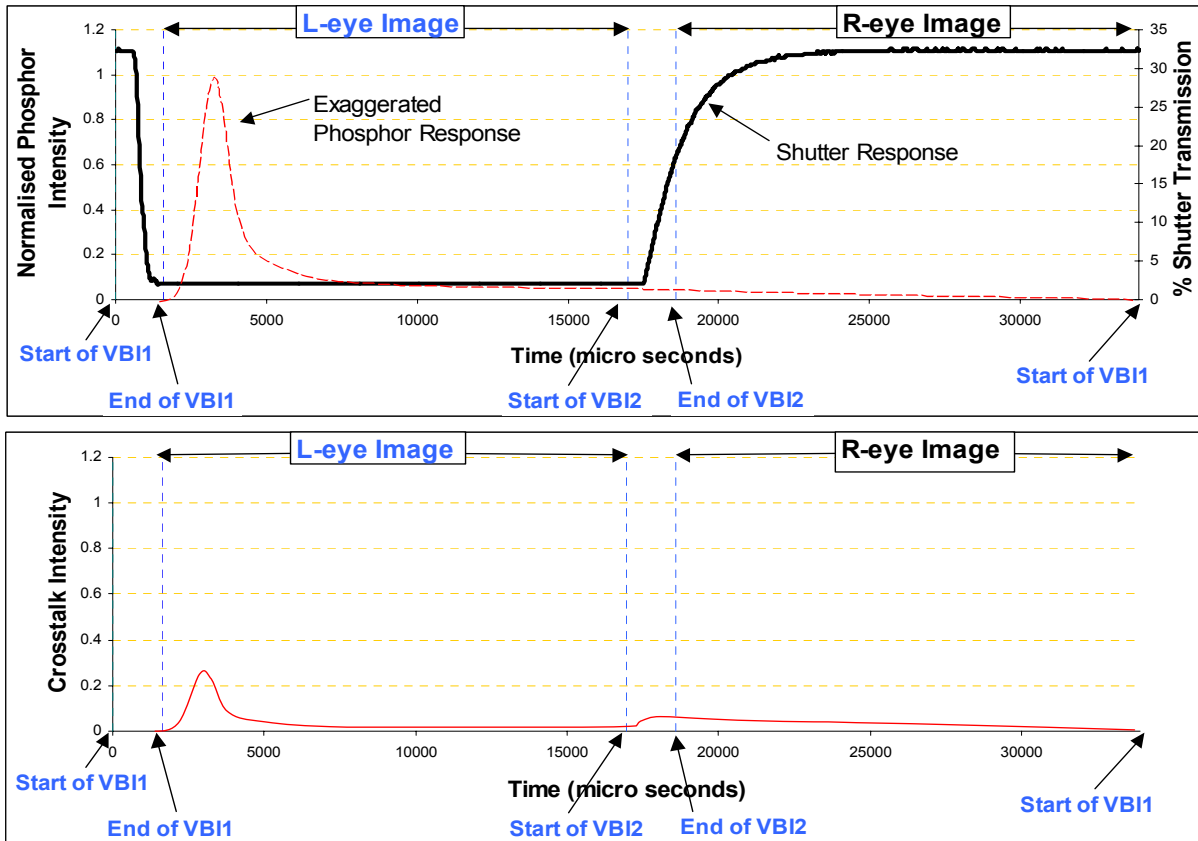


Figure 7: Illustration of the crosstalk model (with exaggerated phosphor response for illustrative purposes). Top: phosphor response and shutter response. Bottom: multiplication of phosphor response by the shutter response to give the amount of crosstalk.

To calculate the crosstalk at another pixel, let's say further down the screen, the above procedure is repeated with the phosphor response delayed in time with respect to the shutter response by the appropriate interval. (This reflects the fact that each pixel on a CRT is excited at a slightly different time. For a typical raster scanning pattern, the cathode ray sweeps horizontal lines down the screen, from the top-left to the bottom-right.) In this iterative fashion, a ghosting profile w.r.t. screen position can be gradually built up.

3. RESULTS

3.1 CROSSTALK MODEL RESULTS

The crosstalk model discussed in Section 2.2 has been prototyped in Excel and uses the input data illustrated in Figures 3 and 5. In this first instance the model has been calculated for a screen refresh rate of 60Hz. The crosstalk model has been run for each of the three colours and also for multiple positions down the screen. The results for each of the three primary colours are shown in Figure 8(a,b,c). The graphs show three parameters: (a) total crosstalk, (b) crosstalk due to shutter leakage, and (c) crosstalk due to phosphor afterglow, plotted versus screen height.

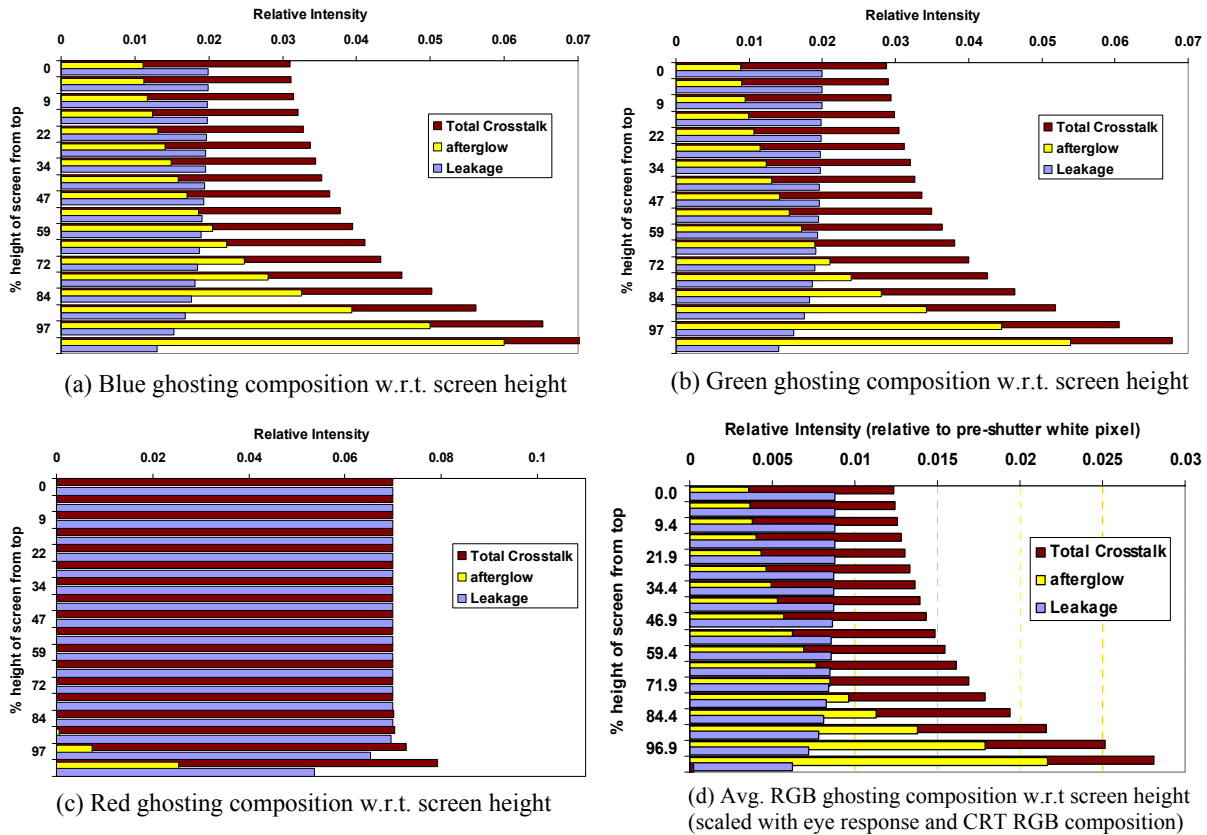


Figure 8: Crosstalk source composition versus screen height for: (a) blue, (b) green, (c) red, and (d) average brightness.

The results for blue and green are remarkably similar - at the top of the screen ghosting is mostly due to shutter leakage, and at the bottom of the screen ghosting is mostly due to phosphor afterglow. The blue and green figures also show a monotonic increase in total crosstalk as we move down the screen. The result for red is quite different from blue and green which is probably due to the high level of transmission during the LCS extinction period for red (see Figure 5). We would have expected the amount of red afterglow (in Figure 8c) to be significantly more but this might be an error due to the limited accuracy of our photodetector system at very low light levels. For all graphs of figure 8, the maximum amount of crosstalk is at the bottom of the screen - which agrees with our perceptual assessment of crosstalk and also with Bos⁵.

The results for the three colours have then been combined into a single average brightness (luminance) result shown in Figure 8(d) by taking into consideration the eye's spectral response¹⁰ as well as a CRT monitor's usual balance between red, green and blue to obtain white light. If we average the crosstalk due to each of the sources over the whole screen (for the average brightness case), we find that shutter leakage and phosphor afterglow are almost even contributors at 51.1% and 48.8% respectively.

It should be emphasised that these results apply only to the particular system that we have measured (LCS glasses, shutter rate, etc). The results for a different system could be significantly different from these results and would require a new set of data to be input into the crosstalk model.

3.2 VALIDATION

To provide us with a quick check that the results from the crosstalk model were close to correct, we used a digital camera to capture the presence of crosstalk on a time-sequential stereoscopic display. Although the digital camera (a Kodak DC625) is by no means a metric device, it would at least provide us with some level of validation.

Figure 9 shows a photograph taken through the right shutter, with the glasses shuttering, the screen was showing a time sequential image, the right image was set to black and the left image was set to full screen 100% green (the other colours were tested separately). The increase of crosstalk toward the bottom of the screen can be clearly observed, and is in accord with the crosstalk model results shown in Figure 8. Figure 10 shows a 3D plot of the data of Figure 9 and shows the nature of the increase in ghost intensity at the bottom of the screen.

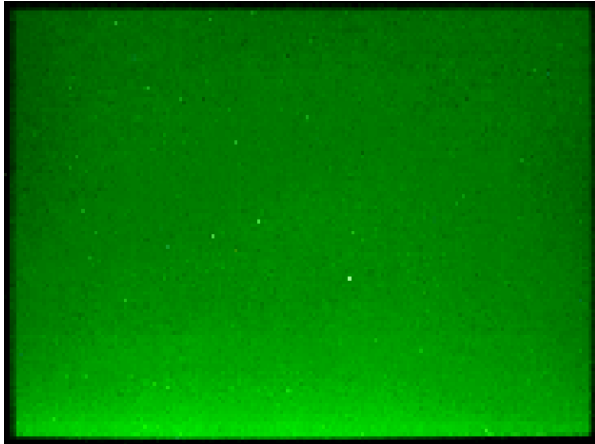


Figure 9: Digital photograph of green ghosting

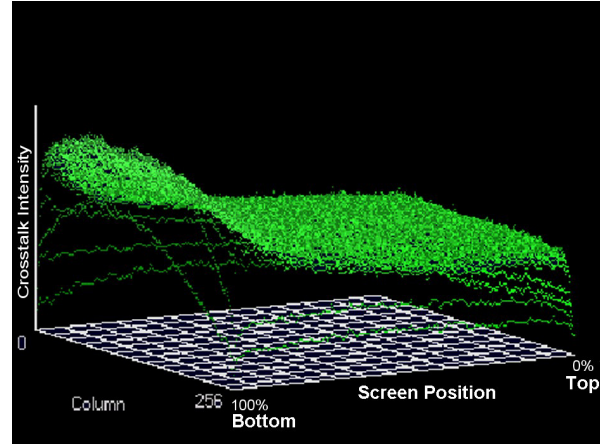


Figure 10: 3D histogram of Figure 9

In order to compare the crosstalk model with the digital camera results for total crosstalk, the ghost to (intended) transmission (G/T) Ratio with respect to screen height was calculated. This ratio was used since the camera's absolute light sensitivity was unknown. Figure 11 shows a comparison of (G/T) ratio calculated from the crosstalk model, and that calculated from data extracted from the digital photographs for each of the three primary colours.

The closest match is with the green response. Although there is an offset between the two curves (modelled and measured), the 'shape' of the two curves is remarkably similar. The similarity of the two curves provides some reassurance as to the accuracy of the crosstalk model for the green case. The offset between the two curves may be due to a scaling, exposure or non-linearity issue with the digital camera or may simply represent an error with the crosstalk model.

The results for blue and red (Figure 11b,c) aren't quite as close but the shape is somewhat similar. An offset between the model and the measured is again present.

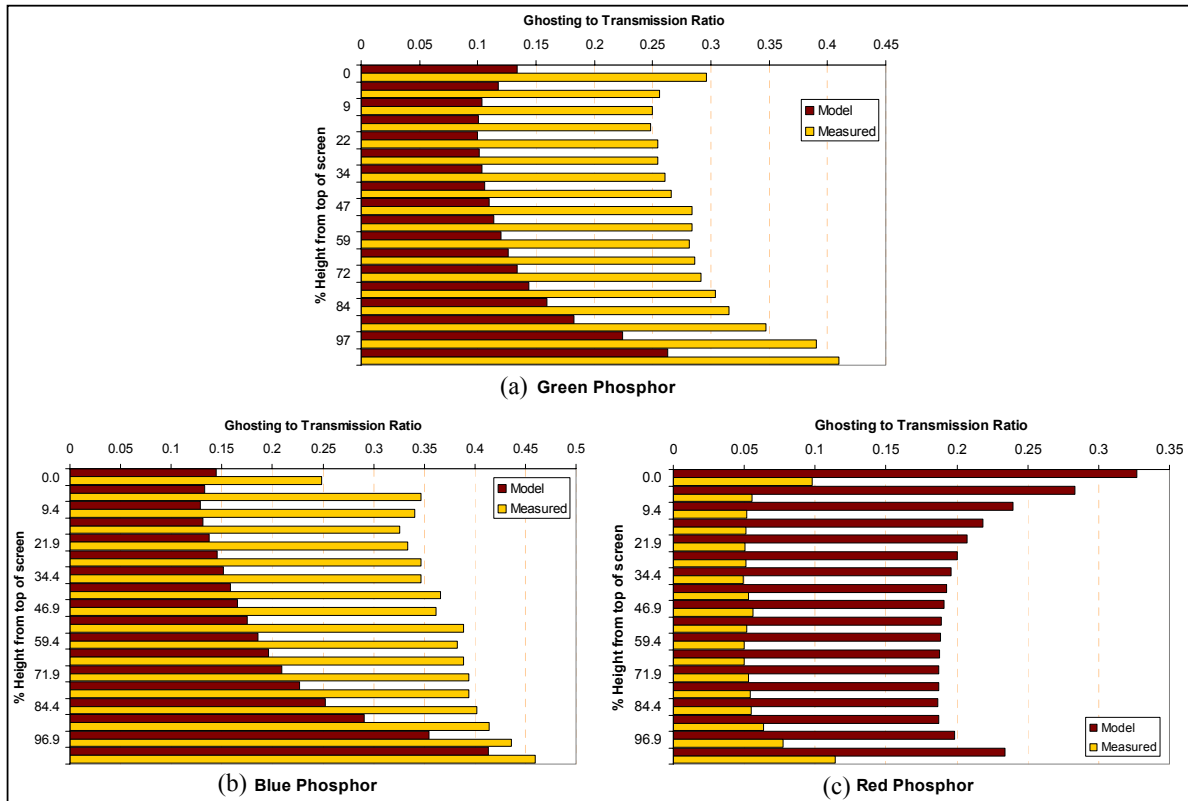


Figure 11: Ghost to Transmission Ratio Comparison for (a) Green, (b) Blue, and (c) Red.

4. CONCLUSION

This paper has discussed the development of a model for crosstalk/ghosting in time-sequential stereoscopic displays. The model provides insight into the mechanisms by which crosstalk occurs. Preliminary validation of the model indicates that it gives a reasonable prediction of crosstalk, however more work is needed for complete validation.

Some of the limitations of the current crosstalk model are: the method used to measure the LCS transmission response in the red channel may not be accurate (because the LED spectral response does not match the red phosphor response), the CRT phosphor afterglow measurements may not be entirely accurate (the photodetector system that we used has limited accuracy in low light levels), and the photodetector system has a bandwidth which is very close to the expected bandwidth of the phosphor afterglow response (hence we may be missing high frequency information for the phosphor time response).

The advantage of the crosstalk model is that it allows the quick simulation of crosstalk under a variety of conditions and hence may be a useful tool to help find ways to reduce crosstalk in stereoscopic displays.

One immediate observation of this study is that the first thing to consider when attempting to reduce crosstalk is to consider changing the LCS glasses (or at least review the performance of the LCS glasses being used). This study found considerable performance variation between various makes and models of LCS glasses. In contrast, very little performance variation was noted between commonly available CRT monitors – hence little change is likely to be obtained by simply swapping monitors. Monitors with short phosphor persistence may well be available by special order but this was beyond the scope of this particular study.

The crosstalk model in its current form isn't particularly user friendly and could be rewritten to improve this aspect. The crosstalk model could also be extended to simulate the use of stereoscopic polarisation modulator panels (such as available from NuVision and StereoGraphics), and could also be modified to simulate the change in crosstalk that would occur with higher field/frame rates. Using a different phosphor time response data set, the model could also simulate the use of CRT projectors for time-sequential stereoscopic display (CRT projectors have a different phosphor time response and spectral response than most CRT monitors).

We have also considered the effect of some of the other sources of crosstalk (as discussed in the introduction), however a full description of these studies is beyond the scope of this paper.⁹

We hope that the reader has gained a better understanding of the mechanisms of stereoscopic image ghosting/crosstalk from the presentation of this research.

REFERENCES

1. T.J. Haven, "A liquid-crystal video stereoscope with high extinction ratios, a 28% transmission state, and 100 μ s switching", in *True Three-Dimensional Imaging Techniques & Display Technologies*, D.F. McAllister, W.E. Robbins, Editors, Proceedings of SPIE vol. 761, pp. 23-26, Bellingham Washington USA, 1987.
2. L. Lipton, J. Halnon, J. Wuopio, B. Dorworth, "Eliminating π -cell artefacts", in *Stereoscopic Displays & Virtual Reality Systems VII*, J.O. Merritt, S.A. Benton. A.J. Woods, M.T. Bolas, Editors, Proceedings of SPIE vol.3957, pp. 264-270, Bellingham Washington USA, 2000.
3. P.J. Bos, T. Haven, "Field-Sequential Stereoscopic Viewing Systems using Passive Glasses", in *SID* Vol. 30/1, pp. 39-43, 1989.
4. J.S. Lipscomb, W.L. Wooten, "Reducing Crosstalk between Stereoscopic Views", in *Stereoscopic Displays & Virtual Reality System*, S.S. Fisher, J.O. Merritt, M.T. Bolas, Editors, Proceedings of SPIE vol.2177, pp. 92-96, Bellingham Washington USA, 1994.
5. P.J. Bos, "Time Sequential Stereoscopic Displays: The Contribution of Phosphor Persistence to the 'Ghost' Image Intensity", in *Three-Dimensional Image Technologies*, H. Kusaka, Editor, Proceedings of ITEC'91, ITE Annual Convention, pp. 603-606, Institute of Television Engineering of Japan, Tokyo, Japan, July 1991.
6. L. Lipton, "The Stereoscopic Cinema: From Film to Digital Projection", in *SMPTE Journal*, pp. 586-593, Sept 2001.
7. L. Lipton, "High Dynamic Range Electro-Optical Shutter for Stereoscopic and other Applications", United States Patent #5 117 302, May 1992.
8. IPL 10530 Integrated Photodiode Amplifiers, Product Data Sheet, Integrated Photomatrix Limited, Dorchester, United Kingdom. [online]: <http://www.ipl-uk.com>
9. S.S.L. Tan, *Sources of Crosstalk in Stereoscopic 3D Displays*, Centre for Marine Science & Technology, Curtin University of Technology, Perth, Australia, 2001.
10. A. Ryer, *International Light Handbook*, pp. 11, International Light Corporation, Newburyport, Massachusetts, USA, 1997. [online]: <http://www.intl-light.com/handbook>

Paper 10 A. J. Woods, T. Rourke (2004) "Ghosting in Anaglyphic Stereoscopic Images" presented at Stereoscopic Displays and Applications XV (SD&A), published in Stereoscopic Displays and Virtual Reality Systems XI, Proceedings of IS&T/SPIE Electronic Imaging, SPIE Vol. 5291, pp. 354-365, San Jose, California, January 2004.

Ghosting in Anaglyphic Stereoscopic Images

Andrew J. Woods*, Tegan Rourke
Centre for Marine Science & Technology (CMST), Curtin University of Technology

ABSTRACT

Anaglyphic 3D images are an easy way of displaying stereoscopic 3D images on a wide range of display types, eg. CRT, LCD, print, etc. While the anaglyphic 3D image method is cheap and accessible, its use requires a compromise in stereoscopic image quality. A common problem with anaglyphic 3D images is ghosting. Ghosting (or crosstalk) is the leaking of an image to one eye, when it is intended exclusively for the other eye. Ghosting degrades the ability of the observer to fuse the stereoscopic image and hence the quality of the 3D image is reduced. Ghosting is present in various levels with most stereoscopic displays, however it is often particularly evident with anaglyphic 3D images. This paper describes a project whose aim was to characterise the presence of ghosting in anaglyphic 3D images due to spectral issues. The spectral response curves of several different display types and several different brands of anaglyph glasses were measured using a spectroradiometer or spectrophotometer. A mathematical model was then developed to predict the amount of crosstalk in anaglyphic 3D images when different combinations of displays and glasses are used, and therefore predict the best type of anaglyph glasses for use with a particular display type.

Keywords: Anaglyph, stereoscopic, 3D, crosstalk, ghosting, image quality.

1. INTRODUCTION

There are many methods of displaying a stereoscopic image, including polarized images, time-sequential alternating frames, two separate images viewed through a binocular lens arrangement, and others. The method used in this project is the anaglyph. Here, the two perspective images are combined into a single image using a complimentary colour coding technique. For example, if a red/cyan anaglyph method is used, the left perspective image is stored in the red channel and the right perspective image is stored in the blue and green colour channels (blue + green = cyan). The observer wears a pair of glasses with one eye's filter coloured red, and the other eye's filter coloured cyan. The filters act to permit the transmission of the correct image to each eye but prevent the transmission of the image not intended for that eye. The brain processes the different perspective images and depth is perceived in the image.

Anaglyphic 3D encoding can be performed using any pair of complimentary colours to store the left and right perspective images. Red/cyan is the most common choice however yellow/blue is also used, and green/magenta is also theoretically possible. The combination of red/blue or red/green can also be used – however brightness is reduced because one of the colour channels is missing in each case.

The main advantages of the anaglyphic 3D method are its simplicity and low cost. All that is required is an anaglyphic 3D image, which can be displayed using almost any colour display method, and a corresponding pair of anaglyphic 3D glasses.

The main disadvantages of anaglyphic images are their inability to accurately depict full-colour images, and the presence of crosstalk. Crosstalk or ghosting is the leaking of an image to one eye, when it is intended exclusively for the other eye. It happens with most stereoscopic displays and results in reduced image quality and difficulty of fusion if the crosstalk is large. Possible sources of crosstalk in anaglyphic images are:

- **Display spectral response**

Most emissive type displays (e.g. CRTs, LCDs, DMDs) work by emitting light in three specific primary colour bands (red, green and blue). The actual spectral content of each light band can vary quite considerably between different display types. If the spectrum of the primary colour bands overlap with each other by any significant

* A.Woods@cmst.curtin.edu.au; phone: +61 8 9266 7920; fax: +61 8 9266 4799; <http://www.cmst.curtin.edu.au>; Centre for Marine Science & Technology, Curtin University of Technology, GPO Box U1987, Perth 6845, AUSTRALIA.

amount, it will be difficult to separate those two colours by the use of colour filters. Ideally the spectral output of each primary colour channel would not overlap.

- **Anaglyph glasses spectral response**

Ideally the filters in anaglyph glasses will only pass light in the selected light bands – e.g. red 600-650nm. If the anaglyph filters still pass light in the undesirable domain, a dim, ghosted image may be seen if the display is still active in those wavelengths.

- **Image compression**

Some image compression formats (e.g. JPEG, MPEG, GIF) can mix information between the three RGB colour channels and hence also introduce crosstalk into anaglyphic 3D images. The amount of crosstalk introduced will depend on the amount of compression used, the type of compression used, and sometimes the particular encoding method used for a particular compression type.

- **Image encoding and transmission**

The two main analogue consumer video formats (NTSC and PAL) encode the colour information as two colour difference signals (at a lower bandwidth than the brightness (luminance) information) multiplexed on top of the luminance signal using a process of Quadrature Amplitude Modulation. Unfortunately this technique also results in the mixing of information between the three RGB colour channels and hence also causes crosstalk

This paper considers the first two points (display spectral response and anaglyphic glasses spectral response).

The reason for this paper is that anaglyphs can often exhibit a lot of ghosting, but the amount of ghosting depends greatly on the type of glasses used and the type of display used. Although ghosting in time-sequential stereoscopic images has been studied^{1,2,3}, relatively few papers have been published on the topic of image quality in anaglyphic 3D images⁴. Our goal was therefore to understand the process of ghosting and hopefully reveal options for reducing ghosting in anaglyphic 3D images.

This paper only examines crosstalk in red/cyan anaglyphic 3D images, although the method discussed could also be applied to the less common blue/yellow anaglyphs or rare green/magenta anaglyphs. Some of the tested glasses were intended for printed anaglyphs, but this paper only considers emissive type displays; other glasses may be better for viewing printed anaglyphs.

2. EXPERIMENTAL METHOD

Figure 1 provides an illustration of the experimental method used in this project. The first step was to characterise the spectral response of the anaglyph display (eg CRT, LCD, or projector). The second step was to characterise the spectral response of the anaglyphic 3D glasses. The third step was to write a computer program to analyse the data from the previous two steps. The computer program (written in Maple 7) calculated a ghosting integral and uncertainties. The fourth step was to generate output from the program that was representative of the crosstalk in the image.

2.1 Measurement of display spectral output

The spectral output of several CRT monitors and a laptop computer LCD were obtained from a previous study^{1,2}. The spectral response of several digital projectors was measured using the irradiance input of a Zeiss Spectroradiometer assembly consisting of an optical fibre bundle inputting to a Zeiss Monolithic Miniature-Spectrometer (MMS) with a sensitive range from UV to just beyond visible (190 to 735 nm). The projectors were connected to a laptop, which displayed a “PowerPoint” slide show, consisting of a plain white slide ($R=G=B=255$), a plain black slide ($R=G=B=0$), a plain red slide ($R=255, G=B=0$), a plain green slide ($R=B=0, G=255$) and a plain blue slide ($R=G=0, B=255$).

2.2 Measurement of spectral transmission of filters

A Hitachi model 150-20 spectrophotometer (SPM) was used to measure the transmission spectrum (restricted to 350–750 nm) of each of the two filters (eg red and cyan) in each of 27 pairs of anaglyph glasses. The SPM compared light sent through the glasses’ filter to a reference beam at each wavelength to determine the percentage transmitted. The resulting printed graphs were scanned and then digitised using Windig 2.5, a program written by Dominique Lovy⁵.

2.3 Data analysis and crosstalk calculation

A computer program was written in Maple to calculate an estimate of the amount of ghosting present when viewing an anaglyphic 3D image displayed on a particular display whilst wearing a particular pair of anaglyphic 3D glasses.

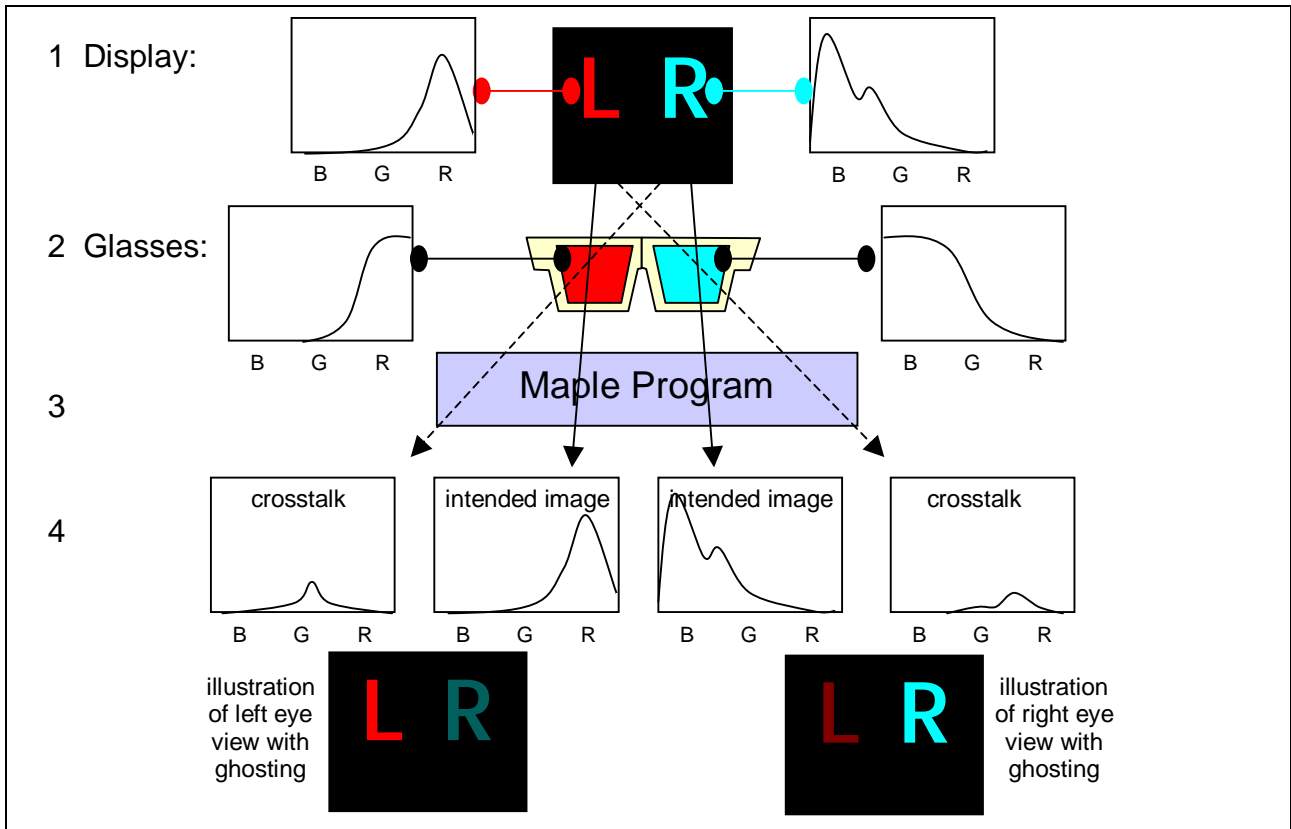


Figure 1: Subset of project plan. Step 1: Characterise display spectral response; Step 2: Characterise glasses spectral response; Step 3: Analyse the data using a computer program; Step 4: Generate estimated output characteristic of crosstalk.

With reference to Figure 1, the program first loads and resamples the display and filter spectral data so that all data is on a common x-axis co-ordinate system. Next, the program determines the display's cyan spectral output by adding the green and blue channel data of the display. The program then multiplies the red display spectrum with the red filter's spectral response to obtain the intended image curve for the red eye, multiplies the cyan display spectrum with the cyan filter's spectrum to obtain the intended image curve for the cyan eye, multiplies the red display spectrum with the cyan filter's spectral response to obtain the crosstalk curve for the cyan eye, and multiplies the cyan display spectrum with the red filter's spectrum to obtain the intended image curve for the red eye.

The program also scales the results to include the human eye's response to light. The human eye has two light detection cell types, rods and cones. Cones, which contain three chemicals that are light-selective pigments, sense colour information. Cones are less sensitive to low light intensities, so are only active in bright or daylight (photopic) vision^{6,7}. Cones are not equally sensitive to all colours. The CIE (Commission Internationale de l'Éclairage or International Commission on Illumination) has published a model that is the standard for simulating photopic (bright light) human eye response, normalised about the peak of 555 nm (see Figure 2)⁸. This standard is the result of physical and psychological experiments relating the output of the human colour vision system with measurements of wavelength and intensity⁹. Figure 2 shows how the cones are more sensitive to yellowish light. This has implications for the ghosting model. If a ghosting level of 2% of image output occurs in the blue light region, this will not be very obvious since the eye is not very sensitive to the light in the blue region.

Figure 3 illustrates the Maple program's analysis of real data. Firstly, (a) display device data and filter data are read into the program. (b) At each wavelength and each display colour, the display intensity, filter response and eye's response are multiplied together. (c) The program calculates the total area under each perceived intensity graph. (d) To find the % crosstalk for a filter, the area under the ghost signal curve is divided by the area under intended signal curve and multiplied by 100.

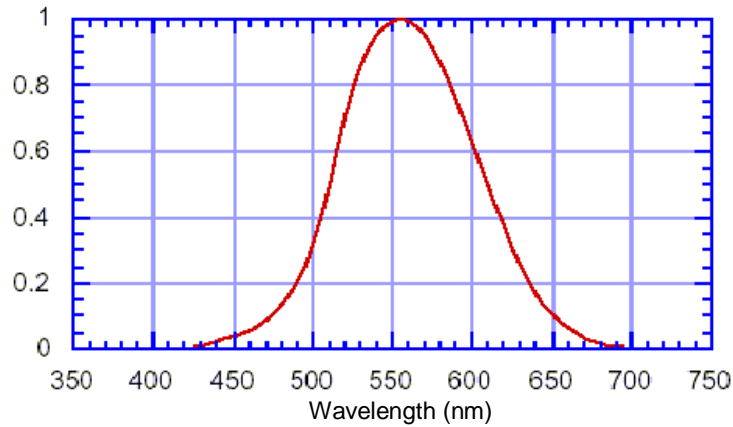


Figure 2: The CIE standard normalised photopic (bright light) human eye response. Figure after Ohno (1999).

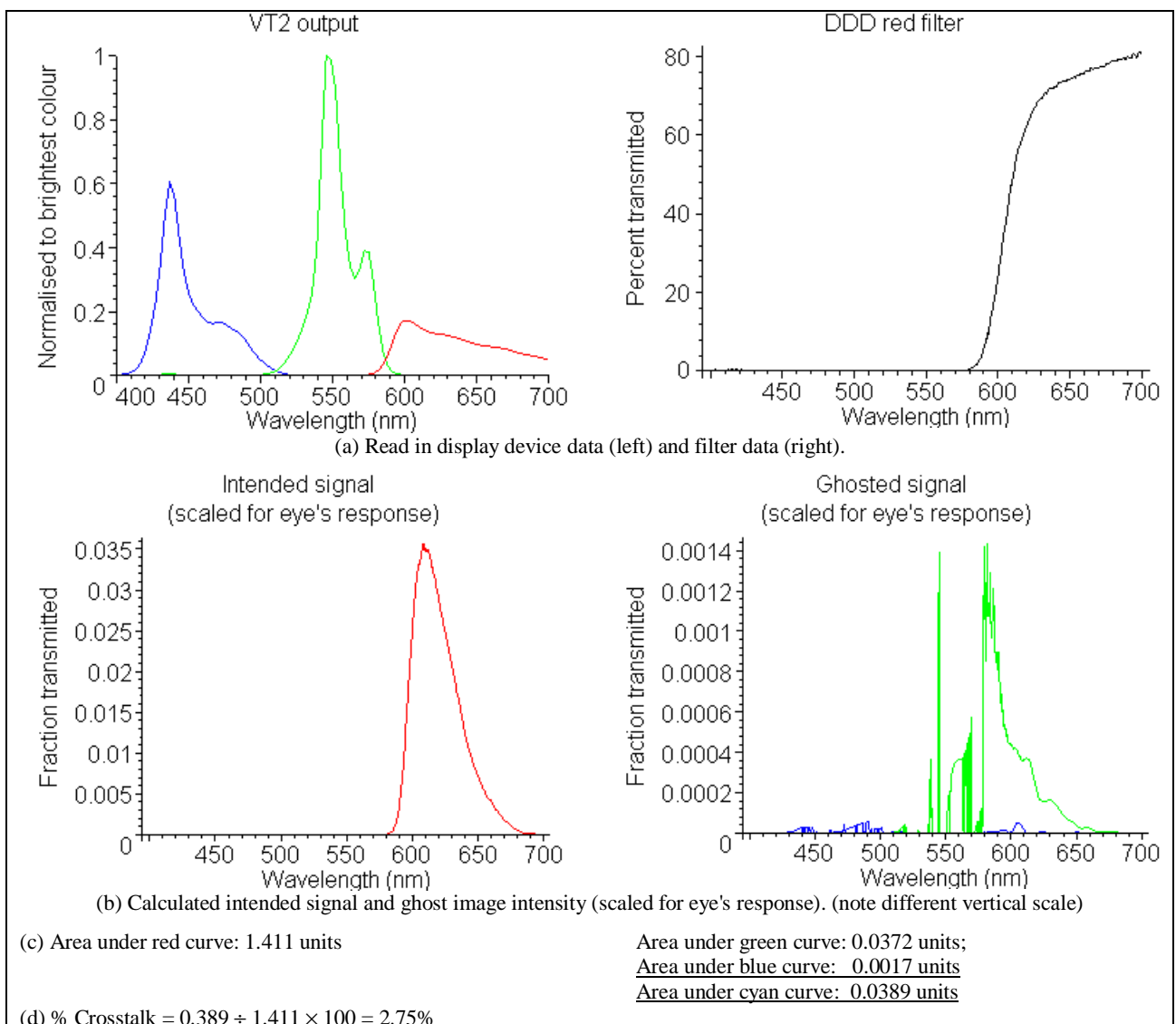


Figure 3: A step-by-step case of the Maple program's analysis of real data.

The overall crosstalk factor for a particular pair of glasses is the sum of the two filter % crosstalk values. It is not a percentage, but rather a number that allows the comparison of any glasses analysed by the Maple program. The program also automates the process of performing a cross comparison of all the displays against all of the glasses.

3. RESULTS

3.1 Display device results

The spectral response of 11 CRT screens and also an LCD were obtained in a previous study^{1,2}. Seven more digital projector spectral outputs were characterised. The details of the displays are summarised in Table 1. As minimal difference was found between the spectral responses of CRTs^{1,2}, only one typical CRT is listed.

Table 1: Summary of the displays whose spectral outputs were characterised.

Display Type	Technology ^α	Brand	Model	Abbreviated Name (used in this paper)
CRT Screen ^{1,2}	P22 RGB Phosphors	Mitsubishi	Diamond View 1772ie	Diamond CRT
LCD Screen ^{1,2}	Liquid Crystal	Acer	Laptop Light	Acer LCD
Digital Projector	1 chip DLP	NEC	MultiSync LT81/G	NEC3
Digital Projector	1 chip DLP	Infocus	LitePro 620	Infocus
Digital Projector	3× LCD TFT Panels	Epson	EMP-5500	Epson
Digital Projector	3× LCD p-Si TFT	NEC	VT540/K	VT2
Digital Projector	3× LCD p-Si TFT	NEC	VT540/K	VT6
Digital Projector	3× LCD TFT Panels	Boxlight	3600	Boxlight 2
Digital Projector	3× LCD TFT Panels	Boxlight	3600	Boxlight 3

PLEASE NOTE: Due to manufacturing variation or experimental error, the results provided in this paper should not be considered to be representative of all displays or projectors of that particular brand or model.

Figure 4 shows the spectral output of the various displays measured in this study. The left column of plots shows the spectral response of all displays for a specific colour primary, eg all displays when showing a red screen. The right column of plots shows the spectral response for all three colour primaries for three specific displays (CRT, laptop LCD, and LCD projector). With reference to Figure 4, it can be seen that the CRT green and blue phosphors outputs are active over a large bell shaped region of the visible spectrum, and overlap the part of the region in which the red phosphor is active. The LCD screen red, blue and green spectra are active throughout the whole visible spectrum, with just an increase in intensity at the wavelengths associated with their colours. Most of the digital projectors have similar shaped curves, though intensity (relative to the brightest colour) varies between projectors.

^α LCD = Liquid Crystal Display; TFT = Thin Film Transistor; DLP= Digital Light Processor (same as Digital Micromirror Device DMD).¹⁰

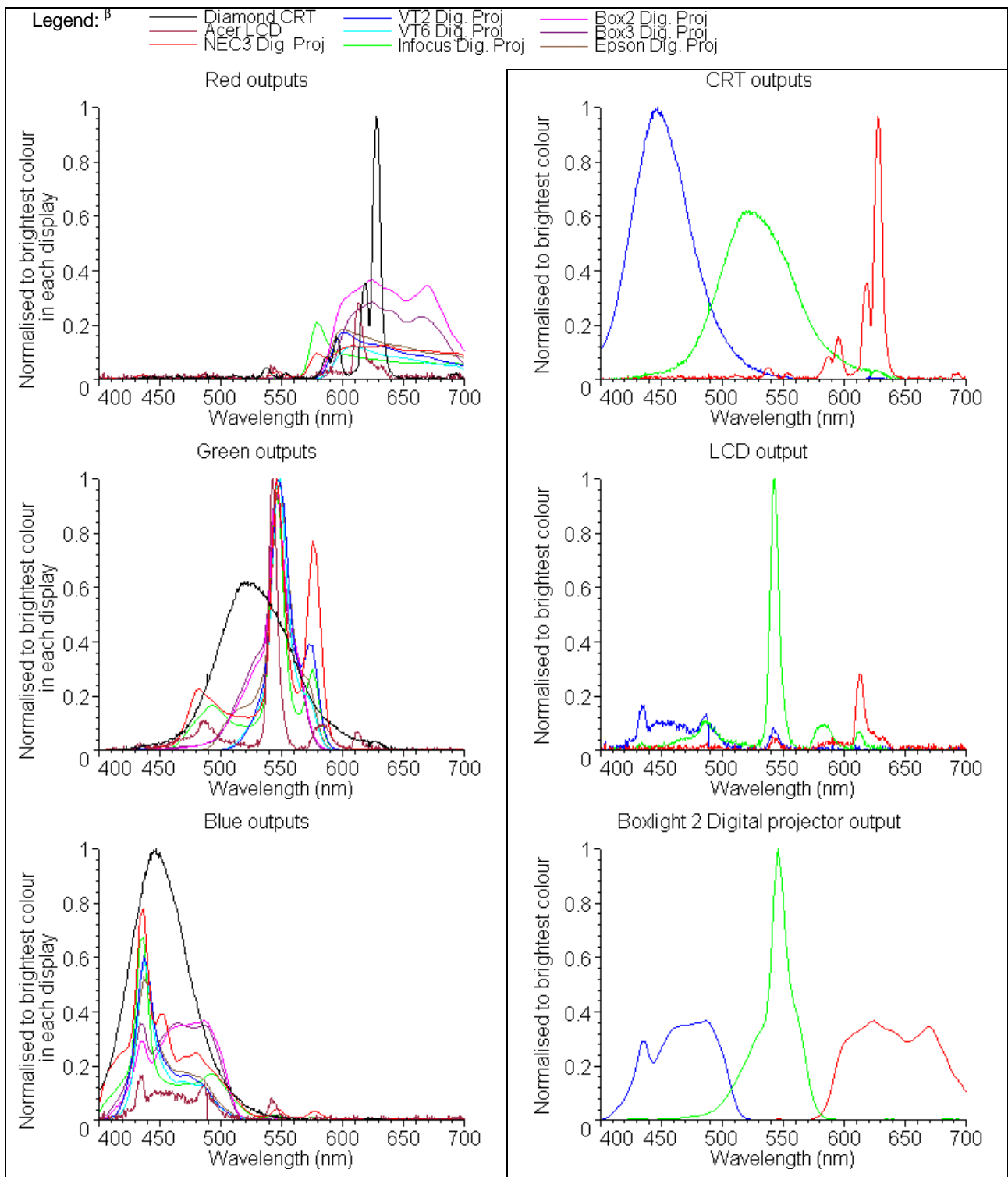


Figure 4: The spectral responses of the various displays tested.

^β We realise the legend of some of the figures in this paper won't be distinguishable when printed in black and white. A colour version of the graphs is available from the primary author's website.

3.2 Anaglyph filter results

To fulfil Step 2 of the plan, data characterising the transmission spectra of various anaglyphic 3D glasses were acquired. Table 2 lists the various red/cyan anaglyphic 3D glasses measured.

Table 2: Red/Cyan Anaglyphic glasses measured.

Glasses Number	Name	Other information on glasses
3DG 2	IMAX/OMNIMAX	"Fujitsu presentation of "We are born of stars"; © IMAX Systems Corp., 1986; Made in USA by Theatric Support, Studio City, California."
3DG 3	National Geographic	Distributed with August 1998 edition of National Geographic Magazine
3DG 4	Sports Illustrated	Distributed with Winter 2000 edition of Sports Illustrated magazine (US edition). "MFGD by Theatric Support."
3DG 6	3D Greets	Attached to a pseudo-colour anaglyph postcard of a Tiger.
3DG 8	Spectacles	"Theatric Support, Studio City CA" Hard-rimmed spectacles purchased from Reel-3D.
3DG 9	Bugs!	From <i>Bugs!</i> magazine series
3DG 11	[no name]	[no identification or writing on glasses – white cardboard]
3DG 14	Reel 3D #1	Purchased from Reel-3D – apparently made by Theatric Support.
3DG 15	Reel 3D #2	Purchased from Reel-3D.
3DG 16	Freddy's Dead	" <i>The Final Nightmare</i> ; New Line Cinema 1991" Distributed at showings of the movie "Freddy's Dead: The Final Nightmare"
3DG 17	3D Video Glasses	"© 1982 3D Video Corp., N. Hollywood, California; for use with 3D Video electronically processed TV programs"
3DG 18	Rhino Home Video	" <i>Cat Women of the Moon</i> ", " <i>Robot Monster</i> " & " <i>The Mask</i> "
3DG 19	DDD	"www.ddd3d.com Dynamic Digital Depth". Supplied by American Paper Optics.
3DG 20	ABC	"96/97 new season premiere; http://abc.com"
3DG 21	Optic Boom	"A DDD Product; ddd.com"
3DG 24	Studio 3D	"Stereoscopic imaging; www.studio3d.com"
3DG 25	Sports Illustrated Australian Edition	Distributed with March 2000 edition of Sports Illustrated magazine (Australian edition).
3DG 26	Substance Comic	Distributed with "3-D Substance #2" Comic, by Jack C. Harris and Steve Ditko and The 3-D Zone. ©1991.
3DG 27	Deep Vision 3D of Hollywood	"For Deep Vision 3-D TV"
3DG 28	Canon ink	Canon Ink (BCI-3e C/M/Y) printed on inkjet transparency sheet
3DG 29	Spy Kids 3D	"© 2003 Miramax Film Corp.; www.spykids.com, Troublemaker Studios, Dimension Films; Mfrd by Playwerks Inc., USA "

PLEASE NOTE: Although a wide selection of glasses was studied, generally only a single pair of glasses of each particular style/brand was sampled. As such, due to manufacturing variations or experimental error, the results provided in this paper should not be considered to be representative of all glasses of that particular style/brand.

Figure 5 shows the combined spectral responses of the filters from the glasses listed in Table 2, grouped according to colour. It is interesting to note that there appears to be a cluster of red and cyan filters in Figure 5 that all trend along the same path. One distinct cyan cluster consists of the cyan filters of the following glasses: 3DG 6, 3DG 15, 3DG 16, 3DG 17, 3DG 19 and 3DG 21. A second distinct cyan cluster consists of the cyan filters of the following glasses: 3DG 3, 3DG 11 and 3DG 20. There are also two distinct red clusters. The first consists of the red filters of the glasses: 3DG 15, 3DG 19 and 3DG 21, and the second consists of the red filters of the glasses: 3DG 4, 3DG 9, 3DG 14 and 3DG 24. It is possible that the same chemicals are used to produce these clustered filters. Three pairs of glasses cluster together in both the red and cyan filters: 3DG 15, 3DG 19 and 3DG 21. These are probably manufactured by the same company and distributed to other companies. The fact that this path presents as a path, and not a single line, could indicate either production variability or be an artefact of the experimental procedure.

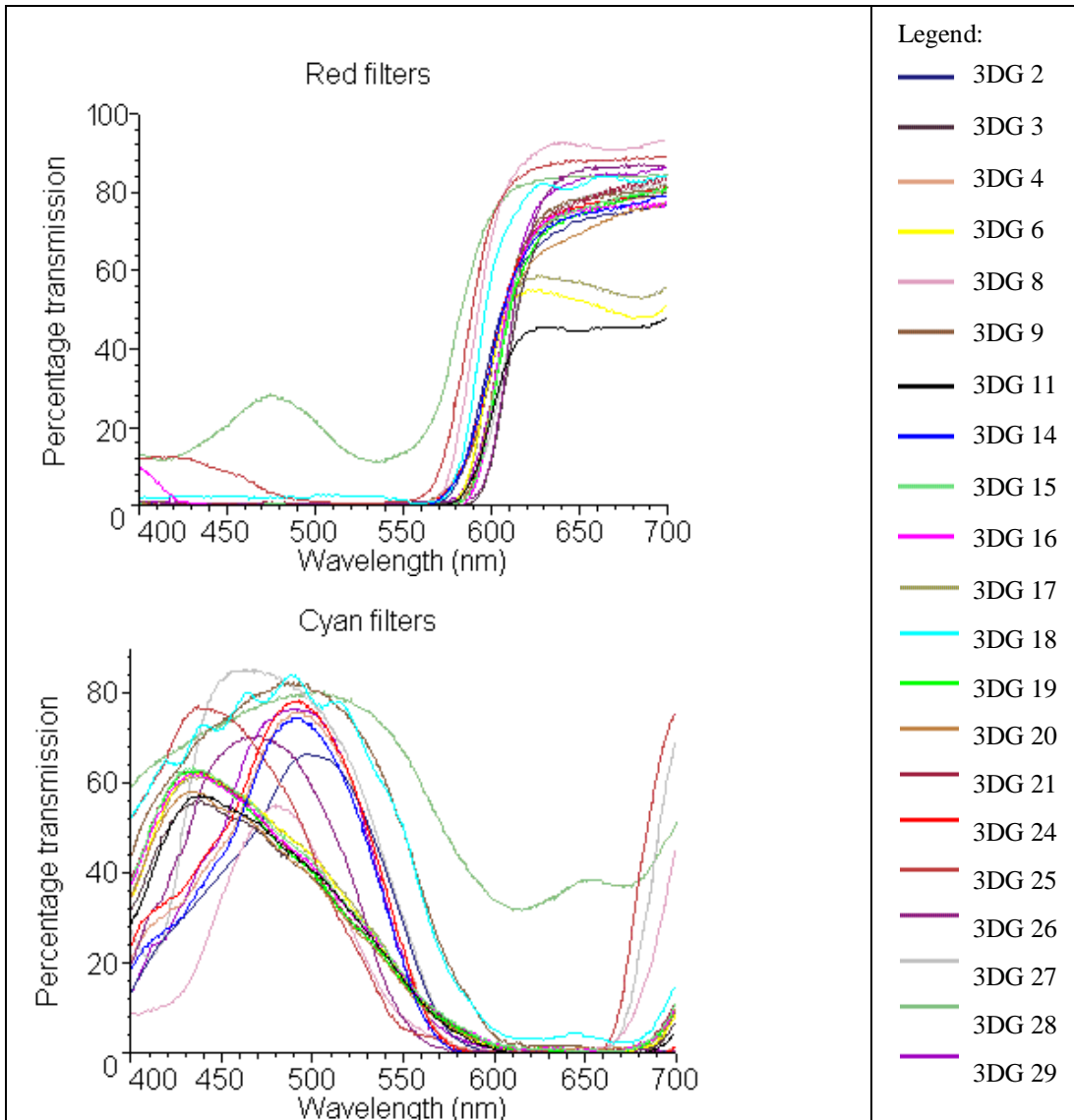


Figure 5: The spectral responses of the anaglyph filters (2 filters per set of glasses).

Figure 6 shows the individual spectral response for three selected pairs of glasses as an example of the variation between pairs of glasses. The red filter of glasses 3DG19 remains at close to 0% transmission from 400 to 570nm (encompassing the green and blue regions) whereas the red filter of glasses 3DG25 has significant leakage in this region (only being close to 0% transmission between 500 and 550 nm). The cyan filter of 3DG25 has a maximum transmission of ~80% in its required pass region, but its transmission also increases rapidly in the >650 nm region. The cyan filter of 3DG19 has a maximum transmission of ~60%, so it will appear dimmer than the cyan filter of 3DG25. The red and cyan filters of 3DG28 are particularly poor but this is understandable due to the use of printing ink.

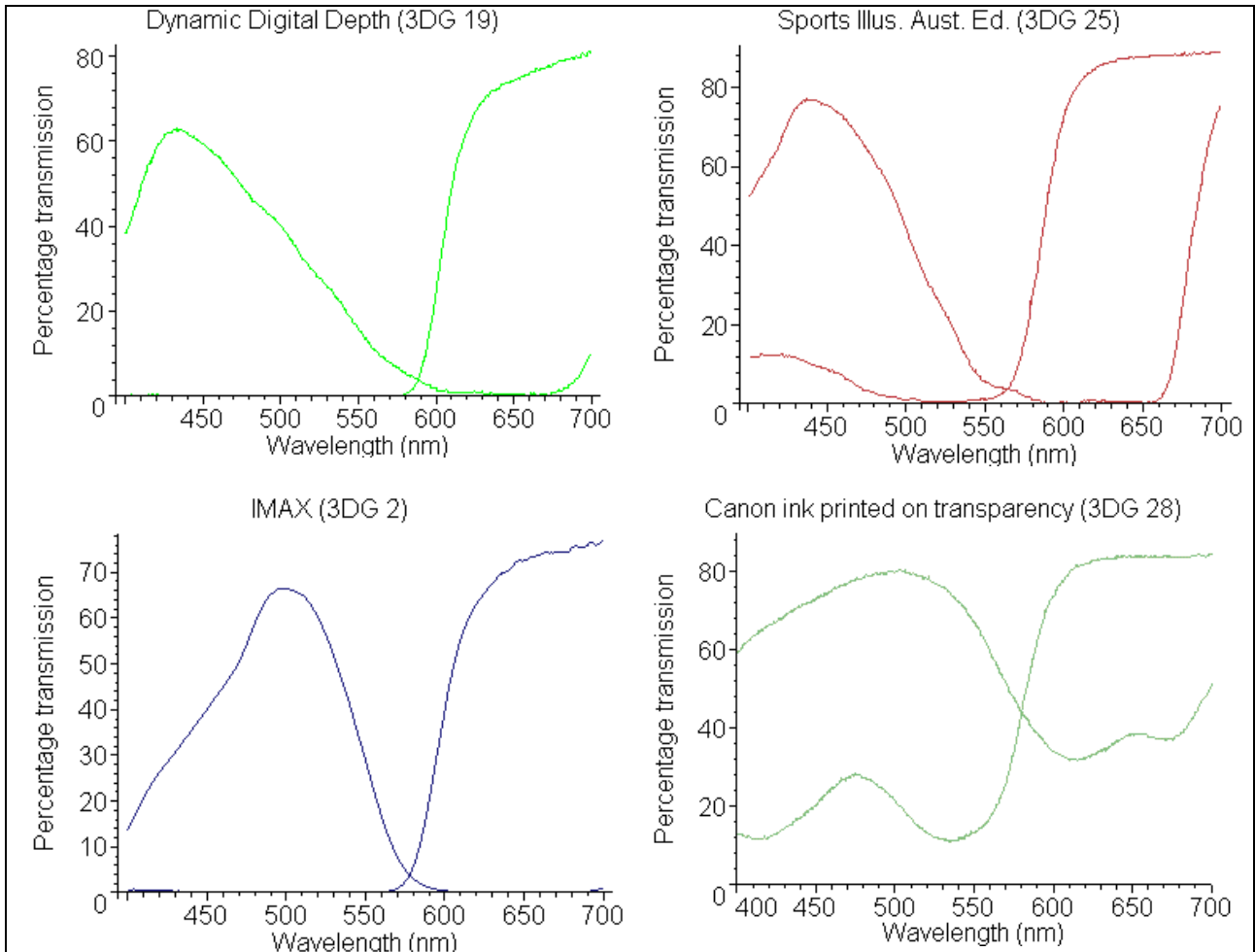


Figure 6: The spectral response of four selected pairs of anaglyph glasses.

3.3 Crosstalk calculation results

The crosstalk results (and uncertainty) calculated by the Maple program for the combination of displays and glasses listed are shown in Table 3. Uncertainties are estimated as 1σ mean error. Note that while the % crosstalk for a filter is a percentage, the overall crosstalk *factor* for a pair of glasses (being the sum of the two filter % crosstalk values) is not a percentage, just a number that allows the comparison of any glasses analysed by the program.

The Maple program also generates a separate table listing the % crosstalk for each individual filter. This allows the user to select the best filters from different glasses and combine them in order to obtain the lowest crosstalk available for that particular display from all available filters. Table 4 summarises this output into lists of the best glasses, best individual filters and corresponding crosstalk factor or percent for each display.

Table 3: Calculated Overall Crosstalk Factor (and uncertainty) for various anaglyph glasses in combination with various RGB display device when viewing *red/cyan* anaglyph 3D images. The lowest crosstalk combinations are highlighted in grey – the worst crosstalk results are highlighted in black. The table is sorted on overall crosstalk factor for CRT displays. Uncertainties are estimated as 1 σ mean error.

Glasses Number	Diamond CRT	Acer LCD Display	NEC3 1DMD Proj	Infocus 1DMD Proj	Epson 3LCD Proj	VT2 3LCD Proj	VT6 3LCD Proj	Boxlight2 3LCD Proj	Boxlight3 3LCD Proj
3DG 19	22.5 ± 0.3	41.6 ± 0.6	20.9 ± 0.3	8.9 ± 0.2	3.92 ± 0.08	4.66 ± 0.09	3.93 ± 0.08	4.21 ± 0.07	5.19 ± 0.09
3DG 16	23.1 ± 0.3	41.2 ± 0.6	20.1 ± 0.3	9.5 ± 0.2	4.58 ± 0.09	5.0 ± 0.1	4.7 ± 0.1	4.72 ± 0.08	5.8 ± 0.1
3DG 15	23.4 ± 0.3	43.0 ± 0.6	22.9 ± 0.3	11.0 ± 0.2	5.2 ± 0.1	6.3 ± 0.1	5.7 ± 0.1	4.85 ± 0.08	5.9 ± 0.1
3DG 21	24.8 ± 0.4	43.2 ± 0.6	22.9 ± 0.3	10.8 ± 0.2	5.15 ± 0.09	5.9 ± 0.1	5.5 ± 0.1	4.97 ± 0.08	6.3 ± 0.1
3DG 20	25.7 ± 0.4	45.7 ± 0.7	26.2 ± 0.4	13.7 ± 0.2	7.1 ± 0.1	8.6 ± 0.1	8.4 ± 0.2	5.57 ± 0.09	7.1 ± 0.1
3DG 11	27.0 ± 0.4	45.2 ± 0.7	28.0 ± 0.4	11.1 ± 0.2	4.03 ± 0.09	6.1 ± 0.1	4.4 ± 0.1	3.14 ± 0.06	4.59 ± 0.09
3DG 29	27.1 ± 0.4	47.2 ± 0.7	31.9 ± 0.4	14.9 ± 0.2	7.6 ± 0.1	10.3 ± 0.2	9.3 ± 0.1	4.81 ± 0.07	7.1 ± 0.1
3DG 27	27.5 ± 0.4	48.8 ± 0.7	33.4 ± 0.5	17.2 ± 0.3	9.0 ± 0.1	11.7 ± 0.2	11.2 ± 0.2	5.40 ± 0.08	8.1 ± 0.1
3DG 26	29.0 ± 0.4	49.7 ± 0.7	38.3 ± 0.6	26.0 ± 0.4	17.3 ± 0.3	20.7 ± 0.3	21.3 ± 0.3	9.4 ± 0.1	13.1 ± 0.2
3DG 03	29.7 ± 0.4	52.4 ± 0.7	37.2 ± 0.6	31.5 ± 0.5	19.3 ± 0.3	21.2 ± 0.3	23.5 ± 0.4	11.0 ± 0.2	14.5 ± 0.2
3DG 06	30.4 ± 0.4	48.8 ± 0.7	30.5 ± 0.4	12.6 ± 0.2	5.1 ± 0.1	7.5 ± 0.1	5.9 ± 0.1	4.04 ± 0.07	5.7 ± 0.1
3DG 14	31.3 ± 0.5	52.2 ± 0.7	49.9 ± 0.7	17.8 ± 0.3	7.5 ± 0.1	14.9 ± 0.2	9.6 ± 0.2	3.08 ± 0.06	5.25 ± 0.09
3DG 24	31.3 ± 0.5	52.2 ± 0.7	50.9 ± 0.7	18.2 ± 0.3	7.6 ± 0.1	15.0 ± 0.2	9.7 ± 0.2	3.15 ± 0.06	5.29 ± 0.09
3DG 09	36.2 ± 0.5	55.4 ± 0.8	54.7 ± 0.8	26.6 ± 0.4	13.5 ± 0.2	20.6 ± 0.3	16.1 ± 0.2	7.2 ± 0.1	9.3 ± 0.1
3DG 17	36.7 ± 0.5	53.6 ± 0.8	33.2 ± 0.5	17.0 ± 0.3	8.5 ± 0.1	10.7 ± 0.2	10.2 ± 0.2	6.13 ± 0.09	8.4 ± 0.1
3DG 08	39.1 ± 0.5	62.3 ± 0.9	73 ± 1	25.8 ± 0.4	11.2 ± 0.2	23.1 ± 0.3	14.5 ± 0.2	4.92 ± 0.08	7.0 ± 0.1
3DG 04	39.7 ± 0.6	57.7 ± 0.8	55.7 ± 0.8	24.2 ± 0.3	12.5 ± 0.2	20.0 ± 0.3	15.8 ± 0.2	5.87 ± 0.09	9.0 ± 0.1
3DG 02	42.5 ± 0.6	61.2 ± 0.8	53.1 ± 0.7	20.1 ± 0.3	9.0 ± 0.1	15.8 ± 0.2	11.8 ± 0.2	4.42 ± 0.07	7.0 ± 0.1
3DG 18	58.6 ± 0.8	75 ± 1	73.5 ± 1.0	45.5 ± 0.6	26.1 ± 0.4	31.8 ± 0.4	33.0 ± 0.5	16.8 ± 0.2	23.4 ± 0.3
3DG 25	62.7 ± 0.9	82 ± 1	92 ± 1	48.5 ± 0.7	31.5 ± 0.4	51.9 ± 0.7	42.6 ± 0.6	14.3 ± 0.2	20.2 ± 0.3
3DG 28	217 ± 2	197 ± 2	275 ± 3	169 ± 2	155 ± 2	190 ± 2	205 ± 2	92.9 ± 0.9	125 ± 1

Table 4: Optimal combinations of the measured displays and 3D glasses for a red/cyan image. When a blue or green filter has the lowest crosstalk, the lowest cyan filter is also given.

Display	Best glasses	Overall Crosstalk factor	Best red filter	% Crosstalk	Best cyan filter	% Crosstalk
Diamond CRT	“DDD”	22.5±0.3	DDD red	19.5±0.3	Reel 3D #1 cyan	2.20±0.03
Acer LCD	“Freddy’s...”	41.2±0.6	Freddy’s. red	34.3±0.5	IMAX cyan	5.63±0.08
NEC3 1DMD Proj	“Freddy’s...”	20.1±0.3	Freddy’s. red	15.4±0.3	Reel 3D #1 cyan	2.92±0.04
Infocus 1DMD Proj	“DDD”	8.9±0.2	DDD red	4.1±0.1	Reel 3D #1 cyan	0.71±0.01
Epson 3LCD Proj	“DDD”	3.92±0.08	DDD red	1.89±0.05	Reel 3D #1 cyan	0.324±0.005
VT2 3LCD Proj	“DDD”	4.66±0.09	DDD red	2.75±0.06	Reel 3D #1 cyan	0.408±0.007
VT6 3LCD Proj	“DDD”	3.93±0.08	DDD red	2.45±0.06	Reel 3D #1 cyan	0.427±0.007
Boxlight2 3LCD Proj	“Reel 3D #1”	3.08±0.06	DDD red	1.63±0.04	Reel 3D #1 cyan	0.480±0.008
Boxlight3 3LCD Proj	“3DG 11”	4.59±0.09	DDD red	2.57±0.05	Reel 3D #1 cyan	1.44±0.02

3.4 Validation

To check that the results from the crosstalk model were sensible, a first order validation test was performed using a CRT display. A pair of rectangles, one red (R=255, G=B=0), one cyan (R=0, G=B=255), which shared an edge were displayed on a CRT screen. An anaglyph filter was held over the intersection. Ideally, if the filter was red, the red half would be bright red and the cyan half would be black (or vice versa for a cyan filter). To a first order approximation, the closer the complimentary side of the filter was to black, the lower the expected percentage crosstalk through that filter.

The model takes into account the brightness of the transmitted colour too, which can also be roughly guessed by the eye. The validation involved holding up two filters of the same colour (eg red) at the same time, and seeing which had a blacker complimentary colour, and how bright the matching colour was, and then estimating which pair of glasses would have a lower % crosstalk. Some filters were very easy to rank, eg the red 3DG18 ($19.5\pm 0.3\%$), 3DG02 ($46.9\pm 0.7\%$) and 3DG04 ($60.5\pm 0.8\%$). The eye's first order observations agree reasonably well with the model being used except where the % crosstalk difference was $<2\%$ at which point many of the glasses were difficult to arrange into sequence by eye anyway. One characteristic the eye has, that the model does not, is the tendency for some colours to seem brighter or dimmer than they really are when placed near certain other colours.⁹ Perhaps this effect distorts perceived brightness enough to overwhelm small differences in crosstalk.

4. DISCUSSION

It is worth mentioning that even a perfect filter (one that transmits 100% of light in the desired wavelength domain and 0% outside it) will have crosstalk if the display's green channel spectral output, say, overlaps the filter's red domain. Hence the perceived crosstalk will vary between display devices, even for the same pair of filters. Glasses will generally produce low ghosting figures if the filters have a low crossover point as well as $\approx 0\%$ transmission outside their desired wavelength region. The wavelength of the crossover point is also important - Ideally, the wavelength of the glasses' crossover point will be close to that of the display device's crossover point.

When choosing a display and filter combination, several aspects must be considered. Firstly, large amounts of crosstalk degrade the quality of the 3D experience, and the images become more difficult for the brain to fuse. This project aimed to highlight possible low-crosstalk combinations, so crosstalk could be reduced. Secondly, intensity is important. If the filter cuts out most of the light, the image will be very dim and hard to see. Lower light levels also make the effect of even small ghosting levels proportionally greater than they might otherwise be. A brightness imbalance between left and right eye can also result in the Pulfrich effect whereby horizontal motion can be interpreted as binocular depth - which is generally undesirable. Brightness levels and imbalance have not been considered in this paper.

Thirdly, colour must be considered. Truly full colour stereoscopic images are not possible with anaglyphs, but a properly constructed anaglyph using complimentary colours can approximate a full colour image. This distorted colour image is usually referred to as a "pseudo-colour anaglyph" or a "polychromatic anaglyph" rather than a "full colour anaglyph". If a non-complimentary combination is used, (e.g. red/blue or red/green) pseudo-colour anaglyphs are impossible, as a large portion of the visible spectrum is missing. The overall image may also be darker. This paper has only considered red/cyan anaglyphs.

For red/cyan anaglyphic 3D images, the minimum overall crosstalk factor in CRTs was very high at 22.5 ± 0.3 . Even mixing and matching the best filters would only reduce the crosstalk factor to just over 21. This is despite the fact that many of the glasses tested were specifically made for watching 3D videos on television CRT screens. The main difficulty here is not the filters, but the large overlapping wavelength domains of the CRT phosphors. This could be reduced by using red/blue only anaglyphs on CRTs, since the crosstalk factor for them decreases to 5.89 ± 0.09 , but this entails other problems as discussed in the previous two paragraphs. The Acer Laptop LCD that was tested has very high crosstalk factors with all tested glasses. Again, there is little a filter can do when the spectral output of the display device is active across so many different wavelengths; Figure 3 shows that when showing a red screen only, for example, the output includes wavelengths all the way into the blue region. It would be near impossible to obtain a filter that matches well with this output. 3-chip LCD projectors exhibited the lowest overall crosstalk factor of all the displays tested. Single chip DMD based projectors (NEC3 and Infocus) gave crosstalk results that were worse than 3-chip LCD projectors but better than CRT displays. These variations between displays are understandable given that each of the different technologies (CRT, LCD, LCD projector, and DMD) use different methods to create the three colour primaries.

We have defined a cyan filter as one that passes a reasonable amount of blue and green (but very little red). If the filter passes blue but very little green and red, it is considered a blue filter. We realise this definition is somewhat approximate - to be more scientific the relative transmission of each of the colour primaries through the filters could be calculated and the filters classified on this bases. This data would also be useful for evaluating the colour balance of the image for image quality purposes and evaluating possible Pulfrich effects. It is also worth noting that the colour

balance of the display will also have an effect on ghosting. It can be seen that a slight colour balance difference between Boxlight2 and Boxlight3 has produced a different set of ghosting results (see Figure 4 and Table 3). In this study we have used the default colour balance of the display, however colour balance effects could also be studied in more detail.

It should be noted that this study only reports on emissive displays. Some of the glasses were intended for use with printed anaglyphs, and hence may perform better with printed anaglyphs than emissive displays. However, testing of anaglyphic 3D ghosting with printed anaglyphs is not reported here.

5. CONCLUSION

This study has revealed that crosstalk in anaglyphic 3D images can be minimised by the appropriate choice of anaglyphic 3D glasses. The study has revealed that there can be considerable variation in the amount of ghosting present when an anaglyphic 3D display is viewed with different anaglyphic 3D glasses.

The study has also revealed that there is considerable variation in the amount of anaglyphic ghosting exhibited by different types of displays – 3 chip LCD projectors were found to offer considerably lower anaglyphic ghosting than the other types of displays tested in this study (CRT displays, LCD screens, and DMD projectors).

The anaglyphic ghosting model works well and generates outputs which appear to agree with subjective assessments of anaglyphic 3D ghosting. The model currently does not take into account the more complicated aspects of colour vision, such as hue perception. However as technological advances, such as functional MRI, are increasing our ability to understand the anatomy, physiology and perception of colour, and non-linear modelling continues⁹, when a complete model is perfected and agreed upon, the program can be modified to include it. The model also does not take into account dimness, brightness imbalance, or pseudo-colour considerations, which are also important to the anaglyph 3D experience.

It should be noted that the results of this paper are not intended to be a leaderboard of one glasses manufacturer versus another - we haven't tested all glasses from all manufacturers, nor have we tested a large sample of each manufacturers glasses. This paper does however highlight that there is significant variation between different anaglyph 3D glasses and displays. Further crosstalk optimisation may be possible by using the model and working with 3D glasses manufacturers.

REFERENCES

1. Tan, Stanley (2001), *Sources of Crosstalk in 3D Stereoscopic Displays*, Centre for Marine Science & Technology, Curtin University of Technology, Bentley, Western Australia.
2. Woods, Andrew & Tan, Stanley (2002), "Characterising Sources of Ghosting in Time- Sequential Stereoscopic Video Displays", presented at *Stereoscopic Displays and Applications XIII*, published in *Stereoscopic Displays and Virtual Reality Systems IX*, Proceedings of SPIE Vol. 4660, pp. 66-77, San Jose, California, 21-23 January 2002.
3. Konrad, J (2000), "Cancellation of image crosstalk in time-sequential displays of stereoscopic video", in *IEEE Transactions on Image Processing*, Vol. 9, No. 5, pp 897-908.
4. Sanders, William & McAllister, David (2003) "Producing Anaglyphs from Synthetic Images", presented at *Stereoscopic Displays and Applications XIV*, published in *Stereoscopic Displays and Virtual Reality Systems X*, Proceedings of SPIE Vol. 5006, pp 348-358, Santa Clara, California, 21-23 January 2003.
5. Lovy, D (1996), *WINDIG 2.5*, Email: lovy@scsun.unige.ch, Dept of Physical Chemistry, University of Geneva, Switzerland.
6. Hollins, Martin (1990) *Medical Physics*, Thomas Nelson & Sons, London, pp26-27.
7. MacDonald & Burns (1975) *Physics for the Life and Health Sciences*, Addison Wesley, USA.
8. Ohno, Yoshi (1999), *OSA Handbook of Optics, Volume III: Visual Optics and Vision*, National Institute of Standards and Technology, Maryland USA.
9. Connolly, C (2003), "Colorimetry: Anatomical Studies Advance", *Photonics Spectra*, Issue Aug 2003, pp 56-66.
10. *HCinema* (not dated), [online], Available: <http://www.projektoren-datenbank.de/pro> [accessed 21st Dec 2003] "Projektoren-Datenbank", "Abkürzungen", "Lexikon", "DLP Projektoren", "LCD Projektoren".

Paper 11 A. J. Woods (2005) "Compatibility of Display Products with Stereoscopic Display Methods" International Display Manufacturing Conference (IDMC), pp. 290-293, Taiwan, February 2005.

Compatibility of Display Products with Stereoscopic Display Methods

Andrew J. Woods

Centre for Marine Science & Technology, Curtin University of Technology,
GPO Box U1987, Perth 6845 AUSTRALIA.

ABSTRACT

Stereoscopic Imaging is coming of age – new high-resolution stereoscopic displays and related stereoscopic equipment are readily available, and a wide range of application areas is making use of stereoscopic imaging technologies. Unfortunately, new display products are not always compatible with existing stereoscopic display methods. This paper discusses the compatibility of current display products with various stereoscopic display methods.

INTRODUCTION

Many stereoscopic specific display products are now readily available in the marketplace. Vendors include Sharp, StereoGraphics, Opticality (formerly X3D), SeeReal, Dimension Technologies Inc. (DTI), VREX, Christie Digital, Barco, and many others. A wide range of supporting stereoscopic compatible hardware and software is also readily available for creating, transmitting, storing, and serving the stereoscopic images (and video) for display on these stereoscopic display products. But more importantly, a wide range of application areas ranging from science to entertainment are increasingly making use of these stereoscopic imaging technologies. For example, stereoscopic 3D DVDs are widely commercially available, thousands of commercially available PC games can be played in stereoscopic 3D by the use of a stereoscopic driver from nVidia, and the 2004 NASA Mars rovers (Spirit and Opportunity) are each fitted with four stereoscopic cameras.

The Cathode Ray Tube (CRT) has been the dominant display technology for many years, however a number of new display technologies have begun to dominate the new display market in recent years (e.g. Liquid Crystal Displays (LCD), Plasma, DLP[†], and many others). These new display products use different display principles and hence their compatibility with various stereoscopic display methods varies from good to bad.

STEREOSCOPIC DISPLAY METHODS

There are many methods available to display stereoscopic images – all of these methods rely on some underlying technique to present each of a person's eyes with a different perspective image. The "underlying technique" is usually based on a method of coding and decoding the multiple stereoscopic views in the same light field – these can be colour, polarisation, time, and/or spatial separation. Summarised below are the main stereoscopic display methods which are currently used in commercial displays:

[†] Digital Light Processing. Developed by Texas Instruments. Also known as the Digital Micro-mirror Device (DMD).

TIME-SEQUENTIAL(FIELD-SEQUENTIAL)

In this method, left and right perspective images are shown alternately(sequentially)on the same display surface. The observer wears a pair of liquid crystal shutter (LCS) 3D glasses whose lenses switch on and off in synchronisation with the left and right perspective images shown on the display such that the left eye only sees the left perspective images and the right eye only sees the right perspective images.

This method is more commonly known as 'field-sequential' or 'frame-sequential' because it is a sequence of fields or frames. It is described here generically as 'time-sequential' because it is a time-sequential sequence of left and right perspective images(which can either be frames or fields).

Time-sequential stereoscopic image quality is dependent upon the persistence and refresh rate of the display and also the quality of the particular LCS 3D glasses used¹. Shorter persistence pixels and faster refresh rates produce better time-sequential stereoscopic image quality. Important 3D image quality factors in time-sequential 3D are ghosting and flicker.

LENTICULAR, PARALLAX BARRIER AND PARALLAX ILLUMINATION

These three stereoscopic display methods are similar in that they require a display whose pixels are spatially-fixed - they rely on the use of an optical element which must accurately align with the pixels of the display. The optical element works to create viewing zones where particular groups of pixels (corresponding to a particular view) are only visible from a particular direction. If an observer's eyes are in two different zones, a stereoscopic image can be observed without the need for 3D glasses.

In the case of Lenticular, the optical element consists of a series of vertical lenslets (lenticules) fitted over the face of the display.

In the case of Parallax Barrier, the optical element consists of a series of opaque vertical strips which are placed over the face of the display.

In the case of Parallax Illumination, a backlight made up of vertical strips of light is fitted behind the display.

In two view systems there is one vertical lenticule/ barrier strip/light strip per two-pixel column. The fitting of the optical element requires accurate registration between the display's pixels and the optical element, hence it is not usually an end-user option. Lenticular and Parallax

Barrier methods can be applied to rear projection displays but are not currently implemented commercially.

SPATIALLY MULTIPLEXED POLARISED

In this method an optical sheet is placed over the face of the display which polarises alternate pixels of the display in orthogonal polarisation states². The viewer wears a pair of polarised 3D glasses to view the stereoscopic image on screen.

This method will only work with displays which have spatially-fixed pixels. The fitting of the optical element requires accurate registration between the display's pixels and the optical element, hence it is not usually an end-user option.

POLARISED PROJECTION

With polarised projection, two displayed images are optically overlaid (e.g. two video projectors projecting onto a single silvered screen) and polarisation is used to code and decode the two views. The observer wears polarised 3D glasses to see the stereoscopic image.

ANAGLYPH

This stereoscopic display method uses colour to separate the two perspective views. Usually the left perspective image is displayed in the red channel of the display and the right perspective image is displayed in the blue and green channels of the display. The observer(s) wears glasses with the left lens red and the right lens cyan. Other combinations of colour primaries are possible.

The anaglyph method is widely used because it is compatible with all full colour displays, however the quality of the perceived stereoscopic image is relatively poor as compared to other stereoscopic methods and truly full-colour stereoscopic images cannot be achieved using anaglyph.

A recent study revealed that anaglyph image quality was dependent upon the spectral colour purity of the display and the glasses³. The study ranked the following displays from best to worst for anaglyph image quality: 3-chip LCD projector, 1-chip DLP projector, CRT display, LCD display.

OTHER METHODS

There are many more methods of displaying stereoscopic images available (plus variations of the methods summarised above), however a full description of all possible stereoscopic display methods is beyond the scope of this paper. For further information, the interested reader is referred to the proceedings of the Stereoscopic Displays and Applications conference⁴.

STEREOSCOPIC COMPATIBILITY

Several factors determine whether a particular display is compatible with a particular stereoscopic display method. These factors include: native polarisation, image pe-

rsistence (sometimes referred to as response time or refresh rate), colour purity, and whether the pixels are spatially-fixed.

The stereoscopic compatibility of the fundamental technology used in a range of different displays is summarised in Figure 1 and described below:

CRT

CRT display technology is fundamentally compatible with time-sequential, polarised projection, and anaglyph methods but incompatible with fixed-pixel methods[‡].

LCD

LCDs are compatible with fixed-pixel methods[‡] (although some care must be taken with native polarisation and the arrangement of the individual colour primary pixels) and polarised projection methods. The colour purity of different LCDs has been found to vary considerably from display to display hence anaglyph compatibility varies from poor to good (notwithstanding the limitations of anaglyph)³.

LCDs are usually incompatible with time-sequential 3D – their long persistence (low refresh rate) usually causes significant stereoscopic image ghosting. Refresh rates of LCDs are steadily improving hence this problem may soon be overcome.

PLASMA

Plasma display technology is fundamentally compatible with time-sequential, and fixed-pixel methods[‡]. Anaglyph compatibility is untested by this author but it is expected to be similar to CRTs. Plasma is currently only used in direct-view displays.

DLP

DLP display technology is fundamentally compatible with time-sequential and polarised projection methods. DLP technology is currently only used in projection displays and hence it is not usually considered for fixed-pixel methods[‡]. The colour purity of different DLP displays varies considerably (usually depending upon the spectral quality of the colour wheel) hence anaglyph compatibility varies from poor to good³.

OTHER DISPLAY PRODUCTS

A range of other display products is also available (or becoming available) in the market, including LED (Light Emitting Diode), OLED (Organic Light Emitting Diode), FELCD (Ferro-Electric Liquid Crystal Display), LCoS (Liquid Crystal on Silicon), and many others. Their compatibility is not discussed in this paper but their own fundamental display properties will determine their compatibility with the various stereoscopic display methods.

[‡] Fixed-Pixel Methods = Lenticular, Parallax Barrier, Parallax Illumination, and Spatially Multiplexed Polarised methods.

	<i>Time-Sequential</i>	<i>Lenticular</i>	<i>Parallax Barrier</i>	<i>Parallax Illumination</i>	<i>Spatially Multiplexed Polarised</i>	<i>Polarised Projection</i>	<i>Anaglyph</i>
<i>Direct View</i>							
<i>CRT</i>	√	X	X	X	X	n/a	<i>Moderate</i>
<i>LCD</i>	X*	√	√	√	√	n/a	<i>Poor to good</i>
<i>PLASMA</i>	√	√	√	X	√	n/a	?
<i>DLP</i>	n/a	n/a	n/a	n/a	n/a	n/a	n/a
<i>Projection (Front and Rear)</i>							
<i>CRT</i>	√	n/a	n/a	n/a	X	√	<i>Moderate</i>
<i>LCD</i>	X*	n/a*	n/a*	n/a	√	√	<i>Poor to good</i>
<i>PLASMA</i>	n/a	n/a	n/a	n/a	n/a	n/a	n/a
<i>DLP</i>	√	n/a*	n/a*	n/a	X	√	<i>Poor to good</i>

Fig. 1. Summary of display method compatibility with stereoscopic display methods. (* = see text)

DISCUSSION

A good number of stereoscopic specific display products are now commercially available. However, there are instances where a consumer would like to use their existing display to view stereoscopic 3D images or video. The stereoscopic display methods which can be most easily retrofitted to an existing display by an end user are anaglyph and time-sequential. Anaglyph will work with all current displays however its 3D image quality is relatively poor. Time-sequential provides much better 3D image quality, however there are several mitigating factors which may prevent that particular display from being used with time-sequential 3D (even though the fundamental display technology may be compatible with time-sequential 3D display). These mitigating factors usually relate to video processing functions performed in the particular display product - such as interlaced to progressive conversion, 50 to 100Hz conversion, frame rate conversion, and image scaling.

INTERLACED TO PROGRESSIVE CONVERSION

Interlaced to progressive conversion (sometimes called deinterlacing) is necessary for displays which are natively progressive (LCD, Plasma and DLP). Several different algorithms for interlaced to progressive conversion are currently in common usage in different display products, and unfortunately some of these algorithms are incompatible with time-sequential 3D (they disrupt the 3D content by mixing the fields). In some instances 'interlaced to progressive' converters also implement reverse 3:2 pulldown however this is also incompatible with time-sequential 3D video. Fortunately there is an interlaced to progressive conversion algorithm which is compatible with field-sequential 3D and a number of display products (and DVD players) use this particular algorithm.

If it is found that a particular display product uses a deinterlacer which is incompatible with field-sequential 3D, the internal deinterlacer can often be bypassed by using an external (3D friendly) deinterlacer, and inputting this signal into the particular display product.

50 TO 100Hz CONVERSION

Some displays include another form of video processing (50 to 100Hz conversion - sometimes called '100Hz Digital Scan') designed to reduce the amount of visible flicker in a television image. Most display products which include 50 to 100Hz conversion use an algorithm which is incompatible with time-sequential 3D, however there is a 50 to 100Hz conversion algorithm which is compatible with time-sequential 3D which could be relatively easily included to maintain time-sequential 3D compatibility.

50 to 100Hz conversion is a very good thing for time-sequential 3D because it overcomes the flicker problem normally associated with viewing field-sequential 3D video (particularly at 50Hz)⁴, however a 3D compatible algorithm needs to be used.

(DLP) FRAME RATE CONVERSION

Some models of DLP projector have a fixed internal operation frequency (usually 60Hz) - a frame rate converter is used to convert a video input signal of any other frame rate to the native frequency of the DLP engine. Unfortunately frame rate conversion usually disrupts the 3D content of a time-sequential 3D video signal. In order to achieve 3D compatibility with these devices, it is necessary to input time sequential 3D video into these display devices at a field-rate or frame-rate which matches the internal operating frequency of the DLP engine.

IMAGE SCALING

In order for display products which have a fixed pixel resolution to display video from a different source resolution, it is necessary for the input video signal to be up-scaled or down-scaled to the resolution of the display. Image scaling will likely disrupt the 3D compatibility of fixed-pixel stereoscopic display methods[‡] but should not affect time-sequential 3D.

For optimal 3D compatibility, it would be desirable if display products which included the video processing functions described above also provided a menu option

which either allowed the device to be switched into a time-sequential 3D compatible mode or disabled the particular video processing function. Interestingly some HD television sets do include a menu option called “game mode” which puts the television into a display mode which is compatible with field-sequential 3D NTSC.

It is also problematic that display product documentation does not usually list whether that display is time-sequential 3D compatible. Third-party listings of products that are compatible and incompatible with time-sequential 3D video are appearing and this should be encouraged.

FIELD-SEQUENTIAL 3D NTSC/PAL

As mentioned in the introduction, a wide range of 3D DVDs is now commercially available – many of these are in field-sequential format (a defacto standard for time-sequential 3D on NTSC and PAL video⁶). Unfortunately a high percentage of new display products are incompatible with time-sequential 3D (in their default mode) and hence more care must now be taken to check or ensure field-sequential 3D will work with particular display products.

Although SD (Standard Definition) video standards such as NTSC and PAL are on the road to retirement, they will remain with us for some time as we gradually transition to HDTV and other formats. Field-sequential 3D will likely remain a useful format during this transition period.

CONCLUSION

The market for stereoscopic compatible display products is increasing and many new stereoscopic specific display products are now available in the market place. This paper has summarised the compatibility of a selection of stereoscopic display methods with a range of display product technologies.

The biggest stereoscopic compatibility problem at the current time is with the time-sequential 3D method - a high percentage of new display products being released are incompatible (in their default mode) with time-sequential 3D. In some cases this incompatibility is due to fundamental display technology limitations (e.g. LCD) but in some cases it is due to the implementation of

advanced video processing features which disrupt the 3D video signal (in some cases this could be relatively easily corrected).

Display manufacturers need to be aware of the growing stereoscopic imaging market and the potential for their display products to be used in stereoscopic display applications.

ACKNOWLEDGEMENTS

The author would like to thank the staff at West Coast Hi-Fi in Cannington, Western Australia for their help in allowing a range of new display products to be tested for stereoscopic compatibility.

REFERENCES

1. A.J. Woods, and S.S.L. Tan (2002) "Characterising Sources of Ghosting in Time-Sequential Stereoscopic Video Displays", in *Stereoscopic Displays and Virtual Reality Systems IX*, Proceedings of SPIE Vol. 4660, San Jose, California, January 2002. www.curtin.edu.au/cmst/publicat/2002-09.pdf
2. S. Faris (1994) “Novel 3-D stereoscopic imaging technology” in *Stereoscopic Displays and Virtual Reality Systems*, Proceedings of SPIE vol. 2177, San Jose, California, February 1994.
3. A.J. Woods, and T. Rourke (2004) "Ghosting in Anaglyphic Stereoscopic Images", in *Stereoscopic Displays and Virtual Reality Systems XI*, Proceedings of SPIE-IS&T Electronic Imaging, SPIE Vol. 5291, San Jose, California, January 2004. www.curtin.edu.au/cmst/publicat/2004-08.pdf
4. The proceedings of the Stereoscopic Displays and Applications conference are published as *Stereoscopic Displays and Virtual Reality Systems*, Proceedings of SPIE, Bellingham, Washington, USA. www.stereoscopic.org/proc
5. A.J. Woods, T. Docherty, and R. Koch, (1991) "The Use of Flicker-Free Television Products for Stereoscopic Display Applications", in *Stereoscopic Displays and Applications II*, Proceedings of SPIE Vol. 1457, San Jose, California, February 1991. www.curtin.edu.au/cmst/publicat/1991-18.pdf
6. “Proposed Standard for Field-Sequential 3D Television” www.stereoscopic.org/standards

Paper 12 A. J. Woods, T. Rourke, K. L. Yuen (2006) "The Compatibility of Consumer Displays with Time-Sequential Stereoscopic 3D Visualisation" (Invited Plenary Paper), in Proceedings of the K-IDS Three-Dimensional Display Workshop 2006, pp. 7-10, Seoul National University, Seoul, South Korea, 21 August 2006.

The Compatibility of Consumer Displays with Time-Sequential Stereoscopic 3D Visualisation

Andrew J. Woods, Tegan Rourke, Ka Lun Yuen

Centre for Marine Science & Technology, Curtin University of Technology,
GPO Box U1987, Perth WA 6845, Australia
Phone: +61 8 9266 7920, Fax: +61 8 9266 4799, E-mail: A.Woods@cmst.curtin.edu.au

Abstract

This paper summarises two recent studies that investigated the suitability of LCD monitors and DLP projectors for use with the time-sequential stereoscopic 3D display method. Fifteen DLP projectors were found that would work with 85Hz time-sequential stereoscopic display, however none of the LCD monitors tested could be used with the conventional time-sequential stereoscopic display method.

1. Introduction

For several years the dominant method for high-quality stereoscopic viewing at personal workstations has been Liquid Crystal Shutter (LCS) 3D glasses on a CRT monitor. A similar process was also used with (3 gun) CRT¹ projectors. However, the CRT is a dying breed and is steadily being replaced by LCD¹ desktop monitors, and in the projection arena, LCD and DLP¹ projectors.

While it used to be reasonable to assume that LCS 3D glasses would work with almost any user's desktop monitor (because it was likely a CRT), the multitude of new (non-CRT) display technologies in the market today means that it is now not easy to know if a particular user's desktop monitor will work with time-sequential stereoscopic display [1].

This is also happening at a time when there is increased interest and activity in stereoscopic imaging and viewing. Users are therefore often interested to know whether their existing display devices can be used for stereoscopic display purposes.

Although the anaglyph 3D method can be used with most new display devices, its quality is usually fairly poor. In contrast, the time-sequential stereoscopic display technique can produce a higher quality

stereoscopic image but it is not compatible with all consumer displays. The time-sequential technique (aka: field-sequential, frame-sequential, alternate field, and sometimes active stereo) works by displaying an alternating sequence of left and right perspective images on the display whilst the user is wearing a pair of LCS 3D glasses. The LCS 3D glasses are driven in synchronisation with the displayed images such that the left eye sees only the left perspective images and similarly for the right eye.

2. LCD Monitors

Historically, LCD monitors have not been usable for time-sequential stereoscopic 3D visualisation due to their slow pixel response rate. With LCD pixel response rates for some monitors now just a few milliseconds it is reasonable to ask whether it is now possible to achieve time-sequential stereoscopic 3D viewing on LCDs.

We tested 15 different LCD monitors to establish their level of compatibility with time-sequential stereoscopic display. Five main properties of LCDs and/or LCS 3D glasses were identified that determine the stereoscopic image quality of time-sequential stereoscopic 3D viewing on LCD monitors [2]:

- LCD and LCS Native Polarisation
- LCD Refresh Rate
- LCD Pixel Response Rate
- LCD Image Update Method
- LCS Duty Cycle

With regard to the above list, if the native polarisation axes of the LCS glasses and the LCD display are orthogonal, the image in that eye will be dark, but this can be easily fixed by using quarter wave or half wave retarders on the glasses.

The refresh rate will determine whether the time-sequential image will be seen with flicker – the higher the frequency the better – 100Hz is usually considered to be the lowest refresh rate required for totally flicker-free operation. The highest refresh rate on the LCD monitors that we tested was 85Hz.

¹ CRT = Cathode Ray Tube, LCD = Liquid Crystal Display, DLP = Digital Light Processing.

If the LCD pixel response rate is greater than the time period of one frame, the pixel will not be able to stabilise in one state before the next time-sequential frame is drawn. With some LCD monitors now providing a pixel response rate of just a few milliseconds, there is sufficient time for each pixel to stabilise within the time period of one frame, but there is another property of (some/most) LCD monitors that prevents them being used for conventional time-sequential stereoscopic display.

In all of the LCDs that we tested, a new image is written to the LCD one line at a time from the top of the screen to the bottom [3]. The time duration to update the whole screen was close to the time period of one frame. This scan-like image update method is illustrated in Figure 1. The vertical axis shows the vertical position on the LCD panel. The horizontal axis shows time. The thin diagonal line represents the addressing of each row of the LCD.

It is evident from Figure 1 that there is no one time when a single image is shown exclusively on the

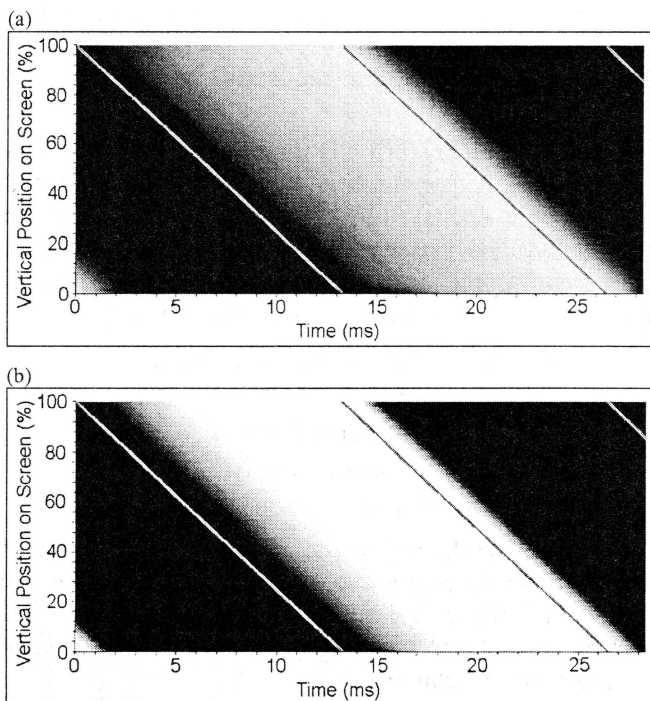


Figure 1: Time domain response of two LCD panels alternating between black and white at 75Hz for (a) a slow pixel response rate panel (21.7ms)² and (b) a fast pixel response rate panel (5.7ms)¹.

² Black-to-White (BTW) plus White-to-Black (WTB) transition time as measured between 10% and 90% thresholds.

whole LCD panel. This means that there is no time when the shutters in LCS glasses could open and reveal exclusively a single perspective image.

In conventional time-sequential systems, LCS glasses are usually driven at ~50% duty cycle (the left shutter is open half of the time and closed the other half of the time, and vice versa for the right shutter). As can be seen from Figure 1, if a pair of LCS glasses operating at 50% duty cycle are used to view a time-sequential image on one of these LCDs, there would be a significant amount of crosstalk between the two perspective views.

We found that by switching the LCS glasses with a very short duty cycle, letterboxing the image (black strips at the top and bottom of the screen), and using a short pixel response rate LCD monitor, we were able to achieve a stereoscopic image on part of the screen, however the image was very dim and is therefore not a practical long-term solution [4][5].

3. DLP Projectors

The capability for some DLP projectors to be used with time-sequential stereoscopic display has been known for some time [6]. This is due to the extremely fast pixel response time (~2µs) of the DMD (Digital Micro-mirror Device) chip [7], the fact that the whole of the screen updates at once, and the capability of some DLP projectors to correctly display an alternating sequence of discrete left and right images.

Several DLP projectors are already available in the marketplace that are advertised as being “stereo-ready” and capable of 120Hz time-sequential stereoscopic display – available from suppliers such as Barco (Galaxy series), Christie Digital (Mirage series), and Infocus / Lightspeed Design Group (DepthQ).

A lesser known fact is that some consumer grade single-chip DLP projectors are also compatible with time-sequential stereoscopic display – although at lower refresh rates.

We tested 44 consumer grade single-chip DLP projectors to determine their level of compatibility with time-sequential stereoscopic display. Each projector was tested to establish: (1) whether the colour wheel synchronised with the incoming video signal, (2) whether there was crosstalk between alternate fields or frames, (3) the maximum frequency

at which the projector would work in stereo, (4) the time delay between the incoming video signal and the displayed images, (5) whether the projector converted interlaced video sources to progressive format in a 3D compatible way, and (6) the colour wheel speed at various video input frequencies.

Fifteen projectors were found to work well at up to 85Hz stereo in VGA mode. 23 projectors would work at 60Hz stereo in VGA mode. 35 projectors were found to be compatible with progressive component video (480P and 576P) at refresh rates of 60Hz and 50Hz [8][9]. In controlled circumstances there will only be a slight amount of flicker visible with 85Hz stereo. Ordinarily, however, 60Hz and 50Hz stereo produce significant flicker³.

The projectors that were found to be compatible with 85Hz VGA time-sequential stereoscopic display are listed in Table 1. The table also lists the time offset (from the trailing edge of the vertical sync signal to the start of image display), and the native resolution of the projector.

Table 1: Consumer DLP projectors found to be compatible with 85Hz VGA time-sequential stereoscopic display.

Projector Make/Model	Time Offset (ms)	Resolution
Acer PD322	0.96	1024x768
Acer PD523	0.96	1024x768
Acer PH110	0.31	854x480
BenQ MP610	0.58	800x600
BenQ PB6240	0.55	1024x768
Boxlight Raven	not measured	800x600
Casio XJ-360	0.35	1024x768
NEC LT35	0.42	1024x768
Optoma EP719	not measured	1024x768
Optoma EP739	not measured	1024x768
Plus U4-237	not measured	1024x768
Plus U5	0.94	1024x768
Sharp XR-10X	0.30	1024x768
Toshiba TDP-S8	0.53	800x600
Yamaha DPX-530	0.42	1024x576

The time offset is important because if the time-offset is significant, and the switching of the LCS glasses is

³ Perceived flicker can be reduced by reducing image brightness and room brightness.

not adjusted accordingly, a significant amount of image crosstalk could occur. The largest time offset measured at 85Hz was 0.96ms, which corresponds to 8% of the time period for one frame – this could result in a noticeable amount of crosstalk if not corrected. A custom LCS glasses driver was developed as a part of this project to allow the switching of the LCS glasses to be time-offset by an adjustable amount.

More details about compatible and incompatible consumer projectors will be available in [8] and [9]. The 120Hz stereo-ready projectors do not appear in Table 1 and can be found by visiting the websites of the companies listed previously.

One other aspect of interest about the operation of most of the 85Hz capable projectors listed above is that the colour wheel speed drops down from 2x at

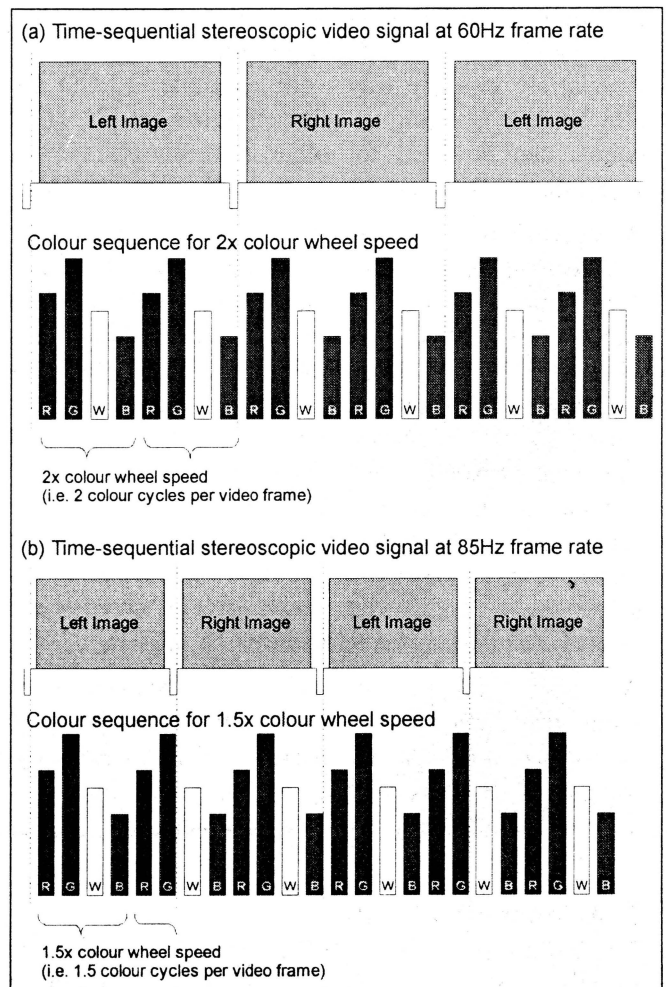


Figure 2: Illustration of (a) 2x and (b) 1.5x colour wheel speed at frame rates of 60Hz and 85Hz respectively (for an example 85Hz stereo capable single-chip DLP projector).

60Hz to 1.5x at 85Hz. “2x colour wheel speed” means that the colour wheel performs two colour cycles per frame. “1.5x colour wheel speed” means that the colour wheel performs one and a half colour cycles per frame. It can be seen in Figure 2 that for 85Hz the left eye will see two red segments and two green segments whereas the right eye will only see one of each. The opposite occurs for the white and blue segments. Images for each eye will therefore have a slightly different colour bias. The effect is noticeable but slight, and may be ameliorated by the auto-white-balance capability of the human eyes.

4. Discussion and Conclusion

This study has revealed that most current generation LCD monitors cannot be used with the time-sequential stereoscopic display technique – this is due to the image-update method. There is continuous development in this area hence there is the possibility that newly released LCD monitors might be 3D compatible in some way - one example is LCD TVs which use a blinking or scanned backlight [3]. LCD panels can be used for other stereoscopic viewing methods and these are summarised in reference [1].

A second study reported in this paper has revealed a relatively large number of consumer single-chip DLP projectors that can be used for time-sequential stereoscopic display – some at image refresh rates as high as 85Hz. Although 60Hz and 85Hz stereo are generally not suitable for situations requiring totally flicker-free stereoscopic viewing, the knowledge that low-cost consumer DLP projectors can be used for time-sequential stereoscopic viewing will open up the range of applications and users of stereoscopic visualisation. Such users and applications can graduate to higher-end flicker-free “stereo-ready” projection systems when requirements dictate.

A wide range of other stereoscopic and autostereoscopic displays are now available in the market or are near to market. With stereoscopic imaging now being used in an increasing number of applications, this is great news for users.

5. Acknowledgements

The work on consumer DLP projectors was supported in part by iVEC (the hub of advanced computing in Western Australia), Jumbo Vision International, and ISA Technologies. We also thank the multitude of

companies and individuals who lent LCD monitors and DLP projectors for testing.

6. References

- [1] A. J. Woods, "Compatibility of Display Products with Stereoscopic Display Methods", in Proceedings of the International Display Manufacturing Conference (IDMC'05), ISBN 957-28522-2-1, Taipei, Taiwan (2005).
- [2] A. J. Woods, and S. S. L. Tan, "Characterising Sources of Ghosting in Time-Sequential Stereoscopic Video Displays", in Stereoscopic Displays and Virtual Reality Systems IX, Proc. SPIE Vol. 4660, San Jose, California (2002).
- [3] A. A. S. Sluyterman, and E. P. Boonekamp, "Architectural Choices in a Scanning Backlight for Large LCD TVs", in SID 05 Digest, pg 996 (2005).
- [4] A. J. Woods, K. L. Yuen, "Compatibility of LCD Monitors with Frame-Sequential Stereoscopic 3D Visualisation", in IMID/IDMC '06 DIGEST, Daegu, South Korea (2006). (in press)
- [5] K. L. Yuen, "Compatibility of LCD Monitors with Stereoscopic Display Methods", Technical Report CMST 2006-34, Curtin University of Technology (2006). (in preparation)
- [6] I. McDowall, M. Bolas, D. Corr, T. Schmidt, "Single and Multiple Viewer Stereo with DLP Projectors", in Stereoscopic Displays and Virtual Reality Systems VIII, Proc. SPIE Vol. 4297, pg 418-425, San Jose, California (2001).
- [7] L. J. Hornbeck, "Current Status and Future Applications for DMD-Based Projection Displays", in Proceedings of the Fifth International Display Workshop IDW '98, Kobe, Japan (1998).
- [8] A. J. Woods, T. Rourke, "The Compatibility of Consumer DLP Projectors with Time-Sequential Stereoscopic 3D Visualisation", to be presented at Stereoscopic Displays and Applications XVIII, San Jose, California, January (2007). (accepted for presentation)
- [9] T. Rourke, A. J. Woods, "Compatibility of Consumer DLP Projectors with Time-Sequential Stereoscopic Visualisation", Technical Report CMST 2006-17, Curtin University of Technology (2006). (in preparation)

Paper 13 A. J. Woods, T. Rourke (2007) "The compatibility of consumer DLP projectors with time-sequential stereoscopic 3D visualization", presented at Stereoscopic Displays and Applications XVIII, published in Stereoscopic Displays and Virtual Reality Systems XIV, Proceedings of IS&T/SPIE Electronic Imaging, SPIE Vol. 6490, pp. 64900V-1 to -7, San Jose, California, January 2007.

The compatibility of consumer DLP projectors with time-sequential stereoscopic 3D visualisation

Andrew J. Woods* and Tegan Rourke
Centre for Marine Science & Technology, Curtin University of Technology,
GPO Box U1987, Perth WA 6845, Australia.

ABSTRACT

A range of advertised "Stereo-Ready" DLP projectors are now available in the market which allow high-quality flicker-free stereoscopic 3D visualization using the time-sequential[†] stereoscopic display method. The ability to use a single projector for stereoscopic viewing offers a range of advantages, including extremely good stereoscopic alignment, and in some cases, portability. It has also recently become known that some consumer DLP projectors can be used for time-sequential stereoscopic visualization, however, it was not well understood which projectors are compatible and incompatible, what display modes (frequency and resolution) are compatible, and what stereoscopic display quality attributes are important. We conducted a study to test a wide range of projectors for stereoscopic compatibility. This paper reports on the testing of 45 consumer DLP projectors of widely different specifications (brand, resolution, brightness, etc). The projectors were tested for stereoscopic compatibility with various video formats (PAL, NTSC, 480P, 576P, and various VGA resolutions) and video input connections (composite, SVideo, component, and VGA). Fifteen projectors were found to work well at up to 85Hz stereo in VGA mode. Twenty-three projectors would work at 60Hz stereo in VGA mode.

Keywords: stereoscopic, field-sequential; time-sequential; DLP projectors; 3D Video

1. INTRODUCTION

The capability for some DLP (Digital Light Processing) projectors to be used with time-sequential stereoscopic display has been known for some time¹. This is due to the extremely fast pixel response time ($\sim 2\mu\text{s}$) of the DMD (Digital Micro-mirror Device) chip², the fact that the whole of the screen updates at once, and the capability of some DLP projectors to correctly display an alternating sequence of discrete left and right images.

Several DLP projectors already available in the market are advertised as being "stereo-ready" and capable of 120Hz time-sequential stereoscopic display. Table 1 lists the (time-sequential) "stereo-ready" projectors available from Barco, Christie, and Infocus at the time of writing this paper.

It also recently became known that some consumer-grade single-chip DLP projectors could be used for time-sequential stereoscopic visualization (although at much lower refresh rates), however, it was not well understood which projector models were compatible and incompatible.

We therefore undertook a research project to sample a wide range of consumer-grade single-chip DLP projectors to determine their level of time-sequential 3D compatibility. The results of the project would provide an improved understanding of the level of 3D compatibility of consumer-grade DLP projectors, which in turn would aid users wishing to use DLP projectors for stereoscopic visualisation purposes. A parallel purpose would be to raise awareness of this stereoscopic capability amongst projector manufacturers with the hope that they would implement time-sequential stereoscopic display compatibility in future models as a standard feature (and list it in their specifications).

* A.Woods@cmst.curtin.edu.au; phone +61 8 9266 7920; fax +61 8 9266 4799; www.cmst.curtin.edu.au

[†] Also known as: field-sequential, frame-sequential, alternate frame, or active stereo.

Table 1: Commercially available (time-sequential) “stereo-ready” DLP projectors

Projector Make/Model	Resolution	Max Freq.	# DMD
Barco DP100	2048 x 1080	144 Hz	3 DMD
Barco Galaxy 7 Classic+	1400 x 1050	118 Hz	3 DMD
Barco Galaxy 12 HB+	1400 x 1050	118 Hz	3 DMD
Christie CP2000	2048 x 1080	144 Hz	3 DMD
Christie Mirage S+2K	1400 x 1050	120 Hz	3 DMD
Christie Mirage S+4K	1400 x 1050	120 Hz	3 DMD
Christie Mirage S+8K	1400 x 1050	120 Hz	3 DMD
Christie Mirage S+14K	1400 x 1050	120 Hz	3 DMD
Infocus DepthQ	800 x 600	120 Hz	1 DMD

2. EXPERIMENTAL METHOD

In this study we tested 45 different consumer-grade single-chip DLP projectors from various manufacturers. The age of the projectors ranged from units that were several years old to projectors that had only been recently released at the time of the tests.

The test equipment layout is shown in Figure 1. Equipment used for testing included: two custom built photodiode sensor pens (based on an Integrated Photomatrix Inc. IPL10530 DAL), an oscilloscope (Goldstar OS-3000), and a custom built LCS 3D glasses driver box capable of adjustable phase and duty cycle. Equipment used to generate the time-sequential 3D video signals consisted of a PC equipped with a stereoscopic capable graphics card (NVIDIA 6600GT) and a Panasonic ‘DMR-E65’ DVD recorder/player. The Panasonic DMR-E65 was chosen because it is known to convert interlaced video signals to progressive in a 3D compatible way when the component progressive output is selected via the internal menu. Software on the PC consisted of Windows XP, the NVIDIA 3D Stereo Driver³, Powerstrip⁴, and Stereoscopic Player⁵.

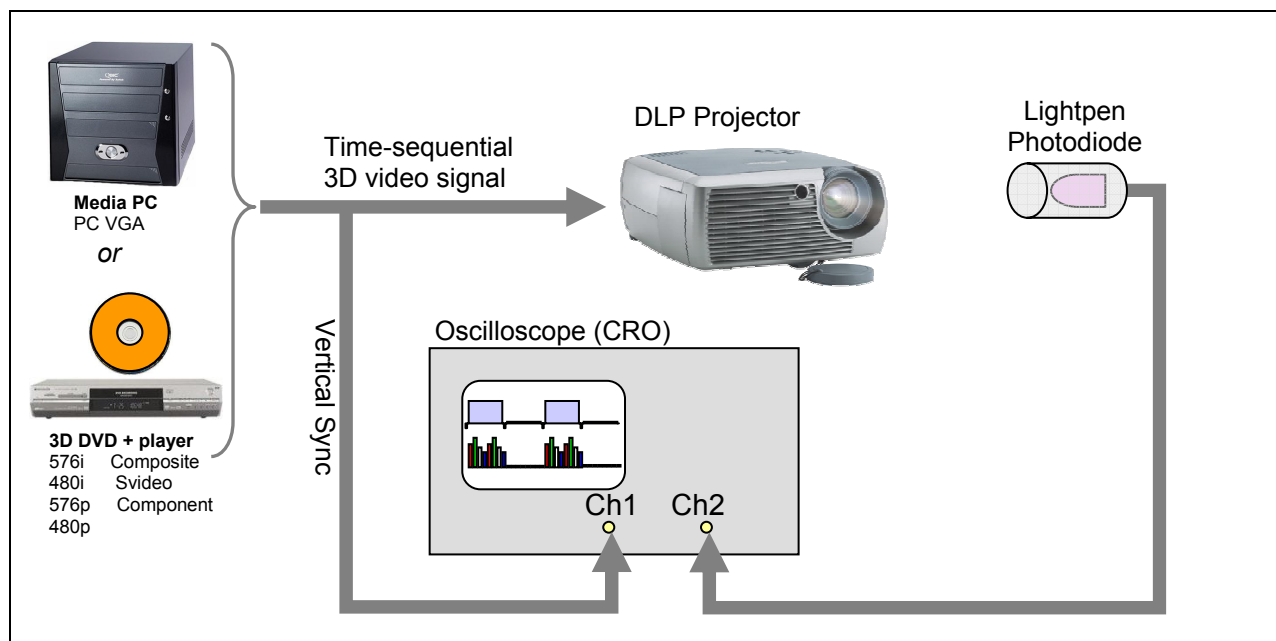


Figure 1: Schematic diagram of the experimental setup.

Test signals consisted of alternating sequences (at field or frame rate) of red and black, blue and black, green and black, white and black, or RGB colour bars and black (i.e., in the case of “red and black”, one field of red, one field of black, and repeat). In the case of the DVD player, custom written NTSC and PAL DVDs were used. In the case of the PC, custom created JPS (Stereoscopic JPEG) files or stereoscopic (side-by-side) AVI files were used.

Each projector was tested to establish: (1) whether the frame rate of the projector synchronized with the incoming video signal, (2) whether the colour-wheel synchronized with the incoming video signal, (3) whether there was crosstalk between alternate fields or frames, (4) the maximum frequency at which the projector would work in stereo (VGA only), (5) the time delay between the incoming video signal and the displayed images, (6) whether the projector converted interlaced video sources to progressive format in a 3D compatible way, and (7) the colour-wheel speed at various video input frequencies. These properties were tested for various video input connections (composite, SVideo, component, and VGA), various video formats (NTSC (480i), PAL (576i), 480P, 576P), and various VGA resolutions/frequencies.

Standard Definition (SD) video formats were tested because there is a reasonable range of commercially available field-sequential 3D DVDs and it is important to know which displays can be used with these 3D DVDs. VGA modes were tested because the projector can be driven at its native resolution and frame rate with this interface. DVI-D input connections were not tested because a method of extracting the vertical sync signal from the DVI-D cable was not available.

3. RESULTS AND DISCUSSION

The 3D compatibility results of the tested projectors were wide and varied. The overall results of the 3D compatibility testing are listed in Table 2. The ‘Composite & SVideo’ column indicates whether the projector would correctly display field-sequential 3D video (PAL or NTSC) entered via the composite and SVideo connector. The results for composite and SVideo are combined in the same column because there was no difference between composite and SVideo results across all the tested projectors. The ‘Component Interlaced’ column indicates whether the projector would correctly display field-sequential 3D video (derived from PAL or NTSC DVD) entered via the component connector. The ‘Component Progressive’ column indicates whether the projector would correctly display frame-sequential 3D video (576P 50Hz or 480P 60Hz) entered via the component connector. There was no difference in 3D compatibility between PAL and NTSC (50/60Hz) in all of the tests for all of the tested projectors so those results are combined in the composite/SVideo and component columns. The VGA 60Hz and 85Hz columns indicate whether the projector would correctly display frame-sequential 3D video entered via the VGA connector (in almost all cases the video resolution was set to the native resolution of the projector). The bottom row of the table indicates the percentage of all tested projectors that were time-sequential 3D compatible in that video mode.

Regarding Table 2, some projectors were totally incompatible with time-sequential 3D video in all video modes and all video connections. This was generally due to the frame output of the projector not synchronizing with the incoming video signal. In most cases where this happened the input video signal was resampled to the native frequency of the projector (usually ~60Hz) – this resampling process usually destroys the 3D video signal.

Some projectors would work with progressive time-sequential 3D video signals but not interlaced time-sequential 3D video signals. This suggests that the projector uses a deinterlacing (interlaced to progressive conversion) routine which is not time-sequential 3D compatible. Fortunately the internal deinterlacer can be bypassed by feeding the projector with a progressive video signal.

In most instances where the projector was 3D incompatible in interlaced mode, it could be seen that the colour-wheel was synchronising to the incoming video signal but the odd and even fields were being mixed during the deinterlacing process. Since DMDs are progressive devices, any interlaced video signal input to the projector must be deinterlaced (converted from interlaced to progressive).

Table 2: Time-sequential 3D compatibility results for the 45 DLP projectors tested. (a green tick indicates that mode was time-sequential 3D compatible, a red cross indicates that mode is not 3D compatible, a dash indicates that mode was not tested, 'n/a' indicates that connection or mode was not available on that projector)

Brand	Model	Composite & S-Video	Component Interlaced	Component Progressive	VGA 60 Hz	VGA 85 Hz
Acer	PD322	x	x	√	√	√
Acer	PD523	x	x	√	√	√
Acer	PD723P	x	x	√	x	x
Acer	PH110	x	x	√	√	√
BenQ	MP 610	x	x	√	√	√
BenQ	PB 6240	x	x	√	√	√
BenQ	PE 7800	x	x	x	x	x
BenQ	PE 8700	x	x	x	x	x
Boxlight	Raven	x	x	√	√	√
Casio	XJ 360	x	x	√	√	√
Casio	XJ 560	x	x	√	x	x
Dell	3200 MP	x	-	-	x	x
IBM	C400	x	n/a	n/a	x	x
Infocus	LitePro 620	√	n/a	n/a	x	x
Liesegang	DDV 2111 Ultra	√	n/a	n/a	x	x
Liesegang	DDV 3200	x	x	√	x	x
Liesegang	e.Motion 4100	x	x	√	x	x
Liesegang	LuxorPlus	x	x	√	x	x
Liesegang	Multi800	x	n/a	√	x	x
Mitsubishi	HC3000	x	x	√	√	x
Mitsubishi	XD450U	x	x	√	x	x
NEC	HT 1100	x	x	√	√	x
NEC	LT 35	x	x	√	√	√
NEC	LT 100	√	√	√	x	x
Optoma	EP719	-	-	-	√	√
Optoma	EP739	-	-	-	√	√
Optoma	EP759	x	x	√	x	x
Optoma	H27	x	x	√	-	-
Optoma	H57	x	x	√	x	x
Optoma	HD72i	x	x	√	√	x
Panasonic	PT-D 5500E	x	x	√	√	x
PLUS	U4-237	x	n/a	n/a	√	√
PLUS	U5-112	x	x	√	√	√
Projection Design	Action! Model 2 Mk2	x	n/a	√	√	x
Projection Design	Evo 2 SX+	x	x	√	√	x
Projection Design	F1+ SX+	x	x	√	√	x
Projection Design	F3 SXGA+	x	x	√	√	x
Sharp	XR10X	x	x	√	√	√
Sharp	XV-Z2000	√	√	√	x	x
Sharp	XV-Z9000E	x	x	√	x	x
Studio Experience	SE 30 HD	x	x	√	x	x
Studio Experience	SE 50 HD	x	x	x	x	x
Toshiba	TDP-S8	x	x	√	√	√
Yamaha	DPX-1300	x	x	√	x	x
Yamaha	DPX-530	x	x	√	√	√
% 3D compatible:		9%	5%	83%	52%	34%

Some projectors were compatible with time-sequential 3D Video (input via the composite, SVideo or component connectors) but not 3D VGA. This would suggest that there is a small quirk in the firmware of the projector. A small change to the firmware could probably allow the projector to work for both 3D Video and 3D VGA. This is not something that 2D projector manufacturers would normally check – but hopefully this will change.

As can be seen in Table 2, 52% of the tested projectors were compatible with 60Hz 3D VGA signals, and 34% of the tested projectors were compatible with 85Hz 3D VGA signals. 85Hz stereo from a consumer projector is a significant result. The problem with 60Hz stereo is that generally this will produce a lot of flicker. With 85Hz stereo, the amount of flicker will be less, but generally not totally flicker-free. Perceived flicker can be reduced by reducing room brightness and image brightness. However, 100Hz or 120Hz stereo is generally required for totally flicker-free operation.

One other specification that was measured during the projector tests was the time offset from the trailing edge of the vertical sync signal to the start of image display by the projector – i.e., the phase of the displayed images relative to the vertical sync pulses. This aspect is important because if the LCS glasses are switched at the incorrect timing relative to the displayed images, a significant amount of ghosting can be introduced. Table 3 lists the time offset for the projectors that were found to be VGA 3D compatible at either 60Hz or 85Hz.

Table 3: Time offset for consumer DLP projectors found to be compatible with 60Hz and/or 85Hz VGA time-sequential stereoscopic display.

Projector Make/Model	Time Offset @ 60Hz (ms)	Time Offset @ 85Hz (ms)	Resolution
Acer PD322	0.28	0.96	1024x768
Acer PD523	0.33	0.96	1024x768
Acer PH110	0.30	0.31	854x480
BenQ MP610	~0.36	0.58	800x600
BenQ PB6240	~0.36	0.55	1024x768
Boxlight Raven	not measured	not measured	800x600
Casio XJ-360	0.29	0.35	1024x768
Mitsubishi HC3000	0.39	x	1280x768
NEC HT 1100	~0.83	x	1024x768
NEC LT35	~0.36	0.42	1024x768
Optoma EP719	not measured	not measured	1024x768
Optoma EP739	not measured	not measured	1024x768
Optoma HD72i	~0.40	x	1280x768
Panasonic PT-D 5500E	~1.02	x	1024x768
PLUS U4-237	not measured	not measured	1024x768
PLUS U5-112	0.32	0.94	800x600
Projection Design Action! Model 2 Mk2	~0.63	x	1280x720
Projection Design Evo 2 SX+	~0.91	x	1400x1050
Projection Design F1+ SX+	~0.91	x	1400x1050
Projection Design F3 SXGA+	not measured	x	1400x1050
Sharp XR-10X	0.26	0.30	1024x768
Toshiba TDP-S8	~0.45	0.53	800x600
Yamaha DPX-530	~0.24	0.42	1024x576

The largest time offset measured at 85Hz was 0.96ms, which corresponds to 8% of the time period for one 85Hz frame (11.8ms) – this could result in a noticeable amount of crosstalk if not corrected. LCS glasses are usually switched very close to the time of the vertical sync pulse (0.1 ms after the trailing edge of the vertical sync pulse for a H3D glasses VGA dongle). With the glasses switching at 0.1ms and the projector switching between views at 0.96ms, this would result in approximately 8% ghosting purely due to the phase difference between the LCS glasses and projector. A custom LCS glasses driver “smart dongle” was developed as part of this project to allow the switching of the LCS glasses to be time-offset by an adjustable amount and hence minimise ghosting due to incorrect LCS switching phase.

It is interesting to note that time offset is vastly different between different projectors and also between different modes of the same projector. The time offsets for other 3D compatible modes were measured but are too complicated to report in this paper - they are reported in Reference 6.

One other item of interest is that the maximum resolution of any consumer projector that was 3D compatible at 85Hz was 1024x768 (XGA). For any projector of a higher resolution than 1024x768, if it would do time-sequential 3D, it would only do so at 60Hz.

One aspect of interest about the operation of most of the 85Hz capable projectors listed above is that the colour-wheel speed drops down from 2x at 60Hz to 1.5x at 85Hz. “2x colour wheel speed” means that the colour wheel performs two colour cycles per frame. “1.5x colour wheel speed” means that the colour wheel performs one and a half colour cycles per frame. It can be seen in Figure 2 that for 85Hz the left eye will see two red segments and two green segments whereas the right eye will only see one of each. The opposite occurs for the white and blue segments. Images for each eye will therefore have a slightly different colour bias. The effect is noticeable but slight, and may be ameliorated by the auto-white-balance capability of the human eyes.

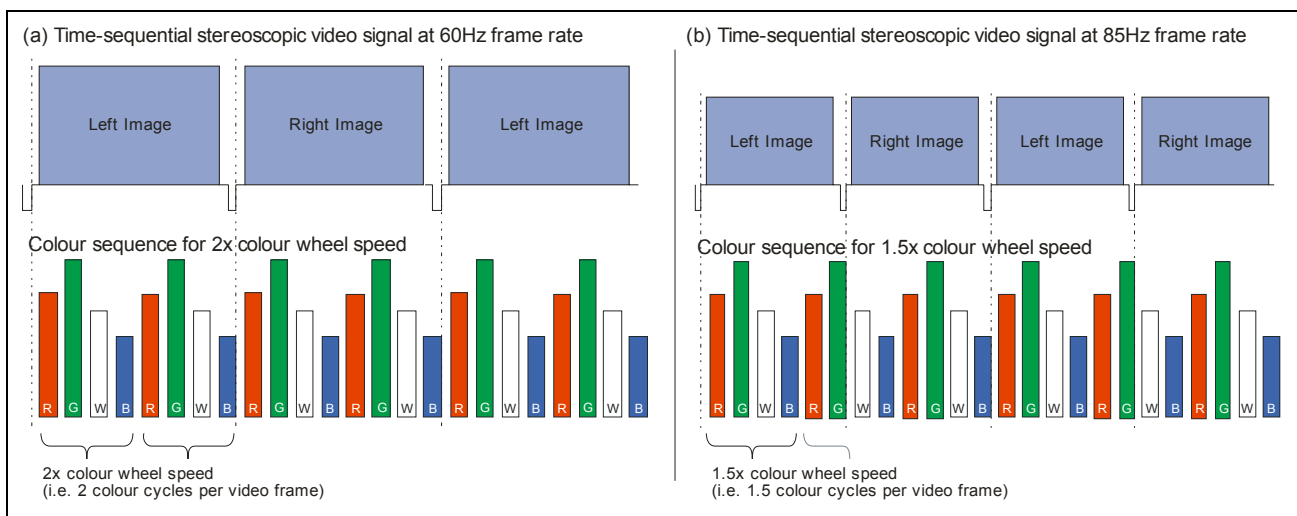


Figure 2: Illustration of (a) 2x and (b) 1.5x colour wheel speed at frame rates of 60Hz and 85Hz respectively (for an example 85Hz stereo capable single-chip DLP projector).

It is fair to ask why some of the projectors are incompatible with time-sequential 3D in various modes. Most of the projectors are incompatible with interlaced sources because they use an interlaced to progressive algorithm which is not time-sequential 3D compatible – an interlaced to progressive algorithm which is optimised for 2D video will not necessarily operate successfully with time-sequential 3D video.

The reason that some projectors are incompatible with progressive 60Hz 3D video sources is usually due to the colour-wheel (and frame rate) of the projector not synchronising with the incoming video signal. Since all DLP projectors are based on the DMD chip from Texas Instruments and likely follow a common reference design, it is thought that this incompatibility is mainly due to a firmware setup issue in the projector configured by the projector manufacturer. It is thought there are two main reasons why not all of the projectors were 85Hz stereo compatible: firstly it could relate to the firmware setup of the projector by the manufacturer, and secondly with resolutions greater than XGA, there is understood to be a bottleneck in the DLP engine which limits the data rate (and therefore the frame rate at higher resolutions). This data bottleneck is also thought to be the reason that correct 120Hz stereo was not possible on any of the projectors tested – however, obviously the designers of the DepthQ projector have been able to overcome this limitation. It is hoped that future DLP chipsets and reference designs will overcome this limitation.

4. CONCLUSION

This study has revealed a relatively large number of consumer single-chip DLP projectors that can be used for time-sequential stereoscopic display – some at image refresh rates as high as 85Hz. Although 85Hz stereo is not generally totally flicker-free, the knowledge that low-cost consumer DLP projectors can be used for time-sequential stereoscopic viewing will open up stereoscopic visualisation to a wider range of users and applications. Such users and applications can graduate to higher-end flicker-free “stereo-ready” projection systems when requirements dictate and funds allow.

Unfortunately most of the projectors tested are not directly compatible with field-sequential 3D DVDs (using common video interfaces: composite, SVideo and component interlaced), however, it was found that 83% of tested projectors could be used to display field-sequential DVDs if the 3D DVD was played back from a 3D compatible progressive output DVD player. Not all progressive output DVD players convert from interlaced to progressive in a 3D compatible way, however, it is known that some Panasonic DVD players do (such as the Panasonic DMR-E65, Panasonic DVD-S55 (NSTC only), and Panasonic DVD-S47 (possibly NTSC only)). It would be useful to develop a list of 3D compatible progressive output DVD players, but that is beyond the scope of this paper.

85Hz stereo via the VGA connector will be of use to a wide range of computer-based stereoscopic imaging applications, the most prominent probably being gaming. Over a thousand different PC games can be played in stereo with the use of an NVIDIA graphics card and the NVIDIA 3D Stereo driver⁷.

Currently the 3D compatibility of consumer DLP projectors is not advertised or listed in product specifications by manufacturers or distributors. Additionally, we did not find any consumer projectors that were capable of 100/120Hz stereo operation. It is hoped that in the near future both of these factors will change.

5. ACKNOWLEDGEMENTS

This work was supported by iVEC (the hub of advanced computing in Western Australia), Jumbo Vision International, and ISA Technologies.

We also wish to thank the multitude of companies and individuals who lent DLP projectors for testing: Kim Kimenkowski, Jumbo Vision International; Sil La Puma and Simon Beard, ISA Technologies; Con Parente, West Coast Hi-Fi O'Connor; David Tuttle, Optoma USA; Geoff Frampton, Essential Office Products; Roger Castle, Castle Funding; Evan Papantoniou, Thames Computer Group; Vaughan Doyle and Adam Thackrah, J Mills Distribution; Nic Beames, Dynamic Digital Depth; Simon, Shriro Australia; Brendan, Perth Audio Visual; Marc Störig, AVCE Liesegang Australia; Will Rossiter and Duncan Boekhold, Yamaha Music; Brian Wood, West Coast Hi-Fi Joondalup; Chris Malcolm, John Curtin Prime Ministerial Gallery; Martin Todd, NEC Australia; Ross Sawatzky and Jayne Schröder, Advanced Visual Design; Alan, Direct National Business Machines; Peter Cutts, PCA Marketing; Adam Byrne, Toshiba Australia; Mike Butler, ComputerCorp; John Voss and Leigh, Rexel Australia; Peter Shilkin, Panasonic Australia; Claudio Cardile, Mitsubishi Australia; Darren Goble, LG Electrical; and Jason Burns, Douglas Hi-Fi.

6. REFERENCES

1. I. McDowall, M. Bolas, D. Corr, T. Schmidt, “Single and Multiple Viewer Stereo with DLP Projectors”, in *Stereoscopic Displays and Virtual Reality Systems VIII*, Proc. SPIE Vol. 4297, pg 418-425, San Jose, California (2001).
2. L. J. Hornbeck, “Current Status and Future Applications for DMD-Based Projection Displays”, in *Proceedings of the Fifth International Display Workshop IDW '98*, Kobe, Japan (1998).
3. NVIDIA 3D Stereo Driver http://www.nvidia.com/object/3d_stereo.html
4. Powerstrip software <http://entechtaiwan.net/util/ps.shtm>
5. Stereoscopic Player software http://www.3dtv.at/Products/Player/Index_en.aspx
6. T. Rourke, A. J. Woods, “Compatibility of Consumer DLP Projectors with Time-Sequential Stereoscopic Visualisation”, Technical Report CMST 2006-17, Curtin University of Technology, Perth, Australia (2006).
7. D. Cook, “Stereoscopic Gaming: Technology and Applications”, Keynote Presentation at *Stereoscopic Displays and Applications XV* conference, 19-21 January 2004, San Jose, California. (Presentation only).

Paper 14 [Reviewed Article]

A. J. Woods (2009) "3-D Displays in the Home" *Information Display*, 7(09), pp. 8-12.

3-D Displays in the Home

There are many predictions that the next stage in the commercial evolution of consumer display technology is the widespread availability of stereoscopic 3-D content for viewing on home 3-D displays. This article describes the types of 3-D displays that are currently available, as well as what technologies are on the horizon.

by Andrew Woods

IN PARALLEL with the widespread deployment of digital 3-D cinema systems and an explosion in the release of 3-D movies into those theaters, there has also been a concerted effort from several consumer-electronics manufacturers to release 3-D TVs and 3-D displays into the consumer marketplace. This article looks at the technologies behind these high-quality 3-D displays that have been released into the consumer marketplace and also answers the often-repeated question: can my existing home TV be used for high-quality 3-D viewing (e.g., by bringing home the 3-D glasses from the movie theater)? While the focus will be mainly on the home-display marketplace for HDTVs or computer monitors, there are a great many more 3-D display products available if the professional-display marketplace is also taken into consideration.

When cathode-ray-tube (CRT) monitors became less commonplace in retail outlets, there was great concern in the stereoscopic-imaging community about what displays could be used for stereoscopic purposes in the

Andrew Woods is a consultant and research engineer based at Curtin University's Centre for Marine Science & Technology in Perth, Australia (www.3d.curtin.edu.au). He has more than 20 years of experience in the design, application, and evaluation of stereoscopic video equipment for underwater, industrial, and entertainment applications. He is also co-chair of the annual Stereoscopic Displays and Applications Conference.

future. Up to that point, CRTs had been the mainstay of stereoscopic display (using active shutter glasses), and the alternative displays such as plasma-display panels (PDPs) or liquid-crystal displays (LCDs) were not directly stereoscopic 3-D compatible. Fortunately, several display manufacturers rose to the challenge. Explanations of how those systems work follow later in this article.

In April of 2007, Samsung became the first to release a stereoscopic 3-D-capable large-screen high-definition television (HDTV) into the home marketplace. The displays used a rear-projection digital-light-processing (DLP) engine designed by Texas Instruments.¹ Several things were remarkable about this product: the very competitive pricing (much less than an equivalent 2-D LCD or PDP); the 3-D capability was included at no extra cost (apart from the 3-D glasses, which had to be purchased separately); the very high quality of the stereoscopic image; the high-definition resolution; and, further, the use in some models of an innovative LED light engine that offered richer colors, longer lamp life, and removal of the rainbow effect. Samsung released a selection of models ranging in size from 46 to 72 in. in 2007 and 2008. Mitsubishi also released a selection of these displays in 2007, 2008, and 2009. Over 2 million of these displays are reported to have been sold into homes in North America to date – the only market in which these particular displays have been directly marketed. It is an open question as to how many of these

displays have been used for 3-D purposes – possibly less than 1% – but there are still some very happy 3-D users out there!

These displays essentially house a single-chip DLP projector that projects onto the rear of a special screen mounted in the front of the display. A color-sequential technique is used to produce full-color images – as with all single-chip DLP solutions. The stereoscopic 3-D method used by these displays is the time-sequential technique, which involves showing left and right images alternately (in this case at 120 Hz) that are viewed using liquid-crystal-shutter (LCS) 3-D glasses that blank the left and right eyes alternately in synchronization with the left and right images shown sequentially on the display. The fast switching time of a DLP (~2 μsec) makes it particularly well-suited to the time-sequential 3-D method. The 3-D input format accepted by these displays, commonly known as the checkerboard format (see Fig. 1), involves multiplexing the left and right images into a single frame in a checkerboard-like layout. This innovatively allows the two left and right image streams to enter the display within a single regular bandwidth video input (albeit at half-resolution per view).

These rear-projection DLP TVs use a half-resolution digital micromirror device (DMD) to achieve a full-resolution image by way of a process called "wobulation."² As shown in Figs. 1(b) and 1(c), in 2-D display mode each frame is broken down into two sub-frames – half of the pixels are displayed in the first sub-

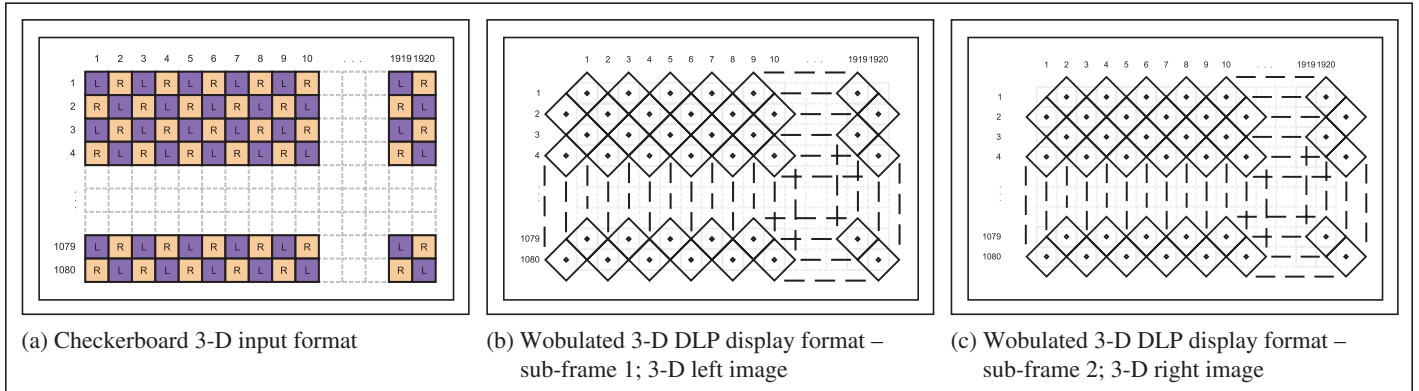


Fig. 1: An illustration of the 3-D input and 3-D display formats of the DLP 3-D HDTVs includes (a) the checkerboard 3-D input format and (b) and (c) the half-resolution DMD with diamond-shaped mirrors that oscillate between two optical positions at 120 Hz to display the full resolution.

frame and the remaining pixels in the second sub-frame. The mirrors of the half-resolution DMD used in these DLP TVs are oriented in a diamond pattern (as opposed to square pixels in a regular DMD), and the centers of the mirrors match the checkerboard pattern shown in Fig. 1(a). The image of the DMD is optically shifted (wobulated) between the two sub-frames in order to display the full-resolution image. In 3-D mode, the two sub-frames are used for the left and right images, respectively. The pixel arrangement of each sub-frame directly corresponds to the checkerboard pattern used for 3-D input, so, in effect, the display internally converts the checkerboard 3-D input to time-sequential 3-D for display, allowing the viewer to wear LCS 3-D glasses to view the 3-D image.

Also in 2007, another class of 3-D displays started to become more widely available and at price points that were affordable to some home users. The micro-polarizer (μ Pol) technique was invented by Sadeg Faris in the early 1990s³ and involves the attachment of a special optical filter to the face of an LCD (Fig. 2), which results in alternate rows of pixels of the display being polarized in two different polarization states – usually left-handed circular and right-handed circular. When the display is viewed using the appropriate passively polarized 3-D glasses, one eye sees all the odd-numbered rows and the other eye sees all the even-numbered rows. When the left and right images are spatially multiplexed onto the odd and even rows respectively, the observer can see a high-quality stereoscopic 3-D image. These types of 3-D displays are now commonly available around the world from

manufacturers including Zalman, Hyundai, Pavonine (under the brands Dimen and Miracube), and JVC in sizes ranging from 22 up to 46 in. The smaller monitors are mainly aimed at the stereoscopic 3-D gaming market, whereas the larger sets are intended for 3-D video or movie viewing. In 3-D mode, these displays have half the 2-D resolution in the vertical axis, and there is also some vertical viewing-angle sensitivity. Some products use a μ Pol variant called Xpol that includes a black mask between rows of pixels to increase the vertical range of the viewing zone and reduce crosstalk. The price premium for the 3-D capability on these sets starts from about 200% on the smaller models and higher for the larger models, so market penetration has not been high.

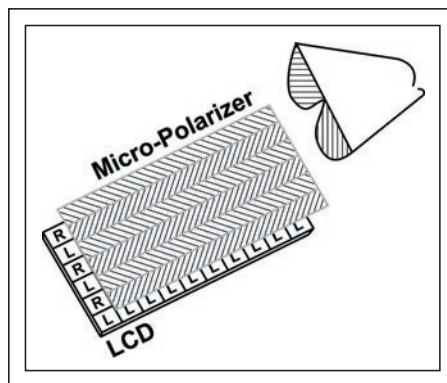


Fig. 2: Shown is an optical layout of a μ Pol 3-D LCD. A micro-polarizer layer over the front of the LCD polarizes alternate rows of pixels into two different polarization states. (Illustration based on Faris.³)

In 2008, Samsung achieved another world's first with the consumer release of two stereoscopic 3-D-capable plasma HDTVs (42 and 50 in.) These displays use the time-sequential 3-D display method and the stereoscopic 3-D images are viewed through LCS 3-D glasses – operating at 120 Hz. Unlike the 3-D DLP HDTVs, which were only released in North America, the 3-D plasma HDTVs were released in many international markets. Recently, Panasonic has been demonstrating time-sequential stereoscopic 3-D-capable plasma displays at various trade shows, and many commentators anticipate they will release a product based on this technology in the near future.

Another 3-D LCD product that has been gaining popularity, particularly in the 3-D gaming market over the last couple of years, uses an innovative dual-panel LCD technique – also known as a variable-polarization-angle display – and is viewed using passive polarized 3-D glasses.⁴ In a conventional LCD, each subpixel in the LCD panel is used as a light-valve controlling the amount of light that travels from the backlight to the observer. But in these 3-D LCDs, the optical function is very different – the optical layout is illustrated in Fig. 3. The first (back) panel (Mod LCD) operates in a somewhat conventional light-valve approach to modulate the brightness of the light at each pixel, except that the image sent to this first panel is an amalgam of the left and right images. Essentially,

$$\sqrt{L^2 + R^2}$$

[see Figs. 4(a)–4(c)]. The second (front) panel (Ang LCD) acts to control the output polariza-

home 3-D displays

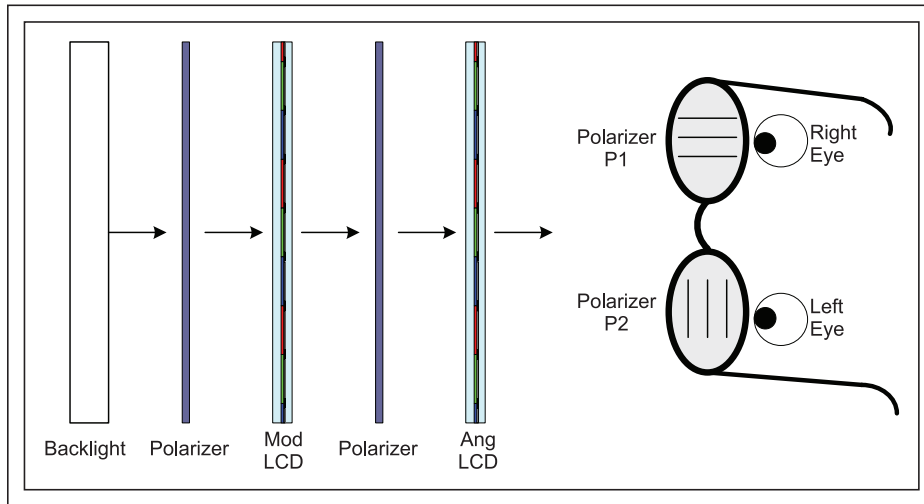


Fig. 3: A basic optical layout of a variable-polarization-angle display is depicted. The modulo LCD controls pixel brightness and the angulo LCD controls the polarization angle of each pixel. (Illustration based on Gaudreau.⁴)

tion angle of each subpixel (using the fundamental function of a liquid-crystal cell as a polarization rotator) and by virtue of this, sending the light from each subpixel to one eye, the other eye, or a mixture of both. The drive signal to the second layer is calculated for each pixel and is approximately $\arctan(L/R)$.⁵ As can be seen in Fig. 4(d), if the image on this second panel was viewed individually, it would be a rather strange experience, but when the display is viewed using the appropriate passive polarized 3-D glasses, the resultant stereoscopic 3-D image can be remarkably good. In 3-D mode, these displays are full resolution (no resolution is sacrificed), but some models do suffer from relatively high amounts of crosstalk (ghosting). Consumer displays using this technique are available from iZ3D, and displays intended for professional appli-

cations are available from MacNaughton, Inc., and Polaris Sensor Technologies.

The most recent consumer 3-D display to hit the market was masterminded by NVIDIA and released as 22-in. 3-D LCDs from Samsung and ViewSonic. These displays use the time-sequential 3-D-display technique and have been specially engineered to be viewed in 3-D by using custom LCS glasses – operating at 120 Hz. The developers had to make some fairly smart changes to the LCD design to allow them to work with LCS 3-D glasses – most LCDs cannot. Again, these displays have been mainly aimed at the 3-D gaming market and they also retain the full resolution of the LCD panel in 3-D mode.

There is also a selection of 3-D displays aimed at the professional and semi-professional markets, available from suppliers

including Planar, Christie, DepthQ, projectiondesign, and others. Large-screen autostereoscopic displays (3-D displays not requiring glasses) are also available in the professional marketplace, but they are believed to be a long way off from being a home consumer-deployed product (especially with Philips having abandoned this market in March 2009⁶). Mobile devices with autostereoscopic displays have been released in Asia by Sharp, Samsung, and Hitachi – but not as yet in the U.S. This article does not even touch on 3-D projection, which is starting to get very exciting with consumer/prosumer product offerings and announcements from ViewSonic, Mitsubishi, Infocus/DepthQ, BenQ, Sharp, and others. (A full summary of all the 3-D displays mentioned above is available from: www.3dmovielist.com/3dhdtvs.html.)

It should be noted that there is a considerable variation in image quality and resolution between these various 3-D displays. For some of the displays, the 3-D resolution is half that of the 2-D resolution. Other image-quality aspects to consider include the amount of crosstalk or ghosting present in the display, display brightness in 3-D mode, as well as regular 2-D measures of image quality.

Can Existing Home TVs Be Used for 3-D Purposes?

A parallel phenomenon with the increased penetration of 3-D displays, and the general consumers' recognition of 3-D TV in the home, is the regular question as to whether a consumer's existing home display(s) can be used for 3-D purposes. For the time being, the short answer is that unless the display is advertised as being "3D-Ready" or "3-D compatible" (see www.3dmovielist.com/

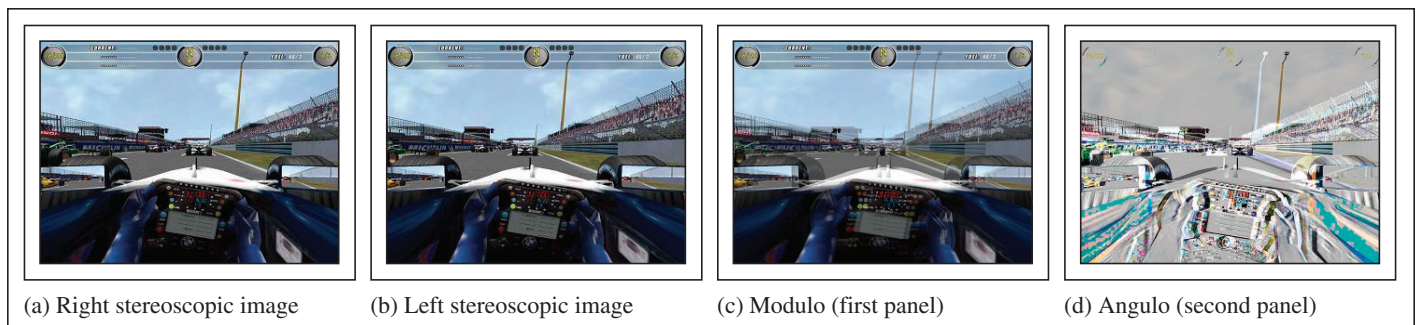


Fig. 4: A left/right stereoscopic image pair [(a) and (b)] is converted to modulo/angulo [(c) and (d)] for display on a variable polarization angle display. (Drive images from Gaudreau.⁴)

3dhdtvs.html) it unfortunately will not be able to be used for high-quality flicker-free full-color stereoscopic 3-D viewing (except in the case of older CRT monitors). Consumers may be tempted to take home the 3-D glasses from the various high-quality 3-D movie screenings, but unfortunately they simply will not work on their conventional home TV. Ignoring the displays that are advertised as being stereoscopic 3-D capable, here is why conventional displays cannot be used for high-quality stereoscopic 3-D viewing.

First, consider the three types of 3-D glasses being used in the theaters – passive polarized glasses, active LCS glasses, and Infitec (Dolby 3-D) glasses.

Polarized 3-D glasses will not work with conventional displays because they output light either in a single polarization direction (e.g., LCDs) or they are unpolarized (e.g., PDPs). An optical filter would need to be added to these displays to provide two polarization states (for the left and right views) – but currently this is not a customer-deployable solution.

LCS 3-D glasses do not work with conventional LCDs for a range of reasons,⁷ but the most significant reason is the image-update method. Unlike CRTs, LCDs are a hold-type display, meaning that each pixel of the display outputs light over the entire frame period – i.e., there is no blanking period. But similar to a CRT, the image on an LCD is updated

row by row from the top of the display to the bottom. The time taken to address the entire display is almost one frame period. What this means is that there is no one time, or period of time, when the display shows one image exclusively across the entire display; i.e., there is no one time when the shutters in a pair of LCS 3-D glasses could be opened so that a left (or right) image would be seen across the entire screen. Figure 5 shows the image-update method of conventional LCDs, which illustrates the problem. As mentioned above, ViewSonic and Samsung have implemented an as-yet-undisclosed modification in their 3-D LCDs to overcome this problem.

Unfortunately, conventional plasma displays also cannot be used with LCS 3-D glasses to produce a high-quality flicker-free 3-D image.⁸ Unlike CRTs or conventional LCDs in which updated pixels are presented sequentially over the course of the frame (see Fig. 5), plasma displays have the nice feature that all of the updated pixels in a frame are illuminated simultaneously. However, the long phosphor persistence of conventional plasma displays means that crosstalk (ghosting) will be high. Additionally, conventional plasma displays can only be driven with a 60-Hz video signal, meaning that even if the crosstalk was ignored, the image seen through the LCS 3-D glasses would flicker excessively. Samsung's 3D-ready plasma displays make use of the checkerboard 3-D input method to

deliver the 3-D video signal and presumably use custom phosphors to reduce the amount of crosstalk due to phosphor persistence.

Even displays that are advertised as being 120 Hz do not solve the problem – 120-Hz (and 240-Hz) technologies are being implemented with a range of LCDs and plasma displays to reduce the problem of image smear in scenes containing fast image motion. Many people recognize that “120 Hz” is often associated with stereoscopic 3-D viewing, but unfortunately the inclusion of 120-Hz refresh rates does not solve all the problems for successfully using time-sequential 3-D on these displays. The most obvious problem is that there is no way of driving them with a true 120-Hz video signal, containing 120 distinct frames per second. Usually, the display accepts only a conventional 60-Hz video signal and the display internally interpolates extra frames. The inability to send 120 unique frames per second to the display would mean that it could not be used for 120-Hz 3-D purposes. So, unless the display is labeled as “3-D-ready” or “3-D compatible,” any mention of 120 Hz currently will not be an advantage to time-sequential 3-D compatibility.⁹

The Infitec system employed in Dolby 3-D cinemas uses special interference filters to divide the visible color spectrum into six narrow bands called R1, R2, G1, G2, B1, and B2 for the purposes of this description.¹⁰ The R1, G1, and B1 bands are used for one eye image and R2, G2, and B2 for the other eye. The human eye is largely insensitive to such fine spectral differences, so this technique is able to generate full-color 3-D images with minimal color differences between the two eyes. Unfortunately, conventional displays lack the ability to modulate light wavelengths at this fine scale, so Infitec/Dolby 3-D glasses also will not work on conventional displays. This may be a possibility in the future with multiprimary-color displays, but there is nothing like this currently in the consumer market.

The only 3-D solution that can be widely deployed to any consumer color display is the anaglyph 3-D method. The anaglyph has been around since the 1800s, and for modern full-color displays involves sending the left and right image views into one or two complementary color channels, respectively. For example, the most common anaglyph technique involves the left perspective image being stored in the red color channel and the right perspective image being stored in the

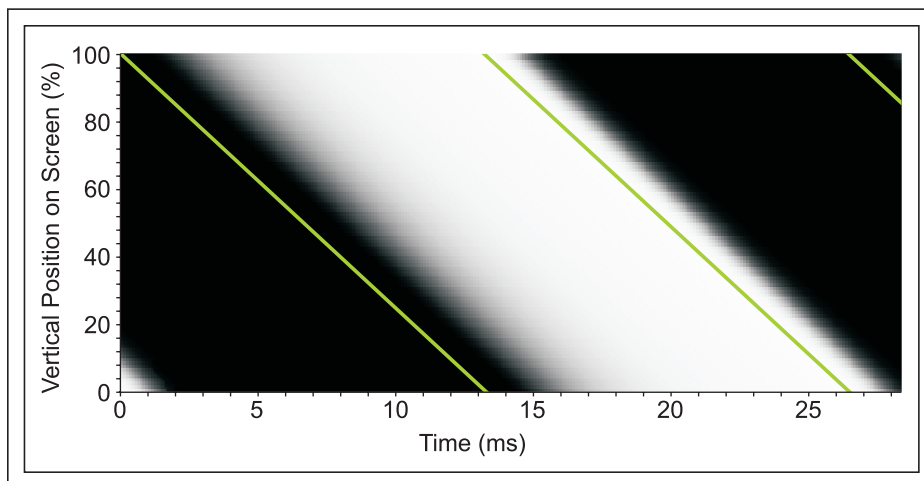


Fig. 5: Time-domain response of an example conventional LCD monitor (with 5.7-msec pixel response rate alternating between black and white frames at 75 Hz). The green line represents the time each row is addressed. It can be seen that there is no point in time when the entire screen shows one image across the entire screen.⁷

home 3-D displays

blue and green (cyan) color channels. The viewer wears red/cyan 3-D glasses to decode the correct image to each eye and sees a 3-D image. Other primary color combinations are possible, including blue/yellow and green/magenta. The main advantages of the anaglyphic 3-D method are its simplicity and low cost. All that is required is an anaglyphic 3-D image source, any full-color display, and a corresponding pair of anaglyphic 3-D glasses. Unfortunately, the anaglyph 3-D method usually suffers from fairly low 3-D image quality – due to fairly high ghosting levels, retinal rivalry, and the inability to reproduce a completely full-color 3-D image.¹¹ Despite these limitations, anaglyph 3-D remains a commonly used format as evidenced by the widespread release of many 3-D DVDs and Blu-ray discs in anaglyph format – albeit leaving many shaking their heads and yearning for something better.

Conclusion

A good (and expanding) range of high-quality 3-D displays is gradually penetrating the home consumer market. The successful roll-out of 3-D cinemas and 3-D movies is probably greatly responsible for the increasing consumer interest in this display category. The next part of the equation that needs attention is the availability of stereoscopic 3-D content for viewing on home 3-D displays. The consumer game market is the greatest source of 3-D content at the present time, with over 300 PC game titles available to be played in stereoscopic 3-D – enabled by 3-D game-software solutions available from NVIDIA, DDD, and iZ3D. There is also talk of game consoles supporting high-quality 3-D displays in the not too distant future. However, probably the most anticipated form of 3-D content is high-definition 3-D movies. Over 300 3-D movies and shorts have been publicly exhibited from 1915 until 2009, but unfortunately only a handful of 3-D movie content is commercially available at the present time (see www.3dmovielist.com) – and none in a high-quality high-definition format. At the present time, most content owners appear to be waiting for the much-talked-about Blu-ray 3-D format to be standardized, which is addressed in another article in this issue. Once that format is standardized, we will probably see another jump in the uptake of stereoscopic 3-D displays.

References

- ¹D. C. Hutchison, “Introducing DLP 3-D TV,” Texas Instruments white paper (2007). [http://dlp.com/downloads/Introducing DLP 3-D HDTV Whitepaper.pdf](http://dlp.com/downloads/Introducing_DLP_3-D_HDTV_Whitepaper.pdf)
- ²W. Allen and R. Ulichney, “Wobulation: Doubling the Addressed Resolution of Projection Displays,” *SID Symposium Digest* **36**, 1514-1517 (2005). http://www.hpl.hp.com/personal/Robert_Ulichney/papers/2005-wobulation-SID.pdf
- ³S. M. Faris, “Novel 3-D stereoscopic imaging technology,” *Stereoscopic Displays and Virtual Reality Systems, Proc. SPIE* **2177**, 180-195 (1994).
- ⁴J. E. Gaudreau, *et al.*, “Innovative stereoscopic display using variable polarized angle,” *Stereoscopic Displays and Virtual Reality Systems XIII, Proc. SPIE* **6055**, 605518 (2006).
- ⁵J. E. Gaudreau, “Stereoscopic displaying method and device,” US Patent 5629798 (1997).
- ⁶C. Chinnock, “Philips Decides to Shut Down 3D Operation,” *Display Daily* (2009), online at <http://displaydaily.com/2009/03/27/>
- ⁷A. J. Woods and K.-L. Yuen, “Compatibility of LCD Monitors with Frame-Sequential Stereoscopic 3-D Visualisation,” (Invited Paper), *Proc. IMID/IDMC '06*, 98-102, (2006). www.3d.curtin.edu.au
- ⁸A. J. Woods and K. S. Karvinen, “The compatibility of consumer plasma displays with time-sequential stereoscopic 3-D visualization,” *Stereoscopic Displays and Applications XIX, Proc. SPIE* **6803**, 68030X (2008). www.3d.curtin.edu.au
- ⁹A. J. Woods and A. Sehic, “The Compatibility of LCD TVs with Time-Sequential Stereoscopic 3-D Visualization,” *Stereoscopic Displays and Applications XX, Proc. SPIE* **7237**, 72370N (2009). www.3d.curtin.edu.au
- ¹⁰H. Jorke and M. Fritz, “Stereo projection using interference filters,” *Stereoscopic Displays and Virtual Reality Systems XIII, Proc. SPIE* **6055**, 60550G (2006).
- ¹¹A. J. Woods, *et al.*, “Characterizing crosstalk in anaglyphic stereoscopic images on LCD monitors and plasma displays,” *J. Soc. Info. Display* **15**, No. 11, 889-898 (November 2007). ■

Paper 15 M. A. Weissman, A. J. Woods (2011) "A simple method for measuring crosstalk in stereoscopic displays" in Stereoscopic Displays and Applications XXII, Proceedings of IS&T/SPIE Electronic Imaging, SPIE Vol. 7863, pp. 786310-1 to -11, Burlingame, California, January 2011.

A simple method for measuring crosstalk in stereoscopic displays

Michael A. Weissman^{*a}, Andrew J. Woods^b

^a TrueVision Systems, Inc., 114 E Haley Street, Santa Barbara, CA 93101, USA

^b Centre for Marine Science & Technology, Curtin University, GPO Box 1987, Perth 6845 Australia

ABSTRACT

Crosstalk (also known as “ghosting”, “leakage”, or “extinction”), a vitally important concept in stereoscopic 3D displays, has not been clearly defined or measured in the stereoscopic literature (Woods^[3]). In this paper, a mathematical definition is proposed which uses a “physical” approach. This derivation leads to a clear definition of left-view or right-view crosstalk and shows that 1), when the display’s black level is not zero, it must be subtracted out and 2), when the source intensities are equal, crosstalk can be measured using observed intensities totally within the respective view. Next, a simple method of measuring crosstalk is presented, one that relies on only viewing a test chart on the display. No electronic or optical instruments are needed. Results of the use of the chart are presented, as well as optical measurements, which did not agree well with chart results. The main reason for the discrepancy is the difficulty of measuring very low light levels. With wide distribution, this tool can lead to the collection of useful performance information about 3D displays and, therefore, to the production of the best stereoscopic displays.

Keywords: crosstalk, extinction, ghosting, stereoscopic displays, 3D displays

1. INTRODUCTION

Maintaining low crosstalk in a stereoscopic display system – that is, reducing, or extinguishing if possible, the amount of “wrong” image in each eye (also known as “ghosting” or “leakage”) – is critically important for comfortable and high-quality 3D viewing. A moderate amount can cause eyestrain; a large amount will prevent fusing the 3D scene. However, when evaluating a stereoscopic display, it is often difficult to measure the amount of crosstalk in the display:

- Due to complexity of the system,
- Due to lack of measurements,
- Due to the reluctance of manufacturers to release data,
- Due to *difficulty* of making the measurement.

Furthermore, we find in the stereoscopic literature (Woods^[3]) that there is much ambiguity and confusion about both the descriptive and mathematical definitions of this important concept. One objective of the current work is to model the stereoscopic image-making process and to come up with a clear mathematical definition.

A second objective is to propose a simple method of measuring the crosstalk fraction and extinction ratio that relies on viewing test patterns on the display without the need for electronic or optical instruments. Our hope is that this tool can be distributed widely and will lead to the collection of consistent information about 3D displays, and therefore, to the production of the best stereoscopic displays possible.

In this paper, we focus on a mathematical definition of crosstalk. As discussed by Woods^[3], mathematical definitions of “crosstalk”, “ghosting”, “leakage”, and “extinction ratio” are quite varied within the stereoscopic literature. Sometimes, when characterizing “white-to-black” crosstalk[†], a simple ratio of the ghost image (the crosstalk contribution) to the white image in the same eye is used^[7]; sometimes this ratio is taken against the white image as seen in the opposite view^{[8][9]}. Sometimes it is taken against the source image rather than the output, observed image^[10]. Sometimes the

* mweissman@truevisionsys.com; www.truevisionsys.com

† A white image is leaked across to a black image.

black level is subtracted out^{[11][12][13][14][15][16][17]}, sometimes not^{[7][8][9][10]}. In order to confirm which formulation is most appropriate, a “physical” model of crosstalk is developed in the next section.

2. DEFINING CROSTALK

A model of the optical process for the formation of stereoscopic images is given in Figure 1. Going from left to right on the diagram, the Left and Right Source Images create source light intensities[‡] that enter into “stereoscopic processing”. This is where the two images are combined – so that they overlap as perfectly as possible in the resultant stereo view – and separated back into each of the viewer’s eyes.

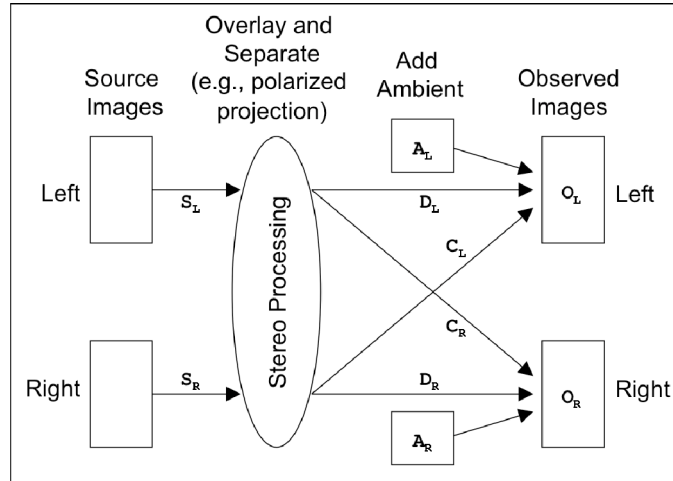


Figure 1. Physical model of the stereoscopic display process, showing light passing from source images, through stereoscopic processing, to observed images. (The variables are defined in the text.)

The combining/separating process takes various forms and technologies. It could be temporally multiplexed (as in time-sequential CRTs, LCDs, or projectors), spatially multiplexed (as in row-interleaved and autostereoscopic displays), or two-channel (as in projector systems or head-mounted displays). A dual projector display, for example, encodes the left and right images with polarized light and overlays them on a (polarization preserving) screen. Polarized glasses are used to decode the two images into the two eyes. The stereoscopic processing part of the display system consists of the projector filters, the screen, and the glasses. The optical processing of any part of this sub-system can be incomplete, leading to crosstalk.

After stereoscopic processing, an observed left or right image is composed mostly of light that was intended for that view, but there can be some “leaked” or “crossed over” contribution from the unintended image. In addition, there could be a contribution from ambient light. Therefore, the observed image intensity for each eye (O_L, O_R) is made up of three components:

$$O_L = D_L + C_L + A_L \quad (1a)$$

$$O_R = D_R + C_R + A_R \quad (1b)$$

where

D = Direct contribution to the observed image.

C = Crossover contribution to the observed image.

A = Ambient light contribution to the observed image.

The direct and crossover contributions can be characterized as portions of the source intensities; i.e., let

[‡] By “intensity”, we are referring to the luminance at some position on the display surface, which is usually measured in cd/m^2 . This emitted light can have any spectral character. For example, in color displays, the formulation could be applied to the red, green, and blue channels separately.

$$\tau_L = D_L/S_L, \quad \tau_R = D_R/S_R \quad (2a, b)$$

$$\chi_{RL} = C_L/S_R, \quad \chi_{LR} = C_R/S_L \quad (3a, b)$$

where S_L, S_R = left and right source image intensities. These fractions can be called

“transmittance” (τ_L and τ_R), the fraction of source image that is intended for each eye, and

“crosstalk” (χ_{RL} and χ_{LR}), the fraction of source image that crosses over or leaks, forming the “ghost” image.

Note the subscript notation “RL” and “LR”. “RL” is used to represent the crosstalk from *Right Image to Left Image*, and vice-versa. This clarifies which crosstalk contribution is being referred to. Both crosstalk and transmittance are simply fractional quantities, not constants. Since the formation of images on stereoscopic displays is sometimes nonlinear, these quantities can be functions of the source intensity levels (as in time-sequential liquid-crystal displays [15][16][17]).

Equations 3 provide a simple, basic, definition of crosstalk: the leaked intensity in one view as a fraction of the source intensity of the other view. Unfortunately, it is often impossible to measure these quantities. The source intensity must be measured before stereo processing; on some displays, such as those with a lenticular or polarizing film, this cannot be done. In addition, the observed intensities (of Equation 1) are the sum of three contributions. Even if we reduce the ambient light to zero, the observed light is the sum of direct and crossed-over light. There are two measured quantities and four unknowns. Theoretically, we could “turn off”, say, the left view and measure only a direct contribution in the right and a crossover contribution in the left. However, in most displays, when black images are presented to the display, the resulting light output is not zero. Thus, the direct contribution in the left and the crossover contribution in the right have not been eliminated.

The light level of a black image (i.e., zero “signal”) is called the black level (BL) of the display. LCDs, in particular, have a relatively high BL, which can be comparable to the crossover contribution. Even for displays having very low intrinsic BL, such as CRTs, plasmas, and OLEDs, there can still be a significant BL if their contrast and/or brightness levels are not adjusted properly.

The conclusion is that a formulation is required that subtracts out any influence of the black level. In addition, it should use quantities measured after stereo processing and, if possible, in only one view. This is presented in the next section.

3. MEASURING CROSSTALK

In most stereoscopic 3D displays, the maximum ghosting[§] occurs when one view has maximum signal level, or a “white” image, and the other has minimum signal level, or a “black” image. This is commonly called white-to-black crosstalk and is the most common way to characterize crosstalk in 3D displays.

As discussed above, white and black image pairs are not sufficient to measure crosstalk when the display has a non-zero black level. A third image pair must be added so that the black level can be properly accounted for. This is illustrated in Figure 2. White and black source image pairs are combined to produce three pairs of observed images. For the left view, for example, there are three resulting observed images: “White”, “Ghost”, and “Black”, as follows,

- White: The observed image is composed of mainly the direct white image with a small crossover component from the black image, plus ambient; i.e., from Equations 1, 2, and 3,

$$O_{WL} = \tau_L (W) + \chi_{RL} (B) + A_L \quad (4a)$$

- Ghost: The observed image is composed of the direct black image plus the crossover white image (these two can be similar in magnitude), plus ambient,

$$O_{GL} = \tau_L (B) + \chi_{RL} (W) + A_L \quad (4b)$$

[§] As discussed by Woods^[3] and others, ghosting, that is, the *perception* of crosstalk, also depends on content. For example, when the disparity (or parallax) of homologous objects is very small or zero, the crossover contribution lies on top of the direct contribution and is therefore not noticeable by the user. However, the contribution is still there and can be measured.

- Black: The observed image is composed of the direct black image plus the crossover black image, plus ambient,

$$O_{BL} = \tau_L(B) + \chi_{RL}(B) + A_L \quad (4c)$$

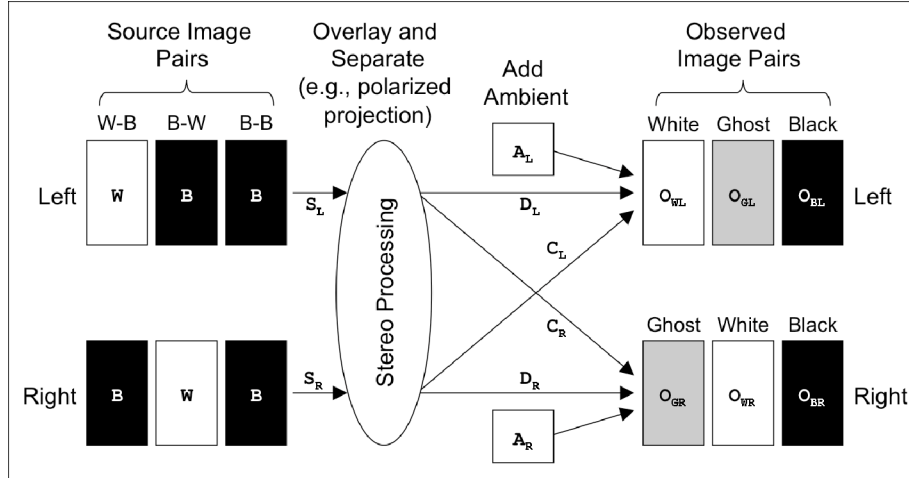


Figure 2. Two white and black Source Images combine to form six Observed Images: “White”, “Ghost”, and “Black” for each view. (Variables are defined in the text.)

where W is the light intensity coming from the white source image and B is the intensity of the black source image. Even though the black image comes from the minimum signal level (e.g., “zero gray-level”), it will not necessarily be zero, because of the black level of the display.

Subtracting Equation 4c from 4a and Equation 4c from 4b, leads to, respectively,

$$O_{WL} - O_{BL} = \tau_L(W - B) \quad (5a)$$

$$O_{GL} - O_{BL} = \chi_{RL}(W - B) \quad (5b)$$

And in turn,

$$\chi_{RL} = \tau_L(O_{GL} - O_{BL}) / (O_{WL} - O_{BL}) . \quad (6a)$$

A similar derivation follows for the right view,

$$\chi_{LR} = \tau_R(O_{GR} - O_{BR}) / (O_{WR} - O_{BR}) . \quad (6b)$$

This result is convenient because all the quantities are measured on the “same side”. However, these equations are *not* convenient because they still require the transmittance factors, which could be difficult to measure. Therefore, the final step is to define an “observed” crosstalk as

$$OCT_{RL} = \chi_{RL} / \tau_L = (O_{GL} - O_{BL}) / (O_{WL} - O_{BL}) \quad (7a)$$

$$OCT_{LR} = \chi_{LR} / \tau_R = (O_{GR} - O_{BR}) / (O_{WR} - O_{BR}) . \quad (7b)$$

This parameter has been called “System Crosstalk” by Huang^[11] and is used by many authors^{[13][14][15][16][17]}. We refer to it here as “observed crosstalk” to emphasize that it uses quantities measured in the observed images and to distinguish it from the crosstalk fraction defined by Equations 3. We suggest the previous crosstalk fraction, χ , be called “intrinsic” crosstalk because it is defined by the source of the crossover contribution. As seen in Equations 7, the difference between observed and intrinsic crosstalk is the transmittance.

Authors will sometimes use the term “extinction ratio” when referring to crosstalk^[3]. The *Extinction Ratio* is the inverse of the crosstalk fraction. That is,

$$ER_{RL} = 1/OCT_{RL} = (O_{WL} - O_{BL}) / (O_{GL} - O_{BL}) \quad (8a)$$

$$ER_{LR} = 1/OCT_{LR} = (O_{WR} - O_{BR}) / (O_{GR} - O_{BR}) \quad (8b)$$

For example, good values for OCT and ER in a stereo display are 1% and 100:1, respectively.

4. RELATING OBSERVED CROSSTALK TO GRAY-LEVELS

Within computers and digital video systems, the “gray-level” is the numerical representation of the brightness of a pixel, usually in the range [0,255]. This is the “signal” that is sent to the display. For legacy reasons that we will not discuss here, the display response, that is, the intensity displayed for a given gray-level, is nonlinear. According to the sRGB color standard (the default for most computers), this nonlinear “transfer curve” from gray-levels (G) to intensity (O) is

$$O/O_{MAX} = (G/G_{MAX})/12.92, \text{ for } G/G_{MAX} < 0.04045 \quad (9a)$$

$$O/O_{MAX} = ((G/G_{MAX}) + 0.055) / (1 + 0.055)^{2.4}, \text{ for } G/G_{MAX} \geq 0.04045 \quad (9b)$$

where O_{MAX} and G_{MAX} are the maximum intensity and gray-level values, respectively.^[4]

This curve is usually approximated as “Gamma 2.2”, or

$$O/O_{MAX} = (G/G_{MAX})^{2.2}, \text{ for } 0 \leq G/G_{MAX} \leq 1 \quad (10)$$

Gamma 2.2 is actually not a good approximation for the low intensity range where crosstalk exists. This is demonstrated in Figure 3. Although these two formulas track well over most of the 0 to 1 range, below about 6% of maximum intensity they diverge. In the range of typical ghost intensities, around 1%, the two curves differ by 40% to 60%.

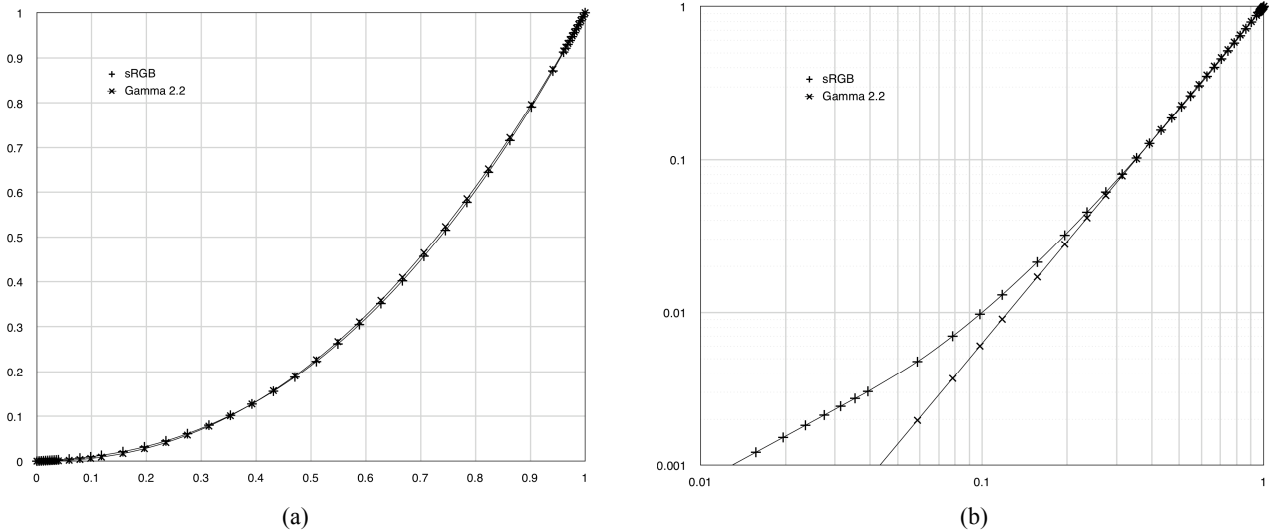


Figure 3. Comparing sRGB to Gamma 2.2: a) linear plot, b) log-log plot. X-axis: scaled gray-level (G/G_{MAX}), Y-axis: scaled intensity (O/O_{MAX}).

Which do we use? Discussions in the literature (e.g., Koren^[6]) indicate that most monitor calibration procedures ignore sRGB, and simply calibrate to Gamma 2.2. Figure 4 shows a calibration of a stereoscopic LCD (JVC GD463D1OU) using the “Spyder3Elite”^[5] colorimeter. (This monitor uses passive glasses with row-interleaved polarization. The calibration was done without polarizing filters on the Spyder.) We see that the calibrated transfer curve is closer to Gamma 2.2 in this low range where the two curves diverge.

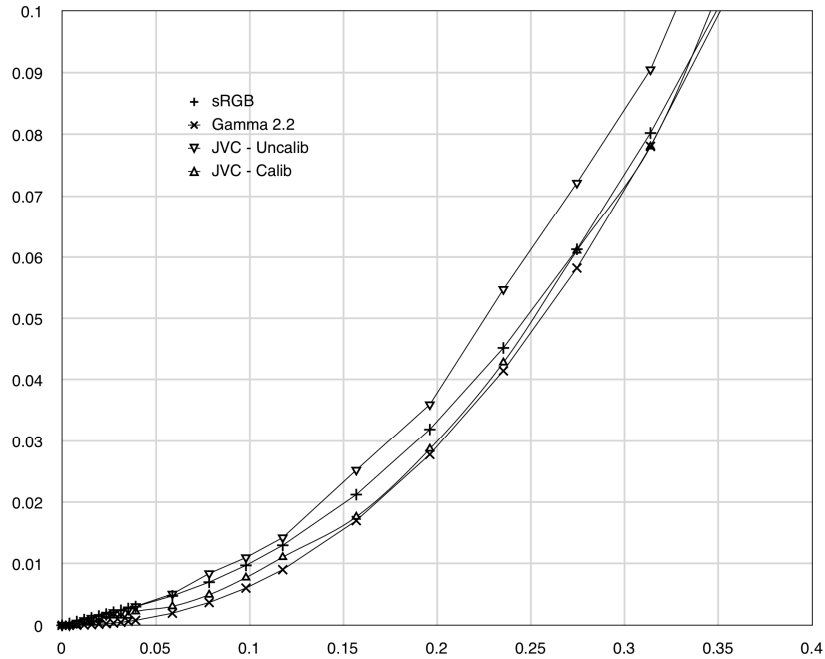


Figure 4. The lower 10% of the transfer curve for a calibrated and uncalibrated 3D monitor, comparing to sRGB and Gamma 2.2. X-axis: scaled gray-level (G/G_{MAX}), Y-axis: scaled intensity ($(O-O_B)/(O_{MAX}-O_B)$).

In the “real world”, a display might suffer from “white crush” and/or “black crush”. That is, the transfer curve might be truncated at top and/or bottom, as illustrated in Figure 5, possibly because of poor adjustment of the display’s contrast and brightness controls. The transfer curves of Figure 4 were performed after removing white and black crush.

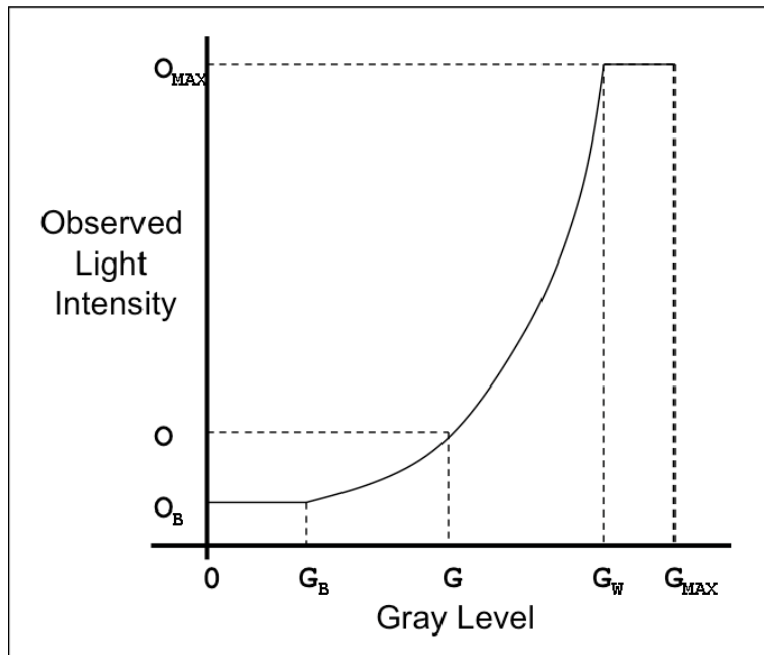


Figure 5. A “real world” display transfer curve.

White and black crush can be removed, or at least minimized, using the display’s brightness and contrast adjustments; however, there is usually a residual black level (which is, of course, large or small depending on the display technology).

This acts as a “pedestal” or bias on which the signal rides. Thus, assuming that Gamma 2.2 is our best estimate for the transfer curve, Equation 10 is modified to read

$$(O - O_B) / (O_{MAX} - O_B) = (G/G_{MAX})^{2.2} \tag{11}$$

where O_B is now the black level of the display, the output intensity for a zero gray-level image. The left-hand side of this equation is “scaled” intensity. This is what is used in Figure 4.

This leads to equations for observed crosstalk in terms of gray-levels:

$$OCT_{RL} = (O_{GL} - O_{BL}) / (O_{WL} - O_{BL}) = (G_{GL}/G_{MAX})^{2.2} \tag{12a}$$

$$OCT_{LR} = (O_{GR} - O_{BR}) / (O_{WR} - O_{BR}) = (G_{GR}/G_{MAX})^{2.2} \tag{12b}$$

That is, if we can estimate the crosstalk intensities in terms of gray-levels, we can actually measure the crosstalk fraction. Note that this result is based on the following assumptions:

1. White and black crush have been eliminated.
2. The display has been calibrated to Gamma 2.2.
3. This calibration is valid after stereo processing.

5. THE TEST CHART

Weissman^[1] and Bloos^[2] have published charts to measure crosstalk (Figure 1). While they do provide a means to compare displays, the numerical results on these charts are in error because the interpretation is in gray-levels rather than intensity values. That is, the nonlinear transfer curve between gray-levels and intensity was neglected. (Weissman’s chart was corrected in 2008.)

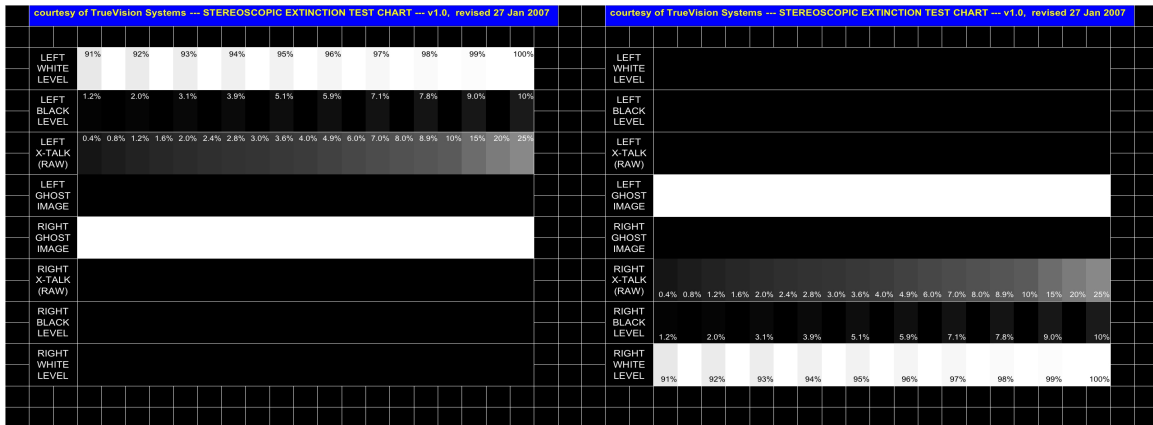


Figure 6a. “Stereoscopic Extinction Test Chart, v1.0” by M.A.Weissman^[1], side-by-side format.

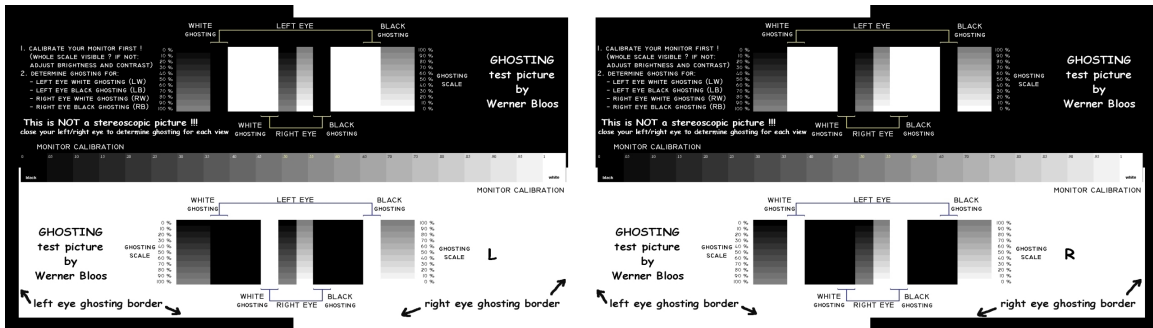
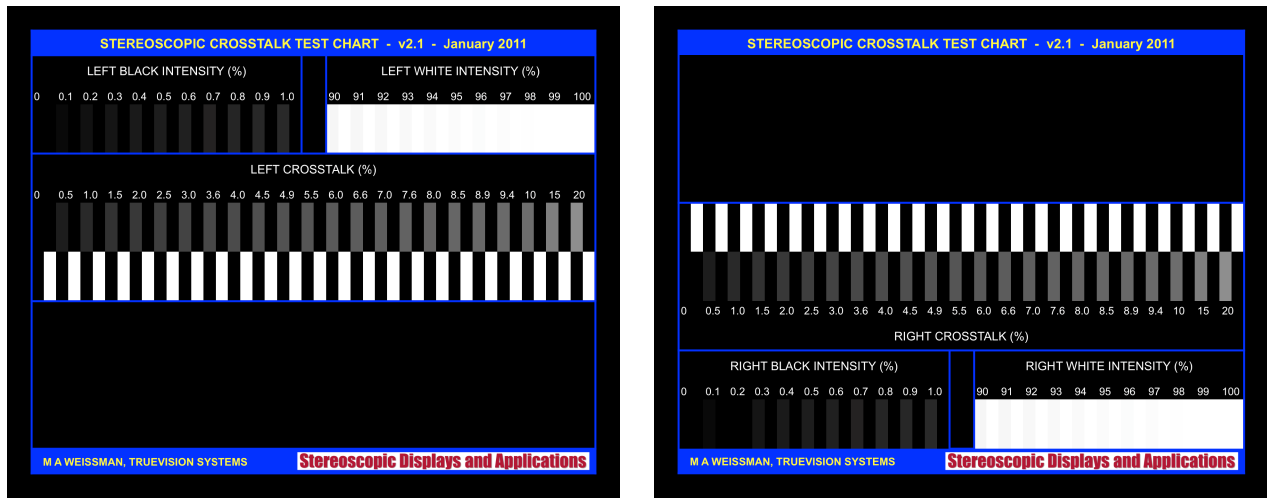


Figure 6b. “Ghost TEST” by W.Bloos^[2], side-by-side format.

The new chart, the “Stereoscopic Crosstalk Test Chart”**, presents all scales as percent intensity and makes it easier to compare the ghost image of the white image with graduated gray patches. As shown in Figure 7, the ghost image comes from the seriated white row of the opposite image and is interleaved with the gray patches for better readability. The gray patches are calibrated according to Equations 12.



(a) Left Image

(b) Right Image

Figure 7. The new version of the Stereoscopic Crosstalk Test Chart. The images may be resized, but, when presented on a stereoscopic display, the left and right images must overlap exactly.

The white and black scales are used to minimize white and black “crush”, the truncation of the transfer curve at the top and/or the bottom. The display’s brightness and contrast levels are adjusted so that these scales are visible. This new version of the chart reports these scales as percent intensity (rather than percent gray-level) and limits them to ranges that are appropriate for sufficient accuracy (10% for white, 1% for black).

The following table gives guidelines for using the chart:

Table 1. How to use the Stereoscopic Crosstalk Test Chart.

1. Adjust brightness and contrast: Put on eyewear or otherwise view in stereo. Using the display’s brightness and contrast controls and the Black Intensity scale, minimize the black level without black crush (if possible!). Using White Intensity scale, maximize the white level without white crush. Repeat as needed.
2. Calibrate display: If possible, calibrate to a gamma value of 2.2 and in stereoscopic mode, that is, after stereo processing.
3. Read Crosstalk: Put on eyewear or otherwise view in stereo. View with either left or right eye (*not both at same time!*). Read the left crosstalk % from the upper interleaved scale at the place where the intensities match and the right crosstalk % from the lower interleaved scale.

6. MEASUREMENTS

6.1 Typical Stereoscopic Crosstalk Test Chart Readings.

The SCT Chart was used to examine the crosstalk of several 3D displays, as listed in Table 2.

** Weissman’s original chart was called “The Stereoscopic *Extinction* Test Chart” because the scale was calibrated as extinction ratio.

Table 2. Typical Stereoscopic Crosstalk Test Chart measurements. The numeric values are percent crosstalk.

	BEFORE MONITOR CALIBRATION		AFTER MONITOR CALIBRATION	
	LEFT EYE	RIGHT EYE	LEFT EYE	RIGHT EYE
JVC GD463D10U (Passive)	0.6	0.4	1.3	1.4
Hyundai S465D (Passive)	3.0	3.3	1.3	1.5
Acer GD235 (Active)	0.3	0.4	0.6	0.6

This table shows different results before and after monitor calibration (using the Spyder3Elite without glasses or filters). Both the JVC and Acer had higher crosstalk readings after calibration; the Hyundai, lower. The before/after change of values is likely due to the direction the transfer curve shifts after calibration, which we have seen lead to both brighter and darker displays. While we do not have transfer curves for the Acer and Hyundai, the JVC before and after curves are given in Figure 6. It can be seen there that, around an intensity level of 0.01 (on the vertical scale), the calibrated curve is about 0.003 darker than the uncalibrated curve. Thus, since the scaled ghost intensity has not changed, the matching gray patch shifts to a higher value on the scale. This accounts for 0.3 of the roughly 0.85 difference in percent CT readings. The rest could be due to 1) poor accuracy of the Spyder at low intensity values and 2) changes in the transfer curves after stereo processing. That is, the curves might not be the same after we put the glasses on.

Even though the polarization process, per se, is linear, there was a shift in color temperature (white point) of the monitor at the low end of the intensity range. According to the Spyder calibration of the JVC, the shift was about 5% between intensity values of about 16% to 38%. It is reasonable to assume there are shifts of this magnitude or larger at the lower (ghost) intensities. A change of the white point could lead to a nonlinear change in luminance readings (due to the changed transmittance of the polarizers) and thus a change in the transfer curve. (A change in color is often observed after putting glasses on.)

6.2 Transfer Curves After Stereoscopic Processing

In an attempt to measure the transfer curve after stereo processing, we mounted left and right circular polarizing filters (the same filters as used in the glasses) in front of the Spyder. Because extinction of a circular filter is a function of rotation in its plane (although not as strong as for a linear polarizer), care was taken to orientate the filters exactly as they are in the glasses.

Row-interleaved monitors are also sensitive to the vertical angle of view; therefore, another important factor is the acceptance angle of the instrument. When viewing by eye, the acceptance angle, defined by the eye's pupil, is very small. The Spyder has a much larger acceptance angle (not measured). Therefore, the instrument was mounted on a tube that was 278 mm long and 44 mm diameter, which restricted the acceptance angle to 9°. While this improved the acceptance angle, it severely limited the luminance, which dropped by a factor of 39. We attempted to measure transfer curves, but the Spyder results were not reliable, especially at the lower intensity levels representative of the ghost image. Therefore, we were not successful at measuring transfer curves after stereoscopic processing, which, for a row-interleaved monitor, requires a more sensitive, more accurate instrument.

6.3 Direct Measurements of Observed Crosstalk

A direct measurement of crosstalk would measure the terms in Equations 7 (O_{GL} , O_{BL} , O_{WL} , O_{GR} , O_{BR} , O_{WR}) after stereoscopic processing (i.e., after glasses or filters). Since the ghost and black intensities can be close in value, they must be measured very accurately. Attempts were made, but, for reasons discussed above, we were not successful with our current equipment, and therefore we could not compare the SCT Chart readings to direct measurements.

7. CONCLUSIONS

In Section 2, we present a physical model of the crosstalk process and introduce the most fundamental definition of crosstalk, "Intrinsic Crosstalk" (Equations 3), which is the ratio of ghost image intensity to its source intensity. However, it is not possible to use this for crosstalk measurements when the source intensity cannot be measured directly or the black level contributes to crosstalk, which is usually the case.

Hence, in Section 3, the model is applied to three stereo pairs ("white-black", "black-white", and "black-black") in order to make measurements on only observed images and to subtract out the black levels. This approach and the resulting

definition of a crosstalk fraction (Equations 7) agree with other authors^{[11][13][14][15][16][17]}. This definition has been called “System Crosstalk” by Huang et al^[11]; however, here we call it “Observed Crosstalk” in order to draw a clear distinction between it and “Intrinsic Crosstalk”. The former uses observed intensities; the latter uses source intensities.

This formulation does not assume the crosstalk fractions or the transmittances are constants; it does, however, assume that 1) the source intensities are “white” and “black” (maximum and minimum image intensities) and 2) the left and right source intensities of image pairs are equal. Both of these restrictions can be lifted within this model. Indeed, the model can be used to study arbitrary source intensities, as in “gray-to-gray” crosstalk^{[15][16][17]}. These topics will be basis for future work.

In Section 4, we consider the relation between observed image intensities and the means of creating images in electronic displays: gray-levels. We show that, even though sRGB (Equations 9) is the standard for computer graphics, displays are generally calibrated to the Gamma 2.2 transfer curve (Equation 10) - assuming that white and black crush are also eliminated. Based on these assumptions, Observed Crosstalk can be direct related to gray-levels, as shown in Equations 12.

Thus, it is possible to create a chart in which ghost images are compared to gray patches calibrated to crosstalk percentages. Such a chart, the “Stereoscopic Crosstalk Test Chart”, is presented in Section 5. The SCT Chart also has white and black scales to be used to minimize white and black crush. This chart will be available soon for general distribution via the Stereoscopic Displays and Applications Conference website (www.stereoscopic.org). In the future, additional versions will be added for color measurements and different formats. Producing the chart as an application will also be considered.

In Section 6, we present some results from attempts to validate the readings of the SCT Chart. First, to illustrate the use of the chart, readings are given before and after monitor calibration (using the Spyder3Elite^[5] colorimeter). There can be significant differences, mainly due to the shift of transfer curve after calibration and the change of white and black levels.

Then we attempted to measure the transfer curve of a row-interleaved monitor after stereoscopic processing, that is, with the polarizing filters (as found in the glasses) in front of the colorimeter. However, this was not successful, because of the reduction of light into the Spyder and the apparatus needed to control the acceptance angle of the device. In short, a much more sensitive instrument is needed for this measurement.

Determination of the transfer curve after stereoscopic processing is very important. In general, when monitors are calibrated to, say, the Gamma 2.2 standard, it is done “with the glasses off”, i.e., before (complete) stereoscopic processing. Thus, if there is any nonlinearity in the system, it is likely the “glasses on” images are not calibrated to the same curve.

Some display systems are known to be nonlinear. For example, time-sequential LCDs have been shown to be nonlinear in its crosstalk characteristics^{[15][16][17]}. That is, the crosstalk percentages are a function of the source intensities. It is likely the transmittance is also a function of source intensity, and therefore a calibration curve “before glasses” will be different from one “after glasses”. In the current study using a row-interleaved monitor, we found indications that the white point could be shifting significantly in the same intensity range as ghost intensities. This means the color channels (R, G, and B) might not be calibrated the same in this region and that the display is not following a standard transfer curve. This is an important area for future research.

Our conclusion from these preliminary measurements is that it could be rare to find a 3D display that is calibrated (post-stereo processing!) to Gamma 2.2 in these low intensity ranges, even after calibration with a colorimeter. Yet, the crosstalk values on the SCT Chart are based on this transfer curve. Are the numbers on the chart still useful?

(The values on the SCT Chart also depend on having no white and black crush. This criterion is easier to achieve, using the contrast and brightness controls of the display.)

Although we could not confirm the accuracy of the crosstalk values given by the SCT Chart, we feel that the numbers are still useful. The numbers on the chart give us a “snapshot” of the system. Yes, they might change if the monitor is calibrated to a gamma of 2.2, but the uncalibrated display might be preferred. The readings from chart can be used as a measure of crosstalk *for those conditions*. (In this case, we would still recommend minimizing white and black crush, as in the guidelines of Table 1, to maintain consistency.)

Whether the display is calibrated or uncalibrated, the SCT Chart indicates the “strength” of the crosstalk component of the image as compared to the maximum image intensity. That is, it is a measure of the influence of the ghost image compared to the intended image, which is, after all, viewed with the same transfer curve, whatever it is. The readings from the SCT Chart express this measure *as if* the transfer curve were Gamma 2.2.

In addition, the chart can always be used in a comparative way. Comparing monitors, changing display parameters, trying different glasses, comparing viewing positions and angles, etc., are all common needs when working with a stereoscopic display system. The chart provides a simple way to do this. If there are special requirements, such as determining the crosstalk at the top of the screen, the chart may be resized and repositioned; however, it is important to keep the two views matched in size and in perfect alignment.

The difficulty we had using a low-end colorimeter (the Spyder) verifies the premise we put forward in the introduction: that measurements of crosstalk are difficult and generally not accessible to users. The SCT Chart alleviates these issues and provides a means to achieve better consistence and performance of stereoscopic 3D displays.

REFERENCES

- [1] M. A. Weissman, “A simple measurement of extinction ratio” presented at Stereoscopic Displays and Applications XVIII, San Jose (2007).
- [2] W. Bloos, “Ghosting test - standard method for determining ghost image,” Stereo Forum, online, dated 5 June 2008. <http://www.stereoforum.org/viewtopic.php?f=16&t=53>.
- [3] A. J. Woods, “How are Crosstalk and Ghosting Defined in the Stereoscopic Literature” in Proc. SPIE Stereoscopic Displays and Applications XXII (in press), Burlingame, 7863, (2011).
- [4] Wikipedia, http://en.wikipedia.org/wiki/SRGB_color_space
- [5] DataColor AG, <http://spyder.datacolor.com/product-mc-s3elite.php>
- [6] N. Koren, <http://www.normankoren.com/makingfineprints1A.html>
- [7] Woods, A. J., Harris, C. R., “Comparing levels of crosstalk with red/cyan, blue/yellow, and green/magenta anaglyph 3D glasses” in Proc. SPIE Stereoscopic Displays and Applications XXI, 7253, 0Q1-0Q12 (2010).
- [8] Chu, Y.-M., Chien, K.-W., Shieh, H.-P. D., Chang, J.-M., Hu, A., and Yang, V., “3D Mobile Display Based on Dual Directional Lightguides” in 4th International Display Manufacturing Conference, Taipei, Taiwan, 799-801 (2005).
- [9] Hong, H.-K., Jang, J.-W., Lee, D.-G., Lim, M.-J., Shin, H.-H., “Analysis of angular dependence of 3-D technology using polarized eyeglasses,” in Journal of the SID, 18(1), 8-12 (2010).
- [10] Huang, K.-C., Tsai, C.-H., Lee, K., Hsueh, W.-J., “Measurement of Contrast Ratios for 3D Display” in Proc. SPIE Input/Output and Imaging Technologies II, 4080, 78-86 (2000).
- [11] Huang, K.-C., Lee, K., Lin, H.-Y., “Crosstalk issue in stereo/autostereoscopic display” in Proc. Int. Display Manufacturing Conference, 2–18 (2009).
- [12] Pala, S., Stevens, R., Surman, P., “Optical crosstalk and visual comfort of a stereoscopic display used in a real-time application” in Proc. SPIE Stereoscopic Displays and Virtual Reality Systems XIV, 6490, 111-1112 (2007).
- [13] Liou, J.-C., Lee, K., Tseng, F.-G., Huang, J.-F., Yen, W.-T., Hsu, W.-L., “Shutter Glasses Stereo LCD with a Dynamic Backlight” in Proc. SPIE Stereoscopic Displays and Applications XX, 7237, 72370X (2009).
- [14] Boher, P., Leroux, T., Bignon, T., Collomb-Patton, V., “Multispectral polarization viewing angle analysis of circular polarized stereoscopic 3D displays” in Proc. SPIE Stereoscopic Displays and Applications XXI, 7253, 0R1-0R12 (2010).
- [15] S.-M. Jung, et al, “Improvement of 3-D Crosstalk with Over-Driving Method for the Active Retarder 3-D Displays” in SID Digest 2010, Seattle, 1264-1267 (2010).
- [16] S. Shestak, et al, “Measuring of Gray-to-Gray Crosstalk in a LCD Based Time-Sequential Stereoscopic Display” in SID Digest 2010, Seattle, 132-135 (2010).
- [17] C.-C. Pan, et al, “Cross-Talk Evaluation of Shutter-Type Stereoscopic 3D Display” in SID Digest 2010, Seattle, 128-131 (2010).

Paper 16 A. J. Woods (2011) "How are crosstalk and ghosting defined in the stereoscopic literature?" in Stereoscopic Displays and Applications XXII, Proceedings of IS&T/SPIE Electronic Imaging, SPIE Vol. 7863, pp. 78630Z-1 to -12, Burlingame, California, January 2011.

How are Crosstalk and Ghosting defined in the Stereoscopic Literature?

Andrew J. Woods*

Centre for Marine Science & Technology, Curtin University, GPO Box U1987, Perth 6845 Australia

ABSTRACT

Crosstalk is a critical factor determining the image quality of stereoscopic displays. Also known as ghosting or leakage, high levels of crosstalk can make stereoscopic images hard to fuse and lack fidelity; hence it is important to achieve low levels of crosstalk in the development of high-quality stereoscopic displays. In the wider academic literature, the terms crosstalk, ghosting and leakage are often used interchangeably and unfortunately very few publications actually provide a descriptive or mathematical definition of these terms. Additionally the definitions that are available are sometimes contradictory. This paper reviews how the terms crosstalk, ghosting and associated terms (system crosstalk, viewer crosstalk, gray-to-gray crosstalk, leakage, extinction and extinction ratio, and 3D contrast) are defined and used in the stereoscopic literature. Both descriptive definitions and mathematical definitions are considered.

Keywords: stereoscopic, crosstalk, cross talk, cross-talk, ghosting, leakage, extinction, 3d contrast.

1. INTRODUCTION

Crosstalk (sometimes also known as ghosting or leakage) is a critical factor affecting the image quality of stereoscopic 3D displays. Crosstalk is the incomplete isolation of the left and right image channels so that one image leaks into the other. This paper reviews the literature on crosstalk and related terms in stereoscopic displays and provides a useful basis for the understanding, further analysis and standardization of the terminology relating to 3D crosstalk. Crosstalk is present in most stereoscopic displays and is often the most important factor affecting the 3D image quality.

To have a constructive discussion about crosstalk, it is necessary to have a common understanding. Surprisingly, very few early papers actually define crosstalk and related terms when they are discussed, many papers use crosstalk and ghosting interchangeably, and even where there are definitions, the definitions are not always consistent between papers.

This paper is related to an earlier paper which reviewed the definition, measurement and mechanisms of crosstalk^[1] but this paper focuses more on the definitions given in the published literature.

Stereoscopic terminology can be used to describe a principle in general terms and can also be used to quantify a physical property – this paper will review both the descriptive and mathematical definitions where applicable.

To obtain an idea of the commonality of the various terms related to crosstalk across the stereoscopic literature, a keyword search was performed across the 1273 documents on the SD&A (Stereoscopic Displays and Applications) 20-year DVD-ROM^[2] for various terms relevant to this paper. The results are detailed in Table 1. Importantly, the use of the term crosstalk is very common, present in over 10% of all stereoscopic documents in the collection.

2. TERMINOLOGY AND DEFINITIONS

2.1 Crosstalk - Descriptive Definition

The term 'crosstalk' (also often written as 'cross-talk'^[3], 'cross talk'^[24] or even 'X-talk'^[3]) is very widely used in the stereoscopic literature (see Table 1). The term 'crosstalk' without an intermediate space or hyphen, is the more commonly used variant so that is what will be used in this paper. It is recommended that authors adopt this as the standard form.

* A.Woods@curtin.edu.au; phone +61 8 9266 7920; www.AndrewWoods3D.com

Table 1: Occurrence of stereoscopic terms across the 1273 documents in the SD&A 20-year DVD-ROM^[2]

Crosstalk	125 documents with 1092 instances
Cross talk and Cross-talk	95 documents with 325 instances
Ghosting	117 documents with 589 instances
Ghost images	30 documents with 56 instances
Leakage	33 documents with 104 instances
Extinction	30 documents with 83 instances
Extinction Ratio	11 documents with 28 instances
3D Contrast	1 document with 30 instances

The term crosstalk has been described variously – here are some examples:

Lipton (1987)^[5]: “Incomplete left and right channel isolation, or *crosstalk*, is of great concern to the designer of a stereoscopic system.”

Veron, et al (1990)^[6]: “The phenomenon of “bleed through” occurs when the left eye also sees the right image, or vice versa. Bleed through is also referred to as optical *crosstalk* between the two images. The metric that characterizes this phenomena is called the interocular *crosstalk* ratio.”

Montgomery, et al (2001)^[7]: “*Cross talk* represents *leakage* of the left eye image data to the right eye and vice versa as a fraction of the window brightness.”

Stevenson, et al (2004)^[8]: “3D *crosstalk* is a measure of how much of the left eye image gets into the right eye and vice versa.”

Stevens (2004)^[9]: “*Cross-talk* ... describes the *leakage* of the optical signal in one channel of the viewing pupil to an adjoining channel”

Kaptein, et al (2007)^[10]: “imperfect separation of the left and right images, a phenomenon known as *crosstalk*”

Pala, et al (2007)^[11]: “optical *crosstalk* ... is *leakage* of the optical signal from the channel corresponding to the right eye to the channel corresponding to the left eye and vice versa.”

Uehara, et al (2008)^[12]: “3D *crosstalk* is defined as the *leakage* of left-eye image to the right eye and vice versa, and is calculated as the ratio of luminance profiles.”

Lipton (2009)^[28]: “*Crosstalk*. Incomplete isolation of the left and right image channels so that one leaks (*leakage*) or bleeds into the other.”

Despite some variations in wording, there is a common theme across these definitions – i.e. the light from one image channel leaking into another.

The terms ‘3D crosstalk’ and ‘interocular crosstalk’ are also sometimes used but they are usually synonymous with ‘crosstalk’.

The following dictionary definition “Cross-talk: unwanted interference between two neighbouring electronic circuits”^[44] is not inconsistent with the definitions quoted above.

In this paper the following descriptive definition will be used (based on Lipton 2009):

Crosstalk: the incomplete isolation of the left and right image channels so that one image leaks into the other.

2.2 Ghosting

In the general stereoscopic literature and the lay media, the terms ‘crosstalk’ and ‘ghosting’ have often been used interchangeably^{[24][25][26][27]}, but in scientific discussion, it is worthwhile to differentiate these terms.

Crosstalk and ghosting appear to have been first documented as separate terms in 1987 by Lenny Lipton: “If the left eye, for example, also sees the right there will be a *perceived* doubling of the image or “*ghosting*.” Incomplete left and right channel isolation, or *crosstalk*, is of great concern to the designer of a stereoscopic system”^[5]

In 2009, Lipton^[28] provided a more formal definition of the two terms: “Crosstalk. Incomplete isolation of the left and right image channels so that one leaks (leakage) or bleeds into the other. Looks like a double exposure. Crosstalk is a physical entity and can be objectively measured, whereas ghosting is a subjective term.” and “Ghosting. The perception of crosstalk is called ghosting.”

‘Ghost’, ‘Ghost Image’ and ‘Ghosting’ have all been used in the stereoscopic literature and are usually used in the context of the perception of crosstalk.

2.3 Leakage

A formal definition for the term “leakage” was not found in the stereoscopic literature as part of this study, however the term is often used within descriptive definitions of “crosstalk”^{[7][9][11][12][28]} (as summarized in Section 2.1). The Macquarie dictionary definition of “leakage” is “1. the act of leaking; leak. 2. that which leaks in or out. 3. the amount that leaks in or out.”^[44] Without a formal definition of leakage in the stereoscopic literature, it therefore seems appropriate to provide the following definition:

Leakage: the (amount of) light that leaks from one stereoscopic image channel to another.

The term ‘crossover contribution’ has also been used.^[45]

Contrary to this definition: Bos^[46] used the term ‘cell leakage ratio’ but it was undefined in the paper and by usage it appears very similar to what most papers call crosstalk. Walworth, et al^[47] used the sentence “visible leakage is least at 560 nm and no more than 0.2% in the red and blue regions” but this usage appears to be the same as the term crosstalk defined above.

2.4 Crosstalk - Mathematical Definition

Crosstalk can also be used as a metric to express how much crosstalk occurs in a particular stereoscopic display system. When expressed as a metric, ‘crosstalk’ is sometimes called ‘crosstalk ratio’.^{[6][11]} There are two mathematical definitions of crosstalk ratio which will be explained below, so when quoting crosstalk values it is important to specify which crosstalk definition is being used. Unfortunately several papers have quoted values of crosstalk without specifying the actual crosstalk definition they are using.^{[3][8][13][14][15]}

Definition 1:

In its simplest form crosstalk can be defined^[16] as:

$$\text{Crosstalk (\%)} = \text{leakage} / \text{signal} \times 100 \quad (1)$$

Where: ‘leakage’ is used here to mean the maximum luminance of light that leaks from the unintended channel to the intended channel, and ‘signal’ is the maximum luminance of the intended channel.

In practice, two luminance measurements are taken (from the intended eye position): (a) black in the intended channel and white in the unintended channel (this corresponds with leakage), and (b) white in the intended channel and black in the unintended channel (this corresponds with signal).

The following two mathematical definitions of crosstalk from the literature essentially agree with this basic definition:

Chu, et al^[17] define:

$$\text{Crosstalk} \equiv \text{luminance measured at one eye} / \text{luminance measured at the other eye} \quad (2)$$

Note that this definition has been developed for a two-view autostereoscopic display and unfortunately uses rather imprecise language. A close look at the paper suggests that they actually mean “luminance of the other channel at the original eye position” for the denominator of (2).

Hong, et al^[18] provides this definition in the context of a micropolarized display: “one test image consists of black data for the even horizontal lines and white data for the odd horizontal lines” (equating to black in the intended eye and white in the unintended eye) ... “the other test image of black data for the odd horizontal lines and white data for even

horizontal lines” (equating to black in the unintended eye and white in the intended eye) ... “The ratio of the measured luminance using these two test images corresponds to 3-D crosstalk.”

The shortcoming of these definitions is that they don’t include the effect of black level. Some displays are incapable of outputting zero luminance for full black (e.g. LCDs[†]) and other displays which can output zero luminance (e.g. CRT, PDP, and OLED displays[†]) might be incorrectly calibrated such that zero pixel value does not output zero luminance. The presence of non-zero black level does not contribute to visible crosstalk / ghosting and if present it would bias the crosstalk calculation using this first definition. If the black level is set at zero luminance, there would be no problem.

Definition 2:

The second mathematical definition of crosstalk takes into consideration non-zero black level by subtracting the black level luminance:

$$\text{Crosstalk (\%)} = (\text{leakage} - \text{black level}) / (\text{signal} - \text{black level}) \times 100 \quad (3)$$

Several papers support this formulation (but with different variable names):

Pala, et al^[11] wrote: “In this work we define the optical crosstalk C as follows.

$$C = \frac{L_G - L_{BL}}{L_M - L_{BL}} \times 100 \quad (4)$$

Where L_M = Luminance of main image, L_G = Luminance of crosstalk (ghost) image, L_{BL} = LCD background luminance”

Liou, et al^[19] provide the following equations:

$$CL = \frac{BW - BB}{WB - BB} \quad \text{and} \quad CR = \frac{WB - BB}{BW - BB} \quad (5,6)$$

Where: “WB = a video stream with all white as left-eye images, and all-black as right-eye images, BW = a video stream with all-black as left-eye images and all-white as right eye images, BB = a video stream with all-black for both left and right eyes (i.e. the black level of the display), and CL and CR = the crosstalk experienced by the left eye and the right eye.”^[19]

Boher, et al^[20] also provide similar equations (reworked here for clarity and also note that the numerator of (8) has been corrected^[21]):

$$\chi_L = \frac{Y_{LKRW}^{GL}(\theta_L, \varphi_L) - Y_{LKRK}^{GL}(\theta_L, \varphi_L)}{Y_{LWRK}^{GL}(\theta_L, \varphi_L) - Y_{LKRK}^{GL}(\theta_L, \varphi_L)} \quad \text{and} \quad \chi_R = \frac{Y_{LWRK}^{GR}(\theta_R, \varphi_R) - Y_{LKRK}^{GR}(\theta_R, \varphi_R)}{Y_{LKRW}^{GR}(\theta_R, \varphi_R) - Y_{LKRK}^{GR}(\theta_R, \varphi_R)} \quad (7,8)$$

Where: “3D crosstalk of right and left eyes χ_R and χ_L ” and “ (θ_R, φ_R) and (θ_L, φ_L) are the right and left eye positions in polar coordinates with regards to the measurement location”. “ Y_{LKRW} is the luminance for white view on right eye and black view on left eye, Y_{LWRK}^{GL} and Y_{LWRK}^{GR} are the luminances for black view on right eye and white view on left eye using GL and GR filters respectively, Y_{RKLK}^{GL} and Y_{RKLK}^{GR} are the luminance for black view on both eyes”^[20]

Additionally, Weissman, et al^[45] use a different technique to obtain a similar result:

$$CT_{RL} = (O_{GL} - O_{BL}) / (O_{WL} - O_{BL}) \quad \text{and} \quad CT_{LR} = (O_{GR} - O_{BR}) / (O_{WR} - O_{BR}) \quad (9,10)$$

Where: CT_{RL} is crosstalk from right channel to left channel (modified here for clarity), O_{GL} is the luminance of the ghost image (black in the left eye and white in the right eye) as measured from the left eye position, O_{BL} is the luminance of the black level as measured from the left eye position, O_{WL} is the luminance of white in the left eye and black in the right eye as measured from the left eye position, and so on.

This definition is sometimes called ‘black-white crosstalk’ since it uses full-black and full-white images in the testing scheme.^[22] Full-white and full-black are used because maximum ghosting usually occurs when the pixels in the desired eye-channel are full-black and the same pixels in the opposite eye-channel are full-white.

[†] LCD = Liquid Crystal Display; CRT = Cathode Ray Tube; PDP = Plasma Display Panel; OLED = Organic Light Emitting Diode.

Crosstalk can initially be thought of as a fairly simple concept but now things start to get more complicated. On some displays crosstalk can vary with: (a) pixel position on the screen, (b) viewing angle (as expressed in equations (7,8)^{[20][23]}, and (c) properties of the eyewear.

In most 3D displays crosstalk is an additive process and is roughly linear. The maximum leakage usually occurs in high-contrast (black/white) areas so measuring black-white crosstalk often determines the display’s overall crosstalk, but, this is not true for all 3D displays, particularly time-sequential 3D on LCDs using active-shutter glasses, or PDPs, and perhaps other stereoscopic displays. This is discussed further in Section 2.6.

2.5 System Crosstalk and Viewer Crosstalk

In 2000, Kuo-Chung Huang, et al^[29] defined two new terms (System Crosstalk and Viewer Crosstalk) in an attempt to disambiguate the terminology relating to crosstalk at that time:

System Crosstalk: *the degree of the unexpected leaking image from the other eye.*

Viewer Crosstalk: *the crosstalk perceived by the viewer.*^[30]

It is important to note that System Crosstalk is independent of the content (determined only by the display), whereas Viewer Crosstalk varies depending upon the content.

These definitions have similarities to the definitions of Crosstalk and Ghosting provided by Lipton^[28] – but are not exactly the same. The definition of Viewer Crosstalk includes the effect of contrast (and indirectly the effect of parallax) but Lipton’s definition of ghosting includes any perception effect.

Mathematical definitions were also provided^[29]:

$$\text{System Crosstalk (left eye)} = \beta 2 / \alpha 1 \quad (11)$$

Where: “ $\alpha 1$ describes the percentage part of the left-eye image observed at the left eye position”, and “ $\beta 2$ describes the percentage part of the right-eye image leaked to the left-eye position”^[29] and vice versa for the other eye.

Viewer Crosstalk is “defined as the ratio of the luminance of unwanted ghost image, which leaks from the image for the other eye, to the luminance of the correct information received by the viewer’s eyes.”^[29] i.e.

$$\text{Viewer Crosstalk (left eye)} = B \beta 2 / A \alpha 1 \quad (12)$$

Where: A is the luminance of a particular point in the left eye image, and B is the luminance of the same corresponding point (same x,y location on the screen) in the right-eye image.

The term Co-location Image Contrast was also introduced to describe the contrast between image points at the same (x,y) location on screen between the left and right eyes, and mathematically defined as:

$$\text{Co-location Image Contrast} = B / A \quad (13)$$

And hence:

$$\text{Viewer Crosstalk} = \text{Co-location Image Contrast} \times \text{System Crosstalk} \quad (14)$$

It is worth noting that equation (11) is similar to crosstalk definition 1 (equation (1)) in that it does not include the effect of black level, however black level is indirectly included in the definition of Viewer Crosstalk by way of the Co-Location Image Contrast term.

In 2009, Huang, et al^[31] provided a revised definition of System Crosstalk which includes the effect of black level:

$$SCT_L = \frac{L_{KWL} - L_{KKL}}{L_{WKL} - L_{KKL}} \quad \text{and} \quad SCT_R = \frac{L_{WKR} - L_{KKR}}{L_{KWR} - L_{KKR}} \quad (15)$$

Where: SCT_L and SCT_R are the system crosstalk for the left and right eyes, L_{KWL} is the luminance measured from the left eye position with black in the left eye image and white in the right eye image, and so on.

As a result of this change it is important to establish which definition of system crosstalk (2000 or 2009) is being used when it appears in a publication.

2.6 Gray-to-Gray Crosstalk

As mentioned in the end of Section 2.4, crosstalk occurs in some displays (particularly time-sequential 3D LCDs) in a non-linear and non-additive fashion. The term ‘gray-to-gray crosstalk’ was therefore developed as a metric to quantify crosstalk in such displays. In essence gray-to-gray crosstalk is the matrix of values of crosstalk ratio for all gray level transition combinations on a display. On a display with linear crosstalk, all the values in the matrix would be the same, however with a 3D display which exhibits non-linearity of crosstalk, the values in the matrix would be mostly different. In the case of time-sequential 3D LCDs, the non-linearity is due in part to the period of time that it takes an LCD pixel to transition from one gray level to another (the pixel response rate), and the fact that the pixel response rate is different for different gray level transitions (i.e. it is a matrix).

Surprisingly, the term gray-to-gray crosstalk was first introduced and defined by three separate papers^{[22][32][33]} very recently at the same conference in May 2010. The three definitions are provided below:

Shestak, et al^[22] defined:

$$C_l(q_1, q_2) = \frac{W_l(q_1, q_2) - W_l(q_1, q_1)}{W_l(q_2, q_2) - W_l(q_1, q_1)} \quad (16)$$

Jung, et al^[32] defined:

$$CT_{i,j} = \frac{|G_{i,j} - G_{i,i}|}{|G_{j,i} - G_{i,i}|} \times 100[\%] \quad (17)$$

Pan, et al^[33] defined:

$$C.T._{i \rightarrow j} = \frac{|L_{j \rightarrow j} - L_{i \rightarrow j}|}{L_{j \rightarrow j} - L_{i \rightarrow i}} \quad (18)$$

Where the variables are defined as follows:

Shestak (2010) Samsung, Korea ^[22]	Jung (2010) LG, Korea ^[32]	Pan (2010) Chi Mei Innolux, Taiwan ^[33]	Variable definitions:
q_1 and q_2	i and j	i and j	are the two specified gray levels between which the gray-to-gray crosstalk is being calculated/measured
$C_l(q_1, q_2)$ and $C_r(q_1, q_2)$	$CT_{i,j}$	$C.T._{i \rightarrow j}$	is the gray-to-gray crosstalk between the specified gray levels (for left (l) and right (r) eyes)
$W_l(q_1, q_2)$ and $W_r(q_1, q_2)$	$G_{i,j}$	$L_{i \rightarrow j}$	is the luminance measurement obtained when the two channels are set to the specified gray levels

The three equations are very similar and apart from minor differences such as the sign of the result, the use of percent notation and variable names, the only difference of significance is that the denominator in equation (17) is slightly different to the denominator of (16) and (18). Specifically, if the denominator in (17) was the same as (16) and (18) it would be written as “ $G_{j,j} - G_{i,i}$ ” rather than the existing “ $G_{j,i} - G_{i,i}$ ”. The existing arrangement of the denominator of (17) is similar in formulation to equations (5,6) used in the definition 2 of crosstalk. The significance of this difference is yet to be fully investigated.

Remembering that the mathematical definition of gray-to-gray crosstalk is a ratio, this formulation needs to be extended to determine the amount of visible crosstalk for different gray levels. The maximum visible crosstalk will not necessarily occur at the same gray levels as the maximum gray-to-gray crosstalk since the co-location image contrast also needs to be considered. To date the extension of ‘gray-to-gray crosstalk’ to ‘gray-to-gray visible crosstalk’ does not appear to have been published.

If you wish to use these equations to relate pixel gray level to display luminance, it will be necessary to consider gamma and the calibration of the display.^[45]

2.7 Extinction and Extinction Ratio

The terms extinction and extinction ratio are not used as commonly in the stereoscopic literature as the term crosstalk (ref. Table 1) but nevertheless it is an important concept. ‘Extinction’ and ‘extinction ratio’ are commonly used without definition however some meaning can often be gained from the context of usage – for example:

Hines (1984)^[34]: “The polarizing filters should be chosen to give a high extinction ratio. Polaroid's HN-38 material works quite nicely with a ratio of 600:1, and their more expensive HN-38s material has a ratio of 2000:1.”

Walworth, et al (1984)^[35]: “Circularly polarized light provides efficient extinction over a wide range of angular rotation”

Haven (1987)^[36]: “extinction ratio measurements made from 470 to 630 nanometers varied between 20:1 and 35:1.”

Lipton (1991)^[37]: “In practice it is possible to closely approach the extinction ratio of the polarizer, which can be 2000:1.”

In the stereoscopic literature, ‘extinction’ usually refers to the process or concept of extinction and ‘extinction ratio’ usually refers to the metric or measurement of extinction – although this distinction should be obvious from the usage.

Some explicit mathematical definitions were found in the stereoscopic literature:

Yeh, et al (1987)^[38]: “Crosstalk was defined by the extinction ratio between the left- and right-eye images and was measured as the ratio of the luminance of the correct eye image to the luminance of the unwanted “ghost” from the image intended for the opposite eye. The higher the extinction ratio, the less the “ghosting” surrounding the stereo images.”

Hodges (1991)^[39]: “extinction ratio (the luminance of the correct eye image divided by the luminance of the opposite eye ghost image)”

Ableah (2011)^[40] defines ‘extinction ratio’ as:

$$X_1 = \frac{L_{1wk}}{L_{1kw}} \quad \text{and} \quad X_2 = \frac{L_{2kw}}{L_{2wk}} \quad (19,20)$$

Where: X_1 and X_2 are the extinction ratio for the left and right eye views, L_{1wk} is the luminance measured from the left eye position with white in the left eye image and black in the right eye image, L_{1kw} is the luminance measured from the left eye position with black in the left eye image and white in the right eye image, L_{2kw} is the luminance measured from the right eye position with black in the left eye image and white in the right eye image, and L_{2wk} is the luminance measured from the right eye position with white in the left eye image and black in the right eye image.

The Yeh definition includes mention of crosstalk but this is inconsistent with other definitions and must be an error. Although the Yeh and Hodges definitions don’t specify the use of maximum (full-white) test signals for correct eye image and ghost image, it is probably fair to assume this. Apart from these two points, the three definitions of extinction ratio are consistent with each other.

Two important points are worth noting here. Firstly, these definitions do not include the effect of black level. High black levels would adversely bias the extinction ratio value using these definitions. Secondly, these definitions of extinction ratio equate to the inverse of crosstalk ratio (definition 1).

2.8 3D Contrast and Stereo Contrast Ratio

Definitions for ‘3D contrast’ and ‘stereo contrast ratio’ were found in the stereoscopic literature as follows:

Boher, et al^[20] define ‘3D contrast’ as:

$$C_L = 1 / \chi_L, \quad C_R = 1 / \chi_R \quad \text{and} \quad C^{3D} = (C_R \times C_L)^{0.5} \quad (21,22,23)$$

Where: C_L and C_R are 3D contrast for the left and right eyes as viewed through the left and right filters, χ_L and χ_R is the 3D crosstalk for left and right eyes (see equations (7,8)), and C^{3D} is the combined 3D contrast for both eyes. Note

that the variable name C in equations (21,22,23) is used for contrast whereas C is used for crosstalk in most other stereoscopic papers.

Abileah (2011)^[40] defines ‘stereo contrast ratio’ as:

$$CR_1 = \frac{L_{1ww}}{L_{1kk}} \quad \text{and} \quad CR_2 = \frac{L_{2ww}}{L_{2kk}} \quad (24,25)$$

Where: CR_1 and CR_2 are ‘stereo contrast ratio’ for the left and right eyes, L_{1ww} is the luminance measured from the left eye position with white in the left eye image and white in the right eye image, and so on.

These two terms ‘3D contrast’ and ‘stereo contrast ratio’ seem very similar by name, but are functionally very different. The definition of ‘3D contrast’ is the inverse of definition 2 of crosstalk ratio (see equation (3)), whereas the definition of ‘stereo contrast ratio’ is essentially the contrast ratio of one channel biased by the amount of crosstalk between channels.

2.9 Other Definitions

Shestak, et al^[22] provide equations for dark crosstalk and light crosstalk specifically relating to crosstalk in time-sequential 3D on LCDs:

$$\text{Dark crosstalk: } C^{\text{dark}} = (W'_2 - W_2) / (W_1 - W_2) \quad (26)$$

$$\text{Light crosstalk: } C^{\text{light}} = (W'_1 - W_1) / (W_2 - W_1) \quad (27)$$

Where: W_1 and W_2 are the original desired luminance for points in the left and right eye view (W_1 is the lower of the two luminances), W'_1 is the displayed luminance affected by crosstalk which brightens the image, and W'_2 is the displayed luminance affected by crosstalk which darkens the image.

Uehara, et al^[41] have investigated crosstalk in multi-view autostereoscopic displays and attempt to make a distinction between ‘interocular crosstalk’ and (for the lack of better term) ‘adjacent-view crosstalk’. In a multi-view autostereoscopic display, the left and right eyes may not be in adjacent views – for example the left eye might see view number 4 and the right eye might see view number 7. A small amount of crosstalk between adjacent views (‘adjacent-view crosstalk’) (e.g. view 4 and 5) can be desirable since it reduces the visibility of the transition as the eye moves between views^[42], however any crosstalk visible between the two views in which the two eyes are located (‘interocular crosstalk’) (e.g. view 4 and view 7 in the example above) is undesirable. The mathematical definition of crosstalk used by Uehara, et al^[41] is equivalent to crosstalk definition 1. In another paper, Uehara, et al^[43] use the term ‘3D crosstalk’ instead of the term ‘adjacent-view crosstalk’ defined here, however this should be avoided because the term ‘3D crosstalk’ is used in some other papers as synonymous to regular ‘crosstalk’.

Chang, et al^[3] describe ‘dynamic crosstalk’ (of moving images) as distinct from the other formulations which are assumed to be ‘static crosstalk’.

The term ‘crosstalk’ is also used in the electronic communications field to refer to the leakage of a signal between one communications channel and another. An attempt was made to find a concise definition of crosstalk from this field for this study but was unsuccessful.

3. DISCUSSION

There is a definite need to standardize the terminology and definitions relating to crosstalk in stereoscopic displays. This paper has revealed considerable variation between definitions in various papers which is detrimental to the ongoing discussion and research of this topic.

There is also a level of ambiguity of language when people talk or write about crosstalk. Are they meaning crosstalk generally? Are they referring to crosstalk ratio? Are they really talking about visible crosstalk or ghosting? Sometimes the context will reveal the meaning, but particularly in written form it is important to use the language of crosstalk carefully and define or specify the meanings being used or refer to a standard.

A major inconsistency found in this study is the differing handling of display black level in the crosstalk ratio and extinction ratio calculations. Displays are trending towards lower black levels which may reduce this discrepancy, however the crosstalk ratio of high-quality displays are also reducing, which will amplify the discrepancy.

It would be worth having a considered discussion about whether the effect of non-zero black level should be included or removed from the mathematical definition of crosstalk ratio – i.e. should definition 1 or definition 2 be used moving forward.

It would be worth analyzing the effect of non-zero black level of current displays on the results of using these definitions to determine how significant the effect is.

The brightness and contrast settings on a display may affect the measurement of crosstalk and would probably need to be calibrated before conducting testing – particularly for the use of test charts to measure crosstalk^[45] and the measurement of gray-to-gray crosstalk.

It is not only important to provide standardized descriptive and mathematical definitions – it is also important to define standardized techniques of measuring these important 3D display quality parameters.

There are a number of standardization efforts underway at the time of writing this paper which may address some of the terminology and definition problems identified in this paper. Activities include:

- The ICDM (International Committee on Display Metrology) (part of SID) is currently working on the “Display Measurements Standard” of which version 1.0 is expected to be released mid-2011. This standard will include a section on 3D display measurement standards.
- The IEC (International Electrotechnical Commission) has established technical committee TC110 (Flat Panel Display Devices) to establish standards relating to “optical measurement methods for 3D displays”. This work includes some coverage of crosstalk measurement.
- The SEMI (Semiconductor Equipment and Materials International) has been working on a document “3D Display Terminology” which includes some definitions of crosstalk related terms.

It will be worth watching for the results of these standardization efforts.

Lastly an open question: How should crosstalk be measured in 3D display systems employing crosstalk cancellation^[1]? Should the crosstalk cancellation be turned off before conducting the measurements or should it be left on? What if the crosstalk cancellation cannot be turned off? In cases where crosstalk cancellation is used, crosstalk will still be present but ghosting may not be visible.

4. TERMINOLOGY SUMMARY

This paper has reviewed the historical meaning of a range of terms in the stereoscopic literature. A summary of descriptive definitions of various stereoscopic terms is offered here for clarity. The definitions provided here are by no means final and the author would welcome the further improvement of these definitions. One shortcoming of some of these definitions is that they may not be easily extensible to multi-view autostereoscopic displays.

Crosstalk: *the incomplete isolation of the left and right image channels so that one image leaks into the other.*

Crosstalk Ratio: *(specifically) the metric of crosstalk.*

Ghosting: *the perception of crosstalk.*

Leakage: *the (amount of) light that leaks from one stereoscopic image channel to another.*

System Crosstalk: *in general terms the same as Crosstalk, but as a metric it specifies the degree of the unexpected leaking image from the other eye using one of two equations (11) or (15).^{[29][31]}*

Viewer Crosstalk: *a measure of the crosstalk perceived by the viewer. cf: ghosting. (See (14))*

Extinction, Extinction Ratio: *a measure of how well the opposite view is blocked in a stereoscopic display; the inverse of crosstalk.*

Gray-to-Gray Crosstalk: *the matrix of values of crosstalk ratio for all gray level transition combinations on a stereoscopic display.*

Cross-talk, Cross Talk, X-talk, Interocular Crosstalk, 3D Crosstalk: *see/use Crosstalk.*

A summary of mathematical definitions is not provided here because there is too much variation in the current mathematical definitions and arbitrary choice of variable names to be able to logically recommend a preferred usage here, apart from saying that: (a) the choice of variable names should follow a logical pattern and avoid overlaps with similar variables in related areas, (b) metrics should account for the presence of display black level, and (c) the standardization of new definitions should take into consideration historical usage. Additionally I don't wish to cut across the results of the standardization efforts currently underway.

5. CONCLUSION

This paper has reviewed the descriptive and mathematical definitions of crosstalk and related terms (ghosting, leakage, system crosstalk, viewer crosstalk, extinction, extinction ratio, and 3D contrast) in the stereoscopic literature. The relatively new term "gray-to-gray crosstalk" has also been described.

The understanding/definition/measurement of crosstalk on 3D displays are all improving rapidly – spurred on by rapid development and deployment of 3D displays and related technologies.

This paper has revealed a high level of ambiguity in relation to the mathematical definition of the crosstalk and extinction terms, and the variables used in these definitions. A well-written and well-researched standard would provide significant benefit to the industry as a whole and the onward improvement of stereoscopic display quality.

Ultimately we need stereoscopic displays which have low crosstalk, and we need the terminology and standards to support that.

6. ACKNOWLEDGEMENTS

The author would like to thank WA:ERA and iVEC for their support of this work. The author would also like to thank the SPIE for producing the SD&A 20-year DVD-ROM^[2], and the SID for making available the SID member publication library, both of which have been incredibly valuable in researching this paper.

REFERENCES

- [1] Woods, A. J., "Understanding Crosstalk in Stereoscopic Displays" (Keynote Presentation) at 3DSA (Three-Dimensional Systems and Applications) conference, Tokyo, Japan (2010). http://www.cmst.curtin.edu.au/publicat/2010-23_understanding_crosstalk_woods.pdf
- [2] Woods, A. J., Merritt, J. O., Fisher, S. S., Bolas, M. T., Benton, S. A., Holliman, N. S., Dodgson, N. A., McDowall, I. E., Dolinsky, M., (editors) [Stereoscopic Displays and Applications 1990-2009: A Complete 20-Year Retrospective and The Engineering Reality of Virtual Reality 1994-2009 (Special Collection)] (DVD-ROM), SPIE (2010).
- [3] Chang, Y.-C., Chiang, C.-Y., Chen, K.-T., Huang, Y.-P., "Investigation of Dynamic Crosstalk for 3D Display" in 2009 International Display Manufacturing Conference, 3D Systems and Applications, and Asia Display (IDMC/3DSA/Asia Display 2009), Taipei, Taiwan, (2009).
- [4] Meyer, L., "Monitor selection criteria for stereoscopic displays" in Proc. SPIE Stereoscopic Displays and Applications III, 1669, 211-214 (1992).
- [5] Lipton, L., "Factors affecting "ghosting" in time-multiplexed piano-stereoscopic CRT display systems" in Proc. SPIE True Three-Dimensional Imaging Techniques and Display Technologies, ed. D.F. McAllister, W.E. Robbins, 0761, 75-78 (1987).
- [6] Veron, H., Southard, D. A., Leger, J. R., Conway, J. L., "Stereoscopic Displays for Terrain Database Visualization" in Proc. SPIE Stereoscopic Displays and Applications, 1256, 124-135 (1990).
- [7] Montgommery, D. J., Woodgate, G. J., Jacobs, A., Harrold, J., Ezra, D., "Analysis of the performance of a flat panel display system convertible between 2D and autostereoscopic 3D modes" in Proc. SPIE Stereoscopic Displays and Virtual Reality Systems VIII, 4297, 148-159 (2001)
- [8] Stevenson, H. and Khazova, M., "Patterned Grating Alignment of Reactive Mesogens for Phase Retarders" in Proceedings of the 24th International Display Research Conference (IDRC) with the 4th International Meeting on Information Display (IMID), Daegu Korea (2004).
- [9] Stevens, R. F., [Cross-talk in 3D displays] Report CETM 56, National Physical Laboratory UK (2004).

- [10] Kaptein, R. and Heynderickx, I., "Effect of Crosstalk in Multi-View Autostereoscopic 3D Displays on Perceived Image Quality" in SID '07 Digest, 1220-1223 (2007).
- [11] Pala, S., Stevens, R., Surman, P., "Optical crosstalk and visual comfort of a stereoscopic display used in a real-time application" in Proc. SPIE Stereoscopic Displays and Virtual Reality Systems XIV, 6490, 1101-1112 (2007).
- [12] Uehara, S., Hiroya, T., Kusanagi, H., Shigemura, K. and Asada, H., "High-visibility 2D/3D LCD with HDDP Arrangement and its Optical Characterization Methods" in IMID/IDMC/ASIA DISPLAY '08 Digest, 147-150 (2008).
- [13] Ealassubramonian, K. and Rajappan, R.P., "Compatible 3-D television: the state of the art" in Proc. SPIE Three-Dimensional Imaging, ed. J.P. Ebbeni, A. Monfils, 0402, 100-106 (1983).
- [14] Morishama, H., Nose, H., Taniguchi, N., Inoguchi, K., Matsumura, S., "An Eyeglass-Free Rear-Cross-Lenticular 3-D Display" in SID Digest 1998, 923-926 (1998).
- [15] Chien, K.-W. and Shieh, H.-P. D., "3D Mobile Display Based on Sequentially Switching Backlight with Focusing Foil" in SID 2004 Digest, 1434-1437 (2004).
- [16] Woods, A. J., Harris, C. R., "Comparing levels of crosstalk with red/cyan, blue/yellow, and green/magenta anaglyph 3D glasses" in Proc. SPIE Stereoscopic Displays and Applications XXI, 7253, 0Q1-0Q12 (2010). <http://cmst.curtin.edu.au/publicat/2010-11.pdf>
- [17] Chu, Y.-M., Chien, K.-W., Shieh, H.-P. D., Chang, J.-M., Hu, A., and Yang, V., "3D Mobile Display Based on Dual Directional Lightguides" in 4th International Display Manufacturing Conference, Taipei, Taiwan, 799-801 (2005).
- [18] Hong, H.-K., Jang, J.-W., Lee, D.-G., Lim, M.-J., Shin, H.-H., "Analysis of angular dependence of 3-D technology using polarized eyeglasses" in Journal of the SID, 18(1), 8-12 (2010).
- [19] Liou, J.-C., Lee, K., Tseng, F.-G., Huang, J.-F., Yen, W.-T., Hsu, W.-L., "Shutter Glasses Stereo LCD with a Dynamic Backlight" in Proc. SPIE Stereoscopic Displays and Applications XX, 7237, 72370X (2009).
- [20] Boher, P., Leroux, T., Bignon, T., Collomb-Patton, V., "Multispectral polarization viewing angle analysis of circular polarized stereoscopic 3D displays," in Proc. SPIE Stereoscopic Displays and Applications XXI, 7253, 0R1-0R12 (2010).
- [21] Boher, P., ELDIM, personal communication, 13 April 2010.
- [22] Shestak, S., et al, "Measuring of Gray-to-Gray Crosstalk in a LCD Based Time-Sequential Stereoscopic Display" in SID 2010, Seattle, 132-135 (2010).
- [23] Boev, A., Gotchev, A., Egiazarian, K., "Crosstalk measurement methodology for autostereoscopic screens" in 3DTV Conference, Kos Island (2007).
- [24] Lane, B., "Stereoscopic displays" in Proc. SPIE Processing and Display of Three-Dimensional Data, ed. J.J. Pearson, 0367, 20-32 (1982)
- [25] Meyer, L., "Monitor selection criteria for stereoscopic displays" in Proc. SPIE Stereoscopic Displays and Applications III, 1669, 211-214 (1992).
- [26] Gorski, A. M., "User evaluation of a stereoscopic display for space training applications" in Proc. SPIE Stereoscopic Displays and Applications III, 1669, 236-243 (1992).
- [27] Woods, A. J. and Tan, S. S. L., "Characterising sources of ghosting in time-sequential stereoscopic video displays" in Proc. SPIE Stereoscopic Displays and Virtual Reality Systems IX, 4660, 66-77 (2002). <http://cmst.curtin.edu.au/publicat/2002-09.pdf>
- [28] Lipton, L., "Glossary" in Lenny Lipton's Blog, online, dated 16 March 2009, accessed 19 March 2010. <http://lennylipton.wordpress.com/2009/03/16/glossary/>
- [29] Huang, K.-C., Tsai, C.-H., Lee, K., Hsueh, W.-J., "Measurement of Contrast Ratios for 3D Display" in Proc. SPIE Input/Output and Imaging Technologies II, 4080, 78-86 (2000).
- [30] Huang, K.-C., Yuan, J.-C., Tsai, C.-H., Hsueh, W.-J., Wang, N.-Y., "A study of how crosstalk affects stereopsis in stereoscopic displays" in Proc. SPIE Stereoscopic Displays and Virtual Reality Systems X, 5006, 247-253 (2003).
- [31] Huang, K.-C., Lee, K., Lin, H.-Y., "Crosstalk issue in stereo/autostereoscopic display" in Proc. Int. Display Manufacturing Conference, 2-18 (2009).
- [32] Jung, S.-M., Lee, Y.-B., Park, H.-J., Lee, S.-C., Jeong, W.-N., Shin, J.-K., Chung, I.-J., "Improvement of 3-D Crosstalk with Over-Driving Method for the Active Retarder 3-D Displays" in SID Digest 2010, Seattle, 1264-1267 (2010).
- [33] Pan, C.-C., Lee, Y.-R., Huang, K.-F., Huang, T.-C., "Cross-Talk Evaluation of Shutter-Type Stereoscopic 3D Display" in SID Digest 2010, Seattle, 128-131 (2010).
- [34] Hines, S. P., "Three-Dimensional Cinematography" in Proc. SPIE Optics in Entertainment II, ed. C.S. Outwater, 0462, 41-47 (1984).

- [35] Walworth, V., Bennett, S., Trapani, G., "Three-dimensional projection with circular polarizers" in Proc. SPIE Optics in Entertainment II, ed. C.S. Outwater, 0462, 64-68 (1984).
- [36] Haven, T. J., "A liquid-crystal video stereoscope with high extinction ratios, a 28 % transmission state, and one-hundred-microsecond switching" in Proc. SPIE True 3D Imaging Techniques and Display Technologies, 761, 23-26 (1987).
- [37] Lipton, L., "Selection devices for field-sequential stereoscopic displays: a brief history" in Proc. SPIE Stereoscopic Displays and Applications II, 1457, 274-282 (1991).
- [38] Yeh, Y.-Y., Silverstein, L. D., "Using electronic stereoscopic color displays: Limits of fusion and depth discrimination" in Proc. SPIE Three-Dimensional Visualization and Display Technologies, ed. S S Fisher, W E Robbins, 1083, 196-204 (1989).
- [39] Hodges, L. F., "Basic principles of stereographic software development" in Proc. SPIE Stereoscopic Displays and Applications II, 1457, 9-17 (1991).
- [40] Abileah, A., "3D Displays – Technologies & Testing Methods" at 3D Imaging Workshop, Stanford University (2011).
- [41] Uehara, S., Ujike, H., Hamagishi, G., Taira, K., Koike, T., Kato, C., Nomura, T., Horikoshi, T., Mashitani, K., Yuuki, A., Izumi, K., Hisatake, Y., Watanabe, N., Umezumi, N., Nakano, Y., "Standardization based on human factors for 3D display: performance characteristics and measurement methods" in Proc. SPIE Stereoscopic Displays and Applications XXI, 7524, 7524071-12 (2010).
- [42] Jain, A., Konrad, J., "Crosstalk in automultiscopic 3-D displays: Blessing in disguise?" in Proc. SPIE Stereoscopic Displays and Virtual Reality Systems XIV, 6490, 6490121-12 (2007).
- [43] Uehara, S., Koike, T., Kato, C., Uchidoi, M., Horikoshi, T., Hamagishi, G., Hisatake, Y., Ujike, H., "Development of Performance Characteristics for 3D Displays" in IMID/IDMC/ASIA DISPLAY 2010 DIGEST, 245-246 (2010).
- [44] [The Macquarie Encyclopedic Dictionary], Macquarie University, Australia (1990).
- [45] Weissman, M. A., Woods, A. J., "A simple method for measuring crosstalk in stereoscopic displays" in Proc. SPIE Stereoscopic Displays and Applications XXII, San Francisco, 7863, (2011). (in press)
- [46] Bos, P. J., "Time sequential stereoscopic displays: The contribution of phosphor persistence to the "ghost" image intensity" in Proc. ITEC'91 Annual Conf., Three-Dimensional Image Tech., H. Kusaka, ed., 603-606 (1991).
- [47] Walworth, V., Bennett, S. and Trapani, G., "Three-dimensional projection with circular polarizers" in Proc. SPIE Optics in Entertainment II, ed. C.S. Outwater, 0462, 64-68 (1984).

Paper 17 [Refereed Conference Paper]

A. J. Woods, J. Helliwell (2012) "Investigating the cross-compatibility of IR-controlled active shutter glasses" in Stereoscopic Displays and Applications XXIII, Proceedings of IS&T/SPIE Electronic Imaging, SPIE Vol. 8288, pp. 82881C-1 to -10, Burlingame, California, January 2012.

Investigating the cross-compatibility of IR-controlled active shutter glasses

Andrew J. Woods* and Jesse Helliwell

Centre for Marine Science & Technology, Curtin University, GPO Box U1987, Perth 6845 Australia

ABSTRACT

Active Shutter Glasses (also known as Liquid Crystal Shutter (LCS) 3D glasses or just Shutter Glasses) are a commonly used selection device used to view stereoscopic 3D content on time-sequential stereoscopic displays. Regrettably most of the IR (infrared) controlled active shutter glasses released to date by various manufacturers have used a variety of different IR communication protocols which means that active shutter glasses from one manufacturer are generally not cross-compatible with another manufacturer's emitter. The reason for the lack of cross-compatibility between different makes of active shutter glasses mostly relates to differences between the actual IR communication protocol used for each brand of glasses. We have characterized eleven different 3D sync IR communications protocols in order to understand the possibility of cross-compatibility between different brands of glasses. This paper contains a summary of the eleven different 3D sync IR protocols as used by a selection of emitters and glasses. The paper provides a discussion of the similarities and differences between the different protocols, the limitations for creating a common 3D sync protocol, and the possibility of driving multiple brands of glasses at the same time.

Keywords: stereoscopic, 3D, active shutter glasses, 3D sync, infrared, protocols, universal.

1. INTRODUCTION

Active Shutter Glasses (also known as Liquid Crystal Shutter (LCS) 3D glasses or just Shutter Glasses) are a commonly used selection device used to view stereoscopic 3D content on time-sequential stereoscopic displays. Time-sequential (or time-multiplexed) stereoscopic 3D displays operate by displaying discrete left and right images in alternating sequence often at image rates of 100, 120 or 144 images per second. The active shutter glasses alternately blank the left and right eyes in sequence with the sequence of images shown on the display such that the left eye only sees the left perspective images and the right eye only sees the right perspective images, ideally without crosstalk. The active shutter glasses usually contain two liquid crystal cells, each acting as a shutter – one in front of each eye.

In order for the active shutter glasses to switch in synchrony with the sequence of left and right images presented on the time-sequential stereoscopic display, some form of timing signal must be sent from the display to the glasses. Most wireless active shutter glasses use an infrared (IR) communication protocol similar to that used for IR remote controls used for TVs and other consumer electronics. In some cases an RF (radio-frequency) communication protocol (such as Bluetooth or ZigBee) are used. The DLP Link™ protocol uses pulses of visible light in its protocol.

Active shutter glasses have been used as a viewing device for time-sequential stereoscopic displays as far back as 1922 for the Teleview¹ system. The first wireless active shutter glasses to be commercially available were the StereoGraphics CrystalEyes which were released in the mid-1980s, used liquid crystal shutters, were battery powered, and used an IR communication protocol for synchronization. Many other brands and designs of IR controlled wireless active shutter glasses have been sold over the years² and in early 2010 the largest consumer release of active shutter glasses occurred with the consumer launch of 3D HDTVs by several consumer electronics manufacturers (including Samsung, Panasonic, Sony, LG, Sharp, and others³).

Regrettably most of the IR controlled active shutter glasses sold to date by various manufacturers have used a variety of different IR communication protocols which means that active shutter glasses from one manufacturer are generally not cross-compatible with another manufacturer's emitter. For example, a pair of 2010 Panasonic active shutter glasses cannot be used directly with a 2010 Samsung 3D HDTV, and vice versa.

* A.Woods@curtin.edu.au; phone +61 8 9266 7920; www.AndrewWoods3D.com

The technical reason for the lack of cross-compatibility between different brands of active shutter glasses mostly relates to differences between the IR communication protocol used for each brand of glasses (other reasons for incompatibility which are discussed in Section 4.1). In this study we have characterized eleven different 3D sync IR communications protocols in order to understand the possibility for implementing cross-compatibility between different brands of 3D glasses and 3D displays.

2. EXPERIMENTAL METHOD

The protocols were measured by connecting the IR protocol emitter (either a stand-alone emitter or an emitter integrated into a 3D display/projector) to a 3D video or 3D sync source. In the case where the IR emitter was integrated into the 3D display/projector, the 3D display/projector was switched into a 3D mode. A high-speed IR photo-sensor (Osram Opto-Semiconductors SFH213 Silicon PIN Photodiode – wavelength range 400-1100nm, 5ns response time) was aimed at the IR emitter and analyzed using a digital storage oscilloscope (TiePie Engineering Handyscope HS3 – 50MHz bandwidth). The timing of the IR pulses was measured relative to the 3D sync signal, the light field emitted by the display, and/or the timing of the shuttering of the eyewear.

Eleven pairs of active shutter glasses were tested in this study and ten of them are shown in Figure 1. Some of the stand-alone emitters tested in this study are shown in Figure 2.



Figure 1: Ten of the eleven active shutter glasses tested in this study: (a) StereoGraphics CrystaleEyes CE-1, (b) ELSA/H3D, (c) NuVision 60GX, (d) NVIDIA 3D Vision, (e) Panasonic TY-EW3D10U, (f) Samsung 2007, (g) Samsung (2010) SSG-2100AB, (h) Sony TDG-BR100, (i) Viewsonic PGD-150 DLP Link, and (j) Xpand X103 Universal. Sharp AN3DG10 not shown.



Figure 2: Some of the stand-alone IR 3D emitters tested: (a) Samsung 2007, (b) NuVision, (c) NVIDIA 3D VISION, (d) CrystalEyes 1, and (e) H3D/ELSA.

In order to verify the accuracy of the protocol measurements, a custom-built universal IR emitter was constructed⁴ and used to send a regenerated version of the various IR protocols to the various active shutter glasses. We were able to reliably drive all of the tested active shutter glasses using the appropriate measured IR protocol. There was only one exception to this testing, which was that we were unable to reliably drive the Xpand X103 universal glasses in the Samsung (2010) protocol mode using our regenerated Samsung 2010 protocol. This might indicate a slight timing error

in our measurement of the Samsung 2010 protocol, however we were able to use this protocol timing to drive an actual pair of the Samsung 2010 active shutter glasses.

3. 3D SYNC PROTOCOLS

The timing diagrams for the eleven protocols measured in this study are detailed below in Figures 3 to 13.

It is important to note that:

- not all of the diagrams are drawn to scale.
- the timings are as measured from commercially released hardware and were not provided or endorsed by the manufacturers.
- there might be timing errors in the measurements and descriptions.
- the Samsung and DLP Link protocols have a subtly different mode of operation which are detailed below.
- all measurements are in units of microseconds (μs).
- the timing of the opening and closing of the left and right shutters is not indicated in these diagrams and do not necessarily coincide exactly with the timing of the tokens. Most notably the Sharp protocol has a 1ms offset between the token and the shutter switching. (In the scope of this paper, a token is defined as a single pulse or group of pulses which define an action for the glasses to perform, e.g. ‘open the left eye’, or ‘close the left eye’ – in the timing diagrams below there is one token per row).
- In a 120fps (frame per second) 3D system, these protocols would repeat every 16.7ms (or every 20ms for a 100fps 3D system) (except Samsung 2010).

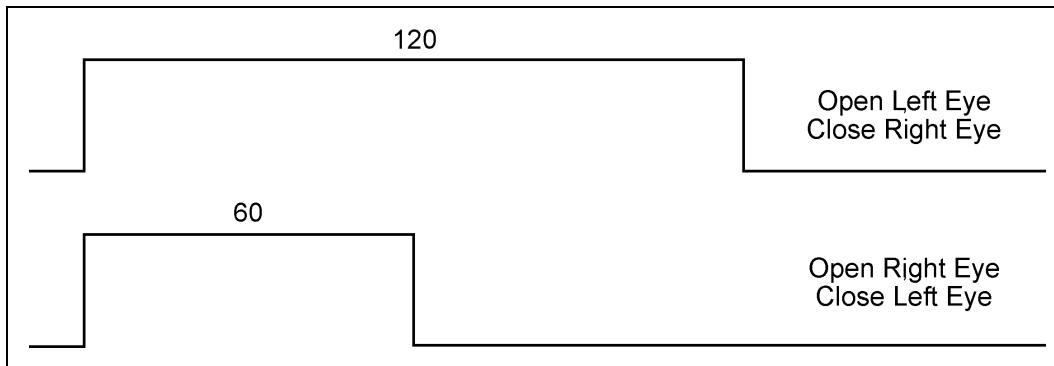


Figure 3: The 3D sync IR protocol for the StereoGraphics Crystaleyes 1 stand-alone emitter and glasses. (Units: μs)

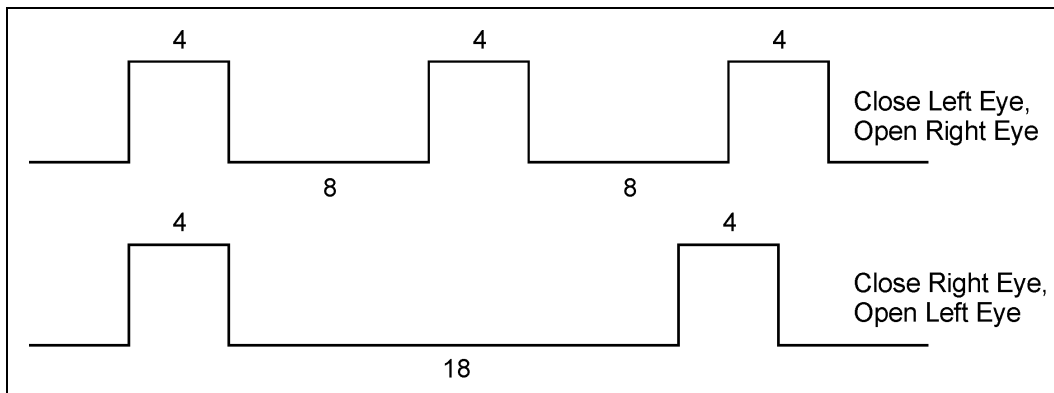


Figure 4: The 3D sync IR protocol for the NuVision stand-alone emitter and 60GX glasses. (Units: μs)

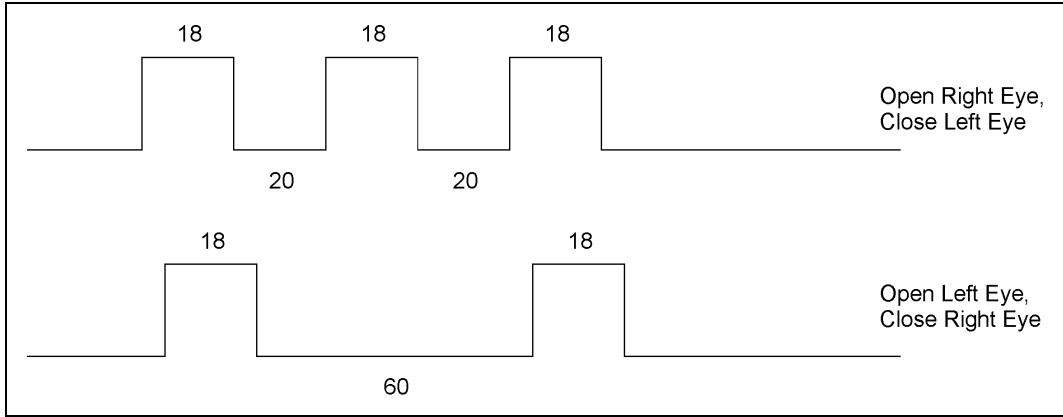


Figure 5: The 3D sync IR protocol for the Xpand stand-alone emitter and glasses. (Units: μs)

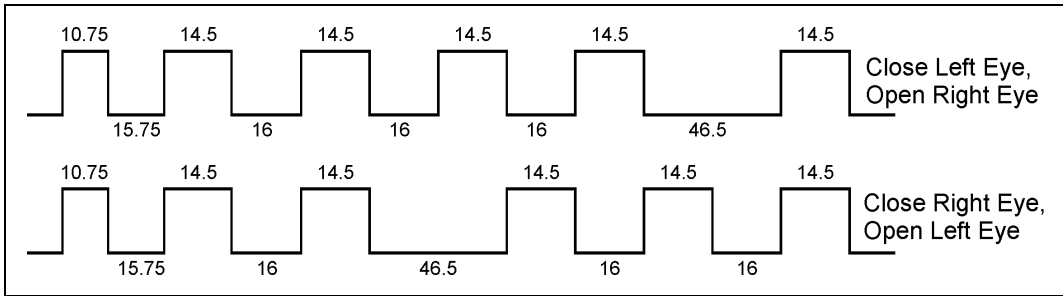


Figure 6: The 3D sync IR protocol for the ELSA/H3D stand-alone emitter and glasses. (Units: μs)

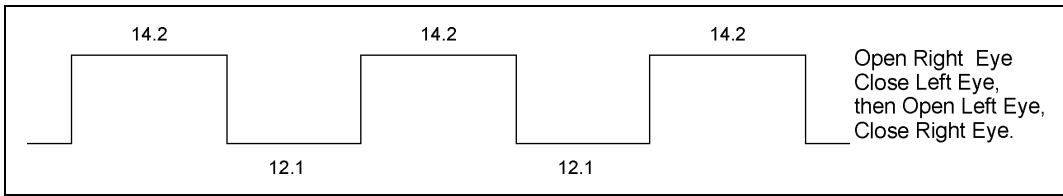


Figure 7: The 3D sync IR protocol for the Samsung 2007 stand-alone emitter and glasses. (Units: μs)
 NB: This is a one token protocol. The single token is output once every right+left frame pair period (at the beginning of the right frame period). The glasses must assume a duty cycle of approximately 50% and calculate the intermediate timing internally.

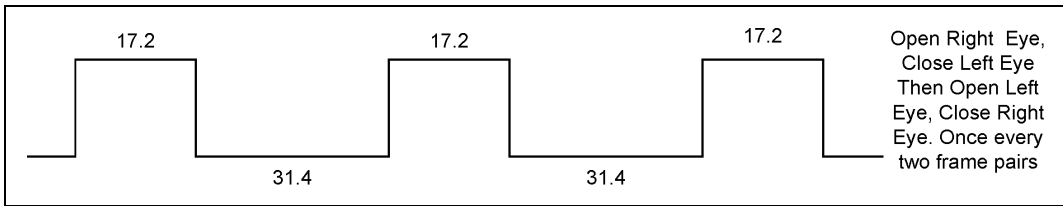


Figure 8: The 3D sync IR protocol for the Samsung 2010 integrated TV emitter and glasses. (Units: μs)
 NB: This is also a one token protocol. The single token is output once every two right+left frame pair periods. The glasses must assume a duty cycle of approximately 50% and calculate the intermediate timing internally.

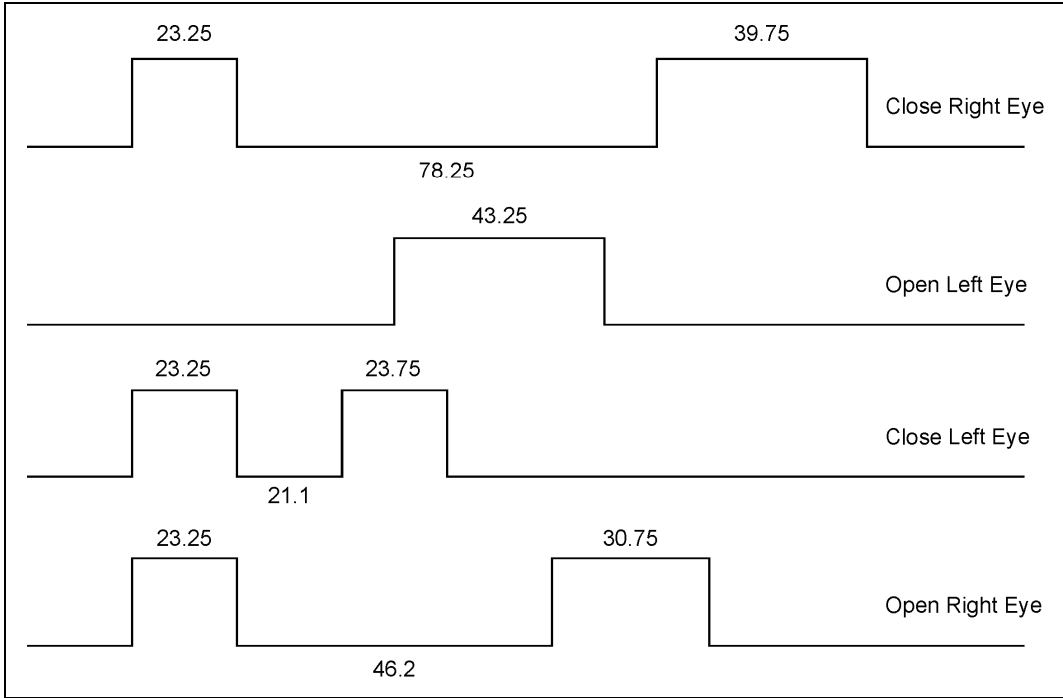


Figure 9: The 3D sync IR protocol for the NVIDIA 3D VISION stand-alone emitter and glasses. (Units: μs)
 NB: This is a four token protocol and hence allows the display to specify the duty cycle for the glasses to operate.

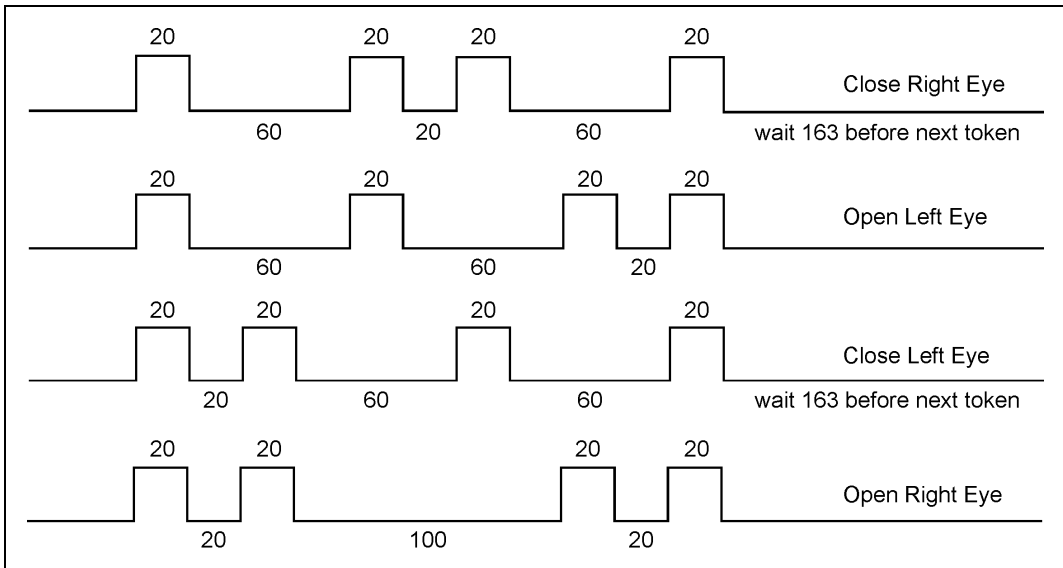


Figure 10: The 3D sync IR protocol for the Panasonic integrated TV emitter and glasses. (Units: μs)
 NB: This is also a four token protocol and allows the display to specify the duty cycle for the glasses to operate.

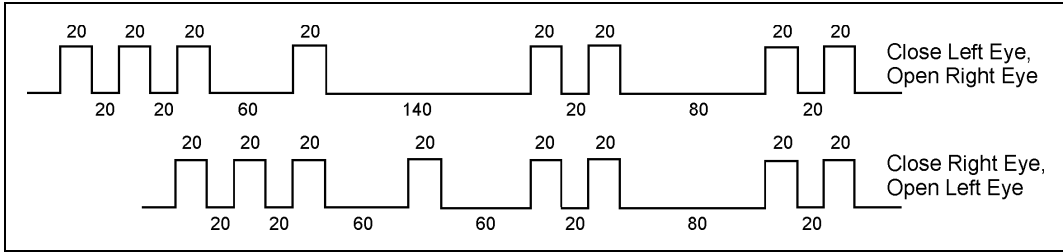


Figure 11: The 3D sync IR protocol for the Sharp integrated emitter and glasses. (Units: μs)

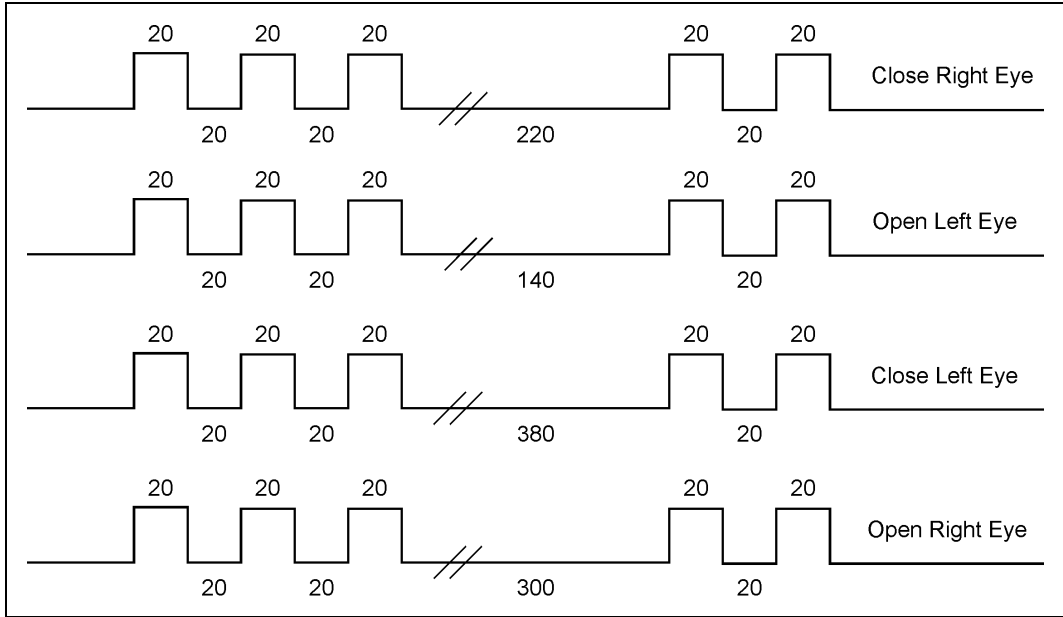


Figure 12: The 3D sync IR protocol for the Sony stand-alone TV emitter and glasses. (Units: μs)
 NB: This is also a four token protocol and allows the display to specify the duty cycle for the glasses to operate.

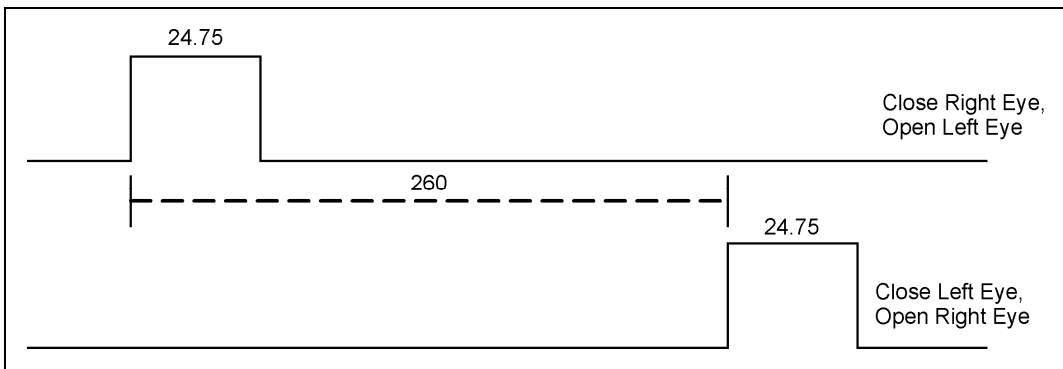


Figure 13: The 3D sync protocol for DLP Link™ projectors and glasses. (Units: μs)
 NB: The left eye token and the right eye token do not differ in width, but in relative timing. The right eye token is delayed relative to the sync reference by $260\mu\text{s}$ as compared to the timing of the left eye pulse. Another way of interpreting this is to say that the timing between pulses for the right perspective image period is $520\mu\text{s}$ ($2 \times 260\mu\text{s}$) less than the timing between pulses for the left perspective image period. Aspects of this protocol appear to be the subject of a US Patent Application⁵.

4. DISCUSSION

4.1 Reasons for Incompatibility

As can be seen in Figures 3-13, there are vast differences between the various 3D sync IR protocols. Even though most current 3D systems use an IR protocol to synchronize the glasses, the differences between the various individual IR protocols severely limits incompatibility between the different brands of glasses. Traditionally most IR controlled shutter glasses have been configured to receive only the IR protocol they are designed for and hence will not receive, or may be confused by, a different 3D sync IR protocol. Needless to say, the incompatibility was there by design. The 3D sync IR protocols are further contrasted in Section 4.2.

In addition to the IR controlled shutter glasses, there are some shutter glasses which use a communication protocol other than IR – specifically: the DLP Link protocol is transmitted in visible light, the Samsung 2011 glasses use the Bluetooth RF (radio frequency) protocol, Bit Cauldron BC5000 glasses use the ZigBee RF protocol, and Volfoni ActiveEyesPro glasses use an unspecified RF protocol (in addition to IR). The use of different electro-magnetic wavelengths to transmit the protocol (i.e. visible light vs. IR vs. ZigBee vs. Bluetooth) will obviously restrict interoperability.

There are also some duty cycle differences between the driving of the shutters for different 3D systems – some use a 50% duty cycle (i.e. the left shutter is open for 50% of the time, and the right shutter is open the other 50% of the time), whereas some glasses use a narrow duty cycle – e.g. 20% (i.e. the left shutter is open for 20% of the cycle, followed by a 30% period when both shutters are closed, followed by the right shutter open for 20% of the cycle, followed by another 30% period when both shutters are closed). Some stereoscopic displays, such as some 3D LCDs, require the use of a reduced duty-cycle switching of the glasses because a full left image (or a full right image) is only visible across the whole display for a short time period⁶. Without this reduced duty cycle operation, severe crosstalk would be evident in the 3D image. In other 3D displays, such as 3D plasma, a slightly reduced duty cycle of the glasses can help reduce crosstalk⁷. A pair of shutter glasses which only supports a 50% duty cycle will therefore not be able to be used on a display which requires reduced duty cycle operation of the glasses.

Finally, some shutter glasses (such as the Sony TDG-BR100) do not use a front polarizer on the shutters – this is a design feature which reduces peripheral ambient flicker while still allowing the 3D LCD TV image to be shuttered to the correct eye because the light emitted by the display is strongly linearly polarized. Glasses without the front polarizer would not be able to be used with Plasma 3D displays or time-sequential 3D projectors, although this limitation can be overcome by the fitting of an appropriate linear polarizer in front of each shutter in the glasses by the user.

4.2 Comparison of IR 3D Protocols

In order to better understand the reasons for incompatibility between the various IR protocols, let's look at the differences and similarities between the protocols shown in Figures 3-13 in more detail. One of the main differences between the various IR protocols is the number of individual tokens per cycle. As mentioned earlier, in the scope of this paper, a token is defined as a single pulse or group of pulses which define an action for the glasses to perform, e.g. 'open the left eye', or 'close the left eye'. Most of the protocols surveyed use a two token protocol, one token to signify switching from left to right, and another token to signify switching from right to left. The three protocols we surveyed which use a four token protocol allow the left and right shutters to be commanded individually (i.e. (1) left shutter open, (2) left shutter closed, (3) right shutter open, (4) right shutter closed). At the opposite end of this spectrum are the two Samsung IR protocols which only use a single token. In this case the token is simply a timing flag sent every one or two cycles to indicate the correct phase and frequency the shutter glasses should operate at and it is up to the glasses to calculate the correct time to switch the left and right shutters using a pre-determined formula. The number of tokens used by each of the sampled 3D sync protocols is summarized in Table 1.

Table 1: The number of tokens used by the various 3D sync protocols (ranked in order of increasing number of tokens).

Glasses	Tokens
Samsung 2007	1
Samsung 2010	1
NuVision	2
Xpand	2
CrystalEyes 1	2
Elsa/H3D	2

Glasses	Tokens
Sharp	2
DLP Link	2
Panasonic	4
NVIDIA	4
Sony	4

It is worth noting that the 4 token protocols are capable of being used to implement custom duty cycle operation of the glasses which is necessary to optimize 3D performance with some displays. As mentioned in section 4.1, some stereoscopic displays require the use of a reduced duty-cycle switching of the glasses for correct operation. The use of a 4 token protocol would therefore seem to offer the most flexibility.

There is a lot of variation in the relative complexity of the various tokens – some use a simple single pulse for each token whereas others use a combination of pulses and some use more pulses than others. The glasses that use a more complex token are less likely to be mis-triggered by spurious IR signals and be able to easily reject other IR signals, however a more complex token also has more chance of being interfered because it has a longer period. Table 2 provides a summary of the number of pulses per token for each of the tested protocols and Table 3 provides a summary of the duration of each token in the eleven protocols.

Table 2: Summary of the number of pulses per token for each protocol (ranked in order of number of pulses per token)

Glasses	Pulses per Token
CrystalEyes 1	1, 1
DLP Link	1, 1
NVIDIA	2, 1, 2, 2
NuVision	3, 2
Xpand	3, 2
Samsung 2007	3

Glasses	Pulses per Token
Samsung 2010	3
Panasonic	4, 4, 4, 4
Sony	5, 5, 5, 5
ELSA/H3D	6, 6
Sharp	8, 8

Table 3: Summary of the duration of each token in the eleven protocols (ranked in order of increasing average duration)

Glasses	Token durations (µs)
DLP Link	24.75, 24.75
NuVision	28, 26
Samsung 2007	66.8
NVIDIA	141.25, 43.25, 68.1, 100.2
Crystaleyes 1	120, 60
Xpand	94, 96

Glasses	Token durations (µs)
Samsung 2010	114.4
ELSA/H3D	195.5, 195.5
Panasonic	220, 220, 220, 220
Sony	380, 300, 540, 460
Sharp	520, 440

Something that is not revealed by the timing diagrams of this paper is the tolerance for signal timing variation of the various glasses. Timing variation can be influenced by manufacturing variation and temperature variation and timing

tolerance should be included in the glasses to allow for this variation. A considerable amount of additional testing would be needed to establish timing tolerance of the glasses and then it would only be valid for a particular set of glasses. Obviously input from the manufacturers would be necessary to establish this tolerance correctly. One example of a large timing tolerance is that the NuVision 60GX glasses can successfully sync to the Xpand protocol, but the Xpand X103 glasses will not accept the NuVision protocol. Tight timing tolerance would mean that a particular pair of glasses would be less likely to be triggered or mis-triggered by the protocol meant for another pair of glasses.

Additionally, some of the glasses will only operate at a certain frame-per-second (fps) range – usually 100-120 fps. This aspect was not tested exhaustively with all the glasses, but it was found that the Panasonic glasses would not operate at some fps rates outside the usual 100-120fps range.

4.3 Cross-Compatibility

The large variation between different protocols described here reveals the main reason for incompatibility between different sets of IR shutter glasses and different 3D displays. There is no doubt the various manufacturers have intentionally used different protocols and this may be for several reasons: to avoid intellectual property problems, to try to ensure consumers only purchase a certain brand of shutter glasses, or to improve quality control.

The current incompatibility between different brands of shutter glasses and displays is a significant problem for consumers and reduces their motivation to purchase multiple pairs of shutter glasses (because they will only work with one brand of display). The improvement or implementation of cross-compatibility of different shutter glasses would be highly desirable for consumers.

Four options for implementing cross-compatibility between shutter glasses and displays are worth considering: (a) configuring displays to output multiple protocols (to drive multiple brands of shutter glasses), (b) a single standardized protocol to be used across multiple vendors, (c) a universal 3D emitter, and (d) the implementation of universal shutter glasses which can be driven by different protocols.

Regarding the output of multiple protocols, we conducted some experiments in this regard and found that some protocols will co-exist while others will not co-exist, meaning whether a single emitter can output two sets of protocols simultaneously and thereby drive two different brands of shutter glasses to view the same 3D display at the same time. The ability for two protocols to co-exist will be determined by the similarity of the two protocols, and the timing tolerance of the glasses. For example, our tests found that the Xpand and Samsung 2010 protocols would not co-exist which will probably be because both protocols use a three-pulse sequence with similar pulse widths – if the glasses are unable to distinguish between the two protocols, they may be confused by the mixture of protocols. This provides another reason to establish the protocol timing tolerance of different glasses, which will determine whether one glasses protocol might drive or mis-trigger another set of glasses, and in turn determine whether a TV can successfully output multiple protocols to drive multiple brands of glasses at the same time. On the other hand, our testing found that the ELSA/H3D and Xpand protocols will co-exist. We were able to successfully allow an audience wearing a combination of ELSA/H3D glasses and Xpand/NuVision glasses to view the same 3D projection display using an emitter which output both ELSA/H3D and Xpand protocols simultaneously. Our testing has also found that the Xpand and Panasonic protocols won't co-exist. The inability for several different protocols to co-exist severely limits the applicability of this option and therefore rules it out as a viable solution for cross-compatibility between shutter glasses.

Regarding a single standardized protocol, in early 2011 the CEA launched an initiative to define a common standardized protocol which would hopefully be adopted by all manufacturers⁸. Also in early 2011, Panasonic and partners announced “The Full HD 3D Glasses Initiative” to license a single common protocol across manufacturers⁹. The difficulty with defining a single standardized protocol is that it ignores all of the displays and glasses which have already been released into the market using other protocols, which hampers its success.

Another option to aid cross-compatibility would be to use a universal 3D emitter - an intermediate device which converts from one 3D sync protocol to another. Examples of such devices are the BitCauldron BC100 and BC010 combination which convert IR 3D sync to Zigbee 3D sync, and the Volfoni ActiveHubPro universal 3D emitter which converts DLP Link 3D sync and IR 3D sync to RF 3D sync.

Regarding the implementation of universal shutter glasses, this would seem the most viable option for implementing cross-compatibility because it has the potential to support a wide range of 3D displays already installed in consumers homes. This would be aided by the industry standardization on a small subset of protocols because it attempts to resolve future cross-compatibility between glasses and displays. One important factor with universal shutter glasses is that they

must correctly implement each of the protocols that they reportedly support. One example of incorrect support is that at least two models of universal shutter that we have tested have not correctly implemented the Sharp 3D sync IR protocol with what should be a 1ms delay between the token and the shutter switching.

In later announcements, the Full HD 3D Glasses Initiative indicated that other protocols have been included in the licensing program which also suggests the use of universal shutter glasses. It will be interesting to see whether the manufacturers support these standardization initiatives and answer consumers' calls for cross-compatibility between shutter glasses.

5. CONCLUSION

The analysis of the various 3D sync IR protocols has certainly been an interesting revelation into what is normally an invisible process. The results have revealed a considerable amount of variation between different 3D sync IR protocols and also some overlap. The paper has outlined options and limitations for cross-compatibility between different brands of 3D displays and 3D shutter glasses.

Please note that the protocol measurements outlined in the document have been provided for research and discussion purposes only. The protocol measurements may be subject to error and should not be used as an actual technical definition of each of the protocols.

6. ACKNOWLEDGEMENTS

We wish to acknowledge the support of iVEC in conducting this research. Product names and trademarks are the property of their respective owners. An earlier version of this manuscript was published as a Curtin University White Paper¹⁰ and submitted to the CEA to assist with their protocol standardization efforts⁸.

REFERENCES

- [1] Symmes, D. L. (2006) "The Chopper" Online: <http://www.3dmovingpictures.com/chopper.html>
Dated: 14 November 2006. Accessed: 29 March 2011.
- [2] Bungert, C. (2005) "Shutterglasses Comparison Chart" Online: <http://stereo3d.com/shutter.htm>
Dated: 1 April 2005. Accessed: 29 March 2011.
- [3] Woods, A. J. (2011) "The Illustrated 3D HDTV list" Online: <http://www.3dmovielist.com/3dhdtvs.html>
Dated: 28 March 2011. Accessed: 29 March 2011.
- [4] Petrus (2011) "Universal shutterglasses controller" (sic) in MTBS3D Forums.
Online: <http://www.mtbs3d.com/phpBB/viewtopic.php?p=55149#p55149>
Dated: 10 Jan 2011. Accessed: 29 March 2011.
- [5] Basile, G. R. and Poradish, F. J. (2006) "System and Method for Synchronizing a Viewing Device" US Patent Application 2008/0151112 A1, dated 22 Dec 2006.
- [6] Woods, A.J., Yuen, K.-L. (2006) "Compatibility of LCD Monitors with Frame-Sequential Stereoscopic 3D Visualisation" (Invited Paper), in IMID/IDMC '06 Digest, (The 6th International Meeting on Information Display, and The 5th International Display Manufacturing Conference), pg 98-102, Daegu, South Korea, 22-25 August 2006. <http://www.cmst.curtin.edu.au/local/docs/pubs/2006-30.pdf>
- [7] Woods, A. J., Karvinen, K. S. (2008) "The compatibility of consumer plasma displays with time-sequential stereoscopic 3D visualization" in Stereoscopic Displays and Applications XIX, Proceedings of SPIE Vol. 6803, SPIE, Bellingham, WA, USA.
http://www.cmst.curtin.edu.au/local/docs/pubs/2008-01_3d-plasma_woods_karvinen.pdf
- [8] CEA (Consumer Electronics Association) (2011) "R4WG16: Active Eyewear Standards IR Sync Request for Proposal (RFP)"
- [9] The Full HD 3D Glasses Initiative. Online: <http://www.fullhd3dglASSES.com/> Accessed: 16 December 2011.
- [10] Woods, A.J., and Helliwell, J. (2011) "White Paper: A Survey of 3D Sync IR Protocols", Curtin University, March 2011. <http://www.cmst.curtin.edu.au/local/docs/pubs/2011-17-woods-helliwell-3D-Sync-IR.pdf>

Paper 18 [Refereed Journal Paper]

A. J. Woods (2013) "3D or 3-D: a study of terminology, usage and style" *European Science Editing*, 39(3), pp. 59-62, August 2013.

Original articles

3D or 3-D: a study of terminology, usage and style

Andrew J. Woods

Centre for Marine Science & Technology, Curtin University, Perth, Australia

Abstract The terms "3D" and "3-D" are two alternative acronyms for the term "three-dimensional". In the published literature both variants are commonly used but what is the derivation of the two forms and what are the drivers of usage? This paper surveys the published stereoscopic literature and examines publication-style policies to understand forces and trends.

Keywords Stereoscopic, 3D, 3-D, three-dimensional, style, terminology.

Background

The term "three-dimensional" has probably been with us since philosophers discovered and discussed the concept of dimensions. The term can be used to refer to anything that has height, width and depth – three dimensions. Conveniently, "three-dimensional" can also be abbreviated to "3-D" or "3D."

The earliest example of the use of the term "three-dimensional" in relation to photography I have been able to locate is Kennedy (1936),¹ who wrote: "It is true that the most fantastic proposals purporting to disclose a short-cut to three-dimensional photography are repeatedly made by persons who claim that by chance or ingenuity they can produce a stereoscopic effect - note the word effect - without taking two pictures and particularly without providing adequate means whereby each eye sees its proper image." However, he doesn't use the abbreviation "3D" or "3-D" in the article.

The earliest example of the abbreviation "3-D" I have located is Spottiswoode et al. (1952),² who wrote: "Up to now the production of three-dimensional (3-D) films has been sporadic." Perhaps there are earlier examples.

Although the acronym "3D" was first used in relation to stereoscopic 3D movies, and can also be used to refer to other stereoscopic topics including 3DTV, 3D displays, 3D cameras and 3D vision, it can also be used to refer to non-stereoscopic technologies including 3D printing (additive manufacturing), 3D computer graphics (using monoscopic depth cues to give a computer-generated image added realism), 3D laser scanning, 3D computer-aided design (CAD), 3D modelling, and DirectX 3D. In order to distinguish stereoscopic 3D from other uses of "3D" some authors use the term "s3D", short for stereoscopic 3D.

It is apparent from the literature that in early times the hyphenated form of "3-D" was used predominantly. For at least the past 30 years, both the hyphenated and non-hyphenated forms "3-D" and "3D" have been in common usage. It seems formal English tends to prefer the hyphenated form, whereas modern usage tends to use the non-hyphenated form, but is there a right and a wrong? Can the two styles co-exist?

Methods

We start this examination by looking at the house styles of various publications relevant to the stereoscopic imaging field. We then consider current trends of usage of language in print. Finally we consider the implications of choosing one style or the other.

Results

First we present the results of the house style survey, and subsequently present the statistical occurrence of the two styles over the past 30 years.

House styles

Many publications have a house style that prescribes the use of the hyphenated version "3-D." A number of publications were surveyed to determine their policy.

IEEE's senior copy editor for IEEE Spectrum magazine, Joe Levine,³ wrote:

IEEE publications like standards, transactions, and proceedings use a more formal style than IEEE Spectrum. While Spectrum doesn't take up all the latest trends, we do consider the styles of mainstream magazines and newspapers. We're encouraged to use a conversational tone. The traditional practice in most house styles is to spell out "three-dimensional" on first reference and then to use "3-D." We only recently started allowing "3-D" to be used in all cases. Our editors urged me to change this, arguing that most of the time people hear in their heads "three dee." And in certain contexts it just sounds odd to spell it out: For example, "three-dimensional television" seems to refer to the object rather than the technology.

I don't think there's an explicit policy on "3-D" vs. "3D" throughout [IEEE] and all [its] societies. I have found that the IEEE Computer Society has its own style guide: <http://www.computer.org/portal/web/publications/styleguide> and they have indeed adopted the no-hyphen style.

With regard to publications from the Society for Information Display (SID), Jay Morreale,⁴ Managing Editor of the Journal of the SID (JSID) wrote:

In both [Information Display] Magazine and JSID, we have been using "3-D" since ID's inception in 1987 and since I became Managing Editor of the Journal back in 1978. My goal is to be consistent until the style dictates a change.

As far as references are concerned, it is policy NOT to change references because it is understood that searches need to be based on "original" paper titles, although I must admit the urge is definitely there to edit the titles of papers in the references.

John Dennis,⁵ the editor of the National Stereoscopic Association magazine *Stereo World*, said:

We follow a style of using “3-D” in articles except when “3D” is used as part of a movie or book title or product name.

Most newspapers use the “3-D” style – although there are some exceptions, or even inconsistencies within the same publication or article. Most newspapers appear to follow *The Associated Press Stylebook*,⁶ which recommends the “3-D” form. In contrast, *The Yahoo! Style Guide*,⁷ which is primarily intended for online publishing, recommends the “3D” form.

SPIE does not apply a preferred style of either “3-D” or “3D” in their proceedings or journals. In the proceedings volumes, the authors are free to choose the form they wish. The same is intended to apply to their journals, however my experience is that well-meaning sub-contracted proof editors often apply “3-D” style unless the author makes a representation otherwise.

The editor of *SPIE Professional*, Kathy Sheehan,⁸ wrote:

Our magazine generally follows AP style. We have a small style list that sometimes over-rides the AP style, which we do in the case of “3D”. Although we would edit an author’s copy, we would not change the name of a previously published book title, article, etc.

Mark Fihn,⁹ editor of *3rd Dimension* newsletter, wrote:

We try to always use “3D”. We don’t give authors any sort of style guide, so we get inputs using either “3D”, “3-D”, or both.

I [usually] do a final edit to change “3-D” to “3D”.

We use “3D” because frequently there’s another hyphen in the equation, such as “3D-enabled” or “pseudo-3D” or some such... It seems awkward to have “3-D-enabled” or “pseudo-3-D”

The evolution of language

Languages evolve over time. Strunk and White¹¹, in their book “*The Elements of Style*,” wrote: “Do not use a hyphen between words that can better be written as one word: water-fowl, waterfowl. Common sense will aid you in the decision, but a dictionary is more reliable.” and particularly “The steady evolution of the language seems to favor union: two words eventually becoming one, usually after a period of hyphenation.”

A survey of 1293 stereoscopic focused papers¹⁰ published by SD&A, IS&T and SPIE over the period 1977-2009 reveals a trend towards the use of the non-hyphenated form. It is important to note that a house style was not applied to these papers so this provides a good unbiased survey of usage amongst a scientific audience. The survey is broken down into roughly decade-long periods:

- 1977-1989: (231 papers containing 1567 pages)
 - “3D” 921 instances in 91 papers
 - “3-D” 1623 instances in 131 papers
- 1990-1989: (407 papers containing 3535 pages)
 - “3D” 3318 instances in 307 papers
 - “3-D” 2003 instances in 165 papers
- 2000-2009: (655 papers containing 6229 pages)
 - “3D” 11627 instances in 573 papers
 - “3-D” 2827 instances in 263 papers

These statistics are illustrated in Figure 1 and Figure 2:

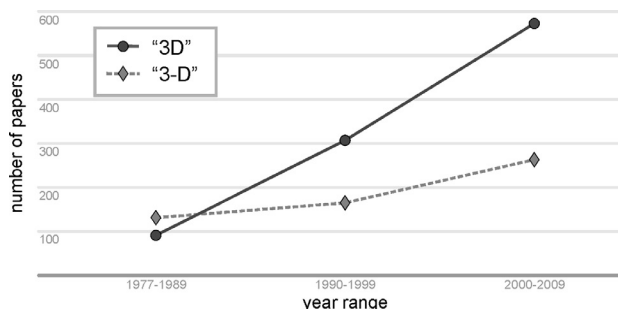


Figure 1: Number of papers in the SD&A 20-year DVD-ROM¹⁰ containing the term “3D” or “3-D” in roughly decade period groups.

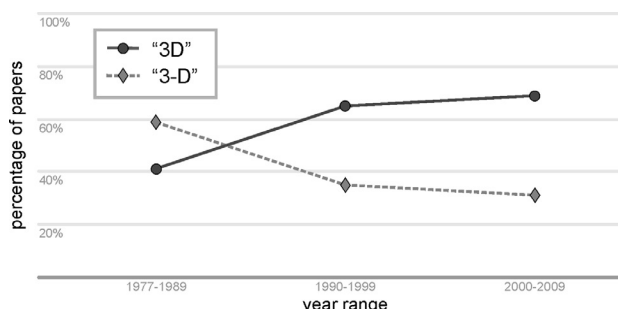


Figure 2: Percentage of number of papers in the SD&A 20-year DVD-ROM¹⁰ containing the term “3D” or “3-D” in roughly decade period groups.

According to this publication record, the “3-D” form was favoured in the 70s and 80s, but over the past couple of decades the unhyphenated “3D” form has become more favoured by scientific authors.

Our next statistic considers the occurrence of “3D” and “3-D” in the May (or April) 2013 issue of several professionally produced publications relevant to the 3D field. Table 1 summarizes counts of “3D” and “3-D”. The count is conducted separately for the text of the publication, which will be affected by the publication’s house style, and in advertisements (adverts), which will not be affected by the publication’s house style.

Table 1: The occurrence of “3D” and “3-D” in various publications. Values greater than 50% are shown in bold.

Publication	Occurrences (count) percentage %			
	in text		in adverts	
	“3-D”	“3D”	“3-D”	“3D”
Stereo World ¹²	(88) 79%	(24) 21%	(12) 14%	(76) 86%
Information Display ¹³	(103) 82%	(23) 18%	(0) 0%	(9) 100%
IEEE Spectrum ¹⁴	(3) 100%	(0) 0%	(0) 0%	(2) 100%
SPIE Professional ¹⁵	(1) 7%	(14) 93%	(0) 0%	(2) 100%
i3 ¹⁶	(0) 0%	(76) 100%	(0) -	(0) -
3rd Dimension ¹⁷	(10) 1%	(718) 99%	(0) 0%	(2) 100%

It can be seen that, not surprisingly, the “3-D” form predominates in the text of the three publications identified earlier which apply a house style of “3-D”. Perhaps tellingly, the occurrence of the non-hyphenated form “3D” predominates in the advertisements appearing in those same publications – indicating the preference of the advertisers or their marketing consultants for the non-hyphenated form. The latter three publications, which are all significantly younger than the earlier three publications, all have a predominance of the “3D” form.

Another statistic that sheds some light on common usage is the incidence of “3D” and “3-D” in Google Searches¹⁸ conducted by the general public as illustrated in Figure 3 and Figure 4.

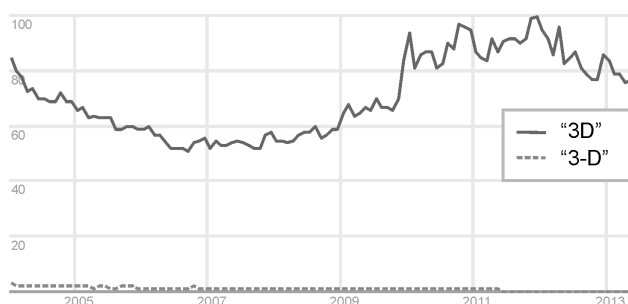


Figure 3: Incidence of “3D” and “3-D” in Google Search statistics plotted together. “3-D” peak is only ~3% of “3D” peak. The number 100 represents the peak search interest.

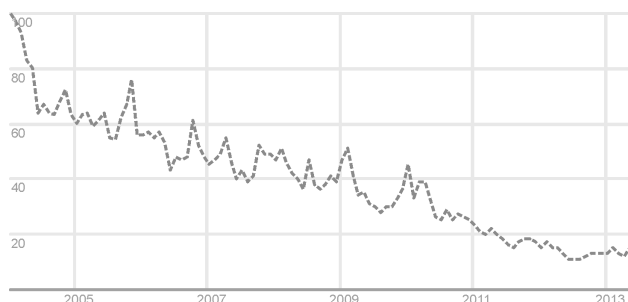


Figure 4: The incidence of “3-D” in Google Search statistics plotted in isolation. 100 represents peak search interest.

Figure 3 reveals that the general public strongly favours “3D” over “3-D” approximately 100:1 in 2013. Although the volume of searches using the term “3D” has had a bit of a wave, over a 9-year period the volume of searches has been fairly steady. Figure 4 reveals that the volume of searches for “3-D” has experienced a heavy decline. These statistics almost function as a popular vote, but importantly reveal that publications using the “3-D” form will miss hits from the vast majority of searches for the “3D” form (unless the search engine automatically combines “3D” and “3-D” results).

Discussion

One could argue that the use of the hyphen in the “3-D” abbreviation is unnecessary. An abbreviation is after all meant to be short, and in this instance the hyphen doesn’t add anything vital to the abbreviation. Furthermore, when “3D” and “3-D” are read aloud, they both sound the same anyway.

As mentioned earlier, some terms already include hyphenation (eg 3D-Ready, 3D-capable, 3D-Con) – the addition of another hyphen for the “3D” in these terms would produce an awkward result. A similar thought applies to extended acronyms such as “3DTV” – “3-DTV” seems awkward.

Regardless of an author’s own preference, when writing a manuscript, he or she should be careful that proper nouns are used in the form defined by the originator (eg “Blu-ray 3D”, not “Blu-ray 3-D”). When citing references, authors should be careful to quote the title exactly as written in the original paper (with or without hyphens) – a change in hyphenation could break automatic citation listing. The hyphenation of email addresses and web addresses should also not be changed – otherwise they may simply be broken. Finally, when authors are checking their manuscript proof before publication, they should be sure to check that the hyphenation of proper nouns, references, web addresses and email addresses have not been changed in the proof editing process - a simple search and replace is tempting but can break all of these items.

It was mentioned earlier that there is some desire to differentiate stereoscopic 3D from other uses of 3D by using the abbreviation “s3D” or “S3D”. Additionally, some authors have suggested that “3-D” could be used for stereoscopic specific discussions, and “3D” used for non-stereoscopic uses.¹⁹ Although this proposal does have some merit, this particular style is not currently in widespread use, and differs from the styles required by most publications.

Conclusion

Is it time to change the conventions and house styles that require the use of the hyphenated form of “3-D”? I propose that the statistics revealed in this paper show the time is right to make that change.

Giving Lenny Lipton,²⁰ author of “Foundations of the Stereoscopic Cinema,”²¹ the last word:

You cannot imagine how passionate some people are about the hyphen. Or maybe you can. Simpler is better and how does 2-D look to you?

References are listed at the bottom of page 62.

References - continued from page 61

- 1 Kennedy C. The Development and Use of Stereo Photography for Educational Purposes. *Journal of the Society for Motion Picture Engineers* 1936;26:3-17. doi: 10.5594/J01280
- 2 Spottiswoode R, Spottiswoode NL, Smith C. Basic Principles of the Three Dimensional Film. *Journal of the Society for Motion Picture and Television Engineers* 1952;59:249-286. doi: 10.5594/J01778
- 3 Joe Levine, IEEE, personal communication, 23 September 2011.
- 4 Jay Morreale, SID, personal communication, 1 September 2011.
- 5 John Dennis, NSA, personal communication, 1 September 2011.
- 6 *The Associated Press Stylebook and Briefing on Media Law*. New York: Associated Press; 2013. ISBN 978-0-917360-57-2.
- 7 *The Yahoo! Style Guide*. New York: Yahoo! Inc; 2010. p. 483. ISBN 978-0312569846.
- 8 Kathy Sheehan, SPIE, personal communication, 29 May 2013.
- 9 Mark Fihn, Veritas et Visus, personal communication, 28 May 2013.
- 10 Woods AJ, Merritt JO, Fisher S, Bolas M, Benton S, Holliman NS, et al. (eds). *Selected SPIE/IS&T papers on DVD-ROM: Stereoscopic Displays and Applications 1990-2009: A Complete 20-Year Retrospective - and The Engineering Reality of Virtual Reality 1994-2009 (CDP51)*. Bellingham (WA): SPIE; 2010. ISBN: 978-0-8194-7659-3
- 11 Strunk W, White EB. *The Elements of Style*. 4th ed. Boston, Massachusetts: Allyn & Bacon; 2000. ISBN: 0-205-30902-X
- 12 *Stereo World*. 38(6) (May/June 2013). Portland, Oregon: National Stereoscopic Association (NSA); 2013. Available at <http://www.stereoworld.org/> [Accessed 19 June 2013].
- 13 *Information Display*. 9(3) (May/June 2013). Campbell, California: Society for Information Display (SID); 2013. Available at <http://informationdisplay.org/> [Accessed 19 June 2013].
- 14 *IEEE Spectrum*. 50(5) (INT) (May 2013). New York: Institute of Electrical and Electronics Engineers (IEEE); 2013. Available at <http://spectrum.ieee.org/> [Accessed 19 June 2013].
- 15 *SPIE Professional*. 8(2) (April 2013). Bellingham, Washington: SPIE; 2013.
- 16 *It Is Innovation (i3)*. 1(3) (May 2013). Arlington, Virginia: Consumer Electronics Association (CEA); 2013. Available at <http://www.ce.org/i3> [Accessed 19 June 2013].
- 17 *3rd Dimension*. 8(2) (May 2013). Temple, Texas: Veritas et Visus; 2013. Available at http://www.veritasetvisus.com/3rd_dimension.htm [Accessed 19 June 2013]
- 18 Google Trends [Internet]. Mountain View, California: Google Inc.; 2013. [updated 30 May 2013; cited 30 May 2013]. Available at www.google.com/trends
- 19 Eric Kurland, 3-DIY, personal communication, 28 May 2013.
- 20 Lenny Lipton, Leonardo IP, personal communication, 8 Nov 2011.
- 21 Lipton L. *Foundations of the Stereoscopic Cinema – A Study in Depth*. New York: Van Nostrand Reinhold Company; 1978.

This is a separator page and is intentionally blank.

Appendix 2 – Statement of Contribution of Candidate to Submitted Publications

- Paper 1** Woods (2012)
Sole Author
- Paper 2** Woods, Yuen, Karvinen (2007)
70% academic contribution
- Paper 3** Woods, Harris (2012)
90% academic contribution
- Paper 4** Woods, Harris, Leggo, Rourke (2013)
80% academic contribution
- Paper 5** Woods, Yuen (2006)
70% academic contribution
- Paper 6** Woods, Karvinen (2008)
70% academic contribution
- Paper 7** Woods, Sehic (2009)
70% academic contribution
- Paper 8** Woods, Harris (2010)
70% academic contribution
- Paper 9** Woods, Tan (2002)
70% academic contribution
- Paper 10** Woods, Rourke (2004)
70% academic contribution
- Paper 11** Woods (2005)
Sole Author
- Paper 12** Woods, Rourke, Yuen (2006)
70% academic contribution
- Paper 13** Woods, Rourke (2007)
70% academic contribution
- Paper 14** Woods (2009)
Sole Author
- Paper 15** Weissman, Woods (2011)
30% academic contribution
- Paper 16** Woods (2011)
Sole Author
- Paper 17** Woods, Helliwell (2012)
70% academic contribution
- Paper 18** Woods (2013)
Sole Author


Signed contribution letters for the co-authored papers are included below.

To Whom It May Concern

I, Andrew James Woods, contributed the content specified below to the following publication:

A. J. Woods, K. L. Yuen, and K. S. Karvinen (2007) "Characterizing crosstalk in anaglyphic stereoscopic images on LCD monitors and plasma displays" in Journal of the Society for Information Display, Volume 15, Issue 11, pp. 889-898, November 2007.

Woods designed the project, and conceived the original measurement, analysis and simulation techniques. The PDP and glasses spectral measurements were collected by Karvinen with assistance from Woods. The LCD spectral measurements were collected by Yuen with assistance from Woods. Karvinen performed most of the data processing with analysis performed by Woods and Karvinen. Karvinen rewrote the simulation software in Matlab from the original framework. The conference paper was written by Woods with input from Karvinen and Yuen. Some of the figures were provided by Karvinen and Yuen and prepared for publication by Woods, other figures were prepared by Woods. For the overall work it is estimated that the academic breakdown was Woods 66%, Karvinen 21%, Yuen 13%; and the labour breakdown was Karvinen 50%, Yuen 30%, Woods 20%.




Andrew J. Woods 22/3/13

I, as Co-Author, endorse that this level of contribution by the candidate indicated above is appropriate.



Kai Karvinen



Ka Lun Yuen 8/4/2013


To Whom It May Concern

I, Andrew James Woods, contributed the content specified below to the following publication:

A. J. Woods, C. R. Harris (2012) "Using cross-talk simulation to predict the performance of anaglyph 3-D glasses" in *Journal of the Society for Information Display*, Vol. 20, No. 6, pp. 304-315.

The project was conducted in two parts. Woods designed the projects and conceived the measurement and analysis techniques for both projects. The first part of the project was conducted by Harris and Woods with Woods providing the academic direction. The data was collected by Harris with the assistance of Woods. The data was collated and processed by Harris and interpreted by Woods and Harris. ~~Harris and Woods jointly conducted the validation test. The second part of the project was conducted solely by Woods. All data was re-measured and re-analysed by Woods. Woods devised and conducted a new validation test with five subjects. The conference paper was written by Woods and reviewed by Harris. The figures and tables were prepared by Woods.~~

For the overall work it is estimated that the academic breakdown was Woods 85%, Harris 15%; and the labour breakdown was Woods 65%, Harris 35%.



Andrew J. Woods 22/3/13

I, as Co-Author, endorse that this level of contribution by the candidate indicated above is appropriate.



Chris R. Harris 12/03/13
date


To Whom It May Concern

I, Andrew James Woods, contributed the content specified below to the following publication:

A. J. Woods, C. R. Harris, D. B. Leggo, T. M. Rourke (2013) "Characterizing and Reducing Crosstalk in Printed Anaglyph Stereoscopic 3D Images" in (Journal of) Optical Engineering, SPIE – accepted for publication in April 2013 issue.


The project was conducted in four parts. Woods designed the projects and conceived the measurement and analysis techniques. The first part of the project involved some initial work to characterise the properties of printed crosstalk and was conducted by Rourke and Woods with Woods providing the academic direction. The data was collected by Rourke with the assistance of Woods. The data was collated and processed by Rourke and interpreted by Woods and Rourke. The second part of the project involved further work to characterise the properties of printed crosstalk and was conducted by Harris and Woods with Woods providing the academic direction. The data was collected by Harris with the assistance of Woods. The data was collated and processed by Harris and interpreted by Woods and Harris. Harris and Woods jointly conducted a validation test. The third part of the project involved an attempt to characterise colour management and its effect on printed crosstalk. This was conducted by Leggo and Woods with Woods providing the academic direction. The data was collected by Leggo with the assistance of Woods. The data was collated and processed by Leggo and interpreted by Woods and Leggo. Leggo conducted a validation test. The fourth part of the project was conducted solely by Woods. All spectral data was re-measured and re-analysed by Woods. Woods devised and conducted a new validation test with five subjects and performed a detailed statistical analysis. The journal paper was written by Woods and reviewed by Harris, Rourke and Leggo. The figures and tables were prepared by Woods.


For the overall work it is estimated that the academic breakdown was Woods 80%, Rourke 5%, Harris 10%, Leggo 5%; and the labour breakdown was Woods 55%, Rourke 10%, Harris 20%, Leggo 15%.


22/3/13
Andrew J. Woods

I, as Co-Author, endorse that this level of contribution by the candidate indicated above is appropriate.


Chris Harris


Dean Leggo 9.4.13


Tegan Rourke 2/4/13

To Whom It May Concern

I, Andrew James Woods, contributed the content specified below to the following publication:

A. J. Woods, K. L. Yuen (2006) "Compatibility of LCD Monitors with Frame-Sequential Stereoscopic 3D Visualisation" (Invited Paper), in IMID/IDMC '06 Digest, (The 6th International Meeting on Information Display, and The 5th International Display Manufacturing Conference), pp. 98-102, Daegu, South Korea, 22-25 August 2006.

Woods designed the project and conceived the measurement, analysis and simulation techniques. The core project was conducted by Yuen and Woods with Woods providing the academic direction. The data was collected by Yuen with the assistance of Woods. The data was processed by Yuen and interpreted by Woods and Yuen. The conference paper was written by Woods with input from Yuen. The figures were provided by Yuen and prepared for publication by Woods, except for Figure 4 generated by Woods which illustrated a key concept to allow LCDs to be able to support time-sequential 3D. For the overall work it is estimated that the academic breakdown was Woods 70%, Yuen 30%; and the labour breakdown was Yuen 75%, Woods 25%.



Andrew J. Woods

5/3/2013

I, as Co-Author, endorse that this level of contribution by the candidate indicated above is appropriate.



Ka Lun Yuen

To Whom It May Concern

I, Andrew James Woods, contributed the content specified below to the following publication:

A. J. Woods, K. S. Karvinen (2008) "The compatibility of consumer plasma displays with time-sequential stereoscopic 3D visualization" in *Stereoscopic Displays and Applications XIX*, Proceedings of IS&T/SPIE Electronic Imaging, SPIE Vol. 6803, pp. 68030X-1 to -9, San Jose, California, January 2008.

Woods designed the project, and conceived the measurement, analysis and simulation techniques. The core project was conducted by Karvinen and Woods with Woods providing the academic direction. The data was collected by Karvinen with the assistance of Woods. The data was processed by Karvinen and interpreted by Woods and Karvinen. The first draft of the conference paper was written by Karvinen. The final paper was extensively revised and completed by Woods. All but one of the figures were provided by Karvinen and prepared for publication by Woods. For the overall work it is estimated that the academic breakdown was Woods 70%, Karvinen 30%; and the labour breakdown was Karvinen 80%, Woods 20%.



Andrew J. Woods

8 Jan 2013.

I, as Co-Author, endorse that this level of contribution by the candidate indicated above is appropriate.



Kai Karvinen

To Whom It May Concern

I, Andrew James Woods, contributed the content specified below to the following publication:

A. J. Woods, A. Sehic (2009) "The compatibility of LCD TVs with time-sequential stereoscopic 3D visualization" in Stereoscopic Displays and Applications XX, Proceedings of IS&T/SPIE Electronic Imaging, SPIE Vol. 7237, pp. 72370N-1 to -9, San Jose, California, January 2009.

Woods designed the project, conceived the analysis technique and also conceived the simulation algorithm. The core project was conducted by Sehic and Woods with Woods providing the academic direction. The data was collected by Sehic with the assistance of Woods. The data was processed by Sehic and interpreted by Woods and Sehic. The conference paper was written by Woods with input from Sehic. All but one of the figures were developed by Sehic and prepared for publication by Woods.

For the overall work it is estimated that the academic breakdown was Woods 70%, Sehic 30%; and the labour breakdown was Sehic 80%, Woods 20%.



Andrew J. Woods

26/3/2013.

I, as Co-Author, endorse that this level of contribution by the candidate indicated above is appropriate.



Adin Sehic

To Whom It May Concern

I, Andrew James Woods, contributed the content specified below to the following publication:


A. J. Woods, C. R. Harris (2010) "Comparing levels of crosstalk with red/cyan, blue/yellow, and green/magenta anaglyph 3D glasses" in Stereoscopic Displays and Applications XXI, Proceedings of IS&T/SPIE Electronic Imaging, SPIE Vol. 7253, pp. 75240Q-1 to -12, San Jose, California, January 2010.

Woods designed the project and conceived the measurement and analysis technique. The core project was conducted by Harris and Woods with Woods providing the academic direction. The data was collected by Harris with the assistance of Woods. The data was collated and processed by Harris and interpreted by Woods and Harris. ~~Harris and Woods jointly conducted the validation test. The first draft of the conference paper was written by Harris and Woods worked up the paper for final publication. The data tables were prepared by Harris and the figures were jointly prepared by Harris and Woods.~~

For the overall work it is estimated that the academic breakdown was Woods 70%, Harris 30%; and the labour breakdown was Harris 80%, Woods 20%.


Andrew J. Woods 27/3/13

I, as Co-Author, endorse that this level of contribution by the candidate indicated above is appropriate.


Chris R. Harris 12/03/13
date

To Whom It May Concern

I, Andrew James Woods, contributed the content specified below to the following publication:

A. J. Woods, S. Tan (2002) "Characterising Sources of Ghosting in Time-Sequential Stereoscopic Video Displays" presented at Stereoscopic Displays and Applications XIII, published in Stereoscopic Displays and Virtual Reality Systems IX, Proceedings of IS&T/SPIE Electronic Imaging, SPIE Vol. 4660, pp. 66-77, San Jose, California, January 2002.

Woods designed the project, conceived the analysis technique and also conceived the simulation algorithm. The core project was conducted by Tan and Woods with Woods providing the academic direction. The data was collected by Tan with the assistance of Woods. The data was processed by Tan and interpreted by Woods and Tan. The simulation was implemented in excel by Tan. The conference paper was written by Woods with input from Tan. The figures were produced by Tan and prepared for publication by Woods. For the overall work it is estimated that the academic breakdown was Woods 70%, Tan 30%; and the labour breakdown was Tan 80%, Woods 20%.



8 JAN 2013.

Andrew J. Woods

I, as Co-Author, endorse that this level of contribution by the candidate indicated above is appropriate.



Stanley Tan


8 Jan 2013.

To Whom It May Concern

I, Andrew James Woods, contributed the content specified below to the following publication:

A. J. Woods, T. Rourke (2004) "Ghosting in Anaglyphic Stereoscopic Images" presented at Stereoscopic Displays and Applications XV (SD&A), published in Stereoscopic Displays and Virtual Reality Systems XI, Proceedings of IS&T/SPIE Electronic Imaging, SPIE Vol. 5291, pp. 354-365, San Jose, California, January 2004.

Woods designed the project and conceived the measurement, analysis and simulation technique. The core project was conducted by Rourke and Woods with Woods providing the academic direction. The data was collected by Rourke with the assistance of Woods. The data was processed by Rourke and interpreted by Woods and Rourke. Rourke implemented the simulation in Excel. The conference paper was written by Woods with input from Rourke. The figures were provided by Rourke and prepared for publication by Woods. For the overall work it is estimated that the academic breakdown was Woods 70%, Rourke 30%; and the labour breakdown was Rourke 80%, Woods 20%.


28/2/13
Andrew J. Woods

I, as Co-Author, endorse that this level of contribution by the candidate indicated above is appropriate.



24/2/13
Tegan Rourke

To Whom It May Concern

I, Andrew James Woods, contributed the content specified below to the following publication:


A.J. Woods, T. Rourke, K. L. Yuen (2006) "The Compatibility of Consumer Displays with Time-Sequential Stereoscopic 3D Visualisation" (Plenary Paper), in Proceedings of the K-IDS Three-Dimensional Display Workshop 2006, pp. 7-10, Seoul National University, Seoul, South Korea, 21 August 2006.

Woods designed the project and conceived the measurement and analysis techniques. The core DLP project was conducted by Rourke and Woods with Woods providing the academic direction. The core LCD project was conducted by Yuen and Woods with Woods providing the academic direction. The DLP data was collected by Rourke with the assistance of Woods. The DLP data was processed by Rourke and interpreted by Woods and Rourke. The LCD data was collected by Yuen with the assistance of Woods. The LCD data was processed by Yuen and interpreted by Woods and Yuen. The conference paper was written by Woods with input from Rourke and Yuen. Figure 1 was provided by Yuen and prepared for publication by Woods. Table 1 was prepared by Rourke. Figure 2 was provided by Woods. For the overall work it is estimated that the academic breakdown was Woods 70%, Rourke 15%, Yuen 15%; and the labour breakdown was Rourke 40%, Yuen 40%, Woods 20%.


Andrew J. Woods 26/3/2013.

I, as Co-Author, endorse that this level of contribution by the candidate indicated above is appropriate.


Tegan Rourke 2/4/13


Ka Lun Yuen 8/4/2013

To Whom It May Concern


I, Andrew James Woods, contributed the content specified below to the following publication:

A. J. Woods, T. Rourke (2007) "The compatibility of consumer DLP projectors with time-sequential stereoscopic 3D visualization", presented at Stereoscopic Displays and Applications XVIII, published in Stereoscopic Displays and Virtual Reality Systems XIV, Proceedings of IS&T/SPIE Electronic Imaging, SPIE Vol. 6490, pp. 64900V-1 to -7, San Jose, California, January 2007.

Woods designed the project and conceived the measurement and analysis technique. The core project was conducted by Rourke and Woods with Woods providing the academic direction. The initial data was collected collaboratively however subsequently the vast majority of the data was collected by Rourke and some data was collected by Woods. The data was collated and processed by Rourke and interpreted by Woods and Rourke. The conference paper was written by Woods with input from Rourke. The data tables were prepared by Rourke and the figures were prepared by Woods. For the overall work it is estimated that the academic breakdown was Woods 70%, Rourke 30%; and the labour breakdown was Rourke 80%, Woods 20%.


28/2/13
Andrew J. Woods

I, as Co-Author, endorse that this level of contribution by the candidate indicated above is appropriate.


24/2/13
Tegan Rourke


To Whom It May Concern

I, Andrew James Woods, contributed the content specified below to the following publication:

M. A. Weissman, A. J. Woods (2011) "A simple method for measuring crosstalk in stereoscopic displays" in Stereoscopic Displays and Applications XXII, Proceedings of IS&T/SPIE Electronic Imaging, SPIE Vol. 7863, pp. 786310-1 to -11, Burlingame, California, January 2011.

Weissman proposed the original technique and developed the initial mathematical analysis with input from Woods. The project was then designed and conducted collaboratively by Weissman and Woods. Optical measurement data to test the technique was collected by Weissman and Woods. The data was processed and interpreted by Weissman and Woods. The first draft of the paper was written by Weissman with input from Woods and finalized for publication collaboratively.

For the overall work it is estimated that the academic breakdown was Woods 30%, Weissman 70%; and the labour breakdown was Woods 30%, Weissman 70%.



Andrew J. Woods date 26/3/2013.

I, as Co-Author, endorse that this level of contribution by the candidate indicated above is appropriate.



Michael A. Weissman date 25 Mar 13

To Whom It May Concern

I, Andrew James Woods, contributed the content specified below to the following publication:


A. J. Woods, J. Helliwell (2012) "Investigating the cross-compatibility of IR-controlled active shutter glasses" in Stereoscopic Displays and Applications XXIII, Proceedings of IS&T/SPIE Electronic Imaging, SPIE Vol. 8288, pp. 82881C-1 to -10, Burlingame, California, January 2012.

Woods designed the projects and conceived the measurement and analysis technique. The core project was conducted by Helliwell and Woods with Woods providing the academic direction. The data was collected by Helliwell with the assistance of Woods. The data was processed by Helliwell and interpreted by Woods and Helliwell. The IR emulator was programmed by Woods and IR codes tested by Woods with Helliwell. The conference paper was written by Woods with input from Helliwell. The figures were provided by Helliwell and prepared for publication by Woods.

For the overall work it is estimated that the academic breakdown was Woods 70%, Helliwell 30%; and the labour breakdown was Woods 50%, Helliwell 50%.


Andrew J. Woods 7/3/13.

I, as Co-Author, endorse that this level of contribution by the candidate indicated above is appropriate.


Jesse Helliwell 7/3/13
date

Appendix 3 – Evidence of Peer-Review Status of Included Publications

Paper 1 – Woods (2012)

Journal of Electronic Imaging

<http://spie.org/x85038.xml>

About the Journal of Electronic Imaging

The *Journal of Electronic Imaging* (JEI) is a print and online journal, copublished by IS&T and SPIE, that publishes papers in all technology areas that make up the fields of design, engineering, and applications of electronic imaging systems. In 1992, inspired by the success of their cosponsored Electronic Imaging conference, the two societies identified a need for a peer-reviewed publication dedicated to the full spectrum of electronic imaging technologies, and JEI was launched as a result.

In addition to contributed research papers, JEI occasionally publishes special sections in key areas of technology. Special sections are assembled by guest editors. See the [Editorial Schedule](#) for a list of forthcoming special section topics and dates.

Why publish in this journal?

JEI is a peer-reviewed journal that addresses technical problems, issues, and progress in the field of electronic imaging. Authors benefit from a rigorous review process, prompt publication times, multimedia integration, and high-resolution online color image display.

Paper 2 – Woods, Yuen, Karvinen (2007)

Paper 3 – Woods, Harris (2012)

Journal of the Society for Information Display

<http://www.sid.org/Publications/JournaloftheSID/InformationforAuthors.aspx>

SCOPE

The *Journal of the Society for Information Display* (*Journal*) publishes original works dealing with the theory and practice of information display. Coverage includes materials, devices and systems; the underlying chemistry, physics, physiology and psychology; measurement techniques, manufacturing technologies; and all aspects of the interaction between equipment and its users. Review articles are also published in all of these areas.

Occasional special issues or sections consist of collections of papers on specific topical areas or collections of full length papers based in part on oral or poster presentations given at conferences sponsored by the Society for Information Display (SID).

EDITORIAL PROCESS

All manuscripts submitted are reviewed by at least two reviewers expert in the subject matter of the manuscript, to assure novelty, accuracy and the appropriate application of scientific and technologic methods. Authors are encouraged to be brief, but not incomplete; effective communication of your ideas is essential

Paper 4 – Woods, Harris, Leggo, Rourke (2013)

Optical Engineering journal

<http://spie.org/x85027.xml>

About Optical Engineering

Optical Engineering (OE) is a print and online journal that publishes peer-reviewed papers reporting on research and development in optical science and engineering and the practical applications of known optical science, engineering, and technology. Contributions addressing issues ranging from fundamental understanding to emerging technologies and applications are within the scope of the journal.

The journal publishes full-length research papers, letters, tutorials, and reviews. In addition to contributed research articles, OE often publishes special sections in key areas of technology. Special sections are assembled by guest editors. See the [Editorial Schedule](#) for a list of forthcoming special section topics and dates.

Why publish in this journal?

Optical Engineering is the flagship journal of SPIE, published since 1962. OE aims to publish highly relevant and high-impact papers. OE is published online as part of the SPIE Digital Library, accessible by researchers at many of the world's leading universities, laboratories, and corporations as well as thousands of individual subscribers.

Paper 5 - Woods, Yuen (2006)

Email from peer-review chair:

<p>From: Byoung-ho Lee [mailto:byoung-ho@snu.ac.kr] Sent: Wednesday, 2 August 2006 7:29 AM To: Andrew Woods Subject: [IMID/IDMC 2006] Paper review</p> <p>Dear Mr. Andrew Woods,</p> <p>Thank you for submitting the paper titled "Compatibility of LCD monitors with frame-sequential stereoscopic 3D visualization" to The 6th International Meeting on Information Display and The International Display Manufacturing Conference (IMID/IDMC 2006).</p> <p>We reviewed your paper. Based on the review comments, we are very pleased to accept your paper as an 'invited paper' for the IMID/IDMC 2006. Your presentation date will be August 23 (Wed). 30 minutes slot will be assigned to each invited paper.</p> <hr/> <p>Review comments</p> <p>This paper tests 15 different LCD monitors for frame-sequential stereoscopic display and identifies five main properties which affect the quality of stereoscopic images. Also, two possible methods of achieving frame-sequential stereo on fast response LCD monitors are proposed. This paper is highly valuable and will attract much attention in the R&D field of frame-sequential stereoscopic display systems. So, I would like to recommend this paper to be presented as an invited paper.</p> <hr/> <p>Thank you and see you in Korea.</p> <p>Sincerely,</p> <p>Byoung-ho Lee Professor, OSA Fellow, SPIE Fellow School of Electrical Engineering Seoul National University Kwanak-Gu Shinlim-Dong Seoul 151-744, Korea Tel: +82 2 880 7245, Fax: +82 2 873 9953 E-mail: byoung-ho@snu.ac.kr http://oeqelab.snu.ac.kr</p>
--

Paper 6 - Woods, Karvinen (2008)

"Introduction" in Stereoscopic Displays and Applications XIX, Proceedings of IS&T/SPIE Electronic Imaging, SPIE Vol. 6803, pp. 68030X-1 to 68030X-9, San Jose, California, January 2008.

<p>This year for the first time the conference committee instituted a process of peer review on selected papers in the proceedings. This process was initiated to facilitate the improved quality of the proceedings, provide authors with constructive feedback on their submissions, and also provide academic authors with additional recognition for their publications. There is an increasing importance of peer reviewed publications in academic circles worldwide and the SD&A conference wishes to remain the most relevant place for stereoscopic imaging papers to be published. This year, two reviewers were sought for each paper for which peer review was requested. A single-blind review process was conducted for those papers, and authors were given a two-week window to respond to the reviewer comments. The chairs reviewed the author responses to the reviews and decided whether the responses to the reviewer comments justified the paper being classified a peer reviewed technical paper. This year the peer reviewed papers were:</p>

- [6803-04] "Methods for improving the quality of user-created stereoscopic content," Lachlan D. Pockett, Sr., Marja Salmimaa, Nokia Research Ctr. (Finland)
- [6803-31] "The compatibility of consumer plasma displays with time-sequential stereoscopic 3D visualization," Andrew J. Woods, Kai S. Karvinen, Curtin Univ. of Technology (Australia)
- [6803-35] "A composition tool for creating comfortable stereoscopic images," Katharina Quintus, Michael W. Halle, Brigham and Women's Hospital
- [6803-36] "Radiation therapy planning using a volumetric 3D display: PerspectaRAD," Joshua Napoli, Sandy Stutsman, Actuality Medical, Inc.; James C. H. Chu, Xing Gong, Rush Univ. Medical Ctr.; Mark J. Rivard, Tufts-New England Medical Ctr.; Gene Cardarelli, Rhode Island Hospital; Thomas P. Ryan, Gregg E. Favalora, Actuality Medical, Inc.

Paper 7 - Woods, Sehic (2009)

Email from peer-review chair:

Dear Author,

Attached below are the anonymous reviewer comments on your paper. The aim of the review process is to provide these to you to help you improve the quality of your presentation at the conference, and in particular the quality of your written paper which will be published in the final conference proceedings.

Please can you read and reflect on the comments from the reviewers and make changes as appropriate. Please resubmit your revised paper as soon as possible.

Best wishes,
Nick Holliman.

Reviewer 1 Comments:

This paper seems well written. It looks at the possibilities of using commercially released displays, that have no been specifically design with 3D in mind, for time-sequential stereo 3D.

Although only minor - the axis writing and labeling on Figures 3, 4, 5 and 7 is unclear and difficult to read.

Some of the websites referenced seem to be missing there date of access.

I would say that the objectives, results and conclusion for the paper are clear.

Reviewer 2 Comments:

Review

Overall, this is a good contribution. I have a number of suggestions for minor improvements.

Section 1, line 1, "aka": this is too informal, you should use "also called" or "also known as".

Section 1, paragraph 2, line 1: "let's" -> "we". This was the only contraction I noticed, it must have slipped through the author's checking process.

Section 2, paragraph 1, line 6, "but what do they do from time-sequential 3-D compatibility?": I prefer not to have rhetorical questions. Can you reword this? What about: "Consider how they could affect time-sequential 3-D compatibility."

Section 3.2, line 2, "100-120 Hz is usually considered necessary for flicker-free viewing with the time sequential 3-D method." I agree with you but can you provide a reference for this?

Section 3.2, final sentence, "however this area will be discussed further later in the paper" -> "This is discussed further in Section ???" (where is it discussed?)

Section 3.6, final sentence: "the 3-D video signal" -> "the frame-sequential 3-D video signal" (to avoid ambiguity)

Section 4, lines 5 and 6: delete "unfortunately" and "even unable" -> "unable"

Section 5.2, line 4, "aka" (again): this is too informal, you should use "also called" or "also known as".

Section 6, Table 1: can you use a proper tick mark rather than a square root sign? In LaTeX try the AMS symbol `\checkmark`

Paper 8 - Woods, Harris (2010)

Email from peer-review chair:

From: Nick Holliman [mailto:n.s.holliman@durham.ac.uk]
Sent: Thursday, 18 February 2010 1:43 AM
To: Andrew Woods
Subject: Re: 7524-25 review

Below are the reviewer's comments:

bw

Nick.

>>>>>>>>>

The paper seems to read well and provides useful information into which glasses and displays to use if Anaglyph is the only option. The work clearly has some limitations but these are well discussed in the final section.

The Paper includes 11 numbered references, but the doesn't seem to be any numbers in the text to link the references to the background work etc. For example in the Introduction the paper refers to Woods and Rourke, however there are multiple papers in the references by Woods and Rourke, so it is unclear as to which paper they are referring to (maybe both). It would be clearer if the references were cited at the relevant places in the text.

The text below Figure 1, refers to 5 points labeled (1) to (5). It maybe clearer if these numbers are also added to the relevant areas of the figure itself.

Given the number of limitations, some idea of what future work should be undertaken might be useful. Is there some way to perform a visual quality assessment of crosstalk for glasses/displays using humans or can the crosstalk simulation algorithm be developed further to address some of the limitations.

Aside from the paper content, there seemed to be some formatting issues, with graphs appearing over tables, but these may simply be down to the fact the paper is written in one version of MS Word and viewed in another.

Also will the paper be printed in colour in the proceedings. Different colours are used and referred to in the text. I printed the paper in B and W and it was sometimes confusing to work out what was being referred too. I realise this problem is mentioned for figures and the reader pointed to the website, but it was the greyed out colours in the results tables which were more confusing.

Somewhat nit picking but... In 4.2 Limitation of this Study, they refer to 'pulfrich effect'. I believe Pulfrich should start with a capital.... Isn't the phenomenon named after Carl Pulfrich, who first described it in the 1920s?

<<<<<<<<<<

Paper 14 - Woods (2009)

Email from special issue associate editor:

From: Brian Schowengerdt
Sent: Wednesday, 27 May 2009 7:45 AM
To: Andrew Woods
Subject: Re: 3D Displays article for ID

Hi Andrew,

The article looks great! Thanks for putting it together under a tight time schedule.

You've presented a very nice cross-section of the relevant technologies. I think the article could be passed along to the copy editors at this point, but I do have a few content-related suggestions that you might consider before we pass it along.

1) Do you think it would be appropriate to include one or two figures and a couple of paragraphs summarizing your findings from your two recent SD&A papers that tested the performance of commercially-available 3D displays? I think that data would nicely compliment the higher-level survey of 3D display options. Perhaps you prefer not to include that data because it's already been published, but if you omitted that element to keep the word count within bounds, I think we can be flexible there.

2) I like your bracketed recommendations for figures. In particular, the figures that present the general layout of the technologies will be quite helpful, I think. The product pictures are less critical, in my view.

3) Currently, you discuss time-sequential stereo on LCDs in two separate sections of your article. First, you mention the NVIDIA effort. Later, you discuss the problems with using conventional 2D-market LCDs. I think it might be helpful to move the paragraph that discusses the NVIDIA effort, to place it directly behind the discussion of the challenges of using LCDs for time-sequential stereo. That way, the logical flow would be 1) many people have LCDs now, so it is tempting to try to use them for stereo, 2) it turns out that LCDs that haven't been specifically engineered for stereo cannot be used successfully, 3) even the newer fast refresh rate LCDs have issues because they are hold-type displays, 4) despite these challenges, some companies are working to enable 3D-ready LCDs. NVIDIA has spearheaded an effort, mostly for the 3D gaming market, while Samsung, Toshiba, and others are demonstrating solutions in the lab (but it is unclear how long it will take to transition them to commercial products).

4) As a follow-on to the above suggestion, you might consider a general merging of your "3D Displays in the Home" section with your "Can I use my existing home TV for 3D purposes?" section, into a single section that surveys the relevant display technologies (both those marketed for 3D applications and those not). This would allow you to group discussions by technology. E.g., regarding plasma TVs, you could start with your paragraph that conventional plasma displays can't be used successfully for stereo, and follow it with your paragraph about the special Samsung plasma television that overcomes limitation of conventional plasmas.

5) I have mixed feelings about the paragraph on the Infitec/Dolby glasses. It might be more detail than is necessary for this 3D home entertainment oriented article. I think it may be sufficient to state that the Dolby glasses are incompatible with all current Home 3D displays. If you would prefer to leave it in, then it might be helpful to expand the discussion to include the possibility of future Dolby-compatible displays. A custom 6-color LCD color filter could be used to create two separate RGB sets for LCD panels, and I recall seeing DLP-based displays that used more than 3 color primaries (I've found some papers out of Samsung on multi-primary displays. Mitsubishi might have also done some work in this area).

The editors are currently reviewing the article by Bill Zou, so I think we are ok for time. If any of my suggestions resonate, or if you would like to make any other revisions, I think a week would be fine--though of course the sooner, the better.

Thanks again,

Brian

Paper 17 - Woods, Helliwell (2012)

Email from peer-review chair:

-----Original Message-----
From: Nicolas Holliman [mailto:n.s.holliman@durham.ac.uk]
Sent: Saturday, 24 December 2011 5:05 AM
To: Andrew Woods
Subject: SDA2012 - reviews for your paper 8228-49

Dear Andrew,

I have received the attached reviews(s) for your paper with comments intended to help you improve the presentation and clarity of your work.

Please could you address all the points raised and upload a new version of the paper to MySpie. Also could you please send me a note explaining what you have done to address the points raised by the reviewer in the revised paper.

If you address all points raised we will list the paper as peer reviewed in the conference proceedings. I may send the revised paper to reviewers again to confirm they are happy with the changes.

Best wishes,
Nick Holliman, SDA2012 Co-chair.

Paper 18 – Woods (2013)

Journal of European Science Editing

http://www.ease.org.uk/sites/default/files/ese_instructions_for_authors_june_2012.pdf

Original articles will be subject to external peer review. Final acceptance or rejection is decided by the Publications Committee. Articles should not exceed 3200 words long and should include an abstract of no more than 200 words. Articles should follow the IMRaD format (Introduction, Methods, Results, and Discussion) and include a structured abstract with four headings: Background, Methods, Results, and Conclusion.

Statement of independence between manager of the peer-review process and the other conference chairs of the Stereoscopic Displays and Applications conference for **Paper 6, Paper 7, Paper 8** and **Paper 17**:

Professor Nick Holliman
Department of Theatre, Film and Television
The University of York
Y010 5GB, United Kingdom

14th October 2013

To whom it may concern

Dear Sir/Madam,

The Stereoscopic Displays and Applications conference has been running a peer-review process since 2008. This was something I felt was a requirement for the conference in the light of recent moves to quality assess research outputs in some countries in the world and has been under my leadership as co-chair of the conference.

The aim of the peer review process, as with any other, is to improve the quality of the proceedings by providing authors with independent critical review of their work and the opportunity to revise their work in the light of the review. It also provides academic authors publishing at the conference a route for additional recognition of the quality of their submission.

In order to maintain the independence of the process I have been the only co-chair involved in the peer review process, acting as the Editor of the peer reviewed papers. I can confirm therefore that Andrew Woods was and is not involved in the peer review process.

Yours sincerely

A black rectangular box redacting the signature of the sender.

Nicolas S. Holliman
BSc (Dunelm), PhD (Leeds), MIEECS, MACM, SMSPIE
Professor of Interactive Media
Head of the Interactive Media Group

Appendix 4 – Copyright Permissions

PERMISSION TO USE COPYRIGHT MATERIAL

I hereby give permission for Andrew Woods to include the below-mentioned materials in his doctoral thesis for Curtin University of Technology, and to communicate this material via the Australasian Digital Thesis Program. This permission is granted on a non-exclusive basis and for an indefinite period.

I confirm that SPIE is the copyright owner of the specified materials.

Permission to use this material is subject to the following conditions: [Delete if not applicable]



SPIE Publisher's permission is hereby granted under the following conditions: ~~(1) you obtain permission of the author(s);~~ (2) the material to be used has appeared in our publication without credit or acknowledgment to another source; and (3) you credit the original SPIE publication. Include the authors' names, title of paper, volume title, SPIE volume number, and year of publication in your credit statement.

Director of Publications

SPIE

Signed:

Name:

Position:

Date:

Eric Pepper, Director of Publications

PO Box 10, Bellingham, WA 98227-0010 USA
360/676-3290 (Pacific Time) eric@spie.org

Date 3/13/2013

Please return signed form to: Andrew Woods, Curtin University, GPO Box U1987, Perth 6845 Australia.

- A. J. Woods, S. Tan (2002) "Characterising Sources of Ghosting in Time-Sequential Stereoscopic Video Displays" presented at Stereoscopic Displays and Applications XIII (SD&A), published in Stereoscopic Displays and Virtual Reality Systems IX, Proceedings of IS&T/SPIE Electronic Imaging, SPIE Vol. 4660, pp. 66-77, San Jose, California, January 2002.
- A. J. Woods, T. Rourke (2004) "Ghosting in Anaglyphic Stereoscopic Images" presented at Stereoscopic Displays and Applications XV (SD&A), published in Stereoscopic Displays and Virtual Reality Systems XI, Proceedings of IS&T/SPIE Electronic Imaging, SPIE Vol. 5291, pp. 354-365, San Jose, California, January 2004.
- A. J. Woods, T. Rourke (2007) "The compatibility of consumer DLP projectors with time-sequential stereoscopic 3D visualization", presented at Stereoscopic Displays and Applications XVIII, published in Stereoscopic Displays and Virtual Reality Systems XIV, Proceedings of IS&T/SPIE Electronic Imaging, SPIE Vol. 6490, pp. 64900V-1 to -7, San Jose, California, January 2007.
- A. J. Woods, K. S. Karvinen (2008) "The compatibility of consumer plasma displays with time-sequential stereoscopic 3D visualization" in Stereoscopic Displays and Applications XIX, Proceedings of IS&T/SPIE Electronic Imaging, SPIE Vol. 6803, pp. 68030X-1 to -9, San Jose, California, January 2008.
- A. J. Woods, A. Sehic (2009) "The compatibility of LCD TVs with time-sequential stereoscopic 3D visualization" in Stereoscopic Displays and Applications XX, Proceedings of IS&T/SPIE Electronic Imaging, SPIE Vol. 7237, pp. 72370N-1 to -9, San Jose, California, January 2009.
- A. J. Woods, C. R. Harris (2010) "Comparing levels of crosstalk with red/cyan, blue/yellow, and green/magenta anaglyph 3D glasses" in Stereoscopic Displays and Applications XXI, Proceedings of IS&T/SPIE Electronic Imaging, SPIE Vol. 7253, pp. 75240Q-1 to -12, San Jose, California, January 2010.
- M. A. Weissman, A. J. Woods (2011) "A simple method for measuring crosstalk in stereoscopic displays" in Stereoscopic Displays and Applications XXII, Proceedings of IS&T/SPIE Electronic Imaging, SPIE Vol. 7863, pp. 786310-1 to -11, Burlingame, California, January 2011.
- A. J. Woods (2011) "How are crosstalk and ghosting defined in the stereoscopic literature?" in Stereoscopic Displays and Applications XXII, Proceedings of IS&T/SPIE Electronic Imaging, SPIE Vol. 7863, pp. 78630Z-1 to -12, Burlingame, California, January 2011.
- A. J. Woods, J. Helliwell (2012) "Investigating the cross-compatibility of IR-controlled active shutter glasses" in Stereoscopic Displays and Applications XXIII, Proceedings of IS&T/SPIE Electronic Imaging, SPIE Vol. 8288, pp. 82881C-1 to -10, Burlingame, California, January 2012.
- A. J. Woods (2012) "Crosstalk in Stereoscopic Displays: a review" in Journal of Electronic Imaging, IS&T/SPIE, Vol. 21, No. 4, pp. 040902 (December 2012).

-end-

PERMISSION TO USE COPYRIGHT MATERIAL AS SPECIFIED BELOW:

- A. J. Woods, T. Rourke, K. L. Yuen (2006) "The Compatibility of Consumer Displays with Time-Sequential Stereoscopic 3D Visualisation" (Plenary Paper), in Proceedings of the K-IDS Three-Dimensional Display Workshop 2006, pp. 7-10, Seoul National University, Seoul, South Korea, 21 August 2006.
- A. J. Woods, K. L. Yuen (2006) "Compatibility of LCD Monitors with Frame-Sequential Stereoscopic 3D Visualisation" (Invited Paper), in IMID/IDMC '06 Digest, (The 6th International Meeting on Information Display, and The 5th International Display Manufacturing Conference), pp. 98-102, Daegu, South Korea, 22-25 August 2006.

I hereby give permission for Andrew Woods to include the below-mentioned materials in his doctoral thesis for Curtin University of Technology, and to communicate this material via the Australasian Digital Thesis Program. This permission is granted on a non-exclusive basis and for an indefinite period.

I confirm that K-IDS is the copyright owner of the specified materials.

Permission to use this material is subject to the following conditions: [Delete if not applicable]

Signed:



Name: *Jin Tang*
Position: *president of KIDS*
Date: *March 14, 2013*

PERMISSION TO USE COPYRIGHT MATERIAL AS SPECIFIED BELOW:

- A. J. Woods, C. R. Harris (2012) "Using cross-talk simulation to predict the performance of anaglyph 3-D glasses" in Journal of the Society for Information Display, Vol. 20, No. 6, pp. 304-315.
- A. J. Woods, K. L. Yuen, and K. S. Karvinen (2007) "Characterizing crosstalk in anaglyphic stereoscopic images on LCD monitors and plasma displays" in Journal of the Society for Information Display, Volume 15, Issue 11, pp. 889-898, November 2007.
- A. J. Woods (2005) "Compatibility of Display Products with Stereoscopic Display Methods" International Display Manufacturing Conference (IDMC), pp. 290-293, Taiwan, February 2005.

I hereby give permission for Andrew Woods to include the below-mentioned materials in his doctoral thesis for Curtin University of Technology, and to communicate this material via the Australasian Digital Thesis Program. This permission is granted on a non-exclusive basis and for an indefinite period.

I confirm that SID is the copyright owner of the specified materials.

Permission to use this material is subject to the following conditions:
- Acknowledge SID as the copyright owner on all applicable pages.

Signed:



Name: Brian Berkeley
Position: President, SID
Date: 13 June, 2013

PERMISSION TO USE COPYRIGHT MATERIAL AS SPECIFIED BELOW:

- A. J. Woods (2009) "3-D Displays in the Home" Information Display, 25(07), pp 8-12, July 2009.

I hereby give permission for Andrew Woods to include the below-mentioned materials in his doctoral thesis for Curtin University of Technology, and to communicate this material via the Australasian Digital Thesis Program. This permission is granted on a non-exclusive basis and for an indefinite period.

I confirm that SID is the copyright owner of the specified materials.

Permission to use this material is subject to the following conditions: [Delete if not applicable]

Signed:



Name:

BRIAN BERKELEY

Position:

PRESIDENT

Date:

10/15/2013

Permission to include **Paper 18** from European Science Editing journal by President of the European Association of Science Editing:

PERMISSION TO USE COPYRIGHT MATERIAL AS SPECIFIED BELOW:

- A. J. Woods 2013 3D or 3-D: a study of terminology, sage and style European Science Editing, 39 3 , pp. 59-62, August 2013.

I hereby give permission for Andrew Woods to include the below-mentioned materials in his doctoral thesis for Curtin University of Technology, and to communicate this material via the Australasian Digital Thesis Program. This permission is granted on a non-exclusive basis and for an indefinite period.

I confirm that EASE is the copyright owner of the specified materials.

Permission to use this material is subject to the following conditions: Delete if not applicable

Signed: Joan Marsh

Name: Joan Marsh

Position: EASE President

Date: 16th October 2013

Appendix 5 – Full List of All Included Publications

The following list of paper numbers and their corresponding full paper citation for all publications included with the thesis is provided to assist the reader.

(Paper Number Order)

- Paper 1** A. J. Woods (2012) "Crosstalk in Stereoscopic Displays: a review" *Journal of Electronic Imaging*, IS&T/SPIE, 21(4), pp. 040902-1 to 040902-21, Oct-Dec 2012.
- Paper 2** A. J. Woods, K. L. Yuen, K. S. Karvinen (2007) "Characterizing crosstalk in anaglyphic stereoscopic images on LCD monitors and plasma displays" *Journal of the Society for Information Display*, 15(11), pp. 889-898, November 2007.
- Paper 3** A. J. Woods, C. R. Harris (2012) "Using cross-talk simulation to predict the performance of anaglyph 3-D glasses" in *Journal of the Society for Information Display*, 20(6), pp. 304-315.
- Paper 4** A. J. Woods, C. R. Harris, D. B. Leggo, T. M. Rourke (2013) "Characterizing and Reducing Crosstalk in Printed Anaglyph Stereoscopic 3D Images" (*Journal of*) *Optical Engineering*, SPIE, 52(4), pp. 043203-1 to 043203-19, April 2013.
- Paper 5** A. J. Woods, K. L. Yuen (2006) "Compatibility of LCD Monitors with Frame-Sequential Stereoscopic 3D Visualisation" (Invited Paper), in *IMID/IDMC '06 Digest*, (The 6th International Meeting on Information Display, and The 5th International Display Manufacturing Conference), pp. 98-102, Daegu, South Korea, 22-25 August 2006.
- Paper 6** A. J. Woods, K. S. Karvinen (2008) "The compatibility of consumer plasma displays with time-sequential stereoscopic 3D visualization" in *Stereoscopic Displays and Applications XIX*, Proceedings of IS&T/SPIE Electronic Imaging, SPIE Vol. 6803, pp. 68030X-1 to 68030X-9, San Jose, California, January 2008.
- Paper 7** A. J. Woods, A. Sehic (2009) "The compatibility of LCD TVs with time-sequential stereoscopic 3D visualization" in *Stereoscopic Displays and Applications XX*, Proceedings of IS&T/SPIE Electronic Imaging, SPIE Vol. 7237, pp. 72370N-1 to 72370N-9, San Jose, California, January 2009.
- Paper 8** A. J. Woods, C. R. Harris (2010) "Comparing levels of crosstalk with red/cyan, blue/yellow, and green/magenta anaglyph 3D glasses" in *Stereoscopic Displays and Applications XXI*, Proceedings of IS&T/SPIE Electronic Imaging, SPIE Vol. 7253, pp. 75240Q-1 to 75240Q-12, San Jose, California, January 2010.
- Paper 9** A. J. Woods, S. Tan (2002) "Characterising Sources of Ghosting in Time-Sequential Stereoscopic Video Displays" presented at *Stereoscopic Displays and Applications XIII (SD&A)*, published in *Stereoscopic Displays and Virtual Reality Systems IX*, Proceedings of IS&T/SPIE Electronic Imaging, SPIE Vol. 4660, pp. 66-77, San Jose, California, January 2002.
- Paper 10** A. J. Woods, T. Rourke (2004) "Ghosting in Anaglyphic Stereoscopic Images" presented at *Stereoscopic Displays and Applications XV (SD&A)*, published in *Stereoscopic Displays and Virtual Reality Systems XI*, Proceedings of IS&T/SPIE Electronic Imaging, SPIE Vol. 5291, pp. 354-365, San Jose, California, January 2004.
- Paper 11** A. J. Woods (2005) "Compatibility of Display Products with Stereoscopic Display Methods" *International Display Manufacturing Conference (IDMC)*, pp. 290-293, Taiwan, February 2005.
- Paper 12** A. J. Woods, T. Rourke, K. L. Yuen (2006) "The Compatibility of Consumer Displays with Time-Sequential Stereoscopic 3D Visualisation" (Invited Plenary Paper), Proceedings of the *K-IDS Three-Dimensional Display Workshop 2006*, pp. 7-10, Seoul National University, Seoul, South Korea, 21 August 2006.
- Paper 13** A. J. Woods, T. Rourke (2007) "The compatibility of consumer DLP projectors with time-sequential stereoscopic 3D visualization" presented at *Stereoscopic Displays and Applications XVIII*, published in *Stereoscopic Displays and Virtual Reality Systems XIV*, Proceedings of IS&T/SPIE Electronic Imaging, SPIE Vol. 6490, pp. 64900V-1 to 64900V -7, San Jose, California, January 2007.
- Paper 14** A. J. Woods (2009) "3-D Displays in the Home" *Information Display*, 25(07), pp 8-12, July 2009.

- Paper 15** M. A. Weissman, A. J. Woods (2011) "A simple method for measuring crosstalk in stereoscopic displays" Stereoscopic Displays and Applications XXII, Proceedings of IS&T/SPIE Electronic Imaging, SPIE Vol. 7863, pp. 786310-1 to -11, Burlingame, California, January 2011.
- Paper 16** A. J. Woods (2011) "How are crosstalk and ghosting defined in the stereoscopic literature?" Stereoscopic Displays and Applications XXII, Proceedings of IS&T/SPIE Electronic Imaging, SPIE Vol. 7863, pp. 78630Z-1 to 78630Z-12, Burlingame, California, January 2011.
- Paper 17** A. J. Woods, J. Helliwell (2012) "Investigating the cross-compatibility of IR-controlled active shutter glasses" Stereoscopic Displays and Applications XXIII, Proceedings of IS&T/SPIE Electronic Imaging, SPIE Vol. 8288, pp. 82881C-1 to 82881C-10, Burlingame, California, January 2012.
- Paper 18** A. J. Woods, (2013) "3D or 3-D: A study of terminology, usage and style" European Science Editing, 39(3), pp. 59-62, August 2013.

(Chronological Order)

- Paper 9** A. J. Woods, S. Tan (2002) "Characterising Sources of Ghosting in Time-Sequential Stereoscopic Video Displays" presented at Stereoscopic Displays and Applications XIII (SD&A), published in Stereoscopic Displays and Virtual Reality Systems IX, Proceedings of IS&T/SPIE Electronic Imaging, SPIE Vol. 4660, pp. 66-77, San Jose, California, January 2002.
- Paper 10** A. J. Woods, T. Rourke (2004) "Ghosting in Anaglyphic Stereoscopic Images" presented at Stereoscopic Displays and Applications XV (SD&A), published in Stereoscopic Displays and Virtual Reality Systems XI, Proceedings of IS&T/SPIE Electronic Imaging, SPIE Vol. 5291, pp. 354-365, San Jose, California, January 2004.
- Paper 11** A. J. Woods (2005) "Compatibility of Display Products with Stereoscopic Display Methods" International Display Manufacturing Conference (IDMC), pp. 290-293, Taiwan, February 2005.
- Paper 12** A. J. Woods, T. Rourke, K. L. Yuen (2006) "The Compatibility of Consumer Displays with Time-Sequential Stereoscopic 3D Visualisation" (Invited Plenary Paper), Proceedings of the K-IDS Three-Dimensional Display Workshop 2006, pp. 7-10, Seoul National University, Seoul, South Korea, 21 August 2006.
- Paper 5** A. J. Woods, K. L. Yuen (2006) "Compatibility of LCD Monitors with Frame-Sequential Stereoscopic 3D Visualisation" (Invited Paper), in IMID/IDMC '06 Digest, (The 6th International Meeting on Information Display, and The 5th International Display Manufacturing Conference), pp. 98-102, Daegu, South Korea, 22-25 August 2006.
- Paper 13** A. J. Woods, T. Rourke (2007) "The compatibility of consumer DLP projectors with time-sequential stereoscopic 3D visualization" presented at Stereoscopic Displays and Applications XVIII, published in Stereoscopic Displays and Virtual Reality Systems XIV, Proceedings of IS&T/SPIE Electronic Imaging, SPIE Vol. 6490, pp. 64900V-1 to 64900V -7, San Jose, California, January 2007.
- Paper 2** A. J. Woods, K. L. Yuen, K. S. Karvinen (2007) "Characterizing crosstalk in anaglyphic stereoscopic images on LCD monitors and plasma displays" Journal of the Society for Information Display, 15(11), pp. 889-898, November 2007.
- Paper 6** A. J. Woods, K. S. Karvinen (2008) "The compatibility of consumer plasma displays with time-sequential stereoscopic 3D visualization" in Stereoscopic Displays and Applications XIX, Proceedings of IS&T/SPIE Electronic Imaging, SPIE Vol. 6803, pp. 68030X-1 to 68030X-9, San Jose, California, January 2008.
- Paper 7** A. J. Woods, A. Sehic (2009) "The compatibility of LCD TVs with time-sequential stereoscopic 3D visualization" in Stereoscopic Displays and Applications XX, Proceedings of IS&T/SPIE Electronic Imaging, SPIE Vol. 7237, pp. 72370N-1 to 72370N-9, San Jose, California, January 2009.
- Paper 14** A. J. Woods (2009) "3-D Displays in the Home" Information Display, 25(07), pp 8-12, July 2009.
- Paper 8** A. J. Woods, C. R. Harris (2010) "Comparing levels of crosstalk with red/cyan, blue/yellow, and green/magenta anaglyph 3D glasses" in Stereoscopic Displays and Applications XXI, Proceedings of IS&T/SPIE Electronic Imaging, SPIE Vol. 7253, pp. 75240Q-1 to 75240Q-12, San Jose, California, January 2010.
- Paper 15** M. A. Weissman, A. J. Woods (2011) "A simple method for measuring crosstalk in stereoscopic displays" Stereoscopic Displays and Applications XXII, Proceedings of IS&T/SPIE Electronic Imaging, SPIE Vol. 7863, pp. 786310-1 to -11, Burlingame, California, January 2011.
- Paper 16** A. J. Woods (2011) "How are crosstalk and ghosting defined in the stereoscopic literature?" Stereoscopic Displays and Applications XXII, Proceedings of IS&T/SPIE Electronic Imaging, SPIE Vol. 7863, pp. 78630Z-1 to 78630Z-12, Burlingame, California, January 2011.
- Paper 17** A. J. Woods, J. Helliwell (2012) "Investigating the cross-compatibility of IR-controlled active shutter glasses" Stereoscopic Displays and Applications XXIII, Proceedings of IS&T/SPIE Electronic Imaging, SPIE Vol. 8288, pp. 82881C-1 to 82881C-10, Burlingame, California, January 2012.

- Paper 3** A. J. Woods, C. R. Harris (2012) "Using cross-talk simulation to predict the performance of anaglyph 3-D glasses" in Journal of the Society for Information Display, 20(6), pp. 304-315.
- Paper 1** A. J. Woods (2012) "Crosstalk in Stereoscopic Displays: a review" Journal of Electronic Imaging, IS&T/SPIE, 21(4), pp. 040902-1 to 040902-21, Oct-Dec 2012.
- Paper 4** A. J. Woods, C. R. Harris, D. B. Leggo, T. M. Rourke (2013) "Characterizing and Reducing Crosstalk in Printed Anaglyph Stereoscopic 3D Images" (Journal of) Optical Engineering, SPIE, 52(4), pp. 043203-1 to 043203-19, April 2013.
- Paper 18** A. J. Woods, (2013) "3D or 3-D: A study of terminology, usage and style" European Science Editing, 39(3), pp. 59-62, August 2013.

(Alphabetical Order by Title)

- Paper 18** A. J. Woods (2013) "3D or 3-D: A study of terminology, usage and style", European Science Editing, 39(3), pp. 59-62, August 2013. [REFEREED JOURNAL PAPER]
- Paper 14** A. J. Woods (2009) "3-D Displays in the Home" Information Display, 25(07), pp 8-12, July 2009. [REVIEWED ARTICLE]
- Paper 15** M. A. Weissman, A. J. Woods (2011) "A simple method for measuring crosstalk in stereoscopic displays" in Stereoscopic Displays and Applications XXII, Proceedings of IS&T/SPIE Electronic Imaging, SPIE Vol. 7863, pp. 786310-1 to -11, Burlingame, California, January 2011. [NON-REFEREED CONFERENCE PAPER]
- Paper 5** A. J. Woods, K. L. Yuen (2006) "Compatibility of LCD Monitors with Frame-Sequential Stereoscopic 3D Visualisation" (Invited Paper), in IMID/IDMC '06 Digest, (The 6th International Meeting on Information Display, and The 5th International Display Manufacturing Conference), pp. 98-102, Daegu, South Korea, 22-25 August 2006.
- Paper 9** A. J. Woods, S. Tan (2002) "Characterising Sources of Ghosting in Time-Sequential Stereoscopic Video Displays" presented at Stereoscopic Displays and Applications XIII (SD&A), published in Stereoscopic Displays and Virtual Reality Systems IX, Proceedings of IS&T/SPIE Electronic Imaging, SPIE Vol. 4660, pp. 66-77, San Jose, California, January 2002. [NON REFEREED CONFERENCE PAPER]
- Paper 4** A. J. Woods, C. R. Harris, D. B. Leggo, T. M. Rourke (2013) "Characterizing and Reducing Crosstalk in Printed Anaglyph Stereoscopic 3D Images" (Journal of) Optical Engineering, SPIE, 52(4), pp. 043203-1 to 043203-19, April 2013.
- Paper 2** A. J. Woods, K. L. Yuen, K. S. Karvinen (2007) "Characterizing crosstalk in anaglyphic stereoscopic images on LCD monitors and plasma displays" Journal of the Society for Information Display, 15(11), pp. 889-898, November 2007.
- Paper 8** A. J. Woods, C. R. Harris (2010) "Comparing levels of crosstalk with red/cyan, blue/yellow, and green/magenta anaglyph 3D glasses" in Stereoscopic Displays and Applications XXI, Proceedings of IS&T/SPIE Electronic Imaging, SPIE Vol. 7253, pp. 75240Q-1 to 75240Q-12, San Jose, California, January 2010.
- Paper 11** A. J. Woods (2005) "Compatibility of Display Products with Stereoscopic Display Methods" International Display Manufacturing Conference (IDMC), pp. 290-293, Taiwan, February 2005. [NON-REFEREED CONFERENCE PAPER]
- Paper 1** A. J. Woods (2012) "Crosstalk in Stereoscopic Displays: a review" Journal of Electronic Imaging, IS&T/SPIE, 21(4), pp. 040902-1 to 040902-21, Oct-Dec 2012.
- Paper 10** A. J. Woods, T. Rourke (2004) "Ghosting in Anaglyphic Stereoscopic Images" presented at Stereoscopic Displays and Applications XV (SD&A), published in Stereoscopic Displays and Virtual Reality Systems XI, Proceedings of IS&T/SPIE Electronic Imaging, SPIE Vol. 5291, pp. 354-365, San Jose, California, January 2004. [NON-REFEREED CONFERENCE PAPER]
- Paper 16** A. J. Woods (2011) "How are crosstalk and ghosting defined in the stereoscopic literature?" in Stereoscopic Displays and Applications XXII, Proceedings of IS&T/SPIE Electronic Imaging, SPIE Vol. 7863, pp. 78630Z-1 to -12, Burlingame, California, January 2011. [NON-REFEREED CONFERENCE PAPER]
- Paper 17** A. J. Woods, J. Helliwell (2012) "Investigating the cross-compatibility of IR-controlled active shutter glasses" in Stereoscopic Displays and Applications XXIII, Proceedings of IS&T/SPIE Electronic Imaging, SPIE Vol. 8288, pp. 82881C-1 to -10, Burlingame, California, January 2012. [REFEREED CONFERENCE PAPER]
- Paper 12** A. J. Woods, T. Rourke, K. L. Yuen (2006) "The Compatibility of Consumer Displays with Time-Sequential Stereoscopic 3D Visualisation" (Plenary Paper), in Proceedings of the K-IDS Three-Dimensional Display Workshop 2006, pp. 7-10, Seoul National University, Seoul, South Korea, 21 August 2006. [NON-REFEREED CONFERENCE PAPER]
- Paper 13** A. J. Woods, T. Rourke (2007) "The compatibility of consumer DLP projectors with time-sequential stereoscopic 3D visualization", presented at Stereoscopic Displays and Applications XVIII, published in Stereoscopic Displays and Virtual Reality Systems XIV, Proceedings of IS&T/SPIE Electronic Imaging, SPIE Vol. 6490, pp. 64900V-1 to -7, San Jose, California, January 2007. [NON-REFEREED CONFERENCE PAPER]

- Paper 7** A. J. Woods, A. Sehic (2009) "The compatibility of LCD TVs with time-sequential stereoscopic 3D visualization" in Stereoscopic Displays and Applications XX, Proceedings of IS&T/SPIE Electronic Imaging, SPIE Vol. 7237, pp. 72370N-1 to 72370N-9, San Jose, California, January 2009.
- Paper 6** A. J. Woods, K. S. Karvinen (2008) "The compatibility of consumer plasma displays with time-sequential stereoscopic 3D visualization" in Stereoscopic Displays and Applications XIX, Proceedings of IS&T/SPIE Electronic Imaging, SPIE Vol. 6803, pp. 68030X-1 to 68030X-9, San Jose, California, January 2008.
- Paper 3** A. J. Woods, C. R. Harris (2012) "Using cross-talk simulation to predict the performance of anaglyph 3-D glasses" in Journal of the Society for Information Display, 20(6), pp. 304-315.